

Drug resistance in breast cancer – mechanisms and approaches to overcome chemoresistance

Edited by

Maria Rosaria De Miglio, Anca Maria Cimpean and Dayanidhi Raman

Published in

Frontiers in Oncology



FRONTIERS EBOOK COPYRIGHT STATEMENT

The copyright in the text of individual articles in this ebook is the property of their respective authors or their respective institutions or funders. The copyright in graphics and images within each article may be subject to copyright of other parties. In both cases this is subject to a license granted to Frontiers.

The compilation of articles constituting this ebook is the property of Frontiers.

Each article within this ebook, and the ebook itself, are published under the most recent version of the Creative Commons CC-BY licence. The version current at the date of publication of this ebook is CC-BY 4.0. If the CC-BY licence is updated, the licence granted by Frontiers is automatically updated to the new version.

When exercising any right under the CC-BY licence, Frontiers must be attributed as the original publisher of the article or ebook, as applicable.

Authors have the responsibility of ensuring that any graphics or other materials which are the property of others may be included in the CC-BY licence, but this should be checked before relying on the CC-BY licence to reproduce those materials. Any copyright notices relating to those materials must be complied with.

Copyright and source acknowledgement notices may not be removed and must be displayed in any copy, derivative work or partial copy which includes the elements in question.

All copyright, and all rights therein, are protected by national and international copyright laws. The above represents a summary only. For further information please read Frontiers' Conditions for Website Use and Copyright Statement, and the applicable CC-BY licence.

ISSN 1664-8714
ISBN 978-2-83251-365-1
DOI 10.3389/978-2-83251-365-1

About Frontiers

Frontiers is more than just an open access publisher of scholarly articles: it is a pioneering approach to the world of academia, radically improving the way scholarly research is managed. The grand vision of Frontiers is a world where all people have an equal opportunity to seek, share and generate knowledge. Frontiers provides immediate and permanent online open access to all its publications, but this alone is not enough to realize our grand goals.

Frontiers journal series

The Frontiers journal series is a multi-tier and interdisciplinary set of open-access, online journals, promising a paradigm shift from the current review, selection and dissemination processes in academic publishing. All Frontiers journals are driven by researchers for researchers; therefore, they constitute a service to the scholarly community. At the same time, the *Frontiers journal series* operates on a revolutionary invention, the tiered publishing system, initially addressing specific communities of scholars, and gradually climbing up to broader public understanding, thus serving the interests of the lay society, too.

Dedication to quality

Each Frontiers article is a landmark of the highest quality, thanks to genuinely collaborative interactions between authors and review editors, who include some of the world's best academicians. Research must be certified by peers before entering a stream of knowledge that may eventually reach the public - and shape society; therefore, Frontiers only applies the most rigorous and unbiased reviews. Frontiers revolutionizes research publishing by freely delivering the most outstanding research, evaluated with no bias from both the academic and social point of view. By applying the most advanced information technologies, Frontiers is catapulting scholarly publishing into a new generation.

What are Frontiers Research Topics?

Frontiers Research Topics are very popular trademarks of the *Frontiers journals series*: they are collections of at least ten articles, all centered on a particular subject. With their unique mix of varied contributions from Original Research to Review Articles, Frontiers Research Topics unify the most influential researchers, the latest key findings and historical advances in a hot research area.

Find out more on how to host your own Frontiers Research Topic or contribute to one as an author by contacting the Frontiers editorial office: frontiersin.org/about/contact

Drug resistance in breast cancer – mechanisms and approaches to overcome chemoresistance

Topic editors

Maria Rosaria De Miglio — University of Sassari, Italy

Anca Maria Cimpean — Victor Babes University of Medicine and Pharmacy, Romania

Dayanidhi Raman — University of Toledo, United States

Citation

De Miglio, M. R., Cimpean, A. M., Raman, D., eds. (2023). *Drug resistance in breast cancer – mechanisms and approaches to overcome chemoresistance*.

Lausanne: Frontiers Media SA. doi: 10.3389/978-2-83251-365-1

Table of contents

05	Editorial: Drug resistance in breast cancer – mechanisms and approaches to overcome chemoresistance Dayanidhi Raman, Anca Maria Cimpean and Maria Rosaria De Miglio
09	miR-27-3p Enhances the Sensitivity of Triple-Negative Breast Cancer Cells to the Antitumor Agent Olaparib by Targeting PSEN-1, the Catalytic Subunit of Γ-Secretase Meng Zhao, Baisheng Sun, Yan Wang, Gengbao Qu, Hua Yang and Pilin Wang
17	STAT5a Confers Doxorubicin Resistance to Breast Cancer by Regulating ABCB1 Zhaoqing Li, Cong Chen, Lini Chen, Dengdi Hu, Xiqian Yang, Wenying Zhuo, Yongxia Chen, Jingjing Yang, Yulu Zhou, Misha Mao, Xun Zhang, Ling Xu, Siwei Ju, Jun Shen, Qinchuan Wang, Minjun Dong, Shuduo Xie, Qun Wei, Yunlu Jia, Jichun Zhou and Linbo Wang
32	Corrigendum: STAT5a Confers Doxorubicin Resistance to Breast Cancer by Regulating ABCB1 Zhaoqing Li, Cong Chen, Lini Chen, Dengdi Hu, Xiqian Yang, Wenying Zhuo, Yongxia Chen, Jingjing Yang, Yulu Zhou, Misha Mao, Xun Zhang, Ling Xu, Siwei Ju, Jun Shen, Qinchuan Wang, Minjun Dong, Shuduo Xie, Qun Wei, Yunlu Jia, Jichun Zhou and Linbo Wang
34	Cytotoxic Effects of Hellebrigenin and Arenobufagin Against Human Breast Cancer Cells Yu Zhang, Bo Yuan, Baolin Bian, Haiyu Zhao, Anna Kiyomi, Hideki Hayashi, Yui Iwatani, Munetoshi Sugiura and Norio Takagi
46	The Role of Non-Coding RNAs in Breast Cancer Drug Resistance Jin-hai Tian, Shi-hai Liu, Chuan-yang Yu, Li-gang Wu and Li-bin Wang
59	High Expression of Complement Component C7 Indicates Poor Prognosis of Breast Cancer and Is Insensitive to Taxane-Anthracycline Chemotherapy Huikun Zhang, Yawen Zhao, Xiaoli Liu, Li Fu, Feng Gu and Yongjie Ma
73	Which Clinicopathologic Parameters Suggest Primary Resistance to Palbociclib in Combination With Letrozole as the First-Line Treatment for Hormone Receptor-Positive, HER2-Negative Advanced Breast Cancer? Ji-Yeon Kim, Jung Min Oh, Yeon Hee Park, Jin Seok Ahn and Young-Hyuck Im
86	MicroRNAs Role in Breast Cancer: Theranostic Application in Saudi Arabia Nouf M. Alyami

- 98 **Advancements in 3D Cell Culture Systems for Personalizing Anti-Cancer Therapies**
Andrew M. K. Law, Laura Rodriguez de la Fuente, Thomas J. Grundy, Guocheng Fang, Fatima Valdes-Mora and David Gallego-Ortega
- 113 **Chidamide Reverses Fluzoparib Resistance in Triple-Negative Breast Cancer Cells**
Xinyang Li, Xiang Yuan, Ziming Wang, Jing Li, Zhiwei Liu, Yukun Wang, Limin Wei, Yuanpei Li and Xinshuai Wang
- 126 **Breast Cancer Stem-Like Cells in Drug Resistance: A Review of Mechanisms and Novel Therapeutic Strategies to Overcome Drug Resistance**
Taniya Saha and Kiven Erique Lukong
- 155 **Pyrotinib-Containing Neoadjuvant Therapy in Patients With HER2-Positive Breast Cancer: A Multicenter Retrospective Analysis**
Xiaoyun Mao, Pengwei Lv, Yiping Gong, Xiujuan Wu, Peng Tang, Shushu Wang, Dianlong Zhang, Wei You, Ouchen Wang, Jun Zhou, Jingruo Li and Feng Jin
- 164 **Augmentation of Extracellular ATP Synergizes With Chemotherapy in Triple Negative Breast Cancer**
Jasmine M. Manouchehri, Jharna Datta, Natalie Willingham, Robert Wesolowski, Daniel Stover, Ramesh K. Ganju, William E. Carson, Bhuvaneswari Ramaswamy and Mathew A. Cherian



OPEN ACCESS

EDITED AND REVIEWED BY

Kara Britt,
Peter MacCallum Cancer Centre,
Australia

*CORRESPONDENCE

Dayanidhi Raman

✉ dayanidhi.raman@utoledo.edu

Anca Maria Cimpean

✉ ancacimpean1972@yahoo.com

✉ acimpeanu@umft.ro

Maria Rosaria De Miglio

✉ demiglio@uniss.it

SPECIALTY SECTION

This article was submitted to
Breast Cancer,
a section of the journal
Frontiers in Oncology

RECEIVED 26 October 2022

ACCEPTED 20 December 2022

PUBLISHED 04 January 2023

CITATION

Raman D, Cimpean AM
and De Miglio MR (2023) Editorial:
Drug resistance in breast cancer –
mechanisms and approaches to
overcome chemoresistance.
Front. Oncol. 12:1080684.
doi: 10.3389/fonc.2022.1080684

COPYRIGHT

© 2023 Raman, Cimpean and De Miglio.

This is an open-access article
distributed under the terms of the
[Creative Commons Attribution License](https://creativecommons.org/licenses/by/4.0/)
(CC BY). The use, distribution or
reproduction in other forums is
permitted, provided the original
author(s) and the copyright owner(s)
are credited and that the original
publication in this journal is cited, in
accordance with accepted academic
practice. No use, distribution or
reproduction is permitted which does
not comply with these terms.

Editorial: Drug resistance in breast cancer – mechanisms and approaches to overcome chemoresistance

Dayanidhi Raman^{1*}, Anca Maria Cimpean^{2,3,4*}
and Maria Rosaria De Miglio^{5*}

¹Department of Cell and Cancer Biology, University of Toledo, Toledo OH, United States,

²Department of Microscopic Morphology/Histology, Victor Babes University of Medicine and Pharmacy, Timisoara, Romania, ³Angiogenesis Research Center Timisoara, Victor Babes University of Medicine and Pharmacy, Timisoara, Romania, ⁴Center of Expertise for Rare Vascular Disease in Children, Emergency Hospital for Children Louis Turcanu, Timisoara, Romania, ⁵Department of Medicine, Surgery and Pharmacy, University of Sassari, Sassari, Italy

KEYWORDS

breast cancer, drug resistance, stem-like cells, non-coding RNAs, triple-negative breast cancer

Editorial on the Research Topic

Drug resistance in breast cancer – mechanisms and approaches to overcome chemoresistance

According to the GLOBOCAN program 2020, breast cancer (BC) had the highest incidence among women worldwide, with an estimated 2.3 million new cases, corresponding to 11.7% of all cancer cases. It is the fifth leading cause of cancer mortality in the world, with 685,000 deaths (1). Conventional therapeutic approaches for BC include radical surgical

resection, radiotherapy, chemotherapy, and endocrine therapies, which induce cancer cell death. Recently, immunotherapy and targeted therapies have altered the prognoses of patients with BC, improving their life quality and survival (2), (3). Despite significant improvement in the outcomes of BC patients, many of them present intrinsic drug resistance, while others are initially drug-sensitive but acquire resistance to anticancer drugs, and frequently multidrug resistance, leading to recurrence and/or metastasis (4–6). Furthermore, growing evidence revealed that patients with the same BC molecular subtype can have different responses to treatment, strongly supporting the high BC heterogeneity. Currently, drug resistance is a major reason for poor prognosis, reducing survival in BC patients (7). If drug resistance could be defeated the impact on BC patient survival would be significant.

Multiple mechanisms linked to drug resistance have been explained in BC treatment, including somatic mutations or epigenetic changes within drug targets, cancer cell heterogeneity, cancer stem cells, cancer-associated macrophages and immune cells modulation, metabolic reprogramming, and interactions among cancer cells and tumor microenvironment (8). Substantial evidence linked therapy resistance to aberrations in miRNA (microRNA, small, single-stranded, non-coding RNA molecules containing 21 to 23 nucleotides) expression levels, which in turn cause dysregulation of gene expression (9). Alyami argued that the main rationale for targeting miRNA is how their involvement in miRNA-mRNA complex networks can manipulate cell apoptosis, cell cycle, epithelial-mesenchymal transition (EMT), and drug resistance, making it an exclusive therapeutic target.

Tian et al. summarized the mechanisms of ncRNAs (non-coding RNA) in chemotherapeutic, endocrine, and targeted drug resistance in BC patients. They described ncRNAs as a target gene of drugs influencing its effects by acting as ceRNAs (competing endogenous RNA that regulate other RNA transcripts by competing for shared miRNAs). This mechanism modulated neoplastic cell sensitivity and drug resistance, regulating cancer apoptosis and cell cycle transfer, and inducing modulation of various signaling pathways. Moreover, Tian et al. suggested that targeting ncRNAs could be a novel strategy for achieving improved treatment outcomes for BC patients.

Recently, the PARP inhibitor Olaparib was approved for the treatment of triple-negative breast cancer (TNBC) with BRCA mutations (10), although differences in the sensitivity of individual patients and resistance to Olaparib have been shown (11). Interesting results of Zhao et al. showed that the sensitivity of TNBC cells to Olaparib can be increased by inducing overexpression in neoplastic cells miR-27-3p, which targets sPSEN-1, the catalytic subunit of γ -secretase, and blocks the activation of the Notch pathway via the inhibition of the cleavage of the Notch protein.

The failure of current therapies and the consequent high mortality in BC patients is greatly ascribed to the therapy-resistant cancer stem cells (CSCs) present in the bulk of the tumor. Often, CSCs increase the drug efflux transporters and

mostly stay in the non-dividing cell-cycle phase (G0) to escape conventional therapeutics, and the induced residual disease is responsible for tumor progression (12). As summarized by Saha et al., the recognition of deregulated miRNAs/ncRNAs/mRNAs signatures in CSCs and their crosstalk with multiple pathways uncovered potential therapeutic targets in drug-resistant BC. Moreover, therapies that can induce alternative mechanisms of cell death, such as ferroptosis, pyroptosis, immunotherapy, drugs targeting CSC metabolism, and nanoparticle therapy, are the upcoming approaches to target the CSCs and overcome drug resistance.

The leading cause of BC death is disease progression due to metastases. Because of this challenge, the identification of unambiguous molecular biomarkers to predict the disease response is needed. Biomarkers are independent and measurable assessments of biological states or diseases that can be critical for the appropriate management of BC during treatment (Saha et al.).

Li et al. identified STAT5a as a key promoter of doxorubicin (DOX)-resistance in BC, inducing overexpression of the multidrug resistance protein ABCB1. Moreover, the use of the STAT5 inhibitor Pimozide, initially approved by the FDA as a psychotropic diseases drug, significantly increased BC cells' sensitivity to DOX both *in vitro* and *in vivo*. STAT5a could be a promising therapeutic target for the treatment of chemoresistant BC, with Pimozide being a likely candidate to reduce chemoresistance. Zhang et al. provided evidence that complement component C7 expression (a 93-kDa serum glycoprotein encoded by the C7 gene, one of the main components of Membrane Attacking Complex-MAC) was an independent poor prognostic factor in triple-negative and luminal B BC subtypes. Furthermore, patients with high C7 expression were insensitive to taxane-anthracycline (TE)-based chemotherapy. These findings highlighted the importance of C7 in BC progression and set a foundation to help clinicians improve the identification of patients for TE chemotherapy by determining C7 expression in the era of precision medicine.

Extracellular adenosine triphosphate (eATP) is abundant in the tumor microenvironment. eATP is highly toxic to BC cells despite being easily degraded by eATPases. Chemotherapy induces further increases in eATP through P2RX channels of cancer cells. Interesting results obtained by Manouchehri et al., demonstrated that eATP is toxic to several TNBC cell lines, and that the purinergic channels P2RX4 and P2RX7 are necessary for this effect. Chemotherapy exposure induced the release of eATP from TNBC cell lines, and inhibitors of eATP metabolism augmented chemotherapy-induced loss of TNBC cell viability.

Cyclin-dependent kinases 4 and 6 (CDK4 and CDK6) are enzymes important in cell division. For ER-positive and HER2-negative metastatic BC, endocrine therapy (ET) combined with CDK4/6 inhibitors is the gold standard for first- and second-line treatment (13). Nevertheless, resistance to this combination therapy frequently develops in this BC subtype. Kim et al. developed a prediction model based on five clinical and

preclinical factors: (i) primary resistance to adjuvant ET; (ii) liver metastasis; (iii) initial CA-15-3 elevation; (iv) weak ER expression, and (v) BRCA2 mutations. Based on this prediction model, patients with ER-positive and HER2-negative metastatic BC may benefit from an initial examination to help identify subgroups at risk of developing primary resistance to the first-line treatment of Palbociclib with Letrozole. In ER-positive and HER2-negative metastatic BC patients, this prediction model-based first evaluation may aid oncologists in the early identification of a group at high risk of acquiring primary resistance to combined therapy with Palbociclib and Letrozole. This group of individuals has a significant propensity for acquiring medication resistance, thus additional treatment options should be considered.

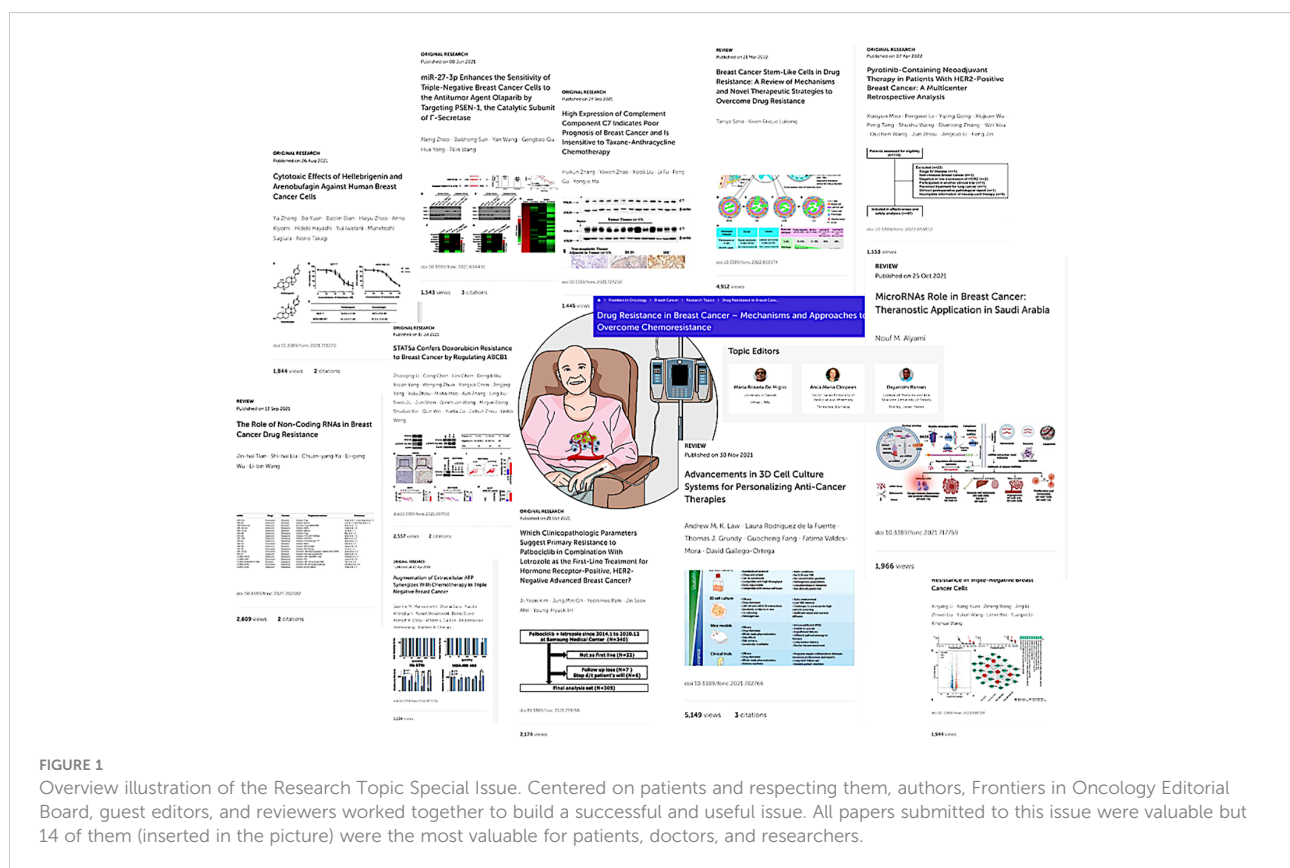
Furthermore, Mao et al. showed that PR-negativity was a significant prognostic factor for total pathological complete response (pCR) or breast pCR rate in HER2 positive BC subtype treated with pyrotinib-containing neoadjuvant therapy.

More frequently, anticancer drug candidates result in translational failures in clinical trials and the main reason for this failure can be attributed to non-accurate preclinical models. Law et al. summarized that to ensure drug efficacy and its mechanism of action has clinical translatability, the complexity of the tumor microenvironment needs to be appropriately modeled. 3D culture models are emerging as powerful

research tools that recapitulate *in vivo* characteristics. Technological advancements in this field show promising applications in improving drug discovery, pre-clinical validation, and precision medicine.

Conclusions

Breast cancer remains one of the most challenging diseases, with unexpected behavior even after several years of remission. Breast cancer molecular classification represented a big step in the elucidation of this malignant heterogeneity, but it seems that it is not enough to explain some hidden sides of the disease, especially the development of therapy resistance. The papers published in the Research Topic -Drug Resistance in Breast Cancer – Mechanisms and Approaches to Overcome Chemoresistance in Frontiers in Oncology (Figure 1) suggested that molecular classification needs to be improved by adding new criteria derived from more accurate experimental and clinical data. Also, this Research Topic highlighted the invasion ability and metastasis of breast cancer stem cells and their response and resistance to current therapies. This Research Topic contains a well-balanced proportion of valuable clinical and experimental



studies in the field of breast cancer, which are extremely useful for both clinicians and academic researchers.

Author contributions

All authors listed have made a substantial, direct, and intellectual contribution to the work and approved it for publication.

Acknowledgments

We are grateful to the Frontiers in Oncology Editorial Team members for their continuous, valuable and helpful support given to us for this Research Topic.

References

1. Sung H, Ferlay J, Siegel RL, Laversanne M, Soerjomataram I, Jemal A, et al. Global cancer statistics 2020: GLOBOCAN estimates of incidence and mortality worldwide for 36 cancers in 185 countries. *CA Cancer J Clin* (2021) 71:209–49. doi: 10.3322/CAAC.21660
2. Esteva FJ, Hubbard-Lucey VM, Tang J, Pusztai L. Immunotherapy and targeted therapy combinations in metastatic breast cancer. *Lancet Oncol* (2019) 20:e175–86. doi: 10.1016/S1470-2045(19)30026-9
3. Masoud V, Pagès G. Targeted therapies in breast cancer: New challenges to fight against resistance. *World J Clin Oncol* (2017) 8:120–34. doi: 10.5306/WJCO.V8.I2.120
4. Abad E, Graifer D, Lyakhovich A. DNA Damage response and resistance of cancer stem cells. *Cancer Lett* (2020) 474:106–17. doi: 10.1016/J.CANLET.2020.01.008
5. Marquette C. Chemotherapy-resistant metastatic breast cancer. *Curr Treat Options Oncol* (2012) 13:263–75. doi: 10.1007/s11864-012-0184-6
6. Brown KA, Andreopoulou E, Andreopoulou P. TOUCH MEDICAL MEDIA endocrine therapy-related endocrinopathies-biology, prevalence, and implications for the management of breast cancer. *Rev Breast Cancer J Publ Date* (2020) 6:17–22. doi: 10.17925/OHR.2020.16.1.17
7. Longley DB, Johnston PG. Molecular mechanisms of drug resistance. *J Pathol J Pathol* (2005) 205:275–92. doi: 10.1002/path.1706
8. Hu W, Tan C, He Y, Zhang G, Xu Y, Tang J. OncoTargets and therapy downregulate functional miRNAs in breast cancer drug resistance. *Onco Targets Ther* (2018) 11:1529–41. doi: 10.2147/OTT.S152462
9. Mulrane L, Mcgee SF, Gallagher WM, O'connor DP. miRNA dysregulation in breast cancer. (2013). doi: 10.1158/0008-5472.CAN-13-1841
10. Eikesdal HP, Yndestad S, Elzawahry A, Llop-Guevara A, Gilje B, Blix ES, et al. Olaparib monotherapy as primary treatment in unselected triple negative breast cancer. *Ann Oncol* (2021) 32:240–9. doi: 10.1016/J.ANNONC.2020.11.009
11. Moustafa D, Abd Elwahed MR, Elsaid HH, Parvin JD. Modulation of early mitotic inhibitor 1 (EMI1) depletion on the sensitivity of PARP inhibitors in BRCA1 mutated triple-negative breast cancer cells. *PloS One* (2021) 16:e0235025. doi: 10.1371/JOURNAL.PONE.0235025
12. Wang J, Liu X, Jiang Z, Li L, Cui Z, Gao Y, et al. A novel method to limit breast cancer stem cells in states of quiescence, proliferation or differentiation: Use of gel stress in combination with stem cell growth factors. *Oncol Lett* (2016) 12:1355–60. doi: 10.3892/OL.2016.4757/HTML
13. Cardoso F, Paluch-Shimon S, Senkus E, Curigliano G, Aapro MS, André F, et al. 5th ESO-ESMO international consensus guidelines for advanced breast cancer (ABC 5). *Ann Oncol* (2020) 31:1623–49. doi: 10.1016/J.ANNONC.2020.09.010

Conflict of interest

The authors declare that the research was conducted in the absence of any commercial or financial relationships that could be construed as potential conflicts of interest.

Publisher's note

All claims expressed in this article are solely those of the authors and do not necessarily represent those of their affiliated organizations, or those of the publisher, the editors and the reviewers. Any product that may be evaluated in this article, or claim that may be made by its manufacturer, is not guaranteed or endorsed by the publisher.



miR-27-3p Enhances the Sensitivity of Triple-Negative Breast Cancer Cells to the Antitumor Agent Olaparib by Targeting PSEN-1, the Catalytic Subunit of γ -Secretase

Meng Zhao¹, Baisheng Sun², Yan Wang¹, Gengbao Qu¹, Hua Yang^{3*} and Pilin Wang^{1*}

¹ Department of Breast Surgery, Beijing Tian Tan Hospital, Capital Medical University, Beijing, China, ² Emergency Department, Fifth Medical Center of the General Hospital of the Chinese People's Liberation Army, Beijing, China,

³ Department of Medical Oncology, Affiliated Hospital of Hebei University, Hebei Key Laboratory of Cancer Radiotherapy and Chemotherapy, Baoding City, China

OPEN ACCESS

Edited by:

Maria Rosaria De Miglio,
University of Sassari, Italy

Reviewed by:

Petra Tesarova,
Charles University, Czechia
Eric Wickstrom,
Thomas Jefferson University,
United States

*Correspondence:

Pilin Wang
wangpilin315@126.com
Hua Yang
huayang2010@aliyun.com

Specialty section:

This article was submitted to
Breast Cancer,
a section of the journal
Frontiers in Oncology

Received: 13 April 2021

Accepted: 21 May 2021

Published: 08 June 2021

Citation:

Zhao M, Sun B, Wang Y, Qu G,
Yang H and Wang P (2021)
miR-27-3p Enhances the Sensitivity of
Triple-Negative Breast Cancer Cells to
the Antitumor Agent Olaparib by
Targeting PSEN-1, the Catalytic
Subunit of γ -Secretase.
Front. Oncol. 11:694491.
doi: 10.3389/fonc.2021.694491

Olaparib has been used in the treatment of triple-negative breast cancer (TNBC) with BRCA mutations. In the present study, we demonstrated the effect of miR-27-3p on the γ -secretase pathway by regulating the sensitivity of TNBC cells to olaparib. miR-27-3p, a microRNA with the potential to target PSEN-1, the catalytic subunit of γ -secretase mediating the second step of the cleavage of the Notch protein, was identified by the online tool miRDB and found to inhibit the expression of PSEN-1 by directly targeting the 3'-untranslated region (3'-UTR) of PSEN-1. The overexpression of miR-27-3p inhibited the activation of the Notch pathway via the inhibition of the cleavage of the Notch protein, mediated by γ -secretase, and, in turn, enhanced the sensitivity of TNBC cells to the antitumor agent olaparib. Transfection with PSEN-1 containing mutated targeting sites for miR-27-3p or the expression vector of the Notch protein intracellular domain (NICD) almost completely blocked the effect of miR-27-3p on the Notch pathway or the sensitivity of TNBC cells to olaparib, respectively. Therefore, our results suggest that the miR-27-3p/ γ -secretase axis participates in the regulation of TNBC and that the overexpression of miR-27-3p represents a potential approach to enhancing the sensitivity of TNBC to olaparib.

Keywords: microRNA-27-3p, Notch pathway, triple-negative breast cancer, olaparib, γ -secretase, PSEN-1

INTRODUCTION

At present, breast cancer (BC) is the most important malignancy threatening female health (1, 2). The main pathological subtypes of BC are endocrine-dependent BC (treated with estrogen receptor- α [ER α] antagonists, including tamoxifen and fulvestrant) and HER2-positive BC (treated with therapeutic antibodies, such as trastuzumab, and small molecules, such as lapatinib) (3–5). The overall prognosis has been significantly improved by the widespread application of effective antitumor drug therapy, but the heterogeneous overall prognosis of triple-negative breast cancer

(TNBC) remains unsatisfactory (6, 7). Recently, the PARP inhibitor olaparib was approved for the treatment of TNBC with BRCA mutations (8–10). Although olaparib is considered to have a beneficial effect on patients with TNBC and prolong the survival of patients, there are differences in the sensitivity of individual patients to olaparib, and there are also reports of olaparib resistance (11, 12). Therefore, research and development regarding strategies to achieve more effective olaparib treatment is of great importance.

The Notch pathway not only functions as the key regulator of the cell-fate decision but also induces the resistance of cancerous cells to antitumor strategies, such as radiation therapy and antitumor agents (13, 14). Increasing data have confirmed that the activation of the Notch pathway relates to the occurrence and progress of human cancers (15, 16). Until now, a total of four types of Notch receptors (Notch protein) has been identified: Notch-1, Notch-2, Notch-3 and Notch-4 (17). Five kinds of Notch's ligands, DLL1, DLL3, DLL4, Jagged1 and Jagged2 bind to Notch protein to activate Notch pathway (18, 19). The Notch-protein is featured as single trans-transmembrane with an extracellular ligand-binding domain and an intracellular domains (NICD) (20). In cancerous cells, the Notch pathway is activated *via* a two-step cleavage process in the presence of ligand-binding (21). ADAMs (a disintegrin and metalloproteinase), including ADAM17 and ADAM10, mediate the first cleavage of Notch, and γ -secretase mediates the second cleavage of Notch; finally, the notch intracellular domain (NICD) is released and translocated to the nucleus to mediate the transcription of certain genes related to drug resistance (22, 23). These genes often encode cellular pro-survival, anti-apoptotic, and epithelial-mesenchymal transition-related factors (24, 25). The activation of the Notch pathway ultimately induces cancerous cells to resist therapeutic strategies (26, 27). Because there are two ADAMs (ADAM17 and ADAM10) that mediate the first cleavage of Notch, the two proteins show mutual compensation in this process, so the second cleavage of Notch, mediated by γ -secretase alone, is an important target for the inhibition Notch pathway activity.

The γ -secretase is considered as an intramembrane aspartate-lyase with multi-subunits, including the PSEN-1, nicastrin subunit (NCSTN), anterior pharynx-defective subunit (APH-1) and presenilin enhancer subunit (PEN-2) (28, 29). Among these subunits, PSEN-1 functions as the catalytic core/subunit for the γ -secretase (30). Inhibition of γ -secretase's activation has the important anti-tumor properties by blocking of the Notch pathway's activation and repressing the expression of PSEN-1 is a promising approach for γ -secretase inhibition.

MicroRNA is a type of small non-coding RNA transcribed by RNA polymerase II (31, 32). It can recognize and bind to the 3'UTR of the target mRNA and degrade the mRNA to achieve gene silencing (33, 34). The use of miRNA to inhibit the expression of tumor-related genes has emerged as an important strategy for antitumor therapy (35). The γ -Secretase is a complex containing multiple protein subunits, including PSEN-1, the catalytic center; Pen-2, the activity regulator subunit; and NCSTN, to stabilize the complex (21). In the present study, miR-27-3p was found to inhibit the activation of

γ -secretase. The overexpression of miR-27-3p enhanced the sensitivity of TNBC cells, MDA-MB-436 or HCC1937, to olaparib by targeting the 3'UTR of PSEN-1.

MATERIALS AND METHODS

Clinical Specimens and Ethical Approval

The use of clinical specimens was approved by the ethics committee of the Beijing Tian Tan Hospital, Capital Medical University. The 30 clinical TNBC specimens (the BRCA mutation subtype) and paired non-tumor tissues were described in our previous publication (35). The usage of the clinical specimens were with the written consent from patients and all the experiments related to the human-derived materials, including clinical specimens and cell lines, were used in accordance with the Helsinki Declaration with the approval from medical ethic committee of Beijing Tiantan Hospital or the/the Hebei Key Laboratory of the Cancer Radiotherapy and Chemotherapy. The sample size used in the present study was adequately powered to detect a pre-specified effect size ($1-\beta$: 0.8; $\alpha/2$: 0.025; $P < 0.05$). The original hypothesis was that the expression of miR-27-3p was not significantly different in healthy tissues as compared with tumor tissue; the alternative hypothesis was that the expression of the targeting gene was significantly different in the healthy tissue as compared with the tumor tissue.

Vectors, Cell Lines, and Reagents

The full-length sequences of PSEN-1, PSEN-1 with mutated miR-27-3p binding sites, and pre-miR-27 were obtained *via* chemical synthesis. These sequences were cloned and prepared as lentivirus vectors. The vector containing the NICD sequence was a gift from Prof. and Dr. Yingshi Zhang of Shenyang Pharmaceutical University (36). The TNBC cell lines with BRCA mutations, HCC1937 (Cat. No.: 3111C0001CCC 000352) or MDA-MB-436 (Cat. No.: 3111C0001CCC 000471), were purchased from the National Infrastructure of Cell Resources, Chinese Academy of Medical Sciences/Peking Union Medical College, a Chinese government center for biological sample collection. The cells were cultured in DMEM (Dulbecco's modification of Eagle's medium) supplemented with 10% FBS. The antitumor agent, olaparib (Cat. No.: S1060), was purchased from Selleck Corporation, Houston, Texas, US. The formulations of olaparib used in the cell-based experiments or animal experiments were described in our previous publication (35).

Quantitative Real-Time Polymerase Chain Reaction

The Notch pathway-related factors in TNBC tissues, including the clinical specimens and the subcutaneous tumors, or TNBC cells were quantitatively examined using previously established qPCR methods (10, 37). Ribonucleic acid was extracted from the TNBC cells or clinical tissues and reverse transcribed into cDNA. The

mRNA expression of these factors was measured *via* qPCR, and β -actin was chosen as the loading control. The primers used in qPCR (37) were (1) CDH1 (E-cadherin), forward primer 5'-CTCCTGAAAAGAGAGTGAAGTGT-3', reverse primer 5'-CCGGATTAATCTCCAGCCAGTT-3'; (2) CDH2 (N-cadherin), forward primer 5'-CCTGGATCGCGAGCAGATA-3', reverse primer 5'-CCATTCCAAACCTGGTGTAAAGAAC-3'; (3) vimentin, forward primer 5'-ACCGCACACAGCAAGGCGAT-3', reverse primer 5'-CGATTGAGGGCTCCTAGCGGTT-3'; (4) ZEB1, forward primer 5'-GATGACCTGCCAACAGACCA-3', reverse primer: 5'-CCCCAGGATTTCTTGCCCTT-3'; (5) fibronectin, forward primer 5'-CAGGATCAC TTACGGAGAAACAG-3', reverse primer 5'-GCCAGTGAC AGCATACACAGTG-3'; (6) SLUG, forward primer 5'-CTTCCTGGTCAAGAAGCA-3', reverse primer 5'-GGGAAATAATCACTGTATGTGTG-3'; (7) TWIST, forward primer 5'-GTACATCGACTTCCTCTACCAG-3', reverse primer 5'-CATCCTCCAGACCGAGAAG-3'; (8) BCL2, forward primer 5'-GATCGTTGCCTTATGCATTGTTTTG-3'; reverse primer, 5'-CGGATCTTTATTTTCATGAGGCACGTTA-3'; (9) BIRC2, forward primer 5'-ACATGCAGCTCGAATGAGAACAT-3'; reverse primer 5'-GATTCCCAACACCTCAAGCCA-3'; (10) BIRC3, forward primer 5'-GTGTTCTAGT TAATCCTGAGCAGCTT-3'; reverse primer 5'-TGGAACCA CTTGGCATGTTGA-3'; (11) BIRC5, forward primer 5'-CAAGGACCACCGCATCTCT-3', reverse primer 5'-AGTCCTTGAAGCAGAAGAAACA-3'; (12) NICD, forward primer 5'-CCGACGCACAAGGTGTCTT-3', reverse primer 5'-GTCGGCGTGTGAGTTGATGA-3'; (13) PSEN-1, forward primer 5'-CCATATTGATCGGCCTGTG-4', reverse primer 5'-GAAGGGCTGCACGAGATAAT-3'; and (14) β -actin, forward primer 5'-CACCATTGGCAATGAGCGGTTC-3', reverse primer 5'-AGGTCTTTGCGGATGTCCACGT-3'. The qPCR results were presented as a heat map of mRNA expression and obtained *via* the method of Ma et al. (19).

Cell Survival Analysis

The MDA-MB-436 and HCC1937 cells were cultured and transfected with the indicated vectors. The cells were harvested, seeded into 96-well plates, and treated with the indicated concentrations of olaparib (3 μ mol/L, 1 μ mol/L, 0.3 μ mol/L, 0.1 μ mol/L, 0.03 μ mol/L, 0.01 μ mol/L, or 0.003 μ mol/L) for 48 h. The number of cells was examined *via* MTT (3-(4,5)-dimethylthiazoliazol (-z-y1) -3,5-di-phenyltetrazoliumromide) assay. The inhibition rates were calculated based on the optical density (OD) of cell samples at 490 nm. The IC_{50} values were calculated based on the rate of inhibition (31, 38).

Subcutaneous Tumor Model and Ethical Approval

All animal experiments were approved by the Animal Care and Ethics Committee of the Beijing Tian Tan Hospital, Capital Medical University (n=10 for each group, with animals randomly allocated into two groups) and were performed in accordance with the UK Animals (Scientific Procedures) Act, 1986, and associated guidelines. The HCC-1937 or MDA-MB-231 cells were cultured

and transfected with the indicated vectors. The cells were injected into nude mice subcutaneously. Then, the mice received olaparib *via* oral administration in accordance with the methods described by Sun HW et al. (39) and Feng et al. (40–42). After olaparib treatment, the samples were harvested from the mice, and the expression of Notch pathway-related factors in tissues was examined by qPCR. The tumor volume was calculated from following equation: (tumor length \times tumor width \times tumor width)/2 (41, 42). The tumor weight was measured using a precision balance. The heat-map of qPCR results was produced following the method described by Ma et al. (25).

The Statistical Analysis

The statistical analysis in the presence work were performed by the Bonferroni's correction with two-way ANOVA methods using SPSS software (Version No. 8.0; IBM Corporation, Armonk, NY, USA). The IC_{50} values of olaparib were calculated by using the Origin Software (version 6.1, OriginLab, Northampton, Massachusetts, USA). The $P < 0.05$ was considered as statistically significant between the results from indicated two groups.

RESULTS

miR-27-3p Targets the 3'UTR of PSEN-1

miR-27-3p was predicted as a microRNA that was potentially able to target the 3'UTR of PSEN-1 and inhibit the activation of the γ -secretase/Notch pathway (Figure 1A). As shown in Figure 1, miR-27-3p could bind the 3'UTR of PSEN-1. The expression of miR-27-3p was lower in the TNBC specimens than in the paired non-tumor tissues (Figure 1B), and the expression of miR-27-3p was negatively correlated with PSEN-1 in TNBC tissues (Figure 1C). To confirm the effect of miR-27-3p on PSEN-1, both Western blots of nuclear or cytoplasmic cellular sub-fractions and qPCR assays were performed. As shown in Figures 1D, E, the overexpression of miR-27-3p decreased the expression of PSEN-1 but not that of PSEN-1 with a mutated miR-27-3p binding site (PSEN-1^{Mut}) in the cytoplasm or the accumulation of NICD in the nucleus of HCC-1937 (Figure 1D) and MDA-MB-436 (Figure 1E) TNBC cells. The overexpression of NICD almost blocked the effect of miR-27-3p on NICD but not the suppressive effect on PSEN-1 (Figures 1D, E). Therefore, miR-27-3p was confirmed to target the 3'UTR of PSEN-1 and thus suppress Notch cleavage.

miR-27-3p Suppresses the Activation of the Notch Pathway by Targeting the 3'UTR of PSEN-1

The effect of miR-27-3p on the Notch pathway was examined *via* qPCR. As shown in Figures 1F, G, the overexpression of miR-27-3p suppressed the expression of pro-survival/anti-apoptosis- or epithelial to mesenchymal transition (EMT)-related downstream genes in the Notch pathway in HCC-1937 (Figure 1G) and MDA-MB-436 (Figure 1H) cells. Moreover,

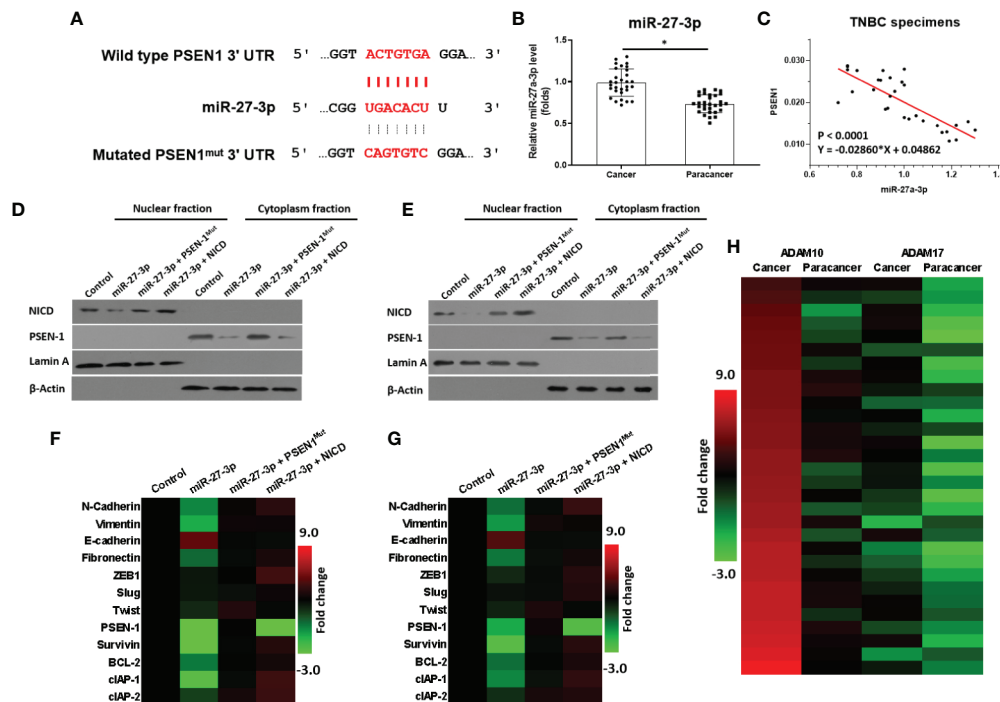


FIGURE 1 | miR-27-3p targets the 3'UTR of PSEN-1. **(A)** miR-27-3p has the potential to target the 3'UTR of PSEN-1. **(B)** The expression of miR-27-3p in TNBC or the paired non-tumor tissues, as determined by qPCR, is presented as a scatterplot. **(C)** The correlation between miR-27-3p and PSEN-1 in TNBC tissues is presented as a scatterplot. **(D, E)** HCC1937 **(D)** or MDA-MB-436 **(E)** TNBC cells were transfected with plasmids, and the subcellular fraction was harvested. The protein expression of PSEN-1 or NICD was examined via western blotting. Lamin A was used to indicate the nuclear material, and β-actin was used to indicate the cytoplasm. **(F, G)** HCC1937 **(F)** or MDA-MB-436 **(G)** TNBC cells were transfected with plasmids and harvested for qPCR. The expression of the downstream genes of the Notch pathway are presented as a heat map. **(H)** The expression of ADAM-17 or ADAM-10 in TNBC tissues was examined by qPCR and is presented as a heat map. *P < 0.05.

to further elucidate the roles of the γ-secretase/Notch axis in TNBC, the expression of ADAM17 and ADAM10 was also examined. As shown in **Figure 1H**, the mRNA expression of ADAM17 and ADAM10 was much higher in TNBC as compared with non-tumor tissues (**Figure 1H**). The expression of ADAM10 was higher than ADAM17 in TNBC cells (**Figure 1H**). Therefore, the elucidation of the roles of miR-27-3p and the γ-secretase/Notch pathway in TNBC is of great significance.

miR-27-3p Enhances the Sensitivity of TNBC Cells to Olaparib by Targeting to the 3'UTR of PSEN-1

The ability of miR-27-3p to enhance the sensitivity of TNBC cells to olaparib was examined by multiple assays. As shown in **Figure 2** and **Table 1**, the antitumor effect of olaparib on the survival of TNBC cells and *in vitro* invasion/migration was enhanced in the presence of miR-27-3p. The overexpression of miR-27-3p also inhibited the expression of downstream genes in the Notch pathway (**Figure 2**). Moreover, the overexpression of PSEN-1^{Mut} or NICD almost blocked the effect of miR-27-3p on the survival of TNBC cells, *in vitro* invasion/migration, and downstream genes of the Notch pathway (**Figure 2**). The *in vivo* growth of TNBC was further examined in a subcutaneous

tumor model (**Figure 3**). The results showed that TNBC cells formed a tumor in the subcutaneous tissue of nude mice (**Figures 3A–D**). The antitumor effect of olaparib on the subcutaneous growth of TNBC cells was enhanced in the presence of miR-27-3p (**Figures 3A–D**). The overexpression of miR-27-3p also inhibited the expression of downstream genes of the Notch pathway in the tumor tissue (**Figure 3B**). Moreover, the overexpression of PSEN-1^{Mut} or NICD almost blocked the effect of miR-27-3p on the survival of TNBC cells, *in vitro* invasion/migration, and the downstream genes of the Notch pathway in the tumor (**Figure 3B**). Therefore, miR-27-3p enhanced the sensitivity of TNBC cells to olaparib by targeting the 3'UTR of PSEN-1.

DISCUSSION

The first antitumor treatment strategies were mainly cytotoxic chemotherapy drugs, such as paclitaxel or doxorubicin (43, 44). However, recent studies have shown that TNBC is heterogeneous and has multiple pathological subtypes (45). The molecularly targeted drug olaparib (a PARP inhibitor) has been approved for the treatment of BRCA-mutated TNBC (46, 47). Given the broad applications of olaparib in clinical treatment, patients with

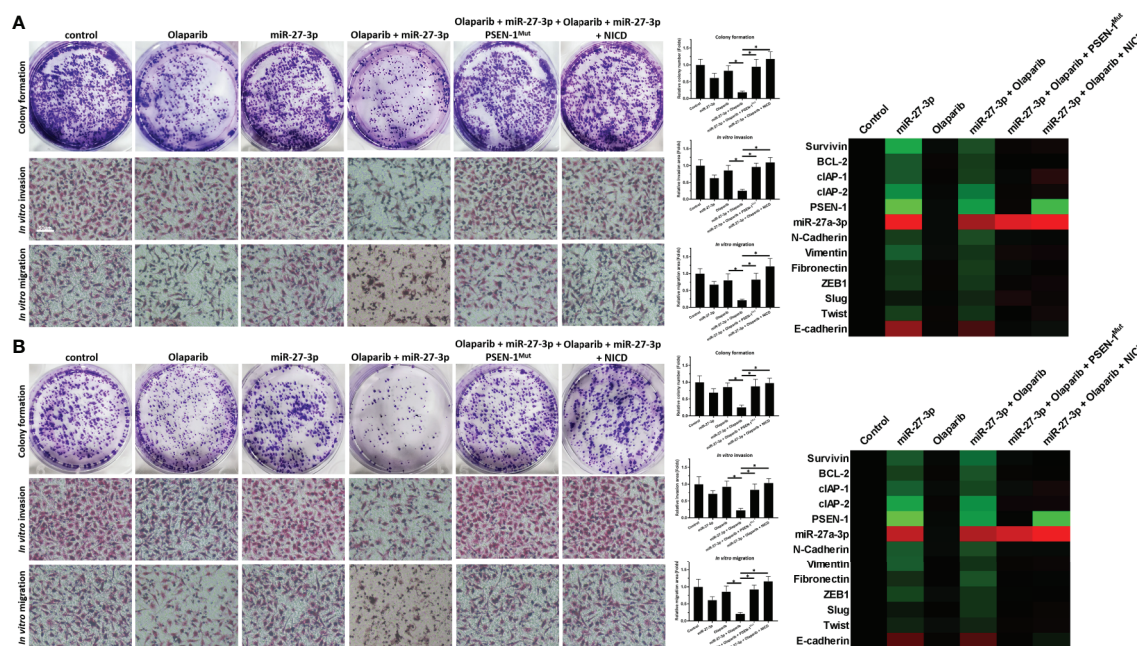


FIGURE 2 | miR-27-3p suppresses the *in vitro* survival or invasion/migration of TNBC cells by targeting the 3'UTR of PSEN-1. **(A, B)** HCC1937 **(A)** or MDA-MB-436 **(B)** TNBC cells were transfected with plasmids or treated with 0.5 $\mu\text{mol/L}$ of olaparib and harvested for colony-formation and Transwell assays. The results are presented as images and quantitative analysis. **(A, B)** The expression of the genes downstream of the Notch pathway in TNBC cells is presented as a heat map. * $P < 0.05$.

TABLE 1 | miR-27-3p enhances the sensitivity of TNBC cells to Olaparib.

Groups	HCC-1937	MDA-MB-436
	IC_{50} values ($\mu\text{mol/L}$)	
control	0.60 ± 0.20	0.74 ± 0.45
miR-27-3p	0.10 ± 0.06	0.17 ± 0.03
miR-27-3p + PSEN-1 ^{Mut}	0.77 ± 0.28	0.96 ± 0.40
miR-27-3p + NICD	1.05 ± 0.69	0.79 ± 0.08

TNBC have also exhibited resistance to olaparib (48). Therefore, it would be of great significance to reverse the resistance of TNBC to olaparib and increase the sensitivity of TNBC cells to olaparib. The results obtained in this study offer several benefits in terms of treatment. Compared with ADAMs, γ -secretase is a better intervention target for the inhibition of the Notch pathway. This will not only help to expand our understanding of the regulation of Notch in TNBC but also provide more options for TNBC treatment.

The γ -Secretase has three main subunits (21). In this study, transfecting TNBC cells with miR-27-3p, which targets PSEN-1, the catalytic subunit of γ -secretase, inhibited the activity of the Notch pathway and upregulated the sensitivity of cells to the molecularly targeted drug olaparib. Preparing miRNAs as lentiviral vectors to interfere with the expression of specific oncogenes and proto-oncogenes has been confirmed as an effective antitumor treatment strategy (49). The effect of miR-27-3p on PSEN-1 was also examined in target-confirmation

studies. The construction of a mutant 3'UTR confirmed the effect of miR-27-3p and the fact that the overexpression of miR-27-3p inhibited the activation of the Notch pathway by targeting PSEN-1. There are four subtypes of Notch protein; these have different extracellular segments (i.e., the N-terminus), but the intracellular segments are highly conserved. Therefore, we prepared nuclear and cytoplasmic sub-fractions and detected the accumulation of the Notch NICD in the nuclear fraction of TNBC cells. Finally, it was confirmed that miR-27-3p regulated Notch protein cleavage, and the influence of miR-27-3p on the Notch pathway was determined by analyzing the EMT, cell pro-survival/anti-apoptosis factors, and other factors downstream of Notch.

Our results mainly focused on the effect of miR-27-3p on Notch pathway in TNBC cells, and miR-27-3p could also regulate some other pathways important for the survival of cancer cells, e.g. MMP13, PPAR γ , Wnt3a, BTG2 or NOVA1 (50–55). In addition to regulating the survival of malignant tumor cells, miR-27-3p may also modify cancer microenvironment by inhibiting fibroblast viability by targeting NOVA1 (55). Moreover, the effect of miR-27-3p by far not limited to the breast cancer and it has been demonstrated that miR-27-3p may also play an important roles in hepatocellular cancer, gastric cancer or osteosarcoma (54–56). Therefore, our results extended our knowledge about the miR-27-3p. Moreover, the presence work concentrate on the usage of miR-27-3p to inhibit the expression of PSEN-1 to inhibit Notch protein cleavage. In addition, there are other miRs that can inhibit the activity of the Notch pathway through other strategies. For

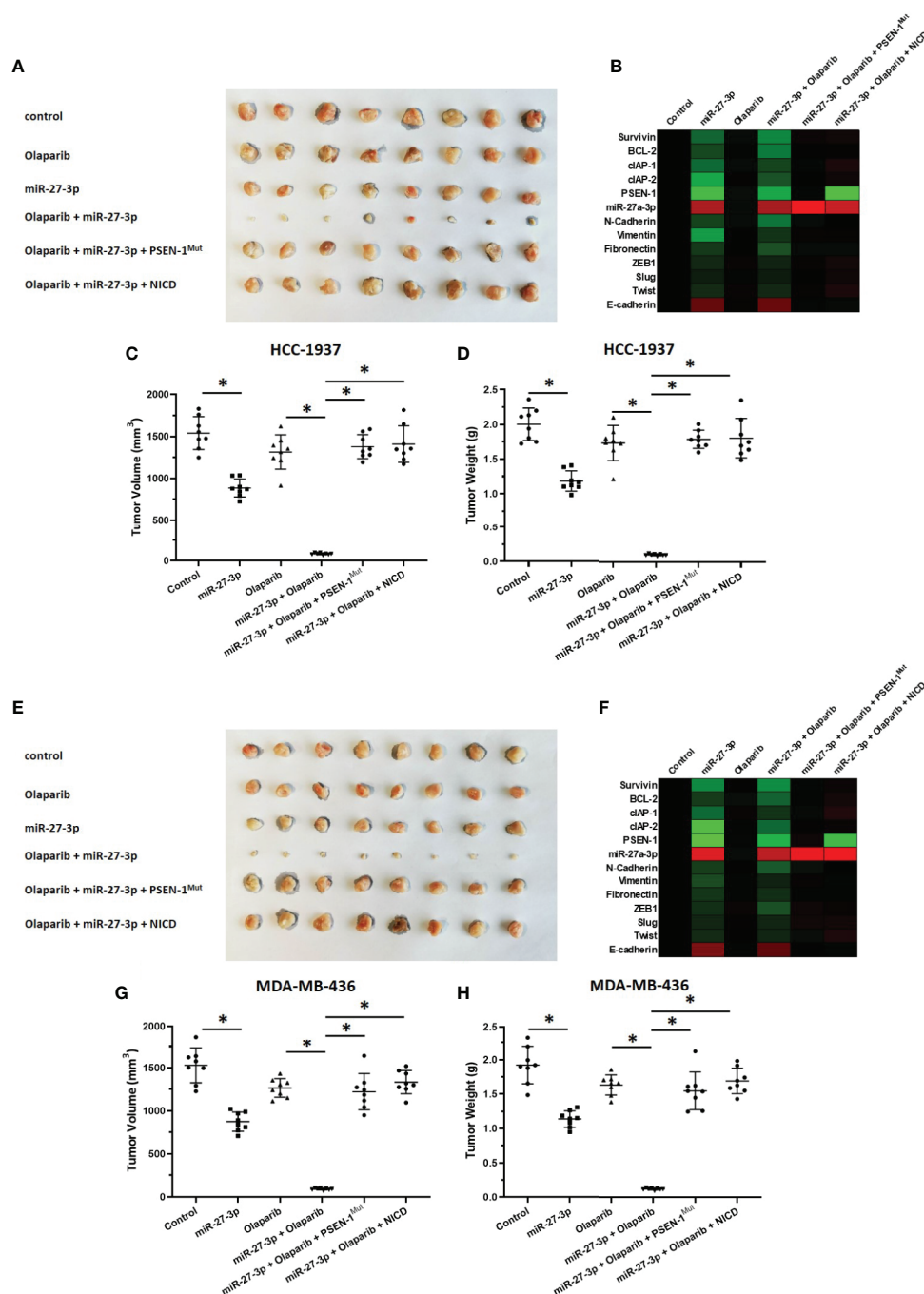


FIGURE 3 | miR-27-3p suppresses the *in vivo* growth of TNBC cells by targeting the 3'UTR of PSEN-1. HCC1937 (A–D) or MDA-MB-436 (E–H) TNBC cells were transfected with plasmids and injected subcutaneously into nude mice. The mice received a 0.5 mg/kg dose of olaparib *via* oral administration. The results are presented as images or the quantitative analysis of tumor tissues (A, C–E, G, H). (B, F) The expression of genes downstream of the Notch pathway in TNBC tissues is presented as a heat map. **P* < 0.05.

example, miR-3163 can inhibit the expression of ADAM17 by acting on the 3'UTR of ADAM17, and finally inhibit the cleavage of Notch protein in HCC cells (49); miR-34a and others can down-regulate the expression level of Notch-1 protein (26). Some previous

publications indicated that miR-27-3p may also interacted with other miRs, e.g. miR-34a-5p (56, 57). These results further confirm the significance of miR-27-3p. In addition to TNBC, Olaparib was also approved for the treatment of ovarian cancer (58, 59). For this

reason, the expression levels of miR-27-3p and PSEN-1 in ovarian cancer tissue samples will be further tested in the future, and whether miR-27-3p can upregulate ovarian cancer cells' sensitivity to Olaparib.

DATA AVAILABILITY STATEMENT

The original contributions presented in the study are included in the article/supplementary material, further inquiries can be directed to the corresponding authors.

ETHICS STATEMENT

The studies involving human participants were reviewed and approved by the ethics committee of the Beijing Tian Tan Hospital, Capital Medical University. The patients/participants provided their written informed consent to participate in this

study. The animal study was reviewed and approved by the ethics committee of the Beijing Tian Tan Hospital, Capital Medical University. Written informed consent was obtained from the individual(s) for the publication of any potentially identifiable images or data included in this article.

AUTHOR CONTRIBUTIONS

MZ, HY and PW designed research. MZ, BS, YW and GQ performed the experiments. HY and PW wrote the manuscript with contributions from all authors. All authors contributed to the article and approved the submitted version.

ACKNOWLEDGMENTS

The authors would like to thank Dr. and Prof. Wei Zhou in Beijing Hospital, Beijing, 100730, PR China, for his advice and supply of materials (the primers used in qPCR).

REFERENCES

- Cortes J, Cescon D, Rugo H, Nowecki Z, Im S, Yusof M, et al. Pembrolizumab Plus Chemotherapy Versus Placebo Plus Chemotherapy for Previously Untreated Locally Recurrent Inoperable or Metastatic Triple-Negative Breast Cancer (KEYNOTE-355): A Randomised, Placebo-Controlled, Double-Blind, Phase 3 Clinical Trial. *Lancet (London England)* (2020) 396:1817–28. doi: 10.1016/s0140-6736(20)32531-9
- Schmid P, Cortes J, Pusztai L, McArthur H, Kümmel S, Bergh J, et al. Pembrolizumab for Early Triple-Negative Breast Cancer. *New Engl J Med* (2020) 382:810–21. doi: 10.1056/NEJMoa1910549
- Fan M, Chen J, Gao J, Xue W, Wang Y, Li W, et al. Triggering a Switch From Basal- to Luminal-Like Breast Cancer Subtype by the Small-Molecule Dipeptidylprolinase G Via Induction of GABARAPL1. *Cell Death Dis* (2020) 11:635. doi: 10.1038/s41419-020-02878-z
- Jiang L, Ren L, Chen H, Pan J, Zhang Z, Kuang X, et al. NCAPG Confers Trastuzumab Resistance Via Activating SRC/STAT3 Signaling Pathway in HER2-Positive Breast Cancer. *Cell Death Dis* (2020) 11:547. doi: 10.1038/s41419-020-02753-x
- Mahboobifard F, Dargahi L, Jorjani M, Ramezani Tehrani F, Pourgholami M. The Role of E α 36 in Cell Type-Specific Functions of Estrogen and Cancer Development. *Pharmacol Res* (2021) 163:105307. doi: 10.1016/j.phrs.2020.105307
- Bertucci F, Ng C, Patsouris A, Droin N, Piscioglio S, Carbuccion N, et al. Genomic Characterization of Metastatic Breast Cancers. *Nature* (2019) 569:560–4. doi: 10.1038/s41586-019-1056-z
- Savas P, Loi S. Expanding the Role for Immunotherapy in Triple-Negative Breast Cancer. *Cancer Cell* (2020) 37:623–4. doi: 10.1016/j.ccell.2020.04.007
- Gu Z, Wang L, Yao X, Long Q, Lee K, Li J, et al. CLC-3/SGK1 Regulatory Axis Enhances the Olaparib-Induced Antitumor Effect in Human Stomach Adenocarcinoma. *Cell Death Dis* (2020) 11:898. doi: 10.1038/s41419-020-03107-3
- Miller A, Garcia P, Yoon K. Developing Effective Combination Therapy for Pancreatic Cancer: An Overview. *Pharmacol Res* (2020) 155:104740. doi: 10.1016/j.phrs.2020.104740
- Wang C, Ding S, Sun B, Shen L, Xiao L, Han Z, et al. Hsa-miR-4271 Downregulates the Expression of Constitutive Androstane Receptor and Enhances In Vivo the Sensitivity of non-Small Cell Lung Cancer to Gefitinib. *Pharmacol Res* (2020) 161:105110. doi: 10.1016/j.phrs.2020.105110
- Moustafa D, Elwahed M, Elsaid H, Parvin J. Modulation of Early Mitotic Inhibitor 1 (EM1) Depletion on the Sensitivity of PARP Inhibitors in BRCA1 Mutated Triple-Negative Breast Cancer Cells. *PLoS One* (2021) 16:e0235025. doi: 10.1371/journal.pone.0235025
- Sun Y, Wu J, Dong X, Zhang J, Meng C, Liu G. MicroRNA-506-3p Increases the Response to PARP Inhibitors and Cisplatin by Targeting EZH2/ β -Catenin in Serous Ovarian Cancers. *Trans Oncol* (2021) 14:100987. doi: 10.1016/j.tranon.2020.100987
- Farooqi A, Butt G, El-Zahaby S, Attar R, Sabitaliyevich U, Jovic J, et al. Luteolin Mediated Targeting of Protein Network and microRNAs in Different Cancers: Focus on JAK-STAT, Notch, mTOR and TRAIL-Mediated Signaling Pathways. *Pharmacol Res* (2020) 160:105188. doi: 10.1016/j.phrs.2020.105188
- Xu Z, Liu C, Zhao Q, Lü J, Ding X, Luo A, et al. Long non-Coding RNA CCAT2 Promotes Oncogenesis in Triple-Negative Breast Cancer by Regulating Stemness of Cancer Cells. *Pharmacol Res* (2020) 152:104628. doi: 10.1016/j.phrs.2020.104628
- Yuan M, Zhao L, Li Y, Gao X, Zhang B, Zhang D, et al. Capsaicin on Stem Cell Proliferation and Fate Determination - A Novel Perspective. *Pharmacol Res* (2021) 167:105566. doi: 10.1016/j.phrs.2021.105566
- Raza W, Luqman S, Meena A. Prospects of Tangeretin as a Modulator of Cancer Targets/Pathways. *Pharmacol Res* (2020) 161:105202. doi: 10.1016/j.phrs.2020.105202
- Zhu QQ, Yang XY, Zhang XJ, Yu CJ, Pang QQ, Huang YW, et al. EGCG Targeting Notch to Attenuate Renal Fibrosis Via Inhibition of TGF β 1/Smad3 Signaling Pathway Activation in Streptozotocin-Induced Diabetic Mice. *Food Funct* (2020) 11(11):9686–95. doi: 10.1039/d0fo01542c
- Durrant CS, Ruscher K, Sheppard O, Coleman MP, Özen I. Beta Secretase 1-Dependent Amyloid Precursor Protein Processing Promotes Excessive Vascular Sprouting Through NOTCH3 Signalling. *Cell Death Dis* (2020) 11(2):98. doi: 10.1038/s41419-020-2288-4
- Wu J, Li H, He J, Tian X, Luo S, Li J, et al. Downregulation of microRNA-9-5p Promotes Synaptic Remodeling in the Chronic Phase After Traumatic Brain Injury. *Cell Death Dis* (2021) 12(1):9. doi: 10.1038/s41419-020-03329-5
- Liu C, Qi M, Li L, Yuan Y, Wu X, Fu J. Natural Cordycepin Induces Apoptosis and Suppresses Metastasis in Breast Cancer Cells by Inhibiting the Hedgehog Pathway. *Food Funct* (2020) 11(3):2107–16. doi: 10.1039/c9fo02879j
- Jia H, Wang Z, Zhang J, Feng F. γ -Secretase Inhibitors for Breast Cancer and Hepatocellular Carcinoma: From Mechanism to Treatment. *Life Sci* (2021) 268:119007. doi: 10.1016/j.lfs.2020.119007
- Kumar V, Vashishta M, Kong L, Wu X, Lu JJ, Guha C, et al. The Role of Notch, Hedgehog, and Wnt Signaling Pathways in the Resistance of Tumors to Anticancer Therapies. *Front Cell Dev Biol* (2021) 9:650772. doi: 10.3389/fcell.2021.650772
- Koo C, Harrison N, Noy P, Szyroka J, Matthews A, Hsia H, et al. The Tetraspanin Tspan15 Is an Essential Subunit of an ADAM10 Scissor Complex. *J Biol Chem* (2020) 295:12822–39. doi: 10.1074/jbc.RA120.012601
- Lu H, Chu H, Tan Y, Qin X, Liu M, Li J, et al. Novel ADAM-17 Inhibitor ZLDI-8 Inhibits the Metastasis of Hepatocellular Carcinoma by Reversing Epithelial-Mesenchymal Transition In Vitro and In Vivo. *Life Sci* (2020) 244:117343. doi: 10.1016/j.lfs.2020.117343

25. Ma Y, Chai N, Jiang Q, Chang Z, Chai Y, Li X, et al. DNA Methyltransferase Mediates the Hypermethylation of the microRNA 34a Promoter and Enhances the Resistance of Patient-Derived Pancreatic Cancer Cells to Molecular Targeting Agents. *Pharmacol Res* (2020) 160:105071. doi: 10.1016/j.phrs.2020.105071
26. Jia H, Yang Q, Wang T, Cao Y, Jiang Q, Ma H, et al. Rhamnetin Induces Sensitization of Hepatocellular Carcinoma Cells to a Small Molecular Kinase Inhibitor or Chemotherapeutic Agents. *Biochim Biophys Acta* (2016) 1860:1417–30. doi: 10.1016/j.bbagen.2016.04.007
27. Kang J, Kim E, Kim W, Seong K, Youn H, Kim J, et al. Rhamnetin and Cirsiliol Induce Radiosensitization and Inhibition of Epithelial-Mesenchymal Transition (EMT) by miR-34a-Mediated Suppression of Notch-1 Expression in non-Small Cell Lung Cancer Cell Lines. *J Biol Chem* (2013) 288:27343–57. doi: 10.1074/jbc.M113.490482
28. Du Z, Li L, Sun W, Zhu P, Cheng S, Yang X, et al. Systematic Evaluation for the Influences of the SOX17/Notch Receptor Family Members on Reversing Enzalutamide Resistance in Castration-Resistant Prostate Cancer Cells. *Front Oncol* (2021) 11:607291. doi: 10.3389/fonc.2021.607291
29. Keyghobadi F, Mehdipour M, Nekoukar V, Firouzi J, Kheimeh A, Nobakht Lahrood F, et al. Long-Term Inhibition of Notch in A-375 Melanoma Cells Enhances Tumor Growth Through the Enhancement of AXIN1, CSNK2A3, and CEBPA2 as Intermediate Genes in Wnt and Notch Pathways. *Front Oncol* (2020) 10:531. doi: 10.3389/fonc.2020.00531
30. Hur JY, Frost GR, Wu X, Crump C, Pan SJ, Wong E, et al. The Innate Immunity Protein IFITM3 Modulates Gamma-Secretase in Alzheimer's Disease. *Nature* (2020) 586(7831):735–40. doi: 10.1038/s41586-020-2681-2
31. Li F, Wei A, Bu L, Long L, Chen W, Wang C, et al. Procaspace-3-activating Compound 1 Stabilizes Hypoxia-Inducible Factor 1 α and Induces DNA Damage by Sequestering Ferrous Iron. *Cell Death Dis* (2018) 9:1025. doi: 10.1038/s41419-018-1038-3
32. Ma D, Qin M, Shi L, Ding X. MicroRNA-6077 Enhances the Sensitivity of Patients-Derived Lung Adenocarcinoma Cells to Anlotinib by Repressing the Activation of Glucose Transporter 1 Pathway. *Cell Signal* (2019) 64:109391. doi: 10.1016/j.cellsig.2019.109391
33. Sargolzaei J, Etemadi T, Alyasin A. The P53/microRNA Network: A Potential Tumor Suppressor With a Role in Anticancer Therapy. *Pharmacol Res* (2020) 160:105179. doi: 10.1016/j.phrs.2020.105179
34. Zhou J, Zhao Y, Li Z, Zhu M, Wang Z, Li Y, et al. miR-103a-3p Regulates Mitophagy in Parkinson's Disease Through Parkin/Ambra1 Signaling. *Pharmacol Res* (2020) 160:105197. doi: 10.1016/j.phrs.2020.105197
35. Yang H, Ren L, Wang Y, Bi X, Li X, Wen M, et al. FBI-1 Enhanced the Resistance of Triple-Negative Breast Cancer Cells to Chemotherapeutic Agents Via the miR-30c/PXR Axis. *Cell Death Dis* (2020) 11:851. doi: 10.1038/s41419-020-03053-0
36. Zhang Y, Li D, Jiang Q, Cao S, Sun H, Chai Y, et al. Novel ADAM-17 Inhibitor ZLDI-8 Enhances the In Vitro and In Vivo Chemotherapeutic Effects of Sorafenib on Hepatocellular Carcinoma Cells. *Cell Death Dis* (2018) 9:743. doi: 10.1038/s41419-018-0804-6
37. Zhou W, Gao Y, Tong Y, Wu Q, Zhou Y, Li Y. Anlotinib Enhances the Antitumor Activity of Radiofrequency Ablation on Lung Squamous Cell Carcinoma. *Pharmacol Res* (2021) 164:105392. doi: 10.1016/j.phrs.2020.105392
38. Guan F, Ding R, Zhang Q, Chen W, Li F, Long L, et al. Wx-132-18B, a Novel Microtubule Inhibitor, Exhibits Promising Anti-Tumor Effects. *Oncotarget* (2017) 8:71782–96. doi: 10.18632/oncotarget.17710
39. Sun H, Feng F, Xie H, Li X, Jiang Q, Chai Y, et al. Quantitative Examination of the Inhibitory Activation of Molecular Targeting Agents in Hepatocellular Carcinoma Patient-Derived Cell Invasion Via a Novel In Vivo Tumor Model. *Anim Model Exp Med* (2019) 2(4):259–68. doi: 10.1002/ame2.12085
40. Feng F, Li X, Li R, Li B. The Multiple-Kinase Inhibitor Lenvatinib Inhibits the Proliferation of Acute Myeloid Leukemia Cells. *Anim Model Exp Med* (2019) 2(3):178–84. doi: 10.1002/ame2.12076
41. Feng Y, Li B, Feng F, Chen Y, Ren Y, Zhang H, et al. Novel Mtor Inhibitor Enhances the Sensitivity of Hepatocellular Carcinoma Cells to Molecular Targeting Agents. *OncoTargets Ther* (2020) 13:7165–76. doi: 10.2147/ott.S244474
42. Feng Y, Gu S, Chen Y, Gao X, Ren Y, Chen J, et al. Virtual Screening and Optimization of Novel Mtor Inhibitors for Radiosensitization of Hepatocellular Carcinoma. *Drug Design Dev Ther* (2020) 14:1779–98. doi: 10.2147/dddt.S249156
43. Di Cosimo S. Advancing Immunotherapy for Early-Stage Triple-Negative Breast Cancer. *Lancet (London England)* (2020) 396:1046–8. doi: 10.1016/s0140-6736(20)31962-0
44. Harbeck N, Gnant M. Breast Cancer. *Lancet (London England)* (2017) 389:1134–50. doi: 10.1016/s0140-6736(16)31891-8
45. Bardia A, Mayer I, Vahdat L, Tolane S, Isakoff S, Diamond J, et al. Sacituzumab Govitecan-hziy in Refractory Metastatic Triple-Negative Breast Cancer. *New Engl J Med* (2019) 380:741–51. doi: 10.1056/NEJMoa1814213
46. Denkert C, Liedtke C, Tutt A, von Minckwitz G. Molecular Alterations in Triple-Negative Breast Cancer-the Road to New Treatment Strategies. *Lancet (London England)* (2017) 389:2430–42. doi: 10.1016/s0140-6736(16)32454-0
47. Eikesdal H, Yndestad S, Elzawahry A, Llop-Guevara A, Gilje B, Blix E, et al. Olaparib Monotherapy as Primary Treatment in Unselected Triple Negative Breast Cancer. *Ann Oncol Off J Eur Soc Med Oncol* (2021) 32:240–9. doi: 10.1016/j.annonc.2020.11.009
48. Fasching P, Link T, Hauke J, Seither F, Jackisch C, Klare P, et al. Neoadjuvant Paclitaxel/Olaparib in Comparison to Paclitaxel/Carboplatinum in Patients With HER2-Negative Breast Cancer and Homologous Recombination Deficiency (GeparOLA Study). *Ann Oncol Off J Eur Soc Med Oncol* (2021) 32:49–57. doi: 10.1016/j.annonc.2020.10.471
49. Yang B, Wang C, Xie H, Wang Y, Huang J, Rong Y, et al. MicroRNA-3163 Targets ADAM-17 and Enhances the Sensitivity of Hepatocellular Carcinoma Cells to Molecular Targeted Agents. *Cell Death Dis* (2019) 10:784. doi: 10.1038/s41419-019-2023-1
50. Chen S, Luo Z, Chen X. Andrographolide Mitigates Cartilage Damage Via miR-27-3p-modulated Matrix metalloproteinase13 Repression. *J Gene Med* (2020) 22(8):e3187. doi: 10.1002/jgm.3187
51. Wang D, He S, Liu B, Liu C. MiR-27-3p Regulates TLR2/4-dependent Mouse Alveolar Macrophage Activation by Targeting Ppargamma. *Clin Sci (Lond)* (2018) 132(9):943–58. doi: 10.1042/CS20180083
52. Ye Z, Hu J, Xu H, Sun B, Jin Y, Zhang Y, et al. Serum Exosomal MicroRNA-27-3p Aggravates Cerebral Injury and Inflammation in Patients With Acute Cerebral Infarction by Targeting Ppargamma. *Inflammation* (2021) 44(3):1035–48. doi: 10.1007/s10753-020-01399-3
53. Zhao Y, Wang P, Meng J, Ji Y, Xu D, Chen T, et al. MicroRNA-27a-3p Inhibits Melanogenesis in Mouse Skin Melanocytes by Targeting Wnt3a. *Int J Mol Sci* (2015) 16(5):10921–33. doi: 10.3390/ijms160510921
54. Zhou L, Liang X, Zhang L, Yang L, Nagao N, Wu H, et al. MiR-27a-3p Functions as an Oncogene in Gastric Cancer by Targeting BTG2. *Oncotarget* (2016) 7(32):51943–54. doi: 10.18632/oncotarget.10460
55. Zhang P, Song X, Dong Q, Zhou L, Wang L. miR-27-3p Inhibition Restore Fibroblasts Viability in Diabetic Wound by Targeting NOVA1. *Aging (Albany NY)* (2020) 12(13):12841–9. doi: 10.18632/aging.103266
56. Li Y, Guo D, Lu G, Mohiuddin Chowdhury ATM, Zhang D, Ren M, et al. Lncrna SNAI3-AS1 Promotes PEG10-Mediated Proliferation and Metastasis Via Decoying of miR-27a-3p and miR-34a-5p in Hepatocellular Carcinoma. *Cell Death Dis* (2020) 11(8):685. doi: 10.1038/s41419-020-02840-z
57. Teteloshvili N, Dekkema G, Boots AM, Heeringa P, Jellema P, de Jong D, et al. Involvement of MicroRNAs in the Aging-Related Decline of CD28 Expression by Human T Cells. *Front Immunol* (2018) 9:1400. doi: 10.3389/fimmu.2018.01400
58. Li Q, Engebrecht J. BRCA1 and BRCA2 Tumor Suppressor Function in Meiosis. *Front Cell Dev Biol* (2021) 9:668309. doi: 10.3389/fcell.2021.668309
59. Li L, Qiu C, Hou M, Wang X, Huang C, Zou J, et al. Ferroptosis in Ovarian Cancer: A Novel Therapeutic Strategy. *Front Oncol* (2021) 11:665945. doi: 10.3389/fonc.2021.665945

Conflict of Interest: The authors declare that the research was conducted in the absence of any commercial or financial relationships that could be construed as a potential conflict of interest.

Copyright © 2021 Zhao, Sun, Wang, Qu, Yang and Wang. This is an open-access article distributed under the terms of the Creative Commons Attribution License (CC BY). The use, distribution or reproduction in other forums is permitted, provided the original author(s) and the copyright owner(s) are credited and that the original publication in this journal is cited, in accordance with accepted academic practice. No use, distribution or reproduction is permitted which does not comply with these terms.



STAT5a Confers Doxorubicin Resistance to Breast Cancer by Regulating ABCB1

OPEN ACCESS

Edited by:

Dayanidhi Raman,
University of Toledo, United States

Reviewed by:

Stan Lipkowitz,
National Cancer Institute,
United States
Benedetta Pellegrino,
University Hospital of Parma, Italy

*Correspondence:

Linbo Wang
linbowang@zju.edu.cn
Jichun Zhou
jichun-zhou@zju.edu.cn

[†]These authors have contributed
equally to this work and
share first authorship

Specialty section:

This article was submitted to
Breast Cancer,
a section of the journal
Frontiers in Oncology

Received: 20 April 2021

Accepted: 29 June 2021

Published: 15 July 2021

Citation:

Li Z, Chen C, Chen L, Hu D, Yang X,
Zhuo W, Chen Y, Yang J, Zhou Y,
Mao M, Zhang X, Xu L, Ju S, Shen J,
Wang Q, Dong M, Xie S, Wei Q, Jia Y,
Zhou J and Wang L (2021) STAT5a
Confers Doxorubicin Resistance to
Breast Cancer by Regulating ABCB1.
Front. Oncol. 11:697950.
doi: 10.3389/fonc.2021.697950

Zhaoqing Li^{1,2,3†}, Cong Chen^{2,3†}, Lini Chen^{2,3†}, Dengdi Hu^{2,3,4}, Xiqian Yang^{2,3,5},
Wenying Zhuo^{2,3,4}, Yongxia Chen^{2,3}, Jingjing Yang^{2,3}, Yulu Zhou^{2,3}, Misha Mao^{2,3},
Xun Zhang^{2,3}, Ling Xu^{2,3}, Siwei Ju^{2,3}, Jun Shen^{2,3}, Qinchuan Wang^{2,3}, Minjun Dong^{2,3},
Shuduo Xie^{2,3}, Qun Wei^{2,3}, Yunlu Jia⁶, Jichun Zhou^{2,3*} and Linbo Wang^{2,3*}

¹ Cancer Institute (Key Laboratory of Cancer Prevention and Intervention, China National Ministry of Education), 2nd Affiliated Hospital, School of Medicine, Zhejiang University, Hangzhou, China, ² Sir Run Run Shaw Hospital, Zhejiang University, Hangzhou, China, ³ Biomedical Research Center and Key Laboratory of Biotherapy of Zhejiang Province, Hangzhou, China, ⁴ Affiliated Cixi Hospital, Wenzhou Medical University, Ningbo, China, ⁵ Breast Surgical Department, Shaoxing Maternity and Child Health Care Hospital, Shaoxing, China, ⁶ The First Affiliated Hospital, Zhejiang University School of Medicine, Hangzhou, China

Chemoresistance is a daunting challenge to the prognosis of patients with breast cancer. Signal transducer and activator of transcription (STAT) 5a plays vital roles in the development of various cancers, but its function in breast cancer is controversial, and its role in chemoresistance in breast cancer remains unexplored. Here we identified STAT5a as a chemoresistance inducer that regulates the expression of ABCB1 in breast cancer and can be targeted by pimozone, an FDA-approved psychotropic drug. First, we found that STAT5a and ABCB1 were expressed at higher levels in doxorubicin-resistant cell lines and chemoresistant patients, and their expression was positively correlated. Then, we confirmed the essential roles of STAT5a and ABCB1 in doxorubicin resistance in breast cancer cells and the regulation of ABCB1 transcription by STAT5a. Subsequently, the efficacy of pimozone in inhibiting STAT5a and sensitizing doxorubicin-resistant breast cancer cells was tested. Finally, we verified the role of STAT5a in doxorubicin resistance in breast cancer and the efficacy of pimozone in reversing this resistance *in vivo*. Our study demonstrated the vital role of STAT5a in doxorubicin resistance in breast cancer. Targeting STAT5a might be a promising strategy for treating doxorubicin-resistant breast cancer. Moreover, repurposing pimozone for doxorubicin resensitization is attractive due to the safety profile of pimozone.

Keywords: breast cancer, STAT5a, ABCB1, pimozone, doxorubicin resistance

Abbreviations: STAT, signal transducer and activator of transcription; DOX, doxorubicin; AC, cyclophosphamide; pCR, pathologic complete response.

INTRODUCTION

Breast cancer is the most common malignant tumor in women. Every year, 1.7 million people are diagnosed worldwide, and approximately half a million people die from this disease (1). Chemoresistance is a main cause of breast cancer-related death, as it results in recurrence and metastasis. Thus, overcoming this issue is critical to improving the prognosis of patients with breast cancer.

Signal transducer and activator of transcription (STAT) 5a belongs to the STAT family, which consists of seven members (STAT1, STAT2, STAT3, STAT4, STAT5a, STAT5b and STAT6) and participates in essential biological behaviors in cells. Similar to other STATs, STAT5 consists of a helical N-terminal domain (ND), a coiled-coil (CC) domain, a DNA-binding domain (DBD), a helical linker (LK), a Src homology 2 (SH2) domain, and a transactivation domain (TAD) located in the C-terminal region (2). STAT5 is mostly present in the cytoplasm in an inactivated state (3). Upon stimulation by a spectrum of cytokines, STAT5 molecules are recruited to the JAK/receptor complex and phosphorylated at tyrosine (Tyr) 694 (STAT5a) or Tyr 699 (STAT5b). Subsequently, STAT5 translocates to the nucleus in the form of dimers and/or tetramers to function as a transcription factor. Stat5a and stat5b derived from distinct but chromosome-linked genes that map to chromosome 17 (bands q11-1 to q22) (4). These two proteins share 94% identity in their amino acid sequences, with the greatest difference in the C-terminal phosphotyrosyl tail and transactivation domain (5). Although STAT5a and STAT5b have some common target genes, they exert nonredundant functions, resulting in unique target gene activation patterns (6, 7). While STAT5a is mainly present in mammary tissue, STAT5b expression is more enriched in muscle and the liver (8). STAT5a plays a vital role in the promotion of cancers, including lung cancer (9), prostate cancer (10), and gastric cancer (11); is involved in chemoresistance in esophageal cancer by negatively regulating miR-29c (12); and is overexpressed in gemcitabine-resistant pancreatic cancer cell lines (13). STAT5 is also activated and localized to the nucleus in a high proportion of breast cancers (14) and promotes cancer progression (15). DNA-damaging agents such as doxorubicin are reported to induce STAT5a expression in breast cancer (16); however, the exact role of STAT5a in chemoresistance in breast cancer remains unknown.

ABCB1 is one of 49 putative members of the superfamily of human adenosine triphosphate (ATP)-binding cassette (ABC) transporters within subfamily B (MDR/TAP) (17). This membrane transporter is known to promote chemoresistance by exporting antitumor drugs out of cancer cells in various cancers, including breast cancer (18–21).

Here, we identified STAT5a as a key promoter of doxorubicin (DOX) resistance in breast cancer *via* upregulation of the expression of ABCB1. An inhibitor of STAT5, pimozone, which is an FDA-approved drug for treatment of psychotropic diseases, significantly sensitized breast cancer cells to DOX both *in vitro* and *in vivo*.

MATERIALS & METHODS

Patient Specimens

Breast cancer specimens were obtained from patients (n = 67) with breast cancer at the Department of Surgical Oncology, Sir Run Run Shaw Hospital. The patient population included people with the luminal A (n=10), luminal B (n=22), HER2-positive (n=15) or triple-negative (n=20) subtype, and the patients received doxorubicin-containing neoadjuvant chemotherapy including doxorubicin plus cyclophosphamide (AC), AC-paclitaxel (T) or AC-T plus Herceptin (H). No residual invasive carcinoma in the breast or lymph nodes (noninvasive breast residuals were allowed) assessed by surgical pathological evaluation was defined as a pathologic complete response (pCR). Patients with pCR were defined as chemosensitive, while those with non-pCR were defined as chemoresistant.

Cell Lines and Regents

The MCF7 cell line was purchased from Cell Bank of the Chinese Academy of Sciences (Shanghai, China) where they were characterized by STR analysis and detection of isozyme, mycoplasma and cell vitality. The cells were maintained in Eagle's Minimum Essential Medium supplemented with 0.01 mg/ml insulin. DOX-resistant MCF7 cells (MCF7/DOX) were established by DOX (D1515, Sigma-Aldrich, St. Louis, MO, USA) challenge at a starting concentration of 1 ng/ml. The concentration of DOX was gradually increased to 1 µg/ml. Cells were cultured in medium containing 10% FBS in a humidified incubator at 37°C.

Western Blotting

Protein samples were subjected to sodium dodecyl sulfate-polyacrylamide gel electrophoresis (Bio-Rad, Hercules, CA, USA) and transferred to a polyvinylidene difluoride membrane (Millipore, Billerica, MA, USA) that was blocked in 0.1% Tween-20 in Tris-buffered saline (TBS) containing 5% skim milk (BD Biosciences, Chicago, IL, USA) for 1 h at room temperature and incubated overnight with primary antibodies against STAT5a (ab32043, Abcam, Cambridge, MA, USA), STAT5b (ab178941; Abcam), p-STAT5 (Tyr694) (ab32364, Abcam), cleaved PARP (9541, Cell Signaling Technology, CST, Danvers, MA, USA), cleaved caspase 7 (9491, CST), cleaved caspase 3 (9664, CST), ABCB1 (13978, CST) and β -actin (sc-477748, Santa Cruz, CA, USA). After three 5-min washes with 0.1% Tween-20 in TBS, the membrane was incubated with a diluted horseradish peroxidase (HRP)-conjugated secondary antibody (1:2000, CST). After three 5-min washes with 0.1% Tween-20 in TBS, the membrane was treated with a Pico ECL kit (FDbio, Hangzhou, Zhejiang, China) and imaged with an Amersham Imager 600 (GE Healthcare, Piscataway, NJ, USA).

RNA Isolation and Quantitative Real-Time PCR

Total RNA was extracted using TRIzol Reagent (Invitrogen, Carlsbad, CA, USA), and the isolated RNA (1 µg) was reverse transcribed with the HiFiScript cDNA Synthesis Kit (CW2569M,

CWBIO, Beijing, China). Quantitative real-time PCR was performed using Ultra SYBR Mixture (CW0957H, CWBIO). Glyceraldehyde 3-phosphate dehydrogenase (GAPDH) was used as the reference gene. The following primers were used:

STAT5a: 5'-ATGCTGTTGCCACGTTTC-3' (sense),
5'-TGTCACCCACCATATCCTAGAC-3' (anti-sense);
ABCB1: 5'-CGAGGTCGGAATGGATCTTGA-3' (sense),
5'-CCAAAGTTCCACACCATATAC-3' (anti-sense); and
GAPDH: 5'-TGACTTCAACAGCGACACCCA-3' (sense),
5'-CACCTGTTGCTGTAGCCAAA-3' (anti-sense).

Results were calculated using the $2^{-\Delta\Delta Ct}$ method.

Transfection of Plasmids and siRNAs and Infection With a Lentivirus

STAT5a- or ABCB1-overexpressing or negative control vectors were designed and synthesized commercially by GeneChem (Shanghai, China). Short interfering RNAs (siRNAs) targeting STAT5a or ABCB1 (si-STAT5a and si-ABCB1) and a scrambled control siRNA were designed and synthesized commercially by RiboBio (Guangzhou, China). The target sequences of the 3 STAT5a-specific siRNAs were as follows:

sequence 1, 5'-TGATGGAGGTGTTGAAGAA-3';
sequence 2, 5'-GCAATGAGCTTGTGTTCCA-3';
sequence 3, 5'-GAGAATTCGACCTGGATGA-3'.

The target sequences of the 3 ABCB1-specific siRNAs were as follows:

sequence 1, 5'-CACTGTTACTCTTAGCAAT-3';
sequence 2, 5'-GAGCTTAACACCCGACTTA-3';
sequence 3, 5'-GTGATAGCTCATCGTTTGT-3'.

Transfection of the plasmids and siRNAs into cells was conducted using Lipofectamine 3000 (Invitrogen) transfection reagents following the manufacturer's instructions. Cells were harvested for total RNA and protein extraction 48 h after transfection and processed for functional assays.

To construct a STAT5a-knockdown MCF7/DOX cell line (MCF7/DOX sh-STAT5a) and corresponding negative control cell line (MCF7/DOX sh-NC), cells were seeded in 6-well plates and incubated for 24 h with lentiviruses (OOBIO, Shanghai, China) carrying shRNA sequences targeting STAT5a (NM_001288718.2, 5'-TGATGGAGGTGTTGAAGAA-3') or a scrambled sequence (5'-CCTAAGGTTAAGTCGCCCTCG-3'). Seventy-two hours after renewal of the medium, 1 μ g/ml puromycin was applied to kill uninfected cells.

Immunohistochemical (IHC) Staining

Breast tumor samples were collected from breast cancer patients at Sir Run Run Shaw Hospital. For immunohistochemical analysis, slides were heated in a pressure cooker containing 10 mM sodium citrate (pH 6.5) for 10 min. Endogenous peroxidases were deactivated by treatment with 3% H₂O₂ for 5 min, and the

slides were blocked with 10% normal goat serum for 30 min at room temperature and probed with primary antibodies against STAT5a (sc-271542X, Santa Cruz), p-STAT5 (Tyr694) (ab32364, Abcam) or ABCB1 (13978, CST) for 1 h at room temperature. The slides were incubated with poly-HRP secondary antibodies for 1 h in the dark at room temperature, and immunodetection was performed using a 3,3'-diaminobenzidine substrate kit. The sections were counterstained with hematoxylin to visualize nuclei. Staining intensity was scored by blinded observers according to intensity and percentage of positive cells. The staining intensity was ranged in four grades: 0 (no staining), 1 (weak staining), 2 (intermediate staining), or 3 (strong staining). The product (percentage of positive cells and respective intensity scores) was used as the final staining score (ranging from 0 to 300).

DOX Efflux Experiment

To assess the accumulation of DOX in cells, pretreated MCF7 or MCF7/DOX cells were treated with the indicated concentration of DOX for 24 h and then imaged under a microscope (ZEISS, Jena, Germany). The mean and total fluorescence intensities were analyzed with ImageJ software (National Institutes of Health, Bethesda, MD, USA).

Chemotherapy Sensitivity Assay

Cells were seeded in 96-well plates at a density of 5×10^3 cells per well in the appropriate medium. The cells were then treated with DOX (at concentrations of 0, 0.01, 0.02, 0.05, 0.1, 0.2, 0.5, 1, and 2 μ g/ml) for 24 h. After the incubation, viability was assessed by a CCK8 (APEXBio, Houston, TX, USA) assay according to the supplier's instructions. The absorbance of each well at 450 nm was measured, and survival rate curves were plotted.

Flow Cytometry

To determine the proportion of apoptotic cells, pretreated cells were collected, washed twice with PBS, and double stained with fluorescein isothiocyanate (FITC)-Annexin V and propidium iodide (PI) (556547, BD Biosciences) according to the supplier's instructions. The apoptosis rate was measured by flow cytometry on a FACScan (BD Bioscience).

Colony Formation Assay

To evaluate colony-forming capacity, 2000 pretreated cells per well were seeded in 6-well plates in medium containing an appropriate concentration of DOX, and the medium was replaced as necessary. After 14 days, the cells were washed with PBS 3 times, fixed in 4% paraformaldehyde (Solarbio, Beijing, China) and stained with 0.1% crystal violet (Solarbio). Colonies were counted, and the results were analyzed.

Luciferase Reporter Assay

A full-length ABCB1 promoter vector was constructed by and purchased from GeneCopoeia (Hangzhou, China). The indicated cells were seeded in 6-well plates and transfected with an ABCB1 reporter plasmid and a STAT5a-overexpressing vector, a negative control vector, STAT5a-specific siRNA, or control siRNA. Forty-eight hours after transfection, the activities of

Gaussia luciferase and secreted alkaline phosphatase were assessed using the Secrete-Pair Gaussia Luciferase Assay Kit (LF031, GeneCopoeia) following the manufacturer's instructions and a 20/20 luminometer (Promega, Madison, WI, USA).

Chromatin Immunoprecipitation (ChIP) Assay

A ChIP assay was performed using the SimpleChIP® Enzymatic Chromatin IP Kit (Magnetic Beads) (9003, CST) as described previously (22). Chromatin was used for immunoprecipitation with an anti-STAT5a, an anti-histone 3, or a normal rabbit IgG antibody. ChIP-enriched DNA was assessed using real-time PCR, and the primer sets for the ABCB1 promoter were designed as follows:

primer 1, 5'-GCGGTCAGGGAGGTTTCACATCAC-3' (forward),
5'-CCCATGCATCCGTTTATAGGCTCT-3' (reverse);
primer 2, 5'-GCTCTTCTACACCTCTTTAGGGT-3' (forward),
5'-GTAACAGTTGCAACAAAAGCTGG-3' (reverse);
primer 3, 5'-CTAATTATTTTTTAGCCAGTGGATAAAGAG-3' (forward),
5'-GCCAGAATAGGCAGAATGAAGATTAGAATC-3' (reverse); and
primer 4, 5'-CTACTTTATTTCAGATATTCTCCAGATTCC-3' (forward),
5'-CCTTACCTTTTATCTGGTTGCTTCCTG-3' (reverse).

Tumor Xenograft Assay

To prove the role of STAT5a in DOX resistance *in vivo*, mice were randomly divided into 2 groups (n=7) and subcutaneously injected with 2×10^6 sh-NC MCF7/DOX or sh-STAT5a MCF7/DOX cells, which were resuspended in 0.1 ml PBS containing 50% Matrigel (Corning, Kennebunk, ME, USA). After one week, the mice were treated with DOX (4 mg/kg, every 3 days, i.p.). To determine the effect of pimozone on STAT5 inhibition and sensitization to DOX, mice were subcutaneously injected with 2×10^6 MCF7/DOX cells as previously described and randomly divided into 4 groups (n=5). After one week, the mice in each group were treated with PBS, pimozone (25 mg/kg, daily, i.p.), DOX (4 mg/kg, every 3 days, i.p.) or both pimozone (25 mg/kg, daily, i.p.) and DOX (4 mg/kg, every 3 days, i.p.). The animals were maintained in laminar flow cabinets under specific pathogen-free conditions. Tumor volumes and mouse body weights were recorded every 3 days. After 21 days, tumor tissue was collected, measured, weighed, fixed in 10% formalin, embedded in paraffin, and processed for hematoxylin and eosin (H&E) and IHC staining.

Statistical Analysis

Quantitative data from at least three independent experiments are expressed as the mean \pm SD. All experimental values were evaluated using GraphPad Prism 9.0.0 (GraphPad Software, Inc., La Jolla, CA, USA). An unpaired t-test was used for statistical

analysis of two experimental groups. The relationships between STAT5a or ABCB1 expression and the pCR rate were tested by Fisher's exact test. Gene expression data obtained from GEO (accession code: GSE87455) were analyzed with GEO2R (23). Patients were divided into STAT5a-low and STAT5a-high groups using the median expression of STAT5a as the cutoff. In all cases, $p < 0.05$ was considered statistically significant.

RESULTS

STAT5a Is Involved in Chemotherapy Resistance in Breast Cancer

Data mining based on GSE87455 was conducted to explore whether STAT5a is involved in chemoresistance in breast cancer (23). STAT5a expression was potentially upregulated in the postchemotherapy group, while STAT5b showed no significant difference, implying a role for STAT5a but not STAT5b in chemoresistance (**Figure 1A**). Then, we verified the data mining results *in vitro* and *in vivo*. First, we compared the IC₅₀ values of wild-type MCF7 and our DOX-resistant MCF7 (MCF7/DOX) cells, which were maintained in medium containing 1 μ g/ml DOX for more than 6 months, by a CCK8 assay. A 32-fold increase in the IC₅₀ of DOX was observed in MCF7/DOX cells compared with MCF7 cells (**Figure 1B**). The mRNA and protein expression of STAT5a but not that of STAT5b was upregulated in the MCF7/DOX cell line, and the level of STAT5a phosphorylation at Tyr694 was also higher in MCF7/DOX cells (**Figures 1C, D**). Additionally, we observed activation of STAT5a upon stimulation of MCF7 cells with DOX, implying a role for STAT5a in the response to chemotherapy stress (**Figure 1E**). Given that STAT5a but not STAT5b was upregulated and activated in chemoresistant patients and cell lines, we focused on STAT5a in the rest of the study. We applied our clinical data to verify the data mining result. IHC was applied to assess the level of STAT5a in breast tumor specimens collected from patients before neoadjuvant treatment. Patients diagnosed as pCR after operation were defined chemo-sensitive, while others chemoresistant. Statistical analysis suggested that patients with STAT5a-positive breast cancer had a lower pCR rate than STAT5a-negative patients (**Figure 1F**). Representative IHC results of STAT5a expression in chemosensitive and chemoresistant patients were shown in **Figure 1G**.

To investigate whether STAT5a can regulate the sensitivity of breast cancer cells to DOX, we knocked down and overexpressed STAT5a *via* siRNA and a plasmid in MCF7/DOX and MCF7 cells, respectively (**Figure 1H**). Si-1 siRNA was selected for subsequent experiments due to its knockdown efficiency. An increased apoptosis rate was observed in STAT5a-knockdown MCF7/DOX cells (**Figures 1I, J**), suggesting a role for STAT5a in cell survival. When STAT5a was overexpressed, MCF7 cells became more resistant to DOX, with the IC₅₀ increasing from 0.7522 μ g/ml to 3.373 μ g/ml (**Figure 1K**). STAT5a knockdown also sensitized MCF7/DOX cells to DOX, decreasing the IC₅₀ from 24.93 μ g/ml to 4.2 μ g/ml, as assessed by CCK8 assays (**Figure 1L**).

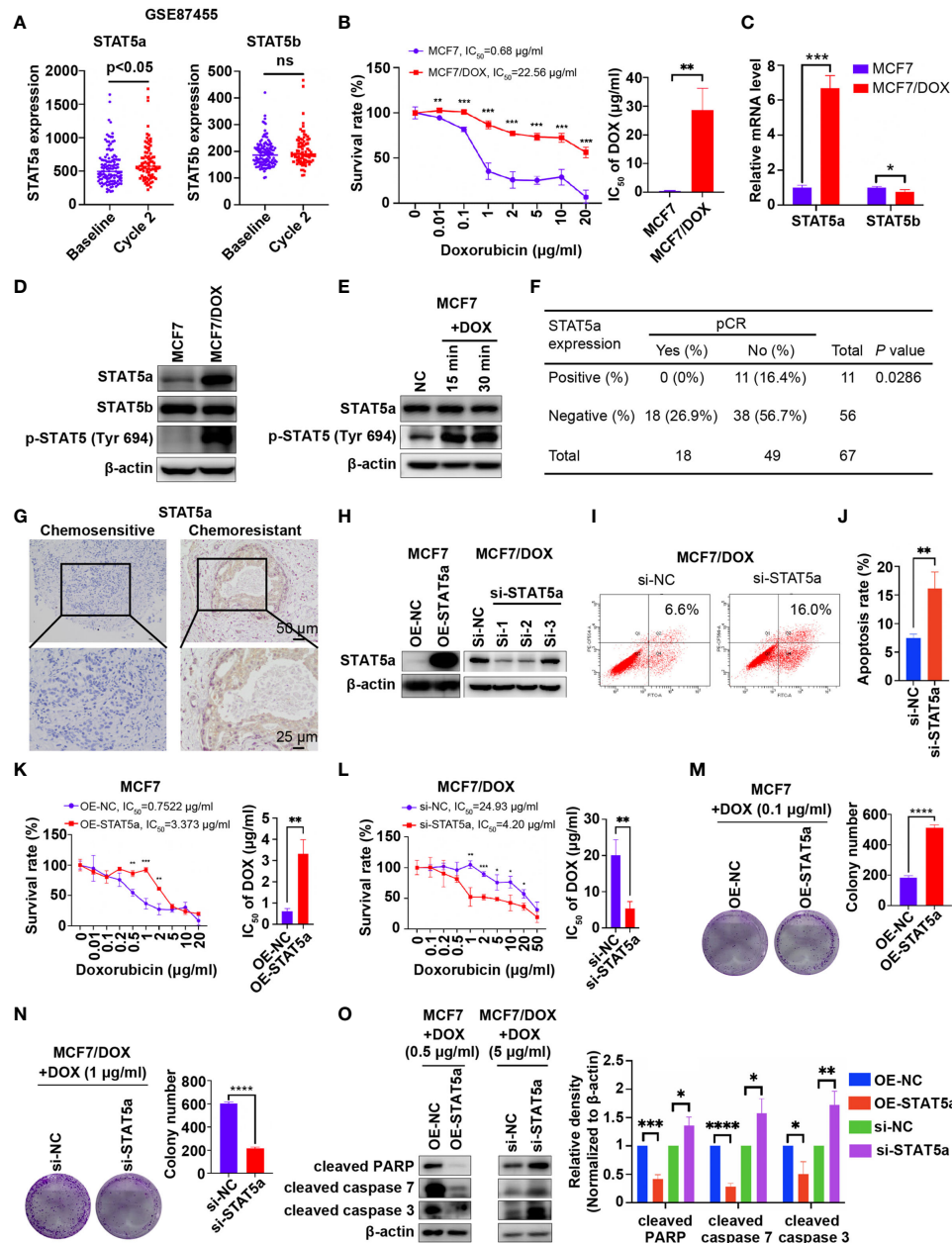


FIGURE 1 | STAT5a is involved in chemoresistance in breast cancer. **(A)** Expression of STAT5a and STAT5b in breast cancer samples collected pre- and postchemotherapy in the dataset GSE87455. **(B)** Survival rates of MCF7 and MCF7/DOX cells after treatment with DOX for 48 h determined by a CCK8 assay. **(C)** mRNA levels of STAT5a and STAT5b in MCF7 and MCF7/DOX cells assessed via qPCR. **(D)** Protein levels of STAT5a, p-STAT5a (Tyr694) and STAT5b in MCF7 and MCF7/DOX cells determined by Western blotting. **(E)** Western blotting was performed to examine the expression of STAT5a and p-STAT5 (Tyr694) in MCF7 cells upon treatment with DOX. **(F)** Correlation between the pCR rate and STAT5a expression in breast cancer samples obtained from 67 patients. **(G)** Representative images of IHC staining for STAT5a in chemoresistant and chemosensitive breast cancer samples. **(H)** Efficiency of vector transfection for overexpression of STAT5a in MCF7 cells and siRNA transfection for knockdown of STAT5a in MCF7/DOX cells determined by Western blotting. **(I, J)** Flow cytometry was performed to assess apoptosis in MCF7/DOX cells after knocking down STAT5a or control treatment **(I)**. Bar graphs showing the percentage of apoptotic cells **(J)**. **(K)** Survival rate and IC_{50} of MCF7 cells transfected with an empty vector or a STAT5a vector after treatment with DOX for 48 h determined by a CCK8 assay. **(L)** Survival rate and IC_{50} of MCF7/DOX cells transfected with scramble siRNA or STAT5a-targeting siRNA after treatment with DOX for 48 h determined by a CCK8 assay. **(M, N)** Representative images and quantification of colonies formed by MCF7 cells transfected with the empty vector or STAT5a vector **(M)** and MCF7/DOX cells transfected with scramble siRNA or STAT5a-targeting siRNA **(N)** in medium containing the indicated concentration of DOX. **(O)** The expression levels of apoptosis markers in MCF7 cells transfected with the empty vector or STAT5a vector and MCF7/DOX cells transfected with scramble siRNA or STAT5a-targeting siRNA under treatment with the indicated concentration of DOX determined by Western blotting. ns, $p > 0.05$; * $p < 0.05$; ** $p < 0.01$; *** $p < 0.001$; **** $p < 0.0001$.

The capacity to form colonies in the presence of DOX was enhanced by STAT5a upregulation in MCF7 cells and attenuated by STAT5a knockdown in MCF7/DOX cells (**Figures 1M, N**). Treatment with DOX induced less apoptosis in STAT5a-overexpressing MCF7 cells and more apoptosis in STAT5a-knockdown MCF7/DOX cells, as indicated by analysis of biomarkers of apoptosis, such as cleaved PARP and cleaved caspase 3/7 (**Figure 1O**). These data suggested that STAT5a could confer DOX resistance in breast cancer.

ABCB1 Is Essential to Chemoresistance in Breast Cancer

ABCB1, a well-known multidrug resistance protein, plays a vital role in chemoresistance in various types of cancers (18–21). ABCB1 expression was significantly increased in patients who received 2 cycles of chemotherapy (“Cycle 2”) compared to prechemotherapy (“Baseline”) expression in the dataset GSE87455 (**Figure 2A**), suggesting the development of chemoresistance after chemotherapy (23). We also investigated the role of ABCB1 in chemoresistance in our study. First, the level of ABCB1 was significantly higher in tumor tissues from patients with chemoresistant breast cancer than in those from chemosensitive patients (**Figure 2B**). Statistical analysis showed that patients with ABCB1-positive breast cancer had a significantly lower pCR rate than those with ABCB1-negative breast cancer (**Figure 2C**). Furthermore, qPCR and Western blot results showed that the mRNA and protein levels of ABCB1 were significantly higher in the MCF7/DOX cell line than in the MCF7 cell line (**Figures 2D, E**). Then, we overexpressed and knocked down ABCB1 *via* a plasmid and siRNA in MCF7 and MCF7/DOX cells, respectively (**Figures 2F, G, J, K**). Si-1 siRNA was selected for subsequent experiments. When the expression of ABCB1 was upregulated, resistance of MCF7 cell to DOX was increased, with the IC₅₀ elevated from 0.59 µg/ml to 2.385 µg/ml (**Figure 2H**), and the colony-forming ability in the presence of DOX was also increased (**Figure 2I**). The expression of biomarkers of apoptosis was significantly reduced in ABCB1-overexpressing MCF7 cells upon treatment with DOX (**Figure 2N**). On the other hand, ABCB1 knockdown in MCF7/DOX cells showed the opposite effects. When ABCB1 was downregulated, MCF7/DOX cells became less resistant to DOX, with the IC₅₀ decreasing from 32.17 µg/ml to 3.32 µg/ml (**Figure 2L**), and fewer colonies formed in the presence of DOX (**Figure 2M**). DOX-induced apoptosis was increased in ABCB1-silenced MCF7/DOX cells, as indicated by assessment of biomarkers of apoptosis (**Figure 2O**). Since ABCB1 confers cell chemoresistance by pumping drugs out of cells, we compared the amount of DOX in MCF7 and MCF7/DOX cells and explored whether the expression of ABCB1 alters the amount of DOX in cells. DOX was monitored *via* fluorescence microscopy due to its intrinsic fluorescence (24). As shown in **Figures 2P, Q**, the amount of DOX in MCF7/DOX cells was significantly lower than that in MCF7 cells, implying that MCF7/DOX cells had a more potent ability to pump out drugs. When ABCB1 was knocked down, the amount of DOX in cells was significantly elevated (**Figures 2R, S**), implying an impaired

ability to pump out drugs. Thus, ABCB1 is essential to chemoresistance in breast cancer cells by pumping drugs out of cancer cells.

STAT5a Modulates Chemoresistance in Breast Cancer by Regulating the Transcription of ABCB1

Data from GSE87455 also showed that the expression level of ABCB1 was significantly higher in the STAT5a-high group (STAT5a level higher than the median) than in the STAT5a-low group (STAT5a level lower than the median) and positively correlated with the expression level of STAT5a (**Figure 3A**). IHC results for our clinical specimens also suggested a significant relationship between STAT5a and ABCB1, with a p value of 0.0006 (**Figure 3B**). Breast cancer specimens with high STAT5a expression showed high ABCB1 expression levels (**Figure 3C**). When STAT5a was knocked down, the ability of MCF7/DOX cells to pump out DOX was attenuated (**Figures 3D, E**). To explore the relationship between STAT5a and ABCB1, we tested whether STAT5a could regulate the expression of ABCB1. The results showed that overexpressing STAT5a in MCF7 cells significantly increased the expression of ABCB1 at both the protein and mRNA levels, and STAT5a knockdown in MCF7/DOX cells had the opposite effect (**Figures 3F–H**).

To further explore how STAT5a modulates ABCB1 expression in breast cancer cells, a 2012-bp fragment of DNA containing ABCB1 sequences from –1686 to 326 relative to the transcription initiation site was subcloned into the Pezx-PG04.1 vector. We cotransfected the ABCB1 promoter vector with a STAT5a expression vector into MCF7 cells or with STAT5a-targeting siRNAs into MCF7/DOX cells. The results in **Figure 3I** indicate that STAT5a overexpression increased ABCB1 promoter activity, while knocking down STAT5a expression attenuated ABCB1 promoter activity. To verify the interactions between STAT5a and five potential STAT5a-binding sites in the ABCB1 promoter region (**Figure 3J**), a chromatin immunoprecipitation (ChIP) assay was performed with MCF7/DOX cells and an anti-STAT5a antibody (**Figure 3K**). The results suggested that STAT5a could promote the transcription of ABCB1 by binding to its promoter region.

Subsequently, a rescue experiment was performed to confirm whether STAT5a modulates chemoresistance in breast cancer cells by regulating ABCB1. As shown in **Figures 3L, M**, upregulation of STAT5a increased resistance to DOX in MCF7 cells, and additional downregulation of ABCB1 significantly suppressed resistance. Similar results are shown in **Figures 3L, N**, where knockdown of STAT5a attenuated the resistance of MCF7/DOX cells to DOX, while additional overexpression of ABCB1 significantly recovered DOX resistance. Taken together, these results suggested that STAT5a conferred DOX resistance to breast cancer cells by regulating the transcription of ABCB1.

STAT5 Inhibitor Pimozide Sensitizes Breast Cancer Cells to DOX

Pimozide, an FDA-approved drug for treatment of psychotropic diseases, has been applied as a potent inhibitor of STAT5 in

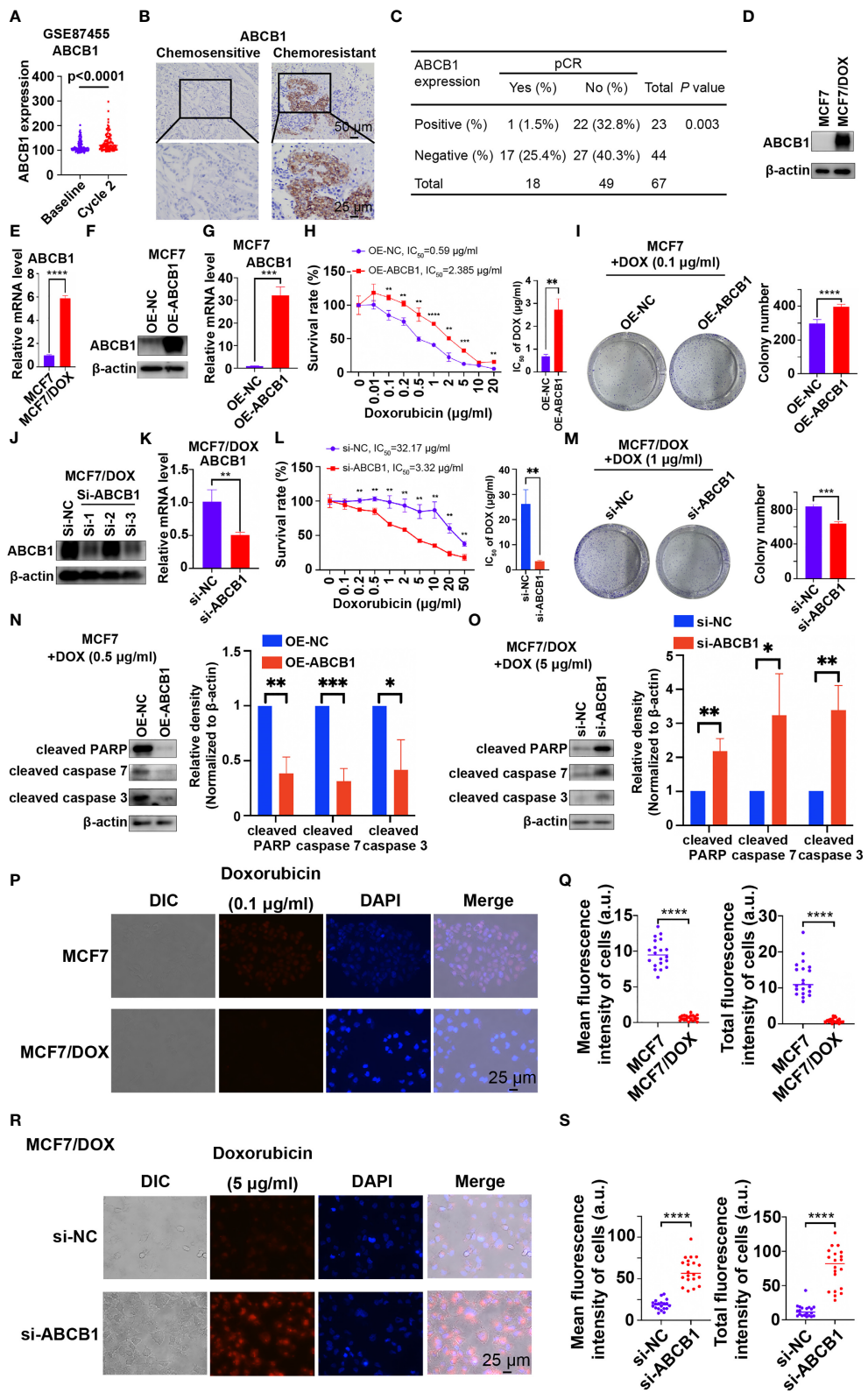


FIGURE 2 | Continued

FIGURE 2 | ABCB1 is essential to chemoresistance in breast cancer. **(A)** Expression of ABCB1 in breast cancer samples collected pre- and postchemotherapy in the dataset GSE87455. **(B)** Representative images of IHC staining for ABCB1 in chemoresistant and chemosensitive breast cancer samples. **(C)** Correlation between the pCR rate and ABCB1 expression in breast cancer samples obtained from 67 patients. **(D, E)** Protein **(D)** and mRNA **(E)** levels of ABCB1 in MCF7 and MCF7/DOX cells determined by Western blotting and qPCR. **(F, G)** Protein **(F)** and mRNA **(G)** levels of ABCB1 in MCF7 cells transfected with an empty vector or ABCB1 vector determined by Western blotting and qPCR. **(H)** Survival rate and IC₅₀ of MCF7 cells transfected with an empty vector or a STAT5a vector after treatment with DOX for 48 h determined by a CCK8 assay. **(I)** Representative images and quantification of colonies formed by MCF7 cells transfected with the empty vector or ABCB1 vector in medium containing DOX. **(J, K)** Protein **(J)** and mRNA **(K)** levels of ABCB1 in MCF7/DOX cells transfected with scramble siRNA or ABCB1-targeting siRNA detected by Western blotting and qPCR. **(L)** Survival rate and IC₅₀ of MCF7/DOX cells transfected with scramble siRNA or ABCB1-targeting siRNA after treatment with DOX for 48 h determined by a CCK8 assay. **(M)** Representative images and quantification of colonies formed by MCF7/DOX cells transfected with scramble siRNA or ABCB1-targeting siRNA in medium containing DOX. **(N, O)** Expression of apoptosis markers in MCF7 cells transfected with the empty vector or ABCB1 vector **(N)** and in MCF7/DOX cells transfected with scramble siRNA or ABCB1-targeting siRNA in the presence of DOX **(O)**. **(P, Q)** Representative images **(P)** and quantification **(Q)** of the accumulation of DOX in MCF7 and MCF7/DOX cells after treatment with DOX. **(R, S)** Representative images **(R)** and quantification **(S)** of the accumulation of DOX in MCF7/DOX cells transfected with scramble siRNA or ABCB1-targeting siRNA after DOX treatment. **p* < 0.05; ***p* < 0.01; ****p* < 0.001; *****p* < 0.0001.

numerous studies (25–27). We also applied pimozone in our study to inhibit the activation of STAT5a and tested whether this treatment sensitizes MCF7/DOX cells to DOX. First, we determined the IC₅₀ of pimozone in MCF7/DOX cells *via* a CCK8 assay. The results showed that the IC₅₀ of pimozone in MCF7/DOX cells was 14.79 μ M and that pimozone exhibited negligible cytotoxicity below a concentration of 5 μ M (**Figure 4A**). WB results showed that pimozone also inhibited STAT5a in MCF7/DOX cells by suppressing the phosphorylation of STAT5a at Tyr694 in a time- and concentration (1 μ M, 2 μ M and 5 μ M)-dependent manner and that the expression of STAT5a and ABCB1 was also repressed by the administration of pimozone (**Figures 4B, C**). Subsequently, we compared the anticancer effects of DOX and a combination of DOX and pimozone. The results showed that pimozone could significantly sensitize MCF7/DOX cells to DOX in a dose-dependent manner (**Figure 4D**). Flow cytometry experiments indicated that the addition of pimozone significantly increased the apoptosis rate of MCF7/DOX cells treated with DOX in a dose-dependent manner (**Figures 4E, F**). The addition of pimozone also increased the levels of apoptosis biomarkers, such as cleaved PARP and cleaved caspase 3/7, as indicated by Western blot analysis (**Figure 4G**). We also analyzed the influence of pimozone on the ability of breast cancer cells to pump out drugs. The results showed that when pimozone was administered, the accumulation of DOX within cells was remarkably increased in MCF7/DOX cells (**Figures 4H, I**). To confirm that pimozone sensitized breast cancer cells by suppressing the STAT5a/ABCB1 pathway, a rescue experiment was conducted. As shown in **Figures 4J, K**, the addition of pimozone to DOX treatment significantly elevated the expression of cleaved PARP and cleaved caspase 3/7 in MCF7/DOX cells, whereas overexpression of STAT5a or ABCB1 restored the expression to low levels. These data suggested that the STAT5 inhibitor pimozone attenuated the ability of cells to pump out drugs and sensitized DOX-resistant breast cancer cells to DOX by suppressing the STAT5a/ABCB1 pathway.

STAT5a Knockdown Sensitizes Breast Cancer Cells to DOX *In Vivo*

To validate our findings *in vivo*, MCF7/DOX sh-NC and MCF7/DOX sh-STAT5a cell lines were constructed, and their

expression of STAT5a and ABCB1 and sensitivity to DOX were validated. The expression of STAT5a and ABCB1 was significantly downregulated in MCF7/DOX sh-STAT5a cells (**Figure 5A**), and these cells showed significantly less resistance to DOX than MCF7/DOX sh-NC cells (**Figure 5B**). These two cell lines were used to establish a xenograft tumor model in nude mice (n=7). The results showed that DOX negligibly suppressed the growth of MCF7/DOX sh-NC tumors due to resistance, while MCF7/DOX sh-STAT5a tumors showed a significantly greater response to DOX (**Figures 5C–E** and **Supplementary Figure 1**). There was no difference in mouse body weight between the 2 groups during the treatment period (**Figure 5F**). IHC results showed decreased expression of STAT5a, p-STAT5a and ABCB1 in MCF7/DOX shSTAT5a tumors (**Figure 5G**). These data suggested that knocking down STAT5a decreased the expression of ABCB1 and sensitized chemoresistant breast cancer cells to DOX *in vivo*.

Pimozone Sensitizes Breast Cancer Cells to DOX *In Vivo*

To verify the efficacy of pimozone in the sensitization of breast cancer cells to chemotherapy *in vivo*, an MCF7/DOX xenograft tumor model was established in nude mice. Mice with xenograft tumors were divided into 4 groups (n=5) and received PBS, DOX, pimozone or a combination of DOX and pimozone as described in the methods. As shown in **Figures 6A–C** and **Supplementary Figure 2**, the volume, growth rate, and weight of tumors in the DOX group were not different from those of tumors in the PBS group, while those of tumors in the pimozone group were significantly lower, and those of tumors in the combination group were the lowest. DOX failed to suppress tumor growth due to resistance, while pimozone exhibited both antitumor activity and efficient sensitization to DOX. Mouse body weights were recorded, and no significant differences were observed among the four groups of mice, implying the drug dose was tolerated (**Figure 6D**). The expression of STAT5a, p-STAT5a and ABCB1 detected by IHC was significantly decreased in tumor tissues from the pimozone group and combination group but did not vary between the DOX group and PBS group (**Figure 6E**), suggesting the potent effect of pimozone on suppressing STAT5a and downstream ABCB1. These results demonstrated that a minimally toxic dose of

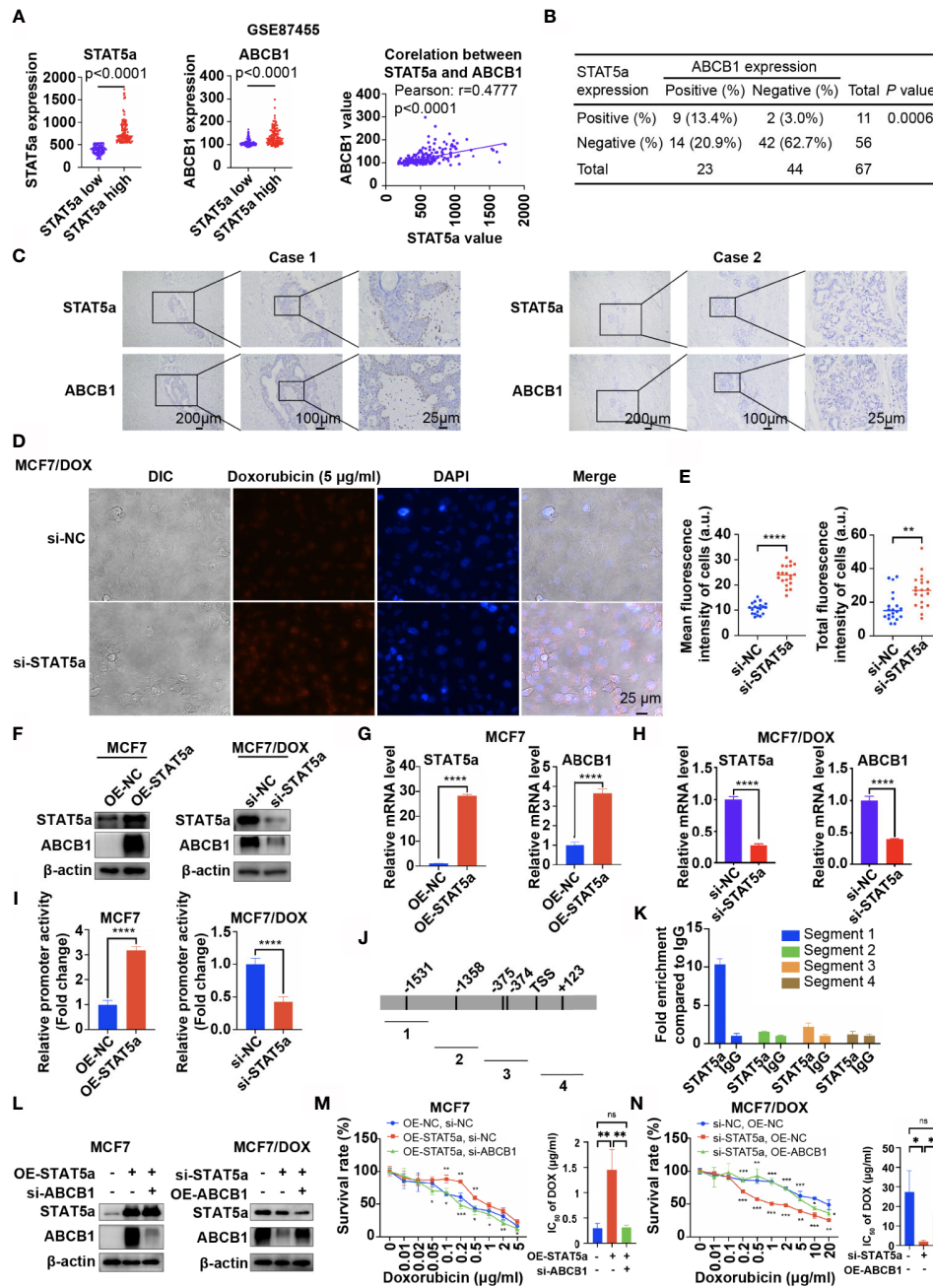


FIGURE 3 | STAT5a modulates chemoresistance in breast cancer by regulating the transcription of ABCB1. **(A)** Data from GSE87455 showed that the expression of ABCB1 was higher in the STAT5a-high group than in the STAT5a-low group in breast cancer, and the expression of STAT5a and ABCB1 was positively correlated. **(B)** Correlation between STAT5a expression and ABCB1 expression in breast cancer samples obtained from 67 patients. **(C)** Representative images of STAT5a and ABCB1 expression levels in breast cancer samples. **(D, E)** Representative images **(D)** and quantification **(E)** of the accumulation of DOX in MCF7/DOX cells transfected with scramble siRNA or STAT5a-targeting siRNA after treatment with DOX. **(F)** Expression levels of STAT5a and ABCB1 in MCF7 cells transfected with an empty vector or a STAT5a vector determined by Western blotting and MCF7/DOX cells transfected with scramble siRNA or STAT5a-targeting siRNA. **(G, H)** mRNA levels of STAT5a and ABCB1 in MCF7/DOX cells transfected with scramble siRNA or STAT5a-targeting siRNA **(G)** and in MCF7/DOX cells transfected with scramble siRNA or STAT5a-targeting siRNA **(H)** determined by qPCR. **(I)** Relative promoter activity in MCF7 cells transfected with the empty vector or STAT5a vector and in MCF7/DOX cells transfected with scramble siRNA or STAT5a-targeting siRNA. **(J)** Four pairs of primers were designed to detect sequences covering five predicted binding sites for STAT5a in the ABCB1 promoter region. **(K)** Binding between STAT5a and the ABCB1 promoter region in sequence 1 was determined by ChIP. **(L)** Levels of STAT5a and ABCB1 in MCF7 cells transfected with the indicated vector or siRNA and in MCF7/DOX cells transfected with the indicated targeting siRNA or vectors. **(M, N)** Survival rates and IC_{50} of MCF7 **(M)** and MCF7/DOX **(N)** cells transfected with the indicated vector or siRNA after treatment with DOX for 48 h determined by a CCK8 assay. ns, $p > 0.05$; * $p < 0.05$; ** $p < 0.01$; *** $p < 0.001$; **** $p < 0.0001$.

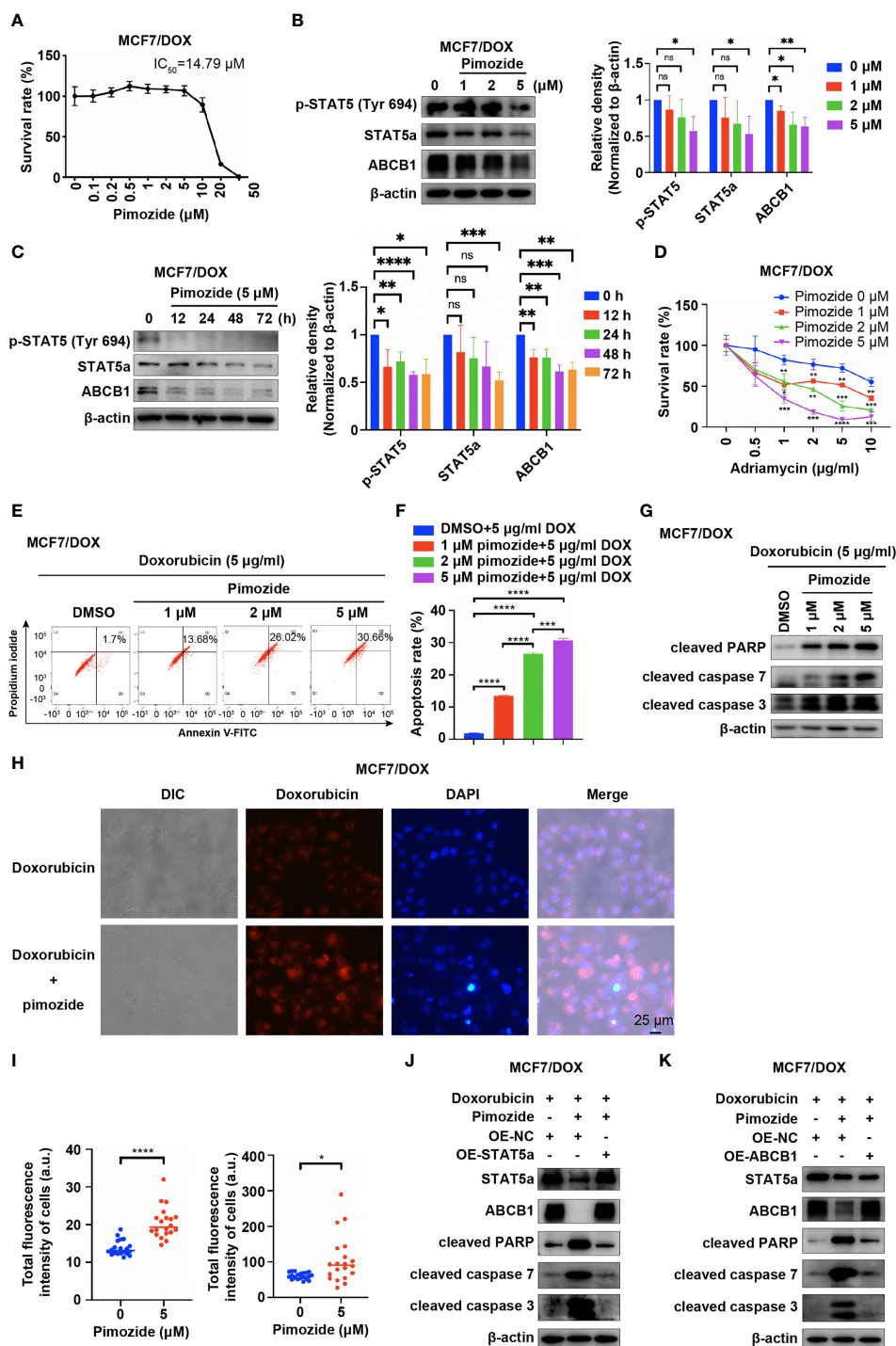


FIGURE 4 | Pimozide sensitizes DOX-resistant cells to DOX by suppressing STAT5a. **(A)** Survival rate of MCF/DOX cells after treatment with pimozide for 48 h, with the IC_{50} calculated to be 14.79 μM . **(B, C)** Expression of p-STAT5 (Try 694), STAT5a and ABCB1 in MCF7/DOX cells after treatment with 0, 1, 2, or 5 μM DOX for 48 h **(B)** or with 5 μM DOX for 0, 12, 24, 48 or 72 h **(C)**. **(D)** Survival rate of MCF7/DOX cells after treatment with a combination of 0, 1, 2 or 5 μM pimozide and the indicated concentration of DOX for 48 h. **(E, F)** Apoptosis rate of MCF7/DOX cells after the indicated treatment assessed by flow cytometry **(E)**; bar graphs showing the percentage of apoptotic cells **(F)**. **(G)** Expression of apoptosis markers in MCF7/DOX cells given the indicated treatments determined by Western blotting. **(H, I)** Accumulation of DOX in MCF7/DOX cells after treatment with DOX or a combination of DOX and pimozide **(H)** and quantification **(I)**. **(J, K)** Western blotting was performed to determine the expression of STAT5a, ABCB1, cleaved PARP, cleaved caspase 7 and cleaved caspase 3 in MCF7/DOX cells treated with DOX and transfected with the indicated vectors. ns, $p > 0.05$; * $p < 0.05$; ** $p < 0.01$; *** $p < 0.001$; **** $p < 0.0001$.

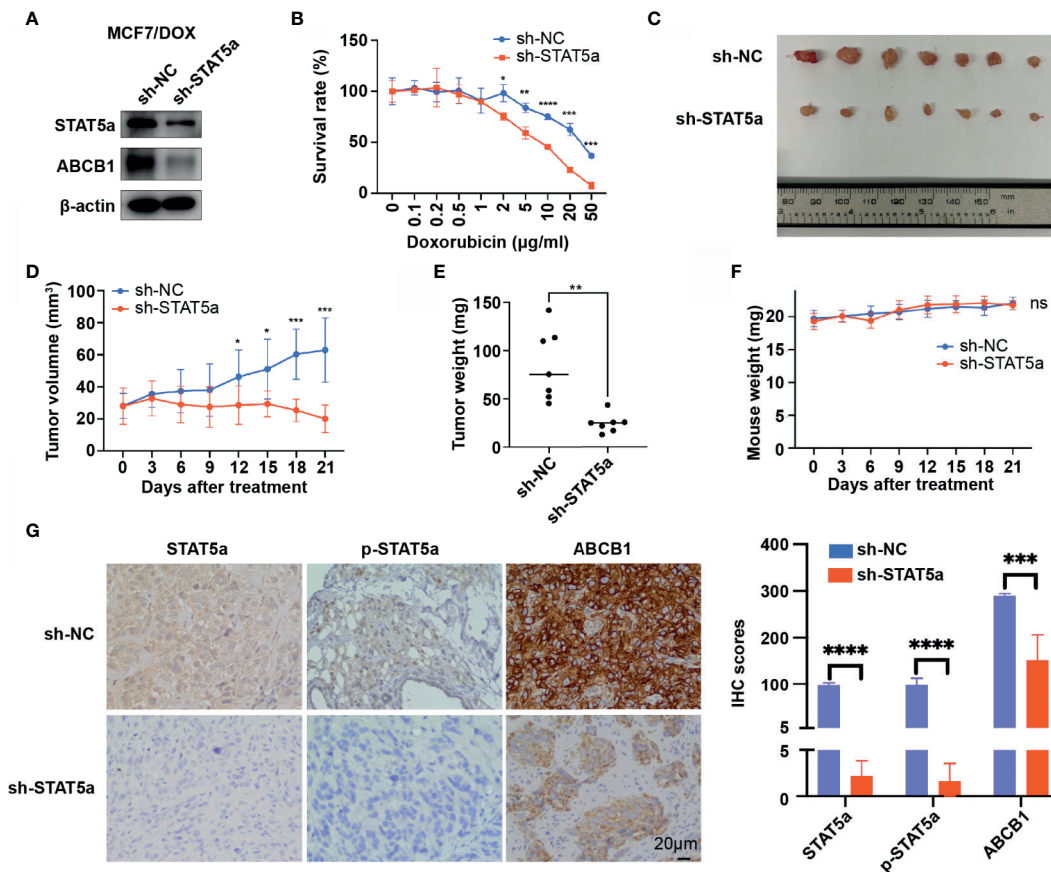


FIGURE 5 | STAT5a knockdown sensitizes breast cancer cells to DOX *in vivo*. **(A)** Expression of STAT5a and ABCB1 in MCF7/DOX sh-NC cells and MCF7/DOX sh-STAT5a cells determined by Western blotting. **(B)** Survival rates of MCF7/DOX sh-NC and MCF7/DOX sh-STAT5a cells after treatment with DOX for 48 h. **(C)** Isolated subcutaneous tumors. **(D)** Tumor growth curves. **(E)** Weights of isolated tumors. **(F)** Nude mouse weight curves. **(G)** Expression of STAT5a, p-STAT5a and ABCB1 in MCF7/DOX sh-NC and MCF7/DOX sh-STAT5a tumors determined by IHC analysis. ns, $p > 0.05$; * $p < 0.05$; ** $p < 0.01$; *** $p < 0.001$; **** $p < 0.0001$.

pimozide had an antitumor effect on breast cancer and was able to sensitize breast cancer to DOX *in vitro* and *in vivo*.

DISCUSSION

Chemoresistance is the leading cause of therapy failure and mortality in breast cancer (28). The drug efflux pump ABCB1 plays a key role in chemoresistance by effluxing various chemotherapeutic agents from tumor cells (21, 28, 29), and its expression is negatively correlated with the prognosis of cancers, including that of breast cancer (30, 31). We verified the function of ABCB1 in chemoresistance in breast cancer cells in our study and proved its regulation by STAT5a.

STAT5a is a member of the STAT family and is highly homologous to STAT5b. STAT5a is mainly present in mammary tissue, while STAT5b is generally expressed in muscle and the liver (8). The role of STAT5a in hematopoietic neoplasms, especially in myeloid cell transformation, is broadly accepted (32), and STAT5a also promotes the development of several other cancers (9–11, 33). However, the role of STAT5a in

the development of breast cancer is controversial (34). On the one hand, STAT5a promotes transformation of mammary epithelial cells and survival of breast cancer cells (35, 36); on the other hand, STAT5a is associated with a relatively good prognosis for patient survival since it promotes mammary epithelial cell differentiation (37–40). The results of our study showed that STAT5a was overexpressed and persistently activated in a chemoresistant breast cancer cell line and upregulated ABCB1 expression by promoting its transcription. The interaction of STAT5a and the promoter of ABCB1 was verified by ChIP in our study, and the interaction of STAT5 with a nearby region was also implied by a previous study (41). The roles of STAT5a and ABCB1 in chemoresistance in breast cancer and their regulation were further confirmed by IHC analysis of breast cancer tissues from 67 patients who received DOX-containing neoadjuvant treatment. The pCR rate was used to measure the sensitivity of patients to chemotherapy. We found that STAT5a- or ABCB1-expressing patients exhibited a significantly lower pCR rate, implying the vital roles of STAT5a and ABCB1 in chemoresistance in breast cancer. Moreover, the expression of STAT5a and ABCB1 was

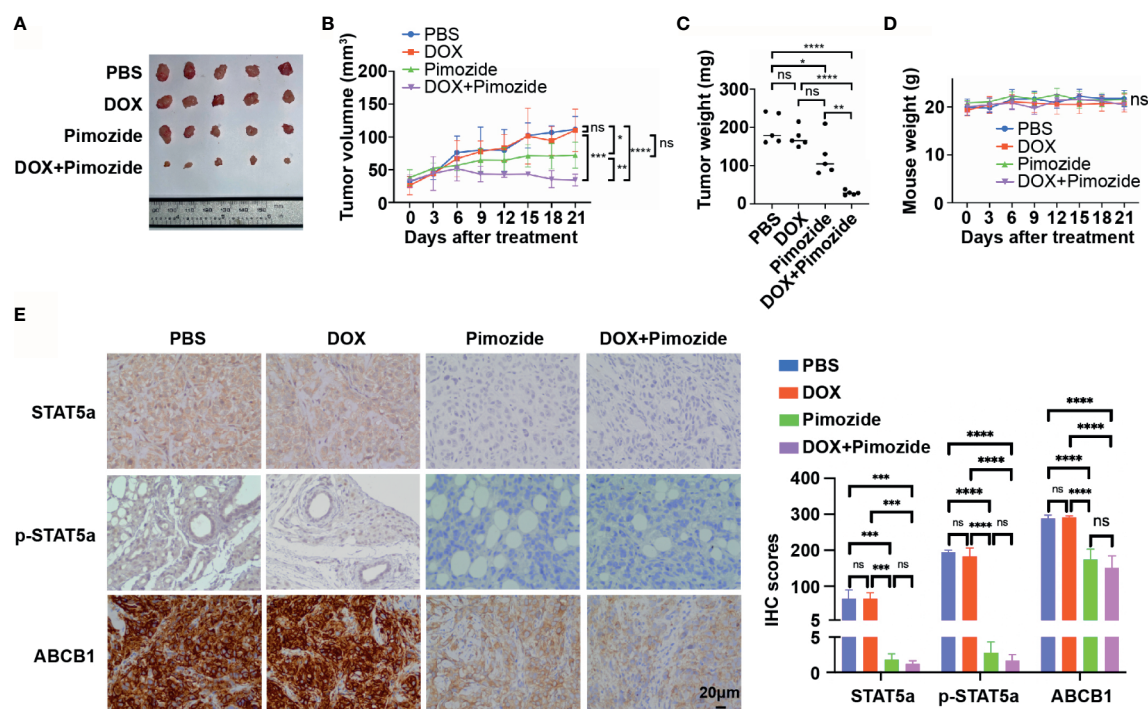


FIGURE 6 | Pimozide sensitizes breast cancer cells to DOX *in vivo*. **(A)** Isolated subcutaneous tumors of each group. **(B)** Growth curves of tumors in each group. **(C)** Weights of isolated tumors in each group. **(D)** Nude mouse weight curves. **(E)** Expression of STAT5a, p-STAT5a and ABCB1 in each group of tumors determined by IHC analysis. ns, $p > 0.05$; * $p < 0.05$; ** $p < 0.01$; *** $p < 0.001$; **** $p < 0.0001$.

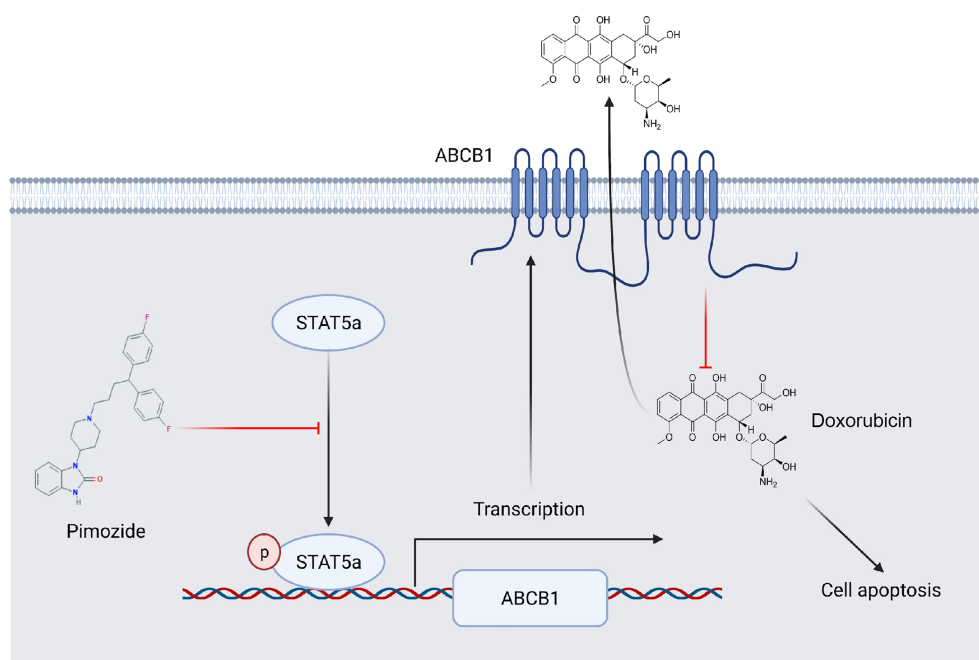


FIGURE 7 | A schematic showing the involvement of STAT5a in DOX resistance in breast cancer. ABCB1 transports DOX out of breast cancer cells to reduce its cellular accumulation. STAT5a promotes the transcription of ABCB1 to confer DOX resistance to cells. Pimozide overcomes this resistance by inhibiting the STAT5a/ABCB1 axis.

positively correlated, which was consistent with our *in vitro* studies.

Pimozide, an FDA-approved psychotropic drug, inactivated STAT5a and downregulated the expression of ABCB1, thus sensitizing MCF7/DOX cells to DOX *in vitro* and *in vivo*, providing a promising strategy for treating patients with chemoresistant breast cancer in the clinic. In fact, pimozide has been found to have antitumor activity mediated by suppressing STAT5 in various types of cancer (25, 42–44). In breast cancer, pimozide has also been proven to promote apoptosis by inhibiting RAN GTPase and AKT and to inhibit epithelial-mesenchymal transition and cell migration (45). Pimozide also acts as a STAT5 inhibitor (46) or STAT3 inhibitor (47) to kill breast cancer cells or sensitize cancer cells to other drugs (48). Additionally, pimozide was found to inhibit ABCB1 in drug-resistant KBV20C oral cancer cells, but the authors did not explain the mechanism (49). Thus, the exact mechanism by which pimozide exerts its anticancer activity remains unclear. In our study, pimozide inhibited STAT5a and ABCB1 in a dose-dependent manner and sensitized breast cancer cells to DOX, which could be rescued by overexpression of STAT5a or ABCB1. The results suggested that the STAT5a/ABCB1 pathway was at least one, if not the main, mechanism by which pimozide functions in drug-resistant breast cancer.

CONCLUSIONS

STAT5a confers breast cancer chemoresistance by upregulating the transcription of ABCB1. Pimozide sensitizes breast cancer cells to DOX by suppressing the activation of STAT5a and downregulating ABCB1 (**Figure 7**). Our study established the vital role of STAT5a in chemoresistance in breast cancer and verified the mechanism. We also identified STAT5a as a therapeutic target for treatment of chemoresistant breast cancer and pimozide as a promising candidate to reduce chemoresistance.

DATA AVAILABILITY STATEMENT

The original contributions presented in the study are included in the article/**Supplementary Material**. Further inquiries can be directed to the corresponding authors.

ETHICS STATEMENT

The studies involving human participants were reviewed and approved by the Ethics Committee of the Sir Run Run Shaw Hospital at the Zhejiang University School of Medicine. The

patients/participants provided their written informed consent to participate in this study. The animal study was reviewed and approved by the Animal Care and Use Committee of Sir Run Run Shaw Hospital, Zhejiang University, Zhejiang, China.

AUTHOR CONTRIBUTIONS

LW, JZ, and ZL designed the study, and ZL, CC, LC, DH, and XY performed the experiments. ZL, WZ, and CC contributed to writing the manuscript. YC, JY, YZ, MM, and LX analyzed the data. XZ, SJ, JS, and QinW contributed to manuscript review and revision. MD, SX, QunW, and YJ provided technical support. All authors contributed to the article and approved the submitted version.

FUNDING

The work was supported by the National Natural Science Foundation of China (No. 81672729, No. 81972597, No. 81602471, No. 81972453, No. 81672840 and No. 82000212), Zhejiang Provincial Natural Science Foundation of China under Grants (No. LY19H160059, No. LY19H160055, No. LY18H160030 and No. LQ21H160022), Zhejiang Provincial Medical and Health Science and Technology Project (No. 2018ZD028 and No. 2021RC003), Ningbo Natural Science Foundation (No. 2019A610315), and Cixi Agricultural and Social Development Science and Technology Project (No. CN2020006). The work was sponsored by the Zheng Shu Medical Elite Scholarship Fund.

ACKNOWLEDGMENTS

BioRender.com was used to create the schematic.

SUPPLEMENTARY MATERIAL

The Supplementary Material for this article can be found online at: <https://www.frontiersin.org/articles/10.3389/fonc.2021.697950/full#supplementary-material>

Supplementary Figure 1 | Tumors formed in nude mice injected with MCF7/DOX sh-NC cells or MCF7/DOX sh-STAT5a cells and treated with doxorubicin (n=7).

Supplementary Figure 2 | Nude mice bearing tumors formed from MCF7/DOX cells were divided into four groups and received the indicated treatment (n=5).

REFERENCES

1. Harbeck N, Gnant M. Breast Cancer. *Lancet* (2017) 389(10074):1134–50. doi: 10.1016/S0140-6736(16)31891-8
2. Szelag M, Piaszyk-Borychowska A, Plens-Galaska M, Wesoly J, Bluysen HA. Targeted Inhibition of STATs and IRFs as a Potential Treatment Strategy in Cardiovascular Disease. *Oncotarget* (2016) 7(30):48788–812. doi: 10.18632/oncotarget.9195

3. Richard AJ, Stephens JM. The Role of JAK-STAT Signaling in Adipose Tissue Function. *Biochim Biophys Acta* (2014) 1842(3):431–9. doi: 10.1016/j.bbdis.2013.05.030
4. Lin JX, Mietz J, Modi WS, John S, Leonard WJ. Cloning of Human Stat5B. Reconstitution of Interleukin-2-Induced Stat5A and Stat5B DNA Binding Activity in COS-7 Cells. *J Biol Chem* (1996) 271(18):10738–44. doi: 10.1074/jbc.271.18.10738
5. Grimley PM, Dong F, Rui H. Stat5a and Stat5b: Fraternal Twins of Signal Transduction and Transcriptional Activation. *Cytokine Growth Factor Rev* (1999) 10(2):131–57. doi: 10.1016/S1359-6101(99)00011-8
6. Basham B, Sathe M, Grein J, McClanahan T, D'Andrea A, Lees E, et al. In Vivo Identification of Novel STAT5 Target Genes. *Nucleic Acids Res* (2008) 36(11):3802–18. doi: 10.1093/nar/gkn271
7. Kanai T, Seki S, Jenks JA, Kohli A, Kawli T, Martin DP, et al. Identification of STAT5A and STAT5B Target Genes in Human T Cells. *PLoS One* (2014) 9(1):e86790. doi: 10.1371/journal.pone.0086790
8. Hennighausen L, Robinson GW. Interpretation of Cytokine Signaling Through the Transcription Factors STAT5A and STAT5B. *Genes Dev* (2008) 22(6):711–21. doi: 10.1101/gad.1643908
9. Xu C, Zhang L, Li H, Liu Z, Duan L, Lu C. MiRNA-1469 Promotes Lung Cancer Cells Apoptosis Through Targeting STAT5a. *Am J Cancer Res* (2015) 5(3):1180–9.
10. Liao Z, Nevalainen MT. Targeting Transcription Factor Stat5a/b as a Therapeutic Strategy for Prostate Cancer. *Am J Transl Res* (2011) 3(2):133–8.
11. Dong SR, Ju XL, Yang WZ. STAT5A Reprograms Fatty Acid Metabolism and Promotes Tumorigenesis of Gastric Cancer Cells. *Eur Rev Med Pharmacol Sci* (2019) 23(19):8360–70. doi: 10.26355/eurrev_201910_19147
12. Li B, Hong P, Zheng CC, Dai W, Chen WY, Yang QS, et al. Identification of miR-29c and its Target FBXO31 as a Key Regulatory Mechanism in Esophageal Cancer Chemoresistance: Functional Validation and Clinical Significance. *Theranostics* (2019) 9(6):1599–613. doi: 10.7150/thno.30372
13. Akada M, Crnogorac-Jurcic T, Lattimore S, Mahon P, Lopes R, Sunamura M, et al. Intrinsic Chemoresistance to Gemcitabine Is Associated With Decreased Expression of BNIP3 in Pancreatic Cancer. *Clin Cancer Res* (2005) 11(8):3094–101. doi: 10.1158/1078-0432.CCR-04-1785
14. Cotala I, Ren S, Zhang Y, Gehan E, Singh B, Furth PA. Stat5a Is Tyrosine Phosphorylated and Nuclear Localized in a High Proportion of Human Breast Cancers. *Int J Cancer* (2004) 108(5):665–71. doi: 10.1002/ijc.11619
15. Zeng Y, Min L, Han Y, Meng L, Liu C, Xie Y, et al. Inhibition of STAT5a by Naa10p Contributes to Decreased Breast Cancer Metastasis. *Carcinogenesis* (2014) 35(10):2244–53. doi: 10.1093/carcin/bgu132
16. Mukhopadhyay UK, Cass J, Raptis L, Craig AW, Bourdeau V, Varma S, et al. STAT5A Is Regulated by DNA Damage Via the Tumor Suppressor P53. *Cytokine* (2016) 82:70–9. doi: 10.1016/j.cyt.2016.01.013
17. Hodges LM, Markova SM, Chinn LW, Gow JM, Kroetz DL, Klein TE, et al. Very Important Pharmacogene Summary: ABCB1 (MDR1, P-Glycoprotein). *Pharmacogenet Genomics* (2011) 21(3):152–61. doi: 10.1097/FPC.0b013e3283385a1c
18. Sharom FJ. The P-glycoprotein Multidrug Transporter. *Essays Biochem* (2011) 50(1):161–78. doi: 10.1042/bse0500161
19. Wang H, Li JM, Wei W, Yang R, Chen D, Ma XD, et al. Regulation of ATP-Binding Cassette Subfamily B Member 1 by Snail Contributes to Chemoresistance in Colorectal Cancer. *Cancer Sci* (2020) 111(1):84–97. doi: 10.1111/cas.14253
20. Jin W, Liao X, Lv Y, Pang Z, Wang Y, Li Q, et al. MUC1 Induces Acquired Chemoresistance by Upregulating ABCB1 in EGFR-Dependent Manner. *Cell Death Dis* (2017) 8(8):e2980. doi: 10.1038/cddis.2017.378
21. Fultang N, Illendula A, Lin J, Pandey MK, Klase Z, Peethambaran B. ROR1 Regulates Chemoresistance in Breast Cancer Via Modulation of Drug Efflux Pump ABCB1. *Sci Rep* (2020) 10(1):1821. doi: 10.1038/s41598-020-58864-0
22. Jia Y, Ying X, Zhou J, Chen Y, Luo X, Xie S, et al. The Novel KLF4/PLAC8 Signaling Pathway Regulates Lung Cancer Growth. *Cell Death Dis* (2018) 9(6):603. doi: 10.1038/s41419-018-0580-3
23. Kimbung S, Markholm I, Bjohle J, Lekberg T, von Wachenfeldt A, Azavedo E, et al. Assessment of Early Response Biomarkers in Relation to Long-Term Survival in Patients With HER2-Negative Breast Cancer Receiving Neoadjuvant Chemotherapy Plus Bevacizumab: Results From the Phase II PROMIX Trial. *Int J Cancer* (2018) 142(3):618–28. doi: 10.1002/ijc.31070
24. Motlagh NS, Parvin P, Ghasemi F, Atiyabi F. Fluorescence Properties of Several Chemotherapy Drugs: Doxorubicin, Paclitaxel and Bleomycin. *BioMed Opt Express* (2016) 7(6):2400–6. doi: 10.1364/BOE.7.002400
25. Nelson EA, Walker SR, Weisberg E, Bar-Natan M, Barrett R, Gashin LB, et al. The STAT5 Inhibitor Pimozide Decreases Survival of Chronic Myelogenous Leukemia Cells Resistant to Kinase Inhibitors. *Blood* (2011) 117(12):3421–9. doi: 10.1182/blood-2009-11-255232
26. Roos A, Dhruv HD, Peng S, Inge LJ, Tuncali S, Pineda M, et al. EGFRvIII-Stat5 Signaling Enhances Glioblastoma Cell Migration and Survival. *Mol Cancer Res* (2018) 16(7):1185–95. doi: 10.1158/1541-7786.MCR-18-0125
27. Nelson EA, Walker SR, Xiang M, Weisberg E, Bar-Natan M, Barrett R, et al. The STAT5 Inhibitor Pimozide Displays Efficacy in Models of Acute Myelogenous Leukemia Driven by FLT3 Mutations. *Genes Cancer* (2012) 3(7-8):503–11. doi: 10.1177/1947601912466555
28. Ji X, Lu Y, Tian H, Meng X, Wei M, Cho WC. Chemoresistance Mechanisms of Breast Cancer and Their Countermeasures. *BioMed Pharmacother* (2019) 114:108800. doi: 10.1016/j.biopha.2019.108800
29. Sui H, Fan ZZ, Li Q. Signal Transduction Pathways and Transcriptional Mechanisms of ABCB1/Pgp-mediated Multiple Drug Resistance in Human Cancer Cells. *J Int Med Res* (2012) 40(2):426–35. doi: 10.1177/147323001204000204
30. Takara K, Sakaeda T, Okumura K. An Update on Overcoming MDR1-Mediated Multidrug Resistance in Cancer Chemotherapy. *Curr Pharm Des* (2006) 12(3):273–86. doi: 10.2174/138161206775201965
31. Koh EH, Chung HC, Lee KB, Lim HY, Kim JH, Roh JK, et al. The Value of Immunohistochemical Detection of P-glycoprotein in Breast Cancer Before and After Induction Chemotherapy. *Yonsei Med J* (1992) 33(2):137–42. doi: 10.3349/ymj.1992.33.2.137
32. Kotecha N, Flores NJ, Irish JM, Simonds EF, Sakai DS, Archambeault S, et al. Single-Cell Profiling Identifies Aberrant STAT5 Activation in Myeloid Malignancies With Specific Clinical and Biologic Correlates. *Cancer Cell* (2008) 14(4):335–43. doi: 10.1016/j.ccr.2008.08.014
33. Tan SH, Dagvadorj A, Shen F, Gu L, Liao Z, Abdulghani J, et al. Transcription Factor Stat5 Synergizes With Androgen Receptor in Prostate Cancer Cells. *Cancer Res* (2008) 68(1):236–48. doi: 10.1158/0008-5472.CAN-07-2972
34. Ferbeyre G, Moriggi R. The Role of Stat5 Transcription Factors as Tumor Suppressors or Oncogenes. *Biochim Biophys Acta* (2011) 1815(1):104–14. doi: 10.1016/j.bbcan.2010.10.004
35. Vafaizadeh V, Klemmt P, Brendel C, Weber K, Doebele C, Britt K, et al. Mammary Epithelial Reconstitution With Gene-Modified Stem Cells Assigns Roles to Stat5 in Luminal Alveolar Cell Fate Decisions, Differentiation, Involvement, and Mammary Tumor Formation. *Stem Cells* (2010) 28(5):928–38. doi: 10.1002/stem.407
36. Yamashita H, Iwase H. The Role of Stat5 in Estrogen Receptor-Positive Breast Cancer. *Breast Cancer* (2002) 9(4):312–8. doi: 10.1007/BF02967610
37. Liu X, Robinson GW, Wagner KU, Garrett L, Wynshaw-Boris A, Hennighausen L. Stat5a Is Mandatory for Adult Mammary Gland Development and Lactogenesis. *Genes Dev* (1997) 11(2):179–86. doi: 10.1101/gad.11.2.179
38. Miyoshi K, Shillingford JM, Smith GH, Grimm SL, Wagner KU, Oka T, et al. Signal Transducer and Activator of Transcription (Stat) 5 Controls the Proliferation and Differentiation of Mammary Alveolar Epithelium. *J Cell Biol* (2001) 155(4):531–42. doi: 10.1083/jcb.200107065
39. Wagner KU, Rui H. Jak2/Stat5 Signaling in Mammogenesis, Breast Cancer Initiation and Progression. *J Mammary Gland Biol Neoplasia* (2008) 13(1):93–103. doi: 10.1007/s10911-008-9062-z
40. Peck AR, Witkiewicz AK, Liu C, Klimowicz AC, Stringer GA, Pequignot E, et al. Low Levels of Stat5a Protein in Breast Cancer Are Associated With Tumor Progression and Unfavorable Clinical Outcomes. *Breast Cancer Res* (2012) 14(5):R130. doi: 10.1186/bcr3328
41. LeBaron MJ, Xie J, Rui H. Evaluation of Genome-Wide Chromatin Library of Stat5 Binding Sites in Human Breast Cancer. *Mol Cancer* (2005) 4(1):6. doi: 10.1186/1476-4598-4-6
42. Goncalves JM, Silva CAB, Rivero ERC, Cordeiro MMR. Inhibition of Cancer Stem Cells Promoted by Pimozide. *Clin Exp Pharmacol Physiol* (2019) 46(2):116–25. doi: 10.1111/1440-1681.13049
43. Subramaniam D, Angulo P, Ponnuram S, Dandawate P, Ramamoorthy P, Srinivasan P, et al. Suppressing STAT5 Signaling Affects Osteosarcoma Growth and Stemness. *Cell Death Dis* (2020) 11(2):149. doi: 10.1038/s41419-020-2335-1

44. Kim U, Kim CY, Lee JM, Ryu B, Kim J, Shin C, et al. Pimozide Inhibits the Human Prostate Cancer Cells Through the Generation of Reactive Oxygen Species. *Front Pharmacol* (2019) 10:1517. doi: 10.3389/fphar.2019.01517
45. Dakir el H, Pickard A, Srivastava K, McCrudden CM, Gross SR, Lloyd S, et al. The Anti-Psychotic Drug Pimozide Is a Novel Chemotherapeutic for Breast Cancer. *Oncotarget* (2018) 9(79):34889–910. doi: 10.18632/oncotarget.26175
46. Mapes J, Anandan L, Li Q, Neff A, Clevenger CV, Bagchi IC, et al. Aberrantly High Expression of the CUB and Zona Pellucida-Like Domain-Containing Protein 1 (CUZD1) in Mammary Epithelium Leads to Breast Tumorigenesis. *J Biol Chem* (2018) 293(8):2850–64. doi: 10.1074/jbc.RA117.000162
47. Dees S, Pontiggia L, Jasmin JF, Mercier I. Phosphorylated STAT3 (Tyr705) as a Biomarker of Response to Pimozide Treatment in Triple-Negative Breast Cancer. *Cancer Biol Ther* (2020) 21(6):506–21. doi: 10.1080/15384047.2020.1726718
48. Xiao Z, Liang J, Deng Q, Song C, Yang X, Liu Z, et al. Pimozide Augments Bromocriptine Lethality in Prolactinoma Cells and in a Xenograft Model Via the STAT5/cyclin D1 and STAT5/BclxL Signaling Pathways. *Int J Mol Med* (2021) 47(1):113–24. doi: 10.3892/ijmm.2020.4784
49. Kim JY, Park Y, Lee BM, Kim HS, Yoon S. P-gp Inhibition by the Anti-Psychotic Drug Pimozide Increases Apoptosis, as Well as Expression of pRb and pH2AX in Highly Drug-Resistant KBV20C Cells. *Anticancer Res* (2018) 38(10):5685–92. doi: 10.21873/anticancer.12905

Conflict of Interest: The authors declare that the research was conducted in the absence of any commercial or financial relationships that could be construed as a potential conflict of interest.

Copyright © 2021 Li, Chen, Chen, Hu, Yang, Zhuo, Chen, Yang, Zhou, Mao, Zhang, Xu, Ju, Shen, Wang, Dong, Xie, Wei, Jia, Zhou and Wang. This is an open-access article distributed under the terms of the Creative Commons Attribution License (CC BY). The use, distribution or reproduction in other forums is permitted, provided the original author(s) and the copyright owner(s) are credited and that the original publication in this journal is cited, in accordance with accepted academic practice. No use, distribution or reproduction is permitted which does not comply with these terms.



Corrigendum: STAT5a Confers Doxorubicin Resistance to Breast Cancer by Regulating ABCB1

Zhaoqing Li^{1,2,3†}, Cong Chen^{2,3†}, Lini Chen^{2,3†}, Dengdi Hu^{2,3,4}, Xiqian Yang^{2,3,5}, Wenying Zhuo^{2,3,4}, Yongxia Chen^{2,3}, Jingjing Yang^{2,3}, Yulu Zhou^{2,3}, Misha Mao^{2,3}, Xun Zhang^{2,3}, Ling Xu^{2,3}, Siwei Ju^{2,3}, Jun Shen^{2,3}, Qinchuan Wang^{2,3}, Minjun Dong^{2,3}, Shuduo Xie^{2,3}, Qun Wei^{2,3}, Yunlu Jia⁶, Jichun Zhou^{2,3*} and Linbo Wang^{2,3*}

OPEN ACCESS

Edited and reviewed by:

Dayanidhi Raman,
University of Toledo, United States

*Correspondence:

Linbo Wang
linbowang@zju.edu.cn
Jichun Zhou
jichun-zhou@zju.edu.cn

[†]These authors have contributed
equally to this work and
share first authorship

Specialty section:

This article was submitted to
Breast Cancer,
a section of the journal
Frontiers in Oncology

Received: 21 February 2022

Accepted: 23 February 2022

Published: 09 March 2022

Citation:

Li Z, Chen C, Chen L, Hu D, Yang X, Zhuo W, Chen Y, Yang J, Zhou Y, Mao M, Zhang X, Xu L, Ju S, Shen J, Wang Q, Dong M, Xie S, Wei Q, Jia Y, Zhou J and Wang L (2022) Corrigendum: STAT5a Confers Doxorubicin Resistance to Breast Cancer by Regulating ABCB1. *Front. Oncol.* 12:880458. doi: 10.3389/fonc.2022.880458

¹ Cancer Institute (Key Laboratory of Cancer Prevention and Intervention, China National Ministry of Education), 2nd Affiliated Hospital, School of Medicine, Zhejiang University, Hangzhou, China, ² Sir Run Run Shaw Hospital, Zhejiang University, Hangzhou, China, ³ Biomedical Research Center and Key Laboratory of Biotherapy of Zhejiang Province, Hangzhou, China, ⁴ Affiliated Cixi Hospital, Wenzhou Medical University, Ningbo, China, ⁵ Breast Surgical Department, Shaoxing Maternity and Child Health Care Hospital, Shaoxing, China, ⁶ The First Affiliated Hospital, Zhejiang University School of Medicine, Hangzhou, China

Keywords: breast cancer, STAT5A, ABCB1, pimozone, doxorubicin resistance

A Corrigendum on

STAT5a Confers Doxorubicin Resistance to Breast Cancer by Regulating ABCB1

By Li Z, Chen C, Chen L, Hu D, Yang X, Zhuo W, Chen Y, Yang J, Zhou Y, Mao M, Zhang X, Xu L, Ju S, Shen J, Wang Q, Dong M, Xie S, Wei Q, Jia Y, Zhou J and Wang L (2021). *Front. Oncol.* 11:697950. doi: 10.3389/fonc.2021.697950

In the original article, there was a mistake in **Figure 1** as published. In **Figure 1F**, the number “42” should be “38”. The corrected **Figure 1** appears below.

The authors apologize for this error and state that this does not change the scientific conclusions of the article in any way. The original article has been updated.

Publisher's Note: All claims expressed in this article are solely those of the authors and do not necessarily represent those of their affiliated organizations, or those of the publisher, the editors and the reviewers. Any product that may be evaluated in this article, or claim that may be made by its manufacturer, is not guaranteed or endorsed by the publisher.

Copyright © 2022 Li, Chen, Chen, Hu, Yang, Zhuo, Chen, Yang, Zhou, Mao, Zhang, Xu, Ju, Shen, Wang, Dong, Xie, Wei, Jia, Zhou and Wang. This is an open-access article distributed under the terms of the Creative Commons Attribution License (CC BY). The use, distribution or reproduction in other forums is permitted, provided the original author(s) and the copyright owner(s) are credited and that the original publication in this journal is cited, in accordance with accepted academic practice. No use, distribution or reproduction is permitted which does not comply with these terms.

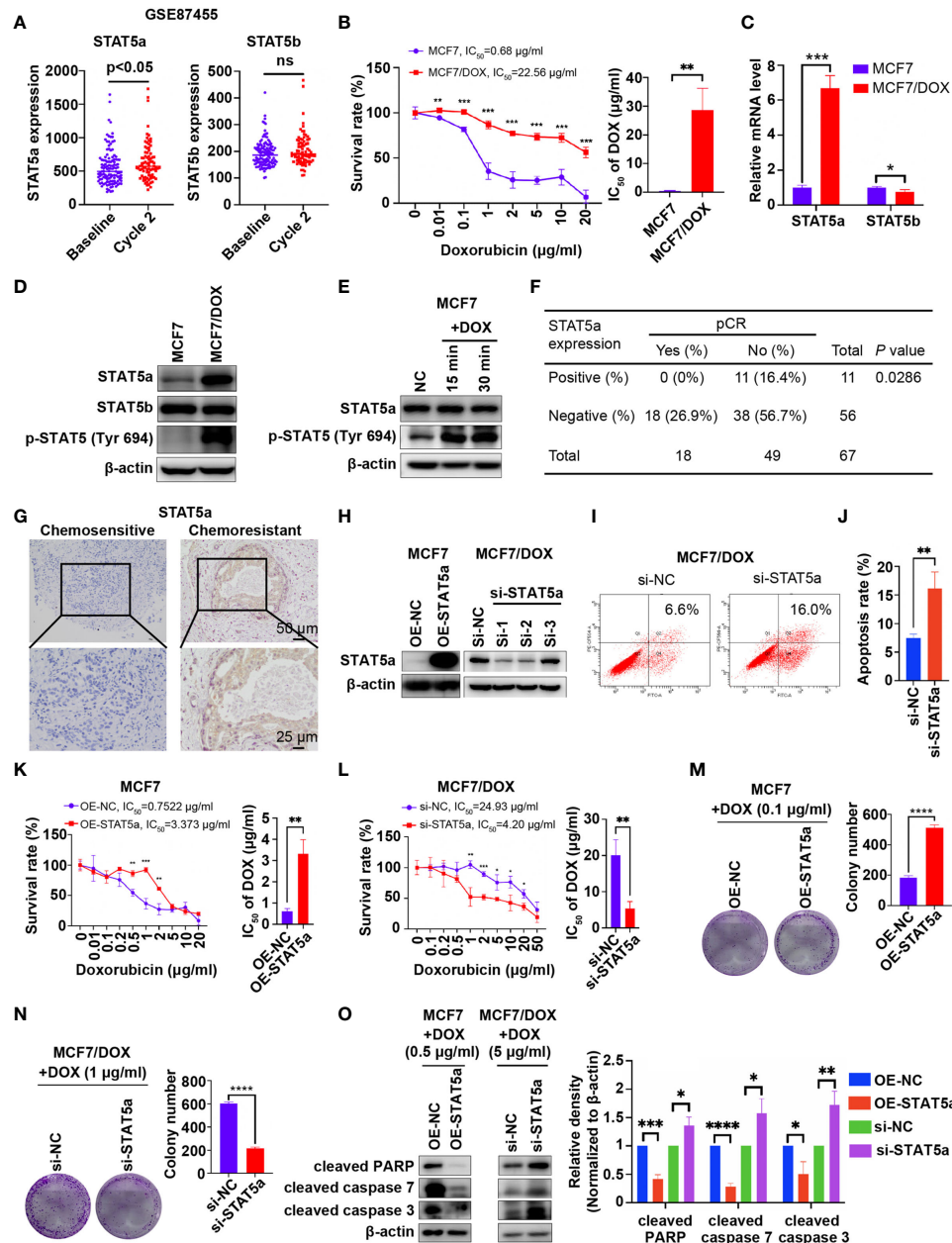


FIGURE 1 | STAT5a is involved in chemoresistance in breast cancer. **(A)** Expression of STAT5a and STAT5b in breast cancer samples collected pre- and postchemotherapy in the dataset GSE87455. **(B)** Survival rates of MCF7 and MCF7/DOX cells after treatment with DOX for 48 h determined by a CCK8 assay. **(C)** mRNA levels of STAT5a and STAT5b in MCF7 and MCF7/DOX cells assessed via qPCR. **(d)** Protein levels of STAT5a, p-STAT5a (Tyr694) and STAT5b in MCF7 and MCF7/DOX cells determined by Western blotting. **(E)** Western blotting was performed to examine the expression of STAT5a and p-STAT5 (Tyr694) in CF7 cells upon treatment with DOX. **(F)** Correlation between the pCR rate and STAT5a expression in breast cancer samples obtained from 67 patients. **(G)** Representative images of IHC staining for STAT5a in chemoresistant and chemosensitive breast cancer samples. **(H)** Efficiency of vector transfection for overexpression of STAT5a in MCF7 cells and siRNA transfection for knockdown of STAT5a in MCF7/DOX cells determined by Western blotting. **(I, J)** Flow cytometry was performed to assess apoptosis in MCF7/DOX cells after knocking down STAT5a or control treatment **(I)**. Bar graphs showing the percentage of apoptotic cells **(J, K)** Survival rate and IC₅₀ of MCF7 cells transfected with an empty vector or a STAT5a vector after treatment with DOX for 48 h determined by a CCK8 assay. **(L)** Survival rate and IC₅₀ of MCF7/DOX cells transfected with scramble siRNA or STAT5a-targeting siRNA after treatment with DOX for 48 h determined by a CCK8 assay. **(M, N)** Representative images and quantification of colonies formed by MCF7 cells transfected with the empty vector or STAT5a vector **(M)** and MCF7/DOX cells transfected with scramble siRNA or STAT5a-targeting siRNA **(N)** in medium containing the indicated concentration of DOX. **(O)** The expression levels of apoptosis markers in MCF7 cells transfected with the empty vector or STAT5a vector and MCF7/DOX cells transfected with scramble siRNA or STAT5a-targeting siRNA under treatment with the indicated concentration of DOX determined by Western blotting. ns, $p > 0.05$; * $p < 0.05$; ** $p < 0.01$; *** $p < 0.001$; **** $p < 0.0001$.



Cytotoxic Effects of Hellebrigenin and Arenobufagin Against Human Breast Cancer Cells

Yu Zhang^{1,2†}, Bo Yuan^{3†}, Baolin Bian², Haiyu Zhao², Anna Kiyomi⁴, Hideki Hayashi¹, Yui Iwatani¹, Munetoshi Sugiura⁴ and Norio Takagi^{1*}

¹ Department of Applied Biochemistry, Tokyo University of Pharmacy & Life Sciences, Hachioji, Japan, ² Institute of Chinese Materia Medica, China Academy of Chinese Medical Sciences, Beijing, China, ³ Laboratory of Pharmacology, School of Pharmacy, Faculty of Pharmaceutical Sciences, Josai University, Sakado, Japan, ⁴ Department of Drug Safety and Risk Management, Tokyo University of Pharmacy & Life Sciences, Hachioji, Japan

OPEN ACCESS

Edited by:

Maria Rosaria De Miglio,
University of Sassari, Italy

Reviewed by:

Melanie Coombs,
Acadia University, Canada
Chun Wai Mai,
International Medical University,
Malaysia
Muhammad Khan,
University of the Punjab, Pakistan

*Correspondence:

Bo Yuan
yuanbo@josai.ac.jp
Norio Takagi
takagino@toyaku.ac.jp

[†]These authors have contributed
equally to this work

Specialty section:

This article was submitted to
Breast Cancer,
a section of the journal
Frontiers in Oncology

Received: 18 May 2021

Accepted: 05 August 2021

Published: 26 August 2021

Citation:

Zhang Y, Yuan B, Bian B, Zhao H,
Kiyomi A, Hayashi H, Iwatani Y,
Sugiura M and Takagi N (2021)
Cytotoxic Effects of Hellebrigenin
and Arenobufagin Against
Human Breast Cancer Cells.
Front. Oncol. 11:711220.
doi: 10.3389/fonc.2021.711220

Development of new therapeutic strategies for breast cancer is urgently needed due to the sustained emergence of drug resistance, tumor recurrence and metastasis. To gain a novel insight into therapeutic approaches to fight against breast cancer, the cytotoxic effects of hellebrigenin (Helle) and arenobufagin (Areno) were investigated in human estrogen receptor (ER)-positive breast cancer cell line MCF-7 and triple-negative breast cancer cell line MDA-MB-231. Helle exhibited more potent cytotoxicity than Areno in both cancer cells, and MCF-7 cells were more susceptible to both drugs in comparison with MDA-MB-231 cells. Apoptotic-like morphological characteristics, along with the downregulation of the expression level of Bcl-2 and Bcl-xL and the upregulation of the expression level of Bad, were observed in Helle-treated MCF-7 cells. Helle also caused the activation of caspase-8, caspase-9, along with the cleavage of poly(ADP-ribose) polymerase in MCF-7 cells. Helle-mediated necrosis-like phenotype, as evidenced by the increased propidium iodide (PI)-positive cells was further observed. G₂/M cell cycle arrest was also induced by Helle in the cells. Upregulation of the expression level of p21 and downregulation of the expression level of cyclin D1, cyclin E1, cdc25C and survivin were observed in MCF-7 cells treated with Helle and occurred in parallel with G₂/M arrest. Autophagy was triggered in MCF-7 cells and the addition of wortmannin or 3-MA, two well-known autophagy inhibitors, slightly but significantly rescued the cells. Furthermore, similar alterations of some key molecules associated with the aforementioned biological phenomena were observed in MDA-MB-231 cells. Intriguingly, the numbers of PI-positive cells in Helle-treated MCF-7 cells were significantly reduced by wortmannin and 3-MA, respectively. In addition, Helle-triggered G₂/M arrest was significantly corrected by wortmannin, suggesting autophagy induction contributed to Helle-induced cytotoxicity of breast cancer cells by modulating necrosis and cell cycle arrest. Collectively, our results suggested potential usefulness of both Helle and Areno in developing therapeutic strategies to treat patients with different types of breast cancer, especially ER-positive breast cancer.

Keywords: breast cancer cells, hellebrigenin, arenobufagin, apoptosis, necrosis, G₂/M arrest, autophagy

INTRODUCTION

According to estimates from the World Health Organization (WHO) in 2020, female breast cancer has surpassed other cancer types as the most commonly diagnosed cancer, with an estimated 2.3 million new cases (1). Estrogen receptor (ER), progesterone receptor (PR) and human epidermal growth factor receptor-2 (HER2) are the most important prognostic and predictive markers for determining the appropriate breast cancer treatment (2, 3). Despite recent advances in early detection, diagnosis, and targeted treatment options such as Herceptin (trastuzumab), breast cancer remains a major health problem and is still the leading cause of cancer death in women worldwide (1, 2). Thus, the development of new therapeutic strategies is urgently needed for the treatment of breast cancer.

Given inseparable relationship between cancer development and inflammation, many anticancer agents have been well characterized by their anti-inflammatory and anticancer activity (4–6). Cinobufacini (also known as Huachansu), a well-known traditional Chinese medicine that comes from the dried skin of *Bufo bufo gargarizans* Cantor, has long been successfully used in clinic as anti-inflammatory and anticancer agents in China (7–9). In line with previous reports, we recently demonstrated that indolealkylamines, a kind of important hydrophilic ingredients of cinobufacini, exhibited protective effect on LPS-induced inflammation in zebrafish (10, 11). Bufadienolides are another kind of important effective constituents of cinobufacini, and we also demonstrated that active bufadienolide compounds such as gamabufotalin, hellebrigenin (Helle) and arenobufagin (Areno) exhibited selective cytotoxic effects against intractable cancer cells (12–14). Furthermore, we recently demonstrated that clinically achieved concentrations of trivalent arsenic derivative (As^{III}) combined with gamabufotalin exhibited synergistic cytotoxicity against glioblastoma cell line U-87, whereas showed much less cytotoxicity to human normal peripheral blood mononuclear cells (PBMCs) (15). These findings thus provide fundamental insight into the mechanisms underlying the anti-inflammatory and anticancer activity of cinobufacini. Although Deng et al. have demonstrated that Areno inhibits the growth of a human breast cancer cell line MCF-7 by inducing apoptosis associated with JNK signaling pathway (16), the cytotoxic effects of Helle and Areno against breast cancer cells as well as the underlying molecular mechanisms remain largely unexplored.

Apoptosis has been characterized by several morphologic features including cell shrinkage and chromatin condensation, all of which are linked to the activation of caspases and their downstream molecules such as poly(ADP-ribose) polymerase (PARP) (17, 18). The activation of caspase-8 and caspase-9 has been closely linked to two major apoptotic machinery, known as the extrinsic and intrinsic apoptotic pathway, respectively (17, 18). A series of Bcl-2 family members, including anti-apoptotic effectors such as Bcl-2/Bcl-xL, and pro-apoptotic effectors such as Bax/Bad, have been demonstrated to regulate apoptosis by modulating mitochondrial membrane permeabilization (18, 19). On the other hand, necrosis has also linked to anticancer activity of chemotherapeutic agents, and has received considerable

attention for the treatment of apoptosis-resistant cancer cells, in which apoptotic pathway is suppressed or absent (20). Cell cycle arrest has been viewed as one of major underlying mechanisms for the cytotoxicity of various anticancer drugs. Cell cycle is known to be sophisticatedly controlled by cyclin-dependent kinases (CDK) paired with their respective cyclin binding partners (CDK/Cyclin complexes) (14, 21, 22). The alteration of p21 Waf1/Cip1 (p21) and p27 Kip1 (p27), known as inhibitors for CDK/Cyclin complexes, also closely links to cell cycle arrest (21–24). Cdc25C, a member of cdc25 family, is known to be associated with cell cycle transition by modulating cdc2/Cyclin B1 (14, 25). Moreover, survivin is highly expressed in most human cancer cells and implicated in cell cycle transitions (12, 14, 26). Besides, induction of autophagic cell death has emerged as a critical mechanism underlying cytotoxic effect of various anticancer drugs (12, 14, 15). Although previous studies have demonstrated that the cytotoxicity of some bufadienolide compounds such as Helle and Areno are attributed to the induction of either of apoptosis/necrosis, cell cycle arrest and autophagy in hepatoma and glioblastoma cells (12, 27, 28), whether and how these biological phenomena contribute to the cytotoxic effects of Helle and Areno in human breast cancer cells remain to be seen.

In this study, cytotoxic effects of Helle and Areno were investigated in the human ER-positive breast cancer cell line MCF-7 and triple-negative breast cancer cell line MDA-MB-231, by focusing on growth inhibition associated with apoptosis/necrosis, cell cycle arrest and autophagic cell death. Key regulatory molecules involved in the above-mentioned biological phenomena were evaluated to further elucidate the underlying mechanisms. Wortmannin and 3-methyladenine (3-MA), two well-known autophagy inhibitors, were also employed to evaluate the correlation between autophagy and apoptosis/necrosis as well as cell cycle transition.

MATERIALS AND METHODS

Materials

Hellebrigenin (Helle) ($\geq 98\%$ purity) and arenobufagin (Areno) ($\geq 98\%$ purity) were purchased from Baoji Herbest Bio-Tech Co., Ltd. (Baoji, China). Fetal bovine serum (FBS) and HEPES were purchased from Sigma Chemical Co. (St. Louis, MO, USA). RPMI-1640 and DMEM medium, 3-methyladenine (3-MA) and wortmannin were obtained from Wako Pure Chemical Industries (Osaka, Japan). 25% glutaraldehyde solution were purchased from Kanto chemical CO., INC. (Tokyo, Japan). WST-1 and 1-Methoxy PMS were obtained from Dojindo Molecular Technologies, Inc. (Tokyo, Japan). Propidium iodide (PI), ribonuclease A (RNaseA), crystal violet (C.I. 42555) Certistain[®] were purchased from Merck KGaA (Sigma-Aldrich; Darmstadt, Germany).

Cell Culture and Treatment

Human breast cancer cell line MCF-7 and MDA-MB-231 were obtained from the American Type Culture Collection (ATCC, Manassas, VA, USA). MCF-7 and MDA-MB-231 were cultured

in RPMI-1640 and DMEM medium (high glucose) supplemented with 10% heat-inactivated FBS and antibiotics (100 U/ml of penicillin and 100 µg/ml of streptomycin (Wako Pure Chemical Industries)) in a humidified 5% CO₂ atmosphere at 37°C, respectively. In experiments using inhibitors, MCF-7 and MDA-MB-231 cells were treated with respective inhibitor at the indicated concentrations for 30 min prior to treatment with indicated concentrations of Helle, in the presence or absence of respective inhibitor for an additional 48 h. Helle and Areno were dissolved in dimethyl sulfoxide (DMSO), and no cytotoxicity of the final concentrations of DMSO (0.02%) was observed in the current experimental system.

Cell Viability and Clonogenic Survival

Following treatment for 48 h with various concentrations of Helle, cell viability was measured by the WST-1 assay as described previously (29). The relative cell viability was expressed as the ratio of the absorbance of each treatment group against those of the corresponding untreated control group. The IC₅₀ values of the drugs were calculated using GraphPad Prism[®]7 software. With respect to the morphological alterations of U-87 cells, the cells were imaged using an inverted microscope (CKX53; Olympus Corporation, Tokyo, Japan) fitted with a digital camera following treatment with various concentrations (3, 10, 30 and 100 nM) of Helle for 48 h. Clonogenic survival assays were performed according to the methods previously described with slight modifications (12, 14, 24). Briefly, MCF-7 and MDA-MB-231 cells were seeded at 2,000 cells/well in 12-well plates, and treated for 24 h with various concentrations (1, 3, 10, 30, 100, 300 and 1000 nM) of Helle and Areno, respectively. The medium was then replaced with fresh media and the cells were allowed to grow for 7–10 days in a humidified 5% CO₂ atmosphere at 37°C. Then, the cells were fixed with 0.25% glutaraldehyde/PBS for 15 min prior to staining with 0.2% crystal violet/PBS for 10 min at room temperature. Following washout of extra crystal violet with water to get an adequate staining pattern, the images of crystal violet-stained cells were scanned into a computer, followed by dissolution of the violet-stained cells in 1% SDS. The absorbance of the cell lysates was determined at 550 nm. The relative colony formation rate was expressed as the ratio of the absorbance at 550 nm of each treatment group against those of the corresponding untreated control group.

Hoechst33342/PI Double Staining Assay

The phenotypic features of cell death were evaluated by use of Hoechst33342/PI double staining assay. After treatment for 48 h with different concentrations (3, 10, 30 and 100 nM) of Helle, MCF-7 cells were washed twice with cold PBS, followed by incubation with 100 µl of staining solution (3 µl/ml of PI and 0.05% Hoechst in PBS) for 15 min at room temperature. The staining images were captured using a BZ-X800 Keyence fluorescence microscope (Keyence, Osaka, Japan) and Leica X software at 100× magnification (Leica, Tokyo, Japan).

Cell Cycle Analysis

After treatment of MCF-7 cells with various concentrations of Helle (10, 30 and 100 nM) for 48 h, cell cycle analysis was

performed using a FACS Canto[™] flow cytometer (Becton Dickinson, CA, USA) according to the methods reported previously (14, 15, 30). Briefly, cells were washed twice with cold PBS, fixed with 1% paraformaldehyde/PBS on ice for 30 min, washed twice again with cold PBS, permeabilized in 70% (v/v) cold ethanol and kept at -20°C for at least 4 h. The cell were then incubated with 0.25% Triton-X 100 for 5 min on ice. After centrifugation (430×g for 5 min at 4°C) and washing with PBS, cells were resuspended in 500 µl of PI/RNase A/PBS (5 µg/ml of PI and 0.1% RNase A in PBS) and incubated for 30 min in the dark at room temperature. A total of 10,000 events were acquired, and FACSDiva[™] software (v6.0; BD Biosciences) and ModFit LT[™] v3.0 (Verity Software House, Inc., Topsham, ME, USA) were used to calculate the number of cells at each G₀/G₁, S and G₂/M phase fraction.

Western Blot Analysis

For preparation of the protein samples, cell pellets (1–2×10⁶ cells per 110 µl buffer) were suspended in Laemmli buffer containing protease inhibitor cocktail tablets (Roche Diagnostics Co., Mannheim, Germany). Protein concentrations of the supernatant were determined according to Bradford's method using the Protein Assay Dye Reagent Concentrate (Bio-Rad Laboratories, Inc.), according to the manufacturer's instructions, using BSA as the standard. Western blot analysis was carried out according to the method previously described (14, 15). Protein bands were detected using the following primary antibodies: Mouse anti-human β-actin (cat. no. A-5441; Sigma-Aldrich; Merck KGaA, Darmstadt, Germany), mouse anti-human Bcl-2 (cat. no. 12741), rabbit anti-human Bcl-xL (cat. no. 2764), rabbit anti-human Bax (cat. no. 2772), rabbit anti-human Bad (cat. no. 9292), mouse anti-human caspase 8 (cat. no. 9746), rabbit anti-human caspase 9 (cat. no. 9502), rabbit anti-human PARP (cat. no. 9542), mouse anti-human p21 (cat. no. 2946), rabbit anti-human p27 (cat. no. 2552), rabbit anti-human cyclin B1 (cat. no. 4135), rabbit anti-human cyclin D1 (cat. no. 2978), rabbit anti-human cyclin E1 (cat. no. 20808), rabbit anti-human Cdc25c (cat. no. 4688), mouse anti-human survivin (cat. no. 2802), rabbit anti-human LC3A/B (cat. no. 12741), rabbit anti-human p-AMPK α (cat. no. 2537), rabbit anti-human AMPK α (cat. no. 2532; all from Cell Signaling Technology, Inc., Danvers, MA, USA)). Blotted protein bands were detected with respective horseradish peroxidase-conjugated secondary antibody (anti-mouse IgG, cat. no. A5906; anti-rabbit IgG, cat. no. A0545; both from Sigma-Aldrich; Merck KGaA) and an appropriate enhanced chemiluminescence (ECL) Western Blot detection kits [(ImmunoStar basic and ImmunoStar zeta (FUJIFILM Wako, Osaka, Japan) or West Femto (Pierce Biotechnology, Thermo Fisher, MA, USA)]. Relative amounts of the immunoreactive proteins obtained were subsequently quantitatively analyzed with the ImageJ software program (Rasband, W.S., ImageJ, U. S. National Institutes of Health, Bethesda, Maryland, USA, <http://rsb.info.nih.gov/ij/>).

Statistical Analysis

Experiments were independently repeated three times, and the results were shown as the means ± standard deviation (SD) of

three assays. The Student's *t*-test was used to compare sample means from two groups, and one-way ANOVA followed by Dunnett's *post hoc* test was used to compare sample means from more than three groups. A probability level of $p < 0.05$ was considered to indicate a statistically significant difference.

RESULTS

Cytotoxic Effects of Helle and Areno Against Human Breast Cancer Cell Lines MCF-7 and MDA-MB-231

A significant decrease in cell viability was observed in a dose-dependent manner in MCF-7 and MDA-MB-231 cells after treatment with various concentrations of Helle for 48 h, and its IC_{50} value was 34.9 ± 4.2 nM and 61.3 ± 9.7 nM, respectively (Figures 1B, C). A similar dose-dependent growth inhibition was also observed in both cells after treatment with various concentrations of Areno for 48 h, and its IC_{50} value was 48.5 ± 6.9 nM and 81.2 ± 10.3 nM, respectively (Figures 1B, C). These results indicated that the cytotoxicity of Helle was more potent than Areno, and that MCF-7 cells were more sensitive to the cytotoxicity of both Helle and Areno, compared to MDA-MB-231 cells.

Inhibition of Colony Formation of MCF-7 and MDA-MB-231 Cells by Helle and Areno

A colony formation assay was conducted to evaluate whether exposure to Helle and Areno suppressed the surviving fraction of MCF-7 and MDA-MB-231 cells. As shown in Figure 2, significant suppression of the colony numbers of MCF-7 and

MDA-MB-231 cells was observed after long-term treatment with Helle at concentrations starting from 30 nM and 10 nM, respectively. In comparison, an inhibitory activity against colony formation of both cells was observed in Areno even at the concentrations as low as 10 nM. These results indicated the superior potency of Helle and Areno against the survival of both MCF-7 and MDA-MB-231 cells.

Phenotypic Features of Cell Death in MCF-7 Cells Treated by Helle

Due to the potent cytotoxic effect of Helle and higher susceptibility of MCF-7 cells to the drug (Figure 1), the mechanism underlying its cytotoxicity was thus further evaluated in the cells. Following treatment for 48 h with various concentrations of Helle (3, 10, 30 and 100 nM), which were determined according to its IC_{50} value, the phenotypic features of cell death were evaluated by use of Hoechst33342/PI staining assay. As shown in Figure 3 and Supplementary Figure 1, following exposure to 10 nM Helle, a non-negligible number of MCF-7 cells showing exclusively apoptotic-like morphology, characterized by cell shrinkage, chromatin condensation as evidenced by a clear increase in the fluorescence intensity of Hoechst33342 in comparison with control group, were observed, although a clear alteration was not recognized after treatment with 3 nM Helle. Intriguingly, a small portion of PI-positive cells were observed after treatment with Helle even at the concentrations as low as 3 nM, indicating that Helle-triggered cytotoxicity was also associated with a necrosis-like phenotype in the cells. Furthermore, these phenomena associated with apoptosis and/or necrosis-like phenotype became more evident when the concentrations were greater than 30 nM.

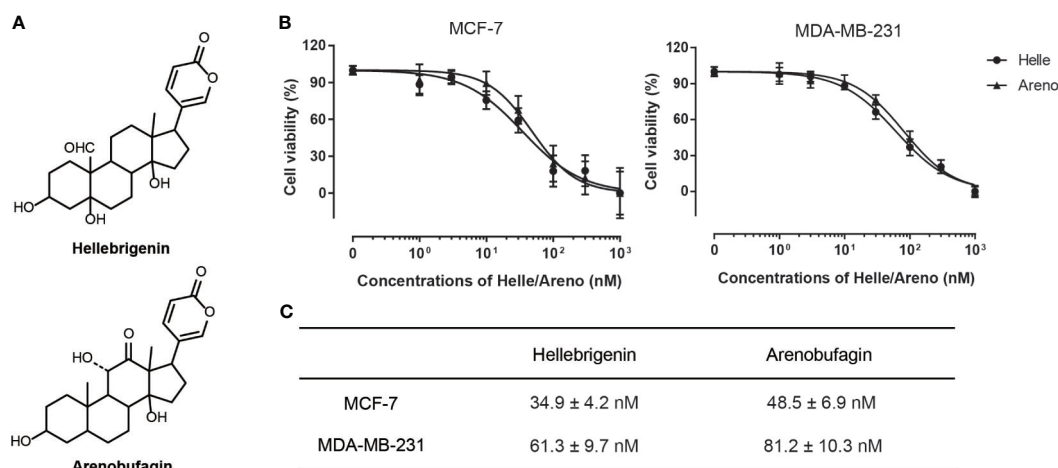


FIGURE 1 | Cytotoxic effects of Helle and Areno against human breast cancer cell lines MCF-7 and MDA-MB-231. Chemical structures of Helle and Areno (A). Cell viability was determined by WST-1 assay after treatment of MCF-7 or MDA-MB-231 (B) with various concentrations of Helle and Areno (1, 3, 10, 30, 100, 300 and 1000 nM) for 48 h. Relative cell viability was calculated as the ratio of the absorbance at 450 nm of each treatment group against those of the corresponding untreated control group. The IC_{50} values of the drugs were calculated using GraphPad Prism[®]7 software (C). Data are shown as the means \pm SD from more than three independent experiments.

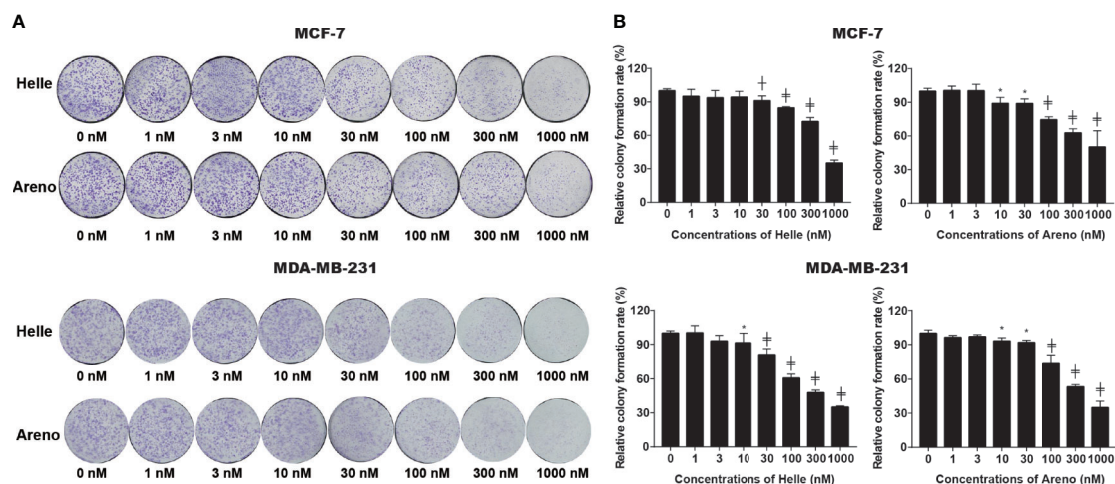


FIGURE 2 | Inhibition of colony formation of MCF-7 and MDA-MB-231 cells by Helle and Areno. The cells were seeded at 2,000 cells/well in 12-well plates following treatment with indicated concentrations (1, 3, 10, 30, 100, 300 and 1000 nM) of Helle and Areno for 24 h. Representative images of the clonogenic assays are shown from three independent experiments (A). The relative colony formation rate was expressed as the ratio of the absorbance at 550 nm of each treatment group against those of the corresponding untreated control group as described in Materials and methods (B). Data are shown as means \pm SD from three independent experiments. * $p < 0.05$; † $p < 0.01$; ‡ $p < 0.0001$ vs. control. Helle, hellebrigenin; Areno, arenobufagin.

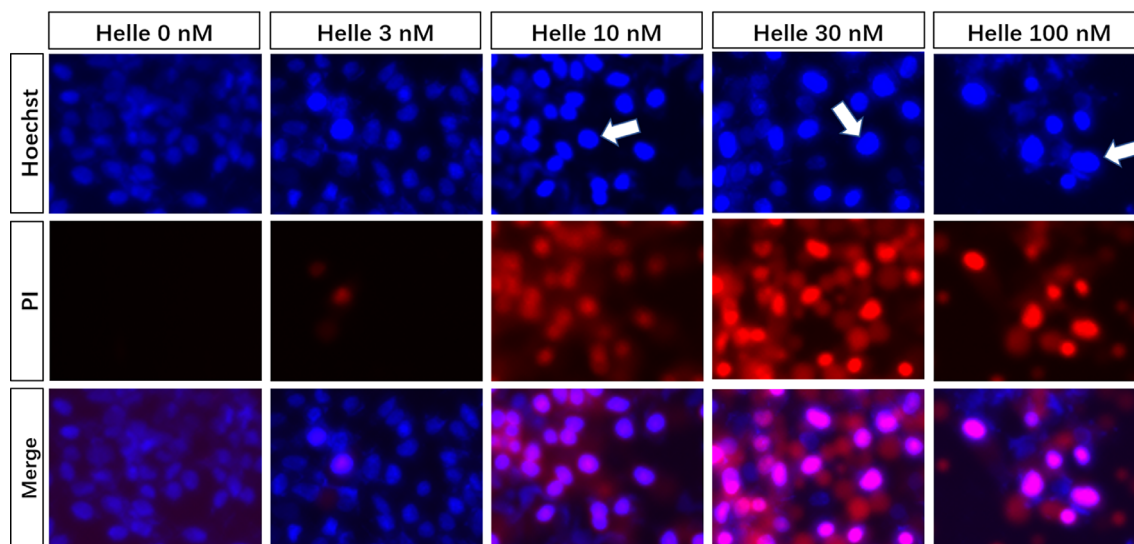


FIGURE 3 | Phenotypic features of cell death in MCF-7 cells treated by Helle. After treatment with various concentrations of Helle (3, 10, 30 and 100 nM) for 48 h, the phenotypic features of cell death were evaluated using the Hoechst 33342 (blue)/PI (red) staining as described in Materials and methods. Cells with condensed nuclei (arrows) and red fluorescence were identified as those undergoing apoptosis and necrosis, respectively. The pink fluorescence represents the merged images of Hoechst 33342 and PI. Images were captured using a BZ-X800 Keyence fluorescence microscope and Leica X software at 100 \times magnification. Helle, hellebrigenin.

Helle-Mediated Activation of Apoptosis Signaling Pathway in MCF-7 Cells

Commitment of cells to apoptosis is closely regulated by Bcl-2 (B-cell leukemia/lymphoma) family, including anti-apoptotic effectors such as Bcl-2/Bcl-xL, and pro-apoptotic effectors such as Bax/Bad (19). As shown in **Figure 4**, in comparison to control

group, a dose-dependent downregulation of the expression level of Bcl-2 and Bcl-xL was induced by Helle. Coincidentally, a dose-dependent upregulation of the expression level of Bad was observed in Helle-treated MCF-7 cells, although almost no significant alteration in the expression level of Bax was detected. At the same time, the exposure to Helle caused a significant downregulation of

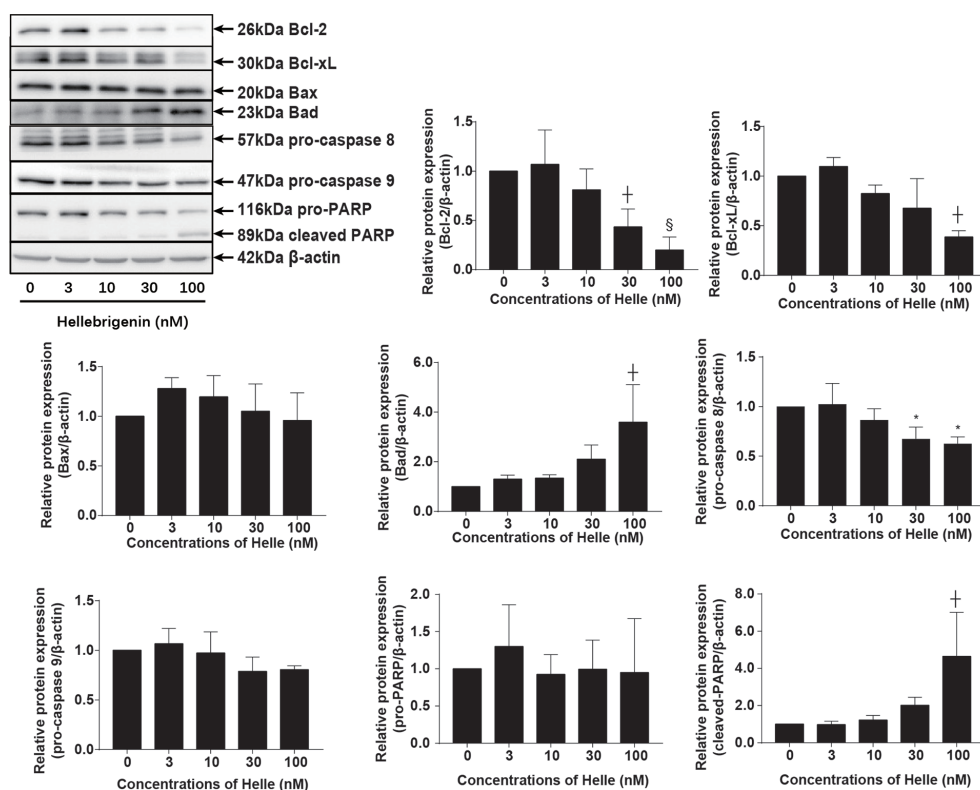


FIGURE 4 | Helle-mediated activation of apoptosis signaling pathway in MCF-7 cells. After treatment with various concentrations of Helle (3, 10, 30 and 100 nM) for 48 h, the expression profile of apoptosis-related proteins was analyzed using western blotting. The relative expression levels were expressed as the ratios between each target gene protein and β -actin protein expression levels, and compared with those of untreated control group, respectively. Data are presented as the means \pm SD from three independent experiments. * $p < 0.05$; † $p < 0.01$; § $p < 0.001$ vs. control.

the expression of pro-caspase-8, which was accompanied by a trend towards downregulation of the expression of pro-caspase-9, indicating the activation of caspase-8 and caspase-9. Furthermore, cleavage of PARP, known as an early marker of chemotherapy-induced apoptosis (31), was observed concomitantly, indicating the onset of apoptosis. In addition, similar downregulation of the expression levels of Bcl-2, Bcl-xL, as well as pro-caspase-8 and -9 was also observed in MDA-MB-231 cells treated by Helle (Supplementary Figure 2).

Effect of Helle on the Cell Cycle Profiling and the Expression Level of Cell Cycle Related-Proteins in MCF-7 Cells

To investigate whether cell cycle arrest is implicated in the cytotoxic effect of Helle, cell cycle analyses were carried out using flow cytometry following treatment with various concentrations of Helle for 48 h. As shown in Figure 5, in comparison to control group, a modest increase in the number of cells in the G_2/M phase along with a significant decrease in the number of cells in the S phase was observed in MCF-7 cells treated with Helle at the concentration starting from 30 nM. An increase in the number of cells in the G_2/M phase was further strengthened following exposure to 100 nM Helle. Concomitantly, a

significant decrease in the number of cells in G_0/G_1 and S phase was also observed. In addition, similar G_2/M arrest was also observed in MDA-MB-231 cells following treatment for 48 h with 60 nM Helle, which was almost equal to its IC_{50} value of the cells (Supplementary Figure 3).

Upregulation of p21 and p27 has been demonstrated to be involved in G_2/M arrest induced by anticancer agents in different types of cancer cells including breast cancer (23, 24, 30). As shown in Figure 6, in line with these previous reports, a significant increase in the expression level of p21 was observed in MCF-7 cells treated with Helle at the concentration starting from 10 nM, although the magnitude of increase was different according to different drug doses. Surprisingly, downregulation of the expression level of p27 was observed in the treated cells, indicating its little involvement in Helle-mediated G_2/M arrest. In addition, downregulation of the expression level of cyclin D1, cyclin E1 and cdc25C was observed in Helle-treated MCF-7 cells in a dose-dependent manner, whereas almost no alteration of cyclin B1 expression was detected. Of note, the exposure to Helle at the concentrations greater than 10 nM potentially downregulated the expression level of survivin. Furthermore, similar downregulation of the expression level of cyclin D1, cyclin E1 as well as cdc25C was observed in Helle-treated MDA-MB-231 cells (Supplementary Figure 4).

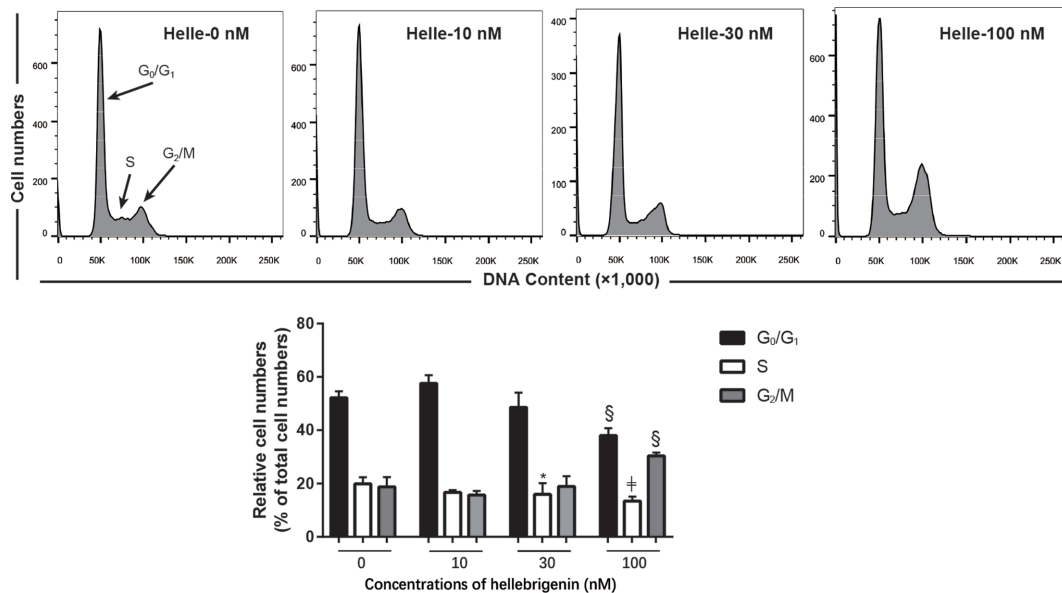


FIGURE 5 | Effect of Helle on the cell cycle profiling in MCF-7 cells. After treatment with various concentrations of Helle (10, 30 and 100 nM) for 48 h, cell cycle analysis was performed using a FACS Canto flow cytometer as described in Materials and methods. A representative FACS histogram from three independent experiments is shown. ModFit LT™ v3.0 was used to calculate the number of cells at each G₀/G₁, S and G₂/M phase fraction. Results are shown as the means ± SD from three independent experiments. **p* < 0.05; §*p* < 0.001; ‡*p* < 0.0001 vs. control. Helle, hellebrigenin.

Involvement of Autophagic Cell Death in Helle-Triggered Cytotoxicity in MCF-7 Cells

Many anticancer agents have been characterized as inducers of autophagy (14, 24, 30), and LC3 has been well known as an established autophagy marker (32, 33). As shown in **Figure 7A**, a modest upregulation of the expression level of LC3 was clearly induced by the treatment with 10 nM Helle compared to control group. Furthermore, exposure to 30 nM Helle significantly upregulated the expression level of LC3. Surprisingly, the magnitude expression level of LC3 dropped when the concentrations of Helle increased up to 100 nM. The drop might be due to the degradation of LC3, as a result of intensive cytotoxicity of 100 nM Helle, although further investigation is obviously needed. Additionally, a similar upregulation of the expression level of LC3 was also observed in MDA-MB-231 cells treated by Helle (**Supplementary Figure 5**). AMP-activated protein kinase (AMPK), a key energy sensor, has been shown to be an upstream promoter of autophagy induction (32, 34). In this regard, a dose-dependent increase in the expression level of phospho-AMPK over the endogenous level was detected in the treated cells, and a statistically significant increase in its expression was further observed in 100 nM Helle-treated cells (**Figure 7B**). Moreover, almost no change in the expression level of total AMPK expression was observed (**Figure 7B**).

Next, two well-known autophagy inhibitor, wortmannin and 3-methyladenine (3-MA) were employed to evaluated whether the induction of autophagy contributed to Helle-mediated cell

growth inhibition. Consistent with **Figure 1**, Helle-triggered dose-dependent growth inhibition was reconfirmed in MCF-7 cells (**Figures 7C, D**). In comparison with control group, the addition of wortmannin significantly abrogated the cytotoxicity of 100 nM Helle, although similar abrogation was not observed when treated with 30 nM Helle (**Figure 7C**). Moreover, the addition of 3-MA rescued the cell from Helle-triggered toxicity, as evidenced by a modest but statistically significant increase in cell viability in the presence of 3-MA, although a slight growth inhibition was induced by 3-MA itself (**Figure 7D**).

Correlation Between Autophagy and Apoptosis, Necrosis as Well as Cell Cycle Arrest in MCF-7 Cells Treated With Helle

Therapeutic effects of anticancer drugs have been attributed to the crosstalk between apoptosis, necrosis and autophagy (17, 35). Wortmannin and 3-MA were thus employed to clarify whether there was a link between autophagy and apoptosis/necrosis as well as G₂/M arrest in Helle-treated MCF-7. Consistent with **Figure 3**, apoptosis and necrosis, as evidenced by chromatin condensation and/or nuclei fragmentation, and the existence of PI-positive cells, were reconfirmed respectively in MCF-7 cells following the exposure to 30 nM Helle for 48 h (**Figure 8A**). In comparison, the numbers of PI-positive cells were significantly reduced by the addition of either wortmannin or 3-MA. On the other hand, almost no alteration was observed in the morphological changes associated with apoptosis regardless of the presence of wortmannin or 3-MA, indicating little relation

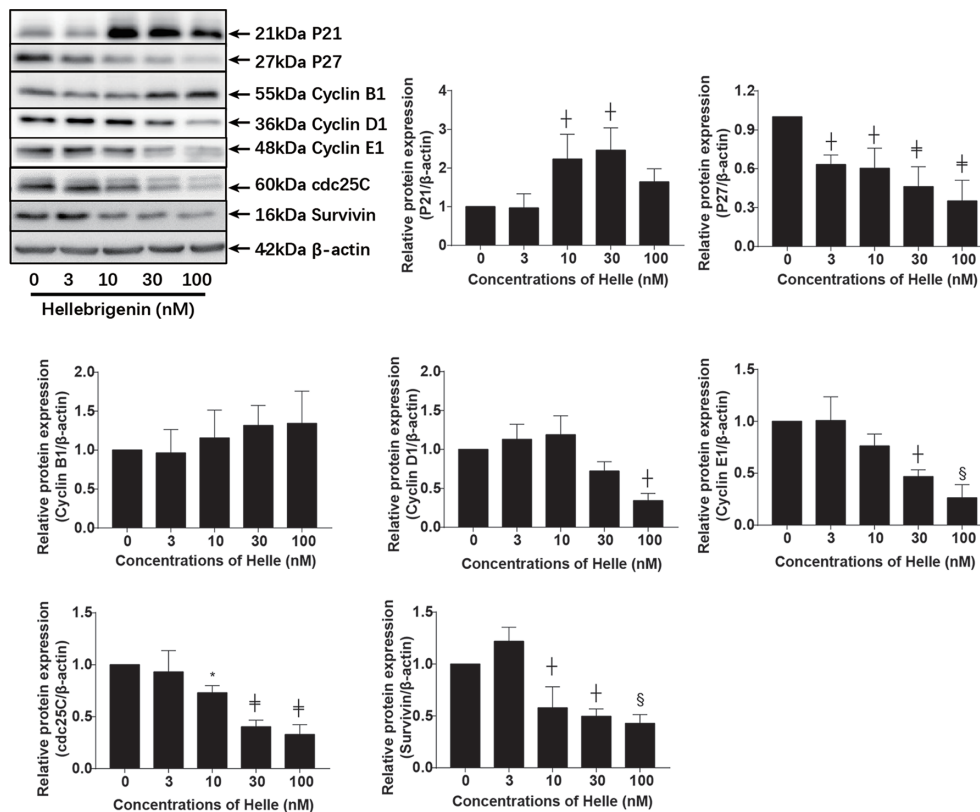


FIGURE 6 | Effect of Helle on the expression level of cell cycle related-proteins in MCF-7 cells. After treatment with various concentrations of Helle (3, 10, 30 and 100 nM) for 48 h, the expression levels of cell cycle-related proteins were analyzed by western blotting. The relative expression levels were expressed as the ratios between each target gene protein and β -actin protein expression levels, and compared with those of untreated control group, respectively. Data are presented as the means \pm SD from three independent experiments. * $p < 0.05$; $^{\dagger}p < 0.01$; $^{\S}p < 0.001$; $^{\ddagger}p < 0.0001$ vs. control.

between autophagy and apoptosis in Helle-treated MCF-7 cells. With respect to cell cycle arrest, G₂/M phase arrest was confirmed in MCF-7 cells treated by 100 nM Helle, accompanied by a significant decrease in the number of cells in G₀/G₁ and S phases (**Figure 8B** and **Supplementary Figure 6**). Again, Helle-triggered G₂/M-phase arrest was also successfully corrected by the addition of wortmannin.

DISCUSSION

Results from this study clearly demonstrated the cytotoxicity of Helle and Areno against human breast cancer cells, and further clarified that MCF-7 cells were more sensitive to the cytotoxicity of both compounds, compared to MDA-MB-231 cells. We have previously demonstrated that both Helle and Areno exhibit selective cytotoxic effects against intractable cancer cells such as glioblastoma cell line U-87 and pancreatic cancer cell line SW1990, rather than noncancerous cells including human normal PBMCs (12–14), suggesting their broad-spectrum utility across different types of cancer cells. Given a clear difference between MCF-7 and MDA-MB-231 cells in terms of

the expression level of ER (24, 30), our results further suggested potential usefulness of both Helle and Areno in developing therapeutic strategies to treat patients with different types of breast cancer, especially ER-positive breast cancer.

It has been demonstrated that high expression of steroid receptor coactivator 3 (SRC-3), known to play a critical role in mammary tumor development and metastasis (36, 37), is correlated with poor survival in ER-positive breast cancer patients (38, 39). A previous study has clarified that bufalin, one of active bufadienolide compounds with similar chemical structure with Helle and Areno, can function as a SRC-3 inhibitor by directly binding to SRC-3 in its receptor interacting domain and selectively promoting SRC-3 protein degradation in ER-positive breast cancer cell lines (40). Intriguingly, both bufalin and Areno have been demonstrated to suppress the proliferation and survival of HER2 overexpressing breast cancer cells, along with the declination of SRC-3 (41), although the effect of Helle on the expression level of SRC-3 still remains unknown. Taking these previous results and our observations into account, we thus suggest that the differential sensitivity of MCF-7 and MDA-MB-231 to both Helle and Areno could be attributed to the inhibitive effect of

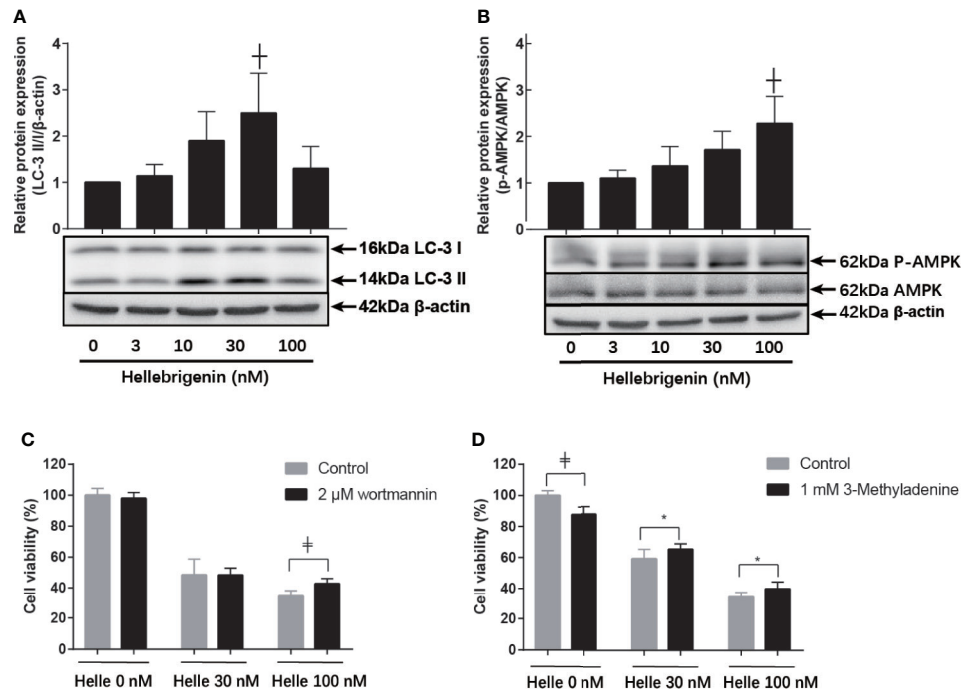


FIGURE 7 | Involvement of autophagic cell death in the cytotoxicity of MCF-7 cells treated with Helle. After treatment with various concentrations of Helle (3, 10, 30 and 100 nM) for 48 h, the expression levels of autophagy induction-related proteins were analyzed by western blotting (**A**, **B**). Cell viability was determined by WST-1 assay after treatment for 48 h with Helle at the concentrations of 30 or 100 nM in the absence or presence of 2 μM wortmannin (**C**) and 1 mM 3-MA (**D**), respectively. Data are presented as the means ± SD from three independent experiments. **p* < 0.05; †*p* < 0.01; ‡*p* < 0.0001 vs. control. Helle, hellebrigenin.

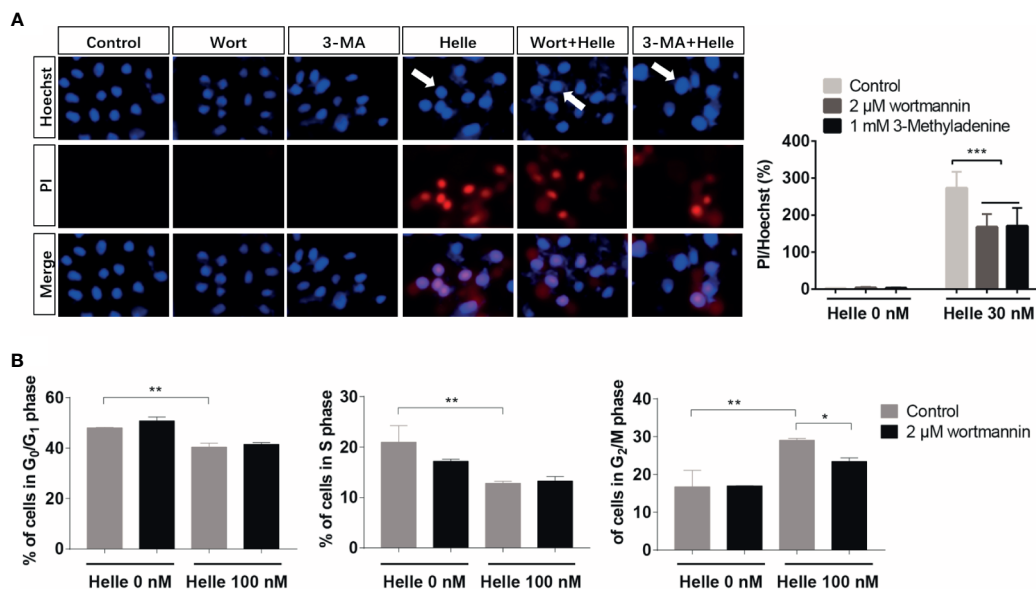


FIGURE 8 | Correlation between autophagy and apoptosis, necrosis as well as cell cycle arrest in MCF-7 cells treated with Helle. (**A**) After treatment for 48 h with 30 nM Helle in the absence or presence of 2 μM wortmannin or 1 mM 3-MA, the phenotypic features of cell death were evaluated using the Hoechst 33342 (blue)/PI (red) staining as described in Materials and methods. The pink fluorescence represents the merged images of Hoechst 33342 and PI. Images were captured using a BZ-X800 Keyence fluorescence microscope and Leica X software at 100×magnification. (**B**) After treatment for 48 h with 100 nM Helle in the absence or presence of 2 μM wortmannin, cell cycle analysis was performed by the same manner as described in the legend of Figure 5. Data are presented as the means ± SD from three independent experiments. **p* < 0.05; ***p* < 0.01; ****p* < 0.001. Helle, hellebrigenin; Wort, wortmannin.

both two compounds on SRC-3, although the alteration of the expression and activity of SRC-3 in breast cancer *in vitro* and *in vivo* obviously warrants further investigation to draw a solid conclusion.

The induction of apoptosis and/or necrosis in cancer cells has been closely linked to the cytotoxic effect of anticancer reagents including bufadienolide compounds such as Helle and Areno (12–14, 16, 27). In line with these previous reports, apoptotic-like morphological characteristics, along with the downregulation of Bcl-2 and Bcl-xL expression and the upregulation of Bad expression, were observed in MCF-7 cells treated with Helle. Similar alterations were also observed in MDA-MB-231 cells. The activation of caspase-8 and -9 as well as their downstream molecule, PARP, was further confirmed. Caspase-8 and -9 have been established as key regulators of intrinsic and extrinsic apoptosis pathway, respectively (18, 22). Collectively, we suggested that apoptosis induction *via* the activation of intrinsic/extrinsic apoptotic signaling pathway contributed to Helle-triggered cytotoxicity of breast cancer cells. Additionally, in agreement with our previous reports showing the necrosis-inducing activities of Helle against glioblastoma and pancreatic cancer cell lines (12, 13), induction of necrosis was also observed in MCF-7 cells. Given that tumor cells can evolve diverse strategies to evade apoptosis during tumor development (20, 42), the potential necrosis-inducing activities of Helle should be beneficial to treat cancer cells harboring the innate and/or adaptive resistance to apoptosis induced by anticancer reagents.

We further demonstrated that Helle-mediated G₂/M arrest was observed in not only MCF-7 but also MDA-MB-231 cells. Similarly, G₂/M arrest of hepatocellular carcinoma HepG2 cells and glioblastoma U-87 cells was also induced by Helle (12, 27), suggesting the generality of the mechanism underlying the cytotoxicity of Helle against different types of cancer cells. Furthermore, upregulation of p21 along with the downregulation of cyclin D1, cyclin E1 and cdc25C was observed in Helle-treated MCF-7 cells. Similar alterations of some aforementioned key molecules in the regulation of cell cycle were also confirmed in Helle-treated MDA-MB-231 cells. Upregulation of p21, a central player in the regulation of cell cycle, has been involved in the G₂/M arrest of various cancer cells induced by diverse anticancer agents including active bufadienolide compounds (12, 14, 22, 24, 43). In addition, previous reports have demonstrated that downregulation of cdc25C occurred in parallel with G₂/M arrest of hepatoma and glioblastoma cells induced by Helle and Areno (12, 27, 44). Downregulation of cyclin D1 and cyclin E1 has also been involved in the G₂/M arrest of prostate cancer cell lines C4-2B and DU145 induced by resveratrol combined with docetaxel (23). Moreover, an ethanol extract of a traditional Chinese medicine, *Eupolyphaga sinensis* Walker induced G₂/M arrest of a chronic myeloid leukemia cell line K562 accompanying through downregulation of cyclin D1, cyclin E1 and cdc25C (21). Besides, the fact that the suppression of survivin expression by Helle in MCF-7 cells was in good agreement with our previous report, in which Helle induced significant downregulation of survivin along with G₂/M arrest of U-87 cells (12). Of note, Li et al. have also demonstrated that silencing of survivin expression causes reduced

proliferation and G₂/M cell cycle arrest in human cancer cells, including HeLa and MCF-7 cells (26). Collectively, our results suggested that Helle triggered G₂/M arrest by modulating aforementioned key players in mitotic progression, and consequently resulted in growth inhibition of cancer cells.

A growing body of evidence has linked autophagic cell death to therapeutic efficacy of various anticancer drugs, and LC3 has been used ubiquitously as autophagy marker (14, 24, 30, 32, 33, 45). In agreement with these previous reports, we demonstrated the activation of AMPK, an upstream promoter of autophagy induction, and the upregulation of LC3 expression in MCF-7 cells treated with Helle. Our results also showed similar upregulation of LC3 expression in Helle-treated MDA-MB-231 cells. We further clarified that the addition of wortmannin and 3-MA slightly but significantly rescued MCF-7 cells. Intriguingly, natural products, which harbor anticancer properties related to their autophagy-inducing activity, have been recently demonstrated to sensitize breast cancer cells such as MDA-MB-231 cells to Taxol by inducing autophagic cell death (46, 47). Magnoflorine, a quaternary alkaloid isolated from Chinese herb, has also been demonstrated to improve the sensitivity of both MCF-7 and MDA-MB-231 cells to doxorubicin *via* inducing apoptosis and autophagy (48). Our results thus suggested that Helle could serve as a promising candidate of potent inducer of apoptosis and/or autophagic cell death, sensitizing breast cancer cells to conventional anticancer drugs such as Taxol and doxorubicin, although further studies will be needed to clarify the molecular details of Helle-triggered cytotoxicity in both cells.

The crosstalk between autophagy, necrosis and cell cycle arrest has received increasing attention to develop new therapeutic approaches for treatment of cancer patients (17, 35, 49, 50). In this regard, we demonstrated a close relation between autophagy and necrosis, as evidenced by a significant reduction of the numbers of PI-positive cells in MCF-7 cells when treated with Helle in the presence of wortmannin or 3-MA. We also demonstrated that Helle-triggered G₂/M arrest was significantly corrected by wortmannin. Taking the previous findings and our results into account, we suggested that autophagy induction contributed to Helle-induced cytotoxicity of breast cancer cells by modulating necrosis induction and cell cycle arrest. Of note, we recently clarified that autophagy induction linked to S-phase arrest, rather than apoptosis and necrosis, in MDA-MB-231 cells treated with the combination of arsenite and tetrandrine, a Chinese plant-derived alkaloid (30, 51). Collectively, whether a correlation exists between autophagy, apoptosis/necrosis and cell cycle arrest seems to be highly dependent on different types of cancer cells and external stimuli.

CONCLUSION

Our results suggest that the generality of the mechanism underlying the cytotoxicity of Helle against both breast cancer cells is linked to its apoptosis-, G₂/M arrest- and autophagy-inducing activity. We further suggest potential usefulness of both

Helle and Arenó, two active bufadienolide compounds, in developing therapeutic strategies to fight against different types of breast cancer, especially ER-positive breast cancer. In addition to apoptosis induction, autophagy appeared to contribute to the cytotoxicity of Helle by modulating both necrosis and cell cycle arrest. Combined treatment has been widely used for cancer chemotherapy, aiming to maximize efficacy of anticancer drugs and minimize their undesirable side effects. In fact, Dong et al. have demonstrated that bufadienolide compounds such as gamabufotalin and bufalin sensitize human breast cancer cells to TRAIL-induced apoptosis (52). We also recently suggested that gamabufotalin could serve as a promising adjuvant therapeutic agent to potentiate therapeutic effect of arsenite in glioblastoma cells (15). The studies on cytotoxic effects of conventional anticancer drugs in combination of Helle or Arenó are ongoing in our laboratory.

DATA AVAILABILITY STATEMENT

The original contributions presented in the study are included in the article/**Supplementary Material**. Further inquiries can be directed to the corresponding authors.

REFERENCES

1. Sung H, Ferlay J, Siegel RL, Laversanne M, Soerjomataram I, Jemal A, et al. Global Cancer Statistics 2020: GLOBOCAN Estimates of Incidence and Mortality Worldwide for 36 Cancers in 185 Countries. *CA Cancer J Clin* (2021) 71(3):209–49. doi: 10.3322/caac.21660
2. Anastasiadi Z, Lianos GD, Ignatiadou E, Harisis HV, Mitsis M. Breast Cancer in Young Women: An Overview. *Updates Surg* (2017) 69(3):313–7. doi: 10.1007/s13304-017-0424-1
3. Waks AG, Winer EP. Breast Cancer Treatment: A Review. *JAMA* (2019) 321(3):288–300. doi: 10.1001/jama.2018.19323
4. Dupre A, Malik HZ. Inflammation and Cancer: What a Surgical Oncologist Should Know. *Eur J Surg Oncol* (2018) 44(5):566–70. doi: 10.1016/j.ejso.2018.02.209
5. Greten FR, Grivennikov SI. Inflammation and Cancer: Triggers, Mechanisms, and Consequences. *Immunity* (2019) 51(1):27–41. doi: 10.1016/j.immuni.2019.06.025
6. Suarez-Carmona M, Lesage J, Cataldo D, Gilles C. EMT and Inflammation: Inseparable Actors of Cancer Progression. *Mol Oncol* (2017) 11(7):805–23. doi: 10.1002/1878-0261.12095
7. Qi J, Tan CK, Hashimi SM, Zulfiker AH, Good D, Wei MQ. Toad Glandular Secretions and Skin Extractions as Anti-Inflammatory and Anticancer Agents. *Evid Based Complement Alternat Med* (2014) 2014:312684. doi: 10.1155/2014/312684
8. Zhang X, Yuan Y, Xi Y, Xu X, Guo Q, Zheng H, et al. Cinobufacini Injection Improves the Efficacy of Chemotherapy on Advanced Stage Gastric Cancer: A Systemic Review and Meta-Analysis. *Evid Based Complement Alternat Med* (2018) 2018:7362340. doi: 10.1155/2018/7362340
9. Jiang Y, Liu LS, Shen LP, Han ZF, Jian H, Liu JX, et al. Traditional Chinese Medicine Treatment as Maintenance Therapy in Advanced Non-Small-Cell Lung Cancer: A Randomized Controlled Trial. *Complement Ther Med* (2016) 24:55–62. doi: 10.1016/j.ctim.2015.12.006
10. Zhang Y, Takagi N, Yuan B, Zhou Y, Si N, Wang H, et al. The Protection of Indolealkylamines on LPS-Induced Inflammation in Zebrafish. *J Ethnopharmacol* (2019) 243:112122. doi: 10.1016/j.jep.2019.112122
11. Zhang Y, Yuan B, Takagi N, Wang H, Zhou Y, Si N, et al. Comparative Analysis of Hydrophilic Ingredients in Toad Skin and Toad Venom Using the UHPLC-HR-MS/MS and UPLC-QqQ-MS/MS Methods Together With the

AUTHOR CONTRIBUTIONS

BY and YZ designed the study and drafted the manuscript. YZ performed the experiments. BB, HZ, AK, YI, and MS assisted interpretation of the results. HH and NT contributed analytical tools and discussed the results. All authors contributed to the article and approved the submitted version.

FUNDING

This work was partially supported by The Japan Society for the Promotion of Science (JSPS) KAKENHI Grant to BY (Grant Numbers 26460233) (Grant Numbers 17K08465). This study was also supported in part by grants from China Scholarship Council (file no. 201908110322).

SUPPLEMENTARY MATERIAL

The Supplementary Material for this article can be found online at: <https://www.frontiersin.org/articles/10.3389/fonc.2021.711220/full#supplementary-material>

- Anti-Inflammatory Evaluation of Indolealkylamines. *Molecules (Basel Switzerland)* (2018) 24(1):86. doi: 10.3390/molecules24010086
12. Han L, Yuan B, Shimada R, Hayashi H, Si N, Zhao HY, et al. Cytocidal Effects of Arenobufagin and Hellebrigenin, Two Active Bufadienolide Compounds, Against Human Glioblastoma Cell Line U-87. *Int J Oncol* (2018) 53(6):2488–502. doi: 10.3892/ijo.2018.4567
13. Yuan B, He J, Kisoh K, Hayashi H, Tanaka S, Si N, et al. Effects of Active Bufadienolide Compounds on Human Cancer Cells and CD4+CD25+Foxp3+ Regulatory T Cells in Mitogen-Activated Human Peripheral Blood Mononuclear Cells. *Oncol Rep* (2016) 36(3):1377–84. doi: 10.3892/or.2016.4946
14. Yuan B, Shimada R, Xu K, Han L, Si N, Zhao H, et al. Multiple Cytotoxic Effects of Gamabufotalin Against Human Glioblastoma Cell Line U-87. *Chem Biol Interact* (2019) 314:108849. doi: 10.1016/j.cbi.2019.108849
15. Yuan B, Xu K, Shimada R, Li J, Hayashi H, Okazaki M, et al. Cytotoxic Effects of Arsenite in Combination With Gamabufotalin Against Human Glioblastoma Cell Lines. *Front Oncol* (2021) 11:628914. doi: 10.3389/fonc.2021.628914
16. Deng LJ, Qi M, Peng QL, Chen MF, Qi Q, Zhang JY, et al. Arenobufagin Induces MCF-7 Cell Apoptosis by Promoting JNK-Mediated Multisite Phosphorylation of Yes-Associated Protein. *Cancer Cell Int* (2018) 18:209. doi: 10.1186/s12935-018-0706-9
17. Nikolettou V, Markaki M, Palikaras K, Tavernarakis N. Crosstalk Between Apoptosis, Necrosis and Autophagy. *Biochim Biophys Acta* (2013) 1833(12):3448–59. doi: 10.1016/j.bbamcr.2013.06.001
18. Su Z, Yang Z, Xu Y, Chen Y, Yu Q. Apoptosis, Autophagy, Necroptosis, and Cancer Metastasis. *Mol Cancer* (2015) 14:48. doi: 10.1186/s12943-015-0321-5
19. Czabotar PE, Lessene G, Strasser A, Adams JM. Control of Apoptosis by the BCL-2 Protein Family: Implications for Physiology and Therapy. *Nat Rev Mol Cell Biol* (2014) 15(1):49–63. doi: 10.1038/nrm3722
20. Xu Y, Lin Z, Zhao N, Zhou L, Liu F, Cichacz Z, et al. Receptor Interactive Protein Kinase 3 Promotes Cisplatin-Triggered Necrosis in Apoptosis-Resistant Esophageal Squamous Cell Carcinoma Cells. *PLoS One* (2014) 9(6):e100127. doi: 10.1371/journal.pone.0100127
21. Dai B, Zhan Y, Qi J, Zhang Y. Eupolyphaga Sinensis Walker Inhibits Human Chronic Myeloid Leukemia Cell K562 Growth by Inducing G2-M Phase Cell Cycle Arrest and Targeting EGFR Signaling Pathway and in S180 Tumor-Bearing Mice. *Environ Toxicol Pharmacol* (2014) 37(3):1177–85. doi: 10.1016/j.etap.2014.04.010

22. Yuan B, Yoshino Y, Kaise T, Toyoda H. Application of Arsenic Trioxide Therapy for Patients With Leukemia. In: H Sun, editor. *Biological Chemistry of Arsenic, Antimony and Bismuth*. Chichester: John Wiley Sons, Ltd (2010). p. 263–92.
23. Singh SK, Banerjee S, Acosta EP, Lillard JW, Singh R. Resveratrol Induces Cell Cycle Arrest and Apoptosis With Docetaxel in Prostate Cancer Cells via a p53/p21WAF1/CIP1 and p27KIP1 Pathway. *Oncotarget* (2017) 8(10):17216–28. doi: 10.18632/oncotarget.15303
24. Yao M, Yuan B, Wang X, Sato A, Sakuma K, Kaneko K, et al. Synergistic Cytotoxic Effects of Arsenite and Tetrandrine in Human Breast Cancer Cell Line MCF-7. *Int J Oncol* (2017) 51(2):587–98. doi: 10.3892/ijo.2017.4052
25. Perdiguer E, Nebreda AR. Regulation of Cdc25C Activity During the Meiotic G2/M Transition. *Cell Cycle (Georgetown Tex)* (2004) 3(6):733–7. doi: 10.4161/cc.3.6.906
26. Li Y, Liu D, Zhou Y, Li Y, Xie J, Lee RJ, et al. Silencing of Survivin Expression Leads to Reduced Proliferation and Cell Cycle Arrest in Cancer Cells. *J Cancer* (2015) 6(11):1187–94. doi: 10.7150/jca.12437
27. Deng LJ, Hu LP, Peng QL, Yang XL, Bai LL, Yiu A, et al. Hellebrigenin Induces Cell Cycle Arrest and Apoptosis in Human Hepatocellular Carcinoma HepG2 Cells Through Inhibition of Akt. *Chem Biol Interact* (2014) 219:184–94. doi: 10.1016/j.cbi.2014.06.003
28. Zhang DM, Liu JS, Deng LJ, Chen MF, Yiu A, Cao HH, et al. Arenobufagin, a Natural Bufadienolide From Toad Venom, Induces Apoptosis and Autophagy in Human Hepatocellular Carcinoma Cells Through Inhibition of PI3K/Akt/mTOR Pathway. *Carcinogenesis* (2013) 34(6):1331–42. doi: 10.1093/carcin/bgt060
29. Ishiyama M, Tominaga H, Shiga M, Sasamoto K, Ohkura Y, Ueno K. A Combined Assay of Cell Viability and *In Vitro* Cytotoxicity With a Highly Water-Soluble Tetrazolium Salt, Neutral Red and Crystal Violet. *Biol Pharm Bull* (1996) 19(11):1518–20. doi: 10.1248/bpb.19.1518
30. Yuan B, Yao M, Wang X, Sato A, Okazaki A, Komuro H, et al. Antitumor Activity of Arsenite in Combination With Tetrandrine Against Human Breast Cancer Cell Line MDA-MB-231 *In Vitro* and *In Vivo*. *Cancer Cell Int* (2018) 18:113. doi: 10.1186/s12935-018-0613-0
31. Kaufmann SH, Desnoyers S, Ottaviano Y, Davidson NE, Poirier GG. Specific Proteolytic Cleavage of Poly(ADP-Ribose) Polymerase: An Early Marker of Chemotherapy-Induced Apoptosis. *Cancer Res* (1993) 53(17):3976–85.
32. Kocaturk NM, Akkoc Y, Kig C, Bayraktar O, Gozuacik D, Kutlu O. Autophagy as a Molecular Target for Cancer Treatment. *Eur J Pharm Sci* (2019) 134:116–37. doi: 10.1016/j.ejps.2019.04.011
33. Kabeya Y, Mizushima N, Ueno T, Yamamoto A, Kirisako T, Noda T, et al. LC3, a Mammalian Homologue of Yeast Apg8p, Is Localized in Autophagosomal Membranes After Processing. *EMBO J* (2000) 19(21):5720–8. doi: 10.1093/emboj/19.21.5720
34. Chiacchiera F, Simone C. The AMPK-FoxO3A Axis as a Target for Cancer Treatment. *Cell Cycle (Georgetown Tex)* (2010) 9(6):1091–6. doi: 10.4161/cc.9.6.11035
35. Amaravadi RK, Thompson CB. The Roles of Therapy-Induced Autophagy and Necrosis in Cancer Treatment. *Clin Cancer Res* (2007) 13(24):7271–9. doi: 10.1158/1078-0432.Ccr-07-1595
36. Qin L, Liao L, Redmond A, Young L, Yuan Y, Chen H, et al. The AIB1 Oncogene Promotes Breast Cancer Metastasis by Activation of PEA3-Mediated Matrix Metalloproteinase 2 (MMP2) and MMP9 Expression. *Mol Cell Biol* (2008) 28(19):5937–50. doi: 10.1128/mcb.00579-08
37. Torres-Arzuay MI, Font de Mora J, Yuan J, Vazquez F, Bronson R, Rue M, et al. High Tumor Incidence and Activation of the PI3K/AKT Pathway in Transgenic Mice Define AIB1 as an Oncogene. *Cancer Cell* (2004) 6(3):263–74. doi: 10.1016/j.ccr.2004.06.027
38. Alkner S, Bendahl PO, Grabau D, Lövgren K, Stål O, Rydén L, et al. AIB1 Is a Predictive Factor for Tamoxifen Response in Premenopausal Women. *Ann Oncol* (2010) 21(2):238–44. doi: 10.1093/annonc/mdp293
39. Osborne CK, Bardou V, Hopp TA, Chamness GC, Hilsenbeck SG, Fuqua SA, et al. Role of the Estrogen Receptor Coactivator AIB1 (SRC-3) and HER-2/Neu in Tamoxifen Resistance in Breast Cancer. *J Natl Cancer Inst* (2003) 95(5):353–61. doi: 10.1093/jnci/95.5.353
40. Wang Y, Lonard DM, Yu Y, Chow DC, Palzkill TG, Wang J, et al. Bufalin Is a Potent Small-Molecule Inhibitor of the Steroid Receptor Coactivators SRC-3 and SRC-1. *Cancer Res* (2014) 74(5):1506–17. doi: 10.1158/0008-5472.Can-13-2939
41. Wang T, Mu L, Jin H, Zhang P, Wang Y, Ma X, et al. The Effects of Bufadienolides on HER2 Overexpressing Breast Cancer Cells. *Tumour Biol* (2016) 37(6):7155–63. doi: 10.1007/s13277-015-4381-3
42. Gong Y, Fan Z, Luo G, Yang C, Huang Q, Fan K, et al. The Role of Necroptosis in Cancer Biology and Therapy. *Mol Cancer* (2019) 18(1):100. doi: 10.1186/s12943-019-1029-8
43. Das CM, Aguilera D, Vasquez H, Prasad P, Zhang M, Wolff JE, et al. Valproic Acid Induces P21 and Topoisomerase-II (Alpha/Beta) Expression and Synergistically Enhances Etoposide Cytotoxicity in Human Glioblastoma Cell Lines. *J Neurooncol* (2007) 85(2):159–70. doi: 10.1007/s11060-007-9402-7
44. Deng LJ, Peng QL, Wang LH, Xu J, Liu JS, Li YJ, et al. Arenobufagin Intercalates With DNA Leading to G2 Cell Cycle Arrest via ATM/ATR Pathway. *Oncotarget* (2015) 6(33):34258–75. doi: 10.18632/oncotarget.5545
45. Tanida I, Ueno T, Kominami E. LC3 and Autophagy. *Methods Mol Biol (Clifton NJ)* (2008) 445:77–88. doi: 10.1007/978-1-59745-157-4_4
46. Lee Y, Na J, Lee MS, Cha EY, Sul JY, Park JB, et al. Combination of Pristimerin and Paclitaxel Additively Induces Autophagy in Human Breast Cancer Cells via ERK1/2 Regulation. *Mol Med Rep* (2018) 18(5):4281–8. doi: 10.3892/mmr.2018.9488
47. Li T, Zhang S, Chen F, Hu J, Yuan S, Li C, et al. Formononetin Ameliorates the Drug Resistance of Taxol Resistant Triple Negative Breast Cancer by Inhibiting Autophagy. *Am J Trans Res* (2021) 13(2):497–514.
48. Wei T, Xiaojun X, Peilong C. Magnoflorine Improves Sensitivity to Doxorubicin (DOX) of Breast Cancer Cells via Inducing Apoptosis and Autophagy Through AKT/mTOR and P38 Signaling Pathways. *BioMed Pharmacother* (2020) 121:109139. doi: 10.1016/j.biopha.2019.109139
49. Mathiasen SG, De Zio D, Cecconi F. Autophagy and the Cell Cycle: A Complex Landscape. *Front Oncol* (2017) 7:51. doi: 10.3389/fonc.2017.00051
50. Zheng K, He Z, Kitazato K, Wang Y. Selective Autophagy Regulates Cell Cycle in Cancer Therapy. *Theranostics* (2019) 9(1):104–25. doi: 10.7150/thno.30308
51. Yu B, Yuan B, Li J, Kiyomi A, Kikuchi H, Hayashi H, et al. JNK and Autophagy Independently Contributed to Cytotoxicity of Arsenite Combined With Tetrandrine via Modulating Cell Cycle Progression in Human Breast Cancer Cells. *Front Pharmacol* (2020) 11:1087. doi: 10.3389/fphar.2020.01087
52. Dong Y, Yin S, Li J, Jiang C, Ye M, Hu H. Bufadienolide Compounds Sensitize Human Breast Cancer Cells to TRAIL-Induced Apoptosis via Inhibition of STAT3/Mcl-1 Pathway. *Apoptosis* (2011) 16(4):394–403. doi: 10.1007/s10495-011-0573-5

Conflict of Interest: The authors declare that the research was conducted in the absence of any commercial or financial relationships that could be construed as a potential conflict of interest.

Publisher's Note: All claims expressed in this article are solely those of the authors and do not necessarily represent those of their affiliated organizations, or those of the publisher, the editors and the reviewers. Any product that may be evaluated in this article, or claim that may be made by its manufacturer, is not guaranteed or endorsed by the publisher.

Copyright © 2021 Zhang, Yuan, Bian, Zhao, Kiyomi, Hayashi, Iwatani, Sugiura and Takagi. This is an open-access article distributed under the terms of the Creative Commons Attribution License (CC BY). The use, distribution or reproduction in other forums is permitted, provided the original author(s) and the copyright owner(s) are credited and that the original publication in this journal is cited, in accordance with accepted academic practice. No use, distribution or reproduction is permitted which does not comply with these terms.



The Role of Non-Coding RNAs in Breast Cancer Drug Resistance

Jin-hai Tian^{1,2†}, Shi-hai Liu^{3†}, Chuan-yang Yu^{1,2}, Li-gang Wu^{4*} and Li-bin Wang^{1,2*}

¹ The Biochip Research Center, General Hospital of Ningxia Medical University, Yinchuan, China, ² The Clinical Medicine College of Ningxia Medical University, Yinchuan, China, ³ Medical Research Center, The Affiliated Hospital of Qingdao University, Qingdao, China, ⁴ Department of Oncology, General Hospital of Ningxia Medical University, Yinchuan, China

OPEN ACCESS

Edited by:

Maria Rosaria De Miglio,
University of Sassari, Italy

Reviewed by:

Yizi Cong,
Yantai Yuhuangding Hospital, China
Alessandra Gennari,
Università del Piemonte Orientale, Italy

*Correspondence:

Li-bin Wang
wanglibin007@126.com
Li-gang Wu
wuligang654321@163.com

[†]These authors have contributed
equally to this work

Specialty section:

This article was submitted to
Breast Cancer,
a section of the journal
Frontiers in Oncology

Received: 29 April 2021

Accepted: 17 August 2021

Published: 13 September 2021

Citation:

Tian J-h, Liu S-h, Yu C-y, Wu L-g and
Wang L-b (2021) The Role of
Non-Coding RNAs in Breast
Cancer Drug Resistance.
Front. Oncol. 11:702082.
doi: 10.3389/fonc.2021.702082

Breast cancer (BC) is one of the commonly occurring malignancies in females worldwide. Despite significant advances in therapeutics, the mortality and morbidity of BC still lead to low survival and poor prognosis due to the drug resistance. There are certain chemotherapeutic, endocrine, and target medicines often used for BC patients, including anthracyclines, taxanes, docetaxel, cisplatin, and fluorouracil. The drug resistance mechanisms of these medicines are complicated and have not been fully elucidated. It was reported that non-coding RNAs (ncRNAs), such as micro RNAs (miRNA), long-chain non-coding RNAs (lncRNAs), and circular RNAs (circRNAs) performed key roles in regulating tumor development and mediating therapy resistance. However, the mechanism of these ncRNAs in BC chemotherapeutic, endocrine, and targeted drug resistance was different. This review aims to reveal the mechanism and potential functions of ncRNAs in BC drug resistance and to highlight the ncRNAs as a novel target for achieving improved treatment outcomes for BC patients.

Keywords: breast cancer, drug resistance, non-coding RNA, micro RNA, long-chain non-coding RNA

INTRODUCTION

Breast cancer (BC), a complicated and heterogeneous disease which has high metastasis and recurrence rate, is a diverse hormone-dependent malignancy carcinoma and is leading in cancer mortality and morbidity globally. More than 20 million BC patients are newly diagnosed in women worldwide (1). Because of the heterogeneity of BC, drug resistance has become one of the major challenges. Although certain advances in research have been applied, the drug resistance of BC is still responsible for the poor prognosis and quite low survival (2). There are certain chemotherapeutic, endocrine, and targeted drugs available which have significantly improved the life quality and overall survival of patients, including anthracyclines, taxanes, cisplatin, and fluorouracil. For these therapeutic drugs, the mechanisms of drug resistance are complicated and have not been fully elucidated.

Non-coding RNAs (ncRNAs), including microRNAs (miRNAs), long-chain non-coding RNAs (lncRNAs), piRNAs, and circle RNAs (circRNAs), a group of RNAs which lack protein-coding regions, only account for about 1% of total genome RNA (3). Although these ncRNAs are less abundant, they exhibited essential performance in transcription, posttranscription, translation, and regulation of cellular processes and signaling pathways in the development and pathology of

different cancer cells (4, 5). Besides, ncRNAs also have a significant influence on the exon gene coding *via* a different mechanism. The ability of ncRNAs to control gene expression makes them as targets or the key regulating genes for the tumor drug resistance (6).

Previous research reported that ncRNAs have the ability to modulate the sensitivity of cancer cell therapy. This ability contributed to the cancer cell drug resistance acquisition. This review summarizes the possible roles of ncRNAs in drug resistance following different mechanisms, highlighting the therapeutic and diagnostic application of ncRNAs for overcoming the BC resistance.

NCRNAS AND ANTHRACYCLINE CHEMORESISTANCE

Anthracyclines are a group of antibiotics that are among the most active chemotherapeutic agents. The commonly used anthracycline antibiotics include doxorubicin, daunorubicin, and epirubicin (7). Anthracyclines exhibited a critical role in treating BC and can be used at all BC stages (8). Unfortunately, these agents also exhibited a well-recognized cardiotoxic profile that limits its clinical application (9). Several studies reported the mechanism of the chemoresistance of anthracycline and showed that ncRNAs exhibited high possibility in regulating BC resistance.

miRNA and Anthracycline Chemoresistance

Chen et al. (10) found that the expression of miR-200c was related to doxorubicin-resistant BC. Upregulation of miR-200c could improve the epirubicin chemoselectivity and is also capable of decreasing the expression of P-glycoprotein (P-gp) and multidrug resistance mRNA in the human MCF-7/ADR cell line. Kopp et al. (11) found that decreased miR-200c expression in doxorubicin-resistant epithelial BC cell line BT474 could make the cells display the mesenchymal cell characteristics. Inhibition and overexpression miR-200c in the cells enhanced its resistance to doxorubicin treatment. Li et al. (12) and Park et al. (13) reported that miR-34a was down-expressed in MCF-7/ADR cells as compared to MCF-7 cells. Overexpression of miR-34a could increase the sensitivity of MCF-7/ADR cells to doxorubicin treatment by targeting NOTCH1. Zheng et al. (14) found that miR-181b performed the function of oncogenes during the development of BC and chemoresistance. Zhao et al. (15) found that downregulation of the miR-302S family genes miR-302d, miR-302c, miR-302b, and miR-302a could increase P-gp expression and enhance the chemoresistance of MCF-7/ADR cells. The enhanced expression of miR-302 facilitated the ADM agglomeration at extracellular and increased the sensitivity of BC cells for ADM. Spindlin1 (SPIN1) is an extremely expressed protein in various cancer types and is also associated with tumor development and genesis. Chen et al. (16) found that SPIN1 was a novel target of the miR-148/152 family; upregulation of miR-148/152 inhibited the SPIN1 expression and induced UGT2B4,

CYP2C8, UGT2B17, and ABCB4 increase. The increase of UGT2B4, CYP2C8, UGT2B17, and ABCB4 is thereby involved in drug metabolism and transport along with enhancement in ADM resistance in BC. Hu et al. (17) reported the abrupt expression of ABCC4 and miR-124-3p in BC and MCF-7/ADR cells. After inhibiting the expression of ABCC4 and miR-124-3p, the sensitivity of the cells toward ADM was significantly increased. Doxorubicin was located in the cytoplasm rather than the nuclei of resistant cells due to the increased nuclear expression of MDR1/P-gp. Bao et al. (18) found that overexpression of miR-298 could inhibit P-gp and increase the P-gp nuclear accumulation and cytotoxicity in doxorubicin-resistant BC cells. The results suggested that miR-298 directly affects P-gp expression and influenced metastatic BC chemoresistance. Shen et al. (19) reported that miR-29a could play an important role in ADM resistance by inhibiting the PTEN/AKT/GSK3 β signaling pathway in BC cells.

Miao et al. (20) revealed that miR-130b induced BC cell chemoresistance and promoted its proliferation through targeting PTEN and PI3K/Akt signaling pathway. Besides, the Wang group showed that miR-222 was capable of decreasing the sensitivity of BC cells to ADM through the PTEN/Akt/p27kip1 signaling pathway (21). The major cause of chemoresistance in BC was the overexpression of multidrug resistance-associated protein 1 (MRP1). Gao et al. (22) found that miR-145 could directly target MRP1 3'-untranslated regions and suppression of MRP1 expression. Overexpression of miR-145 could inhibit MRP1 expression and improve the extracellular doxorubicin accumulation. Jiang et al. (23) illustrated that the EMT-related chemoresistance in BC cells was mediated by miR-489. In their report, the EMT features and chemoresistance of ADM resistance cells (MCF-7/ADM) were reversed by overexpression of miR-489 through targeting Smad3. Meanwhile, Hu et al. (24) observed that overexpression of miR-760 increased the sensitivity of BC cells for certain anticancer agents *via* improved EMT transfer. The results proved that miR-760 was capable of modulating the chemoresistance of BC cells through EMT. Zhang et al. (25) explored the role of miRNA-192-5p in doxorubicin-resistant BC cells. They found that miR-192-5p overexpression was capable of activating JNK, augmenting Bad and caspase9, and suppressing the expression of Bcl-2 and PPIA. Zhao et al. (26) reported the correlation between miR-221 expression and the status of the hormone receptor (HR). In the research, they found that the patients with an increased miR-221 level in the plasma were considered to be HR-negative, and miR-221 can be a biomarker for evaluating the sensitivity of BC patients who previously received neoadjuvant chemotherapy.

LncRNAs in Anthracycline Chemoresistance

LncRNAs comprise a group of over 200 nucleotides containing non-coding RNA molecules, while microRNAs include almost 21 nucleotides containing non-coding regulatory transcripts. It was reported that LncRNAs are involved in various drug resistance- and carcinogenesis-related genomics and cellular processes. The significance of LncRNAs was also discussed in the BC resistance against multiple drugs. For example, the

expression of lnc00518 and multidrug resistance protein 1 (MRP1) was observed in MDR breast cells (MCF-7/ADR) compared with the normal MCF-7 line (27). lnc00518 was capable of reducing the apoptosis through inhibiting the miR-199a/MRP1 axis and increasing the resistance of MCF-7/ADR cells to VCR and ADM. Liang et al. (28) suggested that overexpression of lncLINP1 was positively related to the proliferation, chemoresistance, and metastasis of BC cells. Knockdown of LINP1 promoted BC cell metastasis and increased its resistance to 5-Fu by decreasing the effects of P53. Yao et al. (29) found that lncRNA NONHSAT101069 acted as ceRNA with miR-129-5p and targeted Twist1 in BC cells. The expression of lncRNA NONHSAT101069 promoted the resistance of BC cells to epirubicin and induced the cell EMT and migration process through the lncRNA NONHSAT101069/miR-129-5p/Twist1 axis. Gooding et al. (30) reported that lncRNABORG promoted the triple-negative BC (TNBC) cell chemoresistance to doxorubicin by activating the NF- κ B signaling pathway. Chen et al. (31) found that lncRNAGAS5 significantly reversed the BC cell drug resistance by suppressing the Wnt/ β -catenin signaling pathway through the miR-221-3p/DKK2 axis (Table 1, Supplement Figure 1).

NCRNA AND TAMOXIFEN RESISTANCE

Tamoxifen is the most commonly used chemotherapeutic agent in the treatment of BC, specifically the estrogen receptor (ER)-positive BC subtype (32). Tamoxifen is considered a pioneering drug due to its ubiquitous use, cost-effectiveness, lifesaving properties, and being devoid of major side effects in the majority of BC patients (33). The ER-positive BC accounted for more than 70% of all breast cancers (34). However, ER-positive patients with metastatic disease poorly responded to tamoxifen therapy, and often with increased dose- and time-developed resistance to tamoxifen (35). For most ER-positive/

progesterone receptor (PR)-negative BC subtypes, the 5-year survival was still quite low (~20%) (36). The increased intrinsic and extrinsic factors are also responsible for the resistance toward chemotherapy in BC cells (37). It is quite urgent to better understand the mechanism of tamoxifen resistance and developed new therapies for BC.

miRNAs in Tamoxifen Resistance

Tamoxifen is often used for ER-positive BC treatment. However, the tumor cells could develop resistance to tamoxifen and limit its application. Gene regulation by miRNAs often leads to activation or dysregulation of various pathways responsible for the development of drug resistance (38). Different miRNAs have been reported to be potential indicators for drug sensitivity in BC cell lines (39). Many miRNAs associated with tamoxifen resistance have been identified and offer new targets for BC therapy (40). Gao et al. (41) reported that the decrease of miR-200b and miR-200c reduced the expression of c-MYB and therefore elevated EMT marker vimentin and ZEB1/2 in tamoxifen-resistant ER-positive MCF-7 cells. Epireregulin (EREG), an EGFR agonist, plays a vital role in enhancing the process of glycolysis by activation of EGFR signaling and its downstream glycolytic genes in tamoxifen-resistant BC cells (42, 43). He et al. (44) found that in tamoxifen-resistant BC cells, EREG as a target of miR-186-3p and miR-186-3p is involved in BC cell resistance to tamoxifen. In HER2-positive tamoxifen-resistant primary human breast tumors, miR-221 and miR-222 directly targeted p27Kip1 and are responsible for increasing cell apoptosis upon exposure with tamoxifen (45). Li et al. (46) reported that miR-449a performed its function by targeting ADAM22 and took part in the underlying mechanism of tamoxifen resistance in BC. Another research reported that overexpression of miR-451a promoted the sensitivity of tamoxifen in BC by regulating the macrophage migration inhibitory factor and 14-3-3 ζ ER α (47, 48). Ye et al. (49) examined the differential miRNA expression profiles between

TABLE 1 | Breast cancer anthracycline chemoresistance-related ncRNAs.

ncRNA	Drugs	Function	Targets/mechanisms	References
miR-200c	Doxorubicin	Sensitivity	Inhibition P-gp	Chen et al. (10) and Kopp et al. (11)
miR-34a	Adriamycin	Sensitivity	Inhibition Notch1	Li et al. (12) and Park et al. (13)
miR-302a/b/c/d	Adriamycin	Sensitivity	Activation P-gp MAPK/ERK	Zhao et al. (15)
miR-148/152	Adriamycin	Resistance	Inhibition SPIN1	Chen et al. (16)
miR-124-3p	Adriamycin	Sensitivity	Inhibition ABCG4	Hu et al. (17)
miR-298	Adriamycin	Resistance	Inhibition P-gp	Bao et al. (18)
miR-29a	Adriamycin	Resistance	Inhibition PTEN/AKT/GSK3 β	Shen et al. (19)
miR-130b	Adriamycin	Resistance	Inhibition PI3K/AKT	Miao et al. (20)
miR-222	Adriamycin	Resistance	Inhibition PTEN/AKT/p27 ^{KIP1}	Wang et al. (21)
miR-145	Doxorubicin	Sensitivity	Inhibition MRP1	Gao et al. (22)
miR-489	Adriamycin	Sensitivity	Inhibition EMT/Smad3	Jiang et al. (23)
miR-760	Doxorubicin	Resistance	Inhibition EMT/Nanog	Hu et al. (24)
miR-192-5p	Doxorubicin	Sensitivity	Activation JNK/Bad/Caspase9, inhibition Bcl-2/PPIA	Zhang et al. (25)
miR-221	Adriamycin	Sensitivity	Inhibition hormone receptor(HR)	Zhao et al. (26)
LncRNA-00518	Adriamycin	Resistance	Inhibition miR-199a/MRP1 axis	Chang et al. (27)
LncRNA-LINP1	Doxorubicin	Resistance	Inhibition P53	Liang et al. (28)
LncRNA-NONHSAT101069	Epirubicin	Resistance	Inhibition miR-129-5p/Twist1/EMT	Yao et al. (29)
LncRNA-BORG	Doxorubicin	Resistance	Activation NF- κ B signaling pathway	Gooding et al. (30)
LncRNA-GAS5	Adriamycin	Resistance	Inhibition Wnt/ β -Catenin	Chen et al. (31)

tamoxifen-resistant (MCF-7C and MCF-7T) and tamoxifen-sensitive (MCF-7) BC cell lines and showed that miR-21, miR-27a, miR-146a, miR-148a, and miR-34a performed a major role in tamoxifen resistance in BC.

LncRNAs in Tamoxifen Resistance

Approximately 70% of BC patients have luminal A/ER-positive (ER+) BC which consists of genes with low proliferation rates and low levels of HER2 (50). A previous study showed that several lncRNAs demonstrated important roles in tamoxifen resistance (51). Li et al. (52) revealed that long non-coding RNA UCA1 conferred tamoxifen resistance in BC endocrine therapy through activation of the EZH2/p21 axis and the PI3K/AKT signaling pathway. Liu et al. (53) reported that lncRNA CYTOR has the function of promoting tamoxifen resistance in BC cells *via* sponging miR-125a-5p. Xue et al. (54) observed that lncRNA HOTAIR was upregulated in tamoxifen-resistant breast cancer tissues compared to their primary counterparts. Overexpression of HOTAIR increased the proliferation BC cells and enhanced their tamoxifen resistance. Ma et al. (55) determined that the expression of lncRNA LINP1 (non-homologous end joining pathway 1) was increased in tamoxifen-resistant BC cells. Knockdown of lncRNA LINP1 significantly attenuated the tamoxifen resistance *in vitro* and *in vivo*. lncRNA HOTAIRM1 has been proved to be involved in myelopoiesis as well as transcription regulation of HOXA genes in embryonic stem cells. In BC cells, lncRNA HOTAIRM1 and HOXA1 are upregulated in tamoxifen-resistant MCF7 (TAMR) cells, and the knockdown of lncRNA HOTAIRM1 downregulated the HOXA1 expression and restored the sensitivity to tamoxifen (56). Cyclin D1 is one of the most important cancer proteins that drive cancer cell proliferation and associate with tamoxifen resistance in BC. Shi et al. (57) proved that lncRNA DILA1 inhibits Cyclin D1 degradation and contributes to tamoxifen resistance in breast cancer. Qu et al. (58) reported that lncRNA BLACAT1 was significantly upregulated in tamoxifen-resistant BC cells MCF-7/TR and T47D/TR, and knockdown of lncRNA BLACAT1 reduced the tamoxifen resistance in the cells. Further study revealed that lncRNA BLACAT1 induced tamoxifen resistance through regulating the miR-503/Bcl-2 axis in BC. Ma et al. (59) reported that lncRNA DSCAM-AS1 enhanced BC cell tamoxifen resistance through acting as a sponge of miR-137. Xu et al. (60) found that tamoxifen-resistant BC cell-derived exosomes contain lncRNA urothelial cancer-associated 1 (UCA1), and the expression of lncRNA UCA1 increased tamoxifen resistance in BC. lncRNA UCA1 was also found to be involved in causing tamoxifen resistance in BC cell lines MCF7 and T47D by activating the Wnt/ β -Catenin signaling pathway (61) and mTOR signaling pathway (62). Shi et al. (63) identified that lncRNA ADAMTS9-AS2 has a lower expression in BC tissues and tamoxifen-resistant BC cells. A low expression of lncRNA ADAMTS9-AS2 inhibited PTEN expression and enhanced tamoxifen resistance through targeting miRNA-130a-5p. Zhang et al. (64) revealed that downregulation of lncRNA ROR inhibited the BC cell EMT and enhanced the cell sensibility to tamoxifen through increasing miR-205 expression.

CircRNAs in Tamoxifen Resistance

CircRNAs are a group of ncRNAs which contributed to the gene regulation by competing the combination with endogenous RNA (ceRNA) mechanisms (65). CircRNAs often serve as transcription regulators, acting as microRNA sponges and expressing peptides under rare circumstances and sequestering RNA-binding proteins (RBPs) (66). Sang et al. (67) found that the expression of hsa_circ_0025202 enhanced tamoxifen efficacy and inhibited the progression of BC cells *via* regulating the miR-182-5p/FOXO3a axis. Liang et al. (68) reported that knockdown of CircBMP2 promoted tamoxifen resistance and inhibited apoptosis of BC cells *via* the circBMP2/miR-553/USP4 axis. Hu et al. (69) showed that circ_UBE2D2 isolated from exosomes enhanced the resistance of BC cells to tamoxifen by binding to miR-200a-3p. Uhr et al. (70) revealed that miR-7 is connected with tamoxifen treatment outcomes in an adjuvant hormone-naïve cohort, and circRNA CDR1-AS regulated miR-7 function in BC. However, circRNA CDR1-AS has negative relevant outcomes in the cohort (Table 2, Supplement Figure 2).

ncRNAs AND TAXANE RESISTANCE

Taxanes are an important class of antineoplastic agents often used for treatment of a wide variety of cancers. Paclitaxel and docetaxel are the most commonly used taxanes, which elicit immediate hypersensitivity reactions (HSRs) in 5% to 10% of patients (71). Almost all patients that experience HSRs can be safely reexposed to taxanes. Taxanes not only strengthen BC treatment but also are capable of developing resistance following mortality and metastatic disease (72). Taxanes are cytotoxic because they inhibit the depolymerization of tubulin microtubules and affect the process of mitosis in the M or G1 phase. Furthermore, it is also reported that the antineoplastic activity of taxanes is significantly involved in certain biological processes including angiogenesis, apoptosis, cell motility, invasiveness, and metalloproteinase production (73). Triple-negative breast cancer (TNBC) is a heterogeneous disease with various prognoses and chemosensitivity profiles, and the standard therapy includes the mainstay treatment with anthracyclines and taxanes (74). Although there have been many studies for exploring the cause of taxane resistance in BC, the mechanism of the process is still unknown. ncRNAs could regulate the expression of drug resistance gene and thereby influence the BC cell progression and development of chemotherapy resistance (75).

ncRNAs in Paclitaxel Resistance

miRNAs in Paclitaxel Resistance

Various miRNAs have been reported to be related to different cancers (76). In BC cells, Lin28/let-7 is related to paclitaxel resistance and the Lin28 miRNA level is intensely improved in tissues of tumors following neoadjuvant chemotherapy (77). Lin28 has conferred specified cancer stem cells to BC cells and help the cells to gain the properties of “stemness” so that they can escape from the effect of chemotherapy. Overexpression of Lin28

TABLE 2 | Breast cancer tamoxifen chemoresistance-related ncRNAs.

ncRNA	Drugs	Function	Targets/mechanisms	References
miR-200b/c	Tamoxifen	Sensitivity	Activation of vimentin/ZEB/EMT	Gao et al. (41)
miR-186-3p	Tamoxifen	Resistance	Activation of EREG/EGFR	He et al. (44)
miR-221/222	Tamoxifen	Resistance	Inhibition of p27 ^{Kip1}	Miller et al. (45)
miR-449a	Tamoxifen	Sensitivity	Inhibition of ADAM22	Li et al. (46)
miR-451a	Tamoxifen	Sensitivity	Inhibition of MIF	Liu and Liu et al. (47, 48)
lncRNA-UCA1	Tamoxifen	Resistance	Activation of PI3K/AKT	Li et al. (52)
lncRNA-CYTOR	Tamoxifen	Resistance	Activation of SRF and Hippo signaling pathway	Liu et al. (53)
lncRNA-HOTAIR	Tamoxifen	Resistance	Activation of ER signaling	Xue et al. (54)
lncRNA-LINP1	Tamoxifen	Sensitivity	Inhibition of ER and EMT	Ma et al. (55)
lncRNA-HOTAIRM1	Tamoxifen	Resistance	Inhibition of HOXA1	Kim et al. (56)
lncRNA-DILA1	Tamoxifen	Sensitivity	Inhibition of Cyclin D1	Shi et al. (57)
lncRNA-BLACAT1	Tamoxifen	Resistance	Activation of miR-503/Bcl-2 axis	Qu et al. (58)
lncRNA-DSCAM-AS1	Tamoxifen	Resistance	Activation of EPS8	Ma et al. (59)
lncRNA-UCA1	Tamoxifen	Resistance		Xu et al. (60)
lncRNA-UCA1	Tamoxifen	Resistance	Activation of Wnt/beta-Catenin signaling pathway	Liu et al. (61)
lncRNA-UCA1	Tamoxifen	Resistance	Inhibition of mTOR signaling pathway	Wu et al. (62)
lncRNA-ADAMTS9-AS2	Tamoxifen	Sensitivity	Inhibition of PTEN	Shi et al. (63)
lncRNA-ROR	Tamoxifen	Resistance	Inhibition of EMT	Zhang et al. (64)
circRNA-0025202	Tamoxifen	Sensitivity	Inhibition of FOXA3a	Sang et al. (67)
circRNA-BMPR2	Tamoxifen	Sensitivity	Inhibition of the miR-553/USP4 axis	Liang et al. (68)
circRNA-UBE2D2	Tamoxifen	Resistance	Inhibited of miR-200a-3p	Hu et al. (69)
circRNA-CDR1-AS	Tamoxifen	Resistance	Inhibition of hsa-miR-7	Uhr et al. (70)

is capable of inducing Rb and p21 expression and decreasing the level of let-7a (78). Tsang also reported that let-7a directly targeted caspase 3 and promoted the resistance in paclitaxel-induced apoptosis (79). Tao et al. (80) proved that downregulation of let-7f was associated with its target thrombospondin-1 (TSP-1) and thus influenced the cell sensibility to paclitaxel in MCF-7 cells. With the help of the miRNA array, Zhou et al. (81) observed the upregulation of miR-125b, miR-221, miR-222, and miR-923 in paclitaxel-resistant BC cells. They also proved that miR-125b can inhibit the paclitaxel-induced apoptosis and cytotoxicity by suppressing the expression of pro-apoptotic Bcl2 antagonist killer 1 (BAK1) in BC cells.

Another miRNA involved in paclitaxel resistance was miR-520h; the increased expression of miR-520h was correlated with negligible prognosis and lymph node metastasis in human BC patients. The expression of miR-520h promoted paclitaxel resistance of human breast cancer cells through suppressing death-associated protein kinase 2 (DAPK2) expression and protecting the cells from paclitaxel-induced apoptosis (82). Gu et al. (83) reported that miR-451 possesses a significant influence to the sensibility of neoadjuvant chemotherapy by inhibiting the expression of Bcl-2 and the process of apoptosis induced by paclitaxel. The luminal A subtype was a special type of BC which exhibited ER⁺/PR⁺ and HER2 (84). In luminal A BC cells, miR100 proved to sensitize the cells to paclitaxel treatment in part by targeting the mTOR signaling pathway. The results showed that microRNA 100 plays important roles for luminal A subtype BC cell resistance to paclitaxel (85). In TNBC cells, overexpression of miR-18a was reported to reduce the expression of DICER and enhance autophagy and paclitaxel resistance by inhibiting the mTOR signaling pathway (86). Liu et al. (87) illustrated that the expression of miR-101 in TNBC cells significantly inhibited the effects of tumorigenesis *in vivo* and growth and apoptosis *in vitro*. Besides, miR-101 also increased

paclitaxel sensitivity by suppressing myeloid cell leukemia-1 (MCL-1) expression in TNBC cells.

LncRNAs in Paclitaxel Resistance

Arun et al. (88) reviewed the function and mechanism of lnc-MALAT1 (MALAT1) in BC and proved that the patients with elevated MALAT1 showed worse prognosis. Yu et al. (89) used MCF-7/Tax (taxane-resistant MCF-7 cells) and MCF-7/Adr (adriamycin-resistant MCF-7 cells) cells as research objects. They found that MALAT1 exhibited a significantly high level in the cells, and knockdown of MALAT1 decreased the sensitivity of the cells to taxane and adriamycin. Zheng et al. (90) found that long non-coding RNA CASC2 (CASC2) regulated the expression of miR-18a-5p/CDK19 and activated paclitaxel resistance in BC. Thus, they highlighted the significance of the CASC2/miR-18a-5p/CDK19 axis in the chemoresistance of BC and provided potential aims to improve the chemotherapy of BC.

Unlike ER⁺ and HER2⁺ BC, TNBC patients are primarily treated with chemotherapy. Paclitaxel is the first-line taxane-based chemotherapeutic agent that is used for the treatment of TNBC patients (91). Si et al. showed that lncRNA H19 was one of the downstream target molecules of ER α . Altered ER α expression could change H19 levels and modulate the apoptosis response to chemotherapy in BC cells. They also suggested that the ER α -H19-BIK signaling axis plays an important role in promoting chemoresistance for ER α ⁺ BC to paclitaxel (92). Raveh et al. (93) found that lncRNA-H19 was elevated in TNBC paclitaxel-resistant cell lines compared to parental cells. LncRNA-H19 was highly expressed during embryonic development but decreased after birth, specifically in mammary tissue. Knockdown of lncRNA-H19 in paclitaxel-resistant TNBC cell lines increased paclitaxel sensitivity by reducing p-AKT (Ser473) and decreasing the apoptotic rate

(94). Chen et al. (95) identified that Linc00839 was localized in the nucleus and upregulated in chemoresistant BC cells and tissues. The expression of Linc00839 was activated by Myc and promoted proliferation and chemoresistance in breast cancer through binding with Lin28B *via* activation of the PI3K/AKT signaling pathway.

CircRNA in Paclitaxel Resistance

circRNAs also play vital roles in the paclitaxel resistance of BC cells. Ma et al. (96) identified that circular RNA angiogenin-like 1 (circAMOTL1) has high correlations with paclitaxel resistance in BC cells. circAMOTL1 regulated the AKT pathway and facilitated the anti-apoptotic protein expression which led to paclitaxel resistance in BC cells. Yang et al. (97) reported that circ-ABCB10 bound with let-7a-5p and promoted paclitaxel sensitivity and apoptosis while suppressing invasion and autophagy of paclitaxel-resistant BC cells. Zang et al. (98) proved that circ-RNF111 was upregulated in paclitaxel-resistant BC tissues and cells. Knockdown of circ-RNF111 reduced the function of paclitaxel on BC cells. They further identified miR-140-5p as a target of circ-RNF111, and circ-RNF111 improved paclitaxel resistance of BC cells by upregulating E2F3 *via* sponging miR-140-5p (Table 3, Supplement Figure 3).

ncRNAs in Docetaxel Resistance

miRNAs in Docetaxel Resistance

Docetaxel (a semi-synthetic paclitaxel analog) was synthesized by the precursor obtained from the needles of the European yew. Paclitaxel and docetaxel both performed their function by inhibiting mitotic activity and suppressed the polymerization of microtubules (99). There are various miRNAs whose downregulation plays a vital role in BC cell docetaxel resistance (100, 101). For example, an *in vitro* study revealed that the elevated level of miR-129-3p was interlinked with docetaxel resistance by directly inhibiting the apoptosis-associated protein eukaryotic translation initiation factor 4E (EIF4E). Downregulation of miR-141 resulted in a decrease of EIF4E/CP110 and provided an apoptosis-inducing effect (102). Another study revealed that miR-129-3p promoted docetaxel resistance of BC cells *via* inhibiting the expression of centriolar coiled-coil protein 110 (CP110) (103). In MCF-7 and MDA-MB-231 BC cell lines, an upregulation of miR-3646 was related to

docetaxel resistance through activating the GSK-3 β / β -catenin signaling pathway (104). Hu et al. (105) observed the expression of miR-663, and miR-452 was increased in docetaxel-resistant BC cell lines MDAMB-231 and MCF-7. MiR-452 contributed to the docetaxel resistance by inhibiting anaphase-promoting complex subunit 4 (APC4) expression, while overexpression of miR-663 caused the downregulation of heparin sulfate proteoglycan 2 (HSPG2) and induced BC cell chemoresistance (106). In extensive research, Kaslt et al. (107) conducted a microarray analysis of MDA-MB-231 and MCF-7 cell lines between docetaxel resistance and miRNA expression. The results showed that miR-141 and miR-34a were increased and miR-16, miR-7, miR-30a, miR-126, and miR-125a-5p were decreased in docetaxel resistance cells. Zhang et al. (108) also analyzed miRNA array and found that miR-139-5p was significantly downregulated in BC cells compared to vicinal typical tissue. The *in vitro* research revealed that miR-139-5p was capable of inhibiting BC cell growth and induced apoptosis by targeting Notch1 and hence decreasing the docetaxel resistance. Besides, miR-205 was reported to increase the sensitivity of MDA-231 and MCF-7 cells against docetaxel *via* inhibition of clonogenic capability and cell proliferation (109).

Xu et al. (110) found that miR-125a was downregulated in docetaxel-resistant BC cells, and overexpression of miR-125a enhanced the cells' docetaxel sensitivity by suppressing the BRCA1 expression. The authors also observed that the level of miR-125a was decreased in the HER-2 and metastatic specimens of BC patients. The outcome provided a novel approach toward increased sensitivity of BC patients against docetaxel *via* overexpression of miR125a. Generally, a combined therapy of docetaxel plus adriamycin is used to treat metastatic and reoccurrence BC patients. However, development of drug resistance remains a latent problem, and miR-222 and miR-29a have been reported to increase in docetaxel plus adriamycin-resistant BC cell lines. Further research proved that the two miRNAs are potential inhibitors that altered the drug resistance and restored their sensitivity by targeting PTEN and activating the Akt/mTOR approach (111).

Exosomes, a group of 40–100-nm-nanosized vesicles that lived in the extracellular space of cells, perform as genome exchange vehicles between heterogeneous tumor cells. Exosomes are also

TABLE 3 | Breast cancer paclitaxel chemoresistance-related ncRNAs.

ncRNA	Drugs	Function	Targets/mechanisms	References
Lin28	Paclitaxel	Resistance	Activation of p21 and Rb; inhibition of Let-7	lv et al. (78)
Let-7a	Paclitaxel	Resistance	Inhibition of caspase-3	Tsang et al. (79)
mi-125b	Paclitaxel	Resistance	Inhibition of BAK1	Zhou et al. (81)
mi-520h	Paclitaxel	Resistance	Inhibition of DAPK2	Su et al. (82)
mi-451	Paclitaxel	Resistance	Inhibition of Bcl-2	Gu et al. (83)
mi-100	Paclitaxel	Sensitivity	Inhibition of the Mtor signaling pathway	Zhang et al. (85)
mi-18a	Paclitaxel	Resistance	Inhibition of the mTOR signaling pathway	Sha et al. (86)
mi-101	Paclitaxel	Sensitivity	Inhibition of MCL-1	Liu et al. (87)
LncRNA-CASC2	Paclitaxel	Resistance	Inhibition miR-18a-5p/CDK19	Zheng et al. (90)
LncRNA-H19	Paclitaxel	Resistance	Inhibition AKT/BIK	Si et al. (92) and Raveh et al. (93) and Han et al. (94)
LncRNA-00839	Paclitaxel	Resistance	Activation PI3K/AKT signaling pathway	Chen et al. (95)
CircRNA-ABCB10	Paclitaxel	Resistance	Inhibition of the let-7a-5p/DUSP7 axis	Yang et al. (97)
CircRNA-RNF111	Paclitaxel	Resistance	Inhibition of miR-140-5p/E2F3	Zang et al. (98)

capable of transferring drug resistance to desired cells through the miRNAs they contained. Chen et al. (112) reported that miR-23a, miR-1246, miR-1469, let-7b, miR-38 and miR-1915 were found in docetaxel-resistant cell exosomes, illustrating that these exosomes play important roles in the drug resistance cells.

LncRNAs in Docetaxel Resistance

Huang et al. (113) performed RNA sequencing and analyzed that mRNAs and lncRNAs contribute to docetaxel resistance in two docetaxel-resistant BC cell lines MCF7-RES and MDA-RES and their docetaxel-sensitive parental cell lines. Co-expression network and location analysis revealed that four lncRNAs might upregulate the expression of ABCB1 and influence the cells' drug resistance. The author also identified the lncRNA EPB41L4A-AS2 (EPB41L4A antisense RNA 2) as a potential biomarker for docetaxel sensitivity BC cells. Shin et al. (114) revealed that the combination of cisplatin or taxol and NEAT1 (lncRNA nuclear paraspeckle assembly transcript 1) knockdown synergistically inhibited the cells' sensitivity to the drug when compared with cisplatin or taxol alone. Overexpression of NEAT1 in cisplatin- and taxol-resistant TNBC cells indicated its function of chemoresistance in BC cells (Table 4, Supplement Figure 4).

ncRNAs IN 5-FLUOROURACIL RESISTANCE

5-Fluorouracil (5-FU) is a classic chemotherapeutic drug, and it has been extensively used to treat different cancers (115). However, patients often exhibited primary or acquired drug resistance during treatments. Although there are many advancements in bioresearch technologies in the past several decades, the molecular mechanisms of 5-FU resistance have not been completely clarified (116). ncRNAs as oncogenes or tumor suppressors often play a vital role in BC cells and contributed to 5-FU drug resistance (117).

miRNAs in 5-FU Resistance

Nandy et al. (118) proved that microRNA-125a influences breast cancer stem cells by posttranscriptionally regulating the leukemia inhibitory factor (LIF) receptor gene expression *via* binding with its 3'-untranslated region (UTR), thus regulating the cells' drug resistance to 5-FU through the Hippo signaling pathway. Zhang

et al. (119) reported that the interaction between miR-508-5p and P-gp or ZNRD1 was responsible for 5-FU chemotherapeutic resistance. Moreover, Yin et al. (120) indicated that the direct repression of Bmi1 expression under the action of miR-200c and miR-203 could alter the Bmi1-mediated 5-FU resistance. Li et al. (121) illustrated that chemotherapeutics like 5-FU was involved in the suppression of miR-488 and which in turn activated the epidermal growth factor receptor (EGFR)/nuclear factor kappaB (NF-κB) signaling approach *via* targeting SATB1.

LncRNAs in 5-FU Resistance

Several studies have been conducted to analyze the 5-FU resistance-related upregulation and downregulation of lncRNAs in BC. Redis et al. (122) reported that upregulation of lnc-CCAT2 correlated with the sensitivity to 5-FU in BC cells. The ncRNA nuclear paraspeckle assembly transcript 1 (NEAT1) present at an elevated level in BC cells, especially in stage III–IV tumors vs. overexpression of lncRNA NEAT1, was related to the poor prognosis and metastasis of BC. Li et al. (123) conducted *in vitro* assays to understand the biological function of lnc NEAT1 and observed that NEAT1 was involved in the sponging of miR-211 and induced BC cell resistance to 5-FU. The group of Chen and Hou reported that overexpression of lncROR was connected with BC cell EMT and therefore improved the cells' invasion capability and resistance to 5-FU. This result suggests that upregulation of lncROR can be considered to be a potential drug resistance marker (124, 125). A recent research by Yao et al. (126) found that the ER stress induced by 5-FU could increase the expression of GRP78 in MCF-7 cells. GRP78 then regulated the expression of lncMIAT and AKT through upregulating Oct4, thereby increasing the BC cells' resistance to 5-FU. The conclusion was that lncMIAT participated in BC cell resistance to 5-FU through the ER stress-mediated GRP78/Oct4/lncRNA MIAT/AKT pathway. Luo et al. (127) reported that overexpression of lncRNA SNORD3A specifically sensitizes breast cancer cells to 5-FU *via* enhancing UMP5 expression. The SNORD3A-UMP5 axis may serve as a potential biomarker and therapeutic target to improve the efficacy of 5-FU-based chemotherapy for BC patients.

CircRNA in 5-FU Resistance

circRNAs are a class of ncRNA which have a circle structure. circRNAs have been discovered in various cancers and acted as

TABLE 4 | Breast cancer docetaxel chemoresistance-related ncRNAs.

ncRNA	Drugs	Function	Targets/mechanisms	References
miR-141	Docetaxel	Sensitivity	Activation of EIF4E/CP110	Yao et al. (102)
miR-129-3p	Docetaxel	Resistance	Inhibition of CP110	Zhang et al. (103)
miR-3646	Docetaxel	Resistance	Activation of the GSK-3β/β-catenin signaling pathway	Zhang et al. (104)
miR-452	Docetaxel	Resistance	Inhibition of APC4	Hu et al. (105)
miR-663	Docetaxel	Resistance	Inhibition of HSPG2	Hu et al. (106)
miR-139-5p	Docetaxel	Resistance	Inhibition of Notch1	Zhang et al. (108)
miR-125a-3p	Docetaxel	Sensitivity	Inhibition of BRCA1	Xu et al. (110)
miR-222/29a	Docetaxel	Resistance	Activation of Akt/mTOR	Zhong et al. (111)
LncRNA-EPB41L4A-AS2	Docetaxel	Sensitivity	Activation of ABCB1	Huang et al. (113)
LncRNA-NEAT1	Docetaxel	Resistance	Activation of Sox2/ALDH	Shin et al. (114)

either promoting tumorigenesis or inhibiting tumor progression (128). Regarding research on circRNAs and BC cell chemoresistance, only Yang et al. reported about circRNA CDR1as, implicating its function in regulating 5-FU sensitivity in BC cells (129). In the study, they found that circRNA CDR1as competitively inhibited miR-7 to regulate CCNE1 expression. The overexpression of circRNA CDR1as reversed the enhancement of 5-FU sensitivity in BC cells caused by overexpression of miR-7. The study proved that circRNA CDR1as regulated the sensitivity of 5-FU-resistant BC cells by inhibiting miR-7 to regulate CCNE1 (Table 5, Supplement Figure 5).

NCRNAS IN TRASTUZUMAB RESISTANCE

The human epidermal growth factor receptor 2 (HER-2) is often used to classify the BC patients with overexpression (known as HER-2 positive) or not (HER-2 negative) (130). There is a high correlation between HER-2 upregulation and BC metastasis as well as poor prognosis (131). Trastuzumab (TRS), a HER-2-targeting humanized monoclonal antibody, is a selective treatment that targets HER-2 (132). ncRNA provides a comprehensive understanding of their mechanism of action and function and crucial contribution in regulating BC drug resistance and metastasis (133).

miRNAs in Trastuzumab Resistance

To validate the mechanism of miRNAs in BC trastuzumab resistance, several studies were conducted *in vivo* and *in vitro*. Gong and De Mattos et al. (134, 135) found that upregulation of miR-21 significantly correlated with BC resistance to trastuzumab by activation of PTEN, inhibition of AKT, and sustenance of EMT. However, Nielsen et al. (136) reported that the expression of miR-21 in primary breast cancer may not predict its resistance to adjuvant trastuzumab treatment. Ye et al. (137) proved that miR-221 promoted HER-2-positive BC against trastuzumab through suppressing PTEN expression. Besides, the circulating level of miR-210 in plasma was found to be correlated with HER-2-positive BC patients who are trastuzumab resistant, indicating that plasma miR-210 could serve as a predictive biomarker in surveillance of the therapeutic responsiveness (138). Bai et al. (139) found that miR-200c counteracts

trastuzumab resistance and metastasis by inhibiting ZNF217 and ZEB1 and TGF-beta signaling pathway expression in BC. Ye and Ma et al. (140, 141) reported that downregulation of miR-5423p and miR-375 contributed to induction of TRS resistance in HER-2-positive breast cancer through inhibition of IGF1R and activation of the PI3K/AKT signaling pathway. Corcoran et al. (142) proved that downregulation of miR-630 tightly connected with HER-2-targeting drugs in HER-2-overexpressing BC by inhibition of IGF1R. Venturutti et al. (143) found that miR-16 was upregulated in HER-2-positive breast cancer and miR-16 mediated trastuzumab and lapatinib response in ErbB-2-positive breast cancer *via* its novel targets CCNJ and FUBP1. Huynh et al. (144) reported that microRNA-7 reversed TRS resistance by HER-2 Delta16 and multiple oncogenic pathways in breast cancer cells.

LncRNAs in Trastuzumab Resistance

LncRNA, as a group of ncRNA, also played an important role in HER2⁺ BC trastuzumab resistance, but its contribution to BC resistance is still unclear. Trastuzumab was considered to be the first-line therapy drug to treat advanced HER2⁺ BC (145). It was reported that LncRNA-SNHG14 was responsible for mediating trastuzumab *via* extracellular exosomes of tumor cells. Exosomal lncRNA-SNHG14 activated the Bcl-2/Bax apoptosis signaling pathway and induced resistance against trastuzumab in BC cells. When treating the cells with trastuzumab-resistant cell-derived exosomes, the cell apoptosis and death were remarkably decreased (146). Dong et al. (147) reported that LncRNA AGAP2-AS1 promoted the growth of BC and trastuzumab resistance by upregulation of MyD88 expression by activating the NF- κ B signaling approach. Based on the microarray analysis, Shi et al. (148) observed that LncRNA-ATB was elevated in five trastuzumab-resistant BC patients. Further study revealed that LncRNA-ATB promoted trastuzumab resistance *via* activating the EMT and TGF- β signaling pathway in BC cells. Li et al. (149) reported the significant downregulation of LncGAS5-activated miR21 and mTOR signaling pathway in trastuzumab-resistant SKBR-3 cells and trastuzumab-resistant BC patients. Han et al. (150) observed that LncZNF649-AS1 was highly expressed in trastuzumab-resistant cells compared to sensitive cells. LncZNF649-AS1 was upregulated by H3K27ac modification in the presence of trastuzumab treatment. Knockdown of ZNF649-AS1 reversed trastuzumab resistance *via* modulating ATG5

TABLE 5 | Breast cancer fluorouracil chemoresistance related ncRNAs.

ncRNA	Drugs	Function	Targets/mechanisms	References
miR-125a	Fluorouracil	Resistance	Inhibition LIF/Hippo signaling pathway	Nandy et al. (118)
miR-508-5p	Fluorouracil	Resistance	Inhibition P-gp or ZNRD1	Zhang et al. (119)
miR-200/203	Fluorouracil	Sensitivity	Inhibition P53/Bmi1	Yin et al. (120)
miR-448	Fluorouracil	Resistance	Inhibition EMT/NFkB	Li et al. (121)
LncRNA-NEAT1	Fluorouracil	Resistance	Inhibition miR-211/HMGA2	Li et al. (123)
LncRNA-RoR	Fluorouracil	Resistance	Activation EMT	Chen et al. (124)
LncRNA-ROR	Fluorouracil	Resistance		Hou et al. (125)
LncRNA-MIAT	Fluorouracil	Resistance	Activation GRP78/OCT4/AKT pathway	Yao et al. (126)
LncRNA-SNORD3A	Fluorouracil	Sensitivity	Activation UMPS	Luo et al. (127)
Circ-CDR1as	Fluorouracil	Resistance	Inhibition miR-7/CCNE1	Yang et al. (129)

TABLE 6 | Breast cancer trastuzumab chemoresistance-related ncRNAs.

ncRNA	Drugs	Function	Targets/mechanisms	References
miR-21	Trastuzumab	Resistance	Activation of PTEN Inhibition of AKT and NF- κ B	Gong and De Mattos et al. (134, 135)
miR-221	Trastuzumab	Resistance	Inhibition of PTEN	Ye et al. (137)
miR-200c	Trastuzumab	Resistance	Inhibition of ZNF217/ZEB1/TGF- β signaling pathway	Bai et al. (139)
miR-375	Trastuzumab	Sensitivity	Inhibition of IGF1R,	Ye et al. (140)
miR-542-3p	Trastuzumab	Sensitivity	Activation of PI3K/AKT	Ma et al. (141)
miR-630	Trastuzumab	Sensitivity	Inhibition of IGF1R	Corcoran et al. (142)
miR-16	Trastuzumab	Sensitivity	Inhibition of CCNJ and FUBP1	Venturutti et al. (143)
miR-7	Trastuzumab	Resistance	Inhibition of EGFR	Huynh et al. (144)
LncRNA-SNHG14	Trastuzumab	Sensitivity	Activation of Bcl-2/Bax	Dong et al. (146)
LncRNA-AGAP2-AS1	Trastuzumab	Resistance	Activation of MyD88/NF- κ B signaling pathway	Dong et al. (147)
LncRNA-ATB	Trastuzumab	Resistance	Activation of EMT/TGF- β signaling	Shi et al. (148)
LncRNA-GAS5	Trastuzumab	Sensitivity	Activation of miR21/mTOR signaling pathway	Li et al. (149)
LncRNA-ZNF649-AS1	Trastuzumab	Resistance	Activation of ATG5/PTBP1	Han et al. (150)
LncRNA-HOTAIR	Trastuzumab	Resistance	Activation of TGF- β signaling pathway	Chen et al. (151)

expression. Chen et al (151) found that LncRNA HOTAIR was highly expressed in trastuzumab-resistant cell line SK-BR-3-TR, and blocking of HOTAIR expression restores the sensitivity. LncRNA HOTAIR is involved in BC cell trastuzumab resistance *via* epigenetic modification of methylation in PTEN and therefore activation of the TGF- β signaling pathway (Table 6, Supplement Figure 6).

CONCLUSION

Drug resistance is one of the main causes of BC therapy failure in clinical settings. It is also a complex process involving multiple factors, multiple steps, and multiple genes. Despite a number of novel agents that have been developed, the truly efficient options with minimal adverse effects for BC treatment remain limited. In this article, we summarized the mechanisms of ncRNAs in BC drug resistance, including chemotherapeutic, endocrine, and targeted drug resistance. Based on the reports, the molecular mechanisms of ncRNAs involved in BC drug resistance include 1) ncRNAs as a target gene of drugs and influencing its effects, 2) ncRNAs acting as ceRNAs to modulate BC cell sensitivity and drug resistance, 3) ncRNAs regulating cancer cell apoptosis and cell cycle transfer, and 4) ncRNAs inducing BC cell drug resistance through NF-KB, mTOR, and Wnt/ β -catenin signaling pathways.

Even though there are many studies about the mechanism of ncRNAs in BC drug resistance, some of them even highlighted ncRNAs as a novel target for achieving improved treatment outcomes for BC patients. The mechanism of ncRNA networks regulating drug resistance and the selection of key targets from numerous candidate ncRNAs remain challenging. Besides, despite that most of current studies used human BC cell lines cultured *in vitro*, there still lack clinical studies to explore the mechanism of ncRNAs in BC drug resistance.

Although we reviewed the most research of ncRNA in BC drug resistance in this article, the details of mechanism still need further exploring. With the development of technology and the new research elucidates, we believe that targeting ncRNAs could

be a novel strategy for achieving improved treatment outcomes for BC patients in the future.

AUTHOR CONTRIBUTIONS

L-bW contributed to the conception and design of this study. The acquisition of data was carried out by S-hL and C-yY. The analysis of data was carried by J-hT. All authors contributed to the article and approved the submitted version.

FUNDING

This study was funded by the Science and Technology Projects of Ningxia Key R&D Programs (No. 2019BFH02012, 2021BEG03089); The National Natural Science Foundation of China (No. 81860470); The Ningxia High Level Science and Technology Innovation Leading Talent Project (No. KJT2019003); The Ningxia Biochip Technology Research and Development Innovation Team (No. 2019-18); The Scientific Research Platform Open Project of the General Hospital of Ningxia Medical University (No. 2020-146); The Science Research Project of Ningxia Medical University (No.XM2018099); The Science Research Project of the General Hospital of Ningxia Medical University (No. XM2020159). The First-Class Discipline Construction Project of NingXia Medical University and the School of Clinical Medicine (No. NXYLXK2017A05).

SUPPLEMENTARY MATERIAL

The Supplementary Material for this article can be found online at: <https://www.frontiersin.org/articles/10.3389/fonc.2021.702082/full#supplementary-material>

Supplementary Figure 1 | The pattern diagram of ncRNAs and Anthracyclines chemoresistance.

Supplementary Figure 2 | The pattern diagram of ncRNAs and Tamoxifen chemoresistance.

Supplementary Figure 3 | The pattern diagram of ncRNAs and Paclitaxel chemoresistance.

Supplementary Figure 4 | The pattern diagram of ncRNAs and Docetaxel chemoresistance.

Supplementary Figure 5 | The pattern diagram of ncRNAs and Fluorouracil chemoresistance.

Supplementary Figure 6 | The pattern diagram of ncRNAs and Trastuzumab chemoresistance.

REFERENCES

- Sung H, Ferlay J, Siegel RL, Laversanne M, Soerjomataram I, Jemal A, et al. Global Cancer Statistics 2020: GLOBOCAN Estimates of Incidence and Mortality Worldwide for 36 Cancers in 185 Countries. *CA Cancer J Clin* (2021) 71(3):209–49. doi: 10.3322/caac.21660
- Koual M, Tomkiewicz C, Cano-Sancho G, Antignac JP, Bats AS, Coumoul X. Environmental Chemicals, Breast Cancer Progression and Drug Resistance. *Environ Health* (2020) 19(1):117–42. doi: 10.1186/s12940-020-00670-2
- Slack FJ, Chinnaiyan AM. The Role of Non-Coding RNAs in Oncology. *Cell* (2019) 179(5):1033–55. doi: 10.1016/j.cell.2019.10.017
- Mendell JT. Targeting a Long Noncoding RNA in Breast Cancer. *N Engl J Med* (2016) 374:2287–9. doi: 10.1056/NEJMcibr1603785
- Yao RW, Wang Y, Chen LL. Cellular Functions of Long Noncoding RNAs. *Nat Cell Biol* (2019) 21:542–51. doi: 10.1038/s41556-019-0311-8
- Uchida S, Adams JC. Physiological Roles of non-Coding RNAs. *Am J Physiol Cell Physiol* (2019) 317(1):C1–2. doi: 10.1152/ajpcell.00114.2019
- Chen F, Chen J, Yang L, Liu J, Zhang X, Zhang Y, et al. Extracellular Vesicle-Packaged HIF-1 α -Stabilizing lncRNA From Tumour-Associated Macrophages Regulates Aerobic Glycolysis of Breast Cancer Cells. *Nat Cell Biol* (2019) 21:498–510. doi: 10.1038/s41556-019-0299-0
- Shah AN, Gradishar WJ. Adjuvant Anthracyclines in Breast Cancer: What Is Their Role? *Oncologist* (2018) 23:1153–61. doi: 10.1634/theoncologist.2017-0672
- Bhagat A, Kleiner ES. Anthracycline-Induced Cardiotoxicity: Causes, Mechanisms, and Prevention. *Adv Exp Med Biol* (2020) 1257:181–92. doi: 10.1007/978-3-030-43032-0_15
- Chen J, Tian W, Cai H, He H, Deng Y. Down-Regulation of microRNA-200c is Associated With Drug Resistance in Human Breast Cancer. *Med Oncol* (2012) 29:2527–34. doi: 10.1007/s12032-011-0117-4
- Kopp F, Oak PS, Wagner E, Roidl A. miR-200c Sensitizes Breast Cancer Cells to Doxorubicin Treatment by Decreasing TrkB and Bmi1 Expression. *PloS One* (2012) 7:e50469. doi: 10.1371/journal.pone.0050469
- Li XJ, Ji MH, Zhong SL, Zha QB, Xu JJ, Zhao JH, et al. MicroRNA-34a Modulates Chemosensitivity of Breast Cancer Cells to Adriamycin by Targeting Notch1. *Arch Med Res* (2012) 43:514–21. doi: 10.1016/j.arcmed.2012.09.007
- Park EY, Chang E, Lee EJ, Lee HW, Kang HG, Chun KH, et al. Targeting of Mir34a-NOTCH1 Axis Reduced Breast Cancer Stemness and Chemoresistance. *Cancer Res* (2014) 74:7573–82. doi: 10.1158/0008-5472.CAN-14-1140
- Zheng Y, Lv X, Wang X, Wang B, Shao X, Huang Y, et al. MiR-181b Promotes Chemoresistance in Breast Cancer by Regulating Bim Expression. *Oncol Rep* (2016) 35:683–90. doi: 10.3892/or.2015.4417
- Zhao L, Wang Y, Jiang L, He M, Bai X, Yu L, et al. MiR-302a/B/C/D Cooperatively Sensitizes Breast Cancer Cells to Adriamycin via Suppressing P-Glycoprotein(P-Gp) by Targeting MAP/ERK Kinase Kinase 1 (MEKK1). *J Exp Clin Cancer Res* (2016) 35:25. doi: 10.1186/s13046-016-0300-8
- Chen X, Wang YW, Gao P. SPIN1, Negatively Regulated by miR-148/152, Enhances Adriamycin Resistance via Upregulating Drug Metabolizing Enzymes and Transporter in Breast Cancer. *J Exp Clin Cancer Res* (2018) 37:100. doi: 10.1186/s13046-018-0748-9
- Hu D, Li M, Su J, Miao K, Qiu X. Dual-Targeting of miR-124-3p and ABCC4 Promotes Sensitivity to Adriamycin in Breast Cancer Cells. *Genet Test Mol Biomarkers* (2019) 23:156–65. doi: 10.1089/gtmb.2018.0259
- Bao L, Hazari S, Mehra S, Kaushal D, Moroz K, Dash S. Increased Expression of P-Glycoprotein and Doxorubicin Chemoresistance of Metastatic Breast Cancer is Regulated by miR-298. *Am J Pathol* (2012) 180:2490–503. doi: 10.1016/j.ajpath.2012.02.024
- Shen H, Li L, Yang S, Wang D, Zhong S, Zhao J, et al. MicroRNA-29a Contributes to Drug-Resistance of Breast Cancer Cells to Adriamycin Through PTEN/AKT/GSK3 β Signaling Pathway. *Gene* (2016) 593:84–90. doi: 10.1016/j.gene.2016.08.016
- Miao Y, Zheng W, Li N, Su Z, Zhao L, Zhou H, et al. MicroRNA-130b Targets PTEN to Mediate Drug Resistance and Proliferation of Breast Cancer Cells via the PI3K/Akt Signaling Pathway. *Sci Rep* (2017) 7:41942. doi: 10.1038/srep41942
- Wang DD, Yang SJ, Chen X, Shen HY, Luo LJ, Zhang XH, et al. miR-222 Induces Adriamycin Resistance in Breast Cancer Through PTEN/Akt/p27(kip1) Pathway. *Tumour Biol* (2016) 37:15315–24. doi: 10.1007/s13277-016-5341-2
- Gao M, Miao L, Liu M, Li C, Yu C, Yan H, et al. miR-145 Sensitizes Breast Cancer to Doxorubicin by Targeting Multidrug Resistance-Associated Protein-1. *Oncotarget* (2016) 7:59714–26. doi: 10.18632/oncotarget.10845
- Jiang L, He D, Yang D, Chen Z, Pan Q, Mao A, et al. MiR-489 Regulates Chemoresistance in Breast Cancer via Epithelial Mesenchymal Transition Pathway. *FEBS Lett* (2014) 588:2009–15. doi: 10.1016/j.febslet.2014.04.024
- Hu SH, Wang CH, Huang ZJ, Liu F, Xu CW, Li XL, et al. miR-760 Mediates Chemoresistance Through Inhibition of Epithelial Mesenchymal Transition in Breast Cancer Cells. *Eur Rev Med Pharmacol Sci* (2016) 20:5002–8.
- Zhang Y, He Y, Lu LL, Zhou ZY, Wan NB, Li GP, et al. miRNA-192-5p Impacts the Sensitivity of Breast Cancer Cells to Doxorubicin via Targeting Peptidylprolyl Isomerase A. *Kaohsiung J Med Sci* (2019) 35:17–23. doi: 10.1002/kjm2.12004
- Zhao R, Wu J, Jia W, Gong C, Yu F, Ren Z, et al. Plasma miR-221 as a Predictive Biomarker for Chemoresistance in Breast Cancer Patients Who Previously Received Neoadjuvant Chemotherapy. *Onkologie* (2011) 34:675–80. doi: 10.1159/000334552
- Chang L, Hu Z, Zhou Z, Zhang H. Linc00518 Contributes to Multidrug Resistance Through Regulating the MiR-199a/MRP1 Axis in Breast Cancer. *Cell Physiol Biochem* (2018) 48:16–28. doi: 10.1159/000491659
- Liang Y, Li Y, Song X, Zhang N, Sang Y, Zhang H, et al. Long Noncoding RNA LINP1 Acts as an Oncogene and Promotes Chemoresistance in Breast Cancer. *Cancer Biol Ther* (2018) 19:120–31. doi: 10.1080/15384047.2017.1394543
- Yao N, Fu Y, Chen L, Liu Z, He J, Zhu Y, et al. Long non-Coding RNA NONHSAT101069 Promotes Epirubicin Resistance, Migration, and Invasion of Breast Cancer Cells Through NONHSAT101069/miR-129-5p/Twist1 Axis. *Oncogene* (2019) 38:7216–33. doi: 10.1038/s41388-019-0904-5
- Gooding AJ, Zhang B, Gunawardane L, Beard A, Valadkhan S, Schieman WP. The lncRNA BORG Facilitates the Survival and Chemoresistance of Triple-Negative Breast Cancers. *Oncogene* (2019) 38:2020–41. doi: 10.1038/s41388-018-0586-4
- Chen Z, Pan T, Jiang D, Jin L, Geng Y, Feng X, et al. The lncRNA-GAS5/miR-221-3p/DKK2 Axis Modulates ABCB1-Mediated Adriamycin Resistance of Breast Cancer via the Wnt/ β -Catenin Signaling Pathway. *Mol Ther Nucleic Acids* (2020) 19:1434–48. doi: 10.1016/j.omtn.2020.01.030
- Chang M. Tamoxifen Resistance in Breast Cancer. *Biomol Ther (Seoul)* (2012) 20:256–67. doi: 10.4062/biomolther.2012.20.3.256
- Shaguftha, Ahmad I. Tamoxifen a Pioneering Drug: An Update on the Therapeutic Potential of Tamoxifen Derivatives. *Eur J Med Chem* (2018) 143:515–31. doi: 10.1016/j.ejmech.2017.11.056
- Siegel RL, Miller KD, Jemal A. Cancer Statistics, 2016. *CA Cancer J Clin* (2016) 66:7–30. doi: 10.3322/caac.21332
- Jensen EV, Jordan VC. The Estrogen Receptor: A Model for Molecular Medicine. *Clin Cancer Res* (2003) 9:1980–9.
- Chen L, Linden HM, Anderson BO, Li CI. Trends in 5-Year Survival Rates Among Breast Cancer Patients by Hormone Receptor Status and Stage. *Breast Cancer Res Treat* (2014) 147:609–16. doi: 10.1007/s10549-014-3112-6
- Elliott T, Sethi T. Integrins and Extracellular Matrix: A Novel Mechanism of Multidrug Resistance. *Expert Rev Anticancer Ther* (2002) 2:449–59. doi: 10.1586/14737140.2.4.449
- Joshi T, Elias D, Stenvang J, Alves CL, Teng F, Lyng MB, et al. Integrative Analysis of miRNA and Gene Expression Reveals Regulatory Networks in Tamoxifen-Resistant Breast Cancer. *Oncotarget* (2016) 7(35):57239–53. doi: 10.18632/oncotarget.11136

39. Uhr K, Prager-van der Smissen WJC, Heine AAJ, Ozturk B, van Jaarsveld MTM, Boersma AWM, et al. MicroRNAs as Possible Indicators of Drug Sensitivity in Breast Cancer Cell Lines. *PLoS One* (2019) 14:e0216400. doi: 10.1371/journal.pone.0216400
40. Zhang W, Xu J, Shi Y, Sun Q, Zhang Q, Guan X. The Novel Role of miRNAs for Tamoxifen Resistance in Human Breast Cancer. *Cell Mol Life Sci* (2015) 72(13):2575–84. doi: 10.1007/s00018-015-1887-1
41. Gao Y, Zhang W, Liu C, Li G. miR-200 Affects Tamoxifen Resistance in Breast Cancer Cells Through Regulation of MYB. *Sci Rep* (2019) 9:18844. doi: 10.1038/s41598-019-54289-6
42. Iijima M, Anai M, Kodama T, Shibasaki Y. Epiregulin-Blocking Antibody Inhibits Epiregulin-Dependent EGFR Signaling. *Biochem Biophys Res Commun* (2017) 489:83–8. doi: 10.1016/j.bbrc.2017.03.006
43. Farooqui M, Bohrer LR, Brady NJ, Chuntova P, Kemp SE, Wardwell CT, et al. Epiregulin Contributes to Breast Tumorigenesis Through Regulating Matrix Metalloproteinase 1 and Promoting Cell Survival. *Mol Cancer* (2015) 14:138. doi: 10.1186/s12943-015-0408-z
44. He M, Jin Q, Chen C, Liu Y, Ye X, Jiang Y, et al. The miR-186-3p/EREG Axis Orchestrates Tamoxifen Resistance and Aerobic Glycolysis in Breast Cancer Cells. *Oncogene* (2019) 38:5551–65. doi: 10.1038/s41388-019-0817-3
45. Miller TE, Ghoshal K, Ramaswamy B, Roy S, Datta J, Shapiro CL, et al. MicroRNA-221/222 Confers Tamoxifen Resistance in Breast Cancer by Targeting p27Kip1. *J Biol Chem* (2008) 283:29897–903. doi: 10.1074/jbc.M804612200
46. Li J, Lu M, Jin J, Lu X, Xu T, Jin S. miR-449a Suppresses Tamoxifen Resistance in Human Breast Cancer Cells by Targeting Adam22. *Cell Physiol Biochem* (2018) 50:136–49. doi: 10.1159/000493964
47. Liu ZR, Song Y, Wan LH, Zhang YY, Zhou LM. Over-Expression of miR-451a can Enhance the Sensitivity of Breast Cancer Cells to Tamoxifen by Regulating 14-3-3zeta, Estrogen Receptor Alpha, and Autophagy. *Life Sci* (2016) 149:104–13. doi: 10.1016/j.lfs.2016.02.059
48. Liu Z, Miao T, Feng T, Jiang Z, Li M, Zhou L, et al. miR-451a Inhibited Cell Proliferation and Enhanced Tamoxifen Sensitive in Breast Cancer via Macrophage Migration Inhibitory Factor. *BioMed Res Int* (2015) 2015:207684. doi: 10.1155/2015/207684
49. Ye P, Fang C, Zeng H, Shi Y, Pan Z, An N, et al. Differential microRNA Expression Profiles in Tamoxifen-Resistant Human Breast Cancer Cell Lines Induced by Two Methods. *Oncol Lett* (2018) 15:3532–9. doi: 10.3892/ol.2018.7768
50. Fan C, Oh DS, Wessels L, Weigelt B, Nuyten DS, Nobel AB, et al. Concordance Among Gene-Expression-Based Predictors for Breast Cancer. *N Engl J Med* (2006) 355:560–9. doi: 10.1056/NEJMoa052933
51. Zhang X, Gao S, Li Z, Wang W, Liu G. Identification and Analysis of Estrogen Receptor α Promoting Tamoxifen Resistance-Related lncRNAs. *BioMed Res Int* (2020) 2020:9031723. doi: 10.1155/2020/9031723
52. Li Z, Yu D, Li H, Lv Y, Li S. Long non-Coding RNA UCA1 Confers Tamoxifen Resistance in Breast Cancer Endocrinotherapy Through Regulation of the EZH2/p21 Axis and the PI3K/AKT Signaling Pathway. *Int J Oncol* (2019) 54(3):1033–42. doi: 10.3892/ijo.2019.4679
53. Liu Y, Li M, Yu H, Piao H. lncRNA CYTOR Promotes Tamoxifen Resistance in Breast Cancer Cells via Sponging Mir-125a-5p. *Int J Mol Med* (2020) 45(2):497–509. doi: 10.3892/ijmm.2019.4428
54. Xue X, Yang YA, Zhang A, Fong KW, Kim J, Song B, et al. lncRNA HOTAIR Enhances ER Signaling and Confers Tamoxifen Resistance in Breast Cancer. *Oncogene* (2016) 35:2746–55. doi: 10.1038/onc.2015.340
55. Ma T, Liang Y, Li Y, Song X, Zhang N, Li X, et al. lncRNA LINP1 Confers Tamoxifen Resistance and Negatively Regulated by ER Signaling in Breast Cancer. *Cell Signal* (2020) 68:109536. doi: 10.1016/j.cellsig.2020.109536
56. Kim CY, Oh JH, Lee JY, Kim MH. The lncRNA HOTAIR Promotes Tamoxifen Resistance by Mediating HOXA1 Expression in ER+ Breast Cancer Cells. *J Cancer* (2020) 11(12):3416–23. doi: 10.7150/jca.38728
57. Shi Q, Li Y, Li S, Jin L, Lai H, Wu Y, et al. lncRNA DILA1 Inhibits Cyclin D1 Degradation and Contributes to Tamoxifen Resistance in Breast Cancer. *Nat Commun* (2020) 11(1):5513. doi: 10.1038/s41467-020-19349-w
58. Qu R, Hu C, Tang Y, Yu Q, Shi G. Long Non-Coding RNA BLACAT1 Induces Tamoxifen Resistance in Human Breast Cancer by Regulating miR-503/Bcl-2 Axis. *Cancer Manag Res* (2020) 12:1771–7. doi: 10.2147/CMAR.S239981
59. Ma Y, Bu D, Long J, Chai W, Dong J. lncRNA DSCAM-AS1 Acts as a Sponge of miR-137 to Enhance Tamoxifen Resistance in Breast Cancer. *J Cell Physiol* (2019) 234(3):2880–94. doi: 10.1002/jcp.27105
60. Xu CG, Yang MF, Ren YQ, Wu CH, Wang LQ. Exosomes Mediated Transfer of lncRNA UCA1 Results in Increased Tamoxifen Resistance in Breast Cancer Cells. *Eur Rev Med Pharmacol Sci* (2016) 20:4362–8.
61. Liu H, Wang G, Yang L, Qu J, Yang Z, Zhou X. Knockdown of Long Non-Coding RNA UCA1 Increases the Tamoxifen Sensitivity of Breast Cancer Cells Through Inhibition of Wnt/beta-Catenin Pathway. *PLoS One* (2016) 11:e0168406. doi: 10.1371/journal.pone.0168406
62. Wu C, Luo J. Long Non-Coding RNA (lncRNA) Urothelial Carcinoma-Associated 1 (UCA1) Enhances Tamoxifen Resistance in Breast Cancer Cells via Inhibiting mTOR Signaling Pathway. *Med Sci Monit* (2016) 22:3860–7. doi: 10.12659/MSM.900689
63. Shi YF, Lu H, Wang HB. Downregulated lncRNA ADAMTS9-AS2 in Breast Cancer Enhances Tamoxifen Resistance by Activating microRNA-130a-5p. *Eur Rev Med Pharmacol Sci* (2019) 23(4):1563–73. doi: 10.26355/eurev_201902_17115
64. Zhang HY, Liang F, Zhang JW, Wang F, Wang L, Kang XG. Effects of Long Noncoding RNA-ROR on Tamoxifen Resistance of Breast Cancer Cells by Regulating microRNA-205. *Cancer Chemother Pharmacol* (2017) 79(2):327–37. doi: 10.1007/s00280-016-3208-2
65. Chen LL, Yang L. Regulation of circRNA Biogenesis. *RNA Biol* (2015) 12(4):381–8. doi: 10.1080/15476286.2015.1020271
66. Hansen TB, Jensen TI, Clausen BH, Bramsen JB, Finsen B, Damgaard C, et al. Natural RNA Circles Function as Efficient microRNA Sponges. *Nature* (2013) 495:384–8. doi: 10.1038/nature11993
67. Sang Y, Chen B, Song X, Li Y, Liang Y, Han D, et al. circRNA_0025202 Regulates Tamoxifen Sensitivity and Tumor Progression via Regulating the miR-182-5p/FOXO3a Axis in Breast Cancer. *Mol Ther* (2019) 27(9):1638–52. doi: 10.1016/j.ymthe.2019.05.011
68. Liang Y, Song X, Li Y, Ma T, Su P, Guo R, et al. Targeting the Circbmr2/miR-553/USP4 Axis as a Potent Therapeutic Approach for Breast Cancer. *Mol Ther Nucleic Acids* (2019) 17:347–61. doi: 10.1016/j.omtn.2019.05.005
69. Hu K, Liu X, Li Y, Li Q, Xu Y, Zeng W, et al. Exosomes Mediated Transfer of Circ_UBE2D2 Enhances the Resistance of Breast Cancer to Tamoxifen by Binding to MiR-200a-3p. *Med Sci Monit* (2020) 26:e922253. doi: 10.12659/MSM.922253
70. Uhr K, Sieuwerts AM, de Weerd V, Smid M, Hammerl D, Foekens JA, et al. Association of microRNA-7 and its Binding Partner CDR1-AS With the Prognosis and Prediction of 1st-Line Tamoxifen Therapy in Breast Cancer. *Sci Rep* (2018) 8(1):9657–65. doi: 10.1038/s41598-018-27987-w
71. Picard M. Management of Hypersensitivity Reactions to Taxanes. *Immunol Allergy Clin North Am* (2017) 37:679–93. doi: 10.1016/j.jiac.2017.07.004
72. Sparano JA. Taxanes for Breast Cancer: An Evidence-Based Review of Randomized Phase II and Phase III Trials. *Clin Breast Cancer* (2000) 1:32–40; discussion 41–32. doi: 10.3816/CBC.2000.n.002
73. Perou CM, Sorlie T, Eisen MB, van de Rijn M, Jeffrey SS, Rees CA, et al. Molecular Portraits of Human Breast Tumours. *Nature* (2000) 406:747–52. doi: 10.1038/35021093
74. Prat A, Parker JS, Karginova O, Fan C, Livasy C, Herschkowitz JL, et al. Phenotypic and Molecular Characterization of the Claudin-Low Intrinsic Subtype of Breast Cancer. *Breast Cancer Res* (2010) 12:R68. doi: 10.1186/bcr2635
75. Yu KD, Zhu R, Zhan M, Rodriguez AA, Yang W, Wong S, et al. Identification of Prognosis-Relevant Subgroups in Patients With Chemoresistant Triple-Negative Breast Cancer. *Clin Cancer Res* (2013) 19:2723–33. doi: 10.1158/1078-0432.CCR-12-2986
76. Bonnefoi H, Piccart M, Bogaerts J, Mauriac L, Fumoleau P, Brain E, et al. TP53 Status for Prediction of Sensitivity to Taxane Versus non-Taxane Neoadjuvant Chemotherapy in Breast Cancer (EORTC 10994/BIG 1-00): A Randomised Phase 3 Trial. *Lancet Oncol* (2011) 12:527–39. doi: 10.1016/S1470-2045(11)70094-8
77. Teng R, Hu Y, Zhou J, Seifer B, Chen Y, Shen J, et al. Overexpression of Lin28 Decreases the Chemosensitivity of Gastric Cancer Cells to Oxaliplatin, Paclitaxel, Doxorubicin, and Fluorouracil in Part via microRNA-107. *PLoS One* (2015) 10:e0143716. doi: 10.1371/journal.pone.0143716
78. Lv K, Liu L, M W, Yu J, Liu X, Cheng Y, et al. Lin28 Mediates Paclitaxel Resistance by Modulating P21, Rb and Let-7a miRNA in Breast Cancer Cells. *PLoS One* (2012) 7:e40008. doi: 10.1371/journal.pone.0040008
79. Tsang WP, Kwok TT. Let-7a microRNA Suppresses Therapeutics-Induced Cancer Cell Death by Targeting Caspase-3. *Apoptosis* (2008) 13:1215–22. doi: 10.1007/s10495-008-0256-z

80. Tao WY, Liang XS, Liu Y, Wang CY, Pang D. Decrease of Let-7f in Low-Dose Metronomic Paclitaxel Chemotherapy Contributed to Upregulation of Thrombospondin-1 in Breast Cancer. *Int J Biol Sci* (2015) 11:48–58. doi: 10.7150/ijbs.9969
81. Zhou M, Liu Z, Zhao Y, Ding Y, Liu H, Xi Y, et al. MicroRNA-125b Confers the Resistance of Breast Cancer Cells to Paclitaxel Through Suppression of Pro-Apoptotic Bcl-2 Antagonist Killer 1 (Bak1) Expression. *J Biol Chem* (2010) 285:21496–507. doi: 10.1074/jbc.M109.083337
82. Su CM, Wang MY, Hong CC, Chen HA, Su YH, Wu CH, et al. miR-520h is Crucial for DAPK2 Regulation and Breast Cancer Progression. *Oncogene* (2016) 35:1134–42. doi: 10.1038/onc.2015.168
83. Gu X, Li JY, Guo J, Li PS, Zhang WH. Influence of MiR-451 on Drug Resistances of Paclitaxel-Resistant Breast Cancer Cell Line. *Med Sci Monit* (2015) 21:3291–7. doi: 10.12659/MSM.894475
84. Guo L, Chen G, Zhang W, Zhou L, Xiao T, Di X, et al. A High-Risk Luminal A Dominant Breast Cancer Subtype With Increased Mobility. *Breast Cancer Res Treat* (2019) 175(2):459–72. doi: 10.1007/s10549-019-05135-w
85. Zhang B, Zhao R, He Y, Fu X, Fu L, Zhu Z, et al. MicroRNA 100 Sensitizes Luminal A Breast Cancer Cells to Paclitaxel Treatment in Part by Targeting mTOR. *Oncotarget* (2016) 7:5702–14. doi: 10.18632/oncotarget.6790
86. Sha LY, Zhang Y, Wang W, Sui X, Liu SK, Wang T, et al. MiR-18a Upregulation Decreases Dicer Expression and Confers Paclitaxel Resistance in Triple Negative Breast Cancer. *Eur Rev Med Pharmacol Sci* (2016) 20:2201–8.
87. Liu X, Tang H, Chen J, Song C, Yang L, Liu P, et al. M.A-101 Inhibits Cell Progression and Increases Paclitaxel Sensitivity by Suppressing MCL-1 Expression in Human Triple-Negative Breast Cancer. *Oncotarget* (2015) 6:20070–83. doi: 10.18632/oncotarget.4039
88. Arun G, Spector DL. MALAT1 Long non-Coding RNA and Breast Cancer. *RNA Biol* (2019) 16:860–3. doi: 10.1080/15476286.2019.1592072
89. Yu J, Jin T, Zhang T. Suppression of Long Non-Coding RNA Metastasis-Associated Lung Adenocarcinoma Transcript 1 (MALAT1) Potentiates Cell Apoptosis and Drug Sensitivity to Taxanes and Adriamycin in Breast Cancer. *Med Sci Monit* (2020) 26:e22672. doi: 10.12659/MSM.922672
90. Zheng P, Dong L, Zhang B, Dai J, Zhang Y, Wang Y, et al. Long Noncoding RNA CASC2 Promotes Paclitaxel Resistance in Breast Cancer Through Regulation of miR-18a-5p/CDK19. *Histochem Cell Biol* (2019) 152:281–91. doi: 10.1007/s00418-019-01794-4
91. Yao H, He G, Yan S, Chen C, Song L, Rosol TJ, et al. Triple-Negative Breast Cancer: Is There a Treatment on the Horizon? *Oncotarget* (2017) 8:1913–24. doi: 10.18632/oncotarget.12284
92. Si X, Zang R, Zhang E, Liu Y, Shi X, Zhang E, et al. LncRNA H19 Confers Chemoresistance in ER α -Positive Breast Cancer Through Epigenetic Silencing of the Pro-Apoptotic Gene BIK. *Oncotarget* (2016) 7(49):81452–62. doi: 10.18632/oncotarget.13263
93. Raveh E, Matouk IJ, Gilon M, Hochberg A. The H19 Long non-Coding RNA in Cancer Initiation, Progression and Metastasis - a Proposed Unifying Theory. *Mol Cancer* (2015) 14:184. doi: 10.1186/s12943-015-0458-2
94. Han J, Han B, Wu X, Hao J, Dong X, Shen Q, et al. Knockdown of lncRNA H19 Restores Chemo-Sensitivity in Paclitaxel-Resistant Triple-Negative Breast Cancer Through Triggering Apoptosis and Regulating Akt Signaling Pathway. *Toxicol Appl Pharmacol* (2018) 359:55–61. doi: 10.1016/j.taap.2018.09.018
95. Chen Q, Shen H, Zhu X, Liu Y, Yang H, Chen H, et al. A Nuclear lncRNA Linc00839 as a Myc Target to Promote Breast Cancer Chemoresistance via PI3K/AKT Signaling Pathway. *Cancer Sci* (2020) 111:3279–91. doi: 10.1111/cas.14555
96. Ma J, Fang L, Yang Q, Hibberd S, Du WW, Wu N, et al. Posttranscriptional Regulation of AKT by Circular RNA Angiomotin-Like 1 Mediates Chemoresistance Against Paclitaxel in Breast Cancer Cells. *Aging (Albany NY)* (2019) 11:11369–81. doi: 10.18632/aging.102535
97. Yang W, Gong P, Yang Y, Yang C, Yang B, Ren L. Circ-ABC10 Contributes to Paclitaxel Resistance in Breast Cancer Through Let-7a-5p/DUSP7 Axis. *Cancer Manag Res* (2020) 12:2327–37. doi: 10.2147/CMAR.S238513
98. Zang H, Li Y, Zhang X, Huang G. Circ-RNF111 Contributes to Paclitaxel Resistance in Breast Cancer by Elevating E2F3 Expression via miR-140-5p. *Thorac Cancer* (2020) 11:1891–903. doi: 10.1111/1759-7714.13475
99. Nabholz JM, Gligorov J. Docetaxel in the Treatment of Breast Cancer: Current Experience and Future Prospects. *Expert Rev Anticancer Ther* (2005) 5:613–33. doi: 10.1586/14737140.5.4.613
100. Jones SE, Erban J, Overmoyer B, Budd GT, Hutchins L, Lower E, et al. Randomized Phase III Study of Docetaxel Compared With Paclitaxel in Metastatic Breast Cancer. *J Clin Oncol* (2005) 23:5542–51. doi: 10.1200/JCO.2005.02.027
101. Qi WX, Shen Z, Lin F, Sun YJ, Min DL, Tang LN, et al. Paclitaxel-Based Versus Docetaxel-Based Regimens in Metastatic Breast Cancer: A Systematic Review and Meta-Analysis of Randomized Controlled Trials. *Curr Med Res Opin* (2013) 29:117–25. doi: 10.1185/03007995.2012.756393
102. Yao YS, Qiu WS, Yao RY, Zhang Q, Zhuang LK, Zhou F, et al. miR-141 Confers Docetaxel Chemoresistance of Breast Cancer Cells via Regulation of EIF4E Expression. *Oncol Rep* (2015) 33:2504–12. doi: 10.3892/or.2015.3866
103. Zhang Y, Wang Y, Wei Y, Li M, Yu S, Ye M, et al. MiR-129-3p Promotes Docetaxel Resistance of Breast Cancer Cells via CP110 Inhibition. *Sci Rep* (2015) 5:15424. doi: 10.1038/srep15424
104. Zhang X, Zhong S, Xu Y, Yu D, Ma T, Chen L, et al. MicroRNA-3646 Contributes to Docetaxel Resistance in Human Breast Cancer Cells by GSK-3 β /Beta-Catenin Signaling Pathway. *PLoS One* (2016) 11:e0153194. doi: 10.1371/journal.pone.0153194
105. Hu Q, Chen WX, Zhong SL, Zhang JY, Ma TF, Ji H, et al. MicroRNA-452 Contributes to the Docetaxel Resistance of Breast Cancer Cells. *Tumour Biol* (2014) 35:6327–34. doi: 10.1007/s13277-014-1834-z
106. Hu H, Li S, Cui X, Lv X, Jiao Y, Yu F, et al. The Overexpression of Hypomethylated miR-663 Induces Chemotherapy Resistance in Human Breast Cancer Cells by Targeting Heparin Sulfate Proteoglycan 2 (HSPG2). *J Biol Chem* (2013) 288:10973–85. doi: 10.1074/jbc.M112.434340
107. Kastl L, Brown I, Schofield AC. miRNA-34a is Associated With Docetaxel Resistance in Human Breast Cancer Cells. *Breast Cancer Res Treat* (2012) 131:445–54. doi: 10.1007/s10549-011-1424-3
108. Zhang HD, Sun DW, Mao L, Zhang J, Jiang LH, Li J, et al. MiR-139-5p Inhibits the Biological Function of Breast Cancer Cells by Targeting Notch1 and Mediates Chemosensitivity to Docetaxel. *Biochem Biophys Res Commun* (2015) 465:702–13. doi: 10.1016/j.bbrc.2015.08.053
109. Cai Y, Yan X, Zhang G, Zhao W, Jiao S. MicroRNA-205 Increases the Sensitivity of Docetaxel in Breast Cancer. *Oncol Lett* (2016) 11:1105–9. doi: 10.3892/ol.2015.4030
110. Xu X, Lv YG, Yan CY, Yi J, Ling R. Enforced Expression of hsa-miR-125a-3p in Breast Cancer Cells Potentiates Docetaxel Sensitivity via Modulation of BRCA1 Signaling. *Biochem Biophys Res Commun* (2016) 479:893–900. doi: 10.1016/j.bbrc.2016.09.087
111. Zhong S, Li W, Chen Z, Xu J, Zhao J. MiR-222 and miR-29a Contribute to the Drug-Resistance of Breast Cancer Cells. *Gene* (2013) 531:8–14. doi: 10.1016/j.gene.2013.08.062
112. Chen WX, Cai YQ, Lv MM, Chen L, Zhong SL, Ma TF, et al. Exosomes From Docetaxel-Resistant Breast Cancer Cells Alter Chemosensitivity by Delivering microRNAs. *Tumour Biol* (2014) 35:9649–59. doi: 10.1007/s13277-014-2242-0
113. Huang P, Li F, Li L, You Y, Luo S, Dong Z, et al. lncRNA Profile Study Reveals the mRNAs and lncRNAs Associated With Docetaxel Resistance in Breast Cancer Cells. *Sci Rep* (2018) 8:17970. doi: 10.1038/s41598-018-36231-4
114. Shin VY, Chen J, Cheuk IW, Siu MT, Ho CW, Wang X, et al. Long non-Coding RNA NEAT1 Confers Oncogenic Role in Triple-Negative Breast Cancer Through Modulating Chemoresistance and Cancer Stemness. *Cell Death Dis* (2019) 10:270. doi: 10.1038/s41419-019-1513-5
115. Wei Y, Yang P, Cao S, Zhao L. The Combination of Curcumin and 5-Fluorouracil in Cancer Therapy. *Arch Pharm Res* (2018) 41(1):1–13. doi: 10.1007/s12272-017-0979-x
116. Zhang W, Feng M, Zheng G, Chen Y, Wang X, Pen B, et al. Chemoresistance to 5-Fluorouracil Induces Epithelial-Mesenchymal Transition via Up-Regulation of Snail in MCF7 Human Breast Cancer Cells. *Biochem Biophys Res Commun* (2012) 417:679–85. doi: 10.1016/j.bbrc.2011.11.142
117. Deng J, Wang Y, Lei J, Lei W, Xiong JP. Insights Into the Involvement of Noncoding RNAs in 5-Fluorouracil Drug Resistance. *Tumour Biol* (2017) 39(4):1–10. doi: 10.1177/1010428317697553
118. Nandy SB, Arumugam A, Subramani R, Pedroza D, Hernandez K, Saltzstein E, et al. MicroRNA-125a Influences Breast Cancer Stem Cells by Targeting Leukemia Inhibitory Factor Receptor Which Regulates the Hippo Signaling Pathway. *Oncotarget* (2015) 6:17366–78. doi: 10.18632/oncotarget.3953
119. Zhang Y, Qu X, Teng Y, Li Z, Xu L, Liu J, et al. Cbl-B Inhibits P-Gp Transporter Function by Preventing its Translocation Into Caveolae in

- Multiple Drug-Resistant Gastric and Breast Cancers. *Oncotarget* (2015) 6:6737–48. doi: 10.18632/oncotarget.3253
120. Yin J, Zheng G, Jia X, Zhang Z, Zhang W, Song Y, et al. A Bmi1-miRNAs Cross-Talk Modulates Chemotherapy Response to 5-Fluorouracil in Breast Cancer Cells. *PLoS One* (2013) 8:e73268. doi: 10.1371/journal.pone.0073268
 121. Li QQ, Chen ZQ, Cao XX, Xu JD, Xu JW, Chen YY, et al. Involvement of NF-KappaB/miR-448 Regulatory Feedback Loop in Chemotherapy-Induced Epithelial-Mesenchymal Transition of Breast Cancer Cells. *Cell Death Differ* (2011) 18:16–25. doi: 10.1038/cdd.2010.103
 122. Redis RS, Sieuwerts AM, Look MP, Tudoran O, Ivan C, Spizzo R, et al. CCAT2, a Novel Long non-Coding RNA in Breast Cancer: Expression Study and Clinical Correlations. *Oncotarget* (2013) 4:1748–62. doi: 10.18632/oncotarget.1292
 123. Li X, Wang S, Li Z, Long X, Guo Z, Zhang G, et al. The lncRNA NEAT1 Facilitates Cell Growth and Invasion via the miR-211/HMGA2 Axis in Breast Cancer. *Int J Biol Macromol* (2017) 105:346–53. doi: 10.1016/j.ijbiomac.2017.07.053
 124. Chen YM, Liu Y, Wei HY, Lv KZ, Fu P. Lnc-ROR Induces Epithelial-Mesenchymal Transition and Contributes to Drug Resistance and Invasion of Breast Cancer Cells. *Tumour Biol* (2016) 37:10861–70. doi: 10.1007/s13277-016-4909-1
 125. Hou P, Zhao Y, Li Z, Yao R, Ma M, Gao Y, et al. LncRNA-ROR Induces Epithelial-to-Mesenchymal Transition and Contributes to Breast Cancer Tumorigenesis and Metastasis. *Cell Death Dis* (2014) 5:e1287. doi: 10.1038/cddis.2014.249
 126. Yao XL, Yi T, Xu YL, Guo XY, Yao F, Zhang XH. Endoplasmic Reticulum Stress Confers 5-Fluorouracil Resistance in Breast Cancer Cell via the GRP78/OCT4/lncRNA MIAT/AKT Pathway. *Am J Cancer Res* (2020) 10(3):838–55.
 127. Luo L, Zhang J, Tang H, Zhai D, Huang D, Ling L, et al. LncRNA SNORD3A Specifically Sensitizes Breast Cancer Cells to 5-FU by Sponging miR-185-5p to Enhance UMP5 Expression. *Cell Death Dis* (2020) 11:329. doi: 10.1038/s41419-020-2557-2
 128. Zhu J, Zhang X, Gao W, Hu H, Wang X, Hao D. LncRNA/ circRNA- miRNA-mRNA ceRNA Network in Lumbar Intervertebral Disc Degeneration. *Mol Med Rep* (2019) 20(4):3160–74. doi: 10.3892/mmr.2019.10569
 129. Yang W, Gu J, Wang X, Wang Y, Feng M, Zhou D, et al. Inhibition of Circular RNA CDR1as Increases Chemosensitivity of 5-FU-Resistant BC Cells Through Up-Regulating miR-7. *J Cell Mol Med* (2019) 23:3166–77. doi: 10.1111/jcmm.14171
 130. Cobleigh MA, Vogel CL, Tripathy D, Robert NJ, Scholl S, Fehrenbacher L, et al. Multinational Study of the Efficacy and Safety of Humanized Anti-HER2 Monoclonal Antibody in Women Who Have HER2-Overexpressing Metastatic Breast Cancer That has Progressed After Chemotherapy for Metastatic Disease. *J Clin Oncol* (1999) 17:2639–48. doi: 10.1200/JCO.1999.17.9.2639
 131. Marty M, Cognetti F, Maraninchi D, Snyder R, Mauriac L, Tubiana-Hulin M, et al. Randomized Phase II Trial of the Efficacy and Safety of Trastuzumab Combined With Docetaxel in Patients With Human Epidermal Growth Factor Receptor 2-Positive Metastatic Breast Cancer Administered as First-Line Treatment: The M77001 Study Group. *J Clin Oncol* (2005) 23:4265–74. doi: 10.1200/JCO.2005.04.173
 132. Esteva FJ, Valero V, Booser D, Guerra LT, Murray JL, Pusztai L, et al. Phase II Study of Weekly Docetaxel and Trastuzumab for Patients With HER-2-Overexpressing Metastatic Breast Cancer. *J Clin Oncol* (2002) 20:1800–8. doi: 10.1200/JCO.2002.07.058
 133. Deepti T, Amit SY, Dhiraj K, Garima B, Gopal CK. Non-Coding RNAs as Potential Therapeutic Targets in Breast Cancer. *Biochim Biophys Acta Gene Regul Mech* (2020) 1863(4):194378. doi: 10.1016/j.bbaggm.2019.04.005
 134. Gong C, Yao Y, Wang Y, Liu B, Wu W, Chen J, et al. Up-Regulation of miR-21 Mediates Resistance to Trastuzumab Therapy for Breast Cancer. *J Biol Chem* (2011) 286:19127–37. doi: 10.1074/jbc.M110.216887
 135. De Mattos Arruda L, Bottai G, Nuciforo PG, Di TL, Giovannetti E, Peg V, et al. MicroRNA-21 Links Epithelial-to-Mesenchymal Transition and Inflammatory Signals to Confer Resistance to Neoadjuvant Trastuzumab and Chemotherapy in HER2-Positive Breast Cancer Patients. *Oncotarget* (2015) 6:37269–80. doi: 10.18632/oncotarget.5495
 136. Nielsen BS, Balslev E, Poulsen TS, Nielsen D, Moller T, Mortensen CE, et al. miR-21 Expression in Cancer Cells may Not Predict Resistance to Adjuvant Trastuzumab in Primary Breast Cancer. *Front Oncol* (2014) 4:207. doi: 10.3389/fonc.2014.00207
 137. Ye X, Bai W, Zhu H, Zhang X, Chen Y, Wang L, et al. MiR-221 Promotes Trastuzumab-Resistance and Metastasis in HER2-Positive Breast Cancers by Targeting PTEN. *BMB Rep* (2014) 47:268–73. doi: 10.5483/BMBRep.2014.47.5.165
 138. Jung EJ, Santarpia L, Kim J, Esteva FJ, Moretti E, Buzdar AU, et al. Plasma microRNA 210 Levels Correlate With Sensitivity to Trastuzumab and Tumor Presence in Breast Cancer Patients. *Cancer* (2012) 118:2603–14. doi: 10.1002/cncr.26565
 139. Bai WD, Ye XM, Zhang MY, Zhu HY, Xi WJ, Huang X, et al. MiR-200c Suppresses TGF-Beta Signaling and Counteracts Trastuzumab Resistance and Metastasis by Targeting ZNF217 and ZEB1 in Breast Cancer. *Int J Cancer* (2014) 135:1356–68. doi: 10.1002/ijc.28782
 140. Ye XM, Zhu HY, Bai WD, Wang T, Wang L, Chen Y, et al. Epigenetic Silencing of miR-375 Induces Trastuzumab Resistance in HER2-Positive Breast Cancer by Targeting IGF1R. *BMC Cancer* (2014) 14:134. doi: 10.1186/1471-2407-14-134
 141. Ma T, Yang L, Zhang J. MiRNA5423p Downregulation Promotes Trastuzumab Resistance in Breast Cancer Cells via AKT Activation. *Oncol Rep* (2015) 33:1215–20. doi: 10.3892/or.2015.3713
 142. Corcoran C, Rani S, Breslin S, Gogarty M, Ghobrial IM, Crown J, et al. miR-630 Targets IGF1R to Regulate Response to HER-Targeting Drugs and Overall Cancer Cell Progression in HER2 Over-Expressing Breast Cancer. *Mol Cancer* (2014) 13:71. doi: 10.1186/1476-4598-13-71
 143. Venturutti L, Cordo Russo RI, Rivas MA, Mercogliano MF, Izzo F, Oakley RH, et al. MiR-16 Mediates Trastuzumab and Lapatinib Response in ErbB-2-Positive Breast and Gastric Cancer via its Novel Targets CCNJ and FUBP1. *Oncogene* (2016) 35:6189–202. doi: 10.1038/onc.2016.151
 144. Huynh FC, Jones FE. MicroRNA-7 Inhibits Multiple Oncogenic Pathways to Suppress HER2Delta16 Mediated Breast Tumorigenesis and Reverse Trastuzumab Resistance. *PLoS One* (2014) 9:1–16. doi: 10.1371/journal.pone.0114419
 145. von Minckwitz G, Huang CS, Mano MS, Loibl S, Mamounas EP, Untch M, et al. Trastuzumab Emtansine for Residual Invasive HER2-Positive Breast Cancer. *N Engl J Med* (2019) 380:617–28. doi: 10.1056/NEJMoa1814017
 146. Dong H, Wang W, Chen R, Zhang Y, Zou K, Ye M, et al. Exosome-Mediated Transfer of Lncnasnhg14 Promotes Trastuzumab Chemoresistance in Breast Cancer. *Int J Oncol* (2018) 53:1013–26. doi: 10.3892/ijo.2018.4467
 147. Dong H, Wang W, Mo S, Chen R, Zou K, Han J, et al. SP1-Induced lncRNA AGAP2-AS1 Expression Promotes Chemoresistance of Breast Cancer by Epigenetic Regulation of Myd88. *J Exp Clin Cancer Res* (2018) 37:202–17. doi: 10.1186/s13046-018-0875-3
 148. Shi SJ, Wang LJ, Yu B, Li YH, Jin Y, Bai XZ. LncRNA-ATB Promotes Trastuzumab Resistance and Invasion-Metastasis Cascade in Breast Cancer. *Oncotarget* (2015) 6:11652–63. doi: 10.18632/oncotarget.3457
 149. Li W, Zhai L, Wang H, Liu C, Zhang J, Chen W. Downregulation of LncRNA GAS5 Causes Trastuzumab Resistance in Breast Cancer. *Oncotarget* (2016) 7:27778–86. doi: 10.18632/oncotarget.8413
 150. Han M, Qian X, Cao H, Wang F, Li X, Han N, et al. LncRNA ZNF649-AS1 Induces Trastuzumab Resistance by Promoting ATG5 Expression and Autophagy. *Mol Ther* (2020) 28(11):2488–502. doi: 10.1016/j.ymthe.2020.07.019
 151. Chen T, Liu Z, Zeng W, Huang T. Down-Regulation of Long non-Coding RNA HOTAIR Sensitizes Breast Cancer to Trastuzumab. *Sci Rep* (2019) 9:19881–9. doi: 10.1038/s41598-019-53699-w

Conflict of Interest: The authors declare that the research was conducted in the absence of any commercial or financial relationships that could be construed as a potential conflict of interest.

Publisher's Note: All claims expressed in this article are solely those of the authors and do not necessarily represent those of their affiliated organizations, or those of the publisher, the editors and the reviewers. Any product that may be evaluated in this article, or claim that may be made by its manufacturer, is not guaranteed or endorsed by the publisher.

Copyright © 2021 Tian, Liu, Yu, Wu and Wang. This is an open-access article distributed under the terms of the Creative Commons Attribution License (CC BY). The use, distribution or reproduction in other forums is permitted, provided the original author(s) and the copyright owner(s) are credited and that the original publication in this journal is cited, in accordance with accepted academic practice. No use, distribution or reproduction is permitted which does not comply with these terms.



High Expression of Complement Component C7 Indicates Poor Prognosis of Breast Cancer and Is Insensitive to Taxane-Anthracycline Chemotherapy

Huikun Zhang^{1,2,3,4}, Yawen Zhao^{1,2,3,4}, Xiaoli Liu^{1,2,3,4}, Li Fu^{2,3,4,5}, Feng Gu^{2,3,4,5} and Yongjie Ma^{1,2,3,4*}

¹ Department of Tumor Cell Biology, Tianjin Medical University Cancer Institute and Hospital, National Clinical Research Center for Cancer, Tianjin, China, ² Tianjin's Clinical Research Center for Cancer, Tianjin Medical University Cancer Institute and Hospital, Tianjin, China, ³ Key Laboratory of Cancer Prevention and Therapy, Tianjin, China, ⁴ Key Laboratory of Breast Cancer Prevention and Therapy, Tianjin Medical University, Ministry of Education, Tianjin, China, ⁵ Department of Breast Cancer Pathology and Research Laboratory, Tianjin Medical University Cancer Institute and Hospital, Tianjin, China

OPEN ACCESS

Edited by:

Maria Rosaria De Miglio,
University of Sassari, Italy

Reviewed by:

Joseph A. Pinto,
Auna Oncosalud, Peru
Ke-Da Yu,
Fudan University, China

*Correspondence:

Yongjie Ma
mayongjie@tjmuch.com

Specialty section:

This article was submitted to
Breast Cancer,
a section of the journal
Frontiers in Oncology

Received: 12 June 2021

Accepted: 01 September 2021

Published: 24 September 2021

Citation:

Zhang H, Zhao Y, Liu X, Fu L, Gu F and
Ma Y (2021) High Expression of
Complement Component C7
Indicates Poor Prognosis of Breast
Cancer and Is Insensitive to Taxane-
Anthracycline Chemotherapy.
Front. Oncol. 11:724250.
doi: 10.3389/fonc.2021.724250

Background: Breast cancer is the most commonly diagnosed cancer worldwide. However, the well-known biomarkers are not enough to meet the needs of precision medicine. Novel targets are desirable and highly valuable for improved patient survival. In this regard, we identified complement component C7 as one of the candidates based on data from the OCOMINE database.

Methods: C7 expression was examined by immunohistochemistry in 331 cases of invasive ductal carcinoma (IDC), 45 cases of ductal carcinoma *in situ* (DCIS), and 52 cases of non-neoplastic tissues adjacent to tumor. Then, C7 expression was further confirmed by Western blot analysis based on IDC specimens and non-neoplastic breast specimens. The relationship between the C7 expression and prognosis of breast cancer patients was analyzed in order to investigate the function of C7 in breast cancer patients. Meanwhile, we also analyzed the relationship between the C7 expression and prognosis of 149 patients treated with conventional TE (taxane and anthracycline)-based chemotherapy. Then, a cohort of patients (22 cases) treated with TE neoadjuvant chemotherapy was used to further confirm the relationship between the C7 expression and TE-based chemosensitivity.

Results: In our present study, we reported for the first time that C7 was an independent prognostic factor of breast cancer and C7 expression of IDC tissues was higher than non-neoplastic tissues adjacent to tumor and DCIS. In a cohort of 331 IDC patients, high expression of C7 indicated poor prognosis especially in the triple negative subtype and luminal B subtype. Furthermore, C7 was also a promoting factor for triple negative subtype patients to develop bone metastasis. Meanwhile, we provided the first evidence that patients with high C7 expression were insensitive to TE (taxane and anthracycline)-based chemotherapy by analyzing a cohort of 149 patients treated

with TE-based chemotherapy and another cohort of 22 patients treated with TE neoadjuvant chemotherapy.

Conclusions: In summary, high expression of C7 may promote breast cancer development and might be insensitive to TE-based chemotherapy. Our present study laid a foundation to help clinicians improve the identification of patients for TE-based chemotherapy by C7 in the era of precision medicine.

Keywords: C7, breast cancer, prognosis, TE chemotherapy, bone metastasis

INTRODUCTION

The incidence and mortality of breast cancer continue to increase and has become the most commonly diagnosed cancer worldwide in 2020 (1–3). However, the well-known biomarkers are not enough to meet the needs of precision medicine. Novel targets are desirable and highly valuable for improved patient survival (4). In this regard, we identified complement component C7 as one of the candidates based on data from the ONCOMINE database.

C7 belonging to the complement system, which is composed of complement natural ingredients, complement control components, and complement receptor, is an important component of the innate immune system and plays a vital role in the coordination of innate and adaptive immune reactions (5, 6). Complement component 7 (C7) is a 93-kDa serum glycoprotein encoded by the C7 gene. C7 interacts with other terminal complement components (C5b, C6, C8, and C9) to form a membrane attack complex (MAC), which functions as the cytolytic effector unit of the complement system (7). Insertion of the C7 into the cell membrane was identified to be the critical step in the formation of the MAC (8).

Emerging evidence indicated that C7 participated in the progression of several malignancies. It was reported that C7 expression was enhanced in normal tissues, but remarkably reduced in carcinoma tissues of human esophagus, colon, and kidney cancers (9). Additionally, C7 mRNA level expression showed a gradual downward trend in normal, benign, borderline, and malignant ovarian tissues, and C7 expression was negatively related to tumor grade in ovarian cancer patients (10). On the contrary, some researchers hold the opinion that C7 could promote cancer progression. C7 expression was upregulated in ovarian cancer, and knockdown expression of C7 led to a decrease of ovarian cell proliferation (11). Furthermore, significant upregulation of C7 protein in liver tumor-initiating cells was required to maintain the stemness (12).

Until the present, the role of C7 in human breast cancer was unknown. In this study, we identified for the first time that C7 was an independent prognostic factor of breast cancer and its expression was significantly higher in invasive ductal carcinoma (IDC) tissues compared with non-neoplastic tissues adjacent to tumor and ductal

carcinoma *in situ* (DCIS). By immunohistochemistry analysis of a large population of 331 IDC cases, we provided the first clinical evidence that a high expression of C7 promoted breast cancer progression. In addition, high expression of C7 was a promoting factor for triple negative subtype patients to develop bone metastasis. Furthermore, we reported for the first time that patients with high C7 expression were insensitive to TE (taxane and anthracycline)-based chemotherapy using a cohort of 149 patients treated with TE-based chemotherapy and another cohort of 22 patients treated with TE neoadjuvant chemotherapy.

MATERIALS AND METHODS

Ethical Statement

All experiments were performed in accordance with relevant guidelines and regulations of the Ethics Committee of Tianjin Medical University Cancer Institute & Hospital. All the patients signed an informed consent for their participation in the study and the use of their biological tissues prior to surgery.

Clinical Information of Patients

Paraffin-embedded specimens of 331 breast cancer patients with invasive ductal carcinoma (IDC) from 2004 to 2009, the details of IDC patients were shown in **Supplementary Table S1**. A total of 45 patients with breast ductal carcinoma *in situ* (DCIS) and 52 patients with benign lesions, diagnosed between 2008 and 2015, were reviewed and randomly selected from the archives of the Department of Breast Cancer Pathology and Research Laboratory, Tianjin Medical University Cancer Institute & Hospital.

A total of 331 IDC patients were women aging from 28 to 89 years (mean 51.6 years) without preoperative chemotherapy or radiation. The information of subgroups is shown in **Supplementary Table S2**. A total of 319 cases were included for prognostic analyses, excluding cases with no follow-up data (12 cases). These patients were followed up with a median of 71.5 months (5–140 months). Recurrences and distant metastasis were recorded for 20 (6.3%) cases and 58 (18.2%) cases, respectively, and 31 (9.7%) patients died. Among the 319 cases, 236 (74.0%) patients were of the luminal subtype, 34 (10.7%) of the HER2-overexpression subtype, and 49 (15.3%) of the triple negative subtype. A total of 149 (46.7%) patients received TE-based chemotherapy after operation and the rest (170 cases, 53.3%) were treated with other chemotherapies (not TE-based

Abbreviations: DAB, 3,3'-diaminobenzidine tetrahydrochloride; DCIS, ductal carcinoma *in situ*; IDC, invasive ductal carcinoma; IHC, Immunohistochemistry; OS, overall survival; PFS, progression-free survival; S-P, streptavidin-peroxidase; TE, taxane and anthracycline.

chemotherapy). The details of patients who received non-TE based chemotherapy were the following: 68 cases (CEF: Cyclophosphamide, Epirubicin, and 5-fluorouracil); 59 cases (CMF: Cyclophosphamide, Methotrexate, and 5-fluorouracil); 14 cases (CAF: Cyclophosphamide, Doxorubicin, and 5-fluorouracil); 6 cases (CEF/CMF); and 23 cases (unknown).

Prognostic Information of Patients

Among the 319 patients with prognostic analyses, 53 patients developed metastasis, recurrence, or death within 5 years; while 165 patients were disease-free over the same 5 years since their diagnosis of breast cancer. A total of 51 patients developed distant metastasis during the follow-up period. In detail, 37 patients developed bone metastasis; 13 patients developed lung metastasis; 13 patients developed liver metastasis; 6 patients developed brain metastasis; and 1 patient developed uterus, kidney, ovarian, and thyroid metastasis, respectively. It was worth noting that multiple organic metastases were noted in 17 patients. Among those 37 IDC patients with bone metastasis, 30 patients were of the luminal subtype, 3 of the HER2-overexpression subtype, and 4 of the triple negative subtype. Among the patients who received TE-based regimens, 28 patients developed metastasis, recurrence, or death within 5 years; while 74 patients were disease-free over the same 5 years.

Information of 22 Core Needle Biopsy Specimens

We also selected another cohort of patients (22 cases) hospitalized during October 2005 to June 2009. All 22 patients were diagnosed with invasive breast cancer by a 14-gauge core needle biopsy and had completed with preoperative neoadjuvant chemotherapy consisting of 2–8 cycles of TE combined chemotherapy without other local or systemic treatment before surgery. Patients were women 28 to 71 years of age (mean age 56.5 years) and had no other malignant tumors or tumor history. The distribution of clinical involvement showed that all the patients had tumors >2.0 cm. These 22 specimens were collected from each core needle biopsy specimens of primary breast tumor patients before neoadjuvant chemotherapy. All specimens were immediately fixed in 10% normal-buffered formalin and embedded in paraffin and stained for the presence of C7 by immunohistochemistry. The pathological response to neoadjuvant chemotherapy was evaluated after surgical resection of the remaining tumor and assessed according to Miller and Payne histological grading system: grade 1, no change or some alteration to individual malignant cells but no reduction in overall cellularity; grade 2, minor loss (up to 30%) of cancer cells but overall cellularity remains high; grade 3, reduction of 30% to 90% of cancer cells; grade 4, more than 90% loss of cancer cells but small clusters or widely dispersed individual cancer cells remain; and grade 5, no malignant cells identifiable in sections from the site of the tumor consisting of vascular fibroblastic stroma, often containing macrophages; however, DCIS may be present (13). The details of these 22 patients were the following: grade 1 responses (7 cases), grade 2 responses (7 cases), grade 3

responses (5 cases), and grade 4 responses (5 cases). In this study, the 22 patients were divided into two groups: one group was pathological response grade 2 to 4 which was regarded as positive and another group was pathological response grade 1 which was regarded as negative.

Immunohistochemistry

C7 expression was examined by IHC and the S-P method. In brief, sections (5- μ m thick) were dewaxed, hydrated, and heated for 2.5 min for antigen retrieval using citrate buffer. Then, 3% H₂O₂ and 10% normal horse serum were applied to reduce endogenous horseradish peroxidase activity and nonspecific staining. Next, sections were incubated with the primary antibody (goat antiserum to human C7, Quidel, USA, A308, 1:3,000) at 4°C overnight. After washing, biotin labeled secondary antibody against goat immunoglobulin was applied for 20 min at room temperature. The slides were rinsed and covered with streptavidin-biotin-peroxidase for 20 min. 3,3'-diaminobenzidine tetrahydrochloride (DAB) was used as the enzyme substrate.

Evaluation of Staining

Immunostaining of C7 was reviewed by two pathologists in a blinded manner. A consensus judgment was adopted for the intensity score of the tumors based on the strength of C7 expression. Staining intensity was scored as: 0 (-), no staining; 1 (+), definite but weak staining; 2 (++), moderate staining, and 3 (+++), strong staining. Percentage of the positive staining was scored as 0–100. H score was ranged from 0 to 300 by multiplying the intensity and the percentage score. According to the H score of C7, patients were categorized into two groups: low C7 expression (0–119) and high C7 expression (120–300).

Western Blot

Frozen breast tumor specimens (13 cases) and non-neoplastic breast tissues adjacent to tumor (13 cases) were collected between 2012 and 2015. All patients were women without preoperative chemotherapy or radiation. Tissues were directly lysed in SDS lysis buffer on ice. Equal amounts of cell lysates were loaded and separated by SDS-PAGE, and proteins were transferred onto nitrocellulose membranes and incubated with the primary antibody (goat antiserum to human C7, Quidel, USA, A308, 1:3,000) overnight at 4°C. Membranes were then treated with secondary antibodies. Blots were analyzed by Licor Odyssey infrared imaging.

Statistical Methods

The GraphPad Prism version 6.0 and the SPSS software Version 19.0 were used for statistical analysis. Mann-Whitney U test and χ^2 test were performed for group comparisons, and Spearman's rank correlation test was performed for correlations between two variables. Overall survival (OS) was calculated from pathological diagnosis to the date of last contact or death from breast carcinoma. Progression-free survival (PFS) was defined as the time from surgery to either first disease progression (recurrence or distant metastasis) or cancer-

specific death. Survival analyses were performed according to the Kaplan-Meier method. The Cox proportional hazards regression model was performed for the identification of relevant prognostic factors. All tests were two-sided and values of $P < 0.05$ were considered as statistically significant.

RESULTS

Bioinformatic and Clinical Analysis Identified C7 Was a Tumor Promoter in Breast Cancer

Firstly, we used a public cancer microarray database, ONCOMINE online (<http://www.oncomine.org>), to analyze the C7 mRNA expression level in breast cancer tissues. The data showed that C7 mRNA expression was upregulated in invasive breast carcinoma ($n = 53$) compared with normal breast tissues ($n = 6$) ($P = 5.22\text{E-}15$, fold change = 3.018, **Figure 1A**). Next, survival analysis of the Kaplan Meier-plotter database showed that breast cancer patients with a higher C7 mRNA expression had a shorter overall survival compared with those with a lower C7 mRNA expression (**Figure 1B**). Then, C7 protein expression was examined by our IHC analysis in 331 cases of IDC, 45 cases of DCIS, and 52 cases of non-neoplastic tissues adjacent to tumor. The intensity of C7 staining was shown in representative images as **Supplementary Figure 1**. In breast tissues, C7 was mainly located in the cytoplasm of epithelial cells of mammary gland ducts. And the immunostaining of C7 was high in tumor cells but much weaker in non-neoplasm in the same section (**Figure 1C**), which was further confirmed by Western blot analysis based on frozen IDC specimens and non-neoplastic breast specimens (**Figure 1D**). In addition, C7 expression of IDC tissues was significantly higher than non-neoplastic tissues adjacent to tumor and DCIS (**Figure 1E** and **Table 1**). A total of 21.2% (11/52) of non-neoplastic tissues adjacent to tumor, 26.7% (12/45) of DCIS, and 63.7% (211/331) of IDC tissue specimens showed a high expression of C7 ($\chi^2 = 48.814$, $P < 0.001$) (**Table 1**). Moreover, our data showed that IDC patients with a high expression of C7 showed a shorter overall survival (OS) and progression-free survival (PFS) (**Figure 1F**). Altogether, these findings suggested that C7 may play as a tumor promoter in breast cancer.

High Expression of C7 Indicated Worse Prognosis in Invasive Ductal Carcinoma Patients, Especially in the Triple Negative Subtype and Luminal B Subtype.

In the following, the total 319 IDC cases were divided into two groups: triple negative subtype (49 cases) and non-triple negative subtype (270 cases). In the triple negative subtype (**Figures 2A, B**) and non-triple negative subtype (**Figures 2C, D**), both the OS and PFS of patients with a high C7 expression were significantly shorter than those with a low C7 expression. Next, Kaplan-Meier analysis was performed in non-triple negative patients with detailed classification. In the HER2-overexpression subtype

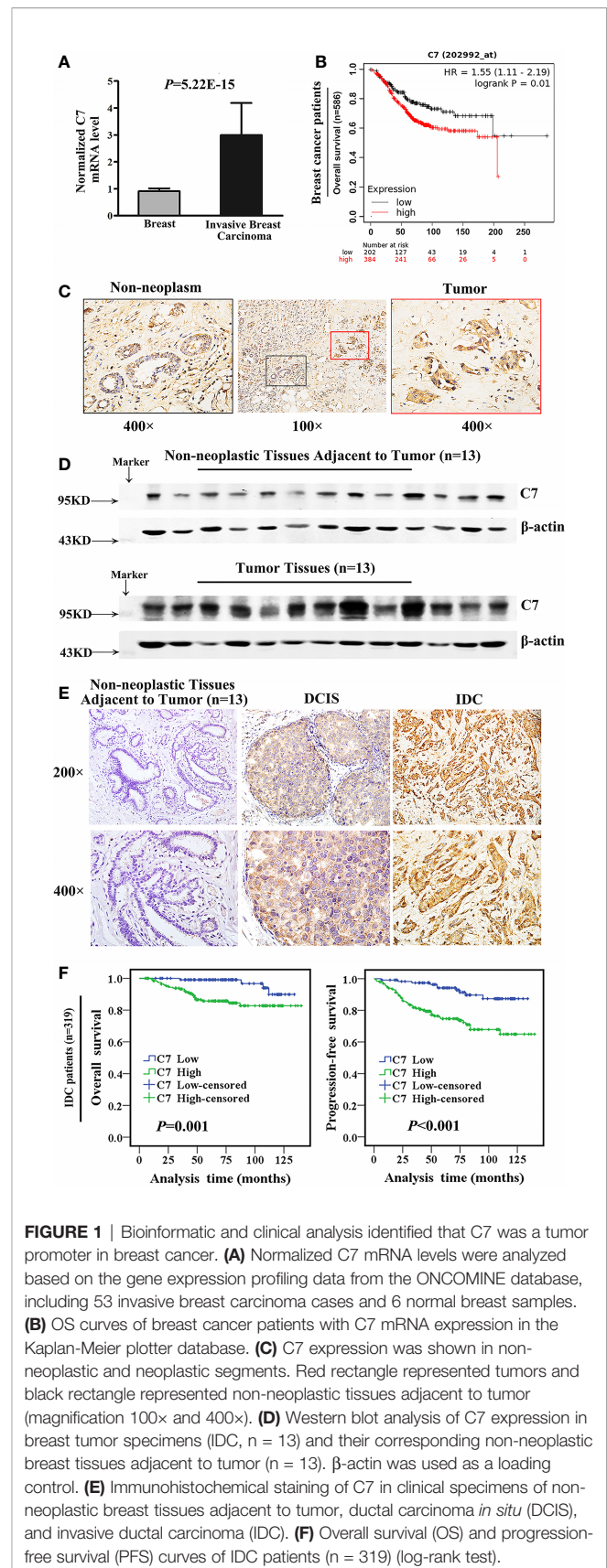


FIGURE 1 | Bioinformatic and clinical analysis identified that C7 was a tumor promoter in breast cancer. **(A)** Normalized C7 mRNA levels were analyzed based on the gene expression profiling data from the ONCOMINE database, including 53 invasive breast carcinoma cases and 6 normal breast samples. **(B)** OS curves of breast cancer patients with C7 mRNA expression in the Kaplan-Meier plotter database. **(C)** C7 expression was shown in non-neoplastic and neoplastic segments. Red rectangle represented tumors and black rectangle represented non-neoplastic tissues adjacent to tumor (magnification 100x and 400x). **(D)** Western blot analysis of C7 expression in breast tumor specimens (IDC, $n = 13$) and their corresponding non-neoplastic breast tissues adjacent to tumor ($n = 13$). β -actin was used as a loading control. **(E)** Immunohistochemical staining of C7 in clinical specimens of non-neoplastic breast tissues adjacent to tumor, ductal carcinoma *in situ* (DCIS), and invasive ductal carcinoma (IDC). **(F)** Overall survival (OS) and progression-free survival (PFS) curves of IDC patients ($n = 319$) (log-rank test).

TABLE 1 | C7 expression in different breast tissue specimens.

Histological type	n	C7 score, n (%)		χ^2	P-value ^d
		Low (0–119)	High (120–300)		
Non-neoplastic tissue ^a	52	41 (78.8)	11 (21.2)	48.814	<0.001***
DCIS ^b	45	33 (73.3)	12 (26.7)		
IDC ^c	331	120 (36.3)	211 (63.7)		

^aNon-neoplastic tissue: non-neoplastic tissues adjacent to tumor.^bDCIS: ductal carcinoma in situ.^cIDC: invasive ductal carcinoma.^dP-value was calculated by Kruskal-Wallis test.Non-neoplastic tissues vs. IDC: $P < 0.001$; DCIS vs. IDC: $P < 0.001$; Non-neoplastic tissues vs. DCIS: $P = 0.587$.*** $P < 0.001$.

($n = 34$, **Figures 2E, F**) and luminal A subtype ($n = 28$, **Figures 2G, H**), we found no correlation between C7 and the OS or PFS. However, the results showed that a high expression of C7 indicated a shorter OS ($P = 0.037$, **Figure 2I**) and PFS ($P = 0.003$, **Figure 2J**) in the luminal B subtype ($n = 208$).

C7 expression was positively correlated with lymph node metastasis ($r_s = 0.162$, $P = 0.003$) and distant metastasis ($r_s = 0.220$, $P < 0.001$) (**Table 2**). Meanwhile, we found that the expression of C7 in patients developing metastasis, recurrence, or death within 5 years (H score: 20.0–250.0, median: 150.0) was higher than those who were disease-free over the same 5 years (H score: 10.0–240.0, median: 120.0, $P = 0.002$, **Figures 3A, B**). Consistently, patients who developed metastasis, recurrence, or death within 5 years exhibited a higher percentage of C7 high expression than those who were disease-free over the same 5 years (**Figure 3C**). Then, the total IDC cases were classified into subgroups according to the molecular subtypes. In the triple negative subtype, the expression of C7 in patients developing metastasis, recurrence, or death within 5 years was higher than those who were disease-free over the same 5 years (**Figure 3D**), and the percentage of high C7 expression in patients who developed metastasis, recurrence, or death within 5 years was significantly higher than those who were disease-free over the same 5 years (**Figure 3E**). Meanwhile, there was a similar trend in the luminal subtype, whereas no such tendency was found in the HER2-overexpression subtype (**Figures 3F–K**). Moreover, in the Cox regression analysis, C7 expression was proved to be an independent prognosis factor for both the OS and PFS in 319 IDC patients (**Table 3**).

High Expression of C7 Promoted Breast Cancer Bone Metastasis.

We further explored the relationship between C7 expression and distant metastasis in IDC patients. C7 expression was weakly correlated with bone metastasis in 319 IDC cases ($r_s = 0.156$, $P = 0.005$), but there was no association between C7 expression and lung metastasis ($r_s = 0.092$, $P = 0.100$), liver metastasis ($r_s = 0.092$, $P = 0.100$), or brain metastasis ($r_s = 0.106$, $P = 0.058$, **Table 4**). Meanwhile, we noticed that the positive association between C7 and bone metastasis might be because there were more events of bone metastasis in breast cancer which made it easier to detect a positive correlation in statistics.

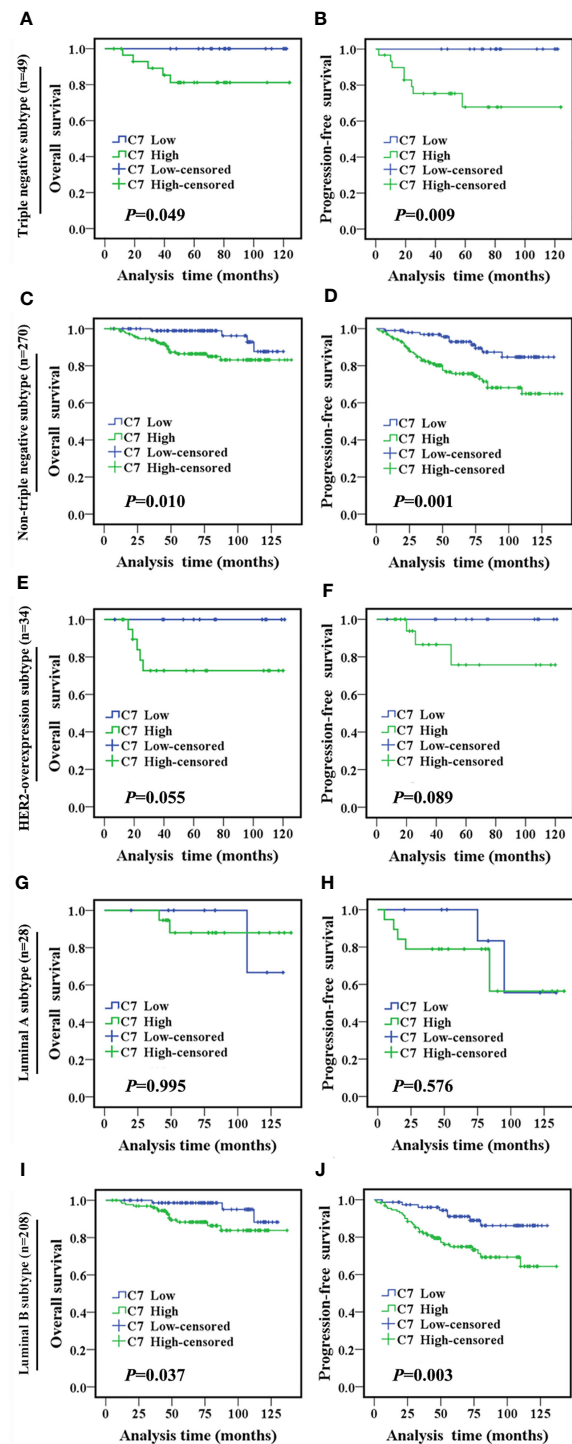


FIGURE 2 | High expression of C7 indicated a shorter survival in IDC patients, especially in the triple negative subtype and luminal B subtype. **(A, B)** OS and PFS curves of patients with triple negative subtype ($n = 49$). **(C, D)** OS and PFS curves of patients with the non-triple negative subtype ($n = 270$). **(E, F)** OS and PFS curves of patients with the HER2-overexpression subtype ($n = 34$). **(G, H)** OS and PFS curves of patients with the luminal A subtype ($n = 28$). **(I, J)** OS and PFS curves of patients with the luminal B subtype ($n = 208$). **(A–J):** log-rank test].

TABLE 2 | C7 expression and pathological features of IDC patients.

Pathological features	n	C7 score, n (%)		r_s	P-value ^e
		Low (0–119)	High (120–300)		
Age, year				0.036	0.514
<50	174	67 (38.5)	107 (61.5)		
≥50	157	55 (35.0)	102 (65.0)		
cTNM stage ^a				0.064	0.249
I	54	21 (38.9)	33 (61.1)		
II	214	83 (38.8)	131 (61.2)		
III–IV	62	18 (29.0)	44 (71.0)		
Histological grade				-0.015	0.779
I	6	1 (16.7)	5 (83.3)		
II	260	97 (37.3)	163 (62.7)		
III	65	24 (36.9)	41 (63.1)		
Tumor size, cm				0.071	0.199
<2	29	12 (41.4)	17 (58.6)		
2–5	250	95 (38.0)	155 (62.0)		
>5	52	15 (28.8)	37 (71.2)		
Lymph node metastasis				0.162	0.003**
0	124	55 (44.4)	69 (55.6)		
1–3	82	33 (50.2)	49 (59.8)		
4–9	53	17 (32.1)	36 (67.9)		
>9	72	17 (23.6)	55 (76.4)		
Distant metastasis				0.220	<0.001***
No	273	114 (41.8)	159 (58.2)		
Yes	58	8 (13.8)	50 (86.2)		
ER status ^b				0.054	0.328
Negative	127	51 (40.2)	76 (59.8)		
Positive	204	71 (34.8)	133 (65.2)		
PR status ^c				0.009	0.876
Negative	123	46 (37.4)	77 (62.6)		
Positive	208	76 (36.5)	132 (63.5)		
HER2 status ^d				0.043	0.431
Negative	219	84 (38.4)	135 (61.6)		
Positive	112	38 (33.9)	74 (66.1)		
Ki-67 status				-0.011	0.846
Negative	45	16 (35.6)	29 (64.4)		
Positive	286	106 (37.1)	180 (62.9)		

^asome missing data.^bER status: estrogen receptor status.^cPR status: progesterone receptor status.^dHER2 status: human epidermal growth factor receptor-2 status.^eP-value was calculated by Spearman's rank-correlation test.** $P < 0.01$, *** $P < 0.001$.

In order to validate the relationship between C7 expression and breast cancer bone metastasis, the total 319 IDC patients were divided into two groups: 37 cases with bone metastasis and 282 cases without bone metastasis. C7 expression in breast cancer patients with bone metastasis (median H score: 155.0) was higher than those without bone metastasis (median H score: 130.0, **Figures 4A, B**). Percentage of high C7 expression in patients who developed BM was higher than those without BM ($P = 0.005$, **Figure 4C**). Furthermore, patients with a high C7 expression showed a shorter interval time (median 26.0 months) from their diagnosis of breast cancer to bone metastasis, compared with those with a low C7 expression (median 77.0 months, $P = 0.026$, **Figure 4D**). While there was no difference in the interval time between patients with a high C7 expression from their diagnosis of breast cancer to ending and those with a low C7 expression ($P = 0.180$, **Figure 4E**). Further analysis

showed that in the triple negative subtype, patients with bone metastasis exhibited a higher C7 expression than those without bone metastasis ($P = 0.044$, **Figure 4F**). While, we did not find a similar trend in the non-triple negative subtype ($P = 0.129$, **Figure 4G**), HER2-overexpression subtype ($P = 0.287$, **Figure 4H**), or luminal B subtype ($P = 0.242$, **Figure 4I**).

High Expression of C7 Indicated a Worse Prognosis of Patients Treated With Taxane and Anthracycline-Based Chemotherapy

TE (taxane and anthracycline)-based chemotherapy is a part of the standard of care in the first line treatment of metastatic breast cancer. Then, we analyzed the relationship between C7 expression and prognosis of patients treated with conventional TE-based chemotherapy ($n = 149$), which were included in 319

IDC specimens. High expression of C7 indicated a shorter OS ($P = 0.003$, **Figure 5A**) and PFS ($P < 0.001$, **Figure 5B**) in patients treated with TE-based chemotherapy. However, no correlations

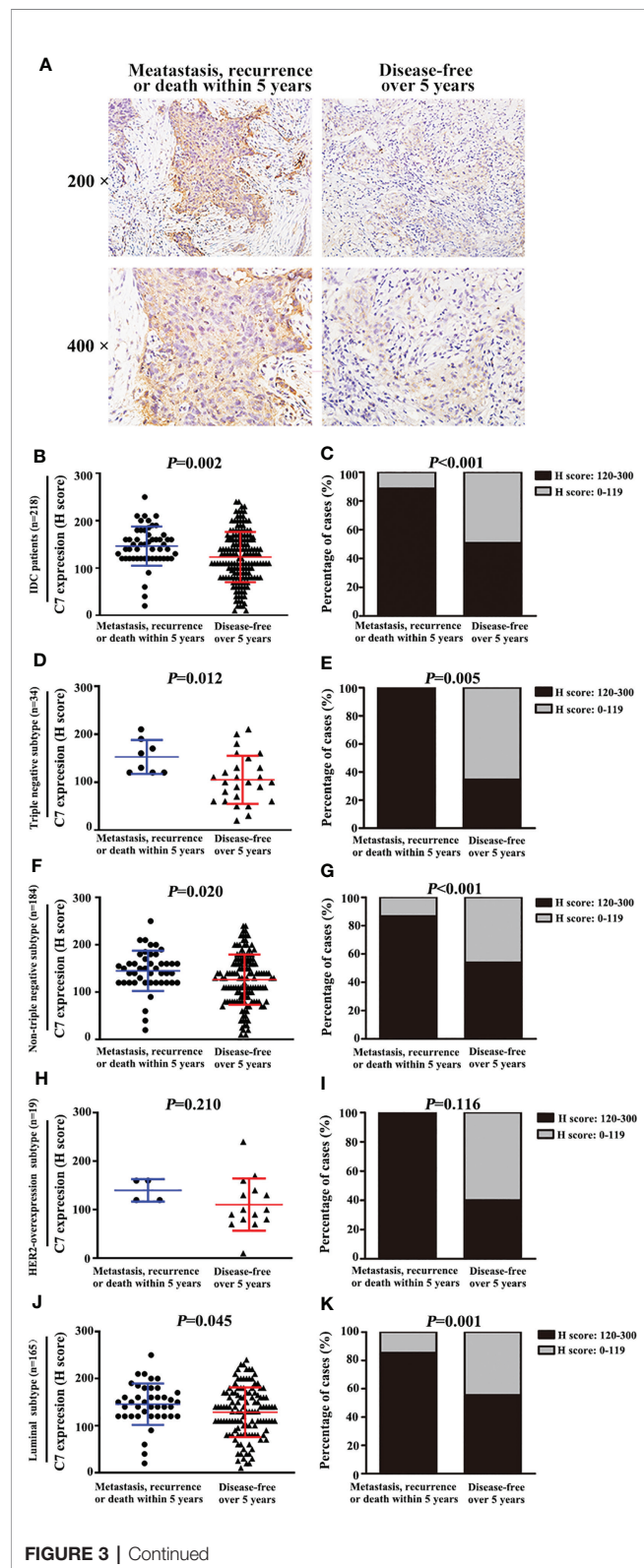


FIGURE 3 | High expression of C7 promoted breast cancer metastasis, recurrence, or death, mainly in the triple negative subtype and luminal B subtype. **(A)** Representative immunohistochemical images of C7 expression in patients who developed metastasis, recurrence, or death within 5 years and patients who were disease-free over 5 years, respectively (magnification 200× and 400×). **(B)** Among 218 IDC patients, C7 expression score in patients who developed metastasis, recurrence, or death within 5 years was higher than those who were disease-free over 5 years (Mann-Whitney U test, $P = 0.002$). **(C)** Among 218 IDC patients, 88.7% (47/53) of patients who developed metastasis, recurrence, or death within 5 years exhibited a high C7 expression, while 50.9% (84/165) of patients who were disease-free over 5 years showed a high C7 expression ($P < 0.001$). **(D, E)** In the triple negative subtype, C7 expression score (**D**) and percentage of high C7 expression (**E**) in patients who developed metastasis, recurrence, or death within 5 years was higher than those who were disease-free over 5 years. **(F, G)** In the non-triple subtype, C7 expression score (**F**) and percentage of high C7 expression (**G**) in patients who developed metastasis, recurrence, or death within 5 years was higher than those who were disease-free over 5 years. **(H, I)** In the HER2-overexpression subtype, there was no difference in the C7 expression score (**H**) or percentage of high C7 expression (**I**) between patients who developed metastasis, recurrence, or death within 5 years and those who were disease-free over 5 years in the luminal B negative subtype, but not in the HER2-overexpression subtype. **(J, K)** In the luminal subtype, C7 expression score (**J**) and percentage of high C7 expression (**K**) in patients who developed metastasis, recurrence, or death within 5 years was higher than those who were disease-free over 5 years. [(B, D, F, H, J): χ^2 test; (C, E, G, I, K): Mann-Whitney U test].

between C7 expression and the OS ($P = 0.115$, **Figure 5C**) or PFS ($P = 0.090$, **Figure 5D**) were found in 170 patients who received non-TE-based chemotherapy. Afterwards, the 149 patients treated with TE-based chemotherapy were classified into subgroups according to the molecular subtypes. The survival analysis showed that C7 expression was not associated with the survival of patients in the triple negative subtype; while a high C7 expression indicated a poor survival in the Luminal B subtype (**Figures 6A–H**).

Moreover, among the 149 patients who received TE-based chemotherapy, patients who developed metastasis, recurrence, or death within 5 years exhibited a higher C7 expression (median H score: 140) than those who were disease-free over the same 5 years (median H score: 110, $P = 0.003$, **Figures 7A, B**). Consistently, among the patients treated with TE-based chemotherapy, patients who developed metastasis, recurrence, or death within 5 years exhibited a higher percentage of C7 high expression than those who were disease-free over the same 5 years (**Table 5**). However, we did not find a similar trend in patients treated with non-TE-based chemotherapy ($P = 0.159$, **Figure 7C**). Meanwhile, among the patients who received TE-based chemotherapy, patients who developed metastasis, recurrence, or death within 5 years exhibited a higher percentage of high C7 expression in the luminal B subtype (**Figures 8A–D**).

Breast Cancer Patients With High Expression of C7 Were Insensitive to Taxane and Anthracycline Neoadjuvant Chemotherapy

Then, a cohort of patients (22 cases) treated with TE neoadjuvant chemotherapy was used to further confirm the relationship

TABLE 3 | Univariate and multivariate analysis for the overall survival (OS) and progression-free survival (PFS) in IDC patients.

Variables	OS (univariate)		OS (multivariate)		PFS (univariate)		PFS (multivariate)	
	HR (95%CI)	P	HR (95%CI)	P	HR (95%CI)	P	HR (95%CI)	P
C7 score	4.691 (1.639–13.425)	0.004	3.822 (1.316–11.098)	0.014*	3.809 (1.930–7.517)	<0.001	3.188 (1.601–6.350)	0.001**
Tumor size	1.293 (0.622–2.668)	0.492	0.718 (0.317–1.624)	0.426	2.114 (1.285–3.478)	0.003	1.270 (0.714–2.257)	0.416
Lymph node metastasis	2.208 (1.567–3.111)	<0.001	2.027 (1.405–2.924)	<0.001	1.718 (1.380–2.138)	<0.001	1.478 (1.153–1.894)	0.002
cTNM	2.045 (1.120–3.734)	0.020	1.260 (0.657–2.418)	0.487	2.296 (1.492–3.535)	<0.001	1.341 (0.803–2.240)	0.261

* $P < 0.05$, ** $P < 0.01$.**TABLE 4 |** Relationship between C7 expression and distant metastasis in IDC patients.

Distant metastasis	n	C7 score, n (%)		r_s	P-value ^a
		Low (0–119)	High (120–300)		
Bone metastasis				0.156	0.005**
No	282	112 (39.7)	170 (60.3)		
Yes	37	6 (16.2)	31 (83.8)		
Lung metastasis				0.092	0.100
No	306	116 (37.9)	190 (62.1)		
Yes	13	2 (15.4)	11 (84.6)		
Liver metastasis				0.092	0.100
No	306	116 (37.9)	190 (62.1)		
Yes	13	2 (15.4)	11 (84.6)		
Brain metastasis				0.106	0.058
No	313	118 (37.7)	295 (62.3)		
Yes	6	0 (0.0)	6 (100)		

^aP-value was calculated by Spearman's rank-correlation test.** $P < 0.01$.

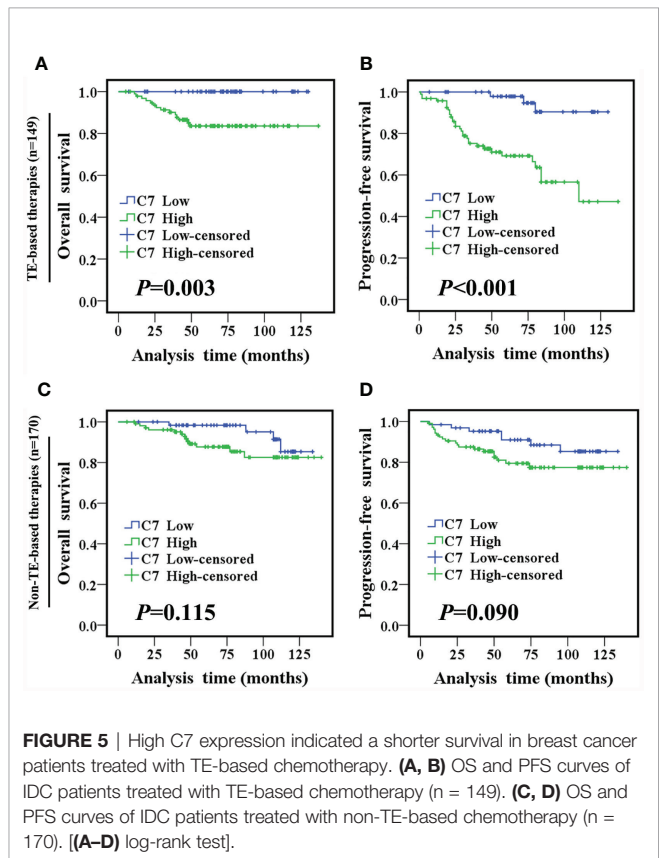
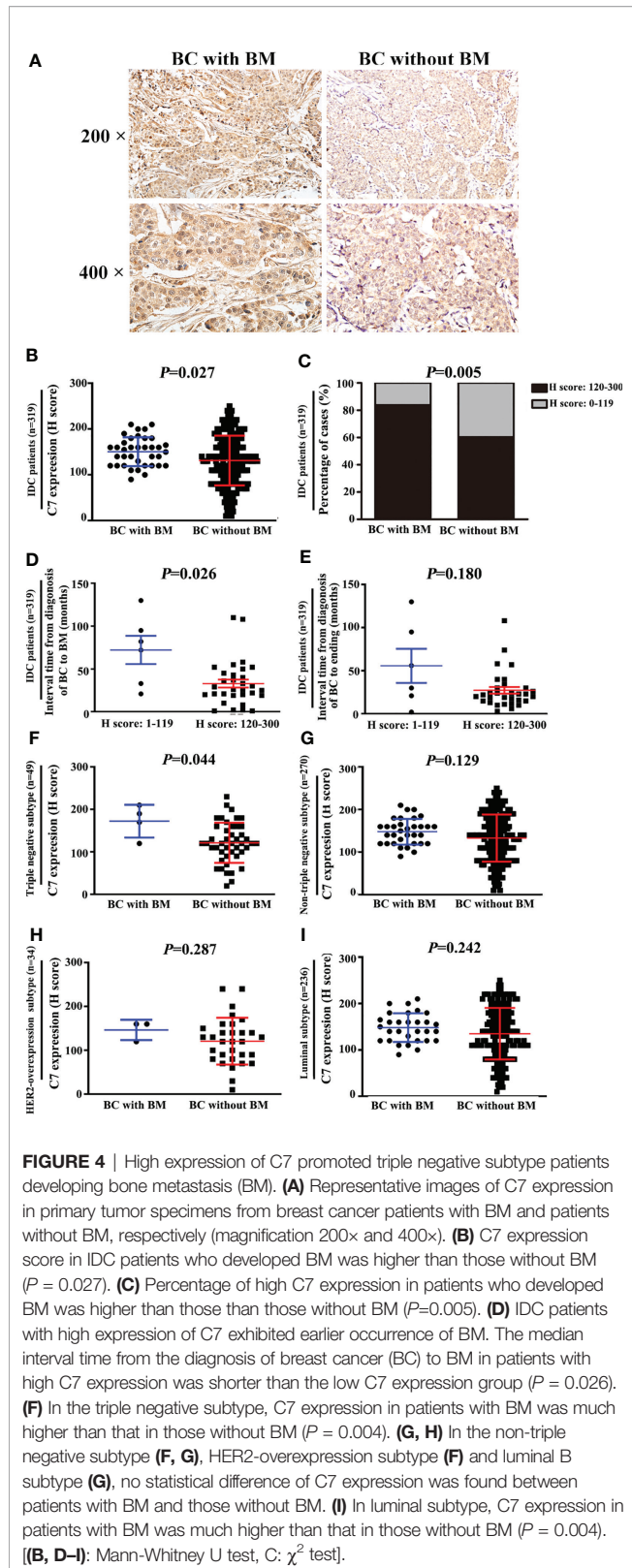
between C7 expression and TE-based chemosensitivity. The 22 patients were divided into two groups: positive pathological response group (15 cases) and negative pathological response group (7 cases). We found that C7 expression in the negative pathological response group (H score: 20 to 190, median: 80) was higher than that in the positive pathological response group (H score: 0–100, median: 40, $P = 0.047$, **Figures 9A, B**).

Gene Set Enrichment Analysis of C7 in The Cancer Genome Atlas Database

To further gain insights into the mechanisms of the role of C7 in breast cancer progression, the analysis of the RNA-seq data of 817 breast cancer patients of the Cancer Genome Atlas (TCGA) was performed. Genes in high and low C7 expression patients were enriched by using the GSEA software for Kyoto Encyclopedia of Genes (KEGG) and Genomes pathway and Gene Ontology (GO) functional enrichment analysis. KEGG analysis suggested that changes were significantly enriched in the “VEGF signaling pathway”, “MAPK signaling pathway”, and “JAK stat signaling pathway” (**Supplementary Figure S2A**). GO analysis showed that changes in the biological process (BP) term were significantly enriched in “positive regulation of MAPK cascade”, “ERK1 and ERK2 cascade”, and “regulation of BMP signaling pathway” (**Supplementary Figure S2B**). It suggested that C7 may promote breast cancer progression by activating the VEGF, MAPK, or JAK stat signaling pathways, and also, C7

promoting breast cancer bone metastasis may be mediated by the bone morphogenetic protein (BMP) signaling pathway.

As well as known, anthracyclines interfere at the interface of Topo II-DNA with their sugar moieties and the cyclohexane ring A, which ultimately results in enzyme-mediated DNA damage in the form of double strand break (DSB) (14, 15). Taxane is a microtubule-stabilizing agent that impairs the proper assembly of mitotic spindles, leading to mitotic arrest and mis-segregation of chromosomes (16). GO analysis suggested that changes in the BP term were significantly enriched in DNA repair and microtubule associated process, such as “regulation DNA repair”, “recombination of DNA repair”, “positive regulation of DNA repair”, “double strand DNA repair”, “microtubule organizing center organization”, “microtubule organizing center localization”, “microtubule cytoskeleton organization involved in mitosis”, and “microtubule-based movement” (**Supplementary Figure S2B**). Changes in the cellular component (CC) term were significantly enriched in “site of damage”, “microtubule”, “microtubule associated complex”, and “DNA repair complex” (**Supplementary Figure S2C**). Changes in the molecular function (MF) term were also significantly enriched in “microtubule motor activity”, “microtubule binding”, “ATP dependent microtubule motor activity”, and “DNA replication origin binding” (**Supplementary Figure S2D**). These results revealed that C7 may regulate the sensitivity of TE-based chemotherapy by affecting DNA repair and microtubule associated process.



DISCUSSION

Our study investigated the clinical and prognostic effects of C7 in breast cancer for the first time. C7 expression of IDC tissues was higher than non-neoplastic tissues adjacent to tumor and DCIS. Moreover, C7 was an independent prognosis factor and a high expression of C7 indicated a poor prognosis of IDC patients. These observations indicated that C7 may act as a tumor promoter, consistent with the study by Saijoh about the role of C7 in ovarian cancer (11). Our further study showed that a high expression of C7 promoted breast cancer bone metastasis. Firstly, we noticed that there was a weak association between C7 and bone metastasis, but there was no difference between C7 expression and lung metastasis, liver metastasis, or brain metastasis (Table 4). In fact, the most common site of breast cancer metastasis is the bone, occurring in about 70% of patients with metastatic breast cancer (17, 18). Consistently, in our cohort, patients with bone metastasis were more than those with lung metastasis, liver metastasis, and brain metastasis, respectively. In order to validate the relationship between C7 expression and breast cancer bone metastasis, the total 319 IDC patients were divided into two groups: 37 cases with bone metastasis and 282 cases without bone metastasis. C7 expression in breast cancer patients

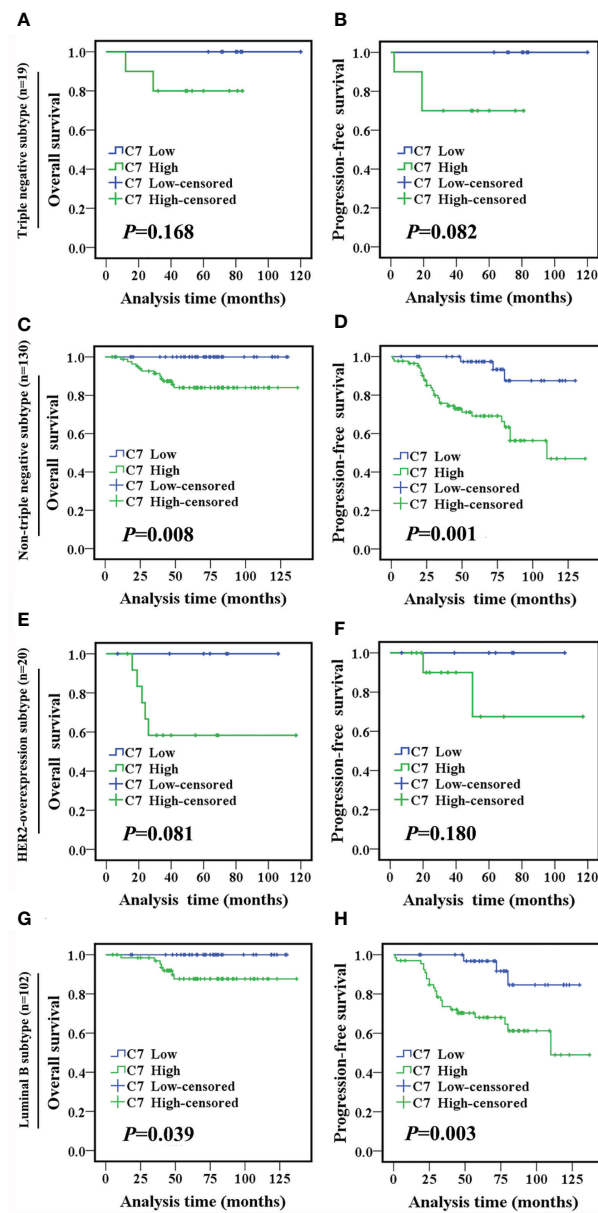


FIGURE 6 | High C7 expression indicated a shorter survival in breast cancer patients treated with TE-based chemotherapy, especially in the luminal B subtype. **(A, B)** OS and PFS curves of triple negative subtype patients who received TE-based chemotherapy (n = 19). **(C, D)** OS and PFS curves of non-triple negative subtype patients who received TE-based chemotherapy (n = 130). **(E, F)** OS and PFS curves of the HER2-overexpression subtype patients who received TE-based chemotherapy (n = 20). **(G, H)** OS and PFS curves of luminal B subtype patients who received TE-based chemotherapy (n = 102). **[(A–H):** log-rank test].

with bone metastasis was higher than those without bone metastasis (**Figures 4A, B**). Furthermore, patients with a high C7 expression showed a shorter interval time from their diagnosis of breast cancer to bone metastasis, compared with those with a low C7 expression (**Figure 4C**). Altogether, these results suggested that a high expression of C7 promoted breast cancer bone metastasis, but further *in vitro* and *in vivo* investigations are needed to confirm these findings.

Although emerging evidence showed the role of C7 in several malignances, little research focused on the mechanism of C7 function in tumor progression. In our present study, KEGG and GO enrichment analysis suggested that C7 may promote breast cancer progression by activating the VEGF, MAPK, or JAK stat signaling pathways. According to these clues, we will perform *in vitro* and *in vivo* assays to confirm the exact mechanism of C7 in breast cancer progression in the further study.

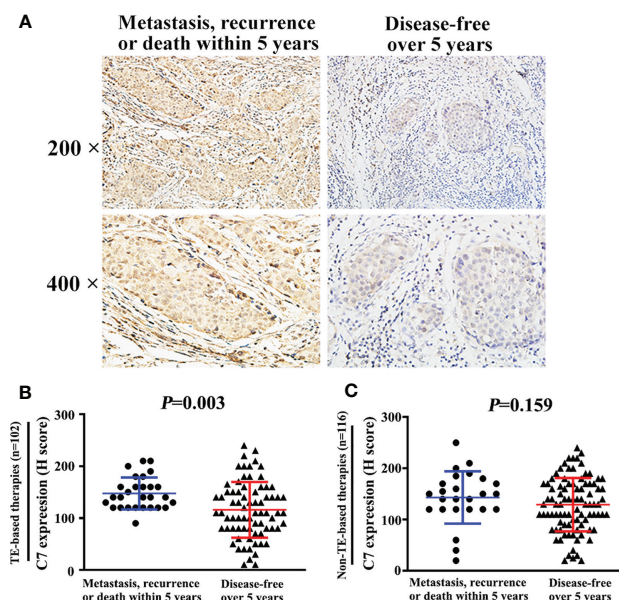


FIGURE 7 | High expression of C7 promoted breast cancer progression in patients treated with TE-based chemotherapy. **(A)** Among 102 patients treated with TE-based chemotherapy, representative images of C7 expression in patients who developed metastasis, recurrence, or death within 5 years and patients who were disease-free over 5 years, respectively (magnification 200× and 400×). **(B)** Among TE-based chemotherapy-treated patients, C7 expression in patients who developed metastasis, recurrence, or death within 5 years was higher than those who were disease-free over 5 years. **(C)** Among non-TE-based chemotherapy-treated cases, no significant difference of C7 expression was found in patients who developed metastasis, recurrence, or death within 5 years and those who were disease-free over 5 years. **[(B, C):** Mann-Whitney U test].

TABLE 5 | Relationship between C7 expression and prognosis of IDC patients treated with TE chemotherapy.

	n	C7 score, n (%)		r_s	P-value ^a
		Low (0–119)	High (120–300)		
Metastasis, recurrence or death within 5 years	28	1 (3.6)	27 (96.4)	-0.459	<0.001***
Disease-free over 5 years	74	40 (54.1)	34 (45.9)		

^aP-value was calculated by Spearman's Rank-Correlation test.

***P < 0.001.

In fact, C7, as a single molecule, may play limited roles in tumor progression. Various studies showed that the membrane attack complex, which is composed of C5b–9 (C5b, C6, C7, C8, C9), could induce the activation of several tumorigenesis signal transduction pathways, including the MAPK family, PKC signaling, Gi protein/PI3K/Akt pathway, and Ras/Raf/ERK1 pathway (19–21). In addition, the sublytic effects of C5b–9 involved cell cycle activation, accomplished by affecting main cell cycle kinases and regulators, such as CDK4, CDK2, p21, CDC2, cyclin D1, and PCNA (22, 23). Moreover, sublytic C5b–9 had an antiapoptotic effect by regulating the phosphorylation of FOXO1 and Bad, and inhibiting the activation of Bid, caspase-8, and NF-κB (24–27). Therefore, it should be better to detect other components, such as C5b, C6, C8, and C9, to provide a more comprehensive information to reveal the roles of the complement in breast cancer progression.

TE-based chemotherapy is a part of the standard of care in the first line treatment of metastatic breast cancer and its clinical use is widespread (28). However, only about 15% patients could achieve pathologic complete response. Therefore, a more detailed classification is necessary to screen a more suitable population to TE chemotherapy (29). A previous study reported that the level of complement C3 α1 (an isoform of cleaved C3 α-chain and a complement activation marker) in breast cancer patients was increased in TE-chemotherapy responders compared with non-responders. The possible explanation may be TE-based chemotherapy induced tumor cells apoptosis to activate the complement system (30). Although the main complement system activation pathways generate C3 convertases efficiently cleaving C3 into C3a and C3b, killing targeted cells finally requires the terminal C5b–9 MAC (membrane attack complex) (31). Therefore, detecting the level of MAC components in breast cancer patients is more reasonable to predict the chemosensitivity.

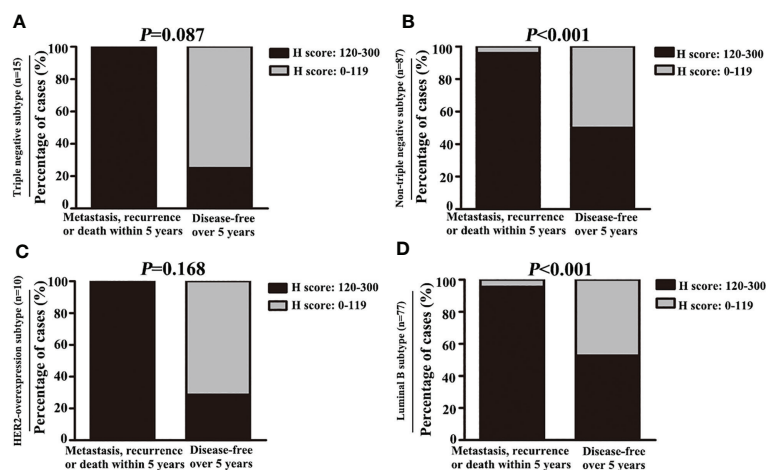


FIGURE 8 | High expression of C7 promoted disease progression in luminal B subtype patients treated with TE-based chemotherapy. **(A, B)** Among patients treated with TE-based chemotherapy, the percentage of high C7 expression in patients who developed metastasis, recurrence, or death within 5 years was higher than those who were disease-free over 5 years in the non-triple negative subtype **(B)**, but not in the triple negative subtype **(A)**. **(C, D)** Among patients treated with TE-based chemotherapy, the percentage of high C7 expression in patients who developed metastasis, recurrence, or death within 5 years was higher than those who were disease-free over 5 years in the luminal B subtype **(D)**, but not in the HER2 overexpression subtype **(C)**. [(A–D): χ^2 test].

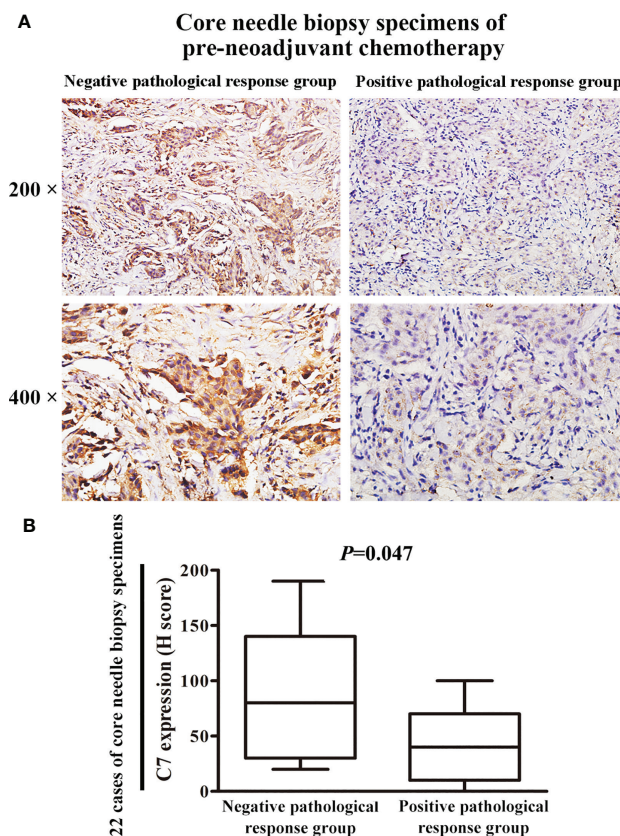


FIGURE 9 | Patients with high C7 expression were insensitive to TE neoadjuvant chemotherapy. **(A)** Representative immunohistochemical images of C7 expression in both positive and negative pathological response groups, respectively (magnification 200x and 400x). **(B)** C7 expression in the negative pathological response group ($n = 7$) was higher than the positive pathological response group ($n = 15$, Mann-Whitney U test, $P = 0.047$).

CONCLUSIONS

Taken together, our study provided the first evidence that C7 expression was an independent prognosis factor in IDC patients. High expression of C7 indicated poor prognosis, especially in the triple negative subtype and luminal B subtype. C7 high expression promoted breast cancer to develop bone-specific metastasis, mainly in the triple negative subtype. Furthermore, patients with high C7 expression were insensitive to TE-based chemotherapy. These findings highlight the importance of C7 in breast cancer progression and lay a foundation to help clinicians improve the identification of patients for TE chemotherapy by C7 in the era of precision medicine.

DATA AVAILABILITY STATEMENT

The raw data supporting the conclusions of this article will be made available by the authors, without undue reservation.

ETHICS STATEMENT

This study was approved by the Institutional Ethics Committee of Tianjin Medical University Cancer Institute and Hospital. The patients/participants provided their written informed consent to participate in this study. Written informed consent was obtained from the individual(s) for the publication of any potentially identifiable images or data included in this article.

REFERENCES

1. Sung H, Ferlay J, Siegel RL, Laversanne M, Soerjomataram I, Jemal A, et al. Global Cancer Statistics 2020: GLOBOCAN Estimates of Incidence and Mortality Worldwide for 36 Cancers in 185 Countries. *CA Cancer J Clin* (2021) 71(3):209–49. doi: 10.3322/caac.21660
2. Lei S, Zheng R, Zhang S, Chen R, Wang S, Sun K, et al. Breast Cancer Incidence and Mortality in Women in China: Temporal Trends and Projections to 2030. *Cancer Biol Med* (2021) 18(3):900–9. doi: 10.20892/j.issn.2095-3941.2020.0523
3. Sun D, Li H, Maomao C, He S, Lei L, Peng J, et al. Cancer Burden in China: Trends, Risk Factors and Prevention. *Cancer Biol Med* (2020) 17(4):879–95. doi: 10.20892/j.issn.2095-3941.2020.0387
4. Dai X, Xiang L, Li T, Bai Z. Cancer Hallmarks, Biomarkers and Breast Cancer Molecular Subtypes. *J Cancer* (2016) 7(10):1281–94. doi: 10.7150/jca.13141
5. Carroll MC. The Complement System in Regulation of Adaptive Immunity. *Nat Immunol* (2004) 5:981–6. doi: 10.1038/ni1113
6. Ricklin D, Hajishengallis G, Yang K, Lambris JD. Complement: A Key System for Immune Surveillance and Homeostasis. *Nat Immunol* (2010) 11:785–97. doi: 10.1038/ni.1923
7. DiScipio RG, Chakravarti DN, Muller-Eberhard HJ, Fey GH. The Structure of Human Complement Component C7 and the C5b-7 Complex. *J Biol Chem* (1988) 263:549–60. doi: 10.1016/S0021-9258(19)57427-0
8. Podack ER, Tschopp J. Membrane Attack by Complement. *Mol Immunol* (1984) 21:589–603. doi: 10.1016/0161-5890(84)90044-0
9. Oka R, Sasagawa T, Ninomiya I, Miwa K, Tanii H, Saijoh K. Reduction in the Local Expression of Complement Component 6 (C6) and 7 (C7) mRNAs in Oesophageal Carcinoma. *Eur J Cancer* (2001) 37:1158–65. doi: 10.1016/S0959-8049(01)00089-2

AUTHOR CONTRIBUTIONS

HZ performed the data analysis, prepared the figures, and wrote the manuscript. YZ contributed to the immunohistochemistry experiments. XL performed the Western blot experiments. LF and FG collected the patient samples and interpreted the data. YM designed the research and wrote the manuscript. All authors contributed to the article and approved the submitted version.

FUNDING

This work was supported by the Scientific Research Program of Tianjin Municipal Education Commission from HZ (2020KJ130).

ACKNOWLEDGMENTS

The authors would like to acknowledge Mrs. Xiaojiao Chen and Mrs. Jing Xu for their help in preparing the paraffin specimens for this study.

SUPPLEMENTARY MATERIAL

The Supplementary Material for this article can be found online at: <https://www.frontiersin.org/articles/10.3389/fonc.2021.724250/full#supplementary-material>

10. Ying L, Zhang F, Pan X, Chen K, Zhang N, Jin J, et al. Complement Component 7 (C7), a Potential Tumor Suppressor, Is Correlated With Tumor Progression and Prognosis. *Oncotarget* (2016) 7:86536–46. doi: 10.18632/oncotarget.13294
11. Suryawanshi S, Huang X, Elishaev E, Budiu RA, Zhang L, Kim S, et al. Complement Pathway Is Frequently Altered in Endometriosis and Endometriosis-Associated Ovarian Cancer. *Clin Cancer Res* (2014) 20:6163–74. doi: 10.1158/1078-0432.CCR-14-1338
12. Seol HS, Lee SE, Song JS, Rhee JK, Singh SR, Chang S, et al. Complement Proteins C7 and CFH Control the Stemness of Liver Cancer Cells via LSF-1. *Cancer Lett* (2016) 372:24–35. doi: 10.1016/j.canlet.2015.12.005
13. Ogston KN, Miller ID, Payne S, Hutcheon AW, Sarkar TK, Smith I, et al. A New Histological Grading System to Assess Response of Breast Cancers to Primary Chemotherapy: Prognostic Significance and Survival. *Breast* (2003) 12:320–7. doi: 10.1016/S0960-9776(03)00106-1
14. Tewey KM, Rowe TC, Yang L, Halligan BD, Liu LF. Adriamycin-Induced DNA Damage Mediated by Mammalian DNA topoisomerase-II. *Science* (1984) 226:466–8. doi: 10.1126/science.6093249
15. Tewey KM, Chen GL, Nelson EM, Liu LF. Intercalative Antitumor Drugs Interfere With the Breakage-Reunion Reaction of Mammalian DNA Topoisomerase-II. *J Biol Chem* (1984) 259:9182–7. doi: 10.1016/S0021-9258(17)47282-6
16. Weaver BA. How Taxol/paclitaxel Kills Cancer Cells. *Mol Biol Cell* (2014) 25:2677e81. doi: 10.1091/mbc.e14-04-0916
17. Brook N, Brook E, Dharmarajan A, Dass CR, Chan A. Breast Cancer Bone Metastases: Pathogenesis and Therapeutic Targets. *Int J Biochem Cell Biol* (2018) 96:63–78. doi: 10.1016/j.biocel.2018.01.003
18. Clément-Demange L, Clézardin P. Emerging Therapies in Bone Metastasis. *Curr Opin Pharmacol* (2015) 22:79–86. doi: 10.1016/j.coph.2015.04.004

19. Niculescu F, Badea T, Rus H. Sublytic C5b-9 Induces Proliferation of Human Aortic Smooth Muscle Cells: Role of Mitogen Activated Protein Kinase and Phosphatidylinositol 3-Kinase. *Atherosclerosis* (1999) 142:47–56. doi: 10.1016/S0021-9150(98)00185-3
20. Niculescu F, Rus H. Mechanisms of Signal Transduction Activated by Sublytic Assembly of Terminal Complement Complexes on Nucleated Cells. *Immunol Res* (2001) 24:191–9. doi: 10.1385/IR.24:2:191
21. Niculescu F, Rus H, van Biesen T, Shin ML. Activation of Ras and Mitogen-Activated Protein Kinase Pathway by Terminal Complement Complexes Is G Protein Dependent. *J Immunol* (1997) 158:4405–12.
22. Fosbrink M, Niculescu F, Rus H. The Role of C5b-9 Terminal Complement Complex in Activation of the Cell Cycle and Transcription. *Immunol Res* (2005) 31:37–46. doi: 10.1385/IR.31:1:37
23. Vlaicu SI, Teglă CA, Cudrici CD, Danoff J, Madani H, Sugarman A, et al. Role of C5b-9 Complement Complex and Response Gene to Complement-32 (RGC-32) in Cancer. *Immunol Res* (2013) 56:109–21. doi: 10.1007/s12026-012-8381-8
24. Fosbrink M, Niculescu F, Rus V, Shin ML, Rus H. C5b-9-Induced Endothelial Cell Proliferation and Migration Are Dependent on Akt Inactivation of Forkhead Transcription Factor FOXO1. *J Biol Chem* (2006) 281:19009–18. doi: 10.1074/jbc.M602055200
25. Soane L, Cho HJ, Niculescu F, Rus H, Shin ML. C5b-9 Terminal Complement Complex Protects Oligodendrocytes From Death by Regulating Bad Through Phosphatidylinositol 3-Kinase/Akt Pathway. *J Immunol* (2001) 167:2305–11. doi: 10.4049/jimmunol.167.4.2305
26. Cudrici C, Niculescu F, Jensen T, Zafranskaia E, Fosbrink M, Rus V, et al. C5b-9 Terminal Complex Protects Oligodendrocytes From Apoptotic Cell Death by Inhibiting Caspase-8 Processing and Up-Regulating FLIP. *J Immunol* (2006) 176:3173–80. doi: 10.4049/jimmunol.176.5.3173
27. Liu L, Li W, Li Z, Kirschfink M. Sublytic Complement Protects Prostate Cancer Cells From Tumour Necrosis Factor-Alpha-Induced Cell Death. *Clin Exp Immunol* (2012) 169:100–8. doi: 10.1111/j.1365-2249.2012.04596.x
28. Giordano SH, Buzdar AU, Smith TL, Kau SW, Yang Y, Hortobagyi GN. Is Breast Cancer Survival Improving? *Cancer* (2004) 100:44–52. doi: 10.1002/cncr.11859
29. Dai K, Qin F, Zhang H, Liu X, Guo C, Zhang M, et al. Low Expression of BMPRII Indicates Poor Prognosis of Breast Cancer and Is Insensitive to Taxane-Anthracycline Chemotherapy. *Oncotarget* (2016) 7:4770–84. doi: 10.18632/oncotarget.6613
30. Michlmayr A, Bachleitner-Hofmann T, Baumann S, Marchetti-Deschmann M, Rech-Weichselbraun I, Burghuber C, et al. Modulation of Plasma Complement by the Initial Dose of Epirubicin/Docetaxel Therapy in Breast Cancer and Its Predictive Value. *Br J Cancer* (2010) 103:1201–8. doi: 10.1038/sj.bjc.6605909
31. Muller-Eberhard HJ. The Membrane Attack Complex of Complement. *Annu Rev Immunol* (1986) 4:503–28. doi: 10.1146/annurev.iy.04.040186.002443

Conflict of Interest: The authors declare that the research was conducted in the absence of any commercial or financial relationships that could be construed as a potential conflict of interest.

Publisher's Note: All claims expressed in this article are solely those of the authors and do not necessarily represent those of their affiliated organizations, or those of the publisher, the editors and the reviewers. Any product that may be evaluated in this article, or claim that may be made by its manufacturer, is not guaranteed or endorsed by the publisher.

Copyright © 2021 Zhang, Zhao, Liu, Fu, Gu and Ma. This is an open-access article distributed under the terms of the Creative Commons Attribution License (CC BY). The use, distribution or reproduction in other forums is permitted, provided the original author(s) and the copyright owner(s) are credited and that the original publication in this journal is cited, in accordance with accepted academic practice. No use, distribution or reproduction is permitted which does not comply with these terms.



Which Clinicopathologic Parameters Suggest Primary Resistance to Palbociclib in Combination With Letrozole as the First-Line Treatment for Hormone Receptor-Positive, HER2-Negative Advanced Breast Cancer?

Ji-Yeon Kim¹, Jung Min Oh², Yeon Hee Park¹, Jin Seok Ahn¹ and Young-Hyuck Im^{1,2*}

OPEN ACCESS

Edited by:

Maria Rosaria De Miglio,
University of Sassari, Italy

Reviewed by:

Norikazu Masuda,
Osaka National Hospital (NHO), Japan
Sung Gwe Ahn,
Yonsei University Health System,
South Korea

*Correspondence:

Young-Hyuck Im
imyh00@skku.edu

Specialty section:

This article was submitted to
Breast Cancer,
a section of the journal
Frontiers in Oncology

Received: 16 August 2021

Accepted: 27 September 2021

Published: 21 October 2021

Citation:

Kim J-Y, Oh JM, Park YH, Ahn JS and
Im Y-H (2021) Which Clinicopathologic
Parameters Suggest Primary
Resistance to Palbociclib in
Combination With Letrozole as the
First-Line Treatment for Hormone
Receptor-Positive, HER2-Negative
Advanced Breast Cancer?
Front. Oncol. 11:759150.
doi: 10.3389/fonc.2021.759150

¹ Division of Hematology-Oncology, Department of Medicine, Samsung Medical Center, Sungkyunkwan University School of Medicine, Seoul, South Korea, ² Biomedical Research Institute, Samsung Medical Center, Sungkyunkwan University School of Medicine, Seoul, South Korea

In this study, we evaluated clinical parameters to predict the primary resistance of palbociclib in combination with endocrine therapy as the first-line treatment in patients with hormone receptor (HR)+, human epidermal growth factor receptor 2 (HER2)-metastatic breast cancer (MBC). We performed a data analysis of patients diagnosed with HR+, HER2-MBC who received palbociclib plus letrozole as the first-line treatment in the metastatic setting from the clinical data warehouse in Samsung Medical Center. In this study, 305 patients were included in the final data analysis. The median follow-up duration was 31 months, and we observed 123 cases of disease progression. The median progression-free survival (PFS) was 28.7 months, and 38 patients (12.5%) had less than a 6-month PFS. The multivariate analysis suggested that primary resistance to adjuvant endocrine therapy (ET) (hazard ratio: 1.91), presence of liver metastasis (hazard ratio: 2.17), initial elevation of serum CA-15-3 (hazard ratio: 1.99), weak positivity of estrogen receptor (ER) (hazard ratio: 2.28), Ki-67 3+ or 4+ (hazard ratios: 2.58 and 10.28), and presence of mutation (hazard ratio: 9.59) were associated with a short PFS duration. A further prediction model was developed with data from 256 patients and 33 cases of disease progression in 6 months. This model included five factors—primary resistance to adjuvant ET (odds ratio, OR: 1.14), liver metastasis (OR: 1.56), initial CA-15-3 elevation (OR: 1.51), weak ER expression (OR: 2.22), and BRCA2 mutation (OR: 2.85)—and the area under the receiver operating characteristic curve was 0.842 (95% CI: 0.775, 0.909; $p < 0.001$). Finally, we divided them into four risk groups according to the prediction model with the five risk factors. These four groups had different PFS ($p < 0.001$) and primary resistance of palbociclib with letrozole [OR of group 2 vs. group 1 (ref): 2.18 ($p = 0.002$), OR of group 3: 3.91 ($p < 0.001$), and OR of group 4: 4.25 ($p < 0.001$)]. We developed a

prediction model of primary resistance to palbociclib with letrozole as the first-line treatment for HR+, HER2-MBC. Our prediction model might be helpful for considering the first-line treatment strategies. Further well-designed clinical trials would be warranted to validate our prediction model.

Keywords: metastatic breast cancer (MBC), hormone receptor positive (HR+), first line, CDK4/6 inhibitor, primary resistance

INTRODUCTION

Hormone receptor (HR)+, human epidermal growth factor 2 (HER2)-breast cancer (BC) is the most commonly diagnosed subset of BC, accounting for 60–70% of all cases (1, 2). Endocrine therapy (ET) is the standard strategy as the initial therapy for metastatic disease in HR+, HER2-BC, even in the presence of visceral metastases, unless visceral crisis is present (3, 4).

Cyclin-dependent kinases (CDKs) play an important role in cell cycle regulation. Cyclin D1, the binding partner of CDK4/6, is often overexpressed in patients with HR+, HER2-BC, leading to the continuous activation of the cyclin D1–CDK4/6 complex (5). The interaction of cyclin D1 with CDK4/6 facilitates the hyperphosphorylation of retinoblastoma (Rb), leading to cell cycle progression through the G1 checkpoint into the S phase (6, 7). Large prospective clinical trials consistently indicate that CDK4/6 inhibitors, in combination with ET, significantly prolong the duration of progression-free survival (PFS) for HR+, HER2-metastatic BC (MBC) (8–13). Moreover, CDK4/6 inhibitors, in combination with ET, demonstrated a benefit in HR+, HER2-MBC overall survival (OS) (14, 15). The development of CDK 4/6 inhibitors has changed the paradigm of HR+, HER2-MBC management. Palbociclib, ribociclib, and abemaciclib, all orally active, highly selective, and reversible inhibitors of CDK4/6, have been approved by the Food and Drug Administration (FDA) for the treatment of HR+, HER2-MBC in combination with ET (7, 16). The current treatment guidelines suggest the combination of CDK4/6 inhibitors with ET to be the first- or second-line treatment for HR+, HER2-MBC unless visceral crisis is present (3, 4).

Despite the widespread use of CDK4/6 inhibitors in HR+, HER2-advanced BC, their efficacy with ET may be limited by the development of *de novo* or acquired resistance. Previous clinical trials showed that approximately 10% of patients with advanced HR+, HER2-BC receiving the first-line treatment consisting of CDK4/6 inhibitors with ET had less than 6 months of PFS, suggesting primary endocrine resistance (8–10). There have been many efforts to unveil the molecular mechanisms of endocrine resistance, including ESR1 mutations, RB1 mutation, overactivation of CDK 4/6, epigenetic alterations, activation of the mammalian target of rapamycin signaling pathway, inactivation of the Hippo pathway including FAT1 loss and YAP activation, and the alterations of somatic genes, such as PIK3KA, FGFR1, and AKT1 (17–23). At present, there are no known biomarkers for primary resistance in patients with HR+, HER2-advanced BC who undergo CDK 4/6 inhibitors with ET as the first-line treatment. Therefore, a new strategy to evaluate the

primary resistance of CDK 4/6 inhibitors with ET as the first-line treatment was needed.

In this study, we aimed to evaluate the clinical parameters to predict the primary resistance of the first-line treatment consisting of palbociclib in combination with ET in patients with HR+, HER2-MBC.

PATIENTS AND METHODS

Patients

We performed a data analysis of anonymized electronic medical records from the clinical data warehouse (CDW) in Samsung Medical Center (SMC). First, we extracted the data of patients who were treated with palbociclib plus aromatase inhibitor from the CDW, and then we excluded the patients who were not treated as the first-line treatment. Finally, data of patients diagnosed with HR+, HER2-MBC who received palbociclib plus an aromatase inhibitor (AI) as the first-line treatment in the metastatic setting at SMC were analyzed. The diagnostic studies for MBC included chest and abdomino-pelvic computed tomography (CT), bone scan or positron emission tomography–CT, and brain magnetic resonance imaging, if indicated, as well as histologic and immunohistochemical (IHC) examinations when the disease recurred during or after adjuvant ET or *de novo*. This study was reviewed and approved by the Institutional Review Board (IRB) of Samsung Medical Center, Seoul, South Korea (IRB no. 2021-07-131). This study was performed in accordance with the Declaration of Helsinki and the Good Clinical Practice guidelines. The requirement for informed consent was waived due to the use of de-identified medical records with clinical data.

Breast Cancer Pathology

Histologic evaluation with hematoxylin and eosin (H&E) staining and estrogen receptor (ER), progesterone receptor (PgR), and HER2 statuses by IHC staining of MBC were assessed by at least two experienced pathologists. ER and PgR positivity were defined as Allred scores in the range of 3–8 according to IHC staining with anti-ER (Immunotech, France) and anti-PgR (Novocastra, UK) antibodies, respectively. HER2 status was evaluated using the appropriate antibody staining (DAKO, CA) or silver *in situ* hybridization (SISH). HER2 grades of 0 and 1 were defined as negative results, while grade 3 was identified as a positive result. HER2 amplification was confirmed by SISH results of 2+. In terms of Ki-67, the pathologists performed their assessment by IHC on the Ventana Discovery autostainer using the MIB-1 antibody as previously

described; (24). We divided the histologic data into four groups based on the level of Ki-67 expression for further analysis: 1+ (0–25%), 2+ (25–50%), 3+ (50–75%), and 4+ (75–100%). Histologic grade and nuclear grade were also evaluated by Bloom–Richardson grading and the World Health Organization grading system, respectively (25).

Statistical Analysis

PFS was defined as the elapsed time from the first day of palbociclib with letrozole treatment as the first-line treatment for metastatic setting to the detection of disease progression. OS was defined as the duration between the first day of palbociclib with letrozole treatment and death. PFS and OS were analyzed using the Kaplan–Meier method. Cox proportional hazard regression was used to estimate hazard ratios and 95% confidence intervals (CIs).

The binary logistic regression method was used for prediction model development. We used the Firth logistic regression method because events were not frequently observed in some variables. Variable weighting was performed by fitting a constant value (α) and coefficients (β) in Firth logistic regression, and we calculated the area under the curve (AUC) of the receiver operating characteristic (ROC) curve as the sum of weighted variables.

$$y = \alpha + \beta_1(\text{factor 1}) + \beta_2(\text{factor 2}) + \beta_3(\text{factor 3}) + \dots$$

For validation, internal validation was performed using bootstrap resampling datasets.

Two-tailed p -values <0.05 were considered statistically significant, and IBM SPSS Statistics, ver. 21 (IBM Co., Armonk, NY), was used for all statistical analyses.

RESULTS

Baseline Characteristics

Between January 2016 and December 2020, 318 patients with MBC were treated with palbociclib and letrozole as the first-line treatment at SMC (Figure 1). Among all 318 patients, seven were lost to follow-up after the first cycle of palbociclib with letrozole

treatment, and six patients wanted to stop the treatment without disease progression or any serious adverse events. Therefore, 305 patients were included in the final analysis.

The clinical and histologic characteristics are described in Table 1. The median age of the patients was 51.6 years. Of all MBC cases, 35.1% were *de novo*, and 64.9% were recurrent. In addition, 58.1% of patients with recurrent MBC had less than 12 months of being disease-free. Visceral metastases were observed in 21.3%, and three or more metastatic sites were found in 15.4%. Regarding previous treatment history, 68.7% of patients had been treated with tamoxifen with or without a GnRH agonist, and 16.7% of patients were treated with AI as adjuvant ET.

With respect to histologic characteristics, strong ER positivity (defined as Allred scores of 7 and 8) was observed in 91.1% of patients, and 5.9% of patients showed weak ER positivity (defined as Allred scores of 3–6). Strong and weak PgR positivity was observed in 48.2 and 24.3% of patients, respectively, and 24.6% of patients had a negative PgR status. In terms of Ki-67, 54.8% of patients had 1+, 27.2% had 2+, 4.6% had 3+, and 1.3% had 4+.

Germline BRCA mutation testing was performed in 61 patients. In these patients, none had BRCA1 mutation, and only five patients harbored BRCA2 mutation (Supplementary Table S1).

Survival Analysis of the First-Line Palbociclib With Letrozole Treatment

We performed a survival analysis of palbociclib with letrozole as the first-line treatment for HR+, HER2-MBC. In this analysis, the median PFS was 28.7 months (95% CI: 22.5, 34.9), and the median OS was not reached (Supplementary Figure S1). The median follow-up duration was 31 months, and we observed 123 cases of disease progression. Thirty-eight patients (12.5%) had a PFS duration of fewer than 6 months, suggesting primary resistance to palbociclib with letrozole, and 17 patients (5.6%) had less than 3 months of PFS.

The Pathologic Characteristics Associated With the Response to Palbociclib With Letrozole

We performed a further subset survival analysis according to baseline characteristics. First, we evaluated the impact of

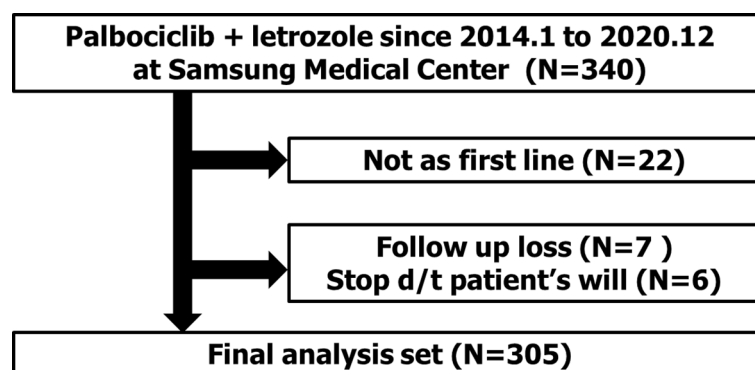


FIGURE 1 | Consort diagram.

TABLE 1 | Baseline patient characteristics (*N* = 305).

Characteristic	<i>N</i> (%)	Characteristic	<i>N</i> (%)
Age		Prior (neo)adjuvant chemotherapy	
Median (range)	51.6 (31.5, 86.7)	Neoadjuvant	41 (13.4)
<40 years old	23 (7.5)	Adjuvant	130 (42.6)
40–60 years old	202 (66.2)	no chemotherapy	134 (43.9)
>60 years old	80 (26.2)	Adjuvant ET (<i>n</i> = 198)	
ECOG PS		Tamoxifen	106 (53.5)
0	177 (58.0)	Tamoxifen + OFS	30 (15.2)
1	122 (40.0)	Anastrozole	14 (7.1)
≥2	5 (1.6)	Letrozole	19 (9.6)
Unknown	1 (0.4)	Unknown	10 (5.1)
Disease status at initial diagnosis		No adjuvant ET	19 (9.6)
<i>De novo</i>	107 (35.1)	Response to adjuvant ET	
Recurred	198 (64.9)	ET naïve	126 (41.3)
Disease-free interval	(<i>n</i> = 198)	Primary resistance ^a	38 (12.5)
<12 months	115 (58.1)	Secondary resistance ^b	58 (19.0)
≥12 months	83 (41.9)	No resistance	83 (27.2)
Metastatic sites		ER status	
Visceral	65 (21.3)	Strong positivity ^c	278 (91.1)
Liver	60 (19.7)	Weak positivity ^d	18 (5.9)
CNS	9 (3.0)	Negative	0
Non-visceral	240 (78.7)	Unknown	9 (3.0)
Bone only	103 (33.8)	PgR status	
Stage IV LN only	29 (8.5)	Strong positivity	147 (48.2)
Number of disease sites		Weak positivity	74 (24.3)
1	158 (51.8)	Negative	75 (24.6)
2	100 (32.8)	Unknown	9 (3.0)
3 or more	47 (15.4)	Ki-67	
Germline BRCA1/2 status		1+	167 (54.8)
Not tested	244 (80.3)	2+	83 (27.2)
Tested	61 (19.7)	3+	14 (4.6)
BRCA1 mutation	0	4+	4 (1.3)
BRCA2 mutation	5 (1.6)	Unknown	37 (12.1)
No BRCA mutation	56 (18.1)		

PS, performance status; CNS, central nervous system; LN, lymph node; ET, endocrine therapy; OFS, ovarian function suppression; ER, estrogen receptor; PgR, progesterone receptor.

^aDefined as breast cancer recurrence within 2 years of adjuvant ET.

^bDefined as breast cancer recurrence either over 2 years since adjuvant ET or within 1 year following adjuvant ET completion.

^cAllred scores 7 and 8.

^dPositive with Allred scores 3–6.

pathologic characteristics on PFS following palbociclib with letrozole treatment. In this analysis, BC with strong ER positivity had better PFS compared with that with weak ER positivity (median PFS, months: 30.3 vs. 11.9; $p = 0.034$). PgR positivity also affected PFS, and those with strong PgR positivity had a tendency to have a longer PFS compared to other groups ($p = 0.111$) (**Figures 2A, B**). Ki-67 grade also impacted PFS. Patients with Ki-67 1+ had the longest PFS among those with other grades (median PFS, months: 31.3; 95% CI: 25.6, 37.1; $p < 0.001$). In this analysis, the inverse correlation between the expression level of Ki-67 and the duration of PFS was statistically significant (**Figure 2C**).

Germline BRCA mutation also affected the efficacy of palbociclib in combination with letrozole. We found five patients harboring germline BRCA2 mutation, and they had a 5.7-month PFS compared to the 37.7-month PFS of those with BRCA wild type and the 29.0-month PFS of those without germline BRCA information ($p < 0.001$), although the number of patients with BRCA mutation was small (**Supplementary Figure S2**). For further analysis, we merged BRCA unknown and germline BRCA wild type as one category because two groups

had similar PFS pattern in previous survival analysis. And we divided germline BRCA status into two categories; BRCA unknown + germline BRCA wild type and germline BRCA mutation (**Figure 2D**).

The Clinical Characteristics Associated With Response to Palbociclib With Letrozole

In terms of clinical characteristics, the Eastern Cooperative Oncology Group (ECOG) performance status (PS) and age (under 50 vs. older than 50 years of age) were not associated with PFS ($p = 0.677$ for ECOG PS; $p = 0.925$ for ECOG age). *De novo* stage IV and recurred BC after curative surgery following palbociclib with letrozole treatment were also not significant in terms of PFS ($p = 0.161$). Among those with recurrent BC, the type of adjuvant endocrine therapy did not affect the efficacy of palbociclib with letrozole ($p = 0.215$).

In terms of endocrine resistance to adjuvant ET, four categories were made: primary resistance, which was defined as disease recurrence after less than 2 years of adjuvant ET; secondary resistance, defined as disease recurrence either 2

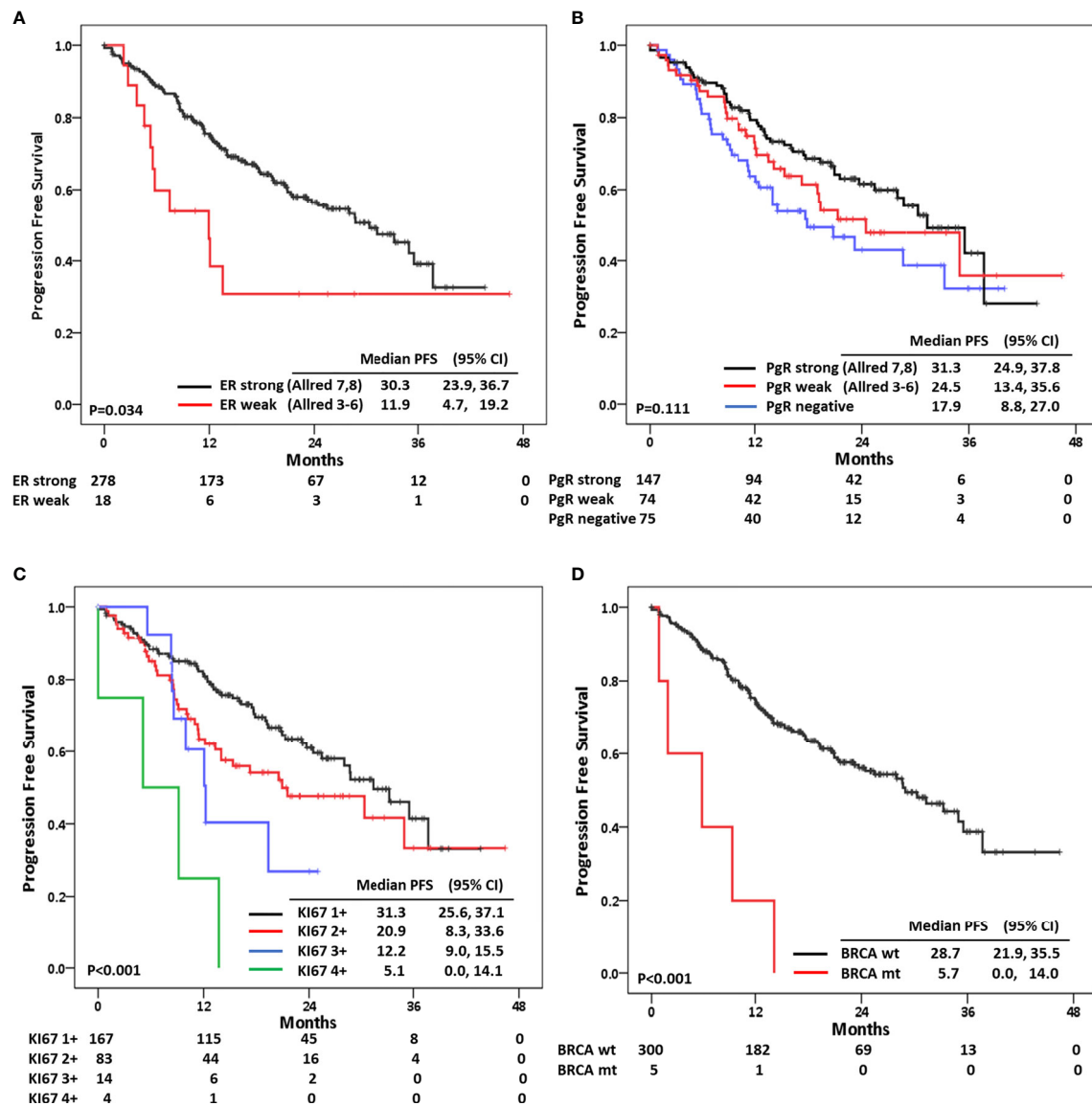


FIGURE 2 | Progression-free survival according to (A) estrogen receptor status, (B) progesterone receptor status, (C) Ki-67 expression status, and (D) germline BRCA mutation.

years or more after adjuvant ET or less than 1 year after the completion of adjuvant ET; no endocrine resistance to adjuvant ET; and endocrine-naïve regardless of *de novo* or recurrent BC. In this analysis, patients with primary resistance to ET had the worst PFS, and the median PFS of these patients was 12.7 months ($p = 0.021$) (Figure 3A). Patients having three or more metastatic sites also had worse prognoses compared to those with one or two metastatic sites (median PFS of one vs. two vs. three or more metastatic sites: 33.3 vs. 23.2 vs. 15.3 months; $p = 0.015$) (Figure 3B).

In 65 patients with visceral metastasis, we observed 60 patients with liver metastasis and nine patients with brain metastasis. Visceral metastasis was associated with poor PFS compared to non-visceral metastasis (median PFS of visceral vs. non-visceral metastasis: 15.3 vs. 31.3 months; $p < 0.001$) (Figure 3C), and liver

metastasis was associated with poor prognosis compared with any other metastatic sites (median PFS of liver metastasis vs. others: 12.7 vs. 31.3 months; $p < 0.001$) (Figure 3D). With regards to metastatic sites, those with lymph node or skin metastases had the longest PFS compared with those having other metastatic lesions (median PFS of lymph node or skin metastases: not reached; $p = 0.001$). In addition, bone-only disease had a superior survival outcome compared to BC with visceral metastasis (median PFS of bone-only disease vs. others vs. visceral metastasis: 29.0 vs. 28.7 vs. 15.3; $p = 0.001$) (Figure 3E).

The elevation of baseline serum tumor markers CA-15-3 and CEA was also associated with short PFS duration ($p = 0.003$ and $p = 0.004$, respectively) (Figure 3F and Supplementary Figure S3).

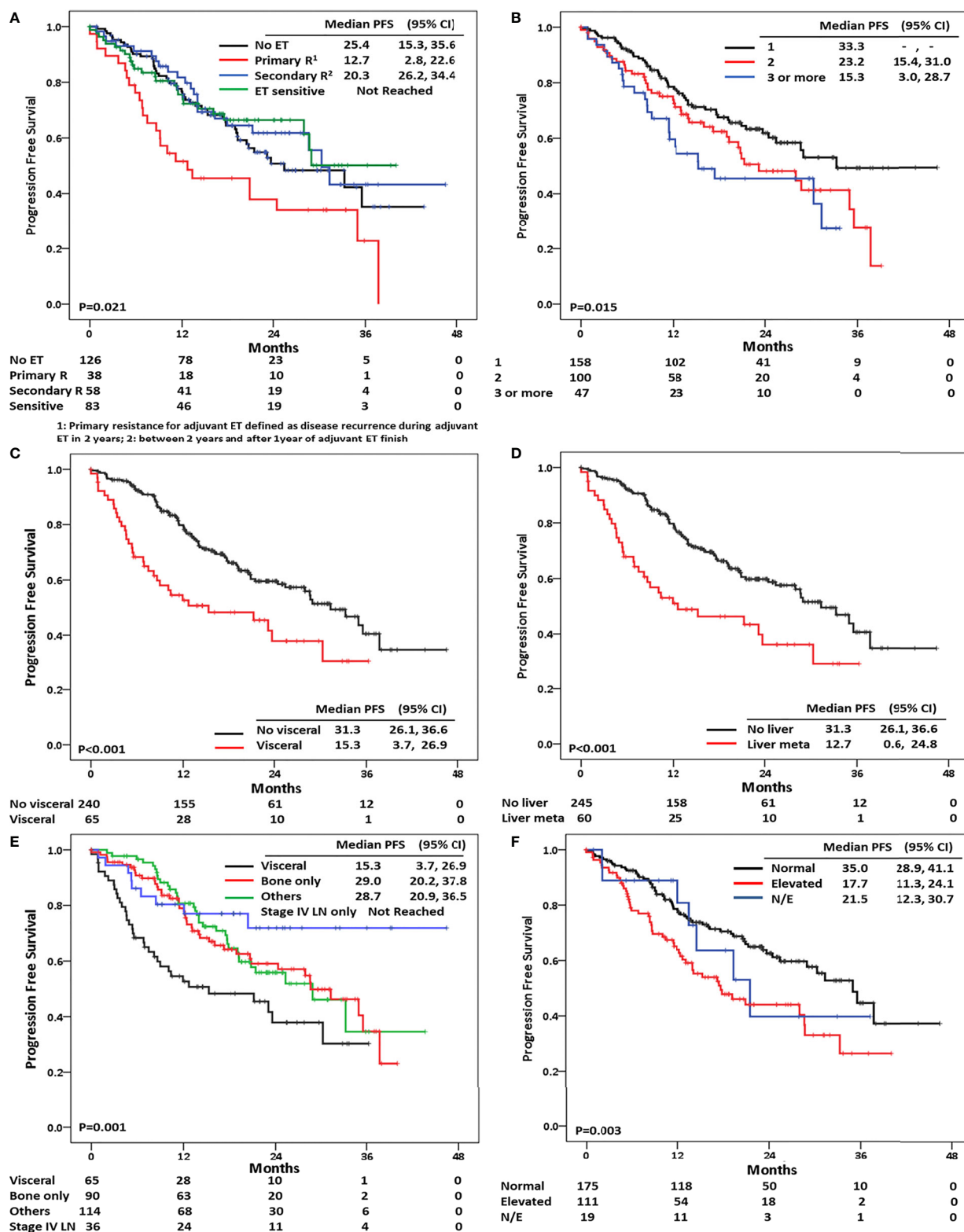


FIGURE 3 | Progression-free survival according to (A) response to adjuvant endocrine treatment, (B) number of metastatic sites, (C) visceral metastasis, (D) liver metastasis, (E) metastatic sites, and (F) baseline CA-15-3 level.

Multivariate Analysis of the Factors Affecting PFS Following Palbociclib With Letrozole

Multivariate analysis was performed using the characteristics affecting PFS following palbociclib in combination with letrozole for the treatment of HR+, HER2-MBC. We excluded visceral metastasis from this analysis because this factor overlapped with liver metastasis. In this analysis, primary resistance to adjuvant ET (hazard ratio: 1.91, 95% CI: 1.13, 3.24; $p = 0.022$), presence of liver metastasis (hazard ratio: 2.17, 95% CI: 1.42, 3.31; $p < 0.001$), initial elevation of serum CA-15-3 level (hazard ratio: 1.99, 95% CI: 1.31, 3.01; $p = 0.005$), weak ER positivity (hazard ratio: 2.28, 95% CI: 1.20, 4.33; $p = 0.024$), Ki-67 3+ or 4+ [hazard ratios: 2.58 (95% CI: 1.17, 5.67) and 10.28 (95% CI: 3.52, 30.09); $p < 0.001$], and presence of BRCA2 mutation (hazard ratio: 9.59, 95% CI: 3.58, 25.70; $p < 0.001$) were associated with short PFS (**Figure 4** and **Supplementary Table S2**).

We excluded the unknown values of six factors and did a binary division of these factors for prediction model development. Therefore, we performed a further multivariate analysis with the values from 256 patients. In this analysis, these six factors consistently had an effect on PFS with statistical significance. The hazard ratio of primary resistance to adjuvant ET for short PFS was 2.27 (95% CI: 1.39, 3.72; $p = 0.001$), that for the presence of liver metastasis was 2.10 (95% CI: 1.35, 3.25; $p =$

0.001), that for the initial elevation of CA-15-3 was 2.26 (95% CI: 1.51, 3.40; $p < 0.001$), that for weak expression of ER status was 2.20 (95% CI: 1.10, 4.41; $p = 0.027$), that for high Ki-67 expression (3+ and 4+) was 3.42 (95% CI: 1.87, 6.56; $p < 0.001$), and that for BRCA2 mutation was 8.54 (95% CI: 2.57, 28.36; $p < 0.001$) (**Table 2**).

Prediction Model for Primary Resistance to Palbociclib With Letrozole

A prediction model for primary resistance to palbociclib with letrozole as the first-line treatment was developed considering patients with HR+, HER2-MBC. We used the values from 256 patients, and 33 events of disease progression in six months were observed.

Firth logistic regression for primary resistance suggested that the five factors—primary resistance to adjuvant ET (odds ratio, OR: 1.14, 95% CI: 0.06, 2.18; $p = 0.038$), liver metastasis (OR: 1.56, 95% CI: 0.71, 2.42; $p < 0.001$), initial elevation of CA-15-3 (OR: 1.51, 95% CI: 0.63, 2.49; $p < 0.001$), weak expression of ER (OR: 2.22, 95% CI: 0.99, 3.51; $p < 0.001$), and BRCA mutation (OR: 2.85, 95% CI: 0.75, 5.31; $p = 0.010$)—affected the 6-month PFS (**Table 3**).

Then, we developed a prediction model for the primary resistance to palbociclib with letrozole. In this analysis, the prediction model with five risk factors had 0.842 in AUC of

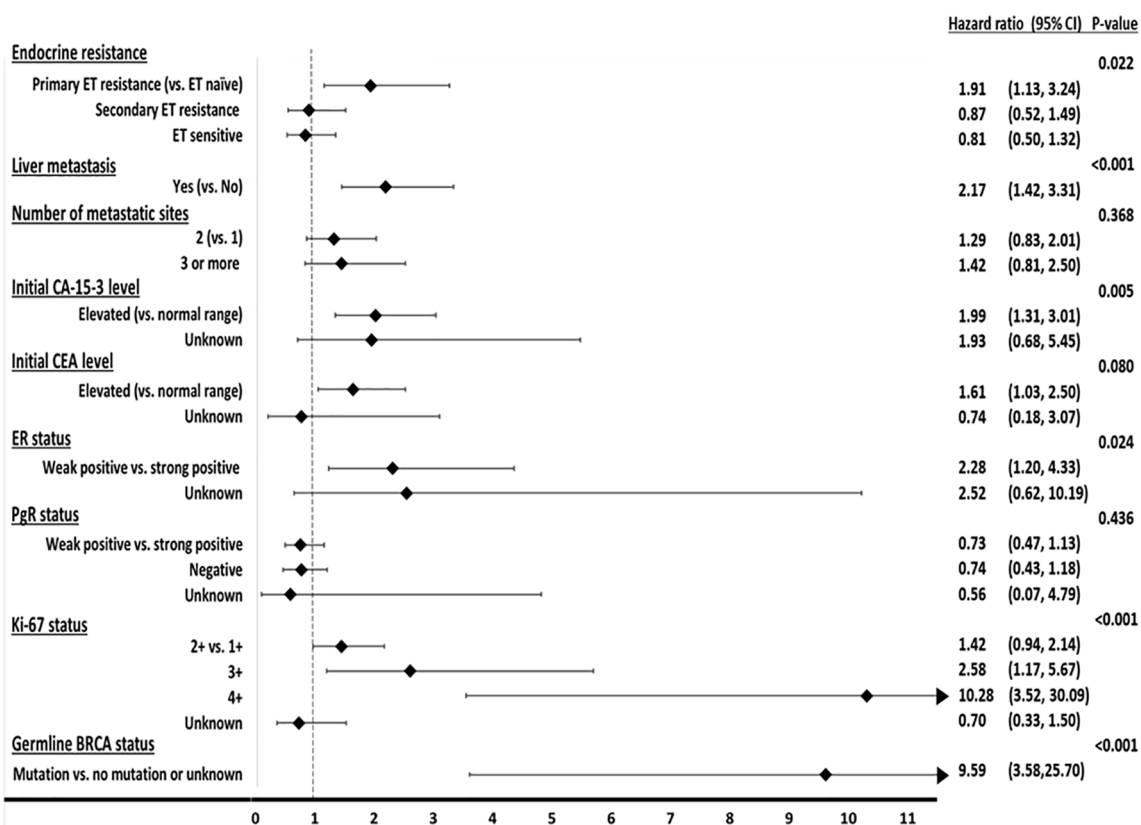


FIGURE 4 | Forest plot of multivariate analysis for factors affecting progression-free survival.

TABLE 2 | Multivariate analysis using binary variables for progression-free survival following palbociclib with letrozole ($N = 256$).

Characteristics	N (%)	Hazard ratio	95% confidence interval		p-value
Resistance to adjuvant ET					0.001
Other	221 (86.3)	Ref			
Primary ET resistance	35 (13.7)	2.27	1.39	3.72	
Liver metastasis					0.001
No	203 (79.3)	Ref			
Yes	53 (20.7)	2.10	1.35	3.25	
Initial elevation of CA-15-3					<0.001
Normal range	156 (60.9)	Ref			
Elevated	100 (39.1)	2.26	1.51	3.40	
Estrogen receptor status					0.027
Strong positivity	242 (94.5)	Ref			
Weak positivity	14 (5.5)	2.20	1.10	4.41	
Ki-67					<0.001
1+, 2+	239 (93.4)	Ref			
3+, 4+	17 (6.6)	3.42	1.87	6.56	
BRCA mutation					<0.001
No mutation or unknown	253 (98.8)	Ref			
BRCA2 mutation	3 (1.2)	8.54	2.57	28.36	

ET, endocrine therapy.

the ROC curve (95% CI: 0.775, 0.909; $p < 0.001$), and the overall model quality was 0.78 (**Figure 5A** and **Supplementary Figure S4A**). Internal validation with bootstrap resampling datasets was performed ($n = 182$). In the validation set, AUC was 0.832 (95% CI: 0.762, 0.901; $p < 0.001$), and the overall model quality was 0.76 (**Supplementary Table S3**, **Figure 5B**, and **Supplementary Figure S4B**).

Primary Resistance Model With the Five Risk Factors

We analyzed the risk of primary resistance of palbociclib with letrozole according to the five risk factors. First, we performed a survival analysis according to the number of risk factors.

In the survival analysis, the median PFS of patients with no risk factor was not reached, and it was 28.0-month PFS in patients with one risk factor, 8.2-months PFS in patients with two risk factors, and 6.8-month PFS in patients who had three risk factors ($p < 0.001$) (**Supplementary Figure S5A**). The primary resistance of palbociclib with letrozole model also suggested that the risk of primary resistance increased as more risk factors existed [OR of one risk factor vs. no risk factor (ref): 2.18, 95% CI: 0.72, 4.41, $p = 0.002$; OR of two risk factors: 4.01, 95% CI: 2.57, 6.25, $p < 0.001$; OR of three risk factors: 4.00, 95% CI: 1.99, 6.50, $p < 0.001$] (**Supplementary Table S4**), and AUC

was 0.830 (95% CI: 0.761, 0.898) ($p < 0.001$) (**Supplementary Figure S5B**).

We also developed a primary resistance model according to the value made of the previous Firth logistic regression with five risk factors. We divided these into four groups: group 1 did not have any risk factors, group 2 had one risk factor except BRCA mutation, group 3 had two risk factors except weak ER positivity, and group 4 consisted of BRCA mutation, three risk factors, and two risk factors including weak ER positivity (**Supplementary Table S5**). The median PFS of group 1 was not reached, and it was 28.0-month PFS in group 2, 10.1-month PFS in group 3, and 5.8-month PFS in group 4 ($p < 0.001$) (**Figure 6A**). The prediction model also precisely expected the primary resistance of palbociclib with letrozole [OR of group 2 vs. 1 (ref): 2.18, 95% CI: 0.72, 4.41, $p = 0.002$; OR of group 3: 3.91, 95% CI: 2.42, 6.16, $p < 0.001$; OR of group 3: 4.25, 95% CI: 2.56, 6.60, $p < 0.001$, and AUC of 0.830 (95% CI: 0.761, 0.898, $p < 0.001$)] (**Table 4** and **Figure 6B**).

Second-Line Treatment After Progression of the First-Line Palbociclib With Letrozole

Of 38 patients with primary resistance to palbociclib in combination with letrozole, 35 patients received second-line treatment. Capecitabine was the most commonly used

TABLE 3 | Predictive model for primary resistance to palbociclib with letrozole as first-line treatment for HR+, HER2-advanced breast cancer using firth logistic regression ($N = 256$).

Characteristics	N (%)	Odds ratio	95% confidence interval		p-value
Disease progression	33 (12.9)				
Primary resistance to adjuvant ET ^a		1.14	0.06	2.18	0.038
Presence of liver metastasis		1.56	0.71	2.42	<0.001
Initial elevation of CA-15-3		1.51	0.63	2.49	<0.001
Estrogen receptor weak positivity ^b		2.22	0.99	3.51	<0.001
Ki-67 3+ or 4+		0.99	0.62	2.24	0.167
Presence of BRCA mutation		2.85	0.75	5.31	0.010

^aEndocrine therapy.

^bWeak or unknown positivity.

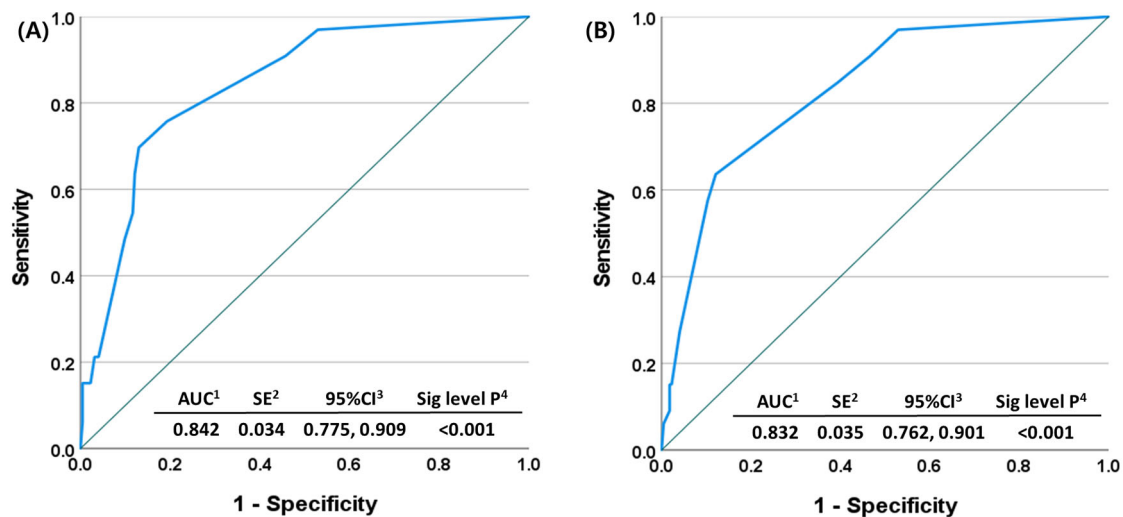


FIGURE 5 | Receiver operating characteristic curve for primary resistance to palbociclib with letrozole as the first-line treatment for HR+ HER2- MBC (A) original set ($n = 256$) and (B) validation set ($n = 182$).

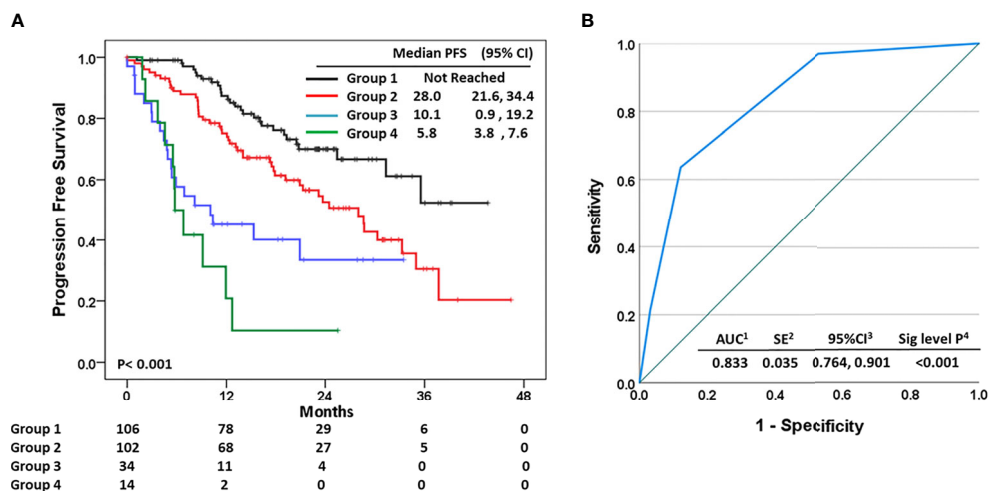


FIGURE 6 | (A) Progression-free survival according to the risk groups of the prediction model. (B) Receiver operating characteristic curve for primary resistance to palbociclib with letrozole as the first-line treatment for HR+ HER2- MBC regarding the risk groups.

therapeutic regimen, followed by taxane, everolimus in combination with exemestane, fulvestrant, and others. The overall 6-month disease control rate was 31.4% (31.3% for capecitabine, 42.9% for taxane, 40.0% for everolimus, and 50.0% for fulvestrant) (Table 5).

DISCUSSION

This study considered the real-world data of palbociclib with letrozole as the first-line treatment for HR+, HER2-MBC. The median PFS was 28.7 months, and primary resistance to adjuvant

ET, liver metastasis, initial elevation of CA-15-3 level, weak ER expression, high expression of Ki-67, and BRCA2 mutation were associated with poor PFS. Our prediction model suggested that these six parameters affected the primary resistance to palbociclib with letrozole, and this model had an AUC of 0.844.

ET is the first-line treatment for HR+, HER2-MBC even in the presence of visceral disease, unless there is visceral crisis (3, 4). In the era of CDK4/6 inhibitor, CDK4/6 inhibitors combined with ET is the standard treatment strategy for HR+, HER2-MBC as the first or second line (3). However, resistance to this combination therapy inevitably develops, and some patients do not benefit from CDK4/6 inhibitor with AI treatment (8–10).

TABLE 4 | Predictive model for primary resistance to palbociclib with letrozole as first-line treatment for HR+, HER2-advanced breast cancer according to risk factor characteristics (N = 256).

Characteristics	N (%)	Odds ratio	95% confidence interval		p-value
Disease progression	33 (12.9)				<0.001
No risk factor (group 1)		Ref	Ref	Ref	Ref
One risk factor (group 2) ^a		2.18	0.72	4.41	0.002
Group 3 ^b		3.91	2.42	6.16	<0.001
Group 4 ^c		4.25	2.56	6.60	<0.001

^aExcept BRCA mutation.^bTwo risk factors except weak estrogen receptor (ER) positivity and BRCA mutation.^cBRCA mutation regardless of the number of risk factors, three risk factors, and two risk factors including weak ER positivity.**TABLE 5 |** Second-line treatment after progression from endocrine therapy with palbociclib and letrozole (N = 38).

Regimen	N (%)	3-month DCR (%)	6-month DCR (%)	12-month DCR (%)
Capecitabine	16 (43.2)	10 (62.5)	5 (31.3)	2 (12.5)
Taxane-based chemotherapy	7 (24.3)	5 (71.4)	3 (42.9)	1 (14.3)
Everolimus with exemestane	5 (13.5)	4 (80.0)	2 (40.0)	1 (20.0)
Fulvestrant	2 (5.4)	1 (50.0)	1 (50.0)	1 (50.0)
Clinical trial	5 (13.5)	2 (40.0)	0 (0.0)	0 (0.0)
No further treatment	3 (7.9)	—	—	—
Total	38 (100.0)	22 (62.9)	11 (31.4)	5 (14.3)

DCR, disease control rate.

In our study, germline BRCA mutation was the most powerful predictive marker for primary resistance to palbociclib with letrozole. Of five patients harboring germline BRCA2 mutation, the median PFS was just 5.7 months, and the hazard ratio for primary resistance in those with BRCA2 mutation was 22.57. However, the number of patients with BRCA mutations in this study was small, and there are currently no other data supporting this association. Further preclinical and clinical research is warranted.

The initial elevation of serum CA-15-3 was also strongly associated with primary resistance to palbociclib with letrozole. The current European Society for Medical Oncology and American Society of Clinical Oncology guideline suggests that CA-15-3 and CEA are not recommended for BC screening, diagnosis, staging, or recurrence evaluation (26, 27). The clinical values of these tumor markers are not well established but might be an aid to evaluate and monitor the response to treatment, particularly in patients with non-measurable metastatic disease with elevation of these markers (3). Many investigators have tried to reveal the clinical values of serum tumor markers, and recent research has suggested CA-15-3 elevation at the time of initial metastasis in 37% of patients with MBC, and 62% of patients had an increase in CA-15-3 level at the diagnosis of metastasis (28). Another study also suggested that the CEA and CA-15-3 levels were useful to detect metastasis early, and their elevations were associated with unfavorable clinicopathologic parameters (29).

In our study, CA-15-3 serum level was associated with primary resistance to palbociclib with letrozole after adjustment through a multivariate analysis. We suggest CA-15-3 to be an independent predictive marker for primary resistance to palbociclib with letrozole, not a secondary finding associated

with clinicopathologic parameters. Moreover, serum CA-15-3 testing had advantages with respect to convenience, easy accessibility, and low cost.

Liver metastasis was already suggested to associate with poor prognosis following CDK4/6 treatment in previous studies (30, 31). Our study also suggested that liver metastasis was associated with poor response to palbociclib with letrozole. Even considering visceral metastasis, including liver metastasis, CDK4/6 inhibition with AI was an effective treatment strategy compared with AI alone, according to previous clinical trials (8–10). However, some patients with visceral metastasis did not benefit from CDK4/6 inhibitors with ET, and cytotoxic chemotherapy would be better than ET for these patients; predictive biomarkers are urgently needed.

ER status was also associated with primary resistance to the first line of palbociclib treatment in combination with letrozole. Even though there was a small number of patients with weak ER+ MBC in this study, they had significantly worse PFS outcomes compared to patients with strong ER+ MBC. Recent guidelines described low ER tumors as having unique molecular features and, therefore, a distinct therapeutic response to endocrine therapy compared with high ER+ BC (32). In this study, ER status was divided into two groups according to Allred score (7 to 8 vs. 3–6). In terms of ER status, no previous studies, including clinical trials, have evaluated the association between ER expression level and the efficacy of CDK 4/6 inhibitors with ET. The results of this study suggested that the expression level of ER should be considered for the treatment of HR+, HER2-MBC with CDK4/6 inhibitors.

Previous research has suggested PgR and Ki-67 state to affect the efficacy of palbociclib (33). Our study also suggested that Ki-67 expression, but not PgR status, was related to PFS following a palbociclib-containing treatment.

Primary resistance to adjuvant ET was associated with primary resistance to the first-line treatment consisting of palbociclib with letrozole for HR+, HER2-MBC. Disease recurrence within 2 years of adjuvant ET was associated with primary resistance to palbociclib, but secondary resistance to ET was not.

Lastly, we developed a prediction model of primary resistance of palbociclib with letrozole as the first-line treatment for metastatic HR+, HER2-MBC. This model suggested that the number and the characteristics of risk factors easily predicted primary resistance and the PFS of a patient. Therefore, this model would be helpful to predict the response of patients to palbociclib with letrozole as the initial treatment.

Our study was a retrospective data analysis with data from about 300 patients in our registry. Therefore, we only performed internal validation to validate our primary resistance model. However, the result of internal validation was similar to that of the original data set with high AUC, and therefore we might suggest that our model was reliable.

Even though the current treatment guidelines recommended CDK 4/6 inhibitors in combination with ET as the first-line treatment in HR+, HER2-MBC, cytotoxic chemotherapy would be more beneficial compared to the use of palbociclib with letrozole in some patients with poor clinico-pathologic parameters. Among 38 patients who underwent disease progression after the first-line palbociclib with letrozole within 6 months, 67.5% of patients had been treated with cytotoxic chemotherapy, and 34.8% of these patients had more than 6 months of PFS following a second-line cytotoxic treatment. Therefore, our prediction model suggested that these clinico-pathologic parameters would be helpful for deciding the first-line treatment in a subset of HR+, HER2-MBC patients. It is necessary to note that these findings are just hypothesis-generating, especially considering that no predictive biomarkers have yet been established related to treatment consisting of CDK 4/6 inhibitors with ET.

In conclusion, we explored palbociclib in combination with letrozole as the first-line treatment for HR+, HER2-MBC and developed a prediction model for primary resistance to the first-line treatment of palbociclib with letrozole. Our prediction model might be helpful for considering the first-line treatment strategies in HR+, HER2-MBC. Further well-designed clinical trials are warranted to validate our prediction model.

DATA AVAILABILITY STATEMENT

The original contributions presented in the study are included in the article/**Supplementary Material**. Further inquiries can be directed to the corresponding author.

ETHICS STATEMENT

This study was reviewed and approved by the Institutional Review Board of Samsung Medical Center, Seoul, South Korea

(IRB no. 2021-07-131). This study was performed in accordance with the Declaration of Helsinki and Good Clinical Practice guidelines. The requirement for informed consent was waived due to the use of de-identified medical records with clinical data. Written informed consent for participation was not required for this study in accordance with the national legislation and the institutional requirements.

AUTHOR CONTRIBUTIONS

J-YK conceived and planned the experiments. J-YK and JO carried out the analyses and experiments. J-YK, YP, JA, and Y-HI contributed to the collection of samples and clinical data. J-YK and Y-HI contributed to the interpretation of the results and took the lead in writing the manuscript. Y-HI supervised the project. All authors contributed to the article and approved the submitted version.

FUNDING

This work was supported by an Institute for Information and Communications Technology Promotion grant funded by the Korean government (2018-0-00861, Intelligent SW Technology Development for Medical Data Analysis), a grant from the Korea Health Technology R and D Project through the Korea Health Industry Development Institute funded by the Ministry of Health and Welfare, Republic of Korea (grant number: HR20C0025), and grants from the National Research Foundation of Korea (NRF-2017R1D1A1B03028446 and NRF-2020R1F1A1072616).

SUPPLEMENTARY MATERIAL

The Supplementary Material for this article can be found online at: <https://www.frontiersin.org/articles/10.3389/fonc.2021.759150/full#supplementary-material>

Supplementary Figure 1 | (A) Progression-free survival and **(B)** overall survival.

Supplementary Figure 2 | Progression-free survival according to germline BRCA mutation, BRCA wild type, and BRCA unknown.

Supplementary Figure 3 | Progression-free survival according to baseline CEA level.

Supplementary Figure 4 | Overall model quality of receiver operating characteristic curve for primary resistance to palbociclib with letrozole as the first-line treatment for HR+ HER2- MBC **(A)** original set ($n = 256$) and **(B)** validation set ($n = 182$).

Supplementary Figure 5 | (A) Progression-free survival according to the number of risk factors. **(B)** Receiver operating characteristic curve for primary resistance to palbociclib with letrozole as the first-line treatment for HR+ HER2- metastatic breast cancer regarding the number of risk factor.

REFERENCES

- Kim JY, Kang D, Nam SJ, Kim SW, Lee JE, Yu JH, et al. Clinical Features and Outcomes of Invasive Breast Cancer: Age-Specific Analysis of a Modern Hospital-Based Registry. *J Glob Oncol* (2019) 5:1–9. doi: 10.1200/JGO.19.00034
- Setiawan VW, Monroe KR, Wilkens LR, Kolonel LN, Pike MC, Henderson BE. Breast Cancer Risk Factors Defined by Estrogen and Progesterone Receptor Status: The Multiethnic Cohort Study. *Am J Epidemiol* (2009) 169:1251–9. doi: 10.1093/aje/kwp036
- Cardoso F, Paluch-Shimon S, Senkus E, Curigliano G, Aapro MS, Andre F, et al. 5th ESO-ESMO International Consensus Guidelines for Advanced Breast Cancer (ABC 5). *Ann Oncol* (2020) 31:1623–49. doi: 10.1016/j.annonc.2020.09.010
- Rugo HS, Rumble RB, Macrae E, Barton DL, Connolly HK, Dickler MN, et al. Endocrine Therapy for Hormone Receptor-Positive Metastatic Breast Cancer: American Society of Clinical Oncology Guideline. *J Clin Oncol* (2016) 34:3069–103. doi: 10.1200/JCO.2016.67.1487
- McDonald ER3rd, de Weck A, Schlabach MR, Billy E, Mavrakis KJ, Hoffman GR, et al. Project DRIVE: A Compendium of Cancer Dependencies and Synthetic Lethal Relationships Uncovered by Large-Scale, Deep RNAi Screening. *Cell* (2017) 170:577–92 e10. doi: 10.1016/j.cell.2017.07.005
- Finn RS, Aleshin A, Slamon DJ. Targeting the Cyclin-Dependent Kinases (CDK) 4/6 in Estrogen Receptor-Positive Breast Cancers. *Breast Cancer Res* (2016) 18:17. doi: 10.1186/s13058-015-0661-5
- Hafner M, Mills CE, Subramanian K, Chen C, Chung M, Boswell SA, et al. Multiomics Profiling Establishes the Polypharmacology of FDA-Approved CDK4/6 Inhibitors and the Potential for Differential Clinical Activity. *Cell Chem Biol* (2019) 26:1067–80 e8. doi: 10.1016/j.chembiol.2019.05.005
- Finn RS, Martin M, Rugo HS, Jones S, Im SA, Gelmon K, et al. Palbociclib and Letrozole in Advanced Breast Cancer. *N Engl J Med* (2016) 375:1925–36. doi: 10.1056/NEJMoa1607303
- Hortobagyi GN, Stemmer SM, Burris HA, Yap YS, Sonke GS, Paluch-Shimon S, et al. Ribociclib as First-Line Therapy for HR-Positive, Advanced Breast Cancer. *N Engl J Med* (2016) 375:1738–48. doi: 10.1056/NEJMoa1609709
- Goetz MP, Toi M, Campone M, Sohn J, Paluch-Shimon S, Huober J, et al. MONARCH 3: Abemaciclib As Initial Therapy for Advanced Breast Cancer. *J Clin Oncol* (2017) 35:3638–46. doi: 10.1200/JCO.2017.75.6155
- Turner NC, Ro J, Andre F, Loi S, Verma S, Iwata H, et al. Palbociclib in Hormone-Receptor-Positive Advanced Breast Cancer. *N Engl J Med* (2015) 373:209–19. doi: 10.1056/NEJMoa1505270
- Slamon DJ, Neven P, Chia S, Fasching PA, De Laurentiis M, Im SA, et al. Phase III Randomized Study of Ribociclib and Fulvestrant in Hormone Receptor-Positive, Human Epidermal Growth Factor Receptor 2-Negative Advanced Breast Cancer: MONALEESA-3. *J Clin Oncol* (2018) 36:2465–72. doi: 10.1200/JCO.2018.78.9909
- Sledge GW Jr., Toi M, Neven P, Sohn J, Inoue K, Pivov X, et al. MONARCH 2: Abemaciclib in Combination With Fulvestrant in Women With HR+/HER2-Advanced Breast Cancer Who Had Progressed While Receiving Endocrine Therapy. *J Clin Oncol* (2017) 35:2875–84. doi: 10.1200/JCO.2017.73.7585
- Cristofanilli M, Rugo HS, Im S-A, Slamon DJ, Harbeck N, Bondarenko I, et al. Overall Survival (OS) With Palbociclib (PAL) + Fulvestrant (FUL) in Women With Hormone Receptor-Positive (HR+), Human Epidermal Growth Factor Receptor 2-Negative (HER2-) Advanced Breast Cancer (ABC): Updated Analyses From PALOMA-3. *J Clin Oncol* (2021) 39(15_suppl):1000. doi: 10.1200/JCO.2021.39.15_suppl.1000
- Slamon DJ, Neven P, Chia SKL, Jerusalem GHM, De Laurentiis M, Im SA, et al. Updated Overall Survival (OS) Results From the Phase III MONALEESA-3 Trial of Postmenopausal Patients (Pts) With HR+/HER2- Advanced Breast Cancer (ABC) Treated With Fulvestrant (FUL) ± Ribociclib (RIB). *J Clin Oncol* (2021) 39(15_suppl):1001. doi: 10.1200/JCO.2021.39.15_suppl.1001
- O'Leary B, Finn RS, Turner NC. Treating Cancer With Selective CDK4/6 Inhibitors. *Nat Rev Clin Oncol* (2016) 13:417–30. doi: 10.1038/nrclinonc.2016.26
- Nayar U, Cohen O, Kapstad C, Cuoco MS, Waks AG, Wander SA, et al. Acquired HER2 Mutations in ER(+) Metastatic Breast Cancer Confer Resistance to Estrogen Receptor-Directed Therapies. *Nat Genet* (2019) 51:207–16. doi: 10.1038/s41588-018-0287-5
- Michaloglou C, Crafter C, Siersbaek R, Delpuech O, Curwen JO, Carnevali LS, et al. Combined Inhibition of mTOR and CDK4/6 Is Required for Optimal Blockade of E2F Function and Long-Term Growth Inhibition in Estrogen Receptor-Positive Breast Cancer. *Mol Cancer Ther* (2018) 17:908–20. doi: 10.1158/1535-7163.MCT-17-0537
- O'Leary B, Cutts RJ, Huang X, Hrebien S, Liu Y, Andre F, et al. Circulating Tumor DNA Markers for Early Progression on Fulvestrant With or Without Palbociclib in ER+ Advanced Breast Cancer. *J Natl Cancer Inst* (2021) 113:309–17. doi: 10.1093/jnci/djaa087
- Saxena NK, Sharma D. Epigenetic Reactivation of Estrogen Receptor: Promising Tools for Restoring Response to Endocrine Therapy. *Mol Cell Pharmacol* (2010) 2:191–202.
- O'Leary B, Cutts RJ, Liu Y, Hrebien S, Huang X, Fenwick K, et al. The Genetic Landscape and Clonal Evolution of Breast Cancer Resistance to Palbociclib Plus Fulvestrant in the PALOMA-3 Trial. *Cancer Discovery* (2018) 8:1390–403. doi: 10.1158/2159-8290.CD-18-0264
- Li Z, Razavi P, Li Q, Toy W, Liu B, Ping C, et al. Loss of the FAT1 Tumor Suppressor Promotes Resistance to CDK4/6 Inhibitors via the Hippo Pathway. *Cancer Cell* (2018) 34:893–905 e8. doi: 10.1016/j.ccell.2018.11.006
- Condorelli R, Spring L, O'Shaughnessy J, Lacroix L, Bailleux C, Scott V, et al. Polyclonal RB1 Mutations and Acquired Resistance to CDK 4/6 Inhibitors in Patients With Metastatic Breast Cancer. *Ann Oncol* (2018) 29:640–5. doi: 10.1093/annonc/mdx784
- Denkert C, Loibl S, Muller BM, Eidtmann H, Schmitt WD, Eiermann W, et al. Ki67 Levels as Predictive and Prognostic Parameters in Pretherapeutic Breast Cancer Core Biopsies: A Translational Investigation in the Neoadjuvant GeparTrio Trial. *Ann Oncol* (2013) 24:2786–93. doi: 10.1093/annonc/mdt350
- Bloom HJ, Richardson WW. Histological Grading and Prognosis in Breast Cancer; a Study of 1409 Cases of Which 359 Have Been Followed for 15 Years. *Br J Cancer* (1957) 11:359–77. doi: 10.1038/bjc.1957.43
- Korde LA, Somerfield MR, Carey LA, Crews JR, Denduluri N, Hwang ES, et al. Neoadjuvant Chemotherapy, Endocrine Therapy, and Targeted Therapy for Breast Cancer: ASCO Guideline. *J Clin Oncol* (2021) 39:1485–505. doi: 10.1200/JCO.20.03399
- Cardoso F, Kyriakides S, Ohno S, Penault-Llorca F, Poortmans P, Rubio IT, et al. Early Breast Cancer: ESMO Clinical Practice Guidelines for Diagnosis, Treatment and Follow-Up. *Ann Oncol* (2019) 30:1194–220. doi: 10.1093/annonc/mdz173
- De Cock L, Heylen J, Wildiers A, Punie K, Smeets A, Weltens C, et al. Detection of Secondary Metastatic Breast Cancer by Measurement of Plasma CA 15.3. *ESMO Open* (2021) 6:100203. doi: 10.1016/j.esmoop.2021.100203
- Uygur MM, Gumus M. The Utility of Serum Tumor Markers CEA and CA 15-3 for Breast Cancer Prognosis and Their Association With Clinicopathological Parameters. *Cancer Treat Res Commun* (2021) 28:100402. doi: 10.1016/j.ctarc.2021.100402
- Odan N, Kikawa Y, Matsumoto H, Minohata J, Suwa H, Hashimoto T, et al. Real-World Outcomes of Treating Advanced Breast Cancer Patients With Palbociclib: A Multicenter Retrospective Cohort Study in Japan-The KBCOG-14 Study. *Breast Cancer (Auckl)*. (2020) 14:1178223420983843. doi: 10.1177/1178223420983843
- Lee J, Park HS, Won HS, Yang JH, Lee HY, Woo IS, et al. Real-World Clinical Data of Palbociclib in Asian Metastatic Breast Cancer Patients: Experiences From Eight Institutions. *Cancer Res Treat* (2021) 53:409–23. doi: 10.4143/crt.2020.451
- Allison KH, Hammond MEH, Dowsett M, McKernin SE, Carey LA, Fitzgibbons PL, et al. Estrogen and Progesterone Receptor Testing in Breast Cancer: ASCO/CAP Guideline Update. *J Clin Oncol* (2020) 38:1346–66. doi: 10.1200/JCO.19.02309
- Shao X, Zheng Y, Cao W, Shen X, Li G, Chen J, et al. Ki67 and Progesterone Receptor Status Predicts Sensitivity to Palbociclib: A Real-World Study. *Ann Transl Med* (2021) 9:707. doi: 10.21037/atm-21-1340

Conflict of Interest: The authors declare that the research was conducted in the absence of any commercial or financial relationships that could be construed as a potential conflict of interest.

Publisher's Note: All claims expressed in this article are solely those of the authors and do not necessarily represent those of their affiliated organizations, or those of the publisher, the editors and the reviewers. Any product that may be evaluated in this article, or claim that may be made by its manufacturer, is not guaranteed or endorsed by the publisher.

Copyright © 2021 Kim, Oh, Park, Ahn and Im. This is an open-access article distributed under the terms of the Creative Commons Attribution License (CC BY). The use, distribution or reproduction in other forums is permitted, provided the

original author(s) and the copyright owner(s) are credited and that the original publication in this journal is cited, in accordance with accepted academic practice. No use, distribution or reproduction is permitted which does not comply with these terms.



MicroRNAs Role in Breast Cancer: Theranostic Application in Saudi Arabia

Nouf M. Alyami*

Department of Zoology, College of Science, King Saud University, Riyadh, Saudi Arabia

OPEN ACCESS

Edited by:

Maria Rosaria De Miglio,
University of Sassari, Italy

Reviewed by:

Vaishali Aggarwal,
University of Pittsburgh, United States
Wei Zhao,
City University of Hong Kong,
Hong Kong, SAR China

*Correspondence:

Nouf M. Alyami
nalyami@ksu.edu.sa

Specialty section:

This article was submitted to
Breast Cancer,
a section of the journal
Frontiers in Oncology

Received: 31 May 2021

Accepted: 30 September 2021

Published: 25 October 2021

Citation:

Alyami NM (2021) MicroRNAs Role in
Breast Cancer: Theranostic
Application in Saudi Arabia.
Front. Oncol. 11:717759.
doi: 10.3389/fonc.2021.717759

Breast cancer is an aggressive silent disease, representing 11.7% of the diagnosed cancer worldwide, and it is also a leading cause of death in Saudi Arabia. Consequently, microRNAs have emerged recently as potential biomarkers to diagnose and monitor such cases at the molecular level, which tends to be problematic during diagnosis. MicroRNAs are highly conserved non-coding oligonucleotide RNA. Over the last two decades, studies have determined the functional significance of these small RNAs and their impact on cellular development and the interaction between microRNAs and messenger RNAs, which affect numerous molecular pathways and physiological functions. Moreover, many disorders, including breast cancer, are associated with the dysregulation of microRNA. Sparingly, many microRNAs can suppress cancer cell proliferation, apoptosis, angiogenesis, invasion, metastasis, and vice versa. Remarkably, microRNAs can be harvested from patients' biofluids to predict disease progression that considered a non-invasive method. Nevertheless, MicroRNAs are currently utilized as anti-cancer therapies combined with other drug therapies or even as a single agents' treatment. Therefore, this review will focus on microRNAs' role in breast cancer as an indicator of disease progression. In addition, this review summarizes the current knowledge of drug sensitivity and methods in detecting microRNA and their application to improve patient care and identifies the current gaps in this field.

Keywords: chemotherapy resistance, breast cancer metastasis, molecular pathways, anticancer therapy, Saudi Arabia, miRNA, circulating biomarkers

1 INTRODUCTION

Breast cancer (BC) is the dominant type of cancer among female patients, reaching 2,261,419 new cases in 2020, representing 11.7% of the yearly diagnosed patients with cancer worldwide. BC incidence has declined dramatically in industrial countries, except for Australia/New Zealand and Western Europe (1). Despite the advances in BC diagnosis, the leading cause of mortality is the disease recurrences due to metastases. Management of disease recurrences and metastasis has modestly improved over the last three last decades (2). Metastasis states the spread of cancer cells through the lymphatic system or bloodstream to distant organs (3). Because of these challenges, the need for sufficient molecular biomarkers to predict the disease response is continued. However,

researchers are examining the utility of MicroRNAs as biomarkers to detect diseases and tumor aggressiveness (4, 5).

MicroRNAs (miRNAs) were discovered in the 1990s in nematodes (6, 7). miRNAs are approximately 19–25 nucleotides (nt) in length and are found in almost all eukaryotes. Since then, many studies have identified miRNAs' functionality and role in disorders and human illnesses such as BC (4). miRNAs can regulate genes by silencing their protein-coding mRNA (messenger RNA) through inducing mRNA turnover. miRNAs are determined to be involved in cellular activities such as tumorigenesis, proliferation, cell survival, apoptosis, and cancer development, affecting cancer progression (5). These small oligonucleotides can function as oncogenes by degrading mRNAs that act as tumor suppressors and *vice versa*. Previous studies showed that many miRNAs impacted Breast cancer development and even drug resistance (8, 9). Due to the heterogeneous nature of the BC, it is considered a challenge, which makes it extremely difficult to classify and treat (2). Concomitantly, many countries, specifically Saudi Arabia, are suffering from recurrent disease conditions due to metastases.

Nonetheless, using blood serum and non-invasive methods that are considered safe and accurate to determine the molecular characterization and create a personalized treatment strategy for each patient to prevent recurrence in the future had been utilized. Therefore, this review focuses on miRNAs' role in breast cancer, wherein they serve as biomarkers to detect tumors, including their progression, treatment resistance, and potential impact on clinical practices.

2 MANUSCRIPT FORMATTING

2.1 Background

Ambros and Ruvkun laboratory discovered the first miRNA and its target in 1993. Ambros's lab has found the *lin-4* gene a fundamental player in *Caenorhabditis Elegans* (*C. elegans*) development. However, the *lin-4* gene does not encode any known cellular protein, but it only generates a short 22 nt RNA. Furthermore, the Ruvkun lab has determined that this small RNA sequence is complementary to the 3'UTR (3'untranslated region) and negatively regulates the *lin-14* gene (6, 7). Seven years later, let-7, a small 21-nt RNA, was discovered and was further identified in various species (10, 11). Since then, thousands of miRNAs and their genetic functions in humans and other animals have been identified (4, 5).

Interestingly, large projects such as FANTOM and ENCODE for genomic annotation and functionality have reported that 80% of mammalian DNA is actively transcribed. The vast majority are noncoding RNA genes (ncRNA) (12, 13). In the past, the main differences between coding and non-coding were based on encoding protein. However, this barrier starts to overlap as particular coding RNA, such as TP53 mRNA, can function as RNA only, significantly impacting much biologic development (14, 15). Furthermore, long non-coding RNA (lncRNA) can regulate gene expression at both genomic and post-transcription levels. At the genomic level by manipulating

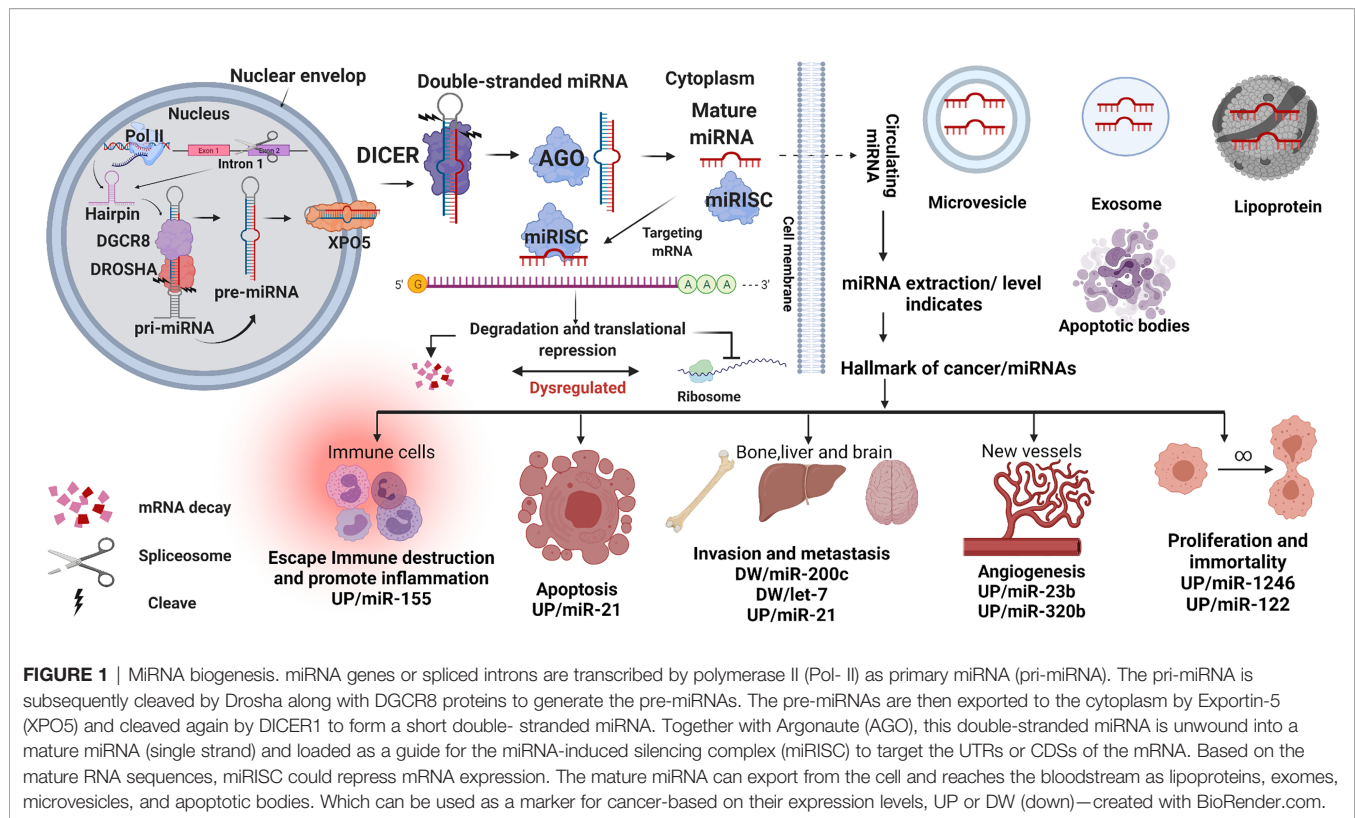
chromatin status and complementary binding to other forms of RNA such as miRNA and mRNA as a post-transcription level (16–19). Also, other studies identified that lncRNA could encode small peptides, but their functions are still unknown (20, 21). Other types of RNA that also function similarly to miRNAs with the exact mechanism (using cytoplasmic processing proteins) are the small interferences RNA (siRNA) (22). They can silence gene expression as miRNA *via* targeting the mRNA but not expressed endogenously as miRNA encoded in the genome. Plus, they can only target one specific mRNA, as for miRNA that can have vast mRNA targets (9, 23). The source of these siRNAs can be viruses as they can manipulate the host gene expression using this tool (23). Nearly 3% of the human genome encodes miRNA genes. These small RNAs play a critical role in various biological processes such as cell apoptosis and development in plants and animals. They function at the translational or mRNA degradation stages (24). Additionally, more than 60% of the *Homo sapiens* mRNA-coding proteins with putative binding sites for miRNA were predicted (25). More than 2,654 mature miRNAs and 1,917 precursor miRNAs are listed for *Homo sapiens*, as reported on the miRBase database (26).

2.2 MicroRNA Biogenesis and Biology

RNA polymerase II (Pol II) generates a transcript identified as pri-miRNA (primary miRNA) during the transcription of the genomic miRNAs in the cell nucleus. Spliced introns of protein-coding genes give rise to approximately 30% of miRNAs. However, most miRNAs encoded gene loci or clusters in the genome. First, the pri-miRNAs comprise more than 1000 bases and stem-loop/hairpin structures with a cap and polyadenylated UTRs. Second, these UTR modifications are cleaved into pre-miRNAs (precursor miRNAs) with 60 to 110 nt by Drosha and DGCR8/Pasha proteins. Pre-miRNAs reportedly binds to XPO5 (Exportin-5) to translocate to the cytosol. The pre-miRNAs are then cleaved by Dicer, generating 15 to 22 nt short double-stranded miRNA duplexes. Finally, DICER and Argonaute (AGO) proteins disassemble the miRNA duplex because of their endoribonuclease activity.

Interestingly, viruses can hijack this process and eventually manipulate the host's gene expression by mimicking the host's short double-stranded miRNA (23). Subsequently, a single strand, called mature miRNA, is assembled into the miRNA-associated RNA-induced silencing complex (miRISC), including DICER and AGO. The miRISC complex can target the UTRs or the coding sequences (CDSs) based on the RNA strand sequence, as illustrated in **Figure 1**. In addition, the miRISC complex suppresses the protein synthesis genes or degrades the mRNAs. The complete alignment with the target mRNA leads to its degradation, whereas the incomplete alignment leads to translation suppression, as shown in **Figure 1** (27).

Furthermore, the mature miRNAs can also exit the cell by different packaging systems. For example, the identification of exosomes containing miR-23b, miR-320, miR-21, let-7a, and miR-1246 are elevated in plasma patients with breast cancer and used as markers for cancer (28, 29). In addition, other proses like lipoproteins, microvesicles, and apoptotic bodies as displayed in **Figure 1** (30–32).



2.3 Methods on Isolating MicroRNAs

Over the last decade, thousands of studies covering miRNA-related discoveries and published. Recent studies have investigated miRNA's role in autoimmune, cardiovascular, and neurological diseases and cancer. Additionally, these studies have identified novel approaches for collecting miRNA from serum to detect metastases and disease prognosis in cancer patients (4). The main goal is to use these miRNAs as biomarkers to develop a fast, non-invasive clinical test for disease diagnosis and prognosis. Many well-known companies currently provide isolation kits using the body biofluids to collect these small circulating non-coding RNA and methods for quantifying them. One study compared six commercial kits and used fresh, frozen, and low volumes of serum to detect sensitivity (33). Another study used serum and cerebrospinal fluids to compare the commercial kit and TRIzol extraction methods for miRNAs recovery and found that TRIzol isolation techniques have low recovery (34). However, many other studies added suggestions and modifications to the TRIzol extraction methods and improved the recovery of the circulating miRNAs over commercial kits (35–37). Quantification of the isolated biomarkers can be performed using *NanoDrop spectrophotometers*. Then using quantification polymerase chain reaction (qPCR) after generating the complementary DNA (cDNA) and for novel miRNA usually using microarray and deep sequencing (34).

2.4 Bioinformatics Analysis

Microarray, qPCR, Next generation-sequencing advancing technologies are becoming more feasible, making them less

expensive than before to quantify miRNA; however, it is only the beginning of any project. Thus, the main challenges are identifying miRNA candidates and their functionality, coding-protein gene targets, and molecular network pathway. Bioinformatics analysis predicts the possible targets for miRNA based on the giving sequences using a specific algorithm. Many databases are available online and always competing on their updates and algorithms. For instance, TargetScan uses the miRNA seeds, which are unique sequences for miRNA, to calculate all the possible binding sites and strength to inhibits the mRNA. Other databases predict targets, such as TarBase, PicTar, and miRBase. Identifying the biological activity and pathways is also available, like; GO (Gene ontology), KEGG, and STRING (38).

2.5 Cancer and MicroRNA

The first study to demonstrate a connotation between miRNAs and tumors was published in 2002. The authors reported that miR-16-1 and miR-15 gene deletions were common in chronic lymphocytic leukemia (CLL) (39). Their expression is inversely correlated with the anti-apoptotic protein and B-cell lymphoma protein (Bcl-2) expression. Both miR-16-1 and miR-15 expressions act as tumor suppressors by suppressing Bcl-2 expression, leading to the induction of apoptosis of leukemic stem cells (40, 41). Interestingly, Bcl-2 was recognized as a suitable biomarker for the prognosis of all molecular subtypes of BCs (42), indicating the potential role of miRNAs in BCs diagnosis. Hence, somatic inhibition of miR-16-1 and miR-15

stimulates leukemogenesis and inhibits cell death (40, 41). Abnormal and dysregulation of miRNA functions have been described in several other cancers, such as lung, breast, colorectal, and leukemia. miRNAs are classified into tumor suppressors or oncogenes (also named oncomir). For example, the miR-30 family, miR-16-1, miR-15, and miR-34 considered tumor suppressors, whereas miR-10, miR-155, and miR-200 family act oncogenes (43). The deregulation of oncomirs or tumor suppressor miRNAs can induce tumorigenesis by manipulating molecular pathways to promote cancer hallmarks, such as proliferation, inhibition of apoptosis, invasion, resistance, and angiogenesis, leading to tumor survival and metastasis (44). Although miRNAs can act as oncomirs or tumor suppressors, studies have also suggested that the global loss of miRNAs can augment tumor progression. Therefore, miRNA dysregulation can promote cellular transformation and carcinogenesis with Dicer, Drosha, and DGCR8 mutation (45).

2.6 MicroRNAs as Diagnostic Marks in Breast Cancer

BC has possible risk factors and lifestyle, family history (genetic alteration in the *BRCA1* and *BRCA2*), age, weight, exposure to radiation, and hormones. In addition, there are two common breast carcinoma types; these are ductal and lobular. Consequently, the treatment strategies are adjusted based on the disease type. Currently, BC is genetically subclassified based on estrogen hormone receptors' levels, human epidermal growth factor receptor (HER2), which can determine the treatment choice (46).

Because BC is remarkably heterogeneous and classified into several subtypes, treatment response and prognosis prediction are challenging. Therefore, new biomarkers are needed (2).

Dysregulation of miRNA was associated with many disorders, including BC. Ongoing studies examine miRNA profiling as a strategy to predict disease progression, improve patient survival, and develop new BC classification strategies (47). Using miRNA expression as a fingerprint would enhance our understanding of disease heterogeneity and novel therapeutics' molecular development. For instance, the expression levels for miRNA cluster miR-125b/miR-99a/let-7c were used as markers to identify luminal A and B subtypes; further, it was correlated with luminal A patients' survival rates (48). Additionally, HER2-encoded miR-4728 expression was precise to detect tumors that are enriched with HER2 receptors. Another cluster, miR-96/182/183, was reported by Zhang et al. and was found to enhance epithelial-to-mesenchymal transition (EMT), which can cause BC cells to be more invasive (49).

Since the 2000s, many more miRNAs have been discovered and linked with BC's development and initiation (50), as described in **Table 1**. Some of the most recognized miRNA families are let-7, miR-200, and miR-10.

The family of let-7 miRNAs in humans includes ten members known to function as tumor suppressors, and they have miR-202, miR-98, and let-7a, b, c, d, e, f, g, and i (72). Let-7 targets multiple molecular pathways contributing to BC heterogeneity and metastases by activating the cancer stem cell (CSC) phenotype (73). On the one hand, a clinical study found the expression of let-7 was considerably lower in patient's serum with BC that developed metastases (74). On the other hand, using Saudi plasma, let-7b-5p, hsa-let-7c-5p, and hsa-let-7i-5p miRNAs were elevated in luminal BC patients and triple-negative BC samples except hsa-let-7c-5p compared to the control (75).

The self-renewing, undifferentiation, and chemotherapy resistance abilities are key CSC features found in BC tumor-

TABLE 1 | Summary of miRNAs associated with drug sensitivity and prognosis in breast cancer.

miRNA	Prognosis	Pathways/Genes	Drug sensitivity/resistance
miR-187-5p and miR-106a-3p	H,PR (51, 52)	HIPK3 and EGFR pathway	Resistant to taxanes, paclitaxel, and docetaxel (53, 54)
miR-182-5p	H,PR (55)	Cx43	Resistant to veliparib (53, 54)
miR-629-5p	H,PR in NSCLC (56)	FOXO3, CXXC4, SFTPC	Resistant to tipifarnib (53, 54)
miR-637	H,PR (57)	Akt1/ β -catenin (cyclin D1) pathway	Resistant to tivantinib (53, 54)
miR-556-5p	H,GR (58)	YAP1	Sensitive to paclitaxel (53, 54)
let-7d-5p and hsa-miR-18a-5p	H,PR (59, 60)	Wnt pathway and BSG	Sensitive to tivantinib (53, 54)
let-7a-5p	H,PR (61)	MYC, HMGA2, H-RAS, HMGA2, DUSP7	Sensitive to bortezomib and paclitaxel (61)
miR-135a-3p	H,PR (62)	HOXA10	Sensitive to JNJ-707 (53, 54)
miR-185-3p	H,GR (63)	E2F1	Sensitive to panobinostat (53, 54)
miR-449	H,GR (64)	TPD52	Sensitive to Doxorubicin (65)
miR-140	H,GR (66)	Wnt1 pathway	Sensitive to fluorouracil, cisplatin, doxorubicin, paclitaxel, and camptothecin (66, 67)
miR-130b	H, PR	PI3K/Akt pathway	Resistant to adriamycin, vincristine, and paclitaxel (68)
miR-29a	H, PR (69)	TET1 and PTEN/AKT/GSK3 β pathway	Resistant to adriamycin (70)
miRNA-132 and miRNA-212	H, PR	PTEN/AKT/NF-KB pathway	Resistant to doxorubicin (71)

High expression (H), Poor Respond (PR), Good Respond (GR), Homeodomain Interacting Protein Kinase 3 (HIPK3), Epidermal Growth Factor Receptor (EGFR), Connexin 43 (Cx43), Non-small-cell lung cancer (NSCLC), Forkhead Box O3 (FOXO3), CXXC Finger Protein 4 (CXXC4), Surfactant Protein C (SFTPC), Yes1 Associated Transcriptional Regulator (YAP1), Basigin (BSG), Homeobox A10 (HOXA10), Tumor Protein D52 (TPD52), Ten Eleven Translocation 1 (TET1).

initiating cell lines (T-IC). Furthermore, let-7 targets the 3'UTR of HMGA2, a high-mobility group protein, and H-RAS mRNA. T-IC cell lines have shown significant expression of both targets due to the loss of let-7 activity. These targets' expression was reduced upon transfection of T-IC cell lines with let-7 lentiviruses (73, 76). Other well-known oncogenes are also targeted by the let-7 family, such as MYC (Myelocytomatosis), KRAS, NRAS, CDK6 (Cell division protein kinase 6), and Cdc25 (Cell division Cycle) (77–79).

The second family is miR-200, consisting of miR-200a, b, c, miR-429, and miR-141. These miRNAs regulate the cell self-renewal *via* B lymphoma Mo-MLV insertion region 1 homolog (BMI1), a known oncogene. This protein, BMI1 at high levels, induces the cell transformation of mammary cells to BC stem cells (80). Furthermore, a report by Jurmeister demonstrated that miR-200c modulates cellular movements. The expression level of miR-200c has been determined to correlate negatively with formin homology 2 domain containing 1 (*FHOD1*) and protein phosphatase, Mg²⁺/Mn²⁺-dependent, 1F (*PPM1F*) levels which are known to promote EMT in BC cell lines by modulating actin formation (81). The ability to move is a sign of aggressiveness, explaining the loss of miR-200c serum in patients diagnosed with triple-negative BC (82).

The third family is miR-10, which was dysregulated in several human cancers, including BC (83). In BC patients, miR-10a was significantly overexpressed in primary tumor samples and cell lines (84). Additionally, the high expression of miR-10b is associated with highly metastatic BC cell lines and in patients with lymph node metastatic (85). In contrast, a study by Ma et al. reported no significant correlation between miR-10b levels and BC patients with distant metastasis (86, 87).

Moreover, many individual miRNAs were also found to interact directly or indirectly with key molecular pathways such as oncomirs or tumor suppressors, modulating BC tumorigenesis. One of the most exceedingly expressed miRNAs in BC has been identified as the oncomir miR-21, which plays a critical role in cancer apoptosis, initiation, migration, and invasion; furthermore, it correlates with tumor development and poor outcomes (88, 89). Such as the significant diagnostic power for miR-21 for BC prediction using Egyptian serum (90). Remarkably, miR-21 targets and suppresses signal transducers and activators of transcription 3 (STAT3) mRNA. Interestingly, STAT3 elevation is an essential biomarker for early detection of 220 BC (8, 91).

MiR-155 is another oncomir that controls many pathways associated with proliferation and reduced survival rates by targeting *BRCA1*, which was identified to play a part in DNA repair and initiation of BC and cell cycle progression (92). Furthermore, miR-155 expression correlates with BC metastasis (93). MiR-155 was also reported to affect apoptosis pathways through caspase 3 by repressing the tumor suppressor gene suppressor of cytokine signaling (SOCS1). Additionally, the activation of miR-155 in BC results in the constitutive stimulation of STAT3 through the JAK network. This pathway induces interleukins and interferons' production, leading to an inflammatory response in BC development (94). This correlated

with the circulating miRNA in mice plasma with breast cancer that decreased significantly when introducing an anti-drug agent miR-155 that reduced inflammation and tumor growth (95). In 2020, a study collected the circulating miR-155 from BC patients and controls that predicted the disease even the grade type (96).

Another miRNA that is often silenced in BC is miR-335, which suppresses all cancer phenotypes except proliferation. miR-335 inhibits metastasis by inhibiting the extracellular matrix protein tenascin-C and transcription factor SOX-4 (97). In addition, miR-335 can reduce cell viability and enhance cell death by modulating the BRCA1 activator network as a metastasis suppressor. However, BRCA1 mutation is the primary pathogenesis for BC and is already nonfunctional even when upregulating miR-335 (98).

Meanwhile, miR-34a is one of the most studied miRNAs that acts as a tumor suppressor and a miR-34b and miR-34c family (99–102). Through targeting silent information regulator 1 (SIRT1), miR-34a induces cell cycle arrest, apoptosis, inhibition of EMT, and proliferation of CSCs (99). Besides, miR-34a targets multiple genes, including Fra-1, LMTK3, Bcl-2, and Notch, implicated in BC tumorigenesis. Although accumulating evidence indicates that miR-34a acts as a tumor suppressor, the suppression of miR-34a was found to promote docetaxel resistance in MCF-7 cells, a known docetaxel-resistant cell (100). However, miR-34a is frequently repressed in BC, which supports BC proliferation and survival (101). Furthermore, this family can also target the mRNA of SIRT1 (silent mating type information regulation 2 homolog) and MYC (102).

MiR-205 is also repressed in metastatic BC. Deregulation of miR-205 enhances BC cell invasion and proliferation (103). The expression of miR-205 was found to inhibit cell growth, clonogenic survival, and enhancement of response to tyrosine kinase suppressors and anchorage-independent cell growth with HER3 (104).

2.7 MicroRNAs as Prognostic Marks in Breast Cancer

Predictive factors give information on whether a patient with cancer will respond to treatment; these are also further used to predict the risk of developing diseases. Unfortunately, despite the marked advances in cancer treatment, chemotherapy resistance remains a significant challenge. Thus, a better comprehension of drug resistance mechanisms is necessary to enhance treatment outcomes. Many factors are associated with drug resistance, such as multidrug resistance protein 1 (MDR1), DNA repair pathways, cell death, and epigenetic modification (105). miRNA can interfere with drug targets that regulate cell survival, apoptotic signaling, and DNA repair pathways. Moreover, miRNAs could modulate cellular responses to anti-cancer treatments (106). Nowadays, prognostic or predictive factors have tremendous potential as biomarkers to guide cancer treatment options. Prognosis predicts the development and disease outcomes and their impact on life quality (107). The most common dysregulated circulating miRNAs are also found in body fluids such as blood. For example, hsa-mir-3662,

hsa-mir-19a, hsa-mir-210, and hsa-mir-7 are located in seven types of cancers. These miRNAs have been determined to significantly impact cancer progression because they regulate critical pathways such as mitogen-activated protein kinases, apoptosis, phosphatidylinositol 3-kinase (PI3K), and Akt/protein kinase B (108).

Interestingly, global dysregulation of miRNAs in many types of cancer can serve as a key prognostic factor. For instance, Dicer and Drosha expression loss are critical in miRNA biogenesis and correlated with poor survival in cancer patients (45).

Collectively, this growing evidence indicates that miRNA profiling and miRNA involvement in drug resistance could help choose the right treatment strategies that most likely will lead to positive outcomes for cancer patients (106). Such as identifying eight miRNAs that can be used as a prognosis after surgery and treatment for triple-negative BC to predict recurrently. They are, miR-20a-5p, miR-455-3p, miR-486-5p, miR-146b-5p, miR-107, miR-324-5p, miR-139-5p and miR-10b-5p (109).

Furthermore, Li et al. identified miR-210 as a therapeutic utility as a biomarker for BC recurrences (110). In 2020, miR-622, a novel miRNA, coupled with poor survival in patients with BC (111). Interestingly, miR-622 was isolated from the patients' plasma in these studies, representing a fast and non-invasive diagnostic method. Similarly, miR-4317 was correlated with lymph node metastasis when it is down-regulated. Sheng et al. used meta-analysis and found candidate targets for miR-4317, and MYD88 mRNA was negatively correlated with a miR-4317 inhibitor that demolished the BC cell lines' ability to migrate, invade, and proliferate shown a significant biomarker value for prognosis (112). Finally, a study demonstrated the potential use of miRNA as an indicator for drug sensitivity and investigated 114 miRNAs and chemotherapy sensitivity in 36 BC lines, as displayed in **Table 1** (53). Also, we integrated the prognosis factor for each of these miRNA using BC patient samples.

2.8 MicroRNAs Reported in BC Patients From Saudi Arabia

BC is still considered a significant disease that affects women, even in developed countries, including Saudi Arabia. More than 1.9 million women are estimated to have BC in 2020, which increased by 18.4% from 2012 (113). According to the Global Cancer Observatory 2018, BC ranked as the most common cancer in Saudi Arabia in both genders; however, it is more common among females. Additionally, BC was identified as the second leading cause of death after leukemia (113). The incidence rate of BC reported between 2010 and 2017 among females ranged from 3 to 8 confirmed cases out of 1000 admitted patients to the Armed Forces Hospital Southern Region, recording the highest rate in 2017 (114). The major cause of death in Saudi BC patients is distal metastases, representing 44.92%, followed by regional metastasis 42.92%; it was determined that 12.15% of deaths had localized diseases (115). These results further highlight the need for improved screening methods. Qattan et al. used a non-invasive method to isolate

circulating miRNAs from Saudi female BC patients' plasma. They identified five significantly elevated miRNAs compared to the control groups. These miRNAs included hsa-let-7i-5p, hsa-miR-25-3p, hsa-miR-16-5p, hsa-let-7b-5p, and hsa-miR-199a-3p. Furthermore, hsa-let-7b-5p, hsa-let-7c-5p, and hsa-let-7i-5p miRNAs were determined to be specifically elevated in luminal BC patients and triple-negative BC samples except for hsa-let-7c-5p. Interestingly, miR-195 was elevated in triple-negative BC (75). Using global miRNA profiling of 23 female BC patients from Saudi Arabia, Hamam et al. were able to identify several circulating miRNAs, including hsa-miR-308, hsa-miR-1290, hsa-miR-188-5p, hsa-miR-1225-5p, hsa-miR-4270, hsa-miR-1202, hsa-miR-1207-5p, hsa-miR-4281, hsa-miR-642b-3p, and hsa-miR-3141. Remarkably, they could concentrate and isolate more miRNAs from the patients' blood samples using a speed vacuum method. The isolated miRNAs were used as a biomarker signature for early-stage detection of BC (116). However, Hamam et al. reported that hsa-miR-155 and hsa-miR-21 were not significantly elevated in the patients' plasma samples, although reported in other cohort studies. Moreover, Alshatwi et al. found that the miRNAs hsa-miR-146a, hsa-miR-499, and hsa-miR-196a2 were significantly upregulated the blood of 92 patients with BC from Saudi Arabia. Additionally, they identified unique genotypic miR-423 (TT) variances in 100 Saudi BC patients compared with matching healthy individuals (117). These genetic variances were associated with metastases and advanced-stage BC (118). Another recent study by Alajez et al., which aimed to discover miRNA biomarkers in samples from Saudi patients to predict metastases (119), reported the downregulation of seven of the miR-200 family of miRNA, including hsa-miR-200a, b, and c in patients with metastasis compared with the primary tumor samples. Other miRNAs identified included hsa-let-7c-5p, hsa-miR-214-3p, hsa-miR-210-3p, and hsa-miR-205-5p, which were also downregulated. The miRNA, hsa-miR-205-5p, was found to modulate Myc, forkhead box O1 (FOXO1), and the amphiregulin (AREG) pathways. Additionally, the expression of hsa-miR-214-3p and hsa-miR-205-5p was correlated with a low survival rate. Furthermore, the global miRNA expression profile confirmed the upregulation of hsa-miR-146a, confirming the findings of Alshatwi et al. reported in Saudi plasma samples, along with other miRNAs such as hsa-miR-150-5p, hsa-miR-155-5p, and hsa-miR-142-5p.

2.9 Clinical Application Using Circulating miRNAs in Breast Cancer Patients

To view the latest clinical pilots (August 2021) approved by the Food and Drug Administration (FDA), and used ClinicalTrials.gov and searched for keywords: circulating, miRNAs, and breast cancer. The results have shown eleven clinical trials with various statuses. However, only five shown are completed; however, these studies did not publish their results. The majority of the studies were completed in France and Italy and one in Poland. Study no. NCT01612871 and NCT03255486 focused on identifying circulating miRNAs correlated with

hormonal treatment and neoadjuvant chemotherapy responses in patients' blood with and without metastases. The other two studies NCT02065908 and NCT02618538 focused on screening women's blood for early detection of breast cancer. Finally, NCT02065908 to detect cardiotoxicity in BC serum patients because of anthracycline chemotherapy administration.

2.10 Strategies in Targeting MicroRNA and Challenges

One of the main rational for targeting miRNA is their ability to crosslink with enormous genes. miRNA's complex networks can manipulate the cell apoptosis, EMT, chemotherapy resistance, and cell cycle, making it a unique therapeutic target. However, few strategies to interfere with these miRNAs were proposed, such as antisense oligonucleotides, locked nucleic acid, miRNA sponges, recovering tumor suppressor miRNA expression.

2.10.1 Antisense Oligonucleotides

MicroRNA based treatment is divided into a first and second generation. The first is synthesized as double-strand small RNA that is antisense (RNA mimicry) to target miRNA. In the second generation, a single strand directly targets the mature miRNA strand, antagomirs. Blocking oncomirs using antisense that is modified and specific to the mature miRNA has shown promising results, demonstrated in **Figure 2**. This approach to block miRNAs was enhanced by adding chemical groups to increases RNA affinity to the target by adding the 2'-O-methoxyethyl group to the antisense oligonucleotides that also stabilized and protect them from nuclease activity. Hutvagner and his team used this principle to successfully silence an endogenous miRNA let-7 *in vivo* and *in vitro* (120).

Similarly, Esau et al., 2006 conjugated the 2'-O-methyl group, and oligonucleotides phosphorothioate reduced the endogenous miR-122 *in vivo* (121). In 2007, Krutzfeldt and his collage used antagomirs, 2'-O-methyl group, oligonucleotides phosphorothioate, and

cholesterol. They injected antagomirs into the tail vein targeting miR-122, which is extremely rich in mice liver. Interestingly, these antagomirs downregulating the endogenous miRNA-122 in 24 hours (122).

2.10.2 Locked Nucleic Acid

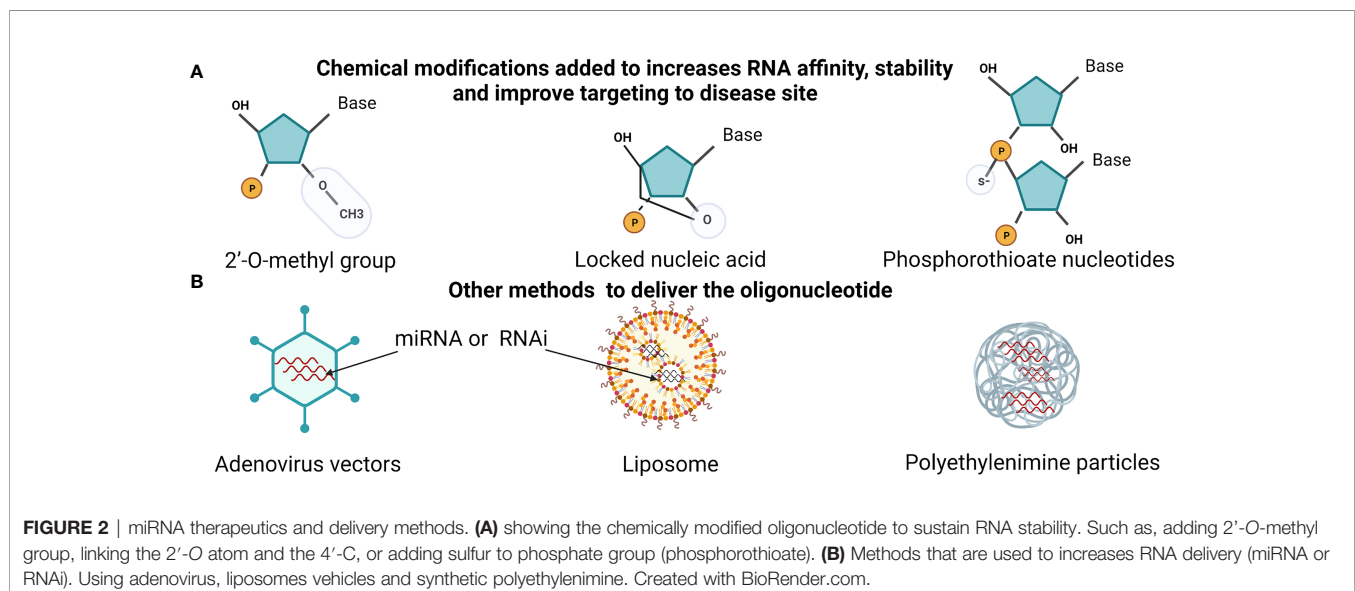
Competing with the antagomirs, the Elmen team also targeted the endogenous miRNA-122 but used a ribose ring locked with methyl group by connecting the 2'-O atom and the 4'-C atom. That gave the molecular more affinity, stability at a significantly lower dose than the conjugated cholesterol by the Krutzfeldt investigation team, illustrated in **Figure 2** (123).

2.10.3 MicroRNA Sponges

"miRNA sponges" was first presented in 2007 by Margaret and colleges. The term "miRNA sponges" is used to describe a vector with a robust mammalian promoter that transcript competitive tandem binding sites to a specific miRNA or a complimentary seed sequence for a family of miRNA. A seed sequence or region is the 2-8nt bases at the 5' of the miRNA complementing a specific subset of targets (mRNA) (124). This seed region is critical and based on it miRNA family is classified. It was successfully introduced in a transgenic animal (*Drosophila* microRNA sponge), demonstrating the miRNA functionality *in vivo* (125).

2.10.4 Recovering Tumor Suppressor MicroRNA Expression

One of the hallmarks of cancer is the inactivation of tumor suppressors. As we showed, many miRNAs can function as tumor suppressors by targeting another oncogene mRNA. Using the same principle as the antisense oligonucleotide, rather than targeting to repress the miRNA replaces the lost one, miRNA mimic. Introducing miR-15a and miR-16 induces cell arrest and apoptosis in prostate tumor xenografts (126). Similarly, miR-29b oligonucleotide on the acute myeloid leukemia xenografts model activates cell death (127). Another method to deliver the



oligonucleotide is using viral vectors. Adenovirus vectors do not intergrade their genome host, making it a great model for providing oligonucleotide. Reducing toxicity and with highly transduction efficiency and accuracy (128). In 2009, Kota and colleges successfully overexpressed miR-26a significantly omitted in hepatocellular carcinoma cell lines using an adenovirus-associated vector. MiR-26a target transcript activates cell cycle, cyclin D2 and E2 making it a great target to investigate *in vivo*. Transduction miR-26a in mouse animal models for hepatocellular carcinoma protected the mice from liver cancer (128).

2.10.5 MicroRNA as a Therapeutic Target and Challenges

Using miRNAs as anti-cancer therapy or targeting their genes could serve as novel treatment strategies to overcome several cancer phenotypes, such as drug resistance and metastases. miRNAs could be targeted by using antisense oligonucleotides specific to certain oncomirs to block their oncogenic activity. Additionally, miRNAs that act as tumor suppressors could be developed as novel therapeutic modalities. To view the latest clinical trials, we used ClinicalTrials.gov and the drug name. A handful of approved miRNA by the FDA had reached the clinical trials, described in **Table 2**. However, over 50 RNA interferences (RNAi) drug treatments are ongoing or completed the clinical test with similar methods in delivery and mechanism as miRNA, explained in **Figure 2** (129). For example, the first RNAi mediated drug that reached the market by Alnylam Pharmaceuticals was for hereditary transthyretin-mediated amyloidosis disease in 2018 and RNAi drug for acute hepatic porphyria in 2019 (130).

Nevertheless, newer or enhanced delivery methods have been developed that increase the efficiency of miRNA therapy reached

clinical trials, such as neutral lipid emulsion, liposomes, and synthetic polyethylenimine demonstrated in **Figures 2** and **3** (131, 132). Moreover, a system using bacterium-derived 400 nm particles conjugated with EGFR antibodies to deliver miR-16 mimics ongoing clinical trials, known as TargomiRs. Similar, small RNA can be linked to N-acetyl-D-galactosamine (GalNAc), another system that uses the cell endocytosis mechanism in phases 1 and 2 and continuing, displayed in **Table 2**. However, the miRNA therapy field is still facing many challenges and young in the therapeutic area similar to RNAi therapeutics, including delivery, stability, off-target effects, and safety (133). Furthermore, miRNAs detected in Saudi Arabia BC patients are still limited, and further studies are needed to provide clinicians with guidelines before applying miRNA-based treatments.

2.11 Conclusion

To date, there have been significant scientific research findings demonstrating the functionality of miRNAs as markers for the prediction, prognosis, and diagnosis of cancer. In addition, accumulating evidence suggests that the suppression of oncomirs or stimulation of tumor-suppressive miRNAs could be used to develop novel treatment strategies, such as RNAi and miRNA-based therapeutics (133). These technologies will significantly lower diagnostic costs, robust the clinical treatment methods, and add molecular targeting to enhance patient prognoses. However, this field is still evolving and still facing many challenges that need to be solved. For example, more profiling for miRNA and identifying their targets, reducing the off-target toxicity, creating a better chemical modification increases cellular uptake to the oligonucleotide, viral delivery efficiency, and safety. However, many preclinical tests are shown promising results as researchers are currently focusing on

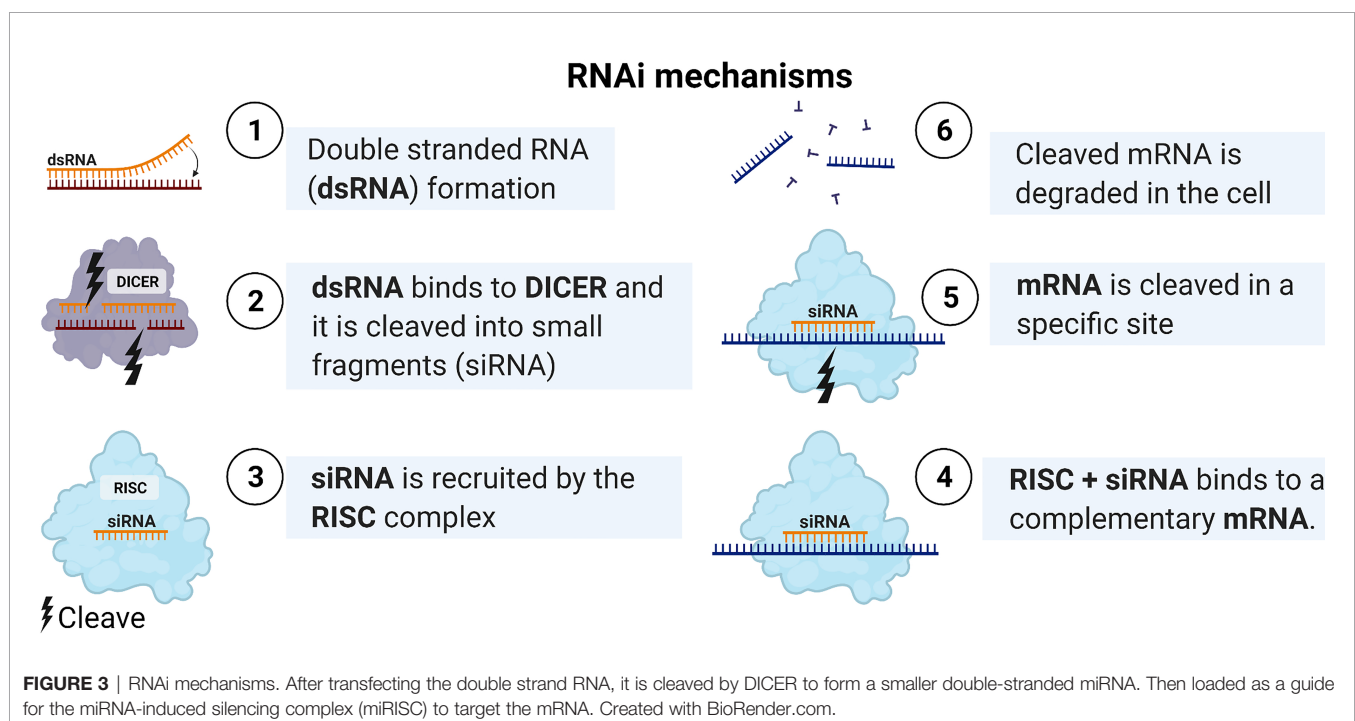


TABLE 2 | Summary of miRNAs drugs FDR-approved in clinical trials.

Drug/company	miRNA	Delivery method	Disease	Phases, status, and Clinical trial no.
MRX34 (Mirna Therapeutics)	miR-34 mimic	Liposomal nanoparticle	Advance solid tumor	Phase I, terminated due to severe immune response, NCT01829971 (134)
MesomiR-1 (EnGenelC)	miR-16 mimic	TargomiRs	Malignant Pleural Mesothelioma and NSCLC	Phase I, ongoing, NCT02369198 (135)
MRG-201 (miRagen Therapeutics)	miR-29 mimic	Cholesterol-conjugated	Keloid	Phase I, ongoing, NCT02603224
MRG-106 (miRagen Therapeutics)	miR-155antagomir	Locked nucleic acid	Cutaneous T-cell Lymphoma, Mycosis Fungoides, Chronic Lymphocytic Leukemia, diffuse large B-cell lymphoma and T-cell leukemia/lymphoma	Phase I, ongoing, NCT02580552
AZD4076 (Regulus Therapeutics)	miR-103/107 antagomir	GalNAc	Type 2 diabetes and non-alcoholic fatty liver	Phase I/II, ongoing, NCT02612662 and NCT02826525
Miravirsen (Hoffmann-La Roche)	miR-122 antagomir	Locked nucleic acid	Chronic hepatitis C	Phase I/II, varies, NCT01646489, NCT01200420, NCT02508090, and NCT02452814

NCT00000000 (ClinicalTrials.gov identifier).

these issues, and pharmaceutical companies show interest in this area presentation opportunities to grow.

AUTHOR CONTRIBUTIONS

The author confirms being the sole contributor of this work and has approved it for publication.

REFERENCES

- Sung H, Ferlay J, Siegel RL, Laversanne M, Soerjomataram I, Jemal A, et al. Global Cancer Statistics 2020: GLOBOCAN Estimates of Incidence and Mortality Worldwide for 36 Cancers in 185 Countries. *CA Cancer J Clin* (2021) 71:209–49. doi: 10.3322/caac.21660
- Sprouffske K, Kerr G, Li C, Prahallad A, Rebmann R, Waehle V, et al. Genetic Heterogeneity and Clonal Evolution During Metastasis in Breast Cancer Patient-Derived Tumor Xenograft Models. *Comput Struct Biotechnol J* (2020) 18:323–31. doi: 10.1016/j.csbj.2020.01.008
- Muller A, Homey B, Soto H, Ge N, Catron D, Buchanan ME, et al. Involvement of Chemokine Receptors in Breast Cancer Metastasis. *Nature* (2001) 410:50–6. doi: 10.1038/35065016
- Li Y, Kowdley KV. MicroRNAs in Common Human Diseases. *Genomics Proteomics Bioinf* (2012) 10:246–53. doi: 10.1016/j.gpb.2012.07.005
- Shah MY, Ferrajoli A, Sood AK, Lopez-Berstein G, Calin GA. microRNA Therapeutics in Cancer - An Emerging Concept. *EBioMedicine* (2016) 12:34–42. doi: 10.1016/j.ebiom.2016.09.017
- Lee RC, Feinbaum RL, Ambros V, The C. Elegans Heterochronic Gene Lin-4 Encodes Small RNAs With Antisense Complementarity to Lin-14. *Cell* (1993) 75:843–54. doi: 10.1016/0092-8674(93)90529-Y
- Wightman B, Ha I, Ruvkun G. Posttranscriptional Regulation of the Heterochronic Gene Lin- 14 by Lin-4 Mediates Temporal Pattern Formation in C. Elegans. *Cell* (1993) 75:855–62. doi: 10.1016/0092-8674(93)90530-4
- Ma JH, Qin L, Li X. Role of STAT3 Signaling Pathway in Breast Cancer. *Cell Commun Signal* (2020) 18:33. doi: 10.1186/s12964-020-0527-z
- Elbashir SM, Harborth J, Lendeckel W, Yalcin A, Weber K, Tuschl T. Duplexes of 21-Nucleotide RNAs Mediate RNA Interference in Cultured Mammalian Cells. *Nature* (2001) 411:494–8. doi: 10.1038/35078107
- Reinhart BJ, Slack FJ, Basson M, Pasquinelli AE, Bettinger JC, Rougvie AE, et al. The 21-Nucleotide Let-7 RNA Regulates Developmental Timing in Caenorhabditis Elegans. *Nature* (2000) 403:901–6. doi: 10.1038/35002607
- Basyuk E, Suavet F, Doglio A, Bordonne R, Bertrand E. Human Let-7 Stem-Loop Precursors Harbor Features of RNase III Cleavage Products. *Nucleic Acids Res* (2003) 31:6593–7. doi: 10.1093/nar/gkg855
- E.P. Consortium. An Integrated Encyclopedia of DNA Elements in the Human Genome. *Nature* (2012) 489:57–74. doi: 10.1038/nature11247
- Hon CC, Ramilowski JA, Harshbarger J, Bertin N, Rackham OJ, Gough J, et al. An Atlas of Human Long Non-Coding RNAs With Accurate 5' Ends. *Nature* (2017) 543:199–204. doi: 10.1038/nature21374
- Candeias MM. The Can and Can't Dos of P53 RNA. *Biochimie* (2011) 93:1962–5. doi: 10.1016/j.biochi.2011.06.010
- Kloc M, Foreman V, Reddy SA. Binary Function of mRNA. *Biochimie* (2011) 93:1955–61. doi: 10.1016/j.biochi.2011.07.008
- Guttman M, Amit I, Garber M, French C, Lin MF, Feldser D, et al. Chromatin Signature Reveals Over a Thousand Highly Conserved Large Non-Coding RNAs in Mammals. *Nature* (2009) 458:223–7. doi: 10.1038/nature07672
- Gong C, Maquat LE. lncRNAs Transactivate STAU1-Mediated mRNA Decay by Duplexing With 3' UTRs via Alu Elements. *Nature* (2011) 470:284–8. doi: 10.1038/nature09701
- Bonasio R, Shiekhattar R. Regulation of Transcription by Long Noncoding RNAs. *Annu Rev Genet* (2014) 48:433–55. doi: 10.1146/annurev-genet-120213-092323
- Yoon JH, Abdelmohsen K, Gorospe M. Functional Interactions Among microRNAs and Long Noncoding RNAs. *Semin Cell Dev Biol* (2014) 34:9–14. doi: 10.1016/j.semcdb.2014.05.015
- Anderson DM, Anderson KM, Chang CL, Makarewich CA, Nelson BR, McAnally JR, et al. A Micropeptide Encoded by a Putative Long Noncoding RNA Regulates Muscle Performance. *Cell* (2015) 160:595–606. doi: 10.1016/j.cell.2015.01.009
- Chng SC, Ho L, Tian J, Reversade B. ELABELA: A Hormone Essential for Heart Development Signals via the Apelin Receptor. *Dev Cell* (2013) 27:672–80. doi: 10.1016/j.devcel.2013.11.002
- Fire A, Xu S, Montgomery MK, Kostas SA, Driver SE, Mello CC. Potent and Specific Genetic Interference by Double-Stranded RNA in Caenorhabditis Elegans. *Nature* (1998) 391:806–11. doi: 10.1038/35888

ACKNOWLEDGMENTS

This manuscript was supported by a grant from the “Research Center of the Female Scientific and Medical Colleges”, Deanship of Scientific Research, King Saud University. Also, the writer would like to thank the RSSU “Research Supporting Unit” at King Saud University.

23. Carthew RW, Sontheimer EJ. Origins and Mechanisms of miRNAs and siRNAs. *Cell* (2009) 136:642–55. doi: 10.1016/j.cell.2009.01.035
24. Bartel DP. MicroRNAs: Genomics, Biogenesis, Mechanism, and Function. *Cell* (2004) 116:281–97. doi: 10.1016/S0092-8674(04)00045-5
25. Friedman RC, Farh KK, Burge CB, Bartel DP. Most Mammalian mRNAs Are Conserved Targets of microRNAs. *Genome Res* (2009) 19:92–105. doi: 10.1101/gr.082701.108
26. Kozomara A, Birgaoanu M, Griffiths-Jones S. Mirbase: From microRNA Sequences to Function. *Nucleic Acids Res* (2019) 47:D155–62. doi: 10.1093/nar/gky1141
27. Ha M, Kim VN. Regulation of microRNA Biogenesis. *Nat Rev Mol Cell Biol* (2014) 15:509–24. doi: 10.1038/nrm3838
28. Hannafon BN, Trigoso YD, Calloway CL, Zhao YD, Lum DH, Welm AL, et al. Plasma Exosome microRNAs Are Indicative of Breast Cancer. *Breast Cancer Res* (2016) 18:90. doi: 10.1186/s13058-016-0753-x
29. Hannafon BN, Carpenter KJ, Berry WL, Janknecht R, Dooley WC, Ding WQ. Exosome-Mediated microRNA Signaling From Breast Cancer Cells is Altered by the Anti-Angiogenesis Agent Docosahexaenoic Acid (DHA). *Mol Cancer* (2015) 14:133. doi: 10.1186/s12943-015-0400-7
30. Axmann M, Meier SM, Karner A, Strobl W, Stangl H, Plochberger B. Serum and Lipoprotein Particle miRNA Profile in Uremia Patients. *Genes (Basel)* (2018) 9:2073–4425. doi: 10.3390/genes9110533
31. Zernecke A, Bidzhikov K, Noels H, Shagdarsuren E, Gan L, Denecke B, et al. Delivery of microRNA-126 by Apoptotic Bodies Induces CXCL12-Dependent Vascular Protection. *Sci Signal* (2009) 2:ra81. doi: 10.1126/scisignal.2000610
32. Li L, Zhu D, Huang L, Zhang J, Bian Z, Chen X, et al. Argonaute 2 Complexes Selectively Protect the Circulating microRNAs in Cell-Secreted Microvesicles. *PLoS One* (2012) 7:e46957. doi: 10.1371/journal.pone.0046957
33. Wright K, de Silva K, Purdie AC, Plain KM. Comparison of Methods for miRNA Isolation and Quantification From Ovine Plasma. *Sci Rep* (2020) 10:825. doi: 10.1038/s41598-020-57659-7
34. McAlexander MA, Phillips MJ, Witwer KW. Comparison of Methods for miRNA Extraction From Plasma and Quantitative Recovery of RNA From Cerebrospinal Fluid. *Front Genet* (2013) 4:83. doi: 10.3389/fgene.2013.00083
35. McDonald JS, Milosevic D, Reddi HV, Grebe SK, Algeciras-Schminich A. Analysis of Circulating microRNA: Preanalytical and Analytical Challenges. *Clin Chem* (2011) 57:833–40. doi: 10.1373/clinchem.2010.157198
36. Shirshova AN, Shamovskaya DA, Boyarskikh UA, Kushlinskii NE, Filipenko ML. One-Phase Phenol-Free Method for microRNA Isolation From Blood Plasma. *MethodsX* (2018) 5:737–43. doi: 10.1016/j.mex.2018.07.002
37. Duy J, Koehler JW, Honko AN, Minogue TD. Optimized microRNA Purification From TRIzol-Treated Plasma. *BMC Genomics* (2015) 16:95. doi: 10.1186/s12864-015-1299-5
38. Zhang GM, Goyal H, Song LL. Bioinformatics Analysis of Differentially Expressed miRNA-Related mRNAs and Their Prognostic Value in Breast Carcinoma. *Oncol Rep* (2018) 39:2865–72.
39. Calin GA, Dumitru CD, Shimizu M, Bichi R, Zupo S, Noch E, et al. Frequent Deletions and Down-Regulation of Micro-RNA Genes Mir15 and Mir16 at 13q14 in Chronic Lymphocytic Leukemia. *Proc Natl Acad Sci U S A* (2002) 99:15524–9. doi: 10.1073/pnas.242606799
40. Pekarsky Y, Croce CM. Role of miR-15/16 in CLL. *Cell Death Differ* (2015) 22:6–11. doi: 10.1038/cdd.2014.87
41. Cimmino A, Calin GA, Fabbri M, Iorio MV, Ferracin M, Shimizu M, et al. miR-15 and miR-16 Induce Apoptosis by Targeting BCL2. *Proc Natl Acad Sci U S A* (2005) 102:13944–9. doi: 10.1038/sj.bjc.6605736
42. Dawson SJ, Makretsov N, Blows FM, Driver KE, Provenzano E, Le Quesne J, et al. BCL2 in Breast Cancer: A Favourable Prognostic Marker Across Molecular Subtypes and Independent of Adjuvant Therapy Received. *Br J Cancer* (2010) 103:668–75. doi: 10.1038/sj.bjc.6605736
43. He Y, Lin J, Kong D, Huang M, Xu C, Kim TK, et al. Current State of Circulating MicroRNAs as Cancer Biomarkers. *Clin Chem* (2015) 61:1138–55. doi: 10.1373/clinchem.2015.241190
44. Hanahan D, Weinberg RA. The Hallmarks of Cancer. *Cell* (2000) 100:57–70. doi: 10.1016/S0092-8674(00)81683-9
45. Hata A, Kashima R. Dysregulation of microRNA Biogenesis Machinery in Cancer. *Crit Rev Biochem Mol Biol* (2016) 51:121–34. doi: 10.3109/10409238.2015.1117054
46. Ellsworth RE, Blackburn HL, Shriver CD, Soon-Shiong P, Ellsworth DL. Molecular Heterogeneity in Breast Cancer: State of the Science and Implications for Patient Care. *Semin Cell Dev Biol* (2017) 64:65–72. doi: 10.1016/j.semcdb.2016.08.025
47. Pham VV, Zhang J, Liu L, Truong B, Xu T, Nguyen TT, et al. Identifying miRNA-mRNA Regulatory Relationships in Breast Cancer With Invariant Causal Prediction. *BMC Bioinf* (2019) 20:143. doi: 10.1186/s12859-019-2668-x
48. Sokilde R, Persson H, Ehinger A, Pirona AC, Ferno M, Hegardt C, et al. Refinement of Breast Cancer Molecular Classification by miRNA Expression Profiles. *BMC Genomics* (2019) 20:503. doi: 10.1186/s12864-019-5887-7
49. Zhang W, Qian P, Zhang X, Zhang M, Wang H, Wu M, et al. Autocrine/Paracrine Human Growth Hormone-Stimulated MicroRNA 96-182-183 Cluster Promotes Epithelial-Mesenchymal Transition and Invasion in Breast Cancer. *J Biol Chem* (2015) 290:13812–29. doi: 10.1074/jbc.M115.653261
50. Fu SW, Chen L, Man YG. miRNA Biomarkers in Breast Cancer Detection and Management. *J Cancer* (2011) 2:116–22. doi: 10.7150/jca.2.116
51. Hu Y, Guo F, Zhu H, Tan X, Zhu X, Liu X, et al. Circular RNA-0001283 Suppresses Breast Cancer Proliferation and Invasion via MiR-187/HIPK3 Axis. *Med Sci Monit* (2020) 26:e921502. doi: 10.12659/MSM.921502
52. Li M, Zhou Y, Xia T, Zhou X, Huang Z, Zhang H, et al. Circulating microRNAs From the miR-106a-363 Cluster on Chromosome X as Novel Diagnostic Biomarkers for Breast Cancer. *Breast Cancer Res Treat* (2018) 170:257–70. doi: 10.1007/s10549-018-4757-3
53. Uhr K, Prager-van der Smissen WJC, Heine AAJ, Ozturk B, van Jaarsveld MTM, Boersma AWM, et al. MicroRNAs as Possible Indicators of Drug Sensitivity in Breast Cancer Cell Lines. *PLoS One* (2019) 14:e0216400. doi: 10.1371/journal.pone.0216400
54. Uhr K, Prager-van der Smissen WJ, Heine AA, Ozturk B, Smid M, Gohlmann HW, et al. Understanding Drugs in Breast Cancer Through Drug Sensitivity Screening. *Springerplus* (2015) 4:611. doi: 10.1186/s40064-015-1406-8
55. Naser Al Deen N, Atallah Lanman N, Chittiboyina S, Lelievre S, Nasr R, Nassar F, et al. A Risk Progression Breast Epithelial 3D Culture Model Reveals Cx43/hsa_circ_0077755/miR-182 as a Biomarker Axis for Heightened Risk of Breast Cancer Initiation. *Sci Rep* (2021) 11:2626. doi: 10.1038/s41598-021-82057-y
56. Liu F, Li T, Hu P, Dai L. Upregulation of Serum miR-629 Predicts Poor Prognosis for Non-Small-Cell Lung Cancer. *Dis Markers* (2021) 2021:8819934. doi: 10.1155/2021/8819934
57. Yang SJ, Wang DD, Zhong SL, Chen WQ, Wang FL, Zhang J, et al. Tumor-Derived Exosomal Circpma1 Facilitates the Tumorigenesis, Metastasis, and Migration in Triple-Negative Breast Cancer (TNBC) Through miR-637/Akt1/beta-Catenin (Cyclin D1) Axis. *Cell Death Dis* (2021) 12:420. doi: 10.1038/s41419-021-03680-1
58. Zhou Y, Liu X, Lan J, Wan Y, Zhu X. Circular RNA Circpph1 Promotes Triple-Negative Breast Cancer Progression via the miR-556-5p/YAP1 Axis. *Am J Transl Res* (2020) 12:6220–34.
59. Nair MG, Prabhu JS, Korlimarla A, Rajarajan S, P SH, Kaul R, et al. miR-18a Activates Wnt Pathway in ER-Positive Breast Cancer and Is Associated With Poor Prognosis. *Cancer Med* (2020) 9:5587–97. doi: 10.1002/cam4.3183
60. Ma L, Li GZ, Wu ZS, Meng G. Prognostic Significance of Let-7b Expression in Breast Cancer and Correlation to Its Target Gene of BSG Expression. *Med Oncol* (2014) 31:773. doi: 10.1007/s12032-013-0773-7
61. Yang W, Gong P, Yang Y, Yang C, Yang B, Ren L. Circ-ABC10 Contributes to Paclitaxel Resistance in Breast Cancer Through Let-7a-5p/DUSP7 Axis. *Cancer Manag Res* (2020) 12:2327–37. doi: 10.2147/CMAR.S238513
62. Chen Y, Zhang J, Wang H, Zhao J, Xu C, Du Y, et al. miRNA-135a Promotes Breast Cancer Cell Migration and Invasion by Targeting HOXA10. *BMC Cancer* (2012) 12:111. doi: 10.1186/1471-2407-12-111
63. Lu G, Li Y, Ma Y, Lu J, Chen Y, Jiang Q, et al. Long Noncoding RNA LINC00511 Contributes to Breast Cancer Tumorigenesis and Stemness by Inducing the miR-185-3p/E2F1/Nanog Axis. *J Exp Clin Cancer Res* (2018) 37:289. doi: 10.1186/s13046-018-0945-6
64. Zhang Z, Wang J, Gao R, Yang X, Zhang Y, Li J, et al. Downregulation of MicroRNA-449 Promotes Migration and Invasion of Breast Cancer Cells by Targeting Tumor Protein D52 (Tpd52). *Oncol Res* (2017) 25:753–61. doi: 10.3727/096504016X14772342320617

65. Tormo E, Ballester S, Adam-Artigues A, Burgues O, Alonso E, Bermejo B, et al. The miRNA-449 Family Mediates Doxorubicin Resistance in Triple-Negative Breast Cancer by Regulating Cell Cycle Factors. *Sci Rep* (2019) 9:5316. doi: 10.1038/s41598-019-41472-y
66. Wu D, Zhang J, Lu Y, Bo S, Li L, Wang L, et al. miR-140-5p Inhibits the Proliferation and Enhances the Efficacy of Doxorubicin to Breast Cancer Stem Cells by Targeting Wnt1. *Cancer Gene Ther* (2019) 26:74–82. doi: 10.1038/s41417-018-0035-0
67. Lu X, Liu R, Wang M, Kumar AK, Pan F, He L, et al. MicroRNA-140 Impedes DNA Repair by Targeting FEN1 and Enhances Chemotherapeutic Response in Breast Cancer. *Oncogene* (2020) 39:234–47. doi: 10.1038/s41388-019-0986-0
68. Miao Y, Zheng W, Li N, Su Z, Zhao L, Zhou H, et al. MicroRNA-130b Targets PTEN to Mediate Drug Resistance and Proliferation of Breast Cancer Cells via the PI3K/Akt Signaling Pathway. *Sci Rep* (2017) 7:41942. doi: 10.1038/srep41942
69. Pei YF, Lei Y, Liu XQ. MiR-29a Promotes Cell Proliferation and EMT in Breast Cancer by Targeting Ten Eleven Translocation 1. *Biochim Biophys Acta* (2016) 1862:2177–85. doi: 10.1016/j.bbdis.2016.08.014
70. Shen H, Li L, Yang S, Wang D, Zhong S, Zhao J, et al. MicroRNA-29a Contributes to Drug-Resistance of Breast Cancer Cells to Adriamycin Through PTEN/AKT/GSK3 β Signaling Pathway. *Gene* (2016) 593:84–90. doi: 10.1016/j.gene.2016.08.016
71. Xie M, Fu Z, Cao J, Liu Y, Wu J, Li Q, et al. MicroRNA-132 and microRNA-212 Mediate Doxorubicin Resistance by Down-Regulating the PTEN-AKT/NF- κ B Signaling Pathway in Breast Cancer. *BioMed Pharmacother* (2018) 102:286–94. doi: 10.1016/j.biopha.2018.03.088
72. Thammaiah CK, Jayaram S. Role of Let-7 Family microRNA in Breast Cancer. *Noncoding RNA Res* (2016) 1:77–82. doi: 10.1016/j.ncrna.2016.10.003
73. Yu F, Yao H, Zhu P, Zhang X, Pan Q, Gong C, et al. Let-7 Regulates Self Renewal and Tumorigenicity of Breast Cancer Cells. *Cell* (2007) 131:1109–23. doi: 10.1016/j.cell.2007.10.054
74. Elghoroury EA, Eldine HG, Kamel SA, Abdelrahman AH, Mohammed A, Kamel MM, et al. Evaluation of miRNA-21 and miRNA Let-7 as Prognostic Markers in Patients With Breast Cancer. *Clin Breast Cancer* (2018) 18:e721–6. doi: 10.1016/j.clbc.2017.11.022
75. Qattan A, Intabli H, Alkhayal W, Eltabache C, Tweigier T, Amer SB. Robust Expression of Tumor Suppressor Mirna's Let-7 and miR-195 Detected in Plasma of Saudi Female Breast Cancer Patients. *BMC Cancer* (2017) 17:799. doi: 10.1186/s12885-017-3776-5
76. Lee YS, Dutta A. The Tumor Suppressor microRNA Let-7 Represses the HMG A2 Oncogene. *Genes Dev* (2007) 21:1025–30. doi: 10.1101/gad.1540407
77. Johnson SM, Grosshans H, Shingara J, Byrom M, Jarvis R, Cheng A, et al. RAS is Regulated by the Let-7 microRNA Family. *Cell* (2005) 120:635–47. doi: 10.1016/j.cell.2005.01.014
78. Sampson VB, Rong NH, Han J, Yang Q, Aris V, Soteropoulos P, et al. MicroRNA Let-7a Down-Regulates MYC and Reverts MYC-Induced Growth in Burkitt Lymphoma Cells. *Cancer Res* (2007) 67:9762–70. doi: 10.1158/0008-5472.CAN-07-2462
79. Trang P, Medina PP, Wiggins JF, Ruffino L, Kelnar K, Omotola M, et al. Regression of Murine Lung Tumors by the Let-7 microRNA. *Oncogene* (2010) 29:1580–7. doi: 10.1038/onc.2009.445
80. Shimono Y, Zabala M, Cho RW, Lobo N, Dalerba P, Qian D, et al. Downregulation of miRNA-200c Links Breast Cancer Stem Cells With Normal Stem Cells. *Cell* (2009) 138:592–603. doi: 10.1016/j.cell.2009.07.011
81. Jurmeister S, Baumann M, Balwierz A, Keklikoglou I, Ward A, Uhlmann S, et al. MicroRNA-200c Represses Migration and Invasion of Breast Cancer Cells by Targeting Actin-Regulatory Proteins FHOD1 and PPM1F. *Mol Cell Biol* (2012) 32:633–51. doi: 10.1128/MCB.06212-11
82. Niedzwiecki S, Piekarski J, Szymanska B, Pawlowska Z, Jezierski A. Serum Levels of Circulating miRNA-21, miRNA-10b and miRNA-200c in Triple-Negative Breast Cancer Patients. *Ginekol Pol* (2018) 89:415–20. doi: 10.5603/GP.a2018.0071
83. Agirre X, Jimenez-Velasco A, San Jose-Eneriz E, Garate L, Bandres E, Cordeu L, et al. Down-Regulation of hsa-miR-10a in Chronic Myeloid Leukemia CD34+ Cells Increases USF2-Mediated Cell Growth. *Mol Cancer Res* (2008) 6:1830–40. doi: 10.1158/1541-7786.MCR-08-0167
84. Zhang L, Huang J, Yang N, Greshock J, Megraw MS, Giannakakis A, et al. microRNAs Exhibit High Frequency Genomic Alterations in Human Cancer. *Proc Natl Acad Sci USA* (2006) 103(24):9136–41. doi: 10.1073/pnas.0508889103
85. Chen W, Cai F, Zhang B, Barekati Z, Zhong XY. The Level of Circulating miRNA-10b and miRNA-373 in Detecting Lymph Node Metastasis of Breast Cancer: Potential Biomarkers. *Tumour Biol* (2013) 34:455–62. doi: 10.1007/s13277-012-0570-5
86. Ma L, Teruya-Feldstein J, Weinberg RA. Tumour Invasion and Metastasis Initiated by microRNA-10b in Breast Cancer. *Nature* (2007) 449:682–8. doi: 10.1038/nature06174
87. Gee HE, Camps C, Buffa FM, Colella S, Sheldon H, Gleadly JM, et al. MicroRNA-10b and Breast Cancer Metastasis. *Nature* (2008) 455:E8–9; author reply E9. doi: 10.1038/nature07362
88. Wang H, Tan Z, Hu H, Liu H, Wu T, Zheng C, et al. microRNA-21 Promotes Breast Cancer Proliferation and Metastasis by Targeting LZTFL1. *BMC Cancer* (2019) 19:738. doi: 10.1186/s12885-019-5951-3
89. Wu Q, Lu Z, Li H, Lu J, Guo L, Ge Q. Next-Generation Sequencing of microRNAs for Breast Cancer Detection. *J BioMed Biotechnol* (2011) 2011:597145. doi: 10.1155/2011/597145
90. Motawi TM, Sadik NA, Shaker OG, El Masry MR, Mohareb F. Study of microRNAs-21/221 as Potential Breast Cancer Biomarkers in Egyptian Women. *Gene* (2016) 590:210–9. doi: 10.1016/j.gene.2016.01.042
91. Zhang C, Liu K, Li T, Fang J, Ding Y, Sun L, et al. miR-21: A Gene of Dual Regulation in Breast Cancer. *Int J Oncol* (2016) 48:161–72. doi: 10.3892/ijo.2015.3232
92. Faraoni I, Antonetti FR, Cardone J, Bonmassar E. miR-155 Gene: A Typical Multifunctional microRNA. *Biochim Biophys Acta* (2009) 1792:497–505. doi: 10.1016/j.bbdis.2009.02.013
93. Mattiske S, Suetani RJ, Neilsen PM, Callen DF. The Oncogenic Role of miR-155 in Breast Cancer. *Cancer Epidemiol Biomarkers Prev* (2012) 21:1236–43. doi: 10.1158/1055-9965.EPI-12-0173
94. Corcoran C, Friel AM, Duffy MJ, Crown J, O'Driscoll L. Intracellular and Extracellular MicroRNAs in Breast Cancer. *Clin Chem* (2011) 57:18–32. doi: 10.1373/clinchem.2010.150730
95. Gorczynski RM, Zhu F, Chen Z, Kos O, Khatiri I. A Comparison of Serum miRNAs Influencing Metastatic Growth of EMT6 vs 4THM Tumor Cells in Wild-Type and CD200R1KO Mice. *Breast Cancer Res Treat* (2017) 162:255–66. doi: 10.1007/s10549-017-4128-5
96. Hosseini Mojahed F, Aalami AH, Poursmaeil V, Amirabadi A, Qasemi Rad M, Sahebkar A. Clinical Evaluation of the Diagnostic Role of MicroRNA-155 in Breast Cancer. *Int J Genomics* (2020) 2020:9514831. doi: 10.1155/2020/9514831
97. Png KJ, Yoshida M, Zhang XH, Shu W, Lee H, Rimner A, et al. MicroRNA-335 Inhibits Tumor Reinitiation and Is Silenced Through Genetic and Epigenetic Mechanisms in Human Breast Cancer. *Genes Dev* (2011) 25:226–31. doi: 10.1101/gad.1974211
98. Heyn H, Engelmann M, Schreek S, Ahrens P, Lehmann U, Kreipe H, et al. MicroRNA miR-335 Is Crucial for the BRCA1 Regulatory Cascade in Breast Cancer Development. *Int J Cancer* (2011) 129:2797–806. doi: 10.1002/ijc.25962
99. Slabakova E, Culig Z, Remsik J, Soucek K. Alternative Mechanisms of miR-34a Regulation in Cancer. *Cell Death Dis* (2017) 8:e3100. doi: 10.1038/cddis.2017.495
100. Li XJ, Ren ZJ, Tang JH. MicroRNA-34a: A Potential Therapeutic Target in Human Cancer. *Cell Death Dis* (2014) 5:e1327. doi: 10.1038/cddis.2014.270
101. Li L, Yuan L, Luo J, Gao J, Guo J, Xie X. MiR-34a Inhibits Proliferation and Migration of Breast Cancer Through Down-Regulation of Bcl-2 and SIRT1. *Clin Exp Med* (2013) 13:109–17. doi: 10.1007/s10238-012-0186-5
102. Yamakuchi M, Ferlito M, Lowenstein CJ. miR-34a Repression of SIRT1 Regulates Apoptosis. *Proc Natl Acad Sci USA* (2008) 105:13421–6. doi: 10.1073/pnas.0801613105
103. Hamam R, Hamam D, Alsaleh KA, Kassem M, Zaher W, Alfayez M, et al. Circulating microRNAs in Breast Cancer: Novel Diagnostic and Prognostic Biomarkers. *Cell Death Dis* (2017) 8:e3045. doi: 10.1038/cddis.2017.440

104. Iorio MV, Casalini P, Piovan C, Di Leva G, Merlo A, Triulzi T, et al. microRNA-205 Regulates HER3 in Human Breast Cancer. *Cancer Res* (2009) 69:2195–200. doi: 10.1158/0008-5472.CAN-08-2920
105. Almeer RS, Abdel Moneim AE. Evaluation of the Protective Effect of Olive Leaf Extract on Cisplatin-Induced Testicular Damage in Rats. *Oxid Med Cell Longevity* (2018) 2018:11. doi: 10.1155/2018/8487248
106. Giovannetti E, Erozcenci A, Smit J, Danesi R, Peters GJ. Molecular Mechanisms Underlying the Role of microRNAs (miRNAs) in Anticancer Drug Resistance and Implications for Clinical Practice. *Crit Rev Oncol Hematol* (2012) 81:103–22. doi: 10.1016/j.critrevonc.2011.03.010
107. Sisic L, Vallbohmer D, Stoecklein NH, Blank S, Schmidt T, Driemel C, et al. Serum microRNA Profiles as Prognostic or Predictive Markers in the Multimodality Treatment of Patients With Gastric Cancer. *Oncol Lett* (2015) 10:869–74. doi: 10.3892/ol.2015.3341
108. Niveditha D, Jasoria M, Narayan J, Majumder S, Mukherjee S, Chowdhury R, et al. Common and Unique microRNAs in Multiple Carcinomas Regulate Similar Network of Pathways to Mediate Cancer Progression. *Sci Rep* (2020) 10:2331. doi: 10.1038/s41598-020-59142-9
109. Hong HC, Chuang CH, Huang WC, Weng SL, Chen CH, Chang KH, et al. A Panel of Eight microRNAs Is a Good Predictive Parameter for Triple-Negative Breast Cancer Relapse. *Theranostics* (2020) 10:8771–89. doi: 10.7150/thno.46142
110. Li Y, Ma X, Zhao J, Zhang B, Jing Z, Liu L. microRNA-210 as a Prognostic Factor in Patients With Breast Cancer: Meta-Analysis. *Cancer Biomark* (2013) 13:471–81. doi: 10.3233/CBM-130385
111. Orlandella FM, Mariniello RM, Mirabelli P, De Stefano AE, Iervolino PLC, Lasorsa VA, et al. miR-622 Is a Novel Potential Biomarker of Breast Carcinoma and Impairs Motility of Breast Cancer Cells Through Targeting NUA1 Kinase. *Br J Cancer* (2020) 20:417–25. doi: 10.1038/s41416-020-0884-9
112. Sheng YW, Hu R, Zhang Y, Luo WJ. MicroRNA-4317 Predicts the Prognosis of Breast Cancer and Inhibits Tumor Cell Proliferation, Migration, and Invasion. *Clin Exp Med* (2020) 20:417–25. doi: 10.1007/s10238-020-00625-4
113. Albeshan SM, Mackey MG, Hossain SZ, Alfuraih AA, Brennan PC. Breast Cancer Epidemiology in Gulf Cooperation Council Countries: A Regional and International Comparison. *Clin Breast Cancer* (2018) 18:e381–92. doi: 10.1016/j.clbc.2017.07.006
114. Asiri S, Asiri A, Ulahannan S, Alanazi M, Humran A, Hummadi A. Incidence Rates of Breast Cancer by Age and Tumor Characteristics Among Saudi Women: Recent Trends. *Cureus* (2020) 12:e6664. doi: 10.7759/cureus.6664
115. Alotaibi RM, Rezk HR, Juliana CI, Guure C. Breast Cancer Mortality in Saudi Arabia: Modelling Observed and Unobserved Factors. *PLoS One* (2018) 13: e0206148. doi: 10.1371/journal.pone.0206148
116. Hamam R, Ali AM, Alsaleh KA, Kassem M, Alfayez M, Aldahmash A, et al. microRNA Expression Profiling on Individual Breast Cancer Patients Identifies Novel Panel of Circulating microRNA for Early Detection. *Sci Rep* (2016) 6:25997. doi: 10.1038/srep25997
117. Alshatwi AA, Shafi G, Hasan TN, Syed NA, Al-Hazzani AA, Alsaif MA, et al. Differential Expression Profile and Genetic Variants of microRNAs Sequences in Breast Cancer Patients. *PLoS One* (2012) 7:e30049. doi: 10.1371/journal.pone.0030049
118. Mir R, Al Balawi IA, Duhier FMA. Involvement of microRNA-423 Gene Variability in Breast Cancer Progression in Saudi Arabia. *Asian Pac J Cancer Prev* (2018) 19:2581–9. doi: 10.22034/APJCP.2018.19.9.2581
119. Elango R AK, Vishnubalaji R, Manikandan M, Ali AM, Abd El-Aziz N, Altheyab A, et al. MicroRNA Expression Profiling on Paired Primary and Lymph Node Metastatic Breast Cancer Revealed Distinct microRNA Profile Associated With LNM. *Front Oncol* (2020) 10:756. doi: 10.3389/fonc.2020.00756
120. Hutvagner G, Simard MJ, Mello CC, Zamore PD. Sequence-Specific Inhibition of Small RNA Function. *PLoS Biol* (2004) 2:E98. doi: 10.1371/journal.pbio.0020098
121. Esau C, Davis S, Murray SF, Yu XX, Pandey SK, Pear M, et al. miR-122 Regulation of Lipid Metabolism Revealed by *In Vivo* Antisense Targeting. *Cell Metab* (2006) 3:87–98. doi: 10.1016/j.cmet.2006.01.005
122. Krutzfeldt J, Kuwajima S, Braich R, Rajeev KG, Pena J, Tuschl T, et al. Specificity, Duplex Degradation and Subcellular Localization of Antagomirs. *Nucleic Acids Res* (2007) 35:2885–92. doi: 10.1093/nar/gkm024
123. Vester B, Wengel J. LNA (Locked Nucleic Acid): High-Affinity Targeting of Complementary RNA and DNA. *Biochemistry* (2004) 43:13233–41. doi: 10.1021/bi0485732
124. Lewis BP, Shih IH, Jones-Rhoades MW, Bartel DP, Burge CB. Prediction of Mammalian microRNA Targets. *Cell* (2003) 115:787–98. doi: 10.1016/S0092-8674(03)01018-3
125. Loya CM, Lu CS, Van Vactor D, Fulga TA. Transgenic microRNA Inhibition With Spatiotemporal Specificity in Intact Organisms. *Nat Methods* (2009) 6:897–903. doi: 10.1038/nmeth.1402
126. Bonci D, Coppola V, Musumeci M, Addario A, Giuffrida R, Memeo I, et al. The miR-15a-miR-16-1 Cluster Controls Prostate Cancer by Targeting Multiple Oncogenic Activities. *Nat Med* (2008) 14:1271–7. doi: 10.1038/nm.1880
127. Garzon R, Heaphy CE, Havelange V, Fabbri M, Volinia S, Tsao T, et al. MicroRNA 29b Functions in Acute Myeloid Leukemia. *Blood* (2009) 114:5331–41. doi: 10.1182/blood-2009-03-211938
128. Kota J, Chivukula RR, O'Donnell KA, Wentzel EA, Montgomery CL, Hwang HW, et al. Therapeutic microRNA Delivery Suppresses Tumorigenesis in a Murine Liver Cancer Model. *Cell* (2009) 137:1005–17. doi: 10.1016/j.cell.2009.04.021
129. Zhang S, Cheng Z, Wang Y, Han T. The Risks of miRNA Therapeutics: In a Drug Target Perspective. *Drug Des Devel Ther* (2021) 15:721–33. doi: 10.2147/DDDT.S288859
130. Mullard A. 2019 FDA Drug Approvals. *Nat Rev Drug Discov* (2020) 19:79–84. doi: 10.1038/d41573-020-00001-7
131. Urban-Klein B, Werth S, Abuharbeid S, Czubayko F, Aigner A. RNAi-Mediated Gene-Targeting Through Systemic Application of Polyethylenimine (PEI)-Complexed siRNA *In Vivo*. *Gene Ther* (2005) 12:461–6. doi: 10.1038/sj.gt.3302425
132. Nishimura M, Jung EJ, Shah MY, Lu C, Spizzo R, Shimizu M, et al. Therapeutic Synergy Between microRNA and siRNA in Ovarian Cancer Treatment. *Cancer Discov* (2013) 3:1302–15. doi: 10.1158/2159-8290.CD-13-0159
133. Esposito CL, Catuogno S, de Francis V. Aptamer-Mediated Selective Delivery of Short RNA Therapeutics in Cancer Cells. *J RNAi Gene Silencing* (2014) 10:500–6.
134. Hong DS, Kang YK, Borad M, Sachdev J, Ejadi S, Lim HY, et al. Phase 1 Study of MRX34, a Liposomal miR-34a Mimic, in Patients With Advanced Solid Tumours. *Br J Cancer* (2020) 122:1630–7. doi: 10.1038/s41416-020-0802-1
135. van Zandwijk N, Pavlakis N, Kao SC, Linton A, Boyer MJ, Clarke S, et al. Safety and Activity of microRNA-Loaded Minicells in Patients With Recurrent Malignant Pleural Mesothelioma: A First-in-Man, Phase 1, Open-Label, Dose-Escalation Study. *Lancet Oncol* (2017) 18:1386–96. doi: 10.1016/S1470-2045(17)30621-6

Conflict of Interest: The author declares that the research was conducted in the absence of any commercial or financial relationships that could be construed as a potential conflict of interest.

Publisher's Note: All claims expressed in this article are solely those of the authors and do not necessarily represent those of their affiliated organizations, or those of the publisher, the editors and the reviewers. Any product that may be evaluated in this article, or claim that may be made by its manufacturer, is not guaranteed or endorsed by the publisher.

Copyright © 2021 Alyami. This is an open-access article distributed under the terms of the Creative Commons Attribution License (CC BY). The use, distribution or reproduction in other forums is permitted, provided the original author(s) and the copyright owner(s) are credited and that the original publication in this journal is cited, in accordance with accepted academic practice. No use, distribution or reproduction is permitted which does not comply with these terms.



Advancements in 3D Cell Culture Systems for Personalizing Anti-Cancer Therapies

Andrew M. K. Law^{1,2†}, Laura Rodriguez de la Fuente^{1,2,3†}, Thomas J. Grundy⁴, Guocheng Fang⁵, Fatima Valdes-Mora^{3,6*} and David Gallego-Ortega^{1,2,5*}

OPEN ACCESS

Edited by:

Maria Rosaria De Miglio,
University of Sassari, Italy

Reviewed by:

Diogo Alpuim Costa,
CUF Oncologia, Portugal
Ahmet Acar,
Middle East Technical University,
Turkey
Valentine Comaills,
Andalusian Center of Molecular
Biology and Regenerative Medicine
(CABIMER), Spain

*Correspondence:

Fatima Valdes-Mora
FValdesMora@ccia.org.au
David Gallego-Ortega
David.GallegoOrtega@uts.edu.au

[†]These authors have contributed
equally to this work

Specialty section:

This article was submitted to
Breast Cancer,
a section of the journal
Frontiers in Oncology

Received: 24 September 2021

Accepted: 11 November 2021

Published: 30 November 2021

Citation:

Law AMK, Rodriguez de la Fuente L,
Grundy TJ, Fang G, Valdes-Mora F
and Gallego-Ortega D (2021)
Advancements in 3D Cell Culture
Systems for Personalizing
Anti-Cancer Therapies.
Front. Oncol. 11:782766.
doi: 10.3389/fonc.2021.782766

¹ Tumour Development Group, The Kinghorn Cancer Centre, Garvan Institute of Medical Research, Darlinghurst, NSW, Australia, ² St. Vincent's Clinical School, Faculty of Medicine, University of New South Wales Sydney, Randwick, NSW, Australia, ³ Cancer Epigenetic Biology and Therapeutics Lab, Children's Cancer Institute, Randwick, NSW, Australia, ⁴ Life Sciences, Inventia Life Science Pty Ltd, Alexandria, NSW, Australia, ⁵ School of Biomedical Engineering, Faculty of Engineering and IT, University of Technology Sydney, Ultimo, NSW, Australia, ⁶ School of Women's and Children's Health, Faculty of Medicine, University of New South Wales Sydney, Randwick, NSW, Australia

Over 90% of potential anti-cancer drug candidates results in translational failures in clinical trials. The main reason for this failure can be attributed to the non-accurate pre-clinical models that are being currently used for drug development and in personalised therapies. To ensure that the assessment of drug efficacy and their mechanism of action have clinical translatability, the complexity of the tumor microenvironment needs to be properly modelled. 3D culture models are emerging as a powerful research tool that recapitulates *in vivo* characteristics. Technological advancements in this field show promising application in improving drug discovery, pre-clinical validation, and precision medicine. In this review, we discuss the significance of the tumor microenvironment and its impact on therapy success, the current developments of 3D culture, and the opportunities that advancements that *in vitro* technologies can provide to improve cancer therapeutics.

Keywords: 3D culture systems, personalised medicine, drug resistance prevention, tumor microenvironment, 3D bioprinting, extracellular matrix, microfluidics

INTRODUCTION

Uncontrolled division of neoplastic cells results in the development of a tumour mass composed of a large variety of cellular and non-cellular components, including the heterogeneous population of cancer cells, infiltrating and resident normal cells, extracellular matrix (ECM) proteins and secreted factors. This complex and highly heterogeneous conglomerate of multiple cell types and extracellular components inside of the tumour mass is known as the tumour microenvironment (TME) (1). The interacting networks established in the TME among cancer cells and the other cell types are the key contributors to the hallmarks of cancer and determine the aggressiveness of the tumour (2–4). Furthermore, this tumour heterogeneity within the TME widely contributes to the extent of patient responses to anti-cancer therapies (5). Resembling the network and the heterogeneity involved in

every type of cancer is considered one of the most challenging practices among oncology researchers globally. However, understanding the molecular features in the TME of each cancer is fundamental for the successful development of clinically translatable anti-cancer drugs.

MODELLING THE PHYSIOLOGY OF TME FOR DRUG TESTING

The complexity within the TME is propagated by the heterogeneous nature of different tumor entities; that is each individual tumor harbors its own unique intricacies comprised of structural, cellular, genetic, and molecular composition. Our continuous effort to improve our understanding of oncology has led to the development of more effective diagnostic and therapeutic approaches. However, we are also simultaneously unravelling the anomalous disease complexities within cancer that challenges clinical success. In a comprehensive survey of clinical success rates by Hay et al., oncology drugs were found to have only a 6.7% success rate of being approved (6), with other studies estimating as low as 3.4% (7). There are various reasons that contribute to this high rate of failure including 1) inadequate

efficacy from poor biodistribution and metabolism of the drug – unsatisfactory therapeutic index; 2) safety concerns associated with significant side effects and off-target toxicities; 3) financial or commercial issues such as insufficient funding or patient recruitment and retention (8–11). Ineffectiveness of therapies is the most common factor (57%) attributed to failure during clinical development (10, 11). Unfortunately, most experimental drugs that were designed through using pre-clinical models to therapeutically target known molecular components are poorly translated to clinical practice.

During the pre-clinical phase, the most commonly employed cancer models are 2D cell cultures before transitioning to *in vivo* mice models (Figure 1) (12). Drug testing in animals prior to clinical trials have been a mainstay for determining drug efficacy and toxicity; however, there are also various issues associated with animal models, from increased costs, logistic demand, limited bioavailability, and an increasing ethical concern (13–15). Although these models have provided us with better insights into tumor biology and have made a significant impact on approaches to cancer healthcare, they do not accurately recapitulate the complex TME and molecular features within a human tumor (16, 17). The dismal results of clinical translatability of drugs developed from pre-clinical models highlight the limitations of our current understanding (16). Currently, one of






	Advantages	Disadvantages
	2D cell culture  <ul style="list-style-type: none"> • Standardised protocol • Cheap and simple • Can be automated • Compatible with high-throughput • Easily expandable • Compatible with various cell types 	<ul style="list-style-type: none"> • Static conditions • No ECM and TME • No concentration gradient • Homogenous populations • Low physiological relevance • Not clinically predictive
	3D cell culture  <ul style="list-style-type: none"> • Efficacy • Drug resistance • Cell-cell and cell-ECM interactions • Sensitivity similar to <i>in vivo</i> • Co-culturing • Heterogenous 	<ul style="list-style-type: none"> • Static environment • Low TME mimicry • Challenges to automate for high content screening • Inefficient waste and nutrient diffusion
	Mice models  <ul style="list-style-type: none"> • Efficacy • Drug resistance • Whole-body pharmacokinetics • Side effects • TME mimicry • Genetically modifiable 	<ul style="list-style-type: none"> • Immunodeficient (PDX) • Unable to upscale • Engraftment failures • Different pathophysiology to humans • Long tumour latency • Murine microenvironment
	Clinical trials  <ul style="list-style-type: none"> • Efficacy • Drug resistance • Whole-body pharmacokinetics • Adverse reactions • Immune response • Route of administration • Highly clinically relevant 	<ul style="list-style-type: none"> • Programs require collaborations between numerous professionals and experts • Long-term follow-ups • Variable patient retention • Challenges in patient recruitment processes • Difficulties in setting trials for rare cancers • Logistical and financial constraints

FIGURE 1 | Advantages and disadvantages of drug development using different pre-clinical models and clinical trials. The physical features when using a pre-clinical model is crucial to ensure physiological relevance. 2D cell cultures is a widely adopted and well-established model that has been used consistently in drug discovery and high throughput screening. However, cancer cells cultured in 2D do not recapitulate the biology of an *in vivo* tumor and thus has very poor performance for clinical prediction. As such, the use of more complex models such as 3D cell culture and mice models has been more representative of clinical cases compared to 2D cell culture. However, the standardized implementation of these models for applications in high content screening and personalised medicine remains a challenge.

the major obstacles for delivering better cancer patient cares is associated with accurate diagnosis and prediction to therapeutic responses (18). As such, the importance of developing more accurate, cost-effective, and efficient pre-clinical technologies for better *in vitro* and *in vivo* models are crucial to creating more efficacious therapies, predicting therapeutic outcomes, and guiding clinical practice.

Bridging the Pre-Clinical Gap: 3D Culture Models

Many researchers use 2D cell cultures as the *in vitro* pre-clinical model for testing anti-tumor drugs before proceeding with *in vivo* trials (13). This is primarily due to the convenience, simplicity and cost-effectiveness of using a 2D cell culture as a model (Figure 2).

However, it is evident that results attained from 2D *in vitro* models have almost no clinical translatability to human tumors (13). The 2D monolayer cultures have been optimized to grow on rigid plastic surfaces and thus fail to capture the crucial elements that make up the complex 3D tissue architecture of the TME, which ultimately affects the cellular response of cells to drugs and the off-target effects. While 2D cultures are still predominantly used for drug discovery due to its simplicity and compatibility with high-content screening platforms, 3D culture systems have numerous advantages over 2D cell culture. Thus the transition to 3D preclinical models have become more appealing as improvement in tissue engineering technology has made 3D cell culture more adaptable and tunable over the microenvironmental factors to better reflect the functional pathology of *in vivo* tumors.

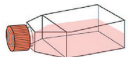








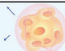




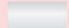

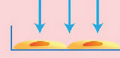



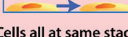
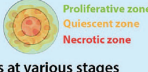


	2D cell culture	3D cell culture
		
Cell-Cell	 Limited cell-cell interaction	 Surrounding cell-cell interaction
Cell-ECM	 No cell-ECM interaction	 Cell-ECM interaction
Cell adhesion	 Restricted on 2D plane	 Dispersed in 3D
Mobility	 Uninhibited dispersion and migration	 Sterically hindered dispersion and migration
Scaffold	 Glass or polystyrene	 Physical structure with matrix
Modification	 Non-modifiable sites	 Modifiable sites
Stiffness	 Untunable - very high (GPa)	 Tunable - low (kPa)
Soluble gradient	 Absent	 Present
Drug resistance	 Non-representative	 Sensitivity similar to <i>in vivo</i>
Cell cycle stage	 Cells all at same stage	 Cells at various stages
Phenotypic diversity	 Conforming	 Diverse

FIGURE 2 | Physiological differences between 2D cell culture and 3D cell culture. Cells develop as a 2D monolayer adopt an apical-basal polarity when plated on a culture flask or a petri dish. The environment that cells are exposed to within the culture flask is a poor representation and does not accurately recapitulate physiological conditions. Comparatively, 3D cultures provide greater biological relevance and cellular response to perturbations are more reflective of *in vivo*.


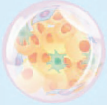
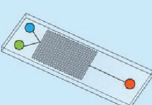

3D Culture Techniques	 Suspension Culture	 Hydrogel Scaffold	 Organ-on-chip	 3D bioprinting
Advantages	<ul style="list-style-type: none"> • Standardised protocols • Cheap and simple • Can be automated • Adaptable for high-throughput • Replicable 	<ul style="list-style-type: none"> • Mimics TME • Relatively cheap and simple • Can be automated • Adaptable for high-throughput • Versatile application and hydrogel availability • Tunable properties 	<ul style="list-style-type: none"> • Dynamic fluidics and perfusion • Simulate physiological processes (eg heartbeat) • Engineered vascularisation • Precise control over microenvironment • Model drug delivery systems 	<ul style="list-style-type: none"> • High precision and resolution (100um) • Construct highly complex tissue structure • Can be automated • Fine tuning of tissue architecture and size • Various bioinks available
Disadvantages	<ul style="list-style-type: none"> • Simple TME • Static • Inefficient nutrient and waste diffusion • Spheroid sizes can vary depending on technique 	<ul style="list-style-type: none"> • Simple architecture • Batch-to-batch variability (Natural hydrogels) • Require biofunctionalisation (Synthetic hydrogels) • Static • Inefficient nutrient and waste diffusion 	<ul style="list-style-type: none"> • High expertise barrier • Difficult to upscale • Requires specialised equipments • Not suitable for long-term experiments 	<ul style="list-style-type: none"> • High expertise barrier • Difficult to upscale • Expensive • Requires specialised equipments • Cell viability can vary depending on technique

FIGURE 3 | Advantages and disadvantages of various 3D culture approaches. The key features of 3D culturing aim to improve the biomimicry and predictive value of pre-clinical models. Suspension cultures and scaffold-based approaches are easier to implement in the lab and upscale for high-throughput. Advancements in microfabrication technology such as microfluidic chips and 3D bioprinting have resulted in more complex and physiologically-relevant models that can be generated.

The emergence of 3D cell culture models as research tools plays a vital role during early pre-clinical drug development. Recently there has been a paradigm shift in the way researchers study the TME; 3D models are able to better mimic the *in vivo* microenvironment compared to 2D cell culture and their applications are simpler, more efficient, versatile, and cost-effective compared to using animal models (13). Currently, intense efforts are taken to generate new cell lines that represent the vast heterogeneity of tumors. Three-dimensional cultures offer a higher chance to represent the genomic diversity and allow testing of new drugs targeting specific signaling pathways. Additionally, 3D culture is a more efficient way to generate new patient-derived cell lines that fail to grow in 2D. For example, in breast cancer and melanoma, tumor circulating cells derived from patients are successfully grown under hypoxia conditions in suspension cultures (19, 20). And in prostate cancer, organoid models from patient-derived xenografts can be also used to assay drug sensitivity (21).

Furthermore, cells embedded within a 3D matrix self-assemble to form structures more similar to their organisation *in vivo* and enable better intercellular contact and communication. Recent advancement in 3D culture has led to the development of new technologies that can generate more complex 3D cell models that aim to bridge the gap between 2D cell culture and animal models. The improved biological relevance of 3D models is due to several key features: dimensionality, presence of ECM, and concentration gradients (Figure 2).

3D Cultures – Dimensionality

3D culture models cultivate a more relevant pathophysiological microenvironment that allows cells to aggregate, proliferate, and display phenotypes as they do within the body. The complex cellular interactions between other cells and the 3D matrix are crucial for maintaining regular cell structure, function and mobility. Since cell migration occurs in three dimensions the matrix provides a topology that mimics the 3D architecture of a tissue, allowing cells attach and interact with their surrounding environment (22). The dynamic tensile forces from the matrix play a crucial role in cell migration and are involved in activating pathological mechanisms associated with invasion, ECM remodeling, and metastasis (23, 24). Kock et al. had conducted a study investigating the biomechanical tractions utilized by various carcinoma cells to invade through a collagen gel. Interestingly, the level of matrix contraction was not associated with invasiveness, but rather the cellular adoption of an elongated spindle-like morphology and the complexity of the collagen deformation (24). Furthermore, fibroblasts were reported to migrate more rapidly on a 3D matrix and maintained a more spindle-like characteristic compared to those that were cultured in 2D (25). Contrarily, cells grown on a 2D plane have much less physical hindrance as they move across a planar surface that is only impeded by surface inhibition (23). As such, 3D cultures have been used to elucidate the mechanisms that drive cancer invasion and metastasis. For example, matrix degradation and ECM remodeling are key

factors involved in invasive malignancy and have been studied in *ex vivo* models to identify potential targets for cancer therapies, such as inhibiting matrix metalloproteinases and invadopodia formation (26–28).

3D Cultures – Extracellular Matrix

The ECM has been well established to influence cell behaviour and response to external factors (29, 30). Cellular phenotypes and functions are dictated by a complex network of signaling that occurs within the context of the microenvironment through cell-cell communications, cell-ECM interactions, soluble factors, and small molecules (29). The importance of these dynamic interactions between cells and its surrounding ECM becomes apparent as cells grown in 3D adopt physical and genetic properties more akin to *in vivo*, such as morphology, phenotype, and expression profiles; whereas 2D monolayers have more vastly different characteristics forced by the unnatural plastic environment (31–33). Additionally, the biomechanical properties of the ECM can modify the signal transductions that occurs within the microenvironment *via* the spatial organisation of cells, stiffness of the matrices, and physical constraints to hinder cell mobility (29, 34). During tumorigenesis, the stiffness of the ECM causes compressive stress that increases the mechanical pressure as the tumor grows and expand. This increased ECM resistance promotes cell-ECM and cell-cell within the tumor communications that can induce hyperactivated mechanotransduction pathways such as RHO/ROCK (35). Consequently, this upregulation of ROCK can increase cancer cell proliferation, migration, epithelial-mesenchymal transition (EMT), and cancer-associated fibroblast (CAF) reprogramming to promote tumor progression (35, 36). Within the ECM various molecules can also regulate the behaviour, differentiation, migration, and phenotypic fates of cells (37). These can include: glycoproteins such as laminin and fibronectin that connects structural molecules together or with cells to orchestrate cell attachment and migration through the ECM; ECM fibres such as collagen and elastin to provide structural elements of tensile strength and elasticity; and proteoglycans such as hyaluronic acid, keratan sulphate, and chondroitin sulphate, that can regulate structural and adhesive properties of the ECM, angiogenesis, and sequester growth factors (37, 38). Additionally, drug sensitivity in cells can be variable based on cell-ECM interactions and spatial positioning of cells relative to the ECM (30, 39, 40). Changes in ECM composition and its biophysical properties do not only alter cell phenotype but can also regulate the cellular response to drugs, such as promoting acquired resistance or reducing drug accumulation within the tumor (41, 42).

3D Cultures – Concentration Gradient

Soluble metabolites, oxygen concentration, and pH throughout the TME can strongly affect the tumor pathophysiology and the efficacy of therapies (39–41). These components exist as a gradient within the tumor; peripheral cells in closer proximity to blood vessels have more access to soluble constituents and oxygen, which decreases as it diffuses through the ECM to the tumor core. The concentration gradients of growth factors, nutrients, wastes, and gases compounds to the intratumoral heterogeneity and influences the signaling within the microenvironment including cell function,

proliferation, morphogenesis, and chemotaxis (30). As such, cells grown in larger 3D aggregates also mimic the *in vivo* condition by existing in various proliferative states based on nutritional access that is restricted by the concentration gradient. From the peripheral to the core of the spheroid is composed of the outer proliferative zone, semi-peripheral quiescent zone, and the central necrotic zone, where each region is in different cell cycle stages (34). This difference in cell cycle stage amongst cancer cells in 3D cultures also contributes to the variable sensitivity of drugs and tumor recurrence from quiescent cells (32, 34). Since blood vessels are unevenly distributed throughout the tumor, regions with low or absent vasculature are hypoxic and acidic and contain high interstitial oncotic pressure (43). In the context of pharmacokinetic, the concentration gradient limits the penetrance of drugs through the tumor and attains a dosage sufficient to exert their therapeutic effects on all the cancer cells (44). In addition, the half-life of drugs also determine the distribution of the agent throughout the tumor; drugs with a long half-life will have more uniform distribution across the tumor even if the rate of the diffusion is low, whereas drugs with a short half-life will have a nonuniform distribution (45). Most research also focuses on the role of mechanisms of action for drugs or therapy resistance, however the physiochemistry of drugs is often neglected (44). As a result, the impeded distribution and diffusion of pharmaceutical agents through the tumor still remains one of the major challenges in anti-cancer treatments. This important, yet often overlooked, the property makes 3D cultures a more accurate model to study the impact of pharmacokinetics and even bacterial biodiversity (46) from concentration gradients (47); compared to cells in 2D cultures which are all homogeneously exposed to nutrients and agents (30).

3D Cultures – Microbiome

The clinical research on the association of microbiota and cancer started in 1868 by William Busch. After centuries of research, increasing evidence implicates that microbiota influences the TME, tumor metabolism, and tumor immunotherapy response (48). For instance, gut microbiota dysbiosis may induce breast tumorigenesis (49). The influence of microbiota in tumorigenesis and tumor progression may differentially impact different types of tumors, as it has been demonstrated the existence of tumour type-specific intracellular bacteria (50). This tumour microbiome diversity, specificity and relevancy provide both challenges and possibilities for tumour treatment (51). Modelling the interactions of microbiota and tumour offers an efficient method to understand the inner correlations and evaluate the microbiota-target drugs.

Compared to the 2D cell models, the 3D culture can replicate the mechanical cues of solid tumors and the chemical gradient (pH, hypoxia, lactate, etc.), which influence the microbiota proliferation, distribution, movement, variety, and metabolism. This, in turn, could affect the metabolite levels in the TME, for instance, by regulating the gene expression (52). Stem-cell derived organoids, relying on 3D culture, have become indispensable tools to investigate the host-microbiota interactions (53). For instance, intestinal organoids usually form luminal structures within the hydrogel's matrix where the bacteria of interest can be microinjected (54). As such, stomach organoids were modelled

with *Helicobacter Pylori* (55). The organ-on-chip approach could also mimic the complexity of 3D tissues or tumors, which attracts more attention to the study of microbiome and disease, an example of this approach has been applied to the gut-microbiome on a chip (56, 57). The bidirectional interactions of drugs with local microbiota manipulate the host response to chemotherapeutic drugs (49, 51, 58, 59), which potentially highlights the importance of 3D cultured models in pharmomicrobiomics. In addition, with the fast development of engineered microbial therapies, 3D cultures become a good candidate for more reliable screening, enabling parallel and long-term monitoring (60).

APPROACHES TO 3D CULTURE MODELS

Anti-cancer drug screening and the development of new personalised therapies are primarily conducted in 2D cultures of cancer cell lines (30). Researchers have generated the Cancer Cell Line Encyclopedia to help provide predictive modelling of anticancer drug sensitivity (61, 62). 2D cultures are a mainstay in biological research and have provided us with a deeper insight and understanding of cancer mechanisms, biomarker discovery, and stratification of tumour profiles. From a drug-development perspective, the improvement of more predictive preclinical models is essential to permit the earlier dismissal of drug candidates from clinical trials and reduce pharmaceutical cost – the development of a new drug is estimated to be \$2.6 billion (63). The disparate response to therapies observed in 2D cultures and in mouse models becomes evident in clinical trials, in which oncology drugs are known to have as low as 3.4% success rate (7). For example, the drug Palifosfamide was a DNA alkylating agent used as a first-line treatment for metastatic soft tissue sarcoma that had failed in Phase III PICASSO 3 trial due to not being able to meet its primary endpoint of progression-free survival in patients (NCT01168791). Within the lab, Palifosfamide demonstrated cytotoxicity in sarcoma cell lines with an IC_{50} range of 0.5–1.5 μ g/mL and treatment in xenograft SCID mice resulted in tumour growth inhibition and improved event-free survival (64).

Recapitulation of the fundamental tissue environment within the human body is essential for the proper evaluation of drug effectiveness. From both the cellular populations to the acellular compositions, such as the ECM, pre-clinical models aim to replicate both pathophysiological and healthy bodily functions. Mimicking the complexities of all the biological processes in a single model is highly challenging. Therefore, researchers are developing new techniques to make 3D culture more applicable and easier to implement (Figure 3). As such, 3D cell cultures are becoming more convenient and accessible while allowing researchers to improve upon the traditional *in vitro* 2D cultures, aiming to model more native-like interactions of tissues to study their mechanisms.

Suspension Cultures

Spheroids are grown as aggregates in suspension and have been applied in various cell types, such as cancer cells, hepatocytes, and stem cells (65). Additionally, they can be grown as a

monoculture or together as a co-culture with other cell types to provide more physiologically relevant interactions. In a study by Courau et al., colon cancer cells were co-cultured with T cells and NK cells to evaluate tumour-lymphocyte communication and test immunomodulatory antibodies (66). Spheroids are able to recapitulate the *in vivo* characteristics of intercellular communications, cell-ECM interaction, and behaviour. The size of spheroids are dictated by the initial seeding cell number; thus it is crucial to optimize the culture conditions to ensure that the spheroids do not become too large and suffer from hypoxia and necrosis from poor nutrient diffusion (30). Spheroids can be generated through 1) hanging drop; 2) low adhesion plates 3) magnetic levitation.

The hanging drop technique is one of the earliest methods of developing 3D cell culture (67). This technique uses specialized hanging drop plates that contain a bottomless well where the droplet of media forms. Cells aggregate within the small droplet of culture media to generate the spheroid over several days. Co-culturing can be conducted by adding cells during the initial dispensing or from consecutive addition of the cells (65). However, transfer of the spheroids from the hanging drop plate to another non-attachment plate will be necessary if growing larger spheroids or downstream assays. The hanging drop technique is relatively facile and efficient and has been adapted for use in various cell lines for toxicity testing and drug screening (68, 69). This technique has very high reproducibility with consistent size spheroids (70).

Low adhesion plates have a low attachment coating on the surface of the wells that reduces cell adherence and promotes cell aggregation into spheroids. The coating can include the non-adherent poly-HEMA or agarose (30). Larger volumes of media can also be used in the low adhesion plate allowing a more efficient generation of tumour spheroids. Furthermore, low adhesion plates are designed for high-throughput screening, allowing 3D cell culturing and assaying within the same, unlike the hanging drop technique (65).

Magnetic levitation generates spheroids through the use of magnetic nanoparticles. Cells are incubated with the nanoparticles for several hours to overnight and are then loaded in a low adhesion plate. The low adhesion plate minimizes cell adhesion to the plate while the application of a magnetic field above the plate incites cells to aggregate and produce the spheroids, which can be maintained without requiring a continuous magnetic force. The spheroids can then be subsequently manipulated using other magnetic tools, such as to accelerate cell migration (71). Magnetic levitation can be scalable for use in high throughput screening and drug discovery (72).

Hydrogel Scaffold Models

Biomimetic scaffolds that model the ECM have been developed over the past few decades to develop microenvironments that can overcome the limitations of traditional 2D cell cultures. In particular, hydrogels have gained interest as physical support that provides the architecture, topology, and biomechanical properties which enables more *in vivo*-like cellular behaviour and communication. Hydrogels can be used to generate various natural and synthetic ECMs that simulate the microenvironment

and stiffness of most soft tissues (29). The internal structures of hydrogels consist of networks of cross-linked polymers that can be moulded through mild gelation conditions that have minimal cytotoxicity (13). Furthermore, hydrogels can be chemically modified to tailor matrix stiffness and viscoelasticity (73–75). Integrin interaction (76, 77), growth factor binding (78), and the 3D organisation of the cells (79) can be tuned through the decoration of hydrogel with a variety of peptides (80, 81). ECM remodeling and cell migration can be facilitated through the inclusion of degradable MMP cleavage sites (76, 77), while the synthetic ECM environment can be enriched with matrix proteins including collagens (82), laminins (83), and fibronectin (84), as well as critical matrix molecules such as hyaluronic acid (hyaluronan) (85). This customizability allows hydrogels to have extensive application and versatility in biological research by offering a range of physical and biochemical characteristics.

Natural hydrogels are derived from sources that are inherently biocompatible (29). Various ECM constituents have been derived from materials such as collagen, fibrin, hyaluronic acid, alginate, and the commercial product Matrigel, a reconstituted basement membrane extracted from murine sarcoma cells (86). These hydrogels have various endogenous factors that promote bioactivity and sustain natural cell function, proliferation, and differentiation. For example, collagen is a widely used ECM that orchestrate controlled cell migration, proliferation, and response to therapies through alteration in stiffness and collagen concentration (87, 88). A study from Puls et al. had studied the progression of metastasis in pancreatic cancer using 3D matrices created with type I collagen and found that exposure to fibrillar collagen induced EMT (89). Increased density of collagen fibril resulted in closer arrangements of cell clusters and matrix stiffness (89). Alginate is also a natural polymer derived from brown algae that can gelate *via* ionic crosslinking of the polysaccharide backbone by divalent cations, such as calcium, magnesium, or barium (73, 90). The stiffness of alginate hydrogel can be modified based on the level of cross-linking that is dictated by the concentration of the crosslinking agent. Importantly, alginate gels are inert as they do not contain any mammalian cell adhesion ligands, and with their low protein adsorption, makes them ideal as a matrix for the encapsulation of cells and tissue (91). Additionally, alginate gels under neutral pH and room temperature, resulting in minimal cellular disruption under gelation conditions (90). Alginate can be biofunctionalized with the addition of adhesive and hydrolytic moieties and has been used as a matrix for various biomedical applications (92–94). A key advantage of alginate matrices is that cells can be easily recovered by dissolving the alginate with a chelating agent, such as sodium citrate. Recently, alginate matrices have been proposed for drug screening in breast cancer tumoroids derived from tumour pieces that retain luminal mechanics (95). Hyaluronic acid is another natural hydrogel that has major biomedical applications due to its high moisture retention and viscoelasticity (96). Hyaluronic acid is a non-immunogenic polysaccharide that is found ubiquitously in the ECM in epithelial and connective tissues and is involved in wound healing, inflammation, and embryonic development (96). It can be modified with functional

groups allowing for a diverse range of applications in regenerative medicine, oncology, and bioengineering (97–101). However, some drawbacks of natural hydrogels can include poor control over the gelation condition, uncontrolled polymer network structures, lower mechanical integrity, and lower experimental reproducibility due to batch-to-batch variations (65, 86).

Synthetic hydrogels are inert scaffolds that permit a higher degree of modification for desired biological or physical conditions, such as biodegradability, porosity, functionalization with adhesive peptide sequences, growth factors or cleavage sites (29, 30). Compared to natural hydrogels, synthetic gels are cheaper and add improved experimental reproducibility as it has a lower batch to batch variation during manufacturing and can be adapted to suit the research need. However, the disadvantage of most synthetic hydrogels is that they act as a minimalistic matrix and have a less complex microenvironment due to the lack of endogenous factors that are generally present in natural hydrogels (29). As such adhesive moieties and catalytic sites need to be crosslinked into the synthetic scaffold to improve their biofunctionality, such as peptides that can mimic fibronectin or laminin-integrin binding (102, 103). Various non-natural sources can be derived to produce these matrices, such as polyethylene glycol (PEG) (104, 105), polyvinyl alcohol, and polylactic acid (PA) (30, 106). PEG has been used for various 3D culturing and tissue engineering applications. For example, PEG has been cultured with breast cancer cells and CAFs to evaluate drug resistance through pathways associated with tumour-stromal interactions (107, 108). In another study, Caiazzo et al. found that PEG can facilitate pluripotency by manipulating the microenvironment of the matrix to create a “reprogramming niche” that promotes MET and increased epigenetic remodeling capable of shifting the somatic cell fate (109). Biomechanical strain and tension induced by the matrix have been reported to modulate the epigenetic and transcriptomic state of cells as a response to their surrounding environment (110–112).

Microfluidics System

The advancement in microfabrication technology has led to the development of microfluidics systems that provides more dynamic microenvironments. These systems are designed with specific structures and scaffolds that can be manufactured through patterning techniques such as soft lithography, photolithography, and micro-contact printing (65). Microfluidics permits precise control over small volumes of fluid through hollow channels that can be smaller than 1µm in diameter (13). These devices or chips have been an essential development in microsystems technology that can generate and manipulate the fluid flow and spatiotemporal gradients to improve the biological relevance of *in vitro* models (113). Nutrients, drugs, and wastes can be readily delivered or removed *via* continuous perfusion through the microchannel (114). Within the microfluidic system, spheroids can be generated at high throughput and with a precision that are uniform in size for both monocultures and co-cultures (115–117).

Microfluidic technology has been used to create more cost-effective and accurate biomedical models to test the

pharmacokinetics, efficacy, and toxicity of treatments. The internal dimensions of a microfluidic chip can be composed of multiple channels – depending on the design and application – where the size of structures can be between the micrometer to millimeter range (118). Generally, microfluidic chips are manufactured using an inert and non-toxic polymer as a base material, such as poly-dimethylsiloxane (PDMS) (23). The microfluidics control and miniaturization of the whole system present several key benefits: 1) high-throughput capabilities; 2) cost-efficient and low consumption of reagents – within the nanoliter to picolitre range; 3) fine-tuning of conditions and automation (118, 119).

A major approach of the microfluidic system is developing organ-on-chip which is able to create a complex *in vitro* model that recapitulates more organ-specific microenvironments. Organ-on-chip focuses on capturing the critical aspects of the normal biological functions or disease states of the organ of interest. This allows researchers to investigate disease phenotypes and pharmacological responses that are clinically relevant and provide more accurate predictions of treatment efficacy (65, 120). Nutrients, growth factors, oxygen, and drugs can be circulated through the chip as a continuous supply *via* dynamic perfusion which can be automated – in addition to waste removal (12). The controlled fluidic motions can also be used to mimic various mechanical signals including shear stress; compressive forces; physiological flow, such as blood flow; and tissue-specific motions, such as cardiac rhythms and respiratory (120–122). Consequently, microfluidics chips have been used to recapitulate aspects of the TME for anti-cancer drug developments, circulating cancer cell detection in blood samples, and personalised organ-on-chips (123–126). The simplest tumour-on-chip models have been applying 3D spheroids within a microfluidics system (127–129). However, more sophisticated tumour-on-chips platforms have been developed that utilizes the dynamic flow of microfluidics. In a study by Chen et al, an *in vitro* breast tumour model was created on a chip to evaluate nanoparticle-based drug delivery systems (130). This chip included a layer of endothelium that lined a microvessel wall, the ECM and tumour spheroids to generate a real-time drug delivery model. Treatments such as doxorubicin – a standard of care therapy for breast cancer – was loaded in carbon dots to study the penetrance of the treatment through the endothelium to the spheroids, where the efficacy and cytotoxicity of the drug delivery were assessed using *in situ* assays within the same system (130). Tumour-on-chips can also contain engineered vascularization as part of the model using perfusable system to imitate the flow of blood vessels to more closely mimic other mechanisms within the TME, including metastasis, angiogenesis, and drug metabolism (131–134). Argwal et al. discovered that vascularized *in vitro* 3D breast tumors exhibited significantly higher resistance to doxorubicin compared to avascular 3D tumors (4.7 times) and 2D culture cells (139.5 times) (135). Interestingly, this high drug resistance could also be overcome *via* a nanoparticle-based drug delivery method (135). The inclusion of vascularization and dynamic flow has also allowed researchers to study the pathophysiology

of blood-based cancer with *in vitro* models, such as lymphoma (136).

3D Bioprinting

The development of *in vitro* 3D models that increase the probability of preclinical drug research representing patient outcomes in drug trials, and potentially remove the need for animal studies, may render preclinical cancer research more cost-effective and accessible. However, the use of novel 3D models in cancer research remains restricted by model reproducibility; a prerequisite for specialized training and limitations relating to throughput. The development and commercialization of 3D bioprinting technologies offer an exciting solution to these challenges. 3D bioprinting is an additive manufacturing process defined by the creation of a 3D structure through controlled and typically automated deposition of a biocompatible material or ‘bioink’. This advanced technology is capable of accurately constructing complex tissue structures that faithfully recapitulate native *in vivo* architecture (137). 3D structures can be created directly from highly viscous or shear-thinning bioinks, where the bioinks can be mixed with the cell suspension to generate functionalized cell models. Alternatively, printed bioinks that are less viscous can be solidified through the addition of other chemicals, cooling, or exposure to light or heat (138).

Bioinks are printable, biocompatible solutions that comprise the necessary elements of a desired 3D microenvironment. Bioinks vary greatly in their composition depending on the printing method and the application. Cells, native proteins, growth factors, and signaling molecules can be combined with synthetic compounds that are both printable and biomimetic. Synthetic molecules can likewise be decorated with peptide sequence (139), MMP degradable ligands and drug molecules (140) so that they are more biocompatible, biodegradable or bioactive. Modifications to the bioink properties and bioprinting methods can be tuned to tailor to the desired applications and studies. For example concentrated bioinks may be necessary for creating dense, stiff structures such as bone biomimetics (141), or dense tumour microenvironment models (142). However, concentrated bioinks are highly viscous and result in increased cell death during printing due to high shear forces. As such, it is also important to optimize these modifications to ensure compatibility with the cell types.

Most 3D bioprinting strategies involve droplet, extrusion, and stereolithographic-based structure creation – for an extensive review on the methods refer to the reviews (138, 143). Commonly employed 3D bioprinting processes include 1) droplet-based 3D bioprinting (DBB), which uses sequential depositions of discrete bioink droplets to create structures (144); 2) drop-on-demand bioprinting (DOD), a subcategory of DBB that controls droplet size and placement by regulating the position and ejection of bioink from a nozzle (145, 146); and 3) laser-assisted bioprinting, an alternative DBB technology that propels bioink droplets from an inverted ‘donor slide’ onto a receiving slide using localized heating of a substrate sensitive to laser radiation (147, 148).

Each 3D bioprinting strategy has various, often interlinked, tradeoffs and downstream applications. For instance, extrusion-

based 3D bioprinters create structures by layering continuous beads of bioink from nozzles, whereas stereolithographic 3D bioprinting uses light to cure regions of bioink precursor within a bath, building a structure layer by layer (143). In this case, stereolithography limits printing to a single bioink at a time but is excellent for creating complex networked microarchitecture. For example, this has been used to create osteoblast and MSC-laden bone biomimetics (141) and replica microvasculature (149), which were seeded with invasive cancer cells to simulate metastasis and investigate cancer cell migration. Furthermore, the placement of ink on a printing surface is less complex in extrusion printing compared to droplet-based systems where droplet size, flight and placement vary with ink properties (150). However, printing with droplets offers an advantage in throughput and high-resolution patterning as the same nozzle set of a DOD system simultaneously creates multiple structures comprising many different bioinks. Extrusion printing has been used in the creation of large 3D structures to investigate glioblastoma-macrophage interactions (151), and meshes of cervical cancer (152), lung adenocarcinoma (153) and mammary epithelial cells (142) for 3D cancer modelling and drug screens. Conversely, the throughput advantage offered by DOD bioprinting has been exploited to create arrays of hepatic and brain cancer cell lines for drug screening (154), and co-culture patterning of ovarian cancer cells and fibroblasts for investigations of cell interactions and paracrine signaling (155).

There is currently a matter of contention in 3D bioprinting created by the conflicting practices of requiring printing processes to be completed quickly, and simultaneously allowing complex 3D models sufficient time to develop and mature. Bioprinting exposes cancer cells to reagents, processes and forces that fall outside their typical environmental niche. As such, reducing the time for which cells are exposed to the reagents and forces improves cell viability and preserves the *in vivo* biology critical to accurate tumour model creation (138). However, the biological processes central to the development of histological micro-architecture are rarely static, proceed slowly and require time to develop. There is a tendency within 3D bioprinting to emphasize time reduction and to prioritize the rapid completion of printing procedures (143). Yet incorporation of time-related factors and processes will be critical as our general understanding and mastery of 3D bioprinting progresses and becomes further integrated into cancer research.

The term '4D bioprinting' has been used to describe 3D bioprinting strategies that integrate the changing of printed structures over time (156). These strategies may rely on organically occurring biological processes such as matrix deposition, tissue self-organisation and cell differentiation (25). Brassard et al. relied on biological dynamics to create complex macro-structures reminiscent of vascular, connective and gastrointestinal tissues (157). These structures were self-assembled from concentrated cell solutions printed into an ECM hydrogel prior to gelation. The creation of *in vitro* organoids is critical for translatable studies into cancer cell behaviour and drug toxicity. Similar concepts are also being embraced to replicate and investigate the tumour microenvironment directly. For example, Yi et al. created an advanced glioblastoma brain cancer model with initial depositions of silicone ink, endothelial and tumour cells

(158). Maturation of the model led to the formation of various features typical of glioblastoma including necrotic foci and pseudopalisades within the tumour cell mass, and leaky endothelial microvessels (159, 160).

In addition to internal biological drivers, externally controlled stimuli can be used to modulate cell behaviour and the printed material surrounding them. The creation of dynamic 3D printed structures is critical for studying the ECM remodeling integral to tumour growth, cell metastasis and drug permeability. Studies have used various stimuli including temperature (161), pH, osmolarity (162), light (163, 164), humidity, magnetic force (165) and electrical charge, to affect material stiffness, size, density, binding affinity (166) and molecular organization (166) of responsive 'smart' materials. Stimuli may cause unidirectional irreversible material responses, or they may be bidirectional and reversible (161). Responses can also be stacked, allowing multiple different material states. In an example of this, Tabriz et al. enabled a multistage crosslinking of printed alginate structures through the addition of sequential Ca^{2+} and Ba^{2+} solutions (167). Each stage further increased the printed structures' durability, facilitating both the initial printability of the bioink, as well as its long-term stability under culture conditions. Aside from material properties, external stimuli can be used to alter the shape of printed structures. Gladman et al., used anisotropic swelling to create complex dimensionality, folds and curvature in 3D planar printed shapes (168). A similar concept was used in a ductal carcinoma study to create geometric mimicry of mammary ducts and acini (169). The impact of responsive bioinks on cancer research is yet to be fully realized. However burgeoning developments in stimulus-responsive geometry and embracing temporal biochemical and biophysical dynamics offer the potential for 3D bioprinted models to be shaped by factors outside of printing complexity (170).

The ability to create representative *in vitro* models is progressing and our understanding of 3D cellular biology continues to grow. To leverage the advances made in these areas within cancer research, the throughput and reproducibility made possible through 3D bioprinting will be critical. Economically viable cancer research requires *in vitro* models that are not only representative of physiological and pathological conditions, but that can be created quickly and efficiently. For this to be possible, we require 3D advanced bioprinting techniques that exploit both intrinsic cell behaviors and innovative biomaterial developments. Synthesis within these areas offers interesting future opportunities for complex 3D model development and the attainment of critical cancer research goals.

LIMITATIONS OF TECHNOLOGY IN 3D MODELS

Although 3D culture has been demonstrated to show great promise as a pre-clinical model, a major drawback of 3D cultures is in their implementation for high-throughput screening; a vital aspect for high-content screening and drug development (171, 172). In particular, three significant technical challenges hamper the adoption of 3D culture technology for high-throughput screening:

1) the automation of liquid handling in 3D culture; 2) culture optimization and assay variability; and 3) automated imaging and visualization of 3D structures. The automation of liquid handling can be conducted in suspension cultures such as through the use of ultra-low-attachment microplates or hanging drop technique (30). However, the application of automated liquid handling translates poorly when using hydrogel-based techniques, such as Matrigel. This is primarily due to the undefined compositions between batches that impact reproducibility and consistency and require highly controlled working environments and rapid processing due to their temperature-sensitive gelation conditions (173). Additionally, this batch-to-batch variation in natural hydrogels considerably impacts cell culture conditions and assay quality and reproducibility; as such it is crucial to ensure consistency between batches when conducting high-throughput screening, such as ECM composition and protein content (103). Finally, 3D models permit co-culturing of multiple cell types and provide a higher morphological complexity compared to 2D cultures; allowing improved multiparametric analysis of cell response to drugs. The additional parameters are particularly valuable as they provide a more accurate evaluation of the efficacy and mechanisms of pharmaceutical agents (174). However, this dimensionality also poses a difficulty in computational image analysis and visualization. The complex topology and thickness of 3D models make them incompatible with most automated imaging systems due to low light penetration and absorption across the multi-layered structures (103). As a result, this can introduce an imaging bias in which only the exterior cells – the layer where cells are exposed to the highest concentration gradient for nutrients and drugs – are imaged and the internal cells are excluded. Despite these challenges, new culture platforms and imaging systems are being developed that aim to overcome these technical difficulties to create 3D cultures that are amenable for high-throughput screening. These developments include using synthetic hydrogels to generate more consistent 3D cell cultures; automated high-resolution imaging using light-sheet microscopy; and integrated computational platforms for data analysis and visualization of 3D cultures (175–177).

CONCLUSIONS

The improvement in 3D culture technology has led to the generation of *in vitro* models that can encompass more

physiological and tissue-specific microenvironments with the aim to overcome the drawbacks observed in other pre-clinical models and have better predictive value for clinical outcomes. 3D culture models allow researchers to recreate specific pathophysiological conditions and tumorigenic processes to identify potential biomarkers for therapeutic targeting or assessing cell response to therapies and drug efficacy. Currently, there has been significant interest in using primary clinical samples in 3D culture for personalised drug screening platforms to improve clinical outcomes and reduce side effects (178, 179). Although there are still practical challenges in the widespread adoption of 3D cultures, advancements in this field will provide researchers with a powerful tool to dissect disease mechanisms, identify new biomarkers, provide valuable data in drug development, and realize the potential in the next generation of personalised medicine.

AUTHOR CONTRIBUTIONS

Writing— original draft preparation, review and editing by AL, LR, TG, GF, FV-M, and DG-O. Figures designed by AL. Supervision by FV-M and DG-O. All authors contributed to the article and approved the submitted version.

FUNDING

AL is supported by a UPA Scholarship from UNSW. LR is supported by a UIPA Scholarship from UNSW Sydney and a PhD top-up award from Kids Cancer Alliance (KCA). FV-M holds a Cancer Institute New South Wales Fellowship (CDF181218). DG-O is holds the Elaine Henry Fellowship from the National Breast Cancer Foundation (NBCF) of Australia (IIRS-21-096) and is supported by a Cancer Council New South Wales (CCNSW) grant (RG18-03).

ACKNOWLEDGMENTS

We thank the members of the Tumour Development Laboratory at Garvan Institute of Medical Research and the Cancer Epigenetics Biology and Therapeutics group at Children's Cancer Institute for helpful discussions.

REFERENCES

- Whiteside TL. The Tumor Microenvironment and Its Role in Promoting Tumor Growth. *Oncogene* (2008) 27(45):5904–12. doi: 10.1038/onc.2008.271
- Hanahan D, Weinberg RA. Hallmarks of Cancer: The Next Generation. *Cell* (2011) 144(5):646–74. doi: 10.1016/j.cell.2011.02.013
- Wang M, Zhao J, Zhang L, Wei F, Lian Y, Wu Y, et al. Role of Tumor Microenvironment in Tumorigenesis. *J Cancer* (2017) 8(5):761–73. doi: 10.7150/jca.17648
- Hanahan D, Coussens LM. Accessories to the Crime: Functions of Cells Recruited to the Tumor Microenvironment. *Cancer Cell* (2012) 21(3):309–22. doi: 10.1016/j.ccr.2012.02.022
- Dagogo-Jack I, Shaw AT. Tumour Heterogeneity and Resistance to Cancer Therapies. *Nat Rev Clin Oncol* (2018) 15(2):81–94. doi: 10.1038/nrclinonc.2017.166
- Hay M, Thomas DW, Craighead JL, Economides C, Rosenthal J. Clinical Development Success Rates for Investigational Drugs. *Nat Biotechnol* (2014) 32(1):40–51. doi: 10.1038/nbt.2786
- Wong CH, Siah KW, Lo AW. Estimation of Clinical Trial Success Rates and Related Parameters. *Biostatistics* (2019) 20(2):273–86. doi: 10.1093/biostatistics/kxx069
- Fogel DB. Factors Associated With Clinical Trials That Fail and Opportunities for Improving the Likelihood of Success: A Review. *Contemp Clin Trials Commun* (2018) 11:156–64. doi: 10.1016/j.conctc.2018.08.001

9. Alavijeh MS, Palmer AM. The Pivotal Role of Drug Metabolism and Pharmacokinetics in the Discovery and Development of New Medicines. *IDrugs* (2004) 7(8):755–63.
10. Hwang TJ, Carpenter D, Lauffenburger JC, Wang B, Franklin JM, Kesselheim AS. Failure of Investigational Drugs in Late-Stage Clinical Development and Publication of Trial Results. *JAMA Intern Med* (2016) 176(12):1826–33. doi: 10.1001/jamainternmed.2016.6008
11. Arrowsmith J, Miller P. Trial Watch: Phase II and Phase III Attrition Rates 2011–2012. *Nat Rev Drug Discovery* (2013) 12(8):569.
12. Tomas-Bort E, Kieler M, Sharma S, Candido JB, Loessner D. 3D Approaches to Model the Tumor Microenvironment of Pancreatic Cancer. *Theranostics* (2020) 10(11):5074–89. doi: 10.7150/thno.42441
13. Lv D, Hu Z, Lu L, Lu H, Xu X. Three-Dimensional Cell Culture: A Powerful Tool in Tumor Research and Drug Discovery. *Oncol Lett* (2017) 14(6):6999–7010. doi: 10.3892/ol.2017.7134
14. Gould SE, Junttila MR, de Sauvage FJ. Translational Value of Mouse Models in Oncology Drug Development. *Nat Med* (2015) 21(5):431–9. doi: 10.1038/nm.3853
15. Joffe AR, Bara M, Anton N, Nobis N. The Ethics of Animal Research: A Survey of the Public and Scientists in North America. *BMC Med Ethics* (2016) 17:17. doi: 10.1186/s12910-016-0100-x
16. Ellis LM, Fidler IJ. Finding the Tumor Copycat. Therapy Fails, Patients Don't. *Nat Med* (2010) 16(9):974–5.
17. Ben-David U, Ha G, Tseng YY, Greenwald NF, Oh C, Shih J. Patient-Derived Xenografts Undergo Mouse-Specific Tumor Evolution. *Nat Genet* (2017) 49(11):1567–75. doi: 10.1038/ng.3967
18. Day CP, Merlino G, Van Dyke T. Preclinical Mouse Cancer Models: A Maze of Opportunities and Challenges. *Cell* (2015) 163(1):39–53. doi: 10.1016/j.cell.2015.08.068
19. Yu M, Bardia A, Aceto N, Bersani F, Madden MW, Donaldson MC, et al. Cancer Therapy. Ex Vivo Culture of Circulating Breast Tumor Cells for Individualized Testing of Drug Susceptibility. *Science* (2014) 345(6193):216–20.
20. Hong X, Roh W, Sullivan RJ, Wong KHK, Wittner BS, Guo H, et al. The Lipogenic Regulator SREBP2 Induces Transferrin in Circulating Melanoma Cells and Suppresses Ferroptosis. *Cancer Discovery* (2021) 11(3):678–95. doi: 10.1158/2159-8290.CD-19-1500
21. Karkampouna S, La Manna F, Benjak A, Kiener M, De Menna M, Zoni E, et al. Patient-Derived Xenografts and Organoids Model Therapy Response in Prostate Cancer. *Nat Commun* (2021) 12(1):1117.
22. Gjorevski N, Piotrowski AS, Varner VD, Nelson CM. Dynamic Tensile Forces Drive Collective Cell Migration Through Three-Dimensional Extracellular Matrices. *Sci Rep* (2015) 5:11458. doi: 10.1038/srep11458
23. Duval K, Grover H, Han LH, Mou Y, Pegoraro AF, Fredberg J, et al. Modeling Physiological Events in 2D vs. 3D Cell Culture. *Physiol (Bethesda)* (2017) 32(4):266–77.
24. Koch TM, Munster S, Bonakdar N, Butler JP, Fabry B. 3d Traction Forces in Cancer Cell Invasion. *PLoS One* (2012) 7(3):e33476. doi: 10.1371/journal.pone.0033476
25. Hakkinen KM, Harunaga JS, Doyle AD, Yamada KM. Direct Comparisons of the Morphology, Migration, Cell Adhesions, and Actin Cytoskeleton of Fibroblasts in Four Different Three-Dimensional Extracellular Matrices. *Tissue Eng Part A* (2011) 17(5–6):713–24. doi: 10.1089/ten.tea.2010.0273
26. Mishra DK, Sakamoto JH, Thrall MJ, Baird BN, Blackmon SH, Ferrari M, et al. Human Lung Cancer Cells Grown in an Ex Vivo 3D Lung Model Produce Matrix Metalloproteinases Not Produced in 2D Culture. *PLoS One* (2012) 7(9):e45308. doi: 10.1371/journal.pone.0045308
27. Wang S, Li E, Gao Y, Wang Y, Guo Z, He J, et al. Study on Invadopodia Formation for Lung Carcinoma Invasion With a Microfluidic 3D Culture Device. *PLoS One* (2013) 8(2):e56448. doi: 10.1371/journal.pone.0056448
28. Goertzen C, Eymael D, Magalhaes M. Three-Dimensional Quantification of Spheroid Degradation-Dependent Invasion and Invadopodia Formation. *Biol Proced Online* (2018) 20:20. doi: 10.1186/s12575-018-0085-6
29. Tibbitt MW, Anseth KS. Hydrogels as Extracellular Matrix Mimics for 3D Cell Culture. *Biotechnol Bioeng* (2009) 103(4):655–63. doi: 10.1002/bit.22361
30. Langhans SA. Three-Dimensional In Vitro Cell Culture Models in Drug Discovery and Drug Repositioning. *Front Pharmacol* (2018) 9:6. doi: 10.3389/fphar.2018.00006
31. Birgersdotter A, Sandberg R, Ernberg I. Gene Expression Perturbation In Vitro—A Growing Case for Three-Dimensional (3D) Culture Systems. *Semin Cancer Biol* (2005) 15(5):405–12. doi: 10.1016/j.semcancer.2005.06.009
32. Kapalczynska M, Kolenda T, Przybyla W, Zajackowska M, Teresiak A, Filas V, et al. 2D and 3D Cell Cultures - A Comparison of Different Types of Cancer Cell Cultures. *Arch Med Sci* (2018) 14(4):910–9.
33. Yamada KM, Cukierman E. Modeling Tissue Morphogenesis and Cancer in 3D. *Cell* (2007) 130(4):601–10. doi: 10.1016/j.cell.2007.08.006
34. Edmondson R, Broglie JJ, Adcock AF, Yang L. Three-Dimensional Cell Culture Systems and Their Applications in Drug Discovery and Cell-Based Biosensors. *Assay Drug Dev Technol* (2014) 12(4):207–18. doi: 10.1089/adt.2014.573
35. Boyle ST, Kular J, Nobis M, Ruskiewicz A, Timpson P, Samuel MS. Acute Compressive Stress Activates RHO/ROCK-Mediated Cellular Processes. *Small GTPases* (2020) 11(5):354–70. doi: 10.1080/21541248.2017.1413496
36. Boyle ST, Poltavets V, Kular J, Pyne NT, Sadow JJ, Lewis AC, et al. ROCK-Mediated Selective Activation of PERK Signalling Causes Fibroblast Reprogramming and Tumour Progression Through a CRELD2-Dependent Mechanism. *Nat Cell Biol* (2020) 22(7):882–95. doi: 10.1038/s41556-020-0523-y
37. Frantz C, Stewart KM, Weaver VM. The Extracellular Matrix at a Glance. *J Cell Sci* (2010) 123(Pt 24):4195–200. doi: 10.1242/jcs.023820
38. Yue B. Biology of the Extracellular Matrix: An Overview. *J Glaucoma* (2014) 23(8 Suppl 1):S20–3. doi: 10.1097/IJG.0000000000000108
39. Lovitt CJ, Shelper TB, Avery VM. Doxorubicin Resistance in Breast Cancer Cells Is Mediated by Extracellular Matrix Proteins. *BMC Cancer* (2018) 18(1):41. doi: 10.1186/s12885-017-3953-6
40. Nunes AS, Barros AS, Costa EC, Moreira AF, Correia IJ. 3D Tumor Spheroids as In Vitro Models to Mimic In Vivo Human Solid Tumors Resistance to Therapeutic Drugs. *Biotechnol Bioeng* (2019) 116(1):206–26. doi: 10.1002/bit.26845
41. Sebens S, Schafer H. The Tumor Stroma as Mediator of Drug Resistance—a Potential Target to Improve Cancer Therapy? *Curr Pharm Biotechnol* (2012) 13(11):2259–72. doi: 10.2174/138920112802501999
42. Sun Y. Tumor Microenvironment and Cancer Therapy Resistance. *Cancer Lett* (2016) 380(1):205–15. doi: 10.1016/j.canlet.2015.07.044
43. Di Paolo A, Bocci G. Drug Distribution in Tumors: Mechanisms, Role in Drug Resistance, and Methods for Modification. *Curr Oncol Rep* (2007) 9(2):109–14. doi: 10.1007/s11912-007-0006-3
44. Minchinton AI, Tannock IF. Drug Penetration in Solid Tumours. *Nat Rev Cancer* (2006) 6(8):583–92. doi: 10.1038/nrc1893
45. Tredan O, Galmarini CM, Patel K, Tannock IF. Drug Resistance and the Solid Tumor Microenvironment. *J Natl Cancer Inst* (2007) 99(19):1441–54. doi: 10.1093/jnci/djm135
46. Biagini F, Calvigioni M, Lapomarda A, Vecchione A, Magliaro C, De Maria C, et al. A Novel 3D In Vitro Model of the Human Gut Microbiota. *Sci Rep* (2020) 10(1):21499. doi: 10.1038/s41598-020-78591-w
47. Knitsch R, AlWahsh M, Raschke H, Lambert J, Hergenroder R. In Vitro Spatio-Temporal NMR Metabolomics of Living 3d Cell Models. *Anal Chem* (2021) 93(40):13485–94. doi: 10.1021/acs.analchem.1c02221
48. Sepich-Poore GD, Zitvogel L, Straussman R, Hasty J, Wargo JA, Knight R. The Microbiome and Human Cancer. *Science* (2021) 371(6536). doi: 10.1126/science.abc4552
49. Alpuim Costa D, Nobre JG, Batista MV, Ribeiro C, Calle C, Cortes A, et al. Human Microbiota and Breast Cancer—Is There Any Relevant Link?—A Literature Review and New Horizons Toward Personalised Medicine. *Front Microbiol* (2021) 12:584332. doi: 10.3389/fmicb.2021.584332
50. Nejman D, Livyatan I, Fuks G, Gavert N, Zwang Y, Geller LT, et al. The Human Tumor Microbiome Is Composed of Tumor Type-Specific Intracellular Bacteria. *Science* (2020) 368(6494):973–80. doi: 10.1126/science.aay9189
51. Alexander JL, Wilson ID, Teare J, Marchesi JR, Nicholson JK, Kinross JM. Gut Microbiota Modulation of Chemotherapy Efficacy and Toxicity. *Nat Rev Gastroenterol Hepatol* (2017) 14(6):356–65. doi: 10.1038/nrgastro.2017.20
52. Kasper SH, Morell-Perez C, Wyche TP, Sana TR, Lieberman LA, Hett EC. Colorectal Cancer-Associated Anaerobic Bacteria Proliferate in Tumor Spheroids and Alter the Microenvironment. *Sci Rep* (2020) 10(1):5321. doi: 10.1038/s41598-020-62139-z

53. Min S, Kim S, Cho SW. Gastrointestinal Tract Modeling Using Organoids Engineered With Cellular and Microbiota Niches. *Exp Mol Med* (2020) 52 (2):227–37. doi: 10.1038/s12276-020-0386-0
54. Puschhof J, Pleguezuelos-Manzano C, Martinez-Silgado A, Akkerman N, Saftien A, Boot C, et al. Intestinal Organoid Cocultures With Microbes. *Nat Protoc* (2021) 16(10):4633–49. doi: 10.1038/s41596-021-00589-z
55. Bartfeld S, Clevers H. Organoids as Model for Infectious Diseases: Culture of Human and Murine Stomach Organoids and Microinjection of *Helicobacter Pylori*. *J Vis Exp* (2015) (105):e53359. doi: 10.3791/53359
56. Jalili-Firoozinezhad S, Gazzaniga FS, Calamari EL, Camacho DM, Fadel CW, Bein A, et al. A Complex Human Gut Microbiome Cultured in an Anaerobic Intestine-on-a-Chip. *Nat BioMed Eng* (2019) 3(7):520–31. doi: 10.1038/s41551-019-0397-0
57. Pocevičiute R, Ismagilov RF. Human-Gut-Microbiome on a Chip. *Nat BioMed Eng* (2019) 3(7):500–1. doi: 10.1038/s41551-019-0425-0
58. Zimmermann M, Zimmermann-Kogadeeva M, Wegmann R, Goodman AL. Mapping Human Microbiome Drug Metabolism by Gut Bacteria and Their Genes. *Nature* (2019) 570(7762):462–7. doi: 10.1038/s41586-019-1291-3
59. Maier L, Pruteanu M, Kuhn M, Zeller G, Telzerow A, Anderson EE, et al. Extensive Impact of non-Antibiotic Drugs on Human Gut Bacteria. *Nature* (2018) 555(7698):623–8. doi: 10.1038/nature25979
60. Harimoto T, Singer ZS, Velazquez OS, Zhang J, Castro S, Hinchliffe TE, et al. Rapid Screening of Engineered Microbial Therapies in a 3D Multicellular Model. *Proc Natl Acad Sci USA* (2019) 116(18):9002–7. doi: 10.1073/pnas.1820824116
61. Barretina J, Caponigro G, Stransky N, Venkatesan K, Margolin AA, Kim S, et al. The Cancer Cell Line Encyclopedia Enables Predictive Modelling of Anticancer Drug Sensitivity. *Nature* (2012) 483(7391):603–7. doi: 10.1038/nature11003
62. Ghandi M, Huang FW, Jane-Valbuena J, Kryukov GV, Lo CC, McDonald ER 3rd, et al. Next-Generation Characterization of the Cancer Cell Line Encyclopedia. *Nature* (2019) 569(7757):503–8. doi: 10.1038/s41586-019-1186-3
63. DiMasi JA, Grabowski HG, Hansen RW. Innovation in the Pharmaceutical Industry: New Estimates of R&D Costs. *J Health Econ* (2016) 47:20–33. doi: 10.1016/j.jhealeco.2016.01.012
64. Hingorani P, Zhang W, Piperdi S, Pressman L, Lin J, Gorlick R, et al. Preclinical Activity of Palifosfamide Lysine (ZIO-201) in Pediatric Sarcomas Including Oxazaphosphorine-Resistant Osteosarcoma. *Cancer Chemother Pharmacol* (2009) 64(4):733–40. doi: 10.1007/s00280-008-0922-4
65. Fang Y, Eglén RM. Three-Dimensional Cell Cultures in Drug Discovery and Development. *SLAS Discovery* (2017) 22(5):456–72.
66. Courau T, Bonnereau J, Chicoteau J, Bottois H, Remark R, Assante Miranda L, et al. Cocultures of Human Colorectal Tumor Spheroids With Immune Cells Reveal the Therapeutic Potential of MICA/B and NKG2A Targeting for Cancer Treatment. *J Immunother Cancer* (2019) 7(1):74. doi: 10.1186/s40425-019-0553-9
67. Simian M, Bissell MJ. Organoids: A Historical Perspective of Thinking in Three Dimensions. *J Cell Biol* (2017) 216(1):31–40. doi: 10.1083/jcb.201610056
68. Andersson TB. Evolution of Novel 3d Culture Systems for Studies of Human Liver Function and Assessments of the Hepatotoxicity of Drugs and Drug Candidates. *Basic Clin Pharmacol Toxicol* (2017) 121(4):234–8. doi: 10.1111/bcpt.12804
69. Tung YC, Hsiao AY, Allen SG, Torisawa YS, Ho M, Takayama S. High-Throughput 3D Spheroid Culture and Drug Testing Using a 384 Hanging Drop Array. *Analyst* (2011) 136(3):473–8. doi: 10.1039/C0AN00609B
70. Kelm JM, Timmins NE, Brown CJ, Fussenegger M, Nielsen LK. Method for Generation of Homogeneous Multicellular Tumor Spheroids Applicable to a Wide Variety of Cell Types. *Biotechnol Bioeng* (2003) 83(2):173–80. doi: 10.1002/bit.10655
71. Shen H, Tong S, Bao G, Wang B. Structural Responses of Cells to Intracellular Magnetic Force Induced by Superparamagnetic Iron Oxide Nanoparticles. *Phys Chem Chem Phys* (2014) 16(5):1914–20. doi: 10.1039/C3CP51435H
72. Timm DM, Chen J, Sing D, Gage JA, Haisler WL, Neeley SK, et al. A High-Throughput Three-Dimensional Cell Migration Assay for Toxicity Screening With Mobile Device-Based Macroscopic Image Analysis. *Sci Rep* (2013) 3:3000. doi: 10.1038/srep03000
73. Caliri SR, Burdick JA. A Practical Guide to Hydrogels for Cell Culture. *Nat Methods* (2016) 13(5):405–14. doi: 10.1038/nmeth.3839
74. Denisin AK, Pruitt BL. Tuning the Range of Polyacrylamide Gel Stiffness for Mechanobiology Applications. *ACS Appl Mater Interfaces* (2016) 8 (34):21893–902. doi: 10.1021/acsami.5b09344
75. Tse JR, Engler AJ. Preparation of Hydrogel Substrates With Tunable Mechanical Properties. *Curr Protoc Cell Biol* (2010) Chapter 10:Unit 10 16. doi: 10.1002/0471143030.cb1016s47
76. Pradhan S, Slater JH. Tunable Hydrogels for Controlling Phenotypic Cancer Cell States to Model Breast Cancer Dormancy and Reactivation. *Biomaterials* (2019) 215:119177. doi: 10.1016/j.biomaterials.2019.04.022
77. Han WM, Anderson SE, Mohiuddin M, Barros D, Nakhai SA, Shin E, et al. Synthetic Matrix Enhances Transplanted Satellite Cell Engraftment in Dystrophic and Aged Skeletal Muscle With Comorbid Trauma. *Sci Adv* (2018) 4(8):eaar4008. doi: 10.1126/sciadv.aar4008
78. Nguyen EH, Daly WT, Le NNT, Farnoodian M, Belair DG, Schwartz MP, et al. Versatile Synthetic Alternatives to Matrigel for Vascular Toxicity Screening and Stem Cell Expansion. *Nat BioMed Eng* (2017) 1(0096):1–14. doi: 10.1038/s41551-017-0096
79. Wee Y, Moore AN, Jia S, Zhou J, Colombo JS, D'Souza RN. A Single-Step Self-Assembly Approach for the Fabrication of Aligned and Multilayered Three-Dimensional Tissue Constructs Using Multidomain Peptide Hydrogel. *SLAS Technol* (2019) 24(1):55–65. doi: 10.1177/2472630318777759
80. Sarwat M, Surrao DC, Huettner N, St John JA, Dargaville TR, Forget A. Going Beyond RGD: Screening of a Cell-Adhesion Peptide Library in 3D Cell Culture. *BioMed Mater* (2020) 15(5):055033. doi: 10.1088/1748-605X/ab9d6e
81. Brosicke N, Sallouh M, Prior LM, Job A, Weberskirch R, Faissner A. Extracellular Matrix Glycoprotein-Derived Synthetic Peptides Differentially Modulate Glioma and Sarcoma Cell Migration. *Cell Mol Neurobiol* (2015) 35(5):741–53. doi: 10.1007/s10571-015-0170-1
82. Ulrich TA, Jain A, Tanner K, MacKay JL, Kumar S. Probing Cellular Mechanobiology in Three-Dimensional Culture With Collagen-Agarose Matrices. *Biomaterials* (2010) 31(7):1875–84. doi: 10.1016/j.biomaterials.2009.10.047
83. Barros D, Conde-Sousa E, Gonçalves AM, Han WM, Garcia AJ, Amaral IF, et al. Engineering Hydrogels With Affinity-Bound Laminin as 3D Neural Stem Cell Culture Systems. *Biomater Sci* (2019) 7(12):5338–49. doi: 10.1039/C9BM00348G
84. Licht C, Rose JC, Anarkoli AO, Blondel D, Roccio M, Haraszti T, et al. Synthetic 3d PEG-Anisogel Tailored With Fibronectin Fragments Induce Aligned Nerve Extension. *Biomacromolecules* (2019) 20(11):4075–87. doi: 10.1021/acs.biomac.9b00891
85. Wang C, Tong X, Yang F. Bioengineered 3D Brain Tumor Model to Elucidate the Effects of Matrix Stiffness on Glioblastoma Cell Behavior Using PEG-Based Hydrogels. *Mol Pharm* (2014) 11(7):2115–25. doi: 10.1021/mp5000828
86. Chaichareonudomrung N, Kunhorm P, Noisa P. Three-Dimensional Cell Culture Systems as an In Vitro Platform for Cancer and Stem Cell Modeling. *World J Stem Cells* (2019) 11(12):1065–83. doi: 10.4252/wjsc.v11.i12.1065
87. Doyle AD, Carvajal N, Jin A, Matsumoto K, Yamada KM. Local 3D Matrix Microenvironment Regulates Cell Migration Through Spatiotemporal Dynamics of Contractility-Dependent Adhesions. *Nat Commun* (2015) 6:8720. doi: 10.1038/ncomms9720
88. Holle AW, Young JL, Spatz JP. In Vitro Cancer Cell-ECM Interactions Inform In Vivo Cancer Treatment. *Adv Drug Delivery Rev* (2016) 97:270–9. doi: 10.1016/j.addr.2015.10.007
89. Puls TJ, Tan X, Whittington CF, Voytik-Harbin SL. 3D Collagen Fibrillar Microstructure Guides Pancreatic Cancer Cell Phenotype and Serves as a Critical Design Parameter for Phenotypic Models of EMT. *PLoS One* (2017) 12(11):e0188870. doi: 10.1371/journal.pone.0188870
90. Lee KY, Mooney DJ. Alginate: Properties and Biomedical Applications. *Prog Polym Sci* (2012) 37(1):106–26. doi: 10.1016/j.progpolymsci.2011.06.003
91. Andersen T, Auk-Emblem P, Dornish M. 3d Cell Culture in Alginate Hydrogels. *Microarrays (Basel)* (2015) 4(2):133–61. doi: 10.3390/microarrays4020133
92. Bidarra SJ, Barrias CC. 3d Culture of Mesenchymal Stem Cells in Alginate Hydrogels. *Methods Mol Biol* (2019) (2002) p:165–80.

93. Cavo M, Caria M, Pulsoni I, Beltrame F, Fato M, Scaglione S. A New Cell-Laden 3D Alginate-Matrigel Hydrogel Resembles Human Breast Cancer Cell Malignant Morphology, Spread and Invasion Capability Observed "In Vivo". *Sci Rep* (2018) 8(1):5333. doi: 10.1038/s41598-018-23250-4
94. Li Y, Kumacheva E. Hydrogel Microenvironments for Cancer Spheroid Growth and Drug Screening. *Sci Adv* (2018) 4(4):eaas8998. doi: 10.1126/sciadv.aas8998
95. Fang G, Lu H, Rodriguez de la Fuente L, Law AMK, Lin G, Jin D, et al. Mammary Tumor Organoid Culture in Non-Adhesive Alginate for Luminal Mechanics and High-Throughput Drug Screening. *Adv Sci (Weinh)* (2021) p:e2102418. doi: 10.1002/advs.202102418
96. Sze JH, Brownlie JC, Love CA. Biotechnological Production of Hyaluronic Acid: A Mini Review. *3 Biotech* (2016) 6(1):67. doi: 10.1007/s13205-016-0379-9
97. Corradetti B, Taraballi F, Martinez JO, Minardi S, Basu N, Bauza G, et al. Hyaluronic Acid Coatings as a Simple and Efficient Approach to Improve MSC Homing Toward the Site of Inflammation. *Sci Rep* (2017) 7(1):7991. doi: 10.1038/s41598-017-08687-3
98. Gurski LA, Jha AK, Zhang C, Jia X, Farach-Carson MC. Hyaluronic Acid-Based Hydrogels as 3D Matrices for In Vitro Evaluation of Chemotherapeutic Drugs Using Poorly Adherent Prostate Cancer Cells. *Biomaterials* (2009) 30(30):6076–85. doi: 10.1016/j.biomaterials.2009.07.054
99. Gerecht S, Burdick JA, Ferreira LS, Townsend SA, Langer R, Vunjak-Novakovic G. Hyaluronic Acid Hydrogel for Controlled Self-Renewal and Differentiation of Human Embryonic Stem Cells. *Proc Natl Acad Sci USA* (2007) 104(27):11298–303. doi: 10.1073/pnas.0703723104
100. Ehlers EM, Behrens P, Wunsch L, Kuhnel W, Russlies M. Effects of Hyaluronic Acid on the Morphology and Proliferation of Human Chondrocytes in Primary Cell Culture. *Ann Anat* (2001) 183(1):13–7. doi: 10.1016/S0940-9602(01)80007-8
101. Suo A, Xu W, Wang Y, Sun T, Ji L, Qian J. Dual-Degradable and Injectable Hyaluronic Acid Hydrogel Mimicking Extracellular Matrix for 3D Culture of Breast Cancer MCF-7 Cells. *Carbohydr Polym* (2019) 211:336–48. doi: 10.1016/j.carbpol.2019.01.115
102. Weber LM, Hayda KN, Haskins K, Anseth KS. The Effects of Cell-Matrix Interactions on Encapsulated Beta-Cell Function Within Hydrogels Functionalized With Matrix-Derived Adhesive Peptides. *Biomaterials* (2007) 28(19):3004–11. doi: 10.1016/j.biomaterials.2007.03.005
103. Booi TH, Price LS, Danen EHJ. 3d Cell-Based Assays for Drug Screens: Challenges in Imaging, Image Analysis, and High-Content Analysis. *SLAS Discovery* (2019) 24(6):615–27. doi: 10.1177/2472555219830087
104. Nagahama K, Oyama N, Ono K, Hotta A, Kawauchi K, Nishikata T. Nanocomposite Injectable Gels Capable of Self-Replenishing Regenerative Extracellular Microenvironments for In Vivo Tissue Engineering. *Biomater Sci* (2018) 6(3):550–61. doi: 10.1039/C7BM01167A
105. Rezaekhani S, Gjorevski N, Lutolf MP. Low-Defect Thiol-Michael Addition Hydrogels as Matrigel Substitutes for Epithelial Organoid Derivation. *Adv Func Mater* (2020) 30(48):1–12. doi: 10.1002/adfm.202000761
106. Raeber GP, Lutolf MP, Hubbell JA. Molecularly Engineered PEG Hydrogels: A Novel Model System for Proteolytically Mediated Cell Migration. *Biophys J* (2005) 89(2):1374–88. doi: 10.1529/biophysj.104.050682
107. Ham SL, Thakuri PS, Plaster M, Li J, Luker KE, Luker GD, et al. Three-Dimensional Tumor Model Mimics Stromal - Breast Cancer Cells Signaling. *Oncotarget* (2018) 9(1):249–67. doi: 10.18632/oncotarget.22922
108. Pape J, Emberton M, Cheema U. 3d Cancer Models: The Need for a Complex Stroma, Compartmentalization and Stiffness. *Front Bioeng Biotechnol* (2021) 9:660502. doi: 10.3389/fbioe.2021.660502
109. Caiazzo M, Okawa Y, Ranga A, Piersigilli A, Tabata Y, Lutolf MP. Defined Three-Dimensional Microenvironments Boost Induction of Pluripotency. *Nat Mater* (2016) 15(3):344–52. doi: 10.1038/nmat4536
110. Downing TL, Soto J, Morez C, Houssin T, Fritz A, Yuan F, et al. Biophysical Regulation of Epigenetic State and Cell Reprogramming. *Nat Mater* (2013) 12(12):1154–62. doi: 10.1038/nmat3777
111. Pickup KE, Pardow F, Carbonell-Caballero J, Lioutas A, Villanueva-Canas JL, Wright RHG, et al. Expression of Oncogenic Drivers in 3D Cell Culture Depends on Nuclear ATP Synthesis by NUDT5. *Cancers (Basel)* (2019) 11(9):1–17. doi: 10.3390/cancers11091337
112. Luca AC, Mersch S, Deenen R, Schmidt S, Messner I, Schafer KL, et al. Impact of the 3D Microenvironment on Phenotype, Gene Expression, and EGFR Inhibition of Colorectal Cancer Cell Lines. *PLoS One* (2013) 8(3):e59689. doi: 10.1371/journal.pone.0059689
113. Huh D, Hamilton GA, Ingber DE. From 3D Cell Culture to Organs-on-Chips. *Trends Cell Biol* (2011) 21(12):745–54. doi: 10.1016/j.tcb.2011.09.005
114. Whitesides GM. The Origins and the Future of Microfluidics. *Nature* (2006) 442(7101):368–73. doi: 10.1038/nature05058
115. Torisawa YS, Mosadegh B, Luker GD, Morell M, O'Shea KS, Takayama S. Microfluidic Hydrodynamic Cellular Patterning for Systematic Formation of Co-Culture Spheroids. *Integr Biol (Camb)* (2009) 1(11–12):649–54. doi: 10.1039/b915965g
116. Torisawa YS, Chueh BH, Huh D, Ramamurthy P, Roth TM, Barald KF, et al. Efficient Formation of Uniform-Sized Embryoid Bodies Using a Compartmentalized Microchannel Device. *Lab Chip* (2007) 7(6):770–6. doi: 10.1039/b618439a
117. Patra B, Chen YH, Peng CC, Lin SC, Lee CH, Tung YC. A Microfluidic Device for Uniform-Sized Cell Spheroids Formation, Culture, Harvesting and Flow Cytometry Analysis. *Biomicrofluidics* (2013) 7(5):54114. doi: 10.1063/1.4824480
118. Cui P, Wang S. Application of Microfluidic Chip Technology in Pharmaceutical Analysis: A Review. *J Pharm Anal* (2019) 9(4):238–47. doi: 10.1016/j.jpha.2018.12.001
119. Kraly JR, Holcomb RE, Guan Q, Henry CS. Review: Microfluidic Applications in Metabolomics and Metabolic Profiling. *Anal Chim Acta* (2009) 653(1):23–35. doi: 10.1016/j.aca.2009.08.037
120. Bhatia SN, Ingber DE. Microfluidic Organs-on-Chips. *Nat Biotechnol* (2014) 32(8):760–72. doi: 10.1038/nbt.2989
121. Esch EW, Bahinski A, Huh D. Organs-On-Chips at the Frontiers of Drug Discovery. *Nat Rev Drug Discovery* (2015) 14(4):248–60. doi: 10.1038/nrd4539
122. El-Ali J, Sorger PK, Jensen KF. Cells on Chips. *Nature* (2006) 442(7101):403–11. doi: 10.1038/nature05063
123. Shang M, Soon RH, Lim CT, Khoo BL, Han J. Microfluidic Modelling of the Tumor Microenvironment for Anti-Cancer Drug Development. *Lab Chip* (2019) 19(3):369–86. doi: 10.1039/C8LC00970H
124. Gogoi P, Sepehri S, Zhou Y, Gorin MA, Paolillo C, Capoluongo E, et al. Development of an Automated and Sensitive Microfluidic Device for Capturing and Characterizing Circulating Tumor Cells (CTCs) From Clinical Blood Samples. *PLoS One* (2016) 11(1):e0147400. doi: 10.1371/journal.pone.0147400
125. Caballero D, Kaushik S, Corrello VM, Oliveira JM, Reis RL, Kundu SC. Organ-On-Chip Models of Cancer Metastasis for Future Personalized Medicine: From Chip to the Patient. *Biomaterials* (2017) 149:98–115. doi: 10.1016/j.biomaterials.2017.10.005
126. van den Berg A, Mummery CL, Passier R, van der Meer AD. Personalised Organs-on-Chips: Functional Testing for Precision Medicine. *Lab Chip* (2019) 19(2):198–205. doi: 10.1039/C8LC00827B
127. Ruppen J, Cortes-Dericks L, Marconi E, Karoubi G, Schmid RA, Peng R, et al. A Microfluidic Platform for Chemoresistive Testing of Multicellular Pleural Cancer Spheroids. *Lab Chip* (2014) 14(6):1198–205. doi: 10.1039/C3LC51093J
128. Fang G, Lu H, Law A, Gallego-Ortega D, Jin D, Lin G. Gradient-Sized Control of Tumor Spheroids on a Single Chip. *Lab Chip* (2019) 19(24):4093–103. doi: 10.1039/C9LC00872A
129. Huang K, Boerhan R, Liu C, Jiang G. Nanoparticles Penetrate Into the Multicellular Spheroid-On-Chip: Effect of Surface Charge, Protein Corona, and Exterior Flow. *Mol Pharm* (2017) 14(12):4618–27. doi: 10.1021/acs.molpharmaceut.7b00726
130. Chen Y, Gao D, Wang Y, Lin S, Jiang Y. A Novel 3D Breast-Cancer-on-Chip Platform for Therapeutic Evaluation of Drug Delivery Systems. *Anal Chim Acta* (2018) 1036:p97–106.
131. Trujillo-de Santiago G, Flores-Garza BG, Tavares-Negrete JA, Lara-Mayorga IM, Gonzalez-Gamboa I, Zhang YS, et al. The Tumor-On-Chip: Recent Advances in the Development of Microfluidic Systems to Recapitulate the Physiology of Solid Tumors. *Materials (Basel)* (2019) 12(18):1–40. doi: 10.3390/ma12182945
132. Shirure VS, Bi Y, Curtis MB, Lezia A, Goedegebuure MM, Goedegebuure SP, et al. Tumor-On-a-Chip Platform to Investigate Progression and Drug Sensitivity in Cell Lines and Patient-Derived Organoids. *Lab Chip* (2018) 18(23):3687–702. doi: 10.1039/C8LC00596F

133. Osaki T, Sivathanu V, Kamm RD. Vascularized Microfluidic Organ-Chips for Drug Screening, Disease Models and Tissue Engineering. *Curr Opin Biotechnol* (2018) 52:116–23. doi: 10.1016/j.copbio.2018.03.011
134. Bray LJ, Werner C. Evaluation of Three-Dimensional in Vitro Models to Study Tumor Angiogenesis. *ACS Biomater Sci Eng* (2018) 4(2):337–46. doi: 10.1021/acsbmaterials.7b00139
135. Agarwal P, Wang H, Sun M, Xu J, Zhao S, Liu Z, et al. Microfluidics Enabled Bottom-Up Engineering of 3D Vascularized Tumor for Drug Discovery. *ACS Nano* (2017) 11(7):6691–702. doi: 10.1021/acsnano.7b00824
136. Mannino RG, Santiago-Miranda AN, Pradhan P, Qiu Y, Mejias JC, Neelapu SS, et al. 3D Microvascular Model Recapitulates the Diffuse Large B-Cell Lymphoma Tumor Microenvironment In Vitro. *Lab Chip* (2017) 17(3):407–14. doi: 10.1039/C6LC01204C
137. Deo KA, Singh KA, Peak CW, Alge DL, Gaharwar AK. Bioprinting 101: Design, Fabrication, and Evaluation of Cell-Laden 3d Bioprinted Scaffolds. *Tissue Eng Part A* (2020) 26(5-6):318–38. doi: 10.1089/ten.tea.2019.0298
138. Ma X, Liu J, Zhu W, Tang M, Lawrence N, Yu C, et al. 3D Bioprinting of Functional Tissue Models for Personalized Drug Screening and In Vitro Disease Modeling. *Adv Drug Delivery Rev* (2018) 132:235–51. doi: 10.1016/j.addr.2018.06.011
139. Chia HN, Vigen M, Kasko AM. Effect of Substrate Stiffness on Pulmonary Fibroblast Activation by TGF- β . *Acta Biomater* (2012) 8(7):2602–11. doi: 10.1016/j.actbio.2012.03.027
140. Sharma R, Smits IPM, de la Vega L, Lee C, Willerth SM. 3d Bioprinting Pluripotent Stem Cell Derived Neural Tissues Using a Novel Fibrin Bioink Containing Drug Releasing Microspheres. *Front Bioeng Biotechnol* (2020) 8:57. doi: 10.3389/fbioe.2020.00057
141. Zhou X, Zhu W, Nowicki M, Miao S, Cui H, Holmes B, et al. 3d Bioprinting a Cell-Laden Bone Matrix for Breast Cancer Metastasis Study. *ACS Appl Mater Interfaces* (2016) 8(44):30017–26. doi: 10.1021/acsami.6b10673
142. Swaminathan S, Hamid Q, Sun W, Clyne AM. Bioprinting of 3D Breast Epithelial Spheroids for Human Cancer Models. *Biofabrication* (2019) 11(2):025003. doi: 10.1088/1758-5090/aaf49
143. Kacarevic ZP, Rider PM, Alkildani S, Retnasingh S, Smeets R, Jung O, et al. An Introduction to 3D Bioprinting: Possibilities, Challenges and Future Aspects. *Materials (Basel)* (2018) 11(11):1–21. doi: 10.3390/ma1112199
144. Gudapati H, Dey M, Ozbolat I. A Comprehensive Review on Droplet-Based Bioprinting: Past, Present and Future. *Biomaterials* (2016) 102:20–42. doi: 10.1016/j.biomaterials.2016.06.012
145. Graham AD, Olof SN, Burke MJ, Armstrong JPK, Mikhailova EA, Nicholson JG, et al. High-Resolution Patterned Cellular Constructs by Droplet-Based 3d Printing. *Sci Rep* (2017) 7(1):7004. doi: 10.1038/s41598-017-06358-x
146. Utama RH, Atapattu L, O'Mahony AP, Fife CM, Baek J, Allard T, et al. A 3d Bioprinter Specifically Designed for the High-Throughput Production of Matrix-Embedded Multicellular Spheroids. *iScience* (2020) 23(10):101621.
147. Koch L, Gruene M, Unger C, Chichkov B. Laser Assisted Cell Printing. *Curr Pharm Biotechnol* (2013) 14(1):91–7.
148. Guillotin B, Souquet A, Catros S, Duocastella M, Pippenger B, Bellance S, et al. Laser Assisted Bioprinting of Engineered Tissue With High Cell Density and Microscale Organization. *Biomaterials* (2010) 31(28):7250–6. doi: 10.1016/j.biomaterials.2010.05.055
149. Huang TQ, Qu X, Liu J, Chen S. 3D Printing of Biomimetic Microstructures for Cancer Cell Migration. *BioMed Microdevices* (2014) 16(1):127–32. doi: 10.1007/s10544-013-9812-6
150. Guillemot F, Souquet A, Catros S, Guillotin B. Laser-Assisted Cell Printing: Principle, Physical Parameters Versus Cell Fate and Perspectives in Tissue Engineering. *Nanomed (Lond)* (2010) 5(3):507–15. doi: 10.2217/nnm.10.14
151. Heinrich MA, Bansal R, Lammers T, Zhang YS, Michel Schiffelers R, Prakash J. 3d-Bioprinted Mini-Brain: A Glioblastoma Model to Study Cellular Interactions and Therapeutics. *Adv Mater* (2019) 31(14):e1806590. doi: 10.1002/adma.201806590
152. Zhao Y, Yao R, Ouyang L, Ding H, Zhang T, Zhang K, et al. Three-Dimensional Printing of HeLa Cells for Cervical Tumor Model In Vitro. *Biofabrication* (2014) 6(3):035001. doi: 10.1088/1758-5082/6/3/035001
153. Wang X, Zhang X, Dai X, Wang X, Li X, Diao J, et al. Tumor-Like Lung Cancer Model Based on 3D Bioprinting. *3 Biotech* (2018) 8(12):501. doi: 10.1007/s13205-018-1519-1
154. Zhang J, Chen F, He Z, Ma Y, Uchiyama K, Lin JM. A Novel Approach for Precisely Controlled Multiple Cell Patterning in Microfluidic Chips by Inkjet Printing and the Detection of Drug Metabolism and Diffusion. *Analyst* (2016) 141(10):2940–7. doi: 10.1039/C6AN00395H
155. Xu F, Celli J, Rizvi I, Moon S, Hasan T, Demirci U. A Three-Dimensional In Vitro Ovarian Cancer Coculture Model Using a High-Throughput Cell Patterning Platform. *Biotechnol J* (2011) 6(2):204–12. doi: 10.1002/biot.201000340
156. Ashammakhi N, Ahadian S, Zengjie F, Suthiwanich K, Lorestani F, Orive G. Advances and Future Perspectives in 4D Bioprinting. *Biotechnol J* (2018) 13(12):e1800148. doi: 10.1002/biot.201800148
157. Brassard JA, Nikolaev M, Hubscher T, Hofer M, Lutolf MP. Recapitulating Macro-Scale Tissue Self-Organization Through Organoid Bioprinting. *Nat Mater* (2021) 20(1):22–9. doi: 10.1038/s41563-020-00803-5
158. Yi HG, Jeong YH, Kim Y, Choi YJ, Moon HE, Park SH, et al. A Bioprinted Human-Glioblastoma-on-a-Chip for the Identification of Patient-Specific Responses to Chemoradiotherapy. *Nat BioMed Eng* (2019) 3(7):509–19. doi: 10.1038/s41551-019-0363-x
159. Alves TR, Lima FR, Kahn SA, Lobo D, Dubois LG, Soletti R, et al. Glioblastoma Cells: A Heterogeneous and Fatal Tumor Interacting With the Parenchyma. *Life Sci* (2011) 89(15-16):532–9. doi: 10.1016/j.lfs.2011.04.022
160. Castaneda CA, Casavilca S, Orrego E, Garcia-Corrochano P, Deza P, Heinike H, et al. Glioblastoma: Molecular Analysis and Its Clinical Implications. *Rev Peru Med Exp Salud Publica* (2015) 32(2):316–25.
161. Stroganov V, Al-Hussein M, Sommer JU, Janke A, Zakharchenko S, Ionov L. Reversible Thermosensitive Biodegradable Polymeric Actuators Based on Confined Crystallization. *Nano Lett* (2015) 15(3):1786–90. doi: 10.1021/nl5045023
162. Hribar KC, Finlay D, Ma X, Qu X, Ondeck MG, Chung PH, et al. Nonlinear 3D Projection Printing of Concave Hydrogel Microstructures for Long-Term Multicellular Spheroid and Embryoid Body Culture. *Lab Chip* (2015) 15(11):2412–8. doi: 10.1039/C5LC00159E
163. Booth MJ, Schild VR, Graham AD, Olof SN, Bayley H. Light-Activated Communication in Synthetic Tissues. *Sci Adv* (2016) 2(4):e1600056. doi: 10.1126/sciadv.1600056
164. Wang LL, Highley CB, Yeh YC, Galarraga JH, Uman S, Burdick JA. Three-Dimensional Extrusion Bioprinting of Single- and Double-Network Hydrogels Containing Dynamic Covalent Crosslinks. *J BioMed Mater Res A* (2018) 106(4):865–75. doi: 10.1002/jbm.a.36323
165. Kokkinis D, Schaffner M, Studart AR. Multimaterial Magnetically Assisted 3D Printing of Composite Materials. *Nat Commun* (2015) 6:8643. doi: 10.1038/ncomms9643
166. Aronsson C, Jury M, Naeimipour S, Boroojeni FR, Christofferson J, Lifwergren P, et al. Dynamic Peptide-Folding Mediated Biofunctionalization and Modulation of Hydrogels for 4D Bioprinting. *Biofabrication* (2020) 12(3):035031. doi: 10.1088/1758-5090/ab9490
167. Tabriz AG, Hermida MA, Leslie NR, Shu W. Three-Dimensional Bioprinting of Complex Cell Laden Alginate Hydrogel Structures. *Biofabrication* (2015) 7(4):045012. doi: 10.1088/1758-5090/7/4/045012
168. Gladman AS, Matsumoto EA, Nuzzo RG, Mahadevan L, Lewis JA. Biomimetic 4D Printing. *Nat Mater* (2016) 15(4):413–8. doi: 10.1038/nmat4544
169. Kwag HR, Serbo JV, Korangath P, Sukumar S, Romer LH, Gracias DH. A Self-Folding Hydrogel In Vitro Model for Ductal Carcinoma. *Tissue Eng Part C Methods* (2016) 22(4):398–407. doi: 10.1089/ten.tec.2015.0442
170. Kuribayashi-Shigetomi K, Onoe H, Takeuchi S. Cell Origami: Self-Folding of Three-Dimensional Cell-Laden Microstructures Driven by Cell Traction Force. *PLoS One* (2012) 7(12):e51085. doi: 10.1371/journal.pone.0051085
171. Ryan SL, Baird AM, Vaz G, Urquhart AJ, Senge M, Richard DJ, et al. Drug Discovery Approaches Utilizing Three-Dimensional Cell Culture. *Assay Drug Dev Technol* (2016) 14(1):19–28. doi: 10.1089/adt.2015.670
172. Montanez-Sauri SI, Beebe DJ, Sung KE. Microscale Screening Systems for 3D Cellular Microenvironments: Platforms, Advances, and Challenges. *Cell Mol Life Sci* (2015) 72(2):237–49. doi: 10.1007/s00018-014-1738-5
173. Ruel-Gariepy E, Leroux JC. In Situ-Forming Hydrogels—Review of Temperature-Sensitive Systems. *Eur J Pharm Biopharm* (2004) 58(2):409–26. doi: 10.1016/j.ejpb.2004.03.019

174. Horvath P, Aulner N, Bickle M, Davies AM, Nery ED, Ebner D, et al. Screening Out Irrelevant Cell-Based Models of Disease. *Nat Rev Drug Discovery* (2016) 15(11):751–69. doi: 10.1038/nrd.2016.175
175. Worthington P, Drake KM, Li Z, Napper AD, Pochan DJ, Langhans SA. Beta-Hairpin Hydrogels as Scaffolds for High-Throughput Drug Discovery in Three-Dimensional Cell Culture. *Anal Biochem* (2017) 535:25–34. doi: 10.1016/j.ab.2017.07.024
176. Eismann B, Krieger TG, Beneke J, Bulkescher R, Adam L, Erfle H, et al. Automated 3D Light-Sheet Screening With High Spatiotemporal Resolution Reveals Mitotic Phenotypes. *J Cell Sci* (2020) 133(11):1–11. doi: 10.1242/jcs.245043
177. Bilgin CC, Fontenay G, Cheng Q, Chang H, Han J, Parvin B. BioSig3D: High Content Screening of Three-Dimensional Cell Culture Models. *PloS One* (2016) 11(3):e0148379. doi: 10.1371/journal.pone.0148379
178. Fong ELS, Toh TB, Yu H, Chow EK. 3d Culture as a Clinically Relevant Model for Personalized Medicine. *SLAS Technol* (2017) 22(3):245–53. doi: 10.1177/2472630317697251
179. Candini O, Grisendi G, Foppiani EM, Brogli M, Aramini B, Masciale V, et al. Author Correction: A Novel 3d In Vitro Platform for Pre-Clinical Investigations in Drug Testing, Gene Therapy, and Immuno-Oncology. *Sci Rep* (2020) 10(1):1845. doi: 10.1038/s41598-020-57846-6

Conflict of Interest: TG is employed by Inventia Life Science Pty Ltd as stated in affiliations.

The remaining authors declare that the research was conducted in the absence of any commercial or financial relationships that could be construed as a potential conflict of interest.

Publisher's Note: All claims expressed in this article are solely those of the authors and do not necessarily represent those of their affiliated organizations, or those of the publisher, the editors and the reviewers. Any product that may be evaluated in this article, or claim that may be made by its manufacturer, is not guaranteed or endorsed by the publisher.

Copyright © 2021 Law, Rodriguez de la Fuente, Grundy, Fang, Valdes-Mora and Gallego-Ortega. This is an open-access article distributed under the terms of the Creative Commons Attribution License (CC BY). The use, distribution or reproduction in other forums is permitted, provided the original author(s) and the copyright owner(s) are credited and that the original publication in this journal is cited, in accordance with accepted academic practice. No use, distribution or reproduction is permitted which does not comply with these terms.



Chidamide Reverses Fluzoparib Resistance in Triple-Negative Breast Cancer Cells

Xinyang Li¹, Xiang Yuan¹, Ziming Wang¹, Jing Li¹, Zhiwei Liu¹, Yukun Wang¹, Limin Wei¹, Yuanpei Li² and Xinshuai Wang^{1*}

¹ Henan Key Laboratory of Cancer Epigenetics, Cancer Hospital, The First Affiliated Hospital, College of Clinical Medicine, Medical College of Henan University of Science and Technology, Luoyang, China, ² Department of Internal Medicine, UC Davis Comprehensive Cancer Center, University of California, Davis, Sacramento, CA, United States

OPEN ACCESS

Edited by:

Maria Rosaria De Miglio,
University of Sassari, Italy

Reviewed by:

Caigang Liu,
ShengJing Hospital of China Medical
University, China
Polly Gravells,
The University of Sheffield,
United Kingdom

*Correspondence:

Xinshuai Wang
xshuaiw@haust.edu.cn

Specialty section:

This article was submitted to
Breast Cancer,
a section of the journal
Frontiers in Oncology

Received: 22 November 2021

Accepted: 19 January 2022

Published: 18 February 2022

Citation:

Li X, Yuan X, Wang Z, Li J,
Liu Z, Wang Y, Wei L, Li Y
and Wang X (2022) Chidamide
Reverses Fluzoparib Resistance in
Triple-Negative Breast Cancer Cells.
Front. Oncol. 12:819714.
doi: 10.3389/fonc.2022.819714

Poly (ADP-ribose) polymerase inhibitor (PARPi) resistance is a new challenge for antitumor therapy. The purpose of this study was to investigate the reversal effects of chidamide on fluzoparib resistance, a PARPi, and its mechanism of action. A fluzoparib-resistant triple-negative breast cancer (TNBC) cell line was constructed, and the effects of chidamide and fluzoparib on drug-resistant cells were studied *in vitro* and *in vivo*. The effects of these drugs on cell proliferation, migration, invasiveness, the cell cycle, and apoptosis were detected using an MTT assay, wound-healing and transwell invasion assays, and flow cytometry. Bioinformatics was used to identify hub drug resistance genes and Western blots were used to assess the expression of PARP, RAD51, MRE11, cleaved Caspase9, and P-CDK1. Xenograft models were established to analyze the effects of these drugs on nude mice. *In vivo* results showed that chidamide combined with fluzoparib significantly inhibited the proliferation, migration, and invasiveness of drug-resistant cells and restored fluzoparib sensitivity to drug-resistant cells. The combination of chidamide and fluzoparib significantly inhibited the expression of the hub drug resistance genes RAD51 and MRE11, arrested the cell cycle at the G2/M phase, and induced cell apoptosis. The findings of this work show that chidamide combined with fluzoparib has good antineoplastic activity and reverses TNBC cell resistance to fluzoparib by reducing the expression levels of RAD51 and MRE11.

Keywords: triple-negative breast cancer, PARP inhibitor resistance, drug resistance reversal, fluzoparib, chidamide

INTRODUCTION

Breast cancer, the most common malignant solid tumor, is the leading cause of cancer deaths among women worldwide, with approximately 2.1 million new cases in 2020 alone (1). Triple-negative breast cancer (TNBC), a subtype of breast cancer that lacks the expression of hormone receptors (estrogen receptor or progesterone receptor) and human epidermal growth factor receptor 2, has a higher degree of virulence and is resistant to various chemotherapeutics and targeted medicine, making it challenging to treat (2, 3). Molecular-targeted precision therapy and predictive

biomarkers associated with the diagnosis and treatment of TNBC are needed to comprehensively treat this malignancy.

Recent research in the field of DNA damage repair has shown that poly (ADP-ribose) polymerase inhibitors (PARPi) that involve the synthetic lethal approach have achieved satisfactory effects and promising prospects in the treatment of various cancers (4–6). PARPi traditionally exert antitumor effects by trapping PARP on DNA, causing DNA replication forks to collapse, disrupting cell mitosis, and inducing cell death, although chemoresistance to PARPi has been reported (7, 8). The mechanisms of PARPi resistance primarily include: (1) restoration of BRCA function or the abnormal expression of DNA repair proteins, leading to the restoration of the homologous recombination repair pathway (9–12); (2) deletion of PTIP, EZH2, and MUS81 expression or increased miR-493-5p expression, leading to stability of the replication fork (13–15); (3) mutations in PARP1 and PARG (16, 17); (4) creation of P-glycoprotein pumps and ATP-binding cassette drug transporters that increase drug outflow (18, 19); and (5) mir-622 overexpression, which inhibits nonhomologous end joining (20). Overcoming PARPi resistance is necessary to permit adequate PARPi antitumor therapy.

The identification of histone deacetylase (HDAC) as a new anticancer therapeutic target has added a new target for novel therapies. HDACs are involved in breast cancer tumorigenesis by regulating the genes of cell cycle factors, differentiation factors, and apoptotic factors (21–23). HDACs can also enhance genes related to angiogenesis, cell invasion, and migration and immune regulation to promote cancer development, such as vascular endothelial growth factor (VEGF), endothelial nitric oxide synthase (eNOS), HIF-1 α , major histocompatibility complex (MHC), and human leukocyte antigens (HLA) (24–29). As a multilayer regulatory protein, HDAC can also affect DNA damage repair by regulating the expression of DNA damage repair-related genes and enhancing the activity of the DNA repair protein complex (30, 31). Most importantly, HDAC inhibitors (HDACi) have exhibited surprising antitumor effects.

Prior works have confirmed that HDACi combined with PARPi has a significant antitumor effect on TNBC cells (32, 33). In addition, HDACi can overcome gemcitabine, tamoxifen, and trastuzumab resistance (34–36). However, no studies on HDACi overcoming PARPi resistance are available. Therefore, based on the multifaceted antitumor activity of HDACi, we hypothesized that chidamide (HDACi) would reverse fluzoparib (PARPi) resistance. We investigated the mechanism behind HDACi reversal of PARPi resistance in breast cancer cells in the present work by constructing fluzoparib-resistant breast cancer cell lines. We demonstrate here that effective antitumor activity can be restored if fluzoparib is combined with chidamide.

MATERIALS AND METHODS

Cell Culture

HCC1937 and MDA-MB-468 triple-negative breast cancer cell line were purchased from the China Center for Type Culture

Collection (CCATCC, China) and cultured according to the instructions provided by the manufacturers. The fluzoparib-resistant cell lines HCC1937-FR and MDA-MB-468-FR were established at our institution.

Chemicals and Antibodies

Fluzoparib is a PARP inhibitor and chidamide is a HDAC inhibitor. PARP, RAD51, MRE11, cleaved Caspase9, GAPDH, and P-CDK1 antibodies were obtained from Abcam Trading Co., Ltd. (Shanghai, China).

Establishment of Drug-Resistant Cell Lines

The fluzoparib-resistant cell lines HCC1937-FR and MDA-MB-468-FR were constructed based on increasing drug concentration. HCC1937 and MDA-MB-468 cells in the logarithmic growth phase were cultured in complete medium at final fluzoparib concentrations of 2 and 5 μ g/ml. After the cells were incubated for 2 days or when cell death reached 50%, the drug-containing medium was removed and the culture medium was passed 3 times or more with drug-free fresh medium. After waiting for the cell state to gradually recover and permit stable passage, the same drug concentration was used again 3 times, with increased drug concentration according to the cell growth. This strategy yielded the fluzoparib-resistant cell lines HCC1937-FR and MDA-MB-468-FR.

Identification and Biological Process Analysis of Differentially Expressed Genes

High-throughput sequencing was used to perform whole-transcriptome sequencing of HCC1937 and HCC1937-FR cells in order to identify differentially expressed genes (DEGs) between parental and drug-resistant cells. Using differential expression analysis, genes with a *p*-value <0.05 and a log₂FC >1 or <-1 were considered DEGs. The biological processes of the enrichment analysis of DEGs were identified using the STRING database (<https://string-db.org/>). Biologic process analysis results were visualized using the ggplot2 package (version 1.26.0). DEGs related to DNA damage repair were selected for further analysis.

Identification of Hub Drug Resistance Genes

DEGs related to DNA damage repair were uploaded to the STRING database in order to obtain the protein–protein interaction network and analyzed visually with Cytoscape software. The top 6 genes with the highest degree of gene association degree were labeled hub drug resistance genes. Based on the gene expression of the 6 hub drug resistance genes, histograms were created and genes of interest were selected for further analysis.

Experimental Efficacy Studies

Experiments regarding the biological function of drug-resistant cells included parental (HCC1937 and MDA-MB-468) and drug-resistant cell lines (HCC1937-FR and MDA-MB-468-FR). Drug efficacy studies using the drug-resistant cell lines utilized PBS, fluzoparib (30 μ g/ml), chidamide (3 or 6 μ g/ml), and the combination of the two drugs (fluzoparib 30 μ g/ml + chidamide 3 or 6 μ g/ml).

Cell Viability Assay

An MTT assay was used to evaluate cell viability. Cells were seeded in 96-well plates at a density of $3\text{--}5 \times 10^3$ cells/well for 24 h, and then treated with the experimental drugs for 48 h according to their experimental group. The cell viability of each well was assessed using a microplate reader (Bio-Tek, Norcross, GA, USA), which measured the absorbance of each well at 570 nm. The mean IC_{50} value of the cells in each experimental group was computed using SPSS. The resistance index was defined as IC_{50} of drug-resistant cells/ IC_{50} of parental cells.

Wound-Healing Assay

The migration ability of drug-resistant cells and drug-treated cells was analyzed using a wound-healing assay. Cells were plated in 6-well plastic culture plates at a density of 5×10^3 cells/well in culture medium until they reached 90% confluence. Either drug-containing or drug-free serum-free medium was added to each Petri well according to the experimental group and observed for 24 h. Cell migration was recorded at 0 and 24 h, and ImageJ software (NIH, Bethesda, MA, USA) was used to quantitatively analyze the degree of cell migration in the different experimental groups.

Transwell Invasion Assays

Cell invasion ability was assessed using Transwell invasion assays. Transwell chambers coated with Matrigel with a bottom membrane aperture size of 8 μm (Sigma-Aldrich, St. Louis, MO, USA) were used to measure cell invasiveness. A total of 200 μl of drug-resistant or parental cells was resuspended in serum-free culture medium with PBS or an experimental drug for 24 h. After washing, fixing, and staining, 10 visual fields were randomly selected and a cell count under a $\times 100$ magnification optical microscope was performed using ImageJ software.

Cell Cycle Analysis

For the cell cycle arrest assay, cells were starved in 6-well plates for 24 h before treatment. Cells were treated with PBS or drug culture medium according to experimental grouping for 24 h. Processed cells were then scraped with PBS, fixed with 70% precooled ethanol for 1 h then washed again and conducted with RNase I for 30 min. The cells treated with PI staining at 4°C for 30 min were then measured using a BD FACS caliber.

Apoptosis Analysis

An Annexin V-FITC/PI apoptosis detection kit was used to measure apoptosis rate. Cells were seeded into 6-well plates and exposed to the experimental drug for 48 h. A BD FACS caliber was used to detect cell apoptosis using the manufacturer's instructions, and the BD CellQuest Pro software was used for analysis.

Animal Tumor Model

BALB/c nude female mice (5–6 weeks old) raised in a specific animal facility were used to construct a xenograft model. HCC1937-FR cells (1×10^7) suspended in 0.2 ml of PBS were inoculated subcutaneously into the backs of the nude mice. Mouse xenograft models were randomly divided into 4 groups and treated for 21 days: fluzoparib (25 mg/kg/bid), chidamide (5 mg/kg/bw), combined (fluzoparib 25 mg/kg/bid + chidamide 5 mg/kg/bw), and controls without any drug

treatment. Xenograft weight and size were measured every 3 days. Tumor volume was calculated according to the formula: $V = (\text{length} \times \text{width}^2)/2$. All animal experiments conformed to the requirements of our institutional ethics committee.

Western Blotting

Cells were treated with the experimental drugs for 48 h, after which their cytoplasm and nuclear protein was extracted (Covin Bio., Beijing, China). Equal amounts of protein, processed using 12% SDS-PAGE (Covin Bio., Beijing, China), were transferred to the PVDF membrane. The membrane, after blocking with 5% skim milk for 2 h, was incubated with a primary antibody at 4°C overnight. After rewarming the next day, the membrane was incubated with a secondary antibody at 37°C for 1 h. The Tanon 2500 chemiluminescence imaging system (Tanon, China) was used to detect the membranes. Further density and quantitative analyses were performed using Image J software.

Cell Transfection

Si-RAD51, si-MRE11, and si-NC vectors for cell transfection were synthesized by Biological Company GenePharma (Shanghai, China). Fluzoparib-resistant cells were cultured in 6-well plastic plates until they reached 80% confluence. Transfection was performed using Lipofectamine 3000 as instructed by the manufacturer.

Quantitative Real-Time Polymerase Chain Reaction

Intracellular mRNA was extracted using the AxyPrep mRNA Small Preparation Kit. cDNA was created *via* reverse transcription using HiScript III RT SuperMix for qPCR(+Gdn wiper). Reverse transcription was performed at 37°C for 15 min and 85°C for 5 s. Quantitative RT-PCR was performed using the ChamQ Universal SYBR qPCR Master Mix (Vazyme, Nanjing, China). Response conditions were as follows: 3 min at 95°C and then 10 s at 95°C for 40 cycles and 3 min at 95°C. mRNA relative expression levels were calculated using the $2^{-\Delta\Delta C_t}$ method. The primers are listed in **Table 1**.

Statistical Analysis

Statistical analyses utilized the IBM SPSS 23.0 software (Armonk, NY, USA). Data statistics were expressed as mean \pm SD. One-way analysis of variance (ANOVA) was used to measure statistically significant differences between the different experimental groups. $p < 0.05$ was considered statistically significant.

RESULTS

HCC1937-FR and MDA-MB-468-FR Fluzoparib Resistance

To evaluate the cytotoxicity of fluzoparib on parental and drug-resistant cell lines, MTT assays were performed to test cell viability after exposure to various concentrations of fluzoparib for 48 h. As shown in **Figure 1A**, with increased fluzoparib concentrations, the growth of parental and drug-resistant cells was significantly reduced and the cell viability of drug-resistant

TABLE 1 | Primers in this study.

	Sequence (5'-3')	Usage
RAD51F	CAACACAGACCACAGACCC	qRT-PCR
RAD51R	AGAAGCATCCGCAGAAACCT	qRT-PCR
MRE11F	TCAGATCTCAGTCAGAGGAGTC	qRT-PCR
MRE11R	AGCCATCTGTTCTGCTAAATCT	qRT-PCR
GAPDHf	ACCACAGTCCATGCCATCAC	qRT-PCR
GAPDHR	TCCACCACCCTGTTGCTGTA	qRT-PCR
Si-RAD51	GCCCUUUAACAGAACAGACUTT AGUCUGUUCUGUAAAGGGCTT	Knockdown
Si-MRE11	GGCCUGUCCAGUUUGAAAUUTT AUUUCAAACUGGACAGGCCTT	Knockdown
NC sense	UUCUCCGAACGUGUCACGUTT	Knockdown
NC antisense	ACGUGACACGUUCGGAGAATT	Knockdown

cell lines was significantly higher than that of parental cell lines. The mean IC₅₀ values of fluzoparib for HCC1937, MDA-MB-468, HCC1937-FR, and MDA-MB-468-FR cells were 6, 15, 60, and 80 µg/ml, respectively. The resistance indices of HCC1937-FR and MDA-MB-468-FR were 10 and 5.33, respectively.

Identification and Biological Function Analysis of DEGs in Drug-Resistant Cells

As shown in the volcano plot (**Figure 1B**), a total of 616 DEGs were developed using high-throughput sequencing, including 393 DEG encoding proteins. When these DEG encoding proteins were uploaded to the STRING database for enrichment analysis, as shown in **Figure 1C**, 95 biological process terms were returned, of which 10 involved DNA damage repair, DNA repair, cellular response to DNA damage, double-strand break repair, double-strand break repair *via* homologous recombination, regulation of response to DNA damage stimulus, regulation of DNA repair, regulation of double-strand break repair, DNA synthesis involved in DNA repair, DNA double-strand break processing, and double-strand break repair *via* nonhomologous end joining. A total of 37 DEGs identified by the enrichment analysis terms were related to DNA damage repair.

Identification of Hub Drug Resistance Genes

The 37 DEGs involved in DNA damage repair were uploaded to the STRING database to analyze their protein–protein interaction network. Visual analysis was performed using Cytoscape. The top 6 genes with the highest gene association (degree ≥ 14) were defined as hub drug resistance genes. As shown in **Figure 1D**, 6 hub drug resistance genes were identified, including RAD51, MRE11, POLA1, RAD54L, RFC4, and MCM10. RAD51 and MRE11 were highly expressed in drug-resistant cells, while POLA1, RAD54L, RFC4, and MCM10 had lower levels of expression (**Figure 1E**). RAD51 and MRE11 were therefore selected for subsequent analysis. As shown in **Figure 1F**, HCC1937-FR and MDA-MB-468-FR had higher levels of RAD51 and MRE11 protein expression than parental controls.

Determine the Optimal Dosage of Chidamide

To assess the cytotoxicity of chidamide on parental and drug-resistant cell lines, cell viability was measured using MTT assays after exposure to various concentrations of chidamide for 48 h.

As shown in **Figure 2A**, the survival rate of both parental and drug-resistant tumor cells gradually decreased with increased concentrations of chidamide. Results demonstrated that the inhibitory effects of chidamide on HCC1937 were better than on HCC1937-FR at a chidamide dose of ≥ 3 µg/ml, while at a dose ≥ 6 µg/ml, its inhibitory effect on MDA-MB-468 was better than on MDA-MB-468-FR. Doses of 3 and 6 µg/ml were therefore selected as subsequent experimental concentrations for HCC1937-FR and MDA-MB-468-FR, as at this concentration chidamide had little effect on their cell viability (cell viability was 85.9% and 85.2%, respectively).

Chidamide Effectively Reverses the Fluzoparib-Resistance of Drug-Resistant Cells

To further evaluate the cytotoxicity of chidamide and fluzoparib on HCC1937-FR and MDA-MB-468-FR, cell viability was again detected using MTT assays after treatment with 3 or 6 µg/ml of chidamide combined with different concentrations of fluzoparib. As shown in **Figure 2B**, chidamide combined with fluzoparib significantly inhibited the proliferation of HCC1937-FR and MDA-MB-468-FR. After statistical analysis of tumor drug concentration-survival rate using SPSS software, the IC₅₀ of HCC1937-FR to fluzoparib decreased from 60 to 9.6 µg/ml, while the IC₅₀ of MDA-MB-468-FR to fluzoparib dropped from 80 to 20 µg/ml. The combined index of chidamide and fluzoparib was calculated using Compusyn software to determine if the combined effects of the two drugs had a coordinating effect. As shown in **Tables 2, 3**, 3 µg/ml chidamide combined with ≥ 3.125 µg/ml fluzoparib had a good synergistic effect on the inhibition of HCC1937-FR cell proliferation, and the proliferation of MDA-MB-468-FR cells was effectively inhibited by ≥ 6 µg/ml chidamide combined with 12.5 µg/ml fluzoparib.

The Ability of Drug-Resistant Cells to Migrate and Invade Was Reduced

The migration ability of parental and drug-resistant cells and the effect of fluzoparib and chidamide on drug-resistant cell migration were measured using wound-healing assays. As shown in **Figures 2C, D**, the migration rates of the parental cells (HCC1937 and MDA-MB-468) were $47.98\% \pm 2.51\%$ and $27.30\% \pm 2.08\%$, compared with $67.64\% \pm 3.10\%$ and $48.17\% \pm 2.98\%$ of the

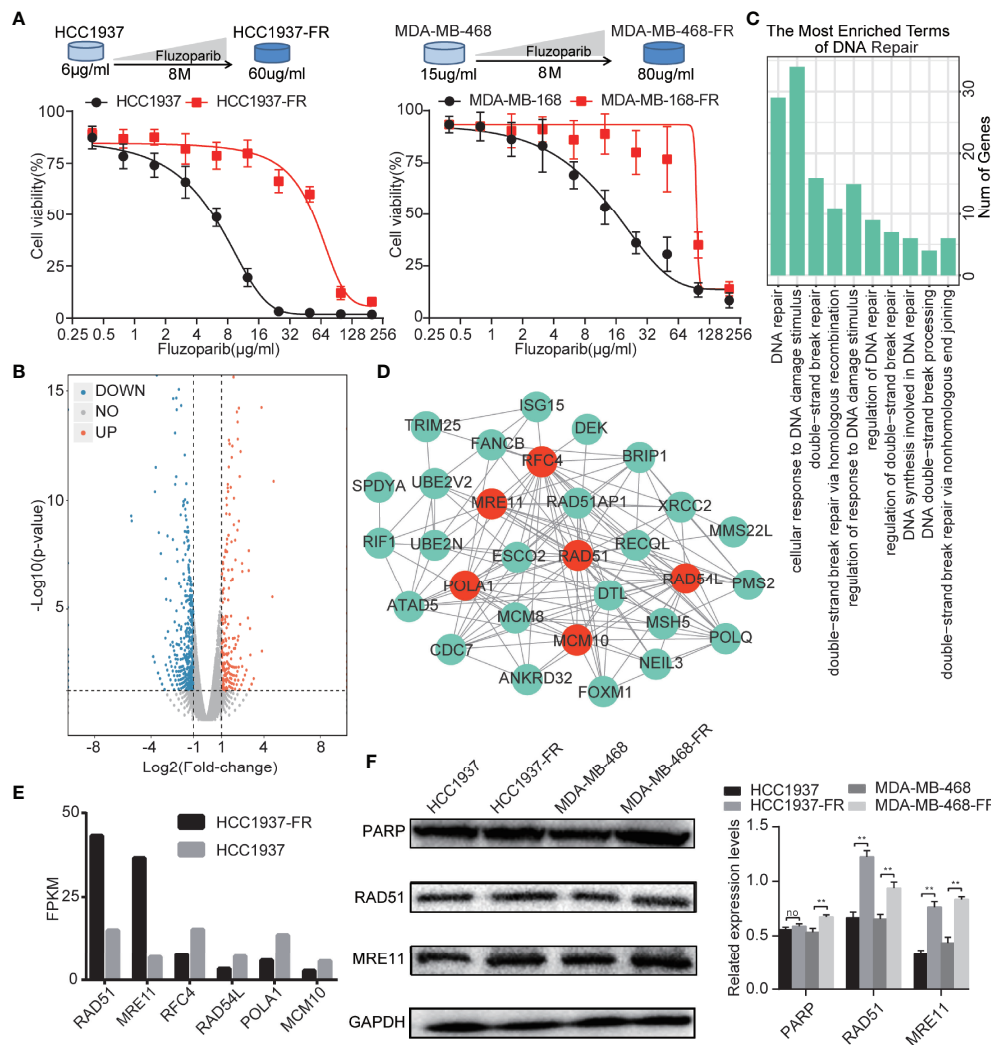


FIGURE 1 | Generation of TNBC cells with acquired resistance to fluzoparib and the identification of key drug resistance genes. **(A)** Schematic plot of the construction of the fluzoparib-resistant HCC1937 and MDA-MB-468 cell lines. Dose-response curves of parental and fluzoparib-resistant HCC1937 and MDA-MB-468 cells treated with different concentrations of fluzoparib for 48 h. **(B)** Volcano plot of the differential gene analysis of parental and fluzoparib-resistant HCC1937 cells via gene sequencing. Red dots represent upregulated genes, and blue dots represent downregulated genes. **(C)** Enrichment analysis related to DNA damage repair. **(D)** Construction of a protein-protein interaction network. The hub drug resistance genes represented by red dots had the highest gene association in the network. **(E)** Gene expression levels of hub drug resistance genes in parental and fluzoparib-resistant HCC1937 cells. **(F)** Immunoblots of RAD51, MRE11, and PARP in parental and fluzoparib-resistant cells. Data are written as mean \pm SD of three independent experiments. ** $p < 0.01$ compared with the parental cell group. No, no significance.

drug-resistant cells (HCC1937-FR and MDA-MB-468-FR), respectively ($p < 0.01$). After 24 h of treatment with fluzoparib and chidamide alone or in combination, the migration rate of HCC1937-FR cells was $46.88\% \pm 3.14\%$ in the fluzoparib single agent, $51.94\% \pm 2.05\%$ in the chidamide single agent, and $37.39\% \pm 2.34\%$ in the combined group. Also, for MDA-MB-468-FR, the migration rate of cancer cells was $38.70\% \pm 3.15\%$ in the fluzoparib single agent, $40.59\% \pm 2.34\%$ in the chidamide single agent, and $30.32\% \pm 2.55\%$ in the combined group. Fluzoparib combined with chidamide significantly inhibited the migration of HCC1937-FR and MDA-MB-468-FR cells ($p < 0.01$).

Similar observations were seen in the Transwell invasion assay. As shown in **Figures 2E, F**, compared with parental cells,

HCC1937-FR and MDA-MB-468-FR cells significantly increased the number of cells that passed through the Transwell chamber, representing significantly enhanced invasiveness ($p < 0.01$). The numbers of invasive cells in the fluzoparib and chidamide groups were significantly decreased compared with controls, and the inhibitory effects of fluzoparib in combination with chidamide were more significant than the single drug groups ($p < 0.01$).

The Antiapoptotic Ability of Drug-Resistant Cells Is Weakened by Antitumor Treatments

Flow cytometry was used to measure the apoptosis rate and cell cycle of parental and drug-resistant cells. Results are shown in

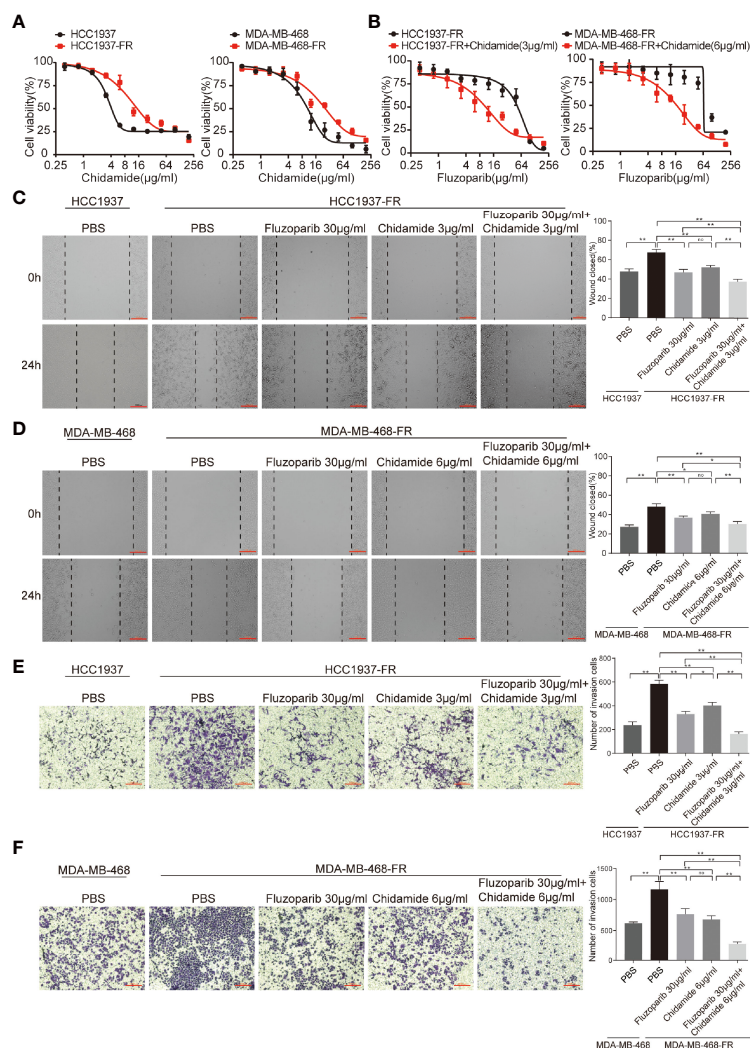


FIGURE 2 | Effects of chidamide and fluzoparib on cell migration. **(A)** Dose-response curves of parental and fluzoparib-resistant cells treated with different concentrations of chidamide for 48 h. **(B)** Dose-response curves of parental and fluzoparib-resistant cells treated with different concentrations of fluzoparib combined with 3 or 6 µg/ml of chidamide. **(C, D)** Wound-healing assay to assess the effects of fluzoparib and chidamide on parental and fluzoparib-resistant HCC1937 and MDA-MB-468 cell migration ability. **(E, F)** Transwell invasion assays assessed the effects of fluzoparib and chidamide on parental and fluzoparib-resistant HCC1937 and MDA-MB-468 invasiveness. Data represent the mean ± SD of three independent experiments. * $p < 0.05$; ** $p < 0.01$. No, no significance.

Figures 3A, B. The apoptosis rates of HCC1937 and MDA-MB-468 cells were 9.51% and 3.29%, respectively, while those of HCC1937-FR and MDA-MB-468-FR cells were 5.7% and 3.81%,

respectively. The antiapoptosis rate of HCC1937-FR cells was significantly higher than that of parental cells ($p < 0.05$), but there was no significant difference in the apoptosis rates of MDA-MB-468-FR and MDA-MB-468. The apoptosis rates of

TABLE 2 | The combination index of different doses of fluzoparib and 3 µg/ml chidamide: HCC1937-FR.

Chidamide (µg/ml)	Fluzoparib (µg/ml)	CI
3	1.5625	1.11351
3	3.125	0.73161
3	6.25	0.55963
3	12.5	0.47928
3	25	0.76496
3	50	0.51067
3	100	0.56623

TABLE 3 | The combination index of different doses of fluzoparib and 6 µg/ml chidamide: MDA-MB-468-FR.

Chidamide (µg/ml)	Fluzoparib (µg/ml)	CI
6	6.25	4.12292
6	12.5	0.50483
6	25	0.60663
6	50	0.26538
6	100	0.18174
6	200	0.10877

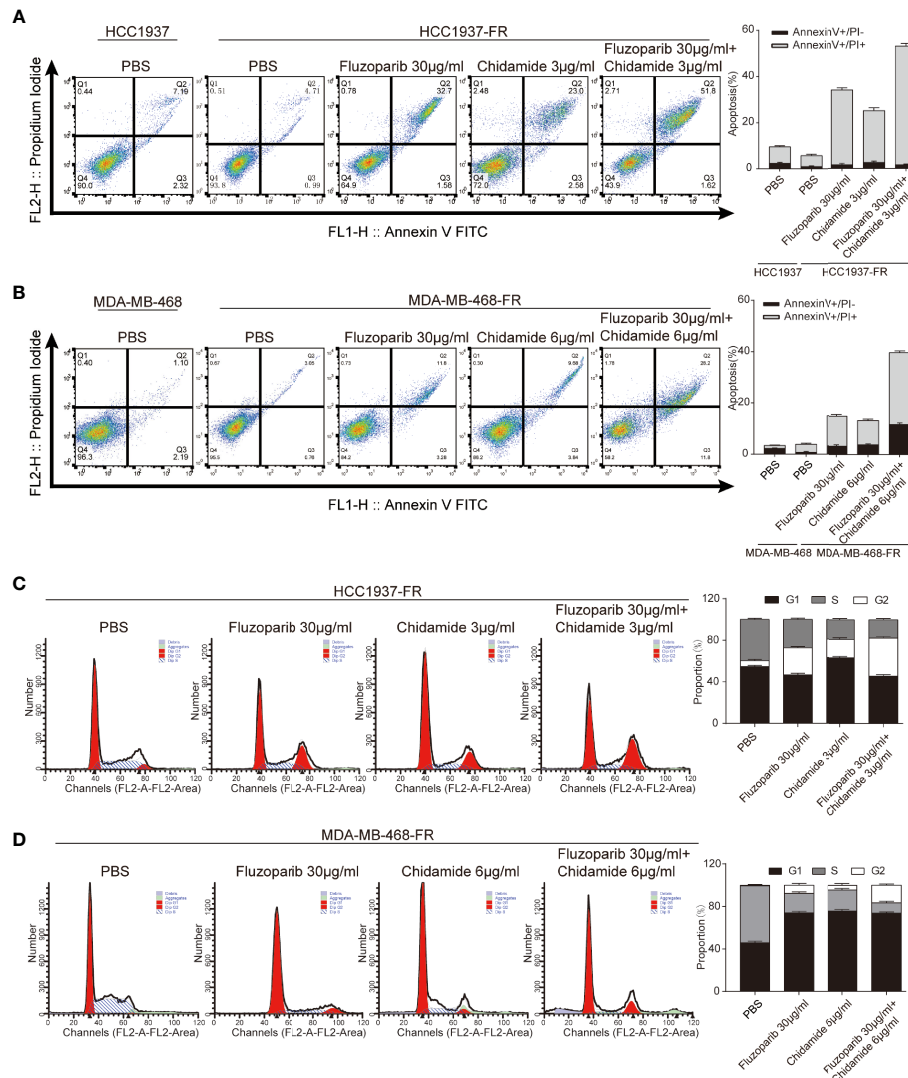


FIGURE 3 | Effects of chidamide and fluzoparib on cell cycle and apoptosis. **(A, B)** Cell apoptosis was detected using Annexin V-FITC/PI double staining followed by flow cytometry for parental and fluzoparib-resistant HCC1937 and MDA-MB-468 cells after incubation with PBS, fluzoparib, chidamide, or a combination treatment (fluzoparib + chidamide) for 24 h. **(C, D)** Cell cycle analysis using PI staining and following flow cytometry for HCC1937-FR and MDA-MB-468-FR cells after incubation with PBS, fluzoparib, chidamide, or a combination treatment (fluzoparib + chidamide) for 24 h. Data represent the mean \pm SD of three independent experiments.

HCC1937-FR cells after fluzoparib single agent, chidamide single agent, and combination exposure were 34.28%, 25.58%, and 53.42%, respectively. The apoptosis rates in the single drug groups were significantly higher than that of the control group ($p < 0.05$). The apoptosis rate of the combined group was also significantly higher than those of the single drug cell groups ($p < 0.05$). The apoptosis rates of MDA-MB-468-FR after fluzoparib single agent, chidamide single agent, and combination exposure were 15.08%, 13.52%, and 40%, respectively. These results were also statistically significant ($p < 0.05$). The cell cycle distributions of HCC1937-FR and MDA-MB-468-FR cells after drug treatment are shown in **Figures 3C, D**. Single drug groups

prolonged the G2/M phase of the drug-resistant cells, while the combination group exerted a greater effect at the G2/M phase ($p < 0.05$).

In Vivo Anticancer Effects of Fluzoparib and Chidamide in HCC1937-FR Breast Cancer Xenograft Models

As shown in **Figure 4**, while both fluzoparib and chidamide inhibited HCC1937-FR breast cancer growth ($p < 0.05$), the combination of these drugs more significantly inhibited neoplasm growth ($p < 0.05$). No general toxicity was observed as no weight loss occurred in any treatment group ($p < 0.05$).

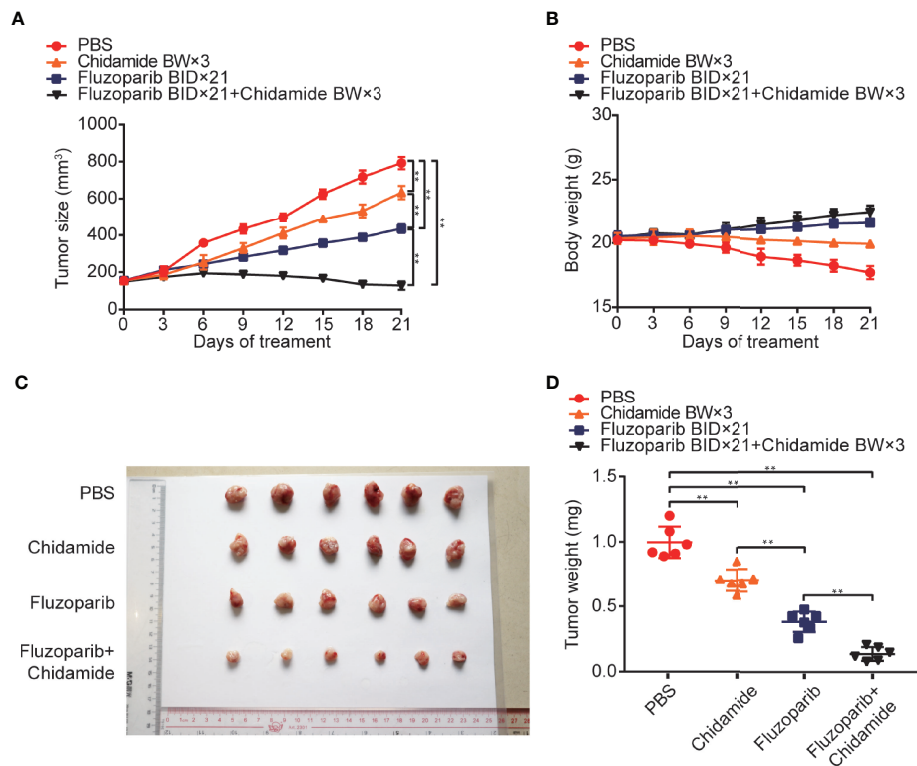


FIGURE 4 | *In vivo* anticancer effects of fluzoparib and chidamide in fluzoparib-resistant HCC1937 breast cancer xenograft models. Randomly grouped nude mice were treated with PBS, fluzoparib (25 mg/kg/bid), chidamide (5 mg/kg/bw), or a combination treatment (fluzoparib 25 mg/kg/bid + chidamide 5 mg/kg/bw) for 21 days. **(A, B)** Tumor growth ratio curve and body weight change every 3 days after the onset of treatment. **(C, D)** Photographs of the exfoliated tumors and weight obtained on day 21 of treatment. ** $p < 0.01$.

Molecular Mechanism of Chidamide Reversing Fluzoparib Resistance

As shown in **Figure 5**, fluzoparib significantly reduced PARP protein expression ($p < 0.05$), while chidamide alone or combined with fluzoparib did not affect PARP expression. The combined effect of the two drugs significantly reduced the expression of the RAD51 and MRE11 proteins in drug-resistant cells. The results of cycle and apoptosis assays showed that the drugs block the cell cycle in the G2/M phase and induce apoptosis. These results suggest that fluzoparib combined with chidamide significantly increased the expression levels of P-CDK1 and cleaved Caspase9.

Genetic Suppression of RAD51 and MRE11 Enhances the Sensitivity of Drug-Resistant Cells to Fluzoparib

Compared with negative controls (NC), the expression of the mRNA and protein of RAD51 and MRE11 were significantly decreased (**Figures 6A, B**). To further study the response of transfected cells to fluzoparib, an MTT assay was used to detect the cell viability of HCC1937-FR and MDA-MB-468-FR cells transfected for 24 h. As shown in **Figure 6C**, the proliferation of transfected cells was significantly inhibited compared with the control group with increased drug concentrations. These data suggest that knockdown of the RAD51 and MRE11 genes could

enhance the sensitivity of HCC1937-FR and MDA-MB-468-FR cells to fluzoparib.

DISCUSSION

The increasing incidence of breast cancer in women is a major women's health problem. First-line treatment options for breast cancer include chemotherapy, hormones, and targeted therapy (37). Immunotherapy drugs have also recently shown promise (38). TNBC, which accounts for approximately 15% of all breast cancers, is insensitive to endocrine and molecular-targeted drugs (39). Precisely targeted therapeutic PARPi have achieved promising results in clinical trials by inhibiting PARP enzyme function and hindering the possibility of DNA repair in tumor cells, thereby accelerating tumor cell death (40). A series of PARP-targeted drugs have been developed, including olaparib, talazoparib, and fluzoparib.

OlympiAD, a randomized, open-label, and phase III trial, evaluated olaparib monotherapy versus a standard chemotherapy regimen (41), reporting that olaparib prolonged PFS from 4.2 to 7.0 months, significantly reduced the risk of disease progression by 42% and was well tolerated (42). EMBRACA, an open-label phase III trial, reported that talazoparib significantly prolonged PFS and

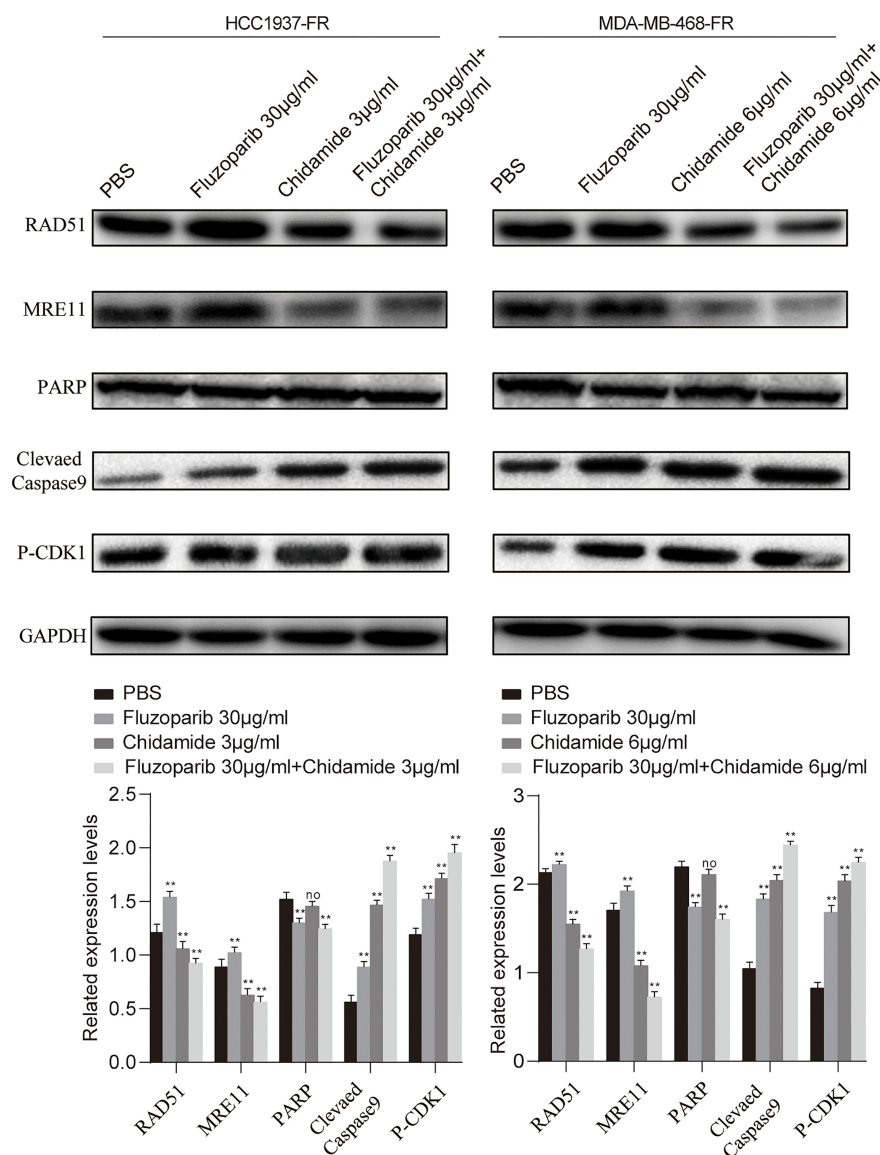


FIGURE 5 | Molecular mechanism studies of fluzoparib-resistant HCC1937 and MDA-MB-468 cells after treatment with PBS, fluzoparib, chidamide, or a combination treatment (fluzoparib + chidamide). Immunoblot analysis of RAD51, MRE11, PARP, BCL-XL, and P-CDK1 and quantitative analysis. Data represent the mean \pm SD of three independent experiments. ** $p < 0.05$ compared with the PBS group. No, no significance. ** $p < 0.01$.

reduced the risk of disease progression, and that the objective response rate of 62.6% in the talazoparib group was more than double that of the chemotherapy group (27.2%) ($p < 0.0001$) (43). Fluzoparib, a synthetic derivative based on olaparib, exhibits antitumor activity against breast cancer as a single agent in a phase 1 study in advanced solid tumors and has a significant antitumor efficacy in combination with apatinib or apatinib and paclitaxel, without extra toxicity (44). Chemotherapy resistance reflects the strong adaptability of tumor cells, so it is important to further explore how to avoid PARPi resistance and develop promising therapeutic strategies. Given the excellent antitumor effects of chidamide against DNA damage repair, we performed

this study to determine if chidamide could reverse fluzoparib resistance.

In this study, we constructed the fluzoparib-resistant triple-negative breast cancer cell lines HCC1937-FR and MDA-MB-468-FR, and further studied the changes in the biological functions of these resistant cells. *In vitro* experiments confirmed that the proliferation, migration, and invasiveness of drug-resistant cells were enhanced compared with parental cells, and that their degree of virility was also increased. Similar studies showed that the migration ability of HCC1937 cells resistant to talazoparib was also enhanced (45). We further investigated the effects of chidamide and fluzoparib on drug-resistant cell lines

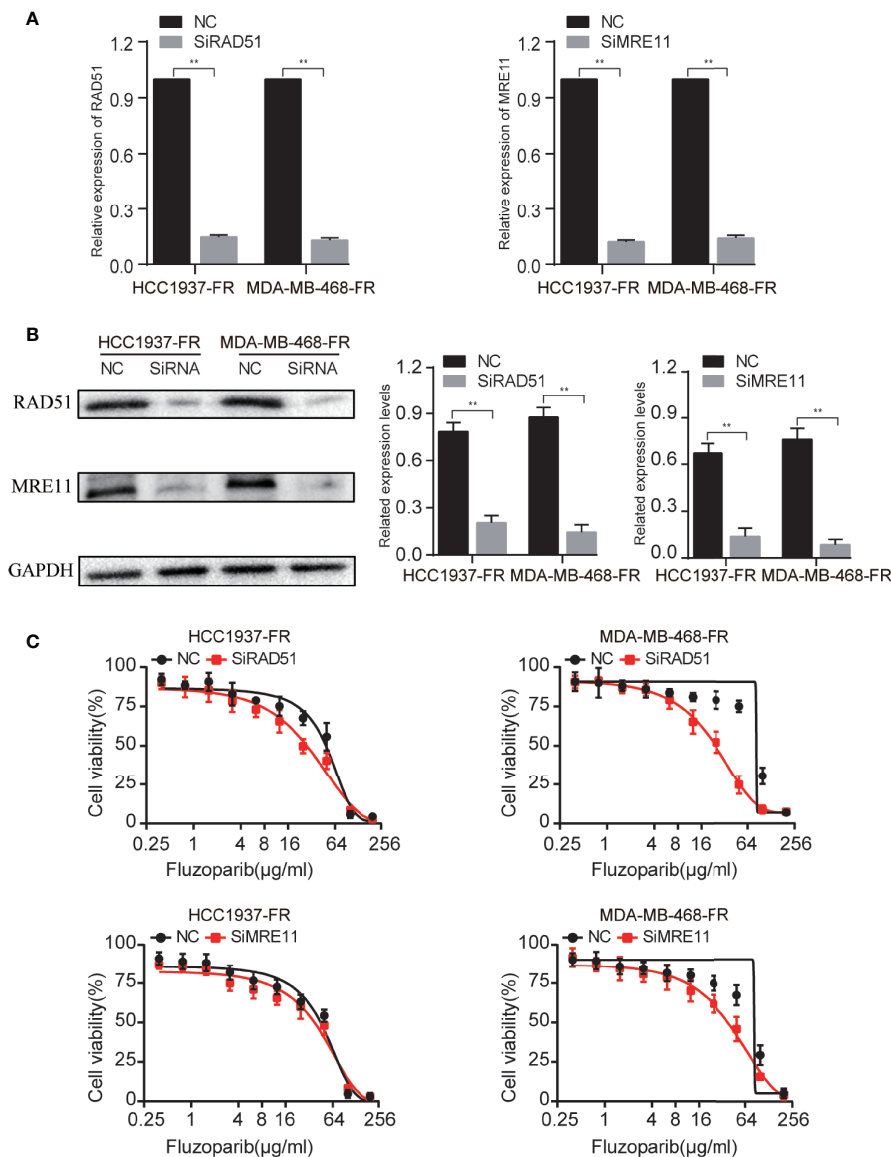


FIGURE 6 | Genetic suppression of RAD51 and MRE11 enhances the sensitivity of drug-resistant cells to fluzoparib. **(A)** qRT-PCR was used to detect RAD51 and MRE11 after transfection with si-RAD51, si-MRE11, and NC in fluzoparib-resistant cells. **(B)** Immunoblots of RAD51 and MRE11 in fluzoparib-resistant cells transfected with si-RAD51, si-MRE11, and NC. **(C)** Dose response of fluzoparib-resistant cells treated with fluzoparib after transfection with si-RAD51, si-MRE11, and NC. NC, negative control. ** $p < 0.01$.

and xenograft models. MTT and flow cytometry results showed that chidamide combined with fluzoparib could significantly inhibit the proliferation of drug-resistant cells and reduce the IC_{50} of fluzoparib. In addition, both chidamide and fluzoparib exhibited certain inhibitory effects on the migration and invasiveness of the drug-resistant cells and, more significantly, the inhibitory effects of the combination of these two drugs were more obvious. Although previous studies have shown that PARPi and HDACi can arrest triple-negative breast cancer cells in the G2/M phase, no works have evaluated the effect of PARPi and HDACi on the drug-resistant cell cycle (32). In the

present study, cycle results showed that all single drugs could arrest drug-resistant cells in the G2/M phase and that the combined group had a more significant effect. Xenograft model results demonstrated that the antitumor treatment effects of the combination groups were greater than any other single drug group, which matched our *in vitro* findings. The nude mice in all treatment groups also did not show significant weight loss.

We performed transcriptome sequencing on drug-resistant and parental cells, identifying DEGs using differential analysis and selecting hub drug-resistant genes related to DNA damage repair. To further explore the potential molecular mechanisms and

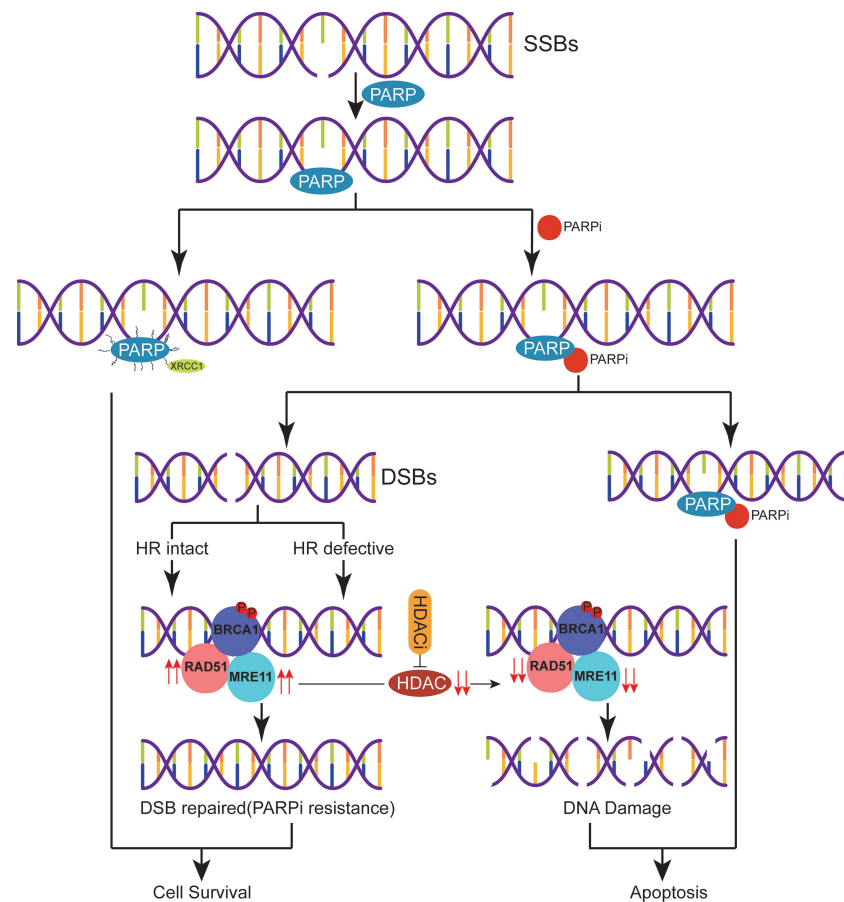


FIGURE 7 | A proposed schematic of PARPi resistance in triple-negative breast cancer. After DNA single-strand breaks (SSBs) occur, PARP binds with the damaged site and recruits related DNA repair proteins to repair the damaged DNA. PARPi can be combined with PARP to inhibit SSB repair leading to apoptosis or process DNA SSBs and initiate homologous recombination (HR) repair. Due to the relative overexpression of the HR repair-related proteins RAD51 and MRE11 in the setting of drug resistance or reduced sensitivity to PARPi, HDACi perpetuates DNA damage by regulating the expression of RAD51 and MRE11, eventually leading to cell apoptosis.

signaling pathways of chidamide reversal of fluzoparib resistance, we used Western blotting (WB) to evaluate molecular changes after drug exposure. We found that both the gene and protein levels of RAD51 and MRE1 were highly expressed in drug-resistant cells, and that their protein levels were significantly downregulated after treatment with chidamide combined with fluzoparib. Min et al. (33) confirmed that HDACi combined with olaparib could downregulate the expression of RAD51 and MRE11 in TNBC. Furthermore, by knocking out the RAD51 and MRE11 genes in fluzoparib-resistant cell lines, transfected cells had enhanced sensitivity to fluzoparib-treated cells. However, the inhibitory effects of RAD51 and MRE11 gene suppression on the proliferation of drug-resistant cell lines were not as significant as that of chidamide. The reason may be that HDACi may affect multiple DNA damage repair proteins at the same time or impact the interactions between HDAC and DNA damage repair proteins. These phenomena suggest that RAD51 and MRE11, as key drug resistance genes, are significantly related to fluzoparib resistance in TNBC cells. RAD51, a key regulator of DNA fidelity, is involved in cell cycle regulation, repair of homologous

recombination, and replication stress response, which are essential for the stability of the genome (46). Human RAD51 has DNA-dependent ATPase activity and performs DNA repair and recombination through homologous pairing and strand exchange between DNA molecules (47). In breast cancer, high expression of RAD51 has been associated with cancer cell metastasis, tumor chemotherapy resistance, and tumor radiotherapy insensitivity (48). MRE11, a nuclear protein, participates in homologous recombination and telomere length maintenance, and has 3' to 5' exonuclease and endonuclease activity (49). MRE11 can form an MRX/MRN complex with RAD50 homologues, which depends on the activity of nucleases to participate in DNA homologous recombination repair (50). Studies have shown that the functional defects and low expression of MRX/MRN and its components were associated with an increased tendency towards sustained DNA damage, cell instability, and malignant transformation and can also affect the sensitivity of cancer cells to chemotherapy and radiotherapy (51). HDACi could downregulate DNA damage repair proteins. The potential mechanism for this may be that HDACi induces

proteasomal deterioration of homologous recombination repair-related proteins, or that HDACi reduces E2F1 binding to the promoters of BRCA1, CHK1, and RAD51, thereby reducing the transcription of these genes (40, 52). The elevated levels of the key regulatory proteins P-CDK1 and cleaved Caspase9 again confirm that the combination of fluzoparib and chidamide can block the cell cycle in the G2/M phase and promote the apoptosis of drug-resistant cells. The present work suggests that the drug resistance or decreased sensitivity of TNBC cells to PARPi is caused by the relative overexpression of the DNA damage repair-related proteins RAD51 and MRE11, while HDACi caused persistent DNA damage by downregulating RAD51 and MRE11, eventually leading to cell apoptosis. As a result, we have proposed a model depicting the molecular mechanisms of chidamide reversal of fluzoparib resistance (Figure 7). There are many kinds of HDAC and PARP inhibitors that are currently available, so the application of these two drugs against drug resistance still requires further study.

In conclusion, this is the first study to provide evidence of PARPi resistance reversal by HDACi *in vivo* and *in vitro* and to propose the molecular mechanism behind the reversal of resistance, providing guidance for breast cancer treatment.

DATA AVAILABILITY STATEMENT

The original contributions presented in the study are included in the article/Supplementary Materials. Further inquiries can be directed to the corresponding author.

REFERENCES

- Sung H, Ferlay J, Siegel RL, Laversanne M, Soerjomataram I, Jemal A, et al. Global Cancer Statistics 2020: GLOBOCAN Estimates of Incidence and Mortality Worldwide for 36 Cancers in 185 Countries. *CA Cancer J Clin* (2021) 71(3):209–49. doi: 10.3322/caac.21660
- Siegel RL, Miller KD, Jemal A. Cancer Statistics, 2019. *CA Cancer J Clin* (2019) 69(1):7–34. doi: 10.3322/caac.21551
- Yin L, Duan JJ, Bian XW, Yu SC. Triple-Negative Breast Cancer Molecular Subtyping and Treatment Progress. *Breast Cancer Res* (2020) 22(1):61. doi: 10.1186/s13058-020-01296-5
- Golan T, Hammel P, Reni M, Van Cutsem E, Macarulla T, Hall MJ, et al. Maintenance Olaparib for Germline BRCA-Mutated Metastatic Pancreatic Cancer. *N Engl J Med* (2019) 381(4):317–27. doi: 10.1056/NEJMoa1903387
- Lord CJ, Ashworth A. Brca1/2 Revisited. *Nat Rev Cancer* (2016) 16(2):110–20. doi: 10.1038/nrc.2015.21
- Lord CJ, Ashworth A. PARP Inhibitors: Synthetic Lethality in the Clinic. *Science* (2017) 355(6330):1152–8. doi: 10.1126/science.aam7344
- Mateo J, Lord CJ, Serra V, Tutt A, Balmaña J, Castroviejo-Bermejo M, et al. A Decade of Clinical Development of PARP Inhibitors in Perspective. *Ann Oncol* (2019) 30(9):1437–47. doi: 10.1093/annonc/mdz192
- D'Andrea AD. Mechanisms of PARP Inhibitor Sensitivity and Resistance. *DNA Repair (Amst)* (2018) 71:172–6. doi: 10.1016/j.dnarep.2018.08.021
- Noordermeer SM, van Attikum H. PARP Inhibitor Resistance: A Tug-of-War in BRCA-Mutated Cells. *Trends Cell Biol* (2019) 29(10):820–34. doi: 10.1016/j.tcb.2019.07.008
- Pishvaian MJ, Biankin AV, Bailey P, Chang DK, Laheru D, Wolfgang CL, et al. BRCA2 Secondary Mutation-Mediated Resistance to Platinum and PARP Inhibitor-Based Therapy in Pancreatic Cancer. *Br J Cancer* (2017) 116(8):1021–6. doi: 10.1038/bjc.2017.40
- Lheureux S, Bruce JP, Burnier JV, Karakasis K, Shaw PA, Clarke BA, et al. Somatic BRCA1/2 Recovery as a Resistance Mechanism After Exceptional

ETHICS STATEMENT

The animal study was reviewed and approved by the Ethics Committee of the First Affiliated Hospital of Henan University of Science and Technology.

AUTHOR CONTRIBUTIONS

Conception and design: XW and XL. Data acquisition and analysis: ZW, JL, and XY. Writing original draft: XL. Writing review and editing: YW, LW, and YL. Data visualization: YL and XL. Supervision: XW and YL. The authors read and approved the final manuscript.

FUNDING

This work was supported in part by Medical Science and Technology project grants of Henan Province (LHGJ20200576).

SUPPLEMENTARY MATERIAL

The Supplementary Material for this article can be found online at: <https://www.frontiersin.org/articles/10.3389/fonc.2022.819714/full#supplementary-material>

- Response to Poly (ADP-Ribose) Polymerase Inhibition. *J Clin Oncol* (2017) 35(11):1240–9. doi: 10.1200/jco.2016.71.3677
- Kondrashova O, Nguyen M, Shield-Artin K, Tinker AV, Teng NNH, Harrell MI, et al. Secondary Somatic Mutations Restoring RAD51C and RAD51D Associated With Acquired Resistance to the PARP Inhibitor Rucaparib in High-Grade Ovarian Carcinoma. *Cancer Discovery* (2017) 7(9):984–98. doi: 10.1158/2159-8290.cd-17-0419
- Rondinelli B, Gogola E, Yücel H, Duarte AA, van de Ven M, van der Sluijs R, et al. EZH2 Promotes Degradation of Stalled Replication Forks by Recruiting MUS81 Through Histone H3 Trimethylation. *Nat Cell Biol* (2017) 19(11):1371–8. doi: 10.1038/ncb3626
- Meghani K, Fuchs W, Detappe A, Drané P, Gogola E, Rottenberg S, et al. Multifaceted Impact of MicroRNA 493-5p on Genome-Stabilizing Pathways Induces Platinum and PARP Inhibitor Resistance in BRCA2-Mutated Carcinomas. *Cell Rep* (2018) 23(1):100–11. doi: 10.1016/j.celrep.2018.03.038
- Ray Chaudhuri A, Callen E, Ding X, Gogola E, Duarte AA, Lee JE, et al. Replication Fork Stability Confers Chemoresistance in BRCA-Deficient Cells. *Nature* (2016) 535(7612):382–7. doi: 10.1038/nature18325
- Pettitt SJ, Krastev DB, Brandsma I, Dréan A, Song F, Aleksandrov R, et al. Genome-Wide and High-Density CRISPR-Cas9 Screens Identify Point Mutations in PARP1 Causing PARP Inhibitor Resistance. *Nat Commun* (2018) 9(1):1849. doi: 10.1038/s41467-018-03917-2
- Gogola E, Duarte AA, de Ruiter JR, Wiegant WW, Schmid JA, de Bruijn R, et al. Selective Loss of PARG Restores Parylation and Counteracts PARP Inhibitor-Mediated Synthetic Lethality. *Cancer Cell* (2018) 33(6):1078–93.e1012. doi: 10.1016/j.ccell.2018.05.008
- Lawlor D, Martin P, Busschots S, Thery J, O'Leary JJ, Hennessy BT, et al. PARP Inhibitors as P-Glycoprotein Substrates. *J Pharm Sci* (2014) 103(6):1913–20. doi: 10.1002/jps.23952
- Patch AM, Christie EL, Etemadmoghadam D, Garsed DW, George J, Fereday S, et al. Whole-Genome Characterization of Chemoresistant Ovarian Cancer. *Nature* (2015) 521(7553):489–94. doi: 10.1038/nature14410

20. Choi YE, Meghani K, Brault ME, Leclerc L, He YJ, Day TA, et al. Platinum and PARP Inhibitor Resistance Due to Overexpression of Microrna-622 in BRCA1-Mutant Ovarian Cancer. *Cell Rep* (2016) 14(3):429–39. doi: 10.1016/j.celrep.2015.12.046
21. Eckschlagner T, Plch J, Stiborova M, Hrabeta J. Histone Deacetylase Inhibitors as Anticancer Drugs. *Int J Mol Sci* (2017) 18(7):1414. doi: 10.3390/ijms18071414
22. Eot-Houllier G, Fulcrand G, Magnaghi-Jaulin L, Jaulin C. Histone Deacetylase Inhibitors and Genomic Instability. *Cancer Lett* (2009) 274(2):169–76. doi: 10.1016/j.canlet.2008.06.005
23. Kim HJ, Bae SC. Histone Deacetylase Inhibitors: Molecular Mechanisms of Action and Clinical Trials as Anti-Cancer Drugs. *Am J Transl Res* (2011) 3(2):166–79.
24. Balliu M, Guandalini L, Romanelli MN, D'Amico M, Paoletti F. HDAC-Inhibitor (s)-8 Disrupts HDAC6-PP1 Complex Prompting A375 Melanoma Cell Growth Arrest and Apoptosis. *J Cell Mol Med* (2015) 19(1):143–54. doi: 10.1111/jcmm.12345
25. Jeong JW, Bae MK, Ahn MY, Kim SH, Sohn TK, Bae MH, et al. Regulation and Destabilization of HIF-1 α by ARD1-Mediated Acetylation. *Cell* (2002) 111(5):709–20. doi: 10.1016/s0092-8674(02)01085-1
26. Montgomery RL, Davis CA, Potthoff MJ, Haberland M, Fielitz J, Qi X, et al. Histone Deacetylases 1 and 2 Redundantly Regulate Cardiac Morphogenesis, Growth, and Contractility. *Genes Dev* (2007) 21(14):1790–802. doi: 10.1101/gad.1563807
27. Setiadi AF, Omilusik K, David MD, Seipp RP, Hartikainen J, Gopaul R, et al. Epigenetic Enhancement of Antigen Processing and Presentation Promotes Immune Recognition of Tumors. *Cancer Res* (2008) 68(23):9601–7. doi: 10.1158/0008-5472.can-07-5270
28. Kortenhorst MS, Wissing MD, Rodriguez R, Kachhap SK, Jans JJ, van der Groep P, et al. Analysis of the Genomic Response of Human Prostate Cancer Cells to Histone Deacetylase Inhibitors. *Epigenetics* (2013) 8(9):907–20. doi: 10.4161/epi.25574
29. Rooney MS, Shukla SA, Wu CJ, Getz G, Hacohen N. Molecular and Genetic Properties of Tumors Associated With Local Immune Cytolytic Activity. *Cell* (2015) 160(1–2):48–61. doi: 10.1016/j.cell.2014.12.033
30. Adimoolam S, Sirisawad M, Chen J, Thiemann P, Ford JM, Buggy JJ. HDAC Inhibitor PCI-24781 Decreases RAD51 Expression and Inhibits Homologous Recombination. *Proc Natl Acad Sci USA* (2007) 104(49):19482–7. doi: 10.1073/pnas.0707828104
31. Kachhap SK, Rosmus N, Collis SJ, Kortenhorst MS, Wissing MD, Hedayat M, et al. Downregulation of Homologous Recombination DNA Repair Genes by HDAC Inhibition in Prostate Cancer Is Mediated Through the E2F1 Transcription Factor. *PLoS One* (2010) 5(6):e11208. doi: 10.1371/journal.pone.0011208
32. Marijon H, Lee DH, Ding L, Sun H, Gery S, de Gramont A, et al. Co-Targeting Poly(ADP-Ribose) Polymerase (PARP) and Histone Deacetylase (HDAC) in Triple-Negative Breast Cancer: Higher Synergism in BRCA Mutated Cells. *BioMed Pharmacother* (2018) 99:543–51. doi: 10.1016/j.biopha.2018.01.045
33. Min A, Im SA, Kim DK, Song SH, Kim HJ, Lee KH, et al. Histone Deacetylase Inhibitor, Suberoylanilide Hydroxamic Acid (SAHA), Enhances Anti-Tumor Effects of the Poly (ADP-Ribose) Polymerase (PARP) Inhibitor Olaparib in Triple-Negative Breast Cancer Cells. *Breast Cancer Res* (2015) 17:33. doi: 10.1186/s13058-015-0534-y
34. Lee HS, Park SB, Kim SA, Kwon SK, Cha H, Lee DY, et al. A Novel HDAC Inhibitor, CG200745, Inhibits Pancreatic Cancer Cell Growth and Overcomes Gemcitabine Resistance. *Sci Rep* (2017) 7:41615. doi: 10.1038/srep41615
35. Huang X, Wang S, Lee CK, Yang X, Liu B. HDAC Inhibitor SNDX-275 Enhances Efficacy of Trastuzumab in ErbB2-Overexpressing Breast Cancer Cells and Exhibits Potential to Overcome Trastuzumab Resistance. *Cancer Lett* (2011) 307(1):72–9. doi: 10.1016/j.canlet.2011.03.019
36. Lee YJ, Won AJ, Lee J, Jung JH, Yoon S, Lee BM, et al. Molecular Mechanism of SAHA on Regulation of Autophagic Cell Death in Tamoxifen-Resistant MCF-7 Breast Cancer Cells. *Int J Med Sci* (2012) 9(10):881–93. doi: 10.7150/ijms.5011
37. Jayaraj R, Nayagam SG, Kar A, Sathyakumar S, Mohammed H, Smiti M, et al. Clinical Theragnostic Relationship Between Drug-Resistance Specific MiRNA Expressions, Chemotherapeutic Resistance, and Sensitivity in Breast Cancer: A Systematic Review and Meta-Analysis. *Cells* (2019) 8(10):1250. doi: 10.3390/cells8101250
38. O'Sullivan H, Collins D, O'Reilly S. Atezolizumab and Nab-Paclitaxel in Advanced Triple-Negative Breast Cancer. *N Engl J Med* (2019) 380(10):986. doi: 10.1056/NEJMc1900150
39. Shen M, Pan H, Chen Y, Xu YH, Yang W, Wu Z. A Review of Current Progress in Triple-Negative Breast Cancer Therapy. *Open Med (Wars)* (2020) 15(1):1143–9. doi: 10.1515/med-2020-0138
40. Xie C, Drenberg C, Edwards H, Caldwell JT, Chen W, Inaba H, et al. Panobinostat Enhances Cytarabine and Daunorubicin Sensitivities in AML Cells Through Suppressing the Expression of BRCA1, CHK1, and Rad51. *PLoS One* (2013) 8(11):e79106. doi: 10.1371/journal.pone.0079106
41. Robson M, Im SA, Senkus E, Xu B, Domchek SM, Masuda N, et al. Olaparib for Metastatic Breast Cancer in Patients With a Germline BRCA Mutation. *N Engl J Med* (2017) 377(6):523–33. doi: 10.1056/NEJMoa1706450
42. Robson ME, Tung N, Conte P, Im SA, Senkus E, Xu B, et al. Olympiad Final Overall Survival and Tolerability Results: Olaparib Versus Chemotherapy Treatment of Physician's Choice in Patients With a Germline BRCA Mutation and HER2-Negative Metastatic Breast Cancer. *Ann Oncol* (2019) 30(4):558–66. doi: 10.1093/annonc/mdz012
43. Litton JK, Rugo HS, Ettl J, Hurvitz SA, Gonçalves A, Lee KH, et al. Talazoparib in Patients With Advanced Breast Cancer and a Germline BRCA Mutation. *N Engl J Med* (2018) 379(8):753–63. doi: 10.1056/NEJMoa1802905
44. Wang L, Yang C, Xie C, Jiang J, Gao M, Fu L, et al. Pharmacologic Characterization of Fluzoparib, a Novel Poly(ADP-Ribose) Polymerase Inhibitor Undergoing Clinical Trials. *Cancer Sci* (2019) 110(3):1064–75. doi: 10.1111/cas.13947
45. Eskiler GG, Cecener G, Dikmen G, Egeli U, Tunca B. Talazoparib Loaded Solid Lipid Nanoparticles: Preparation, Characterization and Evaluation of the Therapeutic Efficacy. *In vitro Curr Drug Deliv* (2019) 16(6):511–29. doi: 10.2174/1567201816666190515105532
46. Bhat KP, Cortez D. RPA and RAD51: Fork Reversal, Fork Protection, and Genome Stability. *Nat Struct Mol Biol* (2018) 25(6):446–53. doi: 10.1038/s41594-018-0075-z
47. Ait Saada A, Lambert SAE, Carr AM. Preserving Replication Fork Integrity and Competence via the Homologous Recombination Pathway. *DNA Repair (Amst)* (2018) 71:135–47. doi: 10.1016/j.dnarep.2018.08.017
48. Bonilla B, Hengel SR, Grundy MK, Bernstein KA. RAD51 Gene Family Structure and Function. *Annu Rev Genet* (2020) 54:25–46. doi: 10.1146/annurev-genet-021920-092410
49. Boeckemeier L, Kraehenbuehl R, Gasasira MU, Vernon EG, Beardmore R, Vågbo CB, et al. Mre11 Exonuclease Activity Removes the Chain-Terminating Nucleoside Analog Gemcitabine From the Nascent Strand During DNA Replication. *Sci Adv* (2020) 6(22):eaaz4126. doi: 10.1126/sciadv.aaz4126
50. Runge KW, Li Y. A Curious New Role for MRN in Schizosaccharomyces Pombe non-Homologous End-Joining. *Curr Genet* (2018) 64(2):359–64. doi: 10.1007/s00294-017-0760-1
51. Situ Y, Chung L, Lee CS, Ho V. MRN (MRE11-RAD50-NBS1) Complex in Human Cancer and Prognostic Implications in Colorectal Cancer. *Int J Mol Sci* (2019) 20(4):816. doi: 10.3390/ijms20040816
52. Ha K, Fiskus W, Choi DS, Bhaskara S, Cerchietti L, Devaraj SG, et al. Histone Deacetylase Inhibitor Treatment Induces 'Brcaness' and Synergistic Lethality With PARP Inhibitor and Cisplatin Against Human Triple Negative Breast Cancer Cells. *Oncotarget* (2014) 5(14):5637–50. doi: 10.18632/oncotarget.2154

Conflict of Interest: The authors declare that the research was conducted in the absence of any commercial or financial relationships that could be construed as a potential conflict of interest.

Publisher's Note: All claims expressed in this article are solely those of the authors and do not necessarily represent those of their affiliated organizations, or those of the publisher, the editors and the reviewers. Any product that may be evaluated in this article, or claim that may be made by its manufacturer, is not guaranteed or endorsed by the publisher.

Copyright © 2022 Li, Yuan, Wang, Li, Liu, Wang, Wei, Li and Wang. This is an open-access article distributed under the terms of the Creative Commons Attribution License (CC BY). The use, distribution or reproduction in other forums is permitted, provided the original author(s) and the copyright owner(s) are credited and that the original publication in this journal is cited, in accordance with accepted academic practice. No use, distribution or reproduction is permitted which does not comply with these terms.



Breast Cancer Stem-Like Cells in Drug Resistance: A Review of Mechanisms and Novel Therapeutic Strategies to Overcome Drug Resistance

Taniya Saha* and Kiven Erique Lukong*

Department of Biochemistry, Microbiology and Immunology, University of Saskatchewan, Saskatoon, SK, Canada

OPEN ACCESS

Edited by:

Dayanidhi Raman,
University of Toledo, United States

Reviewed by:

Syn Kok Yeo,
University of Cincinnati, United States
Ahmet Acar,
Middle East Technical University,
Turkey

*Correspondence:

Taniya Saha
tanyya11@gmail.com
Kiven Erique Lukong
kiven.lukong@usask.ca

Specialty section:

This article was submitted to
Breast Cancer,
a section of the journal
Frontiers in Oncology

Received: 18 January 2022

Accepted: 21 February 2022

Published: 21 March 2022

Citation:

Saha T and Lukong KE (2022) Breast
Cancer Stem-Like Cells in Drug
Resistance: A Review of Mechanisms
and Novel Therapeutic Strategies to
Overcome Drug Resistance.
Front. Oncol. 12:856974.
doi: 10.3389/fonc.2022.856974

Breast cancer is the most frequent type of malignancy in women worldwide, and drug resistance to the available systemic therapies remains a major challenge. At the molecular level, breast cancer is heterogeneous, where the cancer-initiating stem-like cells (bCSCs) comprise a small yet distinct population of cells within the tumor microenvironment (TME) that can differentiate into cells of multiple lineages, displaying varying degrees of cellular differentiation, enhanced metastatic potential, invasiveness, and resistance to radio- and chemotherapy. Based on the expression of estrogen and progesterone hormone receptors, expression of human epidermal growth factor receptor 2 (HER2), and/or BRCA mutations, the breast cancer molecular subtypes are identified as TNBC, HER2 enriched, luminal A, and luminal B. Management of breast cancer primarily involves resection of the tumor, followed by radiotherapy, and systemic therapies including endocrine therapies for hormone-responsive breast cancers; HER2-targeted therapy for HER2-enriched breast cancers; chemotherapy and poly (ADP-ribose) polymerase inhibitors for TNBC, and the recent development of immunotherapy. However, the complex crosstalk between the malignant cells and stromal cells in the breast TME, rewiring of the many different signaling networks, and bCSC-mediated processes, all contribute to overall drug resistance in breast cancer. However, strategically targeting bCSCs to reverse chemoresistance and increase drug sensitivity is an underexplored stream in breast cancer research. The recent identification of dysregulated miRNAs/ncRNAs/mRNAs signatures in bCSCs and their crosstalk with many cellular signaling pathways has uncovered promising molecular leads to be used as potential therapeutic targets in drug-resistant situations. Moreover, therapies that can induce alternate forms of regulated cell death including ferroptosis, pyroptosis, and immunotherapy; drugs targeting bCSC metabolism; and nanoparticle therapy are the upcoming approaches to target the bCSCs overcome drug resistance. Thus, individualizing treatment strategies will eliminate the minimal residual disease, resulting in better pathological and complete response in drug-resistant scenarios. This review summarizes basic understanding of breast cancer subtypes, concept of bCSCs, molecular basis of drug resistance,

dysregulated miRNAs/lncRNAs patterns in bCSCs, and future perspective of developing anticancer therapeutics to address breast cancer drug resistance.

Keywords: breast cancer, drug resistance, BCSCs, miRNAs, therapeutic strategy, cancer stem-like cells

INTRODUCTION

Breast cancer (BC) is the most frequent type of malignancy in women worldwide. BC has now eclipsed lung cancer as the leading cause of global cancer incidence in 2020, with an estimated 2.3 million new cases, representing 11.7% of all cancer cases (1). Drug resistance in BC patients appears to be the major challenge in breast cancer research. Despite significant advances in BC treatment, many patients with malignant BC experience aggressive disease progression due to *de novo* and acquired drug resistance. *De novo* resistance occurs even before drug exposure, while acquired resistance emerges from initially drug-sensitive tumors. The mechanisms associated with *de novo* drug resistance significantly contribute to failure to eradicate the residual disease, thus facilitating the development of acquired drug resistance (2).

The failure of the current treatment therapies as well as the high mortality in metastatic BC patients is highly attributed to the existence of therapy-resistant breast cancer stem-like cells (bCSCs). The emerging concept of CSC origin supports the hierarchical organization of CSC-like cells, sitting at the top of the hierarchy, having the unique ability to give rise to diverse lineages of cancer cells that forms the tumor. Although the CSC-like cells occupy only a very minor fraction of the total tumor mass (around 2%), they are mainly responsible for establishing the intratumor heterogeneity (3). The concept of “tumor heterogeneity” refers to the genetic variation existing between tumor cells within and across the BC patients. According to the CSC concept, the CSC-like cells possess three main characteristics: (1) potent tumor initiation potential to regenerate the tumor, (2) self-renewal feature *in vivo* that would inevitably allow them to form a phenotypically indistinguishable heterogeneous tumor, when transplanted in secondary or tertiary recipients, and (3) finally, they must reflect the differentiation ability so that they can re-establish a phenocopy of the original tumor. Hajj et al. first identified and isolated the bCSCs (CD44+CD24–/lowLineage–) from the phenotypically diverse population of BC cells. This fraction of breast tumor cells can form a new tumor with additional CD44+CD24–/lowLineage– bCSCs along with phenotypically different nontumorigenic cells (4). If the therapy in question fails to specifically target and kill the bCSCs, they would persist as the residual disease, which can regenerate tumors in the future. Frequently, the bCSCs overexpress the drug efflux transporters and spend most of the time in the nondividing cell-cycle phase (G0) to escape from the conventional therapeutics (5). Hence, targeting the bCSCs in any subtype, such as luminal A, luminal B, human epidermal growth factor receptor 2 (HER2)-enriched, and triple-negative (TNBC), is the key strategy to conquer therapeutic resistance in BC. The complex communication between bCSCs and the stromal cells; resistance to

chemotherapeutic drugs (paclitaxel, anthracycline, platinum), endocrine therapies (tamoxifen, fulvestrant), and HER2-targeted drugs (trastuzumab, lapatinib); rewiring of hedgehog (Hh), Notch, Wnt/ β -catenin, and phosphoinositide 3-kinase (PI3K)/Akt/mTOR signaling networks; and enhancing DNA repair mechanism, contribute to the overall drug resistance in bCSCs (6).

MicroRNAs (miRNAs) also add another dimension to the complexity of BC disease progression and therapeutic resistance, through maintenance of the bCSC population. MiRNAs are a group of small noncoding RNAs (ncRNAs) that influence the expression of their target genes at the posttranscriptional level by binding to the 3′-untranslated regions (3′-UTR) of mature mRNA transcripts. Two different types of miRNAs—tumor suppressor miRNAs (miR34, Let-7, miR30, miR200 family, miR600) and Onco-miRs (miR-22, miR155, miR181, miR221/222 cluster)—have been identified in bCSCs, having either tumor-suppressive or oncogenic functions, respectively. Interestingly, miRNAs have been implicated in the regulation of many different signaling networks, contributing to the development and maintenance of bCSCs (3, 7). Moreover, locoregional tumor burden along with the metastatic patterns in BC patients also influence the efficacy of the treatment strategies. In the case of early-stage BC, the tumor is restricted in the breast or local axillary lymph node, and the success rate for relapse-free survival is around 70%–80% (8). However, in the case of advanced BC, where metastatic dissemination from the primary tumor site leads to the re-establishment of secondary tumors involving other organs like lung, brain, liver, and bones, complete cure is not possible. In that scenario, much emphasis is given to prolonging the patient survival to exert a low degree of treatment-associated cytotoxicity to improve the quality of life.

Due to the lack of specific molecular targets in TNBC and increased resistance to the anti-HER2 therapies in HER2+ breast tumors, cytotoxic chemotherapy is the common alternative for treating these two most resistant subtypes of BC. However, there is an increasing search for therapeutic strategies that would sensitize the drug-resistant bCSCs to programmed cell death. Immunotherapy, based on the immune checkpoint inhibitor molecules (ICIs), specific for programmed cell death protein 1 (PD-1), programmed death ligand 1 (PD-L1), and CTLA-4, which are either administered as a single agent or in combination with either a humanized monoclonal antibody, such as trastuzumab, in HER2+ BC settings, or any other chemotherapeutic drug in the TNBC scenario, have been the recent candidates in clinical trials (8). Other immunotherapy approaches like the chimeric antigen receptor T-cell (CAR-T) therapy, dendritic cell (DC) vaccine, and oncolytic viral therapies, specific for bCSC immune targeting, are also gaining significant momentum in recent years (9). Nanoparticle-based

bCSC-targeting platform is also appearing as an upcoming approach to deliver small molecules, antibodies, and miRNAs to affect the signaling networks implicated in bCSC self-renewal and differentiation; interfering with drug-efflux transporters; and targeting bCSC metabolism (10). In this review, we focused on the mechanisms of resistance to chemo-, endocrine, and targeted therapies, the contribution of bCSCs in exerting drug resistance, and the factors influencing bCSC-mediated drug resistance and, finally, we emphasized the alternative forms of upcoming treatment platforms to overcome CSC-related drug resistance in BC patients.

BREAST ARCHITECTURE, BC SUBTYPES, AND ADVANCEMENT OF TECHNOLOGIES TO IDENTIFY BC

The breast architecture mainly involves glandular tissue including the breast lobes and ducts, supportive fibrous connective tissue, and fatty tissues that largely fill in the gaps between the glandular and fibrous tissues. An adult woman's breast consists of 15–20 lobes, each lobe further containing 20–40 lobules. The lobules resemble a grape-like structure, where each of the lobules is attached to a small milk duct, and finally these small ducts join, eventually forming a larger collecting duct. There are around 10 ductal systems present in each breast that finally open at the nipple. A cross-section of a milk duct shows a basement membrane layer, the basal or myoepithelial layer, and the luminal or epithelial layer, from outside to inside (**Figures 1A–C**). In 20%–25% of cases, the tumor is restricted at the site of its origin (*in situ* or preinvasive); whereas, in 75%–80% of cases, the tumors are malignant (invasive) whereby the malignant cells invade the basement membrane and penetrate the stroma.

Histological and Molecular Subtypes

BCs are generally divided according to histological grade and stage, which define the aggressiveness and metastatic potential of the tumor. Histologically, the breast tumors are distinguished into preinvasive and invasive subtypes involving the ductal and lobular compartments. Ductal and lobular subtype is classified as ductal carcinoma *in situ* (DCIS), invasive ductal carcinoma (IDC), lobular carcinoma *in situ* (LCIS), and invasive lobular carcinoma (ILC), respectively (**Figures 1D–H**) (11). At the molecular level, breast tumors are categorized into 4 main subtypes, based on the presence/absence of markers that include estrogen receptors (ER), progesterone receptors (PR), and HER2, as well as their proliferative index according to Ki67 expression (12). These molecular subtypes include TNBC (ER–, PR–, HER2–), HER2-enriched (ER–, PR–, HER2+), luminal A (ER+ and/or PR+, but HER2–, Ki67 <14%), and luminal B (ER+ and/or PR+, HER2+ or HER2–, Ki67 >14%) (refer to **Figure 1I**). ER+ breast tumors are targeted using selective estrogen receptor modulators (SERMs), aromatase inhibitors, cyclin-dependent kinases 4 and 6 (CDK4/6) inhibitors, and ER degraders also called selective estrogen receptor downregulators (SERDs) (13).

HER2-enriched breast tumors are candidates for HER2-targeted monoclonal antibodies. However, TNBC accounts for the most therapy-resistant subtype of heterogeneous basal-like tumors (15%–20% of all breast tumors), which frequently reflects a high mutational burden including tumor suppressor p53 (TP53 gene, 74.5%–82.8%), breast cancer type-1 and/or type-2 susceptibility gene (BRCA1, 1.96%–21.55%; BRCA2, 1.63%–18.10%), and phosphatidylinositol 3-kinase catalytic alpha polypeptide (PI3K α , 8.6%–23.2%) (9, 14–16). However, another compelling piece of evidence from Maristany et al. suggests the concept of phenotypic switching between BC molecular subtypes, as evident from the gene expression studies before, during, and after neoadjuvant therapy with lapatinib and trastuzumab in HER2+/HER2-enriched tumors of the PAMELA trial and BC cell lines (17). Dual blockade of HER2 pathway in HER2-enriched settings leads to a subtype switching to a low-proliferative luminal A phenotype both in the patients' tumor samples and *in vitro* models. Strikingly, this subtype switching from HER2-enriched to luminal A phenotype increased the sensitivity toward CDK4/6 inhibitors; although, this switching is reversible upon stopping the anti-HER2 treatment. Moreover, integrated analysis of copy number and gene expression studies of 2,000 breast tumors by Curtis et al. reveals the existence of novel molecular stratification among the BC population, resulting from the impact of somatic copy number aberrations (CNAs) on the transcriptome (18). A similar study of somatic CNAs revealed an advanced stratification of BC cases into integrative clusters and prototypical patterns of single-nucleotide variants, shaping the clinical courses and response to BC therapies (19). Therefore, in addition to the conventional BC molecular subtypes discussed above, the genomic and transcriptomic architecture of BC samples further add another dimension, yielding novel BC subgroups with distinct clinical outcomes. Moreover, the emerging evidence on the inter- and intratumoral heterogeneity within a breast tumor not only acknowledges the probability that multiple different BC subtypes can coexist within a single tumor but also demonstrates that plasticity between divergent subtypes is possible rather than being static (20). Interconversion between the different subtypes within a breast tumor contributes to disease progression, metastasis, and therapeutic resistance. Therefore, therapeutic decision making must be designed based on the genomic and transcriptomic inputs along with the changing molecular phenotypes even in an individual patient's tumor.

Solid Tissue Biopsy and Liquid Biopsy

Solid tissue biopsy is the standard method of choice in clinical oncology that provides information on tumor histology, molecular profiling and subtyping, and biomarkers targeted for treatment planning (21). However, it does not reveal the complete genomic landscape of the tumor, as the tissue is collected from a specific biopsy area. The heterogeneous nature of the tumor is validated when tumor cells collected from multiple regions from a single patient are subjected to exome sequencing, ploidy profiling, and chromosome aberration analysis. Gerlinger et al., for example, noted that approximately

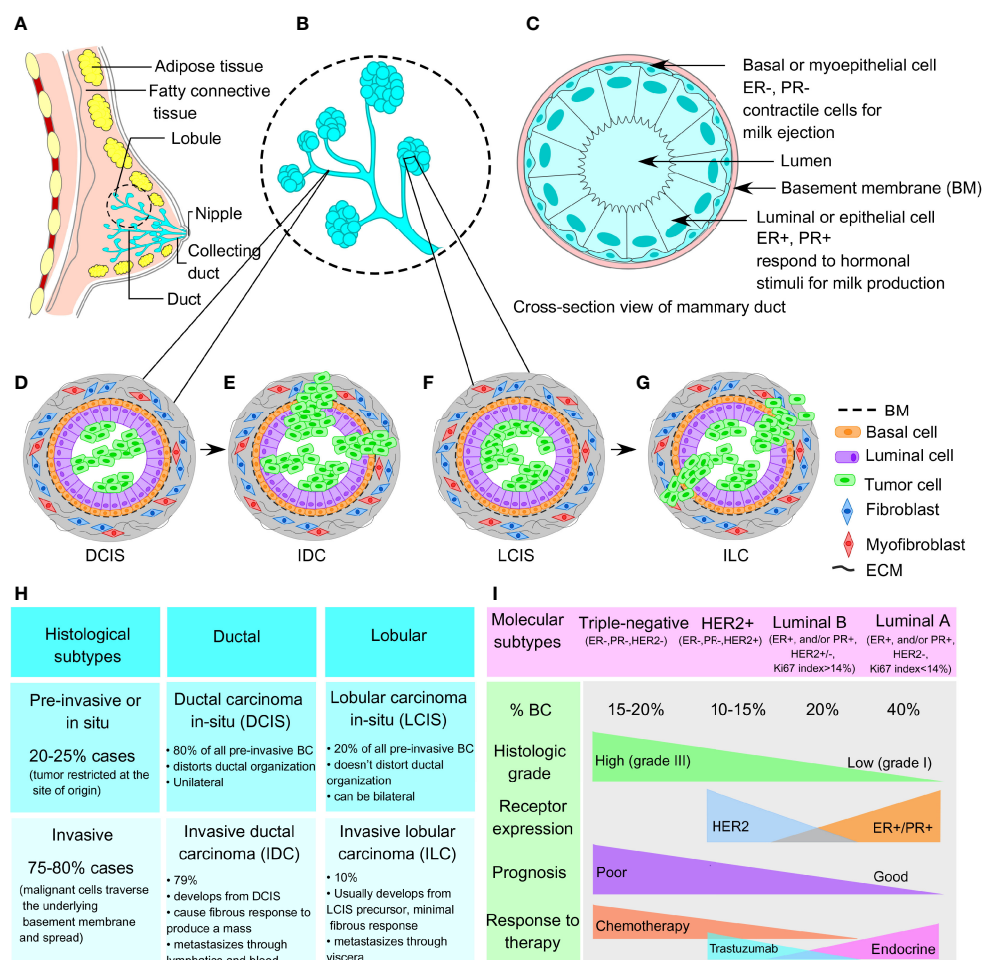


FIGURE 1 | Normal breast architecture and breast cancer subtypes. **(A)** Representative image of breast architecture showing lobular and ductal system. **(B)** Magnified view of milk duct showing detailed lobular and ductal structure as an inset image. **(C)** Cross-sectional view of normal mammary duct showing basement membrane, basal myoepithelial cell layer, and luminal or epithelial cell layer from outside to inside. **(D)** Representative images of ductal carcinoma *in situ* (DCIS) and **(E)** invasive ductal carcinoma (IDC). **(F)** Representative images of lobular carcinoma *in situ* (LCIS) and **(G)** invasive lobular carcinoma (ILC). **(H)** Histological subtypes (preinvasive and invasive) and **(I)** molecular subtypes (triple-negative, HER2+, luminal A, and luminal B) of breast cancer.

63%–69% of the mutations observed in tumor tissue obtained from a single biopsy derived from the same patient are not homogeneous throughout the tumor. This observation strongly indicates the importance of “multiregion biopsy” for the diagnosis of cancer (22).

To bypass this limitation, in 2020, the Food and Drug Administration (FDA) approved the use of “liquid biopsy” where DNA from circulating breast tumor cells (ctDNA) shed from the primary tumor site is isolated from the patient’s blood and then subjected to microfluidic-based single-cell transcriptional profiling (23, 24). CtDNAs released into the systemic circulation can be theoretically defined as an admixture of tumor DNA samples from different metastatic sites, thus fully reflecting the tumor heterogeneity. A very recent work from Kingston et al. represents the application of plasma ctDNA sequencing to define the genomic profile of metastatic BC in 800 patients in the plasmaMATCH trial (25).

With this novel approach, diverse resistance mutations including enrichment of HER2 mutations in HER2+ tumors, ESR1 and MAPK pathway mutations in ER+ HER2– tumors, and multiple PI3KCA mutations in ER+ tumors, have been successfully demonstrated. Particularly, this study utilizes the ctDNA analysis platform in a large clinical trial to denote the subclonal diversification of pretreated advanced BC, categorizing unique mutational processes in ER+ BC and identifying novel therapeutic directions. This noninvasive methodology enables the detection of early stages of BC, monitoring of treatment efficacy and therapeutic resistance, and identification of minimum residual disease (MRD) and risk of relapse (24, 26). Circulating tumor RNAs are also released into the bloodstream of BC patients, which provides another analytic platform through the liquid biopsy method (27). Next-generation sequencing (NGS) is also increasingly applied for high-throughput BC mutational profiling (28, 29).

BCSCs AND DRUG RESISTANCE

BCSCs can escape the conventional therapies through adaptation to several strategies, where the breast cancer stem-like cells can remain dormant or “quiescent”, turn off the apoptotic pathways, and increase DNA repair mechanisms, along with expelling chemotherapy (chemo) drugs out of the cell, manipulating TME, and managing the intracellular load of reactive oxygen and nitrogen species (ROS and RNS) (30). Although the dormant bCSCs maintain themselves in the G0 state, they still retain the ability to enter the cell division cycle in response to mitotic stimulation (31). As chemotherapy and radiation therapy exclusively target the proliferating fraction of tumor cells, the bCSCs can evade systemic therapies, and in turn, develop drug resistance. Thus, drug resistance confers the bCSCs with a selective advantage over the non-CSCs that supports the “survival of the fittest” hypothesis applicable for CSC-like cells within TME. Moreover, epithelial-mesenchymal transition (EMT) plasticity that enables bCSCs to dynamically switch between intermediate cellular states of varying epithelial/mesenchymal traits, also contributes to bCSC-mediated therapeutic resistance (32–34). A study by Liu et al. demonstrates that bCSCs exhibit plasticity that allows them to transition between a proliferative epithelial-like state (E-bCSCs), characterized by a high aldehyde dehydrogenase activity, and a quiescent, mesenchymal-like, invasive state (M-bCSCs), characterized by CD44+CD24– expression (35). This switching from E- to the M-state closely mimics the EMT program, which is associated with CSC properties and drug resistance. This observation strongly proposes that distinct bCSCs coexist within the same tumor, and thus novel combinatorial approaches targeting both CSC phenotypic states are essential to eliminate different types of bCSCs within the same tumor to reverse drug resistance phenomena. In trastuzumab-resistant HER2+ BC, combinatorial targeting of both HER2 (with trastuzumab) and IL-6 receptor (with tocilizumab) synergistically interferes with the tumor progression and metastasis by eradicating both E- and M-bCSCs (36); whereas, in the TNBC scenario, no such approach is available so far.

How the bCSCs Originate Within a Tumor (Clonal Versus Stem Cell Model)

There has been a great deal of debate on how CSCs originate. Clonal evolution theory and the cancer stem cell theory are the two most popular theories that shed light on the origin of this CSCs. Apart from this, CSCs are thought to be one of the determining factors establishing intratumoral heterogeneity, and both clonal evolution theory and stem cell model account for the same (37). The clonal evolution model holds an example of a nonhierarchical model where individual tumor cells are thought to undergo stochastic genetic/epigenetic changes as a function of time and serves as the platform for adaptation and selection of the fittest clones (38). Thus, each cell gets the chance to become tumorigenic or drug resistant if it accumulates enough episodes of genetic/epigenetic modifications. These changes contribute to intratumoral heterogeneity as a result of natural selection and evolution of bCSCs with better survival fitness, where those clones will expand and survive, out-compete the

other nontumorigenic clones with less fitness, eventually making them extinct. This landmark theory was proposed by Peter Nowell in 1976 (39). Furthermore, these clones may change spatially and temporally and develop into a complex subclonal architecture, contributing to tumor heterogeneity. However, the dynamic CSC model represents a hierarchical model, which holds that only the CSC-like cells can develop a tumor, based on their infinite self-renewal and tumorigenic properties (refer to **Figure 2A**). According to this model, a CSC-like cell can either symmetrically divide giving rise to two new CSCs or can asymmetrically divide into a differentiated daughter cancer cell and a CSC (refer to **Figure 2B**). Hence, CSCs contribute to intratumoral heterogeneity through a differentiation program generating a range of distinct cell types within a tumor. However, this differentiation hierarchy is not only a one-way route but can also be reversible or plastic where the terminally differentiated pool of cancer cells can reverse their phenotype and acquire CSC-like properties through a dedifferentiation program, termed as “phenotype reversal”. Recent studies also indicate that different subpopulations of CSCs with varying biochemical, biophysical, and metabolic signatures may exist within a tumor, contributing to tumor heterogeneity, varied dissemination, and drug resistance potential (40). Treatment with the available chemotherapeutic drugs can kill the nonstem-like tumor cells while sparing the drug-resistant bCSCs, allowing them to survive, which eventually repopulate and develop into a tumor, leading to distant metastasis (refer **Figure 2C**). Therefore, treating a hierarchical tumor with some therapeutic agents that can specifically target and eradicate bCSCs can be the only option to get rid of CSCs and tumor recurrence. However, even if the CSC fraction is eliminated out of the TME, the remaining tumor cells may undergo phenotype reversal to replenish the CSC-like population and lead to tumor regrowth (10). Moreover, a failed radiotherapy can stimulate the transition of dormant CSCs into the “awakened state”, whereby they can enter the cell cycle and start proliferating (41).

Characterization of bCSCs

Since bCSCs are phenotypically different from the rest of the cells present within TME, bCSCs can be identified and sorted based on some classical bCSC-specific markers like CD44, CD133, aldehyde dehydrogenase 1 (ALDH1) activity, epithelial cell adhesion molecule (EpCAM), CXCR4, ABCG2, CD34, CD49f, CD90, CD61, and breast cancer resistance protein (BRCP). However, due to the low specificity of these markers, a combination of CSC-like markers is frequently used. However, the combination of a high CD44/CD24 ratio and ALDH1+ is considered to be the most accurate and consistent way of defining bCSCs (42).

CD44

CD44 is a cell-surface hyaluronan acid (HA) receptor that contains an HA-binding site in its extracellular domain. Notably, HA is the major component of ECM. Hence, the CD44-HA interaction not only contributes to the cell adhesion to ECM components but also to tyrosine phosphorylation of cytoskeletal proteins, activation of RhoA/RhoC, Rac1, and Cdc42, fueling invasion and metastasis (43). Activation of these signaling pathways is essential for actin

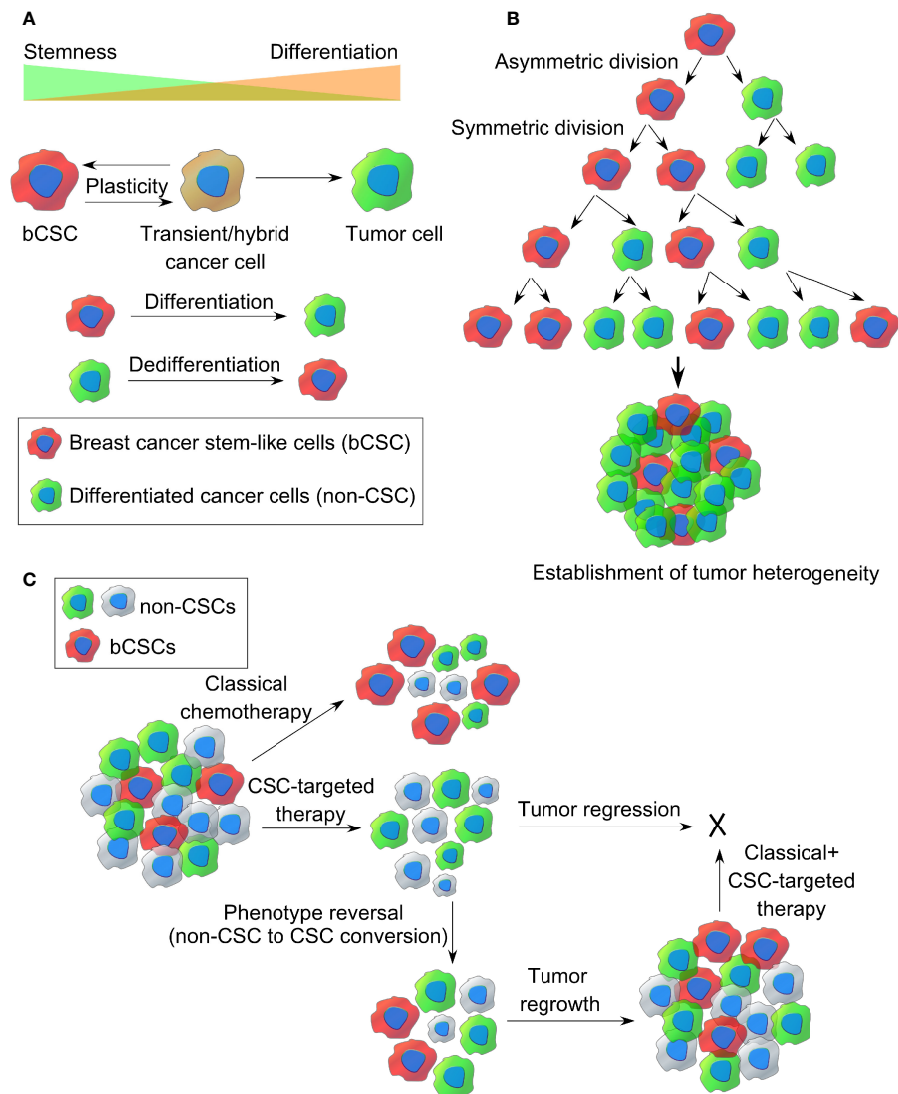


FIGURE 2 | The origin of breast CSCs within a tumor. **(A)** Dynamic cancer stem cell (CSC) model of cancer cell plasticity showing switching between CSC-like state and differentiated cancer cell states (non-CSCs) through differentiation and dedifferentiation pathways. **(B)** Establishment of intratumor heterogeneity in breast cancer, resulting from symmetric and asymmetric cell divisions of breast CSCs. **(C)** Representative images of classical chemotherapy, CSC-targeted therapy, phenotype reversal, and combination therapy for target killing of breast cancer stem-like cells from TME.

cytoskeletal remodeling, actin filament assembly, tumor cell migration, and invasion. CD44 is overexpressed in bCSCs and interestingly involves the Src kinase family proteins to initiate BC progression *via* Twist signaling (44). Moreover, CD44 contributes to chemoresistance since it upregulates the expression of multidrug resistance receptors by activating Nanog (45).

CD133

CD133 is another bCSC-specific marker found to be enriched in basal-like, HER2+, luminal, and TNBC subtypes. CD133-high bCSCs have been documented in tumor cell proliferation, vasculogenic mimicry, invasion, metastasis, and drug resistance (6). Croker et al. identified CD44+CD133+ALDH^{high} bCSC-like

cells as crucial mediators of BC metastasis (46). BRCA1-associated murine breast tumors consist of CD44+/CD24- and CD133+ cells with bCSC-like features, showing a greater intrinsic colony-forming potential that can regenerate breast tumors in NOD/SCID mice (47). Interestingly, CD133-high bCSCs augments endocrine resistance in metastatic BC *via* the IL-6/Notch signaling (48). Xenograft initiating CD44+CD49^{high}CD133/2^{high} cells display self-renewal *in vivo* and greater tumorigenicity in ER- breast cancer (49).

ALDH1

Aldehyde dehydrogenase 1 is a member of NAD(P)⁺-dependent cytosolic isoenzymes, which is critically responsible for the

oxidation of retinol to retinoic acid, required for early differentiation of stem cells. ALDH1 is a general marker of both human normal mammary stem cells and malignant mammary stem-like cells, and high ALDH1 activity is an independent predictor of poor clinical outcome and survival of BC patients (50). Interestingly, only a fraction of CD44+CD24-/low bCSC BC cells are ALDH1+ and display the highest tumorigenic potential, when compared with ALDH1- population (50). Moreover, ALDHhighCD44+CD24- and ALDHhighCD44+CD133+ bCSCs, isolated from MDA-MB-231 and MDA-MB-468 cell lines, respectively, demonstrated enhanced growth, adhesion, migration, colony formation, and invasion profile, compared with ALDHlowCD44-/low cells (46). Therefore, inhibition of ALDH activity can effectively reverse doxorubicin/paclitaxel resistance of ALDHhighCD44+ human bCSCs (51). ALDH+ bCSCs with an increased expression of interleukin-1 receptor (IL1R1) are enriched following antiestrogen therapy and held responsible for the treatment failure (52). Hence, targeting the ALDH+IL1R1+ bCSCs is crucial to reverse the drug resistance exerted by antiestrogens.

EpCAM

EpCAM is a glycosylated type 1 glycoprotein, expressed by human epithelial cells, and functions as an oncogenic signal transducer (53). Al-Hajj et al. showed that EpCAM+CD44+CD24-/lowLineage- fraction had a >10-fold higher frequency of tumor-initiating cells compared with EpCAM-CD44+CD24-/lowLineage- fraction (4). Interestingly, EpCAM overexpressing BC cells can withstand greater radiation stress compared with EpCAMlow cells (54). Hence, EpCAMhigh BC cells retain the ability to form a higher number of mammospheres. Activation of the AKT pathway is also observed in EpCAM overexpressing ZR-75-1 breast cancer cell line, compared with parental cell line. Moreover, EpCAM overexpression also reflects a higher percentage of cells with an E/M hybrid state, encouraging EMT, invasion, and metastasis. EpCAM+ circulating tumor cells isolated from primary human luminal BC patients' blood contain metastasis-initiating cells, leading to bone, lung, and liver metastasis in mice (55). Since survivin has a crucial role in bCSC chemoresistance, EpCAM aptamer-mediated survivin silencing can sensitize bCSCs to doxorubicin and reverse chemoresistance (56).

CXCR4

The chemokine receptor C-X-C chemokine receptor type 4 (CXCR4) is considered to be a prognostic marker of bCSCs. The metastatic cascade is initiated *via* a series of sequential steps that include local invasion and intravasation (transendothelial migration) of cancer cells from the primary tumor site into the circulation, followed by extravasation at distant sites and subsequent organ colonization (homing) (57). Cancer cells at the growing front of the tumor undergo EMT, which degrades the underlying basement membrane and ECM before intravasation. The CXCR4 receptor and its ligand, CXCL12 (SDF-1) play an important role in the dissemination of BC cells from the primary site, transendothelial migration, and eventually trafficking and homing of bCSCs. Chemokines are

8–12-kDa chemoattractant cytokines that contribute to differentiation, cell activation, and trafficking. Notably, the chemoattractant CXCL12 provides directional guidance to CXCR4+ bCSCs toward the secondary metastatic site and initiates metastasis (58–60). Hence, targeting the CXCR4-CXCL12 signaling axis could serve as an alternative approach to restrict bCSC-driven drug resistance. Additionally, CXCR4+ bCSCs show a higher vimentin/E-cadherin ratio, indicating EMT. Interestingly, CXCR4 inhibition can enhance the infiltration of cytotoxic T-cell lymphocytes (CTLs) and improve the responses to immune checkpoint blockers in metastatic BC (61). A quantitative phosphoproteomic study by Yang et al. validated the importance of CXCR4-SDF1 signaling in bCSCs and also identified several important signaling pathways in bCSCs, downstream of CXCR4-SDF1 (62).

Evidence on Therapy-Induced bCSC Enrichment and Drug Resistance

Several studies indicate evidence on bCSC enrichment postanticancer therapy, although the underlying molecular mechanisms leading to bCSC enrichment are largely unknown. Since radiation treatment preferentially kills actively proliferating non-CSCs, there is a natural enrichment of bCSCs posttherapy. Furthermore, radiation can induce reversible transformation between CSC and non-CSC phenotype such that more CSC-like cells, with an increased level of stemness and tumorigenic potential, are generated from both normal stem cells as well as neoplastic nonstem-like cells, which ultimately leads to an increase in the absolute number of bCSCs within TME (41, 63, 64). It is hypothesized that in advanced cancer cases, the majority of the CSCs remain “dormant”, thus remaining unaffected by radiotherapy. Moreover, it is the unique potential of CSCs that can modify divisional dynamics, favoring symmetrical division, generating two identical CD44+CD24-/low daughter cells with higher radioresistance, postradiotherapy (65, 66). The number of tumor-initiating bCSCs also increases along with Notch upregulation, following a brief period of fractionated irradiation (66). Moreover, a study on non-CSCs isolated from the BC patients indicates that ionizing radiation (IR) reprograms the phenotype of differentiated BC cells and converts them into induced bCSC (i-bCSC). These i-bCSCs reflect a greater tumorigenic and mammosphere formation potential, along with a higher expression of stemness-related genes, OCT-4, Sox2, Nanog, and Klf4 (67). Furthermore, in response to IR, non-CSCs undergo radiation-induced EMT and show an increased migratory potential leading to metastasis and disease relapse, thus closely mimicking the CSC-like phenotype (68). Altogether, this evidence strongly suggests that acquisition of CSC phenotype by differentiated BC cells is an example of a direct effect of anticancer therapy, rather than a random event. Another study on glioma and breast cancer suggests that around one-third of the CSCs remain in dormancy and do not enter the cell cycle until challenged with IR (69). This refers to a mechanism whereby more “awakened CSCs” are generated from “dormant CSCs”. Moreover, radiotherapy favors oncogenic metabolism in CSCs upon their conversion from a slow-cycling “dormant” to “awakened” state, which increases their therapeutic resistance (68). Chemotherapy

treatment also enhances the percentage of CD44+CD24-/low BC cells, indicative of innate chemoresistance exerted by bCSCs (70). Hence, despite eradicating the CSCs from the tumor, anticancer therapies including chemo- and radiation therapy rather help the dormant bCSCs to survive by increasing their intrinsic resistance and finally leading to tumor recurrence. Recently, an intricate link between the dormant disseminated tumor cells (DTCs) and therapeutic resistance has been documented, in the course of metastasis (71). DTCs also spread *via* the metastatic cascade and enter the blood or lymphatic circulation (57). During circulation, the DTCs undergo a reversible mitotic arrest program, followed by a long period of dormancy, termed as “quiescence”, when they remain viable but do not increase in number (72). It is hypothesized that a percentage of breast DTCs are indeed bCSCs with long half-lives (73), capable of evading immune surveillance through expression of PD-L1 and show innately higher resistance toward standard radiation, chemo-, and even immunotherapy (74). Upon reaching the distant organs, DTCs infiltrate into the local tissue stroma, although they cannot form micrometastases until dormancy is over. This period is termed as “metastatic cancer dormancy” which reflects the period between the initial therapy and disease relapse. Once the dormant DTCs get adjusted to the new microenvironment, they “awaken” from their dormant state, gain the ability to re-enter the cell cycle, and proliferate, ensuing the metastatic outgrowth (72). Interestingly, ~62% of all deaths from BC happen after 5-year survival mark, emphasizing the contribution of dormant DTCs in disease recurrence (75). Several molecular targets, including integrin $\alpha 5 \beta 1$, $\beta 1$, $\alpha 2$, $\alpha v \beta 3$, FAK, PKC, STAT3, and Cox1/2 have been identified to DTCs’ reawakening program, for which specific therapeutic agents are designed (72). Therefore, if the bCSCs could be targeted before they awaken from dormancy, metastatic dissemination and drug resistance can be potentially restricted.

Factors Contributing to bCSC Drug Resistance Against Conventional Therapeutic Drugs

Vasculogenic Mimicry

Vasculogenic mimicry (VM) is a recently defined pattern of tumor microvascularization that refers to the ability of cancer cells to organize themselves into vascular-like structures to procure nutrients and oxygen independently of normal blood vessels (76, 77). Unlike the concept of angiogenesis or vasculogenesis where the endothelial cells participate in blood vessel formation, VM particularly depends on the participation of highly aggressive tumor cells, having the endothelial phenotype, to form vessel-like structures (**Figure 3A**). VM has been reported in different types of solid aggressive tumors including BC (78–80). CD133+ breast CSCs reflect VM, with a higher expression of vascular endothelial-cadherin (VE-cadherin), along with an upregulated expression of matrix metalloproteinase, MMP-2, and MMP-9 in TNBC (81). Notably, both MMP-2 and MMP-9 are critical players in cellular plasticity and VM formation. According to Sun et al., it is the bCSCs that line the VM channels in breast tumor tissues

from TNBC patients (82). Additionally, bCSCs produce more VM-related molecules like CD133 and ALDH1, to synergize VM formation (82, 83). However, cells participating in VM formation lack the classical endothelial marker CD31, and thus, administration of angiogenesis inhibitors does not affect VM formation. In this context, a phytochemical, thymoquinone (TQ), has been reported to exhibit an inhibitory effect on VM and promotes mesenchymal–epithelial transition (MET) in bCSCs derived from MDA-MB-231, in a dose-dependent manner. Moreover, CD44+CD24- bCSCs when incubated with TQ can interfere with rhodamine-123 efflux and decrease stemness. This observation indirectly denotes that thymoquinone relieves the drug-resistance properties of bCSCs (84). Mechanistically, TQ suppresses the PI3K and Wnt3a signaling, leading to the reduction of the p-Akt/Akt ratio, and has the potential to reduce the number of bCSCs.

Decreased Ferroptosis in bCSCs

Ferroptosis is an iron-dependent mechanism of regulated cell death, which is characterized by the intracellular accumulation of lipid-based ROS, ultimately resulting in the loss of membrane integrity (**Figure 3B**) (85). Notably, lipid-ROS is detoxified in a GPX4-catalyzed enzymatic reaction, which uses glutathione as a reducing agent. Hence, ferroptosis can be triggered either by inhibiting GPX4 enzymatic activity or depleting glutathione. Type I ferroptosis-inducing compounds, including sulfasalazine and erastin block the amino acid transporter required for cysteine import to synthesize glutathione. Type II drugs, such as RSL3, interfere with GPX4 peroxidase activity. Mechanistically, the execution of ferroptosis requires a high concentration of intracellular iron. Ferritin, the intracellular iron-storing protein, can release iron to initiate ferroptosis. The released iron can yield lipid-ROS in an autoamplifying manner. Ferroptosis can be inhibited by the presence of iron chelators and activated by transferrin and its receptor (86). Hence, sensitizing tumor cells to ferroptosis appears as a possible therapeutic approach for BC treatment. Notably, drug-tolerant BC cells show a dependency on the GPX4 activity, thus inhibition of GPX4 can potentially overcome BC drug resistance (87). Taylor et al. reported an array of ferroptosis-inducing small molecules that can selectively kill bCSCs with the mesenchymal phenotype *in vitro* (88). TNBC cells are highly susceptible to cysteine starvation, leading to ferroptosis and necroptosis, *via* the GCN2-eIF2 α -ATF4-CHAC1 pathway (89). Since cysteine serves as the substrate for glutathione synthesis to prevent ferroptosis, depleting the pool of cysteine can sensitize BC cells to ferroptosis (89). Another synthetic derivative from salinomycin, ironomycin (AM5), can trigger cell death in bCSCs, both *in vitro* and *in vivo*, by sequestering iron in lysosomes, which further indicates that iron homeostasis plays a crucial role in bCSC survival (90). A novel nanoparticle, ferritin-bound erastin, and rapamycin (NFER) has shown robust ferroptosis-inducing properties by interfering GPX4 in 4T1 orthotopic BC mouse model (91).

Increased Autophagy in bCSCs and Drug Resistance

Autophagy is an evolutionarily conserved self-degradation process that recycles intracellular nutrients, growth factors, and

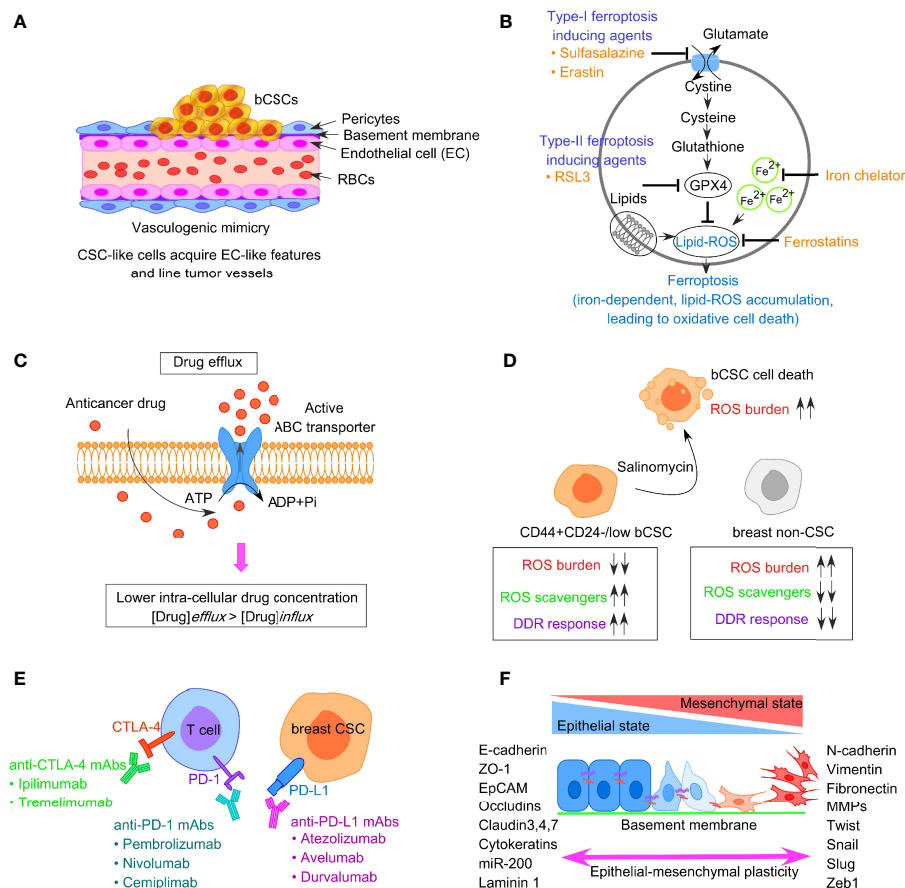


FIGURE 3 | Factors responsible for bCSC-mediated drug resistance against traditional anticancer therapeutics. **(A)** Concept of vascuogenic mimicry observed in breast CSCs leading to drug resistance. **(B)** Representative image of ferroptosis pathway involving generation of lipid-ROS in an iron-dependent manner, leading to oxidative cell death of tumor cells. **(C)** Increased drug efflux due to enhanced expression of ABC transporters in bCSCs, resulting in lower intracellular chemotherapeutic drug concentration. **(D)** Low ROS burden and enhanced DNA damage repair in bCSCs. **(E)** Restoration of T-cell activity by targeting immune-checkpoint molecules like PD-1, PD-L1, and CTLA-4 to reverse CSC-mediated immune escape in breast cancer. **(F)** Epithelial-mesenchymal transition (EMT) plasticity indicating the gradual transition of cancer cells from epithelial state to mesenchymal state and the transcription factors associated with the process.

energy to sustain survival and cellular activities during stress like hypoxia, nutrient deprivation, and ischemia (92). Autophagy provides bCSCs with metabolic flexibility that becomes a prerequisite for their survival in oxygen- or nutrient-poor TME (93). Autophagy contributes to bCSC dormancy, stemness, maintenance, and drug resistance (94–96). Chaperone-mediated autophagy (CMA) and macroautophagy are two different modes of the autophagy process, documented in mammalian cells. Autophagy can elevate bCSC number, and thus develop drug resistance to conventional chemotherapies (97). Furthermore, autophagy-related genes (ATGs) such as ATG4A, ATG5, ATG12, LC3-B, and Beclin1 are expressed in dormant bCSCs, promoting bCSC survival and sustaining bCSCs over the progression of BC (96). Expression of Beclin1 is noted to be higher in mammospheres derived from BC cell lines, MCF-7 and BT474, compared with the adherent cultures (98). Moreover, the expression of lysosome-associated membrane protein type 2A (LAMP2A), involved in the CMA pathway, is augmented in

the course of BC metastasis (99). Autophagy of cancer-associated fibroblasts (CAFs) also contributes to TNBC proliferation and progression. Notably, autophagy-relevant Beclin1 and LC3-II/I protein conversion levels are higher in CAFs, compared with the normal fibroblasts in TNBC (100). Since autophagy serves as one of the factors in malignant growth, inhibition of autophagy can suppress tumor growth. Pharmacological targeting of the autophagic flux with salinomycin can reduce bCSC-driven drug resistance, interfere with their stemness, and also compromise the bCSC tumorigenic potential (101).

Enhanced Drug-Efflux in bCSCs

CSCs often express a higher level of ATP-binding cassette (ABC) transporters that facilitate them to survive chemotherapy, aiding in the survival of drug-resistant CSCs (102). ABC transporters can efficiently expel chemo drugs like anthracycline or taxanes out of the cells and can eventually lead to the acquisition of drug resistance phenotype in bCSCs (Figure 3C). This group of

proteins is located on the cell membrane and thus can allow transmembrane transportation of different toxic molecules. Notably, CSCs exhibit a higher expression of ABC transporters, such as ABCB1 (MDR1), ABCG2 (BCRP1), ABCC11 (MRP8), and ABCB, which are positively correlated with CSC-mediated drug resistance (103, 104). The activity of drug efflux proteins can be monitored through the transport of fluorescent dyes like rhodamine and Hoechst 33342 (105). Based on this property, the CSCs can be isolated from non-CSCs by fluorescent-activated cell sorter (FACS). This fraction of cells termed as “side population” (SP), is identified as CSCs since these cells fall along the side of the cellular distribution on the FACS profile. Downregulating ABCG2 with wedelolactone-encapsulated PLGA nanoparticles increases the chemosensitivity of bCSCs (106). The Sox2-ABCG2-TWIST1 axis contributes to chemoresistance and stemness in TNBC, indicating the importance of ABCG2 as a potential bCSC-specific target in TNBC patients (107). Moreover, simultaneous blocking of ABCG2 and antiapoptotic gene BCL2 with SiRNA in bCSCs leads to better chemotherapeutic response to doxorubicin (108). Dofequidar, an ABC transporter inhibitor, increases the chemosensitivity of bCSCs in advanced or recurrent BC patients, when administered in combination with chemo drugs like doxorubicin, fluorouracil, and cyclophosphamide (109). ABC transporters not only participate in establishing the drug resistance *via* increased efflux of chemo drugs but also contribute to EMT (110). ABCB1 is another group of ABC transporter implicated in the chemoresistant nature of CSCs and induction of EMT (111, 112). Therefore, the combined application of chemotherapeutic drugs and ABC inhibitors should be employed to kill the bCSCs (111).

Enhanced DNA Repair in bCSCs

Although cancer cells show a reduced DNA damage repair (DDR) mechanism and reflect many mutations and genomic instability, CSC-like cells exhibit a highly dynamic DDR system that protects the DNA effectively (113). Both chemotherapy drugs and radiotherapy can induce DNA damage. Mechanistically, radiotherapy contributes to DNA damage through the production of water-derived free radicals and ROS that avidly interacts with DNA, protein, and lipids. The generation of ROS, in turn, switches on the DDR pathway. However, in contrast to non-CSCs, CSCs have a low ROS burden and augmented DNA repair system (refer to **Figure 3D**). An increased level of ROS scavengers in CSCs maintains low levels of ROS that protect the CSCs from ROS-mediated DNA damage and apoptosis. The ROS scavenger, N-acetylcysteine, can restore both CSC and EMT phenotypes (114). A novel compound, salinomycin, can effectively target the CSC niche and kill CD44^{high}CD24⁻/low bCSCs as it upregulates the ROS levels (115). The radioresistance property of CSC-like cells is linked with cell-cycle kinetics, which is reflected by a significant increase in the doubling time and Chk1/Chk2 basal activation level (116). The elongated cell-cycle window, therefore, offers more time to repair the genetic defects in CSCs. When the DNA defects are corrected, CSCs again enter into the cell cycle from the quiescent state and escape apoptosis. Therefore, targeting DDR could reverse therapeutic resistance.

Frizzled 5 (FZD5), a member of the FZD family, contributes to DDR, G1/S transition, proliferation, stemness, and chemoresistance in TNBC (117). FZD5 knockdown suppresses the expression of CD133, ALDH, EpCAM, and Oct-4, thus potentially overcoming chemoresistance and recurrence in TNBC. Likewise, CCR5 directs the DDR mechanism and bCSC expansion (118). CCR5 antagonists, vicriviroc and maraviroc, can substantially increase cell death caused by DNA-damaging chemo drugs. MYC and MCL1 also cooperatively function in bCSC maintenance in TNBC patients *via* increasing ROS production and HIF-1 α expression (119).

Immune Escape in bCSCs and Drug Resistance

CSCs are a crucial driver in immune evasion, metastasis, and drug resistance. Substantial evidence suggests a reciprocal interaction between CSCs and immune cells, and that CSCs adopt different strategies to circumvent immune attacks mediated by different immune cell types within TME. This, in turn, contributes to CSC expansion and mediate protumorigenic immune function, leading to CSC-specific avoidance of immune detection and destruction of immune cells. Tumor-associated macrophages (TAMs), tumor-associated neutrophils (TANs), myeloid-derived suppressor cells (MDSCs), DCs, tumor-infiltrating lymphocytes (TILs), B cells, natural killer (NK) cells, and T regulatory (Treg) cells, and proinflammatory cytokines secreted by these cells, are therefore crucial for maintaining an immune-resistant phenotype. Treatment of bCSCs with conditioned medium from TAMs results in an upregulated expression of Oct3/4, Sox2, Nanog, and ALDH1 activity (120). MDSCs also lead to the enrichment of bCSCs *via* IL-6/STAT3 and NO/Notch signaling, leading to the suppression of T-cell activation (121). The T-cell inhibitory molecule, PD-L1 is overexpressed on the bCSC cell surface, compared with their differentiated counterparts, and is dependent on PI3K/AKT and Notch signaling pathway (122). Interestingly, PD-L1 expression is upregulated in response to EMT induction and facilitates the immune escape of bCSCs (123, 124). Moreover, bCSCs are not only resistant to chemotherapy but also immunotherapy (125). Therefore, restoring the T-cell activity by manipulating immune checkpoint molecules, targeting either PD-1/PD-L1 (nivolumab/pembrolizumab) or CTLA-4 (ipilimumab) can be an effective strategy (**Figure 3E**). Also, immunosuppressive cytokines secreted by breast CSCs (IL-4, IL-6, IL-8, IL-10, and IL-13) result in therapeutic resistance, increased EMT, metastasis, and recruitment of immunosuppressive immune cell types like Treg and MDSCs (126). A high circulating level of IL-6 contributes to disease recurrence, tamoxifen resistance in luminal BC, and trastuzumab resistance in HER-2 enriched BC. Targeting IL-6 receptor with monoclonal antibody tocilizumab, hence, suppresses metastatic potential of bCSCs and enhances the cytotoxicity of cisplatin against TNBC (127).

bCSC-Driven EMT, Metastasis, and Drug Resistance

Like normal tissue stem cells, EMT and the reverse process MET are critical to CSC features. Substantial evidence exists that correlates EMT plasticity to the emergence of dedifferentiated cells with CSC phenotype, ultimately driving metastasis and drug

resistance (128, 129). EMT inducers such as TGF- β and receptor tyrosine kinase (RTK) ligands modulate gene expression patterns through complex signaling networks (112). This results in the upregulation of transcriptional repressors like Snail, Slug, Zeb1/2, Twist, and E47. This group of proteins, then, interacts with the promoter sequence of adherens junction protein, E-cadherin, recruits histone deacetylases (HDACs), and induces its chromatin condensation, leading to transcriptional repression of E-cadherin. EMT involves the dissolution of cell-cell adherens junction barriers, loss of apico-basolateral polarity of epithelial cells, along with increased expression of mesenchymal markers such as fibronectin and vimentin (**Figure 3F**) (128). This, in turn, aids in gaining motile characteristics of cancer cells post-EMT. Mani et al. indicated that when the EMT program is induced in immortalized human mammary epithelial cells through ectopic expression of Twist, Snail, or TGF- β treatment, the cells exhibited mesenchymal appearances, developed many stem-like properties, and had the potential to form mammary tumors in mice (128). Importantly, the metastatic cancer cells with mesenchymal-like features generated post-EMT, exhibited CD44^{high}/CD24^{low} signature, and formed mammospheres whereas CD44^{low}/CD24^{high} cells could not. Al-Hajj et al. reported that disseminated BC cells found in pleural effusions are enriched in CD44^{high}CD24^{low} bCSCs (4). Interestingly, the EMT-associated emergence of bCSCs is induced by CD8⁺T cells that stimulate dedifferentiation of BC cells into bCSCs (130). An increased expression of stroma cell-related genes, attributed to the EMT program, could be linked to drug resistance in BC (131). Hence, blocking the EMT program can eventually interfere with CSC maintenance and innate or acquired drug resistance (70). Therapeutic intervention of micro-RNAs can provide an additional strategy to disrupt the EMT-CSC deadly axis. Application of HDAC inhibitors and “differentiation-inducing” agents are also believed to fetch clinical benefits to BC patients.

MECHANISM OF BCSC-MEDIATED DRUG RESISTANCE TO CANCER THERAPY

Resistance to Chemotherapy

Chemotherapy involves chemo drugs given to the BC patients either intravenously or orally, along with other treatments like surgery, radiation, or hormonal therapy. Through the bloodstream, the chemo drugs reach the cancer cells and kill them. Adjuvant and neoadjuvant chemotherapies are two different modes of chemotherapies. In adjuvant chemotherapy (following surgery), the chemo drug is given to kill the cancer cells that have been left behind or could not be seen in imaging tests; whereas, in neoadjuvant chemotherapy, the chemo drug is given to shrink the breast tumor to reduce the requirement of extensive surgery. However, several lines of evidence indicate bCSC enrichment following exposure to chemo drugs, resulting in multidrug resistance (MDR). Here, we focus on the variety of chemo drugs (refer to **Table 1**), their mode of action, and potential mechanisms of chemoresistance exerted by bCSCs.

Paclitaxel Resistance

Paclitaxel, a first-line therapeutic agent for the treatment of metastatic BC, is a microtubule-stabilizing agent. It interferes with microtubule dynamic instability at nanomolar concentrations, thus leading to G2/M mitotic arrest and apoptosis in BC cells (**Figure 4A**). Paclitaxel resistance seems to be one of the primary obstacles that lead to chemotherapeutic failure in BC. HER2/ β -catenin pathway mediates paclitaxel resistance in BC cells, and hence suppression of the HER2/ β -catenin signaling can overcome paclitaxel resistance (132). Penfluridol (PFL) treatments that suppress both HER2/ β -catenin pathways significantly inhibit the survival of paclitaxel-resistant BC cells. Notably, paclitaxel resistance increases both CD44⁺CD24[−] bCSC content and sphere-forming ability in the paclitaxel-resistant SUM159 metastatic TNBC cell line (133). According to this report, dasatinib, an Src family kinase inhibitor, induces epithelial differentiation of mesenchymal TNBC cells and sensitizes TNBC cells to paclitaxel therapy through targeting bCSCs. An increased association of ALDH1 expression has been noted in paclitaxel-resistant BC patients (134). TNBC cell lines, such as MDA-MB-231, SUM-149, and SUM-159 show an enhanced activity of hypoxia-inducible factors (HIFs) and their target gene products, with chronic exposure to paclitaxel therapy. Furthermore, chemotherapy-induced HIF activation results in bCSC enrichment through IL-6 and IL-8 signaling and enhanced expression of MDR-1 (135). Hence, combinatorial therapies including HIF inhibitors along with paclitaxel chemotherapy are being tested in clinical trials to explore its efficacy in BC patients.

Platinum Resistance

Platinum-based chemotherapeutic drugs, such as cisplatin, oxaliplatin, carboplatin, nedaplatin, and lobaplatin are frequently the choice of drugs for treating advanced BC cases, including TNBC (136, 137). Mechanistically, platinum-based drugs interact with guanine and adenine nucleotides, forming platinum-DNA nonfunctional adducts, disrupting DNA double-helical structure, and eventually inhibiting cell division (**Figure 4B**) (138). However, drug resistance associated with platinum therapy and the numerous side effects that it causes have been a long-standing concern for BC patients. According to Sledge et al., only 47% of the BC patients with metastatic BC are partially sensitive to platinum therapy (139). Several lines of evidence indicate a crucial contribution of bCSCs in developing and maintenance of platinum resistance. In this context, a novel drug disulfiram (DSF) can reverse cisplatin resistance in different BC cell lines through inhibiting ALDH enzymatic activity and interfering with the expression of Oct4, Sox2, and Nanog in bCSCs. IL-6 secreted by breast tumor-derived mesenchymal stem-like cells (MSCs), augments cisplatin resistance *via* STAT3 signaling (140). Although neutralizing IL-6 can partially interfere with the IL6-STAT3 axis and reverse the cisplatin resistance, the specific role of bCSCs remains unclear. Notably, there is the active involvement of PI3K/AKT/NF- κ B signaling in enrichment as well as maintenance of breast CSCs. Cisplatin is known to stimulate transcriptional upregulation of PI3KCA, thereby triggering PI3K/AKT signaling in platinum-

TABLE 1 | Different chemotherapeutic modalities in clinical practice and novel therapeutic drugs being developed against BC subtypes and their mechanism of action.

Breast cancer subtype	Drug	Biological target (mechanism of action)
Hormone positive	In clinical practice	
	Tamoxifen	Competitively inhibits interaction between ER and estrogen
	Fulvestrant	SERD, competitively inhibits estrogen to occupy ER, ER degradation
	Aromatase inhibitors (AIs) (exemestane, anastrozole, letrozole)	Blocks conversion of androgens to estrogens
	Leuprolide	Reduces production of estrogen and progesterone by the ovary by blocking effects of GnRH on the pituitary gland
	Goserelin	Luteinizing hormone-releasing hormone (LHRH) agonist, stops LH production, blocks release of estrogen
	Palbociclib (FDA approval: February 2015)	CDK4/6 inhibitors for advanced stage BC along with letrozole
	Ribociclib (FDA approval: March 2017)	CDK4/6 inhibitors for advanced stage BC along with letrozole
	Abemaciclib or verzenio (FDA approval: October 2021)	CDK4/6 inhibitors for treatment of early-stage BC
	Everolimus (FDA approval: July 2012)	mTOR inhibitor, sensitizes hormone-receptor-positive BC to exemestane
	In pipeline	
	Buparlisib (BKM120)	Pan-class I PI3K inhibitor, combination therapy with fulvestrant, phase III trial (NCT01610284)
	Alpelisib	PI3K inhibitor, inhibiting p110 alpha; combination therapy with fulvestrant, phase III trial (NCT02437318)
	Taselisib	Alpha-specific PI3K inhibitor; combination therapy with fulvestrant, phase III trial (NCT02340221)
	Entinostat	HDAC inhibitor, phase II trial with exemestane (NCT02115282)
	Vorinostat	HDAC inhibitor, in combination with tamoxifen, terminated (NCT01194427)
	Irosustat	Steroid sulfatase inhibitor with AI, phase II trial completed (NCT01785992)
HER2 enriched	In clinical practice	
	Trastuzumab	Anti-HER2 mAb interacting with extracellular domain IV of HER2
	Pertuzumab	Anti-HER2 mAb targeting HER2 extracellular domain II, inhibiting HER2 heterodimerization with EGFR, HER3, and HER4
	Lapatinib	Tyrosine kinase inhibitor (TKI) targeting both EGFR and HER2, interacts at ATP-binding site of kinases
	Ado-trastuzumab emtansine	Anti-HER2 mAb conjugated with microtubule inhibitor emtansine
	Margetuximab (FDA approval: December 2020)	HER2-targeted antibody for metastatic HER2+ BC
	Tucatinib (FDA approval: April 2020)	HER2 inhibitor, used in combination with trastuzumab and capecitabine (Xeloda) in metastatic HER2+ BC
	In pipeline	
	Patritumab	Anti-HER3 mAb in combination with trastuzumab and paclitaxel in phase I/II trial completed (NCT01276041)
	Buparlisib with lapatinib and pilaralisib with trastuzumab	Pan class-I PI3K inhibitors, phase I/II trial (NCT01589861), phase I/II trial (NCT01042925)
	Lonafarnib	Inhibits Ras activity, combination therapy with trastuzumab and paclitaxel, phase I completed (NCT00068757)
	NeuVax + trastuzumab	Immunotherapy for treatment of early-stage HER2+ BC; phase IIb trial (NCT02297698)
	Ridaforolimus with trastuzumab	mTOR inhibitors, phase II trial completed (NCT00736970)
	Sirolimus with trastuzumab	mTOR inhibitors, phase II trial completed (NCT00411788)
Triple-negative	MK-2206	Allosteric pan-Akt inhibitor; combination therapy with trastuzumab and lapatinib, terminated (NCT00963547)
	In clinical practice	
	Anthracyclines	Topoisomerase II inhibitors, stabilize DNA breaks and ensuing tumor cell death
	Taxanes	Microtubule-stabilizing agent, stabilize GDP-bound tubulin in microtubule, G2/M arrest, cell death
	Olaparib	PARP inhibitor, blocks repair of single-strand DNA breaks by base excision repair (BER) system
	Talazoparib	PARP inhibitor
	Bevacizumab	Antiangiogenic mAb against VEGF bevacizumab + docetaxel anti-VEGF mAb
	Atezolizumab (FDA approval: March 2019)	Anti PD-L1 antibody as first-line therapy to locally advanced or metastatic PD-L1-positive TNBC patients
	Pembrolizumab (FDA approval: October 2021)	Anti PD-1 antibody for high-risk early-stage TNBC
	Trodely (sacituzumab) (FDA approval: 2020)	Trop-2 directed antibody and topoisomerase inhibitor drug conjugate for metastatic TNBC patients
	In pipeline	
	Cetuximab + cisplatin or carboplatin	Anti-EGFR mAb for metastatic TNBC, phase II completed (NCT00463788)
	Glembatumumab vedotin	mAb-cytotoxic drug conjugate targeting glycoprotein NMB in TNBC, phase II completed (NCT01997333)
	Dasatinib + cetuximab + cisplatin	Src inhibitors, tested in TNBC cell lines

The clinical trial number for the drugs in pipeline has been mentioned according to *ClinicalTrials.gov*.

resistant cells. However, a recent report emphasizes that mechanistically cisplatin leads to CSC enrichment in platinum-resistant cells through the NF- κ B-TNF- α -PI3KCA loop (141).

Anthracycline Resistance

Anthracyclines, antibiotics extracted from *Streptomyces* bacteria, administered as broad-spectrum chemotherapeutic drugs in BC patients, are topoisomerase II inhibitors (**Figure 4C**) (142). Since, topoisomerases modify DNA topology by breaking or rejoining DNA double strands, inhibiting its catalytic activity stabilizes DNA breaks, eventually causing cell death. This class of drugs includes doxorubicin, daunorubicin, and epirubicin. Resistance to anthracyclines has been linked with multiple factors, such as the acquisition of MDR due to overexpression of drug efflux pumps and permeability glycoprotein-1, alteration of topoisomerase II activity, CSC enrichment, altered DNA repair, and metabolic reprogramming (143). A 4-day exposure to doxorubicin and paclitaxel, followed by a 2-day recovery, leads to significant enrichment of CD44^{high}CD24⁻/low bCSCs (144). In this context, cardamonin, a small molecule, significantly prevents bCSC enrichment, when administered along with chemotherapeutic drugs, *via* downregulation of IL-6, IL-8, NF- κ B, and STAT3 signaling (144). Knockdown of Annexin A3 also influences the drug sensitivity of bCSCs to doxorubicin *via* an upregulation of drug uptake, inhibits metastasis, and exhibits a change in heterogeneity and plasticity in bCSCs (145).

Resistance to Endocrine Therapy

Endocrine therapy is an effective mode of treatment for the ER+ BC cases that blocks ER signaling, depriving the growing tumor of estrogen (146, 147). ER signaling plays a crucial role in BC proliferation, invasion, and angiogenesis. Mechanisms, through which the endocrine therapy works (refer to **Table 1**), can be categorized into (1) SERMs, (2) aromatase inhibitors (AIs), (3) CDK4/6 inhibitors, and (4) SERDs (**Figure 4D**) (148, 149). SERMs function by sitting in the ER of breast tissues, blocking the estrogen from interacting with the ER, and hence the cells can no longer grow and multiply (150). AIs work by blocking the function of the aromatase enzyme that converts androgen into estrogen (151). CDK4/6 inhibitors are generally used in combination with endocrine therapy to treat hormone-receptor-positive but HER-2 negative metastatic BC (152, 153). CDK4/6 is required by BC cells for cell-cycle division. BCSCs develop resistance to endocrine therapy in ER+ BC and are mainly responsible for the failure of endocrine therapy (154). Therefore, specific targeting of drug-resistant bCSCs could serve as a potential therapeutic strategy in overcoming hormonal therapy resistance.

Tamoxifen Resistance

ER- α -positive BC cases constitute around 70%–75% of overall BC incidence. Although, tamoxifen (TAM) has been the fundamental mode of endocrine therapy for the treatment of ER+ BC patients for the last three decades, acquired TAM resistance is frequently held accountable for the disease relapse (155). TAM competitively inhibits the interaction of estrogen

ligand with ERs (**Figure 4E**). Most importantly, an increased proportion of bCSCs in advanced BC patients have a potential contribution to TAM resistance and breast tumorigenesis (156). Poorly differentiated breast tumors contain a higher percentage of CSC-like cells than well-differentiated breast tumors (157). TAM-resistant BC cells retain stem-like properties (158). Notably, TAM-resistant MCF-7 cells showed increased proliferation rate, enhanced mammosphere formation ability, increased mRNA expression of OCT-4, SOX-2, and CD133, and increased EMT signature, compared with wild-type MCF-7 cells (158). In a parallel study, Wang et al. indicated that TAM-resistant MCF-7 cells contain a higher proportion of CD44⁺CD24⁻/low bCSCs, exhibit lesser sensitivity to Adriamycin compared with wild-type MCF-7 cells, and express SOX-2 as a biomarker for TAM resistance (159). Serine phosphorylation, particularly at Serine 118, has been documented for activating the N-terminal transcriptional function of ER- α . SOX-2 can reprogram the non-genomic estrogen signaling and augment bCSC proportion through phosphorylation of ER- α at serine 118, making it hypersensitive to circulating estrogen (160). Phosphorylation, ubiquitination, and other posttranslational modifications play an important role in activating ER and its coregulators and can influence the sensitivity to different endocrine therapies (161). Therefore, inhibition of SOX-2 could restore the sensitivity of BC cells to TAM (162). Furthermore, ER splicing variants, including estrogen-related receptors (ERRs), and the recently identified estrogen receptor α -variant (ER- α 36) are involved in TAM resistance and estrogen hypersensitivity (163). However, the contribution of ER- β in bCSC-mediated TAM resistance is still under investigation. Upregulation of different growth factors including HER2, epidermal growth factor receptor (EGFR), and insulin-like growth factor 1 receptor (IGF1R) has been documented in BC endocrine resistance, although direct evidence has been found in support of PI3K-mediated TAM resistance (164). Hence, targeting PI3K and IGF1R is considered a major therapeutic target to reverse TAM resistance in bCSCs. Different signaling pathways, such as Wnt and Notch, induce TAM resistance, promoting bCSC activity in TAM-resistant MCF-7 cells, while inhibition of these pathways could overcome TAM resistance (165, 166). A positive correlation has been noted between activation of Hedgehog (Hh) signaling and reduction in disease-free or recurrence-free survival in BC patients, which can even result in TAM resistance (167). The intervention of Hedgehog (Hh) signaling, thus, can potentially interfere with bCSC proliferation, migration, and invasion and reverse TAM resistance. Therefore, inhibition of Notch, Hedgehog (Hh), and Wnt/ β -catenin signaling pathways should serve as another strategy to overcome TAM resistance in bCSCs.

Fulvestrant Resistance

Fulvestrant is a selective estrogen receptor degrader (SERD) administered in both first and subsequent lines of treatment in ER- α + metastatic BC patients (149, 168). Fulvestrant competitively inhibits estrogen to occupy the ER, eventually promotes degradation of the receptor, and thus interferes with

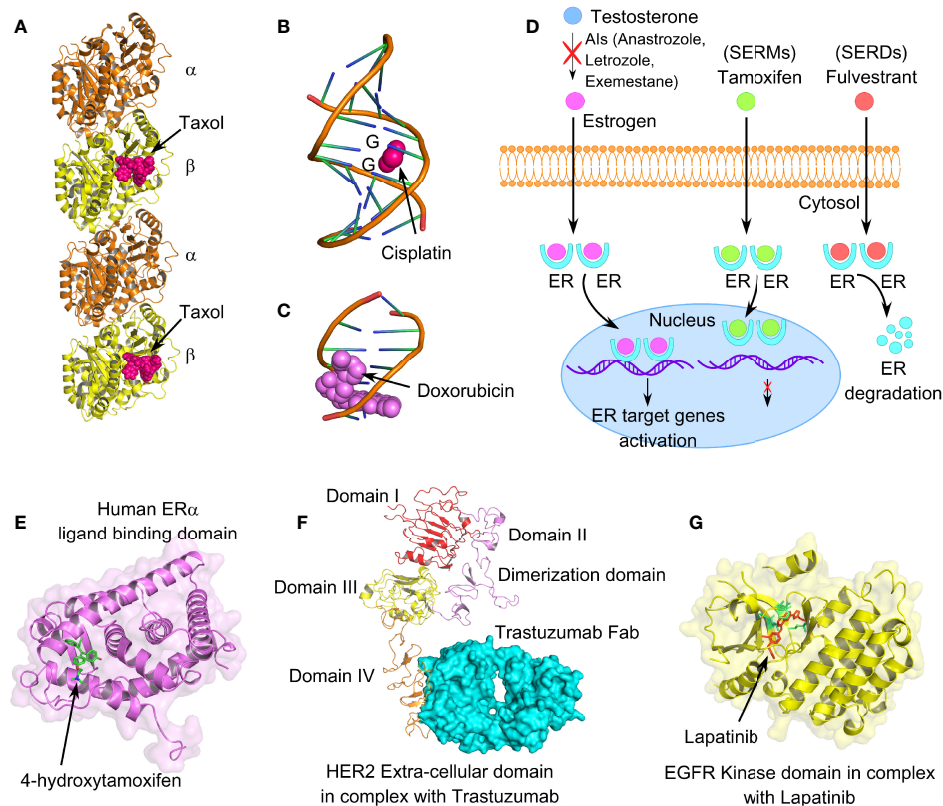


FIGURE 4 | Mechanism of action of different anticancer drugs for the treatment of breast cancer. **(A)** Tubulin dimers stabilized with microtubule-stabilizing drug paclitaxel (PDB code: 6WVR). **(B)** Interaction of chemo drug cisplatin with double-stranded DNA (PDB code: 1AIO), forming major adducts of cisplatin with guanine nucleotides. **(C)** Doxorubicin intercalation with DNA base pairs (PDB code: 2DES). **(D)** Cartoon representation of mechanism of action of endocrine therapeutic drugs, such as selective estrogen receptor modulators (SERMs), selective estrogen receptor degrader (SERDs), and aromatase inhibitors (AIs). **(E)** Human ER- α -ligand-binding domain in complex with tamoxifen (PDB code: 3ERT). **(F)** Extracellular domain IV of HER2 in association with recombinant humanized IgG1 monoclonal antibody, trastuzumab (PDB code: 6OGE). **(G)** EGFR kinase domain in complex with lapatinib, a selective receptor tyrosine kinase inhibitor, targeting both EGFR and HER2 (PDB code: 1XKK). Lapatinib interacts in the ATP-binding pocket of EGFR (L718, V726, A743, M793, and L844); highlighted in lemon green.

estrogen signaling in breast tumor tissues (169). Unfortunately, there has not been extensive research done on fulvestrant resistance in bCSCs as well as the molecular mechanisms responsible for the resistance. Dysregulation of both G protein-coupled estrogen receptor-1 (GPER) and CDK6 are associated with fulvestrant resistance in BC (170). Notably, GPER-induced signaling is essential for the survival of bCSCs (171). Very recently, Kaminska et al. reported that cyclin E2 overexpression has been recognized as a biomarker for persistent fulvestrant-resistant metastatic BC and reduced disease-free survival (172). However, AI-resistant BC cells, having a higher proportion of bCSC-like cells and increased stemness, are inhibited by fulvestrant (173). Several signaling pathways, such as MEK/ERK, NF- κ B, EGFR, PI3K/AKT, and β -catenin have been implicated so far to fulvestrant resistance in BC. MiRNA-221/222 confers estrogen-independent growth and fulvestrant resistance in BC through multiple signaling networks. Strikingly, miR-221/222 contributes to acquired fulvestrant resistance through activation of the β -catenin pathway, and miR-221/222 has recently been documented in CD44+CD24⁻/low bCSCs (174).

Aromatase Inhibitor Resistance

AIs constitute the first-line therapeutic approach for the treatment of ER+ BC in postmenopausal women (175, 176). AIs deplete the circulating level of estrogen in the human body by interfering with estrogen biosynthesis through blocking aromatase activity (177). Hence, in the presence of AIs, estrogen production is inhibited, which slows down tumor progression in ER+ BC settings. When treating early-stage ER+ BC, AIs are frequently the choice of hormonal therapy over TAM due to the fewer side effects it causes. However, acquired AI resistance may develop in over 20% of early-stage BC patients and found to be inevitable in metastatic BC patients (178). Acquired AI resistance involves a switch from dependence on ER signaling to growth-factor-mediated signaling, such as HER2 signaling (179). Both cancer-cell intrinsic (enhanced activity of FGFR, ERBB2, and IGF1R and the downstream signaling of PI3K-AKT-mTOR and MAPK pathways) and extrinsic mechanisms (interaction of TME with other cell types) cumulatively coordinate the development and maintenance of AI resistance (180). AIs are classified into 2 subtypes—steroidal

(type I) and nonsteroidal (type II). The three different AIs anastrozole (nonsteroidal), letrozole (nonsteroidal), and exemestane (steroidal) are being used in adjuvant therapy as the first line of treatment modality for both early and metastatic BC in postmenopausal women. BCSCs in ER- α + settings reflect an activated PI3K signaling, which confers endocrine resistance including AI resistance (181). Notably, different PI3K inhibitors such as alpelisib, buparlisib, and taselisib (<https://clinicaltrials.gov/ct2/show; ClinicalTrials.gov Identifier: NCT02437318, NCT01610284, and NCT02340221>) are being administered as novel therapeutic drugs in phase III clinical trials for the treatment of breast cancer AI resistance (**Table 1**). The expression of HIF-1 α has also been recognized as a biomarker and therapeutic target that promotes AI resistance (179).

Resistance to Targeted Therapy

HER2 is an oncogenic RTK, which is frequently genetically amplified or overexpressed in around 15%–20% of invasive BC cases (182). However, although the emergence of anti-HER2 drugs, trastuzumab and lapatinib, significantly improved the clinical outcome in HER2-enriched BC, the associated drug resistance problem poses challenges to effective treatment. Resistance to anti-HER2 drugs occurs due to the presence of bCSCs in the tumor milieu that can remain “hidden” from the activity of these drugs (111). Therefore, we need to understand the mechanisms responsible for the associated drug resistance followed by the application of anti-HER2 drugs to encounter the involvement of bCSCs in therapeutic resistance (refer to **Table 1**).

Trastuzumab Resistance

Amplification of ERBB2 (HER2) is associated with clinically aggressive breast tumors, shorter disease/recurrence-free survival, and poor overall survival (183). Trastuzumab is a recombinant humanized IgG1 monoclonal antibody that interacts with extracellular domain IV of ERBB2, inhibiting dimerization between ERBB2 and other EGFR family members (**Figure 4F**) (184). Although HER2+ BC responds quite well to trastuzumab (HerceptinTM) therapy plus chemotherapy in the early stages of the disease, acquired resistance, however, to trastuzumab after 1–2 years of treatment is a frequent event following metastasis (185). Factors like HER2 degradation, overexpression of other RTKs, mutation of PI3KCA (PI3K catalytic subunit p110 α), and loss of Phosphatase and Tensin Homolog Deleted on Chromosome 10 (PTEN) tumor-suppressive function have been linked with trastuzumab resistance (186). Continued application of trastuzumab in HER2+ cells with loss of PTEN encourages EMT and transforms HER2+ BC to TNBC (187). Strikingly, these transformed cells frequently exhibit mesenchymal features along with mesenchymal-specific gene expression profile, although the parental HER2+ cells show epithelial morphology with epithelial-specific gene signature. Since bCSCs exhibit chemoresistance to small-molecule targeted therapy, exploring the mechanism of trastuzumab resistance must have clinical implications. BCSCs confer drug resistance by activation of

different prosurvival pathways, such as PI3K/AKT, NF κ B, and JAK/STAT pathways (188). Thus, CD44+CD24–/low bCSC phenotype serves as a prognostic factor for clinical outcome and predictive factor for poor trastuzumab response in patients with HER2+ BC. Importantly, PI3K/AKT/mTOR activation has been implicated in both *de novo* and acquired trastuzumab resistance (189). Since PTEN loss and mutation of PI3KCA lead to aberrant downstream activation of PI3K/AKT/mTOR pathway, which in turn sustains bCSC population, both the factors correlate with trastuzumab resistance (190). Therefore, combining PI3K/AKT/mTOR inhibitors along with HER2 targeting drugs to overcome trastuzumab resistance provides an active area of research. Pan-class I PI3K inhibitors, such as buparlisib and pilaralisib when administered with trastuzumab (189), lapatinib (191), or trastuzumab and paclitaxel (192), are proven to be safer and successful in HER2+ advanced stage BC patients. IL-6-mediated bCSC expansion is another independent mechanism resulting in trastuzumab resistance (36). Moreover, STAT3 activation also stimulates breast cancer stem-like properties resulting in HER2 overexpression and trastuzumab resistance (193). Hence, targeting JAK/STAT3 pathway or administering IL-6 receptor-targeted antibody should overcome the trastuzumab resistance by reducing the bCSC burden. Additionally, CD47 blockade with trastuzumab also eliminates HER2+ BC cells, overcoming trastuzumab tolerance (194).

Lapatinib Resistance

Lapatinib is a reversible and selective receptor tyrosine kinase inhibitor, targeting both epidermal growth factor receptor (EGFR) and HER2 (195). In contrast to trastuzumab, lapatinib blocks kinases' active ATP-binding site, thus interfering with receptor phosphorylation (**Figure 4G**). However, despite the initial response in HER2-overexpressing BC, acquired resistance to lapatinib turns out to be a frequent event in the course of treatment. Liu et al. have isolated and characterized several lapatinib-resistant HER2/ER+ BC clones from lapatinib-sensitive BT474 cells through chronic exposure to lapatinib. This group has identified that activation of AXL is associated with lapatinib resistance in these resistant BT474 clones (196). Evidence indicates a close association of breast CSCs in exerting lapatinib resistance. In this context, a recent study suggests that miR-205-5p is highly expressed in bCSCs. miR-205-5p represses ERBB/HER receptors in bCSCs, leading to resistance to targeted therapy (197). Silencing miR-205-5p in bCSCs, followed by lapatinib treatment, significantly reduces BC proliferation, resensitizing BC cells toward EGFR/anti-HER2 treatments. Furthermore, knockdown of miR-205-5p by locked oligonucleotides significantly reduces EMT and metastatic potential exerted by bCSCs (198). TGF- β -SMAD3 signaling also contributes to trastuzumab and lapatinib resistance, maintaining CSC phenotype in HER2+ settings (199). CD24 supports the expression of HER2 along with activation of PI3K/AKT signaling, resulting in lapatinib resistance (200). Hence, small-molecule inhibitors of SMAD3, or targeting CD24, can attenuate lapatinib resistance and increase the sensitivity of HER2+ BC cells to lapatinib.

BCSC-RELATED miRNA SIGNATURE MODULATING STEMNESS AND DRUG RESISTANCE

The regulation of bCSCs by miRNAs (~less than 25 nucleotides) is emerging as an innovative tool to deal with bCSC-driven drug resistance. Tumor suppressor miRNAs and OncomiRs have been implicated to play an essentially important role in the regulation of bCSC self-renewal, differentiation, tumor initiation, EMT, metastasis, and therapeutic resistance (3, 7, 201). In this section, we will briefly discuss these 2 types of bCSC-related microRNA signature, either suppressing or favoring drug resistance, through their regulation of multiple signaling networks.

Tumor Suppressor miRs in bCSCs

Several miRNAs, miR-30, miR-34, miR-200 family, miR-223, let-7, and miR-600 have been documented for tumor suppressive function (201). miR-223 is downregulated in CD44+CD24-/low bCSC in TNBC compared with non-CSCs (202). Thus, overexpression of miR-223 sensitizes the TNBC cells to tumor necrosis factor-related apoptosis-inducing ligand (TRAIL)-induced apoptosis (202). miRNA expression profiling indicates that miR-200 family (miR-200a, miR-200b, miR-200c, miR-141, miR-429) is significantly downregulated in bCSCs (203). Overexpression of miR-200c inhibits clonogenicity and tumor-initiation potential of bCSCs, mainly through suppressing Notch signaling and its component JAG1 (201, 204). Similarly, miR-205 and miR-200 families are significantly downregulated in post-EMT metastatic BC, and thus overexpression of the miR200 family prevents TGF- β -induced EMT by negatively regulating both ZEB1 and ZEB2 (205). Let-7 miRNA, downregulated in bCSCs, is mainly engaged in restricting cell-cycle progression, self-renewal, and pluripotency of bCSCs by regulating factors like H-RAS, E2F2, and HMGA2 (206). Let-7 miRNA can block self-renewal of bCSCs in ER+ BC background by targeting the Wnt/ β -catenin pathway (207). Similarly, miR-30 negatively regulates the stemness of bCSCs and is significantly downregulated in bCSCs. Hence, overexpression of miR-30 diminishes anoikis resistance and self-renewal potential of bCSCs by directly targeting integrin β 3 and ubiquitin-conjugating enzyme 9 (208). Overexpression of miR-600 inhibits bCSC self-renewal and decreases *in vivo* tumorigenicity by inhibiting the Wnt/ β -catenin pathway, as it targets the enzyme, SCD1, essential for producing active WNT proteins (209). Therefore, in absence of miR-600, the activated Wnt signaling promotes self-renewal, whereas overexpression of miR-600 induces bCSC differentiation into BC cells. Likewise, miR-34a restricts bCSC stemness and chemoresistance to doxorubicin *via* directly inhibiting the Notch signaling pathway. Notably, miR-34a is downregulated in bCSCs, and hence, overexpression of miR-34a inhibits the Notch signaling pathway, sensitizes bCSCs to paclitaxel, and inhibits BC proliferation, migration, and invasion (210). Similarly, miR-34c has reduced expression in breast CSCs, and overexpressing it significantly interferes with EMT, migration, and self-renewal properties through targeting Notch4 (211).

Oncogenic miRNAs (OncomiR) in bCSCs

Unlike tumor suppressor miRs, oncomiRs such as miR-21, miR-22, miR-155, miR-181, miR-9, and miR-221/222 cluster, show aberrant expression, and stimulate breast tumor growth, by suppressing apoptotic pathways, allowing proliferation, migration, invasion, and cell-cycle progression (3). Hence, strategies that target oncomiR can effectively block bCSC survival and function. miR-155 stimulates bCSC chemoresistance to doxorubicin by targeting CD44, CD90, and ABCG2, and inhibiting miR-155 resensitizes MDA-MB-231 BC cells to doxorubicin (212). Similarly, miR-181 also offers to be a promising therapeutic target to restrict bCSC function as it stimulates bCSC self-renewal potential and colony-formation properties (213). The miR-181/BRCA1 axis has been suggested to promote bCSC phenotypes in primary BC settings. Interestingly, a positive correlation is found between TGF- β expression level and miR-181/BRCA1 pathway activation in primary breast tumor samples (214). TGF- β pathway promotes bCSC population by inducing miR-181 at the posttranscriptional level and downregulating ATM kinase (215). An upregulated expression of miR-21 is positively correlated with poor prognosis, metastasis, and advanced stages of BC (216). miR-21 stimulates proliferation of BC cells and inhibition of apoptosis *via* suppressing tumor suppressors like PTEN, tropomyosin α 1 (TPM1), and programmed cell death protein 4 (PDCD4) (7, 217, 218). Importantly, in BC cells, miR-21 regulates EMT through inhibition of PTEN function *via* p-AKT and p-ERK pathways, and re-expression of miR-21 leads to the acquisition of EMT phenotype in bCSCs with the activation of mesenchymal markers (vimentin, N-cadherin, α -SMA) (219, 220). Another important piece of evidence recognizes miR-22 as a crucial epigenetic modifier, regulating stemness, EMT, and metastasis in BC by silencing TET family-dependent chromatin remodeling (221). Importantly, two other oncomiRs, miR-9 and miR-221, are associated with poor clinical outcomes in BC patients. An enhanced expression of both miR-9 and miR-221 leads to an increase in the SP colonies with CSC-like features, and radically increasing bCSC stemness, migration, and invasion *via* upregulating Oct-4, Nanog, and CD133. However, knockdown of both miR-9 and miR-221 reduced the number of SP colonies and accordingly reduced bCSC self-renewal potency, migration, and invasion (222). Therefore, drugs targeting this class of drug-resistant oncomiRs can resensitize the BC cells to chemotherapies. Recently, MSC-released exosomes, containing specific miRNA sequences, are being utilized for the targeted killing of chemoresistant bCSCs (201, 223).

MECHANISMS AND APPROACHES TO OVERCOME MULTIMODAL DRUG RESISTANCE

In this section, we review the recent development of bCSC-targeting therapeutic platforms, based on small-molecule inhibitors, nanotherapeutics, molecules affecting different BC

signaling networks, and bCSC-specific immunotherapy for targeting breast cancer-associated multidrug resistance.

ALDH1 Inhibitors, HIF1 α Inhibitors, and EGFR/HER2 Inhibitors

The previously established bCSC marker, ALDH, is a prerequisite for the maintenance of the drug-tolerant breast cancer stem-like population as it protects them from ROS-associated toxic effects (224). Since the ALDH^{high}CD44⁺ subpopulation reflects higher metastatic ability both *in vitro* and *in vivo* relative to ALDH^{low}CD44[−] and shows resistance to standard cancer therapies, inhibition of ALDH activity through all-trans retinoic acid (ATRA) or diethylaminobenzyldehyde (DEAB) sensitizes this population to treatment (51). ATRA reduces the activity of both ALDH1A1 and ALDH3A1 and stimulates CSC differentiation. Hence, combination therapy of ATRA with a standard chemotherapy regimen could fetch promising results for eliminating bCSCs. The HIF family members, HIF1 α and HIF2 α , are crucial regulators of cancer stemness (135). Mechanistically, HIF1 α activates the survival genes in hypoxic conditions, whereas HIF2 α interacts with the promoter of Oct4 and Nanog. Hence, HIFs are critical for the chemoresistance exerted by bCSCs (135). This study proposes that the treatment of human BC cells with chemotherapeutic agents such as paclitaxel and gemcitabine leads to survival and enrichment of bCSCs, which in turn depends on the HIFs. Studies involving mice breast tumor models further elaborated that chemotherapy along with HIF inhibitors, such as digoxin (interferes with HIF1 α translation) or acriflavine (inhibits dimerization of HIF1 α or HIF2 α with HIF1 β), might improve the survival of BC patients (225–227). Several HIF1 inhibitors including 2-methoxyestradiol, BAY 87-2243, and PX-478 2HCI are, therefore, undergoing clinical trials (228). Moreover, inhibition of the EGFR/HER2 signaling axis by lapatinib blocked the expression of ABC transporter proteins, ABCB1 and ABCG2, which sensitizes MCF-7 tumor spheres to doxorubicin (229).

Targeting Signaling Pathways in bCSCs

There is an intricate relationship between bCSC maintenance and Notch, PI3K/AKT/mTOR, Wnt/ β -catenin, and Hedgehog signaling pathways. The interplay between these signaling pathways also influences the disease outcomes in BC progression. Therefore, targeting these pathways serve as an essential strategy to restrict bCSC expansion and overcome drug resistance phenomena.

Notch Signaling

Deregulated Notch signaling in bCSCs represents poor clinical outcomes in drug-resistant BC. Evolutionarily conserved Notch signaling is linked with cell differentiation and cell fate decisions. Notch signaling pathways include 4 receptors (Notch1–4) and 5 ligands such as delta-like ligand (DLL)1, DLL3, DLL4, JAG1, and JAG2 (230, 231). Interaction with the Notch ligand leads to the release of its intracellular domain (NICD), which then translocates to the nucleus and impacts gene expression in association with different transcription factors. Studies have established links between bCSCs, aberrant Notch signaling, and radio-/endocrine-/chemoresistance. A significantly higher

expression of activated Notch1 is noted in the culture media of bCSCs, postradiation (66). A substantial induction of the JAG1 ligand is also evident on the surface of nonadherent bCSCs after fractionated radiation (232). Both JAG1 and Notch pathway contributes to chemoresistance in BC metastasizing to bone (233). Moreover, suppression of Notch1 signaling enhances antitumor efficacy of chemotherapy agents *via* reduction of bCSCs in TNBC (234). Notably, Notch ligand DLL1+ quiescent bCSCs drive chemoresistance *via* NF κ B pathway in BC (235), and disease progression in ER+ BC is dependent on DLL1-mediated Notch1 signaling in bCSCs (236). Notch1 ligands, JAG1, and JAG2 are also overexpressed in endocrine-resistant luminal BC, resulting in an increased bCSC activity (237). Therefore, the blockade of Notch signaling is of clinical importance to eradicate resistant bCSCs and offer long-term disease-free survival.

PI3K/AKT/mTOR Signaling

PI3K is a family of lipid kinases that phosphorylate phosphatidylinositol (PI) at the intracellular membrane and plasma membranes. An increased PI3K/AKT/mTOR signaling in bCSCs has been documented over the years, contributing to survival, proliferation, metastasis, and drug resistance in BC cells (238, 239). Mutations, specifically in its catalytic domain, p110 α , are the most frequent genetic events, affecting around one-third of BC patients. Alterations in the PI3K/AKT/mTOR pathway in bCSCs result in the TAM resistance in ER+ BC (240, 241). The interaction between PI3K and Wnt/ β -catenin pathway is responsible for stemness and self-renewal abilities of bCSCs (242). Therefore, small-molecule inhibitors targeting the key players, PI3K, AKT, and mTOR can reverse the drug resistance and self-renewal abilities of breast cancer stem-like cells. Pan-PI3K inhibitors, such as buparlisib and pictilisib (inhibiting p110 α / β / γ / δ); PI3K isoform-specific inhibitors such as alpelisib and taselisib (inhibiting p110 α and p110 α / γ / δ , respectively); AKT inhibitors such as ipatasertib, capivasertib (AZD5363), and vevorisertib (MK-2206); PI3K/AKT dual inhibitor gedatolisib (PF-05212384); and mTOR inhibitors such as everolimus, vistusertib, and sapanisertib are currently available for the treatment of BC (243). B591, a novel PI3K inhibitor, has shown promising results in targeting breast CSCs in the mouse xenograft model, affecting both its self-renewal potential and EMT (244). However, despite substantial preclinical evidence, the innate and acquired resistance has limited the application of this group of inhibitors in BC.

Wnt/ β -Catenin Signaling

Wnt/ β -catenin signaling contributes to self-renewal, migration, and invasion of bCSCs, leading to systematic dissemination in BC. A significantly higher level of Wnt/ β -catenin signaling is noted in bCSCs compared with the bulk of the tumor (245). Hence, Wnt/ β -catenin signaling serves as a novel target for restricting BC progression. A highly potent small-molecule inhibitor CWP232228 can preferentially inhibit bCSC proliferation *via* antagonizing the binding of β -catenin to T-cell factor (TCF) in the nucleus (246). Another natural product, gomisins M2, downregulates Wnt/ β -catenin signaling and

inhibits bCSC proliferation, mammosphere formation, and self-renewal (247). Studies indicate multiple interaction points or crosstalk between Notch and Wnt/ β -catenin signaling pathways, and thus it is essential to focus on Notch-Wnt synergies in BC progression (248). In a normal mammary setting, in response to Notch ligand DLL1, macrophages express Wnt ligands (Wnt3, Wnt10A, and Wnt16), important for mammary stem cell numbers and activity (249). Thus, the proteins exerting regulatory effects on both these pathways should serve as a novel therapeutic target and targeted in BC. GSK3 β is one such protein that regulates β -catenin stability as well as phosphorylates Notch ICD (250).

Hedgehog Signaling

The Hh signaling is another novel target in BC since it is frequently upregulated in bCSCs and contributes to CSC self-renewal and stemness maintenance. The cancer-associated fibroblasts (CAFs) within TME support the maintenance of CSC function in breast tumors *via* their regulation of both Wnt/ β -catenin and Hh signaling. Briefly, CAFs promote BC progression through proliferation, invasion, matrix remodeling (*via* matrix production and crosslinking, matrix stiffness, force-mediated matrix remodeling), macrophage, and endothelial cell crosstalk (*via* secretion of VEGF, exosomes, HGF production), chemoresistance, and immunosuppression (251–253). Notably, BC shows divergent CAF phenotypes, including FAP-positive (fibroblast-activating protein α 1) CAFs driving immunosuppression and resistance to PD-L1 therapy (254). According to Friedman et al., two distinct subpopulations of CAFs (S100A4+ and PDPN+) exist in human breast tumors, where their ratio decides the clinical outcomes across subtypes and is highly correlated with BRCA mutations in TNBC (255). The interaction between the breast cancer cell and fibroblasts also induces the CAF phenotype through activation of Notch signaling (256). Hence, understanding the full repertoire of CAFs and the dynamic changes as breast tumors evolve can improve the precision of treatment and reverse drug resistance. BCSCs secrete the Hedgehog ligand, SHH, which controls CAFs through activation of Hh signaling (257). The CAFs, in turn, secrete some factors that result in the expansion and self-renewal of bCSCs. Therapeutic targeting of CAFs using the inhibitor molecule of Smoothed, the main effector molecule of the Hh pathway, sensitizes TNBC xenograft models to docetaxel (258). Tetraspanin 8 (TSPAN8), a membrane glycoprotein, enhances BC stemness by activating SHH signaling (259). Activation of Hh signaling results in salinomycin resistance in tumor spheres, generated from the MCF-7 cell line (260). However, the inhibition of the Hh pathway by cyclopamine can sensitize the MCF-7 cells to paclitaxel. Therefore, exploring the detailed mechanisms of Hh-driven bCSC signaling can help in the designing of novel drug candidates to reverse BC drug resistance.

Targeting bCSC Metabolism

Maintenance of a reduced level of ROS through metabolic reprogramming is one of the strategies adopted by bCSCs to avoid oxidative stress, which is attributed to the higher expression of ROS scavengers including glutathione peroxidase, superoxide dismutase, and catalase. There is a close association

between ROS levels and bCSC-driven radioresistance. Pharmacological inhibition of ROS scavengers in bCSCs distinctly reduces their clonogenicity potential, resulting in radiosensitization (261). Moreover, ROS generating drugs can target drug-resistant bCSCs through induction of premature senescence (262). To mitigate a higher energy demand of fast-growing tumor cells, bCSCs further reshape their metabolic machinery. BCSCs are metabolically plastic, which allows them to dynamically switch their metabolic state to favor glycolysis or oxidative phosphorylation (OXPHOS). Unlike the non-CSCs that majorly depend on glycolysis, bCSCs can favor either glycolysis or OXPHOS, depending on the niche. The glycolytic switch in CSCs, in general, contributes to stemness. Metabolic switching from OXPHOS to glycolytic phenotype, known as the Warburg effect, is another survival adaptation exhibited by bCSCs, to sustain growth in nutrient-deprived or hypoxic environments (263–265). Since BCL-2 protein is a crucial regulator of mitochondrial respiration, inhibition of BCL-2 prevents OXPHOS (266). This, in turn, reduces the bCSC burden that depends on OXPHOS. Several OXPHOS-targeting compounds, such as atovaquone, arsenic trioxide, and phenformin are undergoing clinical trials for different solid tumors (267, 268). Interestingly, CSCs with metastatic potential follows a distinct metabolic signature. According to Luo et al., metabolic or oxidative stress plays a crucial role concerning bCSCs' plasticity between quiescent mesenchymal-like (M) state and proliferative epithelial-like (E) state. Oxidative stress produced due to H₂O₂, 2DG, and hypoxia regulates the transition from ROS^{low} M-bCSCs into ROS^{High} E-bCSCs (269). Importantly, hexokinase 2, which catalyzes the initial step of glucose metabolism, is a major target of metformin for altering bCSC metabolism. Therefore, exploiting the metabolic switching of bCSCs could essentially provide a novel platform targeting the multidrug-resistant bCSC population.

Nanotherapeutics Against bCSCs

Nanoparticle-based drug carriers (nanocarriers) are often used to specifically deliver chemotherapeutic drugs, siRNAs, miRNAs, and antibodies, designed based on identifying antibodies/aptamers against bCSC-specific markers (**Figure 5A**) (270, 271). Due to the site-specific delivery and improved stability and bioavailability, nanocarriers are appearing as novel platforms for targeting (1) bCSC-specific antigens such as CD44 and ALDH1, (2) drug-efflux ABC transporters (ABCB1 and ABCG2), (3) self-renewing signaling pathways, (4) autophagy process, (5) metabolism, and (6) TME. Sahli et al. developed a triple-drug delivery platform, composed of paclitaxel, verteporfin, and combretastatin (CA4) inside polymer-lipid hybrid nanoparticles to target bCSCs and associated tumor vasculature (272). Gao et al. have further improvised these smart platforms to simultaneously target bCSCs and bulk breast tumor cells by encapsulating the combination of bCSC-specific inhibitor with a chemotherapeutic agent, along with a phytochemical agent or RNA-based therapy (273). HA-modified mesoporous silica nanoparticles loaded with 8 hydroxyquinoline consisting of docetaxel have been designed to eliminate bCSCs (274). This HA modification enables an enhanced uptake of nanoparticles by bCSCs. Another novel

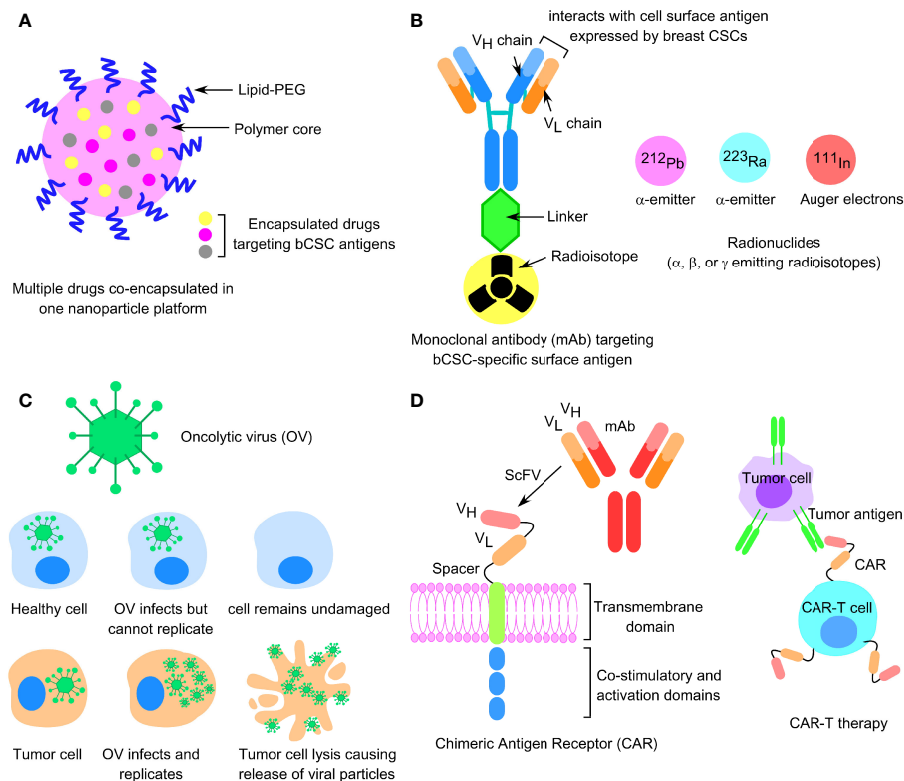


FIGURE 5 | Novel upcoming strategies to reverse bCSC drug resistance. **(A)** Cartoon structure of a nanoparticle-based drug carrier encapsulated with multiple chemotherapeutic drugs targeting bCSC antigens. **(B)** α- or β-emitting radionuclide conjugated with monoclonal antibody targeting breast CSC-specific antigens. **(C)** Design of oncolytic viral particles targeting tumor cells. **(D)** Cartoon representation of chimeric antigen receptor (CAR-T therapy) against CSC surface antigens.

chitosan-decorated doxorubicin-encapsulated nanocarrier has been developed to target CD44 surface receptors of bCSCs (275). Recently, a nanocarrier system using PEG-PLA copolymers has been designed for the delivery of autophagy inhibitor molecule, chloroquine, in complex with doxorubicin and docetaxel to eliminate both bCSCs and non-bCSCs (276). Since bCSCs require a specialized niche to survive, nanoparticle-based platforms targeting ECM modifying enzyme lysyl oxidase result in TME disruption (277). A novel HA-based platform encapsulating CD44-targeted docetaxel conjugate is another example of nanocarrier, killing both bCSCs and non-bCSCs (278).

bCSC-Targeting Strategy Focusing on Immunotherapy

Since CSCs exhibit distinct immune characteristics and express specific immune markers, targeting those molecules as a part of immunotherapy is employed to target CSCs. Different strategies like DC vaccine, adoptive T-cell transfer, oncolytic virus, ICIs, and combination therapies are recent approaches to target bCSCs.

DC-Based Vaccine

DCs loaded with CSC lysate or mRNA, administered as vaccines, are capable of eliciting cancer-specific immune responses (279).

Notably, DCs are the professional antigen-presenting cells (APCs) that process the antigenic material and present peptide antigens to T cells and activate them. Interestingly, DCs in BC patients exhibit decreased antigen uptake, reduced antigen processing, reduced expression of costimulators, weak migration profile, along decreased IL-12 production (280, 281). Patients with advanced breast and ovarian cancers can be successfully vaccinated by DC loaded with HER2/Neu- or MUC1-derived antigenic peptides (282). Phase-I clinical trial with metastatic BC showed that fusion of breast tumor cells with DCs resulted in immunological and clinical antitumor responses (283). DC pulsed with breast tumor lysate has proved to be a standard method for a source of BC antigen, capable of eliciting anticancer immune responses (284). BCSC-RNA-pulsed DC vaccine also effectively kills breast tumor cells through activation of CD4⁺ T_H lymphocytes and CD8⁺ cytotoxic T cells. This study highlights the efficacy of bCSC-RNA for priming DC cells in evoking immune response against drug-resistant CSC populations. However, DC-based vaccines present a few drawbacks; they are both cost-effective and time-consuming for patient-specific treatment. Factors like antigenic peptide or CSC-RNA loading on DC, route of administration, and doses are yet to be standardized to resolve these technical limitations.

Adoptive T-Cell Therapy

Adoptive T-cell therapy is a personalized mode of immunotherapy to target CSCs. Here, tumor immune lymphocytes (TILs) with intrinsic antitumor activity are isolated from cancer-bearing patients. Following isolation, TILs are cultured in the presence of IL-2 so that they can recognize tumor-associated antigens on cancer cells, and eventually release cytotoxic cytokines, perforin, and granzymes (285). The recent approach focuses on designing CAR-T cells against the CSC surface antigens in different cancer models to achieve complete regression of tumor (286). CARs generally constitute the extracellular binding domain, a single-chain variable fragment (scFv) specific for a tumor antigen, an extracellular spacer domain, a transmembrane domain, followed by an intracellular signaling domain (**Figure 5D**). EGFR-specific CAR-T cells have shown promising results in high EGFR-expressing TNBC cell lines and patient-derived xenograft mouse models (287). Another recent report highlights promising results for HER2-specific second-generation CAR-T therapy for the treatment of breast-to-brain metastasis (288). Other bCSC markers targeted by CAR-T therapy include c-Met, CD133, CD166, CD47, EpCAM, and LGR5 (55, 289, 290). Despite the remarkable clinical success of CAR-T therapy in hematologic cancers, its application is limited in solid tumors. Due to the lack of chemokine expression required for the infiltration of CAR-T cells into the tumor tissues and dense fibrotic matrix in solid tumors, the ability of CAR to get recruited at the tumor site and infiltrate is considerably affected (291). Frequently, CAR-T cells fail to penetrate the tumor tissues through the vascular endothelium (292). Therefore, instead of systemic administration, regional administration of CAR-T cells in solid cancers will be more effective. Altogether, the major limitation of this approach includes burdensome and expensive preparation to isolate the patient-derived T cells and the major side effects resulting from cytokine release syndrome.

Oncolytic Viral Therapy

Oncolytic viruses (OVs), a novel class of DNA/RNA-attenuated viruses that selectively infect, replicate inside the tumor cells, and eventually kill them either through modulating the TME or *via* antitumor response (**Figure 5C**) (293). These naturally occurring or genetically engineered viruses have the potential to convert an “immunologically cold” TME into an “immunologically hot” one by increasing the net influx of TILs, consisting of CD4+ and CD8+ T cells, B cells, and NK cells (293, 294). Activated CD8+ cytotoxic T cells and NK cells are associated with a good prognosis, whereas the presence of Foxp3+ Treg cells within the breast TME is associated with a poor prognosis, due to their role in immunosuppression. Immunologically “cold” tumors exhibit a low mutational burden, poor MHC presentation of tumor antigen, poor migration of TILs, and also have reduced expression of PD-L1 on the surface of tumor cells, thus making the response to ICIs inadequate (295). Interestingly, OVs induce a strong antiviral tumor immune response through the production of cytokines like type-1 interferon that in turn promotes PD-L1 expression on tumor cells and also cytokines, such as CCL3 and CCL4, attracting PD-1+ or CTLA-4+ immune

cells within TME (296). Eriksson et al. indicated that OVs, Ad5/3-Delta24 and Ad5.pk7-Delta 24, can selectively kill CD44+ CD24-/low bCSC population. Oncolytic herpes simplex virus, oHSV G47A, effectively kills bCSCs both *in vitro* and *in vivo*, derived from SK-BR-3 and primary human BC cells (297). A randomized phase II study by Bernstein et al. reported that the combination of oncolytic reovirus (pelareorep) with paclitaxel significantly increased survival of metastatic BC patients (298). Combining pelareorep with paclitaxel, along with anti-PD-L1 antibody, avelumab (NCT04215146) is presently undergoing phase II clinical study in BC patients (299).

Immune Checkpoint Inhibitors

Immune checkpoint ligands such as PD-L1 and PD-L2 are highly expressed on CSCs. The immune cells, on the other hand, express the receptor for these ligands, PD-1. Now, the interaction between PD-1 and PD-L1/PD-L2 interferes with T-cell proliferation and activity, leading to tumor immune suppression, thus serving as a strategy to immune escaping of CSCs (300). Therefore, immune checkpoint blockade of PD-L1/PD-L2 is emerging as a novel therapeutic approach, whereby these CSC-specific ligands are engaged by ICIs, thus making it possible to target CSCs for programmed cell death. Notably, multiple clinical trials on ICIs, targeting CTLA-4, PD-1, and PD-L1 are in progress that are either administered as a single agent or in combination with trastuzumab or with chemotherapeutic drugs, in HER2-enriched and TNBC settings, respectively. In March 2019, FDA has approved the clinical application of anti-PD-L1 antibody, atezolizumab, in combination with nab-paclitaxel, to be administered as the first-line therapy to metastatic or locally advanced PD-L1+ TNBC patients (301). A recent phase Ib clinical study by Nanda et al. explored the antitumor efficacy and safety profile of PD-1 inhibitor molecule pembrolizumab in advanced TNBC patients (302). Furthermore, certain drugs that stimulate PD-L1 degradation can be administered as a combination therapy with ICIs to significantly enhance the efficacy of cancer immunotherapy (303).

CONCLUSION AND PERSPECTIVES

Despite ongoing efforts using novel chemotherapeutics, ICIs, small-molecule inhibitors, or combinations of these innovative therapeutic platforms, bCSC-driven drug resistance remains a public health concern globally. Exploring better bCSC-targeting substitutes is thus the way forward. Radionuclides conjugated with monoclonal antibodies (mAb), administered in radioimmunotherapy (RIT), involve highly potent α - or β -particles to deliver cytotoxic radiation to cancer cells or TME (**Figure 5B**) (304). ^{212}Pb -TCMC-trastuzumab using lead-212 (α -particle emitter), is undergoing phase I clinical trial to study its antitumor effects in HER2+ intraperitoneal cancer patients (305, 306). Another isotope, ^{111}In -NLS-trastuzumab, is being administered to kill trastuzumab-resistant BC cell lines *via* the emission of Auger electrons (307). Recently, radionuclide therapy using ^{223}Ra (α -particle emitter) has been successful in delaying the growth of DTCs in early-stage BC (308). Radioactive

iodine therapy with single-domain antibodies targeting HER2 (^{131}I -GMIB-anti-HER2-VHH1) documents the first-in-human study, demonstrating the safety profile and efficacy of radionuclide in the treatment of HER2+ BC (309). Importantly, RIT is advantageous in the management of MRD, residual tumor margins following surgery, and CTCs in hematologic malignancy, compared with external beam radiation therapy. Likewise, nanobiotechnology should be fully explored to precisely target bCSC-specific novel antigens, to eliminate the same. The efficacy of synthetic nanoparticles, such as silver (AgNPs) (310), gold (AuNPs) (311), and selenium (SeNPs) (312), has been studied extensively in different types of solid cancers. Notably, AgNPs (313) and AuNPs (314) both have shown encouraging results in BC, although the potency of the same in target killing of breast

CSCs is not known. Hence, the potential of this family of radionuclides and nanoparticles should be considered in the targeted killing of bCSCs. In conclusion, cotargeting of multiple signaling networks contributing to bCSC survival and proliferation, by virtue of multimodal targeted therapeutics, will lay the foundation to overcome BC drug resistance.

AUTHOR CONTRIBUTIONS

TS has written the manuscript and prepared the figures and table for the manuscript. KEL has edited the manuscript and provided valuable suggestions and inputs in modifying the manuscript. All authors listed have made a substantial, direct, and intellectual contribution to the work and approved it for publication.

REFERENCES

- Sung H, Ferlay J, Siegel RL, Laversanne M, Soerjomataram I, Jemal A, et al. Global Cancer Statistics 2020: GLOBOCAN Estimates of Incidence and Mortality Worldwide for 36 Cancers in 185 Countries. *CA A Cancer J Clin* (2021) 71:209–49. doi: 10.3322/caac.21660
- Abad E, Graifer D, Lyakhovich A. DNA Damage Response and Resistance of Cancer Stem Cells. *Cancer Lett* (2020) 474:106–17. doi: 10.1016/j.canlet.2020.01.008
- Niu T, Zhang W, Xiao W. MicroRNA Regulation of Cancer Stem Cells in the Pathogenesis of Breast Cancer. *Cancer Cell Int* (2021) 21:31. doi: 10.1186/s12935-020-01716-8
- Al-Hajj M, Wicha MS, Benito-Hernandez A, Morrison SJ, Clarke MF. Prospective Identification of Tumorigenic Breast Cancer Cells. *Proc Natl Acad Sci* (2003) 100:3983–8. doi: 10.1073/pnas.0530291100
- Wang J, Liu X, Jiang Z, Li L, Cui Z, Gao Y, et al. A Novel Method to Limit Breast Cancer Stem Cells in States of Quiescence, Proliferation or Differentiation: Use of Gel Stress in Combination With Stem Cell Growth Factors. *Oncol Lett* (2016) 12:1355–60. doi: 10.3892/ol.2016.4757
- Zheng Q, Zhang M, Zhou F, Zhang L, Meng X. The Breast Cancer Stem Cells Traits and Drug Resistance. *Front Pharmacol* (2020) 11:599965. doi: 10.3389/fphar.2020.599965
- O'Bryan S, Dong S, Mathis JM, Alahari SK. The Roles of Oncogenic miRNAs and Their Therapeutic Importance in Breast Cancer. *Eur J Cancer* (2017) 72:1–11. doi: 10.1016/j.ejca.2016.11.004
- Quagliano E, Conti L, Cavallo F. Breast Cancer Stem Cell Antigens as Targets for Immunotherapy. *Semin Immunol* (2020) 47:101386. doi: 10.1016/j.smim.2020.101386
- Dees S, Ganesan R, Singh S, Grewal IS. Emerging CAR-T Cell Therapy for the Treatment of Triple-Negative Breast Cancer. *Mol Cancer Ther* (2020) 19:2409–21. doi: 10.1158/1535-7163.MCT-20-0385
- Zhao Y, Alakhova DY, Kabanov AV. Can Nanomedicines Kill Cancer Stem Cells? *Adv Drug Deliv Rev* (2013) 65:1763–83. doi: 10.1016/j.addr.2013.09.016
- Harbeck N, Penault-Llorca F, Cortes J, Gnant M, Houssami N, Poortmans P, et al. Breast Cancer. *Nat Rev Dis Primers* (2019) 5:66. doi: 10.1038/s41572-019-0111-2
- Sorlie T, Perou CM, Tibshirani R, Aas T, Geisler S, Johnsen H, et al. Gene Expression Patterns of Breast Carcinomas Distinguish Tumor Subclasses With Clinical Implications. *Proc Natl Acad Sci* (2001) 98:10869–74. doi: 10.1073/pnas.191367098
- Lukong KE. Understanding Breast Cancer – The Long and Winding Road. *BBA Clin* (2017) 7:64–77. doi: 10.1016/j.bbacli.2017.01.001
- Kumar P, Aggarwal R. An Overview of Triple-Negative Breast Cancer. *Arch Gynecol Obstet* (2016) 293:247–69. doi: 10.1007/s00404-015-3859-y
- Prat A, Pineda E, Adamo B, Galván P, Fernández A, Gaba L, et al. Clinical Implications of the Intrinsic Molecular Subtypes of Breast Cancer. *Breast* (2015) 24 Suppl 2:S26–35. doi: 10.1016/j.breast.2015.07.008
- Foulkes WD, Smith IE, Reis-Filho JS. Triple-Negative Breast Cancer. *N Engl J Med* (2010) 363:1938–48. doi: 10.1056/NEJMra1001389
- Brasó-Maristany F, Griguolo G, Pascual T, Paré L, Nuciforo P, Llombart-Cussac A, et al. Phenotypic Changes of HER2-Positive Breast Cancer During and After Dual HER2 Blockade. *Nat Commun* (2020) 11:385. doi: 10.1038/s41467-019-14111-3
- METABRIC Group, Curtis C, Shah SP, Chin S-F, Turashvili G, Rueda OM, et al. The Genomic and Transcriptomic Architecture of 2,000 Breast Tumours Reveals Novel Subgroups. *Nature* (2012) 486:346–52. doi: 10.1038/nature10983
- Russnes HG, Lingjaerde OC, Børresen-Dale A-L, Caldas C. Breast Cancer Molecular Stratification. *Am J Pathol* (2017) 187:2152–62. doi: 10.1016/j.ajpath.2017.04.022
- Turner KM, Yeo SK, Holm TM, Shaughnessy E, Guan J-L. Heterogeneity Within Molecular Subtypes of Breast Cancer. *Am J Physiol Cell Physiol* (2021) 321:C343–54. doi: 10.1152/ajpcell.00109.2021
- Russano M, Napolitano A, Ribelli G, Iuliani M, Simonetti S, Citarella F, et al. Liquid Biopsy and Tumor Heterogeneity in Metastatic Solid Tumors: The Potentiality of Blood Samples. *J Exp Clin Cancer Res* (2020) 39:95. doi: 10.1186/s13046-020-01601-2
- Gerlinger M, Rowan AJ, Horswell S, Larkin J, Endesfelder D, Gronroos E, et al. Intratumor Heterogeneity and Branched Evolution Revealed by Multiregion Sequencing. *N Engl J Med* (2012) 366:883–92. doi: 10.1056/NEJMoa1113205
- Alimirzaie S, Bagherzadeh M, Akbari MR. Liquid Biopsy in Breast Cancer: A Comprehensive Review. *Clin Genet* (2019) 95:643–60. doi: 10.1111/cge.13514
- Alba-Bernal A, Lavado-Valenzuela R, Domínguez-Recio ME, Jiménez-Rodríguez B, Queipo-Ortuño MI, Alba E, et al. Challenges and Achievements of Liquid Biopsy Technologies Employed in Early Breast Cancer. *EBioMedicine* (2020) 62:103100. doi: 10.1016/j.ebiom.2020.103100
- Kingston B, Cutts RJ, Bye H, Beaney M, Walsh-Crestani G, Hrebien S, et al. Genomic Profile of Advanced Breast Cancer in Circulating Tumour DNA. *Nat Commun* (2021) 12:2423. doi: 10.1038/s41467-021-22605-2
- Diehl F, Schmidt K, Choti M, Romans K, Goodman S, Li M, et al. Circulating Mutant DNA to Assess Tumor Dynamics. *Nat Med* (2008) 14:985–90. doi: 10.1038/nm.1789
- Yuan T, Huang X, Woodcock M, Du M, Dittmar R, Wang Y, et al. Plasma Extracellular RNA Profiles in Healthy and Cancer Patients. *Sci Rep* (2016) 6:19413. doi: 10.1038/srep19413
- Desmedt C, Voet T, Sotiriou C, Campbell PJ. Next-Generation Sequencing in Breast Cancer: First Take Home Messages. *Curr Opin Oncol* (2012) 24:597–604. doi: 10.1097/CCO.0b013e328359554e
- Roy-Chowdhuri S, de Melo Gagliato D, Routbort MJ, Patel KP, Singh RR, Broadus R, et al. Multigene Clinical Mutational Profiling of Breast Carcinoma Using Next-Generation Sequencing. *Am J Clin Pathol* (2015) 144:713–21. doi: 10.1309/AJCPWDEQYCYC92JQ

30. Steinbichler TB, Dudás J, Skvortsov S, Ganswindt U, Riechelmann H, Skvortsova I-I. Therapy Resistance Mediated by Cancer Stem Cells. *Semin Cancer Biol* (2018) 53:156–67. doi: 10.1016/j.semcancer.2018.11.006
31. Kleffel S, Schatton T. Tumor Dormancy and Cancer Stem Cells: Two Sides of the Same Coin? *Adv Exp Med Biol* (2013) 734:145–79. doi: 10.1007/978-1-4614-1445-2_8
32. Morel A-P, Lièvre M, Thomas C, Hinkal G, Ansieau S, Puisieux A. Generation of Breast Cancer Stem Cells Through Epithelial-Mesenchymal Transition. *PLoS One* (2008) 3:e2888. doi: 10.1371/journal.pone.0002888
33. Pinto CA, Widodo E, Waltham M, Thompson EW. Breast Cancer Stem Cells and Epithelial Mesenchymal Plasticity – Implications for Chemoresistance. *Cancer Lett* (2013) 341:56–62. doi: 10.1016/j.canlet.2013.06.003
34. Kröger C, Afeyan A, Mraz J, Eaton EN, Reinhardt F, Khodor YL, et al. Acquisition of a Hybrid E/M State Is Essential for Tumorigenicity of Basal Breast Cancer Cells. *Proc Natl Acad Sci USA* (2019) 116:7353–62. doi: 10.1073/pnas.1812876116
35. Liu S, Cong Y, Wang D, Sun Y, Deng L, Liu Y, et al. Breast Cancer Stem Cells Transition Between Epithelial and Mesenchymal States Reflective of Their Normal Counterparts. *Stem Cell Rep* (2014) 2:78–91. doi: 10.1016/j.stemcr.2013.11.009
36. Korkaya H, Kim G, Davis A, Malik F, Henry NL, Ithimakin S, et al. Activation of an IL6 Inflammatory Loop Mediates Trastuzumab Resistance in HER2+ Breast Cancer by Expanding the Cancer Stem Cell Population. *Mol Cell* (2012) 47:570–84. doi: 10.1016/j.molcel.2012.06.014
37. Prasetyanti PR, Medema JP. Intra-Tumor Heterogeneity From a Cancer Stem Cell Perspective. *Mol Cancer* (2017) 16:41. doi: 10.1186/s12943-017-0600-4
38. Greaves M, Maley CC. Clonal Evolution in Cancer. *Nature* (2012) 481:306–13. doi: 10.1038/nature10762
39. Nowell PC. The Clonal Evolution of Tumor Cell Populations: Acquired Genetic Lability Permits Stepwise Selection of Variant Sublines and Underlies Tumor Progression. *Science* (1976) 194:23–8. doi: 10.1126/science.959840
40. Thankamony AP, Saxena K, Murali R, Jolly MK, Nair R. Cancer Stem Cell Plasticity – A Deadly Deal. *Front Mol Biosci* (2020) 7:79. doi: 10.3389/fmolb.2020.00079
41. Liu Y, Yang M, Luo J, Zhou H. Radiotherapy Targeting Cancer Stem Cells “Awakens” Them to Induce Tumour Relapse and Metastasis in Oral Cancer. *Int J Oral Sci* (2020) 12:19. doi: 10.1038/s41368-020-00087-0
42. Li W, Ma H, Zhang J, Zhu L, Wang C, Yang Y. Unraveling the Roles of CD44/CD24 and ALDH1 as Cancer Stem Cell Markers in Tumorigenesis and Metastasis. *Sci Rep* (2017) 7:13856. doi: 10.1038/s41598-017-14364-2
43. Bourguignon LYW, Wong G, Earle C, Krueger K, Spevak CC. Hyaluronan-CD44 Interaction Promotes C-Src-Mediated Twist Signaling, microRNA-10b Expression, and RhoA/RhoC Up-Regulation, Leading to Rho-Kinase-Associated Cytoskeleton Activation and Breast Tumor Cell Invasion. *J Biol Chem* (2010) 285:36721–35. doi: 10.1074/jbc.M110.162305
44. Ponti D, Costa A, Zaffaroni N, Pratesi G, Petrangolini G, Coradini D, et al. Isolation and *In Vitro* Propagation of Tumorigenic Breast Cancer Cells With Stem/Progenitor Cell Properties. *Cancer Res* (2005) 65:5506–11. doi: 10.1158/0008-5472.CAN-05-0626
45. Bourguignon LYW, Spevak CC, Wong G, Xia W, Gilad E. Hyaluronan-CD44 Interaction With Protein Kinase C(epsilon) Promotes Oncogenic Signaling by the Stem Cell Marker Nanog and the Production of microRNA-21, Leading to Down-Regulation of the Tumor Suppressor Protein PDCD4, Anti-Apoptosis, and Chemotherapy Resistance in Breast Tumor Cells. *J Biol Chem* (2009) 284:26533–46. doi: 10.1074/jbc.M109.027466
46. Croker AK, Goodale D, Chu J, Postenka C, Hedley BD, Hess DA, et al. High Aldehyde Dehydrogenase and Expression of Cancer Stem Cell Markers Selects for Breast Cancer Cells With Enhanced Malignant and Metastatic Ability. *J Cell Mol Med* (2009) 13:2236–52. doi: 10.1111/j.1582-4934.2008.00455.x
47. Wright MH, Calcagno AM, Salcido CD, Carlson MD, Ambudkar SV, Varticovski L. Brca1 Breast Tumors Contain Distinct CD44+/CD24- and CD133+ Cells With Cancer Stem Cell Characteristics. *Breast Cancer Res* (2008) 10:R10. doi: 10.1186/bcr1855
48. Sansone P, Ceccarelli C, Berishaj M, Chang Q, Rajasekhar VK, Perna F, et al. Self-Renewal of CD133(hi) Cells by IL6/Notch3 Signalling Regulates Endocrine Resistance in Metastatic Breast Cancer. *Nat Commun* (2016) 7:10442. doi: 10.1038/ncomms10442
49. Meyer MJ, Fleming JM, Lin AF, Hussain SA, Ginsburg E, Vonderhaar BK. CD44posCD49fhiCD133/2hi Defines Xenograft-Initiating Cells in Estrogen Receptor-Negative Breast Cancer. *Cancer Res* (2010) 70:4624–33. doi: 10.1158/0008-5472.CAN-09-3619
50. Ginestier C, Hur MH, Charafe-Jauffret E, Monville F, Dutcher J, Brown M, et al. ALDH1 is a Marker of Normal and Malignant Human Mammary Stem Cells and a Predictor of Poor Clinical Outcome. *Cell Stem Cell* (2007) 1:555–67. doi: 10.1016/j.stem.2007.08.014
51. Croker AK, Allan AL. Inhibition of Aldehyde Dehydrogenase (ALDH) Activity Reduces Chemotherapy and Radiation Resistance of Stem-Like ALDHhiCD44+ Human Breast Cancer Cells. *Breast Cancer Res Treat* (2012) 133:75–87. doi: 10.1007/s10549-011-1692-y
52. Sarmiento-Castro A, Caamaño-Gutiérrez E, Sims AH, Hull NJ, James MI, Santiago-Gómez A, et al. Increased Expression of Interleukin-1 Receptor Characterizes Anti-Estrogen-Resistant ALDH+ Breast Cancer Stem Cells. *Stem Cell Rep* (2020) 15:307–16. doi: 10.1016/j.stemcr.2020.06.020
53. Munz M, Baeuerle PA, Gires O. The Emerging Role of EpCAM in Cancer and Stem Cell Signaling. *Cancer Res* (2009) 69:5627–9. doi: 10.1158/0008-5472.CAN-09-0654
54. Mal A, Bukhari AB, Singh RK, Kapoor A, Barai A, Deshpande I, et al. EpCAM-Mediated Cellular Plasticity Promotes Radiation Resistance and Metastasis in Breast Cancer. *Front Cell Dev Biol* (2021) 8:597673. doi: 10.3389/fcell.2020.597673
55. Bacelli I, Schneeweiss A, Riethdorf S, Stenzinger A, Schillert A, Vogel V, et al. Identification of a Population of Blood Circulating Tumor Cells From Breast Cancer Patients That Initiates Metastasis in a Xenograft Assay. *Nat Biotechnol* (2013) 31:539–44. doi: 10.1038/nbt.2576
56. Wang T, Gantier MP, Xiang D, Bean AG, Bruce M, Zhou S-F, et al. EpCAM Aptamer-Mediated Survivin Silencing Sensitized Cancer Stem Cells to Doxorubicin in a Breast Cancer Model. *Theranostics* (2015) 5:1456–72. doi: 10.7150/thno.11692
57. Chaffer CL, Weinberg RA. A Perspective on Cancer Cell Metastasis. *Science* (2011) 331:1559–64. doi: 10.1126/science.1203543
58. Müller A, Homey B, Soto H, Ge N, Catron D, Buchanan ME, et al. Involvement of Chemokine Receptors in Breast Cancer Metastasis. *Nature* (2001) 410:50–6. doi: 10.1038/35065016
59. Liang Z, Yoon Y, Votaw J, Goodman MM, Williams L, Shim H. Silencing of CXCR4 Blocks Breast Cancer Metastasis. *Cancer Res* (2005) 65:967–71. doi: 10.1007/b101891
60. Chatterjee S, Behnam Azad B, Nimmagadda S. The Intricate Role of CXCR4 in Cancer. *Adv Cancer Res* (2014) 124:31–82. doi: 10.1016/B978-0-12-411638-2.00002-1
61. Chen IX, Chauhan VP, Posada J, Ng MR, Wu MW, Adstamongkonkul P, et al. Blocking CXCR4 Alleviates Desmoplasia, Increases T-Lymphocyte Infiltration, and Improves Immunotherapy in Metastatic Breast Cancer. *Proc Natl Acad Sci USA* (2019) 116:4558–66. doi: 10.1073/pnas.1815515116
62. Yi T, Zhai B, Yu Y, Kiyotsugu Y, Raschle T, Eitzkorn M, et al. Quantitative Phosphoproteomic Analysis Reveals System-Wide Signaling Pathways Downstream of SDF-1/CXCR4 in Breast Cancer Stem Cells. *Proc Natl Acad Sci* (2014) 111:E2182–90. doi: 10.1073/pnas.1404943111
63. Chaffer CL, Brueckmann I, Scheel C, Kaestli AJ, Wiggins PA, Rodrigues LO, et al. Normal and Neoplastic Nonstem Cells can Spontaneously Convert to a Stem-Like State. *Proc Natl Acad Sci* (2011) 108:7950–5. doi: 10.1073/pnas.1102454108
64. Gupta PB, Chaffer CL, Weinberg RA. Cancer Stem Cells: Mirage or Reality? *Nat Med* (2009) 15:1010–2. doi: 10.1038/nm0909-1010
65. Reid PA, Wilson P, Li Y, Marcu LG, Bezak E. Current Understanding of Cancer Stem Cells: Review of Their Radiobiology and Role in Head and Neck Cancers. *Head Neck* (2017) 39:1920–32. doi: 10.1002/hed.24848
66. Phillips TM, McBride WH, Pajonk F. The Response of CD24(-/Low)/CD44+ Breast Cancer-Initiating Cells to Radiation. *J Natl Cancer Inst* (2006) 98:1777–85. doi: 10.1093/jnci/djj495
67. Lagadec C, Vlasi E, Della Donna L, Dekmezian C, Pajonk F. Radiation-Induced Reprogramming of Breast Cancer Cells. *Stem Cells* (2012) 30:833–44. doi: 10.1002/stem.1058
68. Lee SY, Jeong EK, Ju MK, Jeon HM, Kim MY, Kim CH, et al. Induction of Metastasis, Cancer Stem Cell Phenotype, and Oncogenic Metabolism in

- Cancer Cells by Ionizing Radiation. *Mol Cancer* (2017) 16:10. doi: 10.1186/s12943-016-0577-4
69. Demicheli R, Miceli R, Moliterni A, Zambetti M, Hrushesky WJM, Retsky MW, et al. Breast Cancer Recurrence Dynamics Following Adjuvant CMF Is Consistent With Tumor Dormancy and Mastectomy-Driven Acceleration of the Metastatic Process. *Ann Oncol* (2005) 16:1449–57. doi: 10.1093/annonc/mdi280
 70. Li X, Lewis MT, Huang J, Gutierrez C, Osborne CK, Wu M-F, et al. Intrinsic Resistance of Tumorigenic Breast Cancer Cells to Chemotherapy. *J Natl Cancer Inst* (2008) 100:672–9. doi: 10.1093/jnci/djn123
 71. Basu S, Dong Y, Kumar R, Jeter C, Tang DG. Slow-Cycling (Dormant) Cancer Cells in Therapy Resistance, Cancer Relapse and Metastasis. *Semin Cancer Biol* (2021) 78:90–103. doi: 10.1016/j.semcancer.2021.04.021 S1044579X2100122X.
 72. Park S-Y, Nam J-S. The Force Awakens: Metastatic Dormant Cancer Cells. *Exp Mol Med* (2020) 52:569–81. doi: 10.1038/s12276-020-0423-z
 73. Banya M, Hartkopf AD, Krawczyk N, Kaiser T, Meier-Stiegen F, Fehm T, et al. Dormancy in Breast Cancer. *Breast Cancer (Dove Med Press)* (2012) 4:183–91. doi: 10.2147/BCTT.S26431
 74. Korentzelos D, Clark AM, Wells A. A Perspective on Therapeutic Pan-Resistance in Metastatic Cancer. *Int J Mol Sci* (2020) 21:E7304. doi: 10.3390/ijms21197304
 75. Sosa MS, Bragado P, Aguirre-Ghiso JA. Mechanisms of Disseminated Cancer Cell Dormancy: An Awakening Field. *Nat Rev Cancer* (2014) 14:611–22. doi: 10.1038/nrc3793
 76. Maniotis AJ, Folberg R, Hess A, Seftor EA, Gardner LMG, Pe'er J, et al. Vascular Channel Formation by Human Melanoma Cells *In Vivo* and *In Vitro*: Vasculogenic Mimicry. *Am J Pathol* (1999) 155:739–52. doi: 10.1016/S0002-9440(10)65173-5
 77. Shirakawa K, Wakasugi H, Heike Y, Watanabe I, Yamada S, Saito K, et al. Vasculogenic Mimicry and Pseudo-Comedo Formation in Breast Cancer. *Int J Cancer* (2002) 99:821–8. doi: 10.1002/ijc.10423
 78. Andonegui-Elguera MA, Alfaro-Mora Y, Cáceres-Gutiérrez R, Caro-Sánchez CHS, Herrera LA, Diaz-Chávez J. An Overview of Vasculogenic Mimicry in Breast Cancer. *Front Oncol* (2020) 10:220. doi: 10.3389/fonc.2020.00220
 79. Liu Z, Sun B, Qi L, Li H, Gao J, Leng X. Zinc Finger E-Box Binding Homeobox 1 Promotes Vasculogenic Mimicry in Colorectal Cancer Through Induction of Epithelial-to-Mesenchymal Transition. *Cancer Sci* (2012) 103:813–20. doi: 10.1111/j.1349-7006.2011.02199.x
 80. Sun T, Zhao N, Zhao X-L, Gu Q, Zhang S-W, Che N, et al. Expression and Functional Significance of Twist1 in Hepatocellular Carcinoma: Its Role in Vasculogenic Mimicry. *Hepatology* (2010) 51:545–56. doi: 10.1002/hep.23311
 81. Liu TJ, Sun BC, Zhao XL, Zhao XM, Sun T, Gu Q, et al. CD133+ Cells With Cancer Stem Cell Characteristics Associates With Vasculogenic Mimicry in Triple-Negative Breast Cancer. *Oncogene* (2013) 32:544–53. doi: 10.1038/onc.2012.85
 82. Sun H, Yao N, Cheng S, Li L, Liu S, Yang Z, et al. Cancer Stem-Like Cells Directly Participate in Vasculogenic Mimicry Channels in Triple-Negative Breast Cancer. *Cancer Biol Med* (2019) 16:299–311. doi: 10.20892/j.issn.2095-3941.2018.0209
 83. Xing P, Dong H, Liu Q, Zhao T, Yao F, Xu Y, et al. ALDH1 Expression and Vasculogenic Mimicry Are Positively Associated With Poor Prognosis in Patients With Breast Cancer. *Cell Physiol Biochem* (2018) 49:961–70. doi: 10.1159/000493227
 84. Haiaty S, Rashidi M-R, Akbarzadeh M, Bazmani A, Mostafazadeh M, Nikanfar S, et al. Thymoquinone Inhibited Vasculogenic Capacity and Promoted Mesenchymal-Epithelial Transition of Human Breast Cancer Stem Cells. *BMC Complement Med Ther* (2021) 21:83. doi: 10.1186/s12906-021-03246-w
 85. Yang WS, SriRamaratnam R, Welsch ME, Shimada K, Skouta R, Viswanathan VS, et al. Regulation of Ferroptotic Cancer Cell Death by GPX4. *Cell* (2014) 156:317–31. doi: 10.1016/j.cell.2013.12.010
 86. Li Z, Chen L, Chen C, Zhou Y, Hu D, Yang J, et al. Targeting Ferroptosis in Breast Cancer. *Biomark Res* (2020) 8:58. doi: 10.1186/s40364-020-00230-3
 87. Hangauer MJ, Viswanathan VS, Ryan MJ, Bole D, Eaton JK, Matov A, et al. Drug-Tolerant Persister Cancer Cells are Vulnerable to GPX4 Inhibition. *Nature* (2017) 551:247–50. doi: 10.1038/nature24297
 88. Taylor WR, Fedorka SR, Gad I, Shah R, Alqahtani HD, Koranne R, et al. Small-Molecule Ferroptotic Agents With Potential to Selectively Target Cancer Stem Cells. *Sci Rep* (2019) 9:5926. doi: 10.1038/s41598-019-42251-5
 89. Chen M-S, Wang S-F, Hsu C-Y, Yin P-H, Yeh T-S, Lee H-C, et al. CHAC1 Degradation of Glutathione Enhances Cystine-Starvation-Induced Necroptosis and Ferroptosis in Human Triple Negative Breast Cancer Cells via the GCN2-Eif2 α -ATF4 Pathway. *Oncotarget* (2017) 8:114588–602. doi: 10.18632/oncotarget.23055
 90. Mai TT, Hamai A, Hienzsch A, Cañeque T, Müller S, Wicinski J, et al. Salinomycin Kills Cancer Stem Cells by Sequestering Iron in Lysosomes. *Nat Chem* (2017) 9:1025–33. doi: 10.1038/nchem.2778
 91. Li Y, Wang X, Yan J, Liu Y, Yang R, Pan D, et al. Nanoparticle Ferritin-Bound Erastin and Rapamycin: A Nanodrug Combining Autophagy and Ferroptosis for Anticancer Therapy. *Biomater Sci* (2019) 7:3779–87. doi: 10.1039/C9BM00653B
 92. Chen N, Karantza-Wadsworth V. Role and Regulation of Autophagy in Cancer. *Biochim Biophys Acta* (2009) 1793:1516–23. doi: 10.1016/j.bbamcr.2008.12.013
 93. Nazio F, Bordini M, Cianfanelli V, Locatelli F, Cecconi F. Autophagy and Cancer Stem Cells: Molecular Mechanisms and Therapeutic Applications. *Cell Death Differ* (2019) 26:690–702. doi: 10.1038/s41418-019-0292-y
 94. Gong C, Song E, Codogno P, Mehrpour M. The Roles of BECN1 and Autophagy in Cancer are Context Dependent. *Autophagy* (2012) 8:1853–5. doi: 10.4161/auto.21996
 95. Wolf J, Dewi DL, Fredebohm J, Müller-Decker K, Flechtenmacher C, Hoheisel JD, et al. A Mammosphere Formation RNAi Screen Reveals That ATG4A Promotes a Breast Cancer Stem-Like Phenotype. *Breast Cancer Res* (2013) 15:R109. doi: 10.1186/bcr3576
 96. Chatterjee M, van Golen KL. Breast Cancer Stem Cells Survive Periods of Farnesyl-Transferase Inhibitor-Induced Dormancy by Undergoing Autophagy. *Bone Marrow Res* (2011) 2011:1–7. doi: 10.1155/2011/362938
 97. Han Y, Fan S, Qin T, Yang J, Sun Y, Lu Y, et al. Role of Autophagy in Breast Cancer and Breast Cancer Stem Cells (Review). *Int J Oncol* (2018) 52:1057–70. doi: 10.3892/ijo.2018.4270
 98. Gong C, Bauvy C, Tonelli G, Yue W, Deloménie C, Nicolas V, et al. Beclin 1 and Autophagy Are Required for the Tumorigenicity of Breast Cancer Stem-Like/Progenitor Cells. *Oncogene* (2013) 32:2261–2272, 2272e.1–11. doi: 10.1038/onc.2012.252
 99. Han Q, Deng Y, Chen S, Chen R, Yang M, Zhang Z, et al. Downregulation of ATG5-Dependent Macroautophagy by Chaperone-Mediated Autophagy Promotes Breast Cancer Cell Metastasis. *Sci Rep* (2017) 7:4759. doi: 10.1038/s41598-017-04994-x
 100. Wang M, Zhang J, Huang Y, Ji S, Shao G, Feng S, et al. Cancer-Associated Fibroblasts Autophagy Enhances Progression of Triple-Negative Breast Cancer Cells. *Med Sci Monit* (2017) 23:3904–12. doi: 10.12659/msm.902870
 101. Yue W, Hamai A, Tonelli G, Bauvy C, Nicolas V, Tharinger H, et al. Inhibition of the Autophagic Flux by Salinomycin in Breast Cancer Stem-Like/Progenitor Cells Interferes With Their Maintenance. *Autophagy* (2013) 9:714–29. doi: 10.4161/auto.23997
 102. Fletcher JI, Haber M, Henderson MJ, Norris MD. ABC Transporters in Cancer: More Than Just Drug Efflux Pumps. *Nat Rev Cancer* (2010) 10:147–56. doi: 10.1038/nrc2789
 103. Lou H, Dean M. Targeted Therapy for Cancer Stem Cells: The Patched Pathway and ABC Transporters. *Oncogene* (2007) 26:1357–60. doi: 10.1038/sj.onc.1210200
 104. Pasello M, Giudice AM, Scotlandi K. The ABC Subfamily A Transporters: Multifaceted Players With Incipient Potentialities in Cancer. *Semin Cancer Biol* (2020) 60:57–71. doi: 10.1016/j.semcancer.2019.10.004
 105. Hirschmann-Jax C, Foster AE, Wulf GG, Nuchtern JG, Jax TW, Gobel U, et al. A Distinct “Side Population” of Cells With High Drug Efflux Capacity in Human Tumor Cells. *Proc Natl Acad Sci* (2004) 101:14228–33. doi: 10.1073/pnas.0400067101
 106. Das S, Mukherjee P, Chatterjee R, Jamal Z, Chatterji U. Enhancing Chemosensitivity of Breast Cancer Stem Cells by Downregulating SOX2 and ABCG2 Using Wedelolactone-Encapsulated Nanoparticles. *Mol Cancer Ther* (2019) 18:680–92. doi: 10.1158/1535-7163.MCT-18-0409
 107. Mukherjee P, Gupta A, Chattopadhyay D, Chatterji U. Modulation of SOX2 Expression Delineates an End-Point for Paclitaxel-Effectiveness in Breast Cancer Stem Cells. *Sci Rep* (2017) 7:9170. doi: 10.1038/s41598-017-08971-2

108. Sun M, Yang C, Zheng J, Wang M, Chen M, Le DQS, et al. Enhanced Efficacy of Chemotherapy for Breast Cancer Stem Cells by Simultaneous Suppression of Multidrug Resistance and Antiapoptotic Cellular Defense. *Acta Biomater* (2015) 28:171–82. doi: 10.1016/j.actbio.2015.09.029
109. Saeki T, Nomizu T, Toi M, Ito Y, Noguchi S, Kobayashi T, et al. Dofequidar Fumarate (MS-209) in Combination With Cyclophosphamide, Doxorubicin, and Fluorouracil for Patients With Advanced or Recurrent Breast Cancer. *J Clin Oncol* (2007) 25:411–7. doi: 10.1200/JCO.2006.08.1646
110. Saxena M, Stephens MA, Pathak H, Rangarajan A. Transcription Factors That Mediate Epithelial–Mesenchymal Transition Lead to Multidrug Resistance by Upregulating ABC Transporters. *Cell Death Dis* (2011) 2:e179–9. doi: 10.1038/cddis.2011.61
111. Kobilite R, Januskeviciene I, Urbanaviciute R, Daniunaite K, Drobnienė M, Ostapenko V, et al. Nongenotoxic ABCB1 Activator Tetraphenylphosphonium Can Contribute to Doxorubicin Resistance in MX-1 Breast Cancer Cell Line. *Sci Rep* (2021) 11:6556. doi: 10.1038/s41598-021-86120-6
112. Singh A, Settleman J. EMT, Cancer Stem Cells and Drug Resistance: An Emerging Axis of Evil in the War on Cancer. *Oncogene* (2010) 29:4741–51. doi: 10.1038/ncr.2010.215
113. Schulz A, Meyer F, Dubrovskaya A, Borgmann K. Cancer Stem Cells and Radioresistance: DNA Repair and Beyond. *Cancers (Basel)* (2019) 11:E862. doi: 10.3390/cancers11060862
114. Zhao H, Duan Q, Zhang Z, Na L, Wu H, Shen Q, et al. Up-Regulation of Glycolysis Promotes the Stemness and EMT Phenotypes in Gemcitabine-Resistant Pancreatic Cancer Cells. *J Cell Mol Med* (2017) 21:2055–67. doi: 10.1111/jcmm.13126
115. Versini A, Colombeau L, Hienzs A, Gaillet C, Retailleau P, Debieu S, et al. Salinomycin Derivatives Kill Breast Cancer Stem Cells by Lysosomal Iron Targeting. *Chemistry* (2020) 26:7416–24. doi: 10.1002/chem.202000335
116. Maugeri-Saccà M, Bartucci M, De Maria R. DNA Damage Repair Pathways in Cancer Stem Cells. *Mol Cancer Ther* (2012) 11:1627–36. doi: 10.1158/1535-7163.MCT-11-1040
117. Sun Y, Wang Z, Na L, Dong D, Wang W, Zhao C. FZD5 Contributes to TNBC Proliferation, DNA Damage Repair and Stemness. *Cell Death Dis* (2020) 11:1060. doi: 10.1038/s41419-020-03282-3
118. Jiao X, Velasco-Velázquez MA, Wang M, Li Z, Rui H, Peck AR, et al. CCR5 Governs DNA Damage Repair and Breast Cancer Stem Cell Expansion. *Cancer Res* (2018) 78:1657–71. doi: 10.1158/0008-5472.CAN-17-0915
119. Lee K-M, Giltneane JM, Balko JM, Schwarz LJ, Guerrero-Zotano AL, Hutchinson KE, et al. MYC and MCL1 Cooperatively Promote Chemotherapy-Resistant Breast Cancer Stem Cells via Regulation of Mitochondrial Oxidative Phosphorylation. *Cell Metab* (2017) 26:633–647.e7. doi: 10.1016/j.cmet.2017.09.009
120. Nnv R, Kundu GC. PO-285 Role of Tumour Associated Macrophages (TAMs) in Regulation of Cancer Stem Cell (CSCs) Enrichment in Breast Cancer. *ESMO Open* (2018) 3:A132. doi: 10.1136/esmoopen-2018-EACR25.316
121. Peng D, Tanikawa T, Li W, Zhao L, Vatan L, Szeliga W, et al. Myeloid-Derived Suppressor Cells Endow Stem-Like Qualities to Breast Cancer Cells Through IL6/STAT3 and NO/NOTCH Cross-Talk Signaling. *Cancer Res* (2016) 76:3156–65. doi: 10.1158/0008-5472.CAN-15-2528
122. Mansour FA, Al-Mazrou A, Al-Mohanna F, Al-Alwan M, Ghebeh H. PD-L1 is Overexpressed on Breast Cancer Stem Cells Through Notch3/mTOR Axis. *Oncotarget* (2020) 9:1729299. doi: 10.1080/2162402X.2020.1729299
123. Akalay I, Janji B, Hasmim M, Noman MZ, André F, De Cremoux P, et al. Epithelial-To-Mesenchymal Transition and Autophagy Induction in Breast Carcinoma Promote Escape From T-Cell-Mediated Lysis. *Cancer Res* (2013) 73:2418–27. doi: 10.1158/0008-5472.CAN-12-2432
124. Dongre A, Rashidian M, Reinhardt F, Bagnato A, Keckesova Z, Ploegh HL, et al. Epithelial-To-Mesenchymal Transition Contributes to Immunosuppression in Breast Carcinomas. *Cancer Res* (2017) 77:3982–9. doi: 10.1158/0008-5472.CAN-16-3292
125. Reiman JM, Knutson KL, Radisky DC. Immune Promotion of Epithelial–Mesenchymal Transition and Generation of Breast Cancer Stem Cells. *Cancer Res* (2010) 70:3005–8. doi: 10.1158/0008-5472.CAN-09-4041
126. Gatti-Mays ME, Balko JM, Gameiro SR, Bear HD, Prabhakaran S, Fukui J, et al. If We Build It They Will Come: Targeting the Immune Response to Breast Cancer. *NPJ Breast Cancer* (2019) 5:37. doi: 10.1038/s41523-019-0133-7
127. Heo T-H, Wahler J, Suh N. Potential Therapeutic Implications of IL-6/IL-6R/Gp130-Targeting Agents in Breast Cancer. *Oncotarget* (2016) 7:15460–73. doi: 10.18632/oncotarget.7102
128. Mani SA, Guo W, Liao M-J, Eaton E, Ayyanan A, Zhou AY, et al. The Epithelial–Mesenchymal Transition Generates Cells With Properties of Stem Cells. *Cell* (2008) 133:704–15. doi: 10.1016/j.cell.2008.03.027
129. Polyak K, Weinberg RA. Transitions Between Epithelial and Mesenchymal States: Acquisition of Malignant and Stem Cell Traits. *Nat Rev Cancer* (2009) 9:265–73. doi: 10.1038/nrc2620
130. Santisteban M, Reiman JM, Asiedu MK, Behrens MD, Nassar A, Kalli KR, et al. Immune-Induced Epithelial to Mesenchymal Transition *In Vivo* Generates Breast Cancer Stem Cells. *Cancer Res* (2009) 69:2887–95. doi: 10.1158/0008-5472.CAN-08-3343
131. Farmer P, Bonnefoi H, Anderle P, Cameron D, Wirapati P, Wirapati P, et al. A Stroma-Related Gene Signature Predicts Resistance to Neoadjuvant Chemotherapy in Breast Cancer. *Nat Med* (2009) 15:68–74. doi: 10.1038/nm.1908
132. Gupta N, Gupta P, Srivastava SK. Penfluridol Overcomes Paclitaxel Resistance in Metastatic Breast Cancer. *Sci Rep* (2019) 9:5066. doi: 10.1038/s41598-019-41632-0
133. Tian J, Raffa FA, Dai M, Moamer A, Khadang B, Hachim IY, et al. Dasatinib Sensitizes Triple Negative Breast Cancer Cells to Chemotherapy by Targeting Breast Cancer Stem Cells. *Br J Cancer* (2018) 119:1495–507. doi: 10.1038/s41416-018-0287-3
134. Tanei T, Morimoto K, Shimazu K, Kim SJ, Tanji Y, Taguchi T, et al. Association of Breast Cancer Stem Cells Identified by Aldehyde Dehydrogenase 1 Expression With Resistance to Sequential Paclitaxel and Epirubicin-Based Chemotherapy for Breast Cancers. *Clin Cancer Res* (2009) 15:4234–41. doi: 10.1158/1078-0432.CCR-08-1479
135. Samanta D, Gilkes DM, Chaturvedi P, Xiang L, Semenza GL. Hypoxia-Inducible Factors Are Required for Chemotherapy Resistance of Breast Cancer Stem Cells. *Proc Natl Acad Sci U S A* (2014) 111:E5429–5438. doi: 10.1073/pnas.1421438111
136. Staudacher L, Cottu PH, Diéras V, Vincent-Salomon A, Guilhaume MN, Escalup L, et al. Platinum-Based Chemotherapy in Metastatic Triple-Negative Breast Cancer: The Institut Curie Experience. *Ann Oncol* (2011) 22:848–56. doi: 10.1093/annonc/mdq461
137. Dent R, Rugo HS. Most Neoadjuvant Chemotherapy for Triple-Negative Breast Cancer Should Include Platinum. *Lancet Oncol* (2021) 22:27–8. doi: 10.1016/S1470-2045(20)30747-6
138. Jung Y, Lippard SJ. Direct Cellular Responses to Platinum-Induced DNA Damage. *Chem Rev* (2007) 107:1387–407. doi: 10.1021/cr068207j
139. Sledge GW, Loehrer PJ, Roth BJ, Einhorn LH. Cisplatin as First-Line Therapy for Metastatic Breast Cancer. *J Clin Oncol* (1988) 6:1811–4. doi: 10.1200/JCO.1988.6.12.1811
140. Xu H, Zhou Y, Li W, Zhang B, Zhang H, Zhao S, et al. Tumor-Derived Mesenchymal-Stem-Cell-Secreted IL-6 Enhances Resistance to Cisplatin via the STAT3 Pathway in Breast Cancer. *Oncol Lett* (2018) 15:9142–50. doi: 10.3892/ol.2018.8463
141. Thakur B, Ray P. Cisplatin Triggers Cancer Stem Cell Enrichment in Platinum-Resistant Cells Through NF- κ B-TNF α -PIK3CA Loop. *J Exp Clin Cancer Res* (2017) 36:164. doi: 10.1186/s13046-017-0636-8
142. Marinello J, Delcuratolo M, Capranico G. Anthracyclines as Topoisomerase II Poisons: From Early Studies to New Perspectives. *Int J Mol Sci* (2018) 19:3480. doi: 10.3390/ijms19113480
143. Capelôa T, Benyahia Z, Zampieri LX, Blackman MCNM, Sonveaux P. Metabolic and Non-Metabolic Pathways That Control Cancer Resistance to Anthracyclines. *Semin Cell Dev Biol* (2020) 98:181–91. doi: 10.1016/j.semcdb.2019.05.006
144. Jia D, Tan Y, Liu H, Ooi S, Li L, Wright K, et al. Cardamonin Reduces Chemotherapy-Enriched Breast Cancer Stem-Like Cells *In Vitro* and *In Vivo*. *Oncotarget* (2016) 7:771–85. doi: 10.18632/oncotarget.5819
145. Du R, Liu B, Zhou L, Wang D, He X, Xu X, et al. Downregulation of Annexin A3 Inhibits Tumor Metastasis and Decreases Drug Resistance in Breast Cancer. *Cell Death Dis* (2018) 9:126. doi: 10.1038/s41419-017-0143-z

146. Nicholson RI, Johnston SR. Endocrine Therapy – Current Benefits and Limitations. *Breast Cancer Res Treat* (2005) 93:3–10. doi: 10.1007/s10549-005-9036-4
147. Leung EY, Askarian-Amiri ME, Sarkar D, Ferraro-Peyret C, Joseph WR, Finlay GJ, et al. Endocrine Therapy of Estrogen Receptor-Positive Breast Cancer Cells: Early Differential Effects on Stem Cell Markers. *Front Oncol* (2017) 7:184. doi: 10.3389/fonc.2017.00184
148. Fan W, Chang J, Fu P. Endocrine Therapy Resistance in Breast Cancer: Current Status, Possible Mechanisms and Overcoming Strategies. *Future Med Chem* (2015) 7:1511–9. doi: 10.4155/fmc.15.93
149. Blancas I, Olier C, Conde V, Bayo JL, Herrero C, Zarcos-Pedrinaci I, et al. Real-World Data of Fulvestrant as First-Line Treatment of Postmenopausal Women With Estrogen Receptor-Positive Metastatic Breast Cancer. *Sci Rep* (2021) 11:4274. doi: 10.1038/s41598-021-83622-1
150. Patel HK, Bihani T. Selective Estrogen Receptor Modulators (SERMs) and Selective Estrogen Receptor Degradable (SERDs) in Cancer Treatment. *Pharmacol Ther* (2018) 186:1–24. doi: 10.1016/j.pharmthera.2017.12.012
151. Smith IE, Dowsett M. Aromatase Inhibitors in Breast Cancer. *N Engl J Med* (2003) 348:2431–42. doi: 10.1056/NEJMra023246
152. Xu B, Fan Y. CDK4/6 Inhibition in Early-Stage Breast Cancer: How Far Is It From Becoming Standard of Care? *Lancet Oncol* (2021) 22:159–60. doi: 10.1016/S1470-2045(20)30757-9
153. Alves CL, Ehmsen S, Terp MG, Portman N, Tuttolomondo M, Gammelgaard OL, et al. Co-Targeting CDK4/6 and AKT With Endocrine Therapy Prevents Progression in CDK4/6 Inhibitor and Endocrine Therapy-Resistant Breast Cancer. *Nat Commun* (2021) 12:5112. doi: 10.1038/s41467-021-25422-9
154. Rodriguez D, Ramkairsingh M, Lin X, Kapoor A, Major P, Tang D. The Central Contributions of Breast Cancer Stem Cells in Developing Resistance to Endocrine Therapy in Estrogen Receptor (ER)-Positive Breast Cancer. *Cancers (Basel)* (2019) 11:E1028. doi: 10.3390/cancers11071028
155. Johnston SR. Acquired Tamoxifen Resistance in Human Breast Cancer—Potential Mechanisms and Clinical Implications. *Anticancer Drugs* (1997) 8:911–30. doi: 10.1097/00001813-199711000-00002
156. Ojo D, Wei F, Liu Y, Wang E, Zhang H, Lin X, et al. Factors Promoting Tamoxifen Resistance in Breast Cancer via Stimulating Breast Cancer Stem Cell Expansion. *Curr Med Chem* (2015) 22:2360–74. doi: 10.2174/0929867322666150416095744
157. Pece S, Tosoni D, Confalonieri S, Mazzarol G, Vecchi M, Ronzoni S, et al. Biological and Molecular Heterogeneity of Breast Cancers Correlates With Their Cancer Stem Cell Content. *Cell* (2010) 140:62–73. doi: 10.1016/j.cell.2009.12.007
158. Liu H, Zhang H, Sun X, Guo X, He Y, Cui S, et al. Tamoxifen-Resistant Breast Cancer Cells Possess Cancer Stem-Like Cell Properties. *Chin Med J (Engl)* (2013) 126:3030–4. doi: 10.3760/cma.j.issn.0366-6999.20130227
159. Wang X. STAT3 Mediates Resistance of CD44+CD24-/Low Breast Cancer Stem Cells to Tamoxifen *In Vitro*. *J BioMed Res* (2012) 26:325–35. doi: 10.7555/JBR.26.20110050
160. Vazquez-Martin A, Cufi S, López-Bonet E, Corominas-Faja B, Cuyàs E, Vellon L, et al. Reprogramming of Non-Genomic Estrogen Signaling by the Stemness Factor SOX2 Enhances the Tumor-Initiating Capacity of Breast Cancer Cells. *Cell Cycle* (2013) 12:3471–7. doi: 10.4161/cc.26692
161. Musgrove EA, Sutherland RL. Biological Determinants of Endocrine Resistance in Breast Cancer. *Nat Rev Cancer* (2009) 9:631–43. doi: 10.1038/nrc2713
162. Piva M, Domenici G, Iriando O, Rábano M, Simões BM, Comaills V, et al. Sox2 Promotes Tamoxifen Resistance in Breast Cancer Cells. *EMBO Mol Med* (2014) 6:66–79. doi: 10.1002/emmm.201303411
163. Zhang X, Wang Z-Y. Estrogen Receptor- α Variant, ER- α 36, Is Involved in Tamoxifen Resistance and Estrogen Hypersensitivity. *Endocrinology* (2013) 154:1990–8. doi: 10.1210/en.2013-1116
164. Chakraborty AK, Welsh A, Digiovanna MP. Co-Targeting the Insulin-Like Growth Factor I Receptor Enhances Growth-Inhibitory and Pro-Apoptotic Effects of Anti-Estrogens in Human Breast Cancer Cell Lines. *Breast Cancer Res Treat* (2010) 120:327–35. doi: 10.1007/s10549-009-0382-5
165. Loh YN, Hedditch EL, Baker LA, Jary E, Ward RL, Ford CE. The Wnt Signalling Pathway Is Upregulated in an *In Vitro* Model of Acquired Tamoxifen Resistant Breast Cancer. *BMC Cancer* (2013) 13:174. doi: 10.1186/1471-2407-13-174
166. Lombardo Y, Faronato M, Filipovic A, Virillo V, Magnani L, Coombes RC. Nicastrin and Notch4 Drive Endocrine Therapy Resistance and Epithelial to Mesenchymal Transition in MCF7 Breast Cancer Cells. *Breast Cancer Res* (2014) 16:R62. doi: 10.1186/bcr3675
167. Ramaswamy B, Lu Y, Teng K-Y, Nuovo G, Li X, Shapiro CL, et al. Hedgehog Signaling Is a Novel Therapeutic Target in Tamoxifen-Resistant Breast Cancer Aberrantly Activated by PI3K/AKT Pathway. *Cancer Res* (2012) 72:5048–59. doi: 10.1158/0008-5472.CAN-12-1248
168. Robertson JFR, Bondarenko IM, Trishkina E, Dvorkin M, Panasci L, Manikhas A, et al. Fulvestrant 500 Mg Versus Anastrozole 1 Mg for Hormone Receptor-Positive Advanced Breast Cancer (FALCON): An International, Randomised, Double-Blind, Phase 3 Trial. *Lancet* (2016) 388:2997–3005. doi: 10.1016/S0140-6736(16)32389-3
169. Wardell SE, Marks JR, McDonnell DP. The Turnover of Estrogen Receptor α by the Selective Estrogen Receptor Degradable (SERD) Fulvestrant Is a Saturable Process That Is Not Required for Antagonist Efficacy. *Biochem Pharmacol* (2011) 82:122–30. doi: 10.1016/j.bcp.2011.03.031
170. Giessrigl B, Schmidt WM, Kalipciyan M, Jeitler M, Bilban M, Gollinger M, et al. Fulvestrant Induces Resistance by Modulating GPER and CDK6 Expression: Implication of Methyltransferases, Deacetylases and the hSWI/SNF Chromatin Remodelling Complex. *Br J Cancer* (2013) 109:2751–62. doi: 10.1038/bjc.2013.583
171. Chan Y-T, Lai AC-Y, Lin R-J, Wang Y-H, Wang Y-T, Chang W-W, et al. GPER-Induced Signaling Is Essential for the Survival of Breast Cancer Stem Cells. *Int J Cancer* (2020) 146:1674–85. doi: 10.1002/ijc.32588
172. Kaminska K, Akrap N, Staaf J, Alves CL, Ehinger A, Ebbesson A, et al. Distinct Mechanisms of Resistance to Fulvestrant Treatment Dictate Level of ER Independence and Selective Response to CDK Inhibitors in Metastatic Breast Cancer. *Breast Cancer Res* (2021) 23:26. doi: 10.1186/s13058-021-01402-1
173. Uchiumi K, Tsuboi K, Sato N, Ito T, Hirakawa H, Niwa T, et al. Cancer Stem-Like Properties of Hormonal Therapy-Resistant Breast Cancer Cells. *Breast Cancer* (2019) 26:459–70. doi: 10.1007/s12282-018-00944-1
174. Rao X, Di Leva G, Li M, Fang F, Devlin C, Hartman-Frey C, et al. MicroRNA-221/222 Confers Breast Cancer Fulvestrant Resistance by Regulating Multiple Signaling Pathways. *Oncogene* (2011) 30:1082–97. doi: 10.1038/onc.2010.487
175. Magnani L, Stoeck A, Zhang X, Lanczky A, Mirabella AC, Wang T-L, et al. Genome-Wide Reprogramming of the Chromatin Landscape Underlies Endocrine Therapy Resistance in Breast Cancer. *Proc Natl Acad Sci* (2013) 110:E1490–9. doi: 10.1073/pnas.1219992110
176. Cardoso F, Costa A, Senkus E, Aapro M, André F, Barrios CH, et al. 3rd ESO-ESMO International Consensus Guidelines for Advanced Breast Cancer (ABC 3). *Ann Oncol* (2017) 28:16–33. doi: 10.1093/annonc/mdw544
177. Miller W. Aromatase Inhibitors: Mechanism of Action and Role in the Treatment of Breast Cancer. *Semin Oncol* (2003) 30:3–11. doi: 10.1016/S0093-7754(03)00302-6
178. Miller WR, Larionov AA. Understanding the Mechanisms of Aromatase Inhibitor Resistance. *Breast Cancer Res* (2012) 14:201. doi: 10.1186/bcr2931
179. Kazi AA, Gilani RA, Schech AJ, Chumsri S, Sabnis G, Shah P, et al. Nonhypoxic Regulation and Role of Hypoxia-Inducible Factor 1 in Aromatase Inhibitor Resistant Breast Cancer. *Breast Cancer Res* (2014) 16:R15. doi: 10.1186/bcr3609
180. Ma CX, Reinert T, Chmielewska I, Ellis MJ. Mechanisms of Aromatase Inhibitor Resistance. *Nat Rev Cancer* (2015) 15:261–75. doi: 10.1038/nrc3920
181. Hardt O, Wild S, Oerlecke I, Hofmann K, Luo S, Wienck Y, et al. Highly Sensitive Profiling of CD44+/CD24- Breast Cancer Stem Cells by Combining Global mRNA Amplification and Next Generation Sequencing: Evidence for a Hyperactive PI3K Pathway. *Cancer Lett* (2012) 325:165–74. doi: 10.1016/j.canlet.2012.06.010
182. Slamon DJ, Clark GM, Wong SG, Levin WJ, Ullrich A, McGuire WL. Human Breast Cancer: Correlation of Relapse and Survival With Amplification of the HER-2/Neu Oncogene. *Science* (1987) 235:177–82. doi: 10.1126/science.3798106
183. Tandon AK, Clark GM, Chamness GC, Ullrich A, McGuire WL. HER-2/Neu Oncogene Protein and Prognosis in Breast Cancer. *J Clin Oncol* (1989) 7:1120–8. doi: 10.1200/JCO.1989.7.8.1120
184. Richard S, Selle F, Lotz J-P, Khalil A, Gligorov J, Soares DG. Pertuzumab and Trastuzumab: The Rationale Way to Synergy. *Acad Bras Cienc* (2016) 88 Suppl 1:565–77. doi: 10.1590/0001-3765201620150178

185. Pohlmann PR, Mayer IA, Mernaugh R. Resistance to Trastuzumab in Breast Cancer. *Clin Cancer Res* (2009) 15:7479–91. doi: 10.1158/1078-0432.CCR-09-0636
186. Nagata Y, Lan K-H, Zhou X, Tan M, Esteva FJ, Sahin AA, et al. PTEN Activation Contributes to Tumor Inhibition by Trastuzumab, and Loss of PTEN Predicts Trastuzumab Resistance in Patients. *Cancer Cell* (2004) 6:117–27. doi: 10.1016/j.ccr.2004.06.022
187. Burnett JP, Korkaya H, Ouzounova MD, Jiang H, Conley SJ, Newman BW, et al. Trastuzumab Resistance Induces EMT to Transform HER2(+) PTEN(-) to a Triple Negative Breast Cancer That Requires Unique Treatment Options. *Sci Rep* (2015) 5:15821. doi: 10.1038/srep15821
188. Seo AN, Lee HJ, Kim EJ, Jang MH, Kim YJ, Kim JH, et al. Expression of Breast Cancer Stem Cell Markers as Predictors of Prognosis and Response to Trastuzumab in HER2-Positive Breast Cancer. *Br J Cancer* (2016) 114:1109–16. doi: 10.1038/bjc.2016.101
189. Saura C, Bendell J, Jerusalem G, Su S, Ru Q, De Buck S, et al. Phase Ib Study of Buparlisib Plus Trastuzumab in Patients With HER2-Positive Advanced or Metastatic Breast Cancer That Has Progressed on Trastuzumab-Based Therapy. *Clin Cancer Res* (2014) 20:1935–45. doi: 10.1158/1078-0432.CCR-13-1070
190. Dong C, Wu J, Chen Y, Nie J, Chen C. Activation of PI3K/AKT/mTOR Pathway Causes Drug Resistance in Breast Cancer. *Front Pharmacol* (2021) 12:628690. doi: 10.3389/fphar.2021.628690
191. Guerin M, Rezaei K, Isambert N, Campone M, Autret A, Pakradouni J, et al. PIKHER2: A Phase IB Study Evaluating Buparlisib in Combination With Lapatinib in Trastuzumab-Resistant HER2-Positive Advanced Breast Cancer. *Eur J Cancer* (2017) 86:28–36. doi: 10.1016/j.ejca.2017.08.025
192. Tolane S, Burris H, Gartner E, Mayer IA, Saura C, Maurer M, et al. Phase I/II Study of Buparlisib (SAR245408) in Combination With Trastuzumab or Trastuzumab Plus Paclitaxel in Trastuzumab-Refractory HER2-Positive Metastatic Breast Cancer. *Breast Cancer Res Treat* (2015) 149:151–61. doi: 10.1007/s10549-014-3248-4
193. Chung SS, Giehl N, Wu Y, Vadgama JV. STAT3 Activation in HER2-Overexpressing Breast Cancer Promotes Epithelial-Mesenchymal Transition and Cancer Stem Cell Traits. *Int J Oncol* (2014) 44:403–11. doi: 10.3892/ijo.2013.2195
194. Upton R, Banuelos A, Feng D, Biswas T, Kao K, McKenna K, et al. Combining CD47 Blockade With Trastuzumab Eliminates HER2-Positive Breast Cancer Cells and Overcomes Trastuzumab Tolerance. *Proc Natl Acad Sci USA* (2021) 118:e2026849118. doi: 10.1073/pnas.2026849118
195. Geyer CE, Forster J, Lindquist D, Chan S, Romieu CG, Pienkowski T, et al. Lapatinib Plus Capecitabine for HER2-Positive Advanced Breast Cancer. *N Engl J Med* (2006) 355:2733–43. doi: 10.1056/NEJMoa064320
196. Liu L, Greger J, Shi H, Liu Y, Greshock J, Annan R, et al. Novel Mechanism of Lapatinib Resistance in HER2-Positive Breast Tumor Cells: Activation of AXL. *Cancer Res* (2009) 69:6871–8. doi: 10.1158/0008-5472.CAN-08-4490
197. De Cola A, Volpe S, Budani MC, Ferracin M, Lattanzio R, Turdo A, et al. miR-205-5p-Mediated Downregulation of ErbB/HER Receptors in Breast Cancer Stem Cells Results in Targeted Therapy Resistance. *Cell Death Dis* (2015) 6:e1823–3. doi: 10.1038/cddis.2015.192
198. De Cola A, Lamolinara A, Lanuti P, Rossi C, Iezzi M, Marchisio M, et al. MiR-205-5p Inhibition by Locked Nucleic Acids Impairs Metastatic Potential of Breast Cancer Cells. *Cell Death Dis* (2018) 9:821. doi: 10.1038/s41419-018-0854-9
199. Chihara Y, Shimoda M, Hori A, Ohara A, Naoi Y, Ikeda J, et al. A Small-Molecule Inhibitor of SMAD3 Attenuates Resistance to Anti-HER2 Drugs in HER2-Positive Breast Cancer Cells. *Breast Cancer Res Treat* (2017) 166:55–68. doi: 10.1007/s10549-017-4382-6
200. Hosonaga M, Arima Y, Sugihara E, Kohno N, Saya H. Expression of CD24 is Associated With HER2 Expression and Supports HER2-Akt Signaling in HER2-Positive Breast Cancer Cells. *Cancer Sci* (2014) 105:779–87. doi: 10.1111/cas.12427
201. Zhang Y, Xu B, Zhang X-P. Effects of miRNAs on Functions of Breast Cancer Stem Cells and Treatment of Breast Cancer. *Onco Targets Ther* (2018) 11:4263–70. doi: 10.2147/OTT.S165156
202. Sun X, Li Y, Zheng M, Zuo W, Zheng W. MicroRNA-223 Increases the Sensitivity of Triple-Negative Breast Cancer Stem Cells to TRAIL-Induced Apoptosis by Targeting HAX-1. *PLoS One* (2016) 11:e0162754. doi: 10.1371/journal.pone.0162754
203. Lim Y, Wright JA, Attema JL, Gregory PA, Bert AG, Smith E, et al. Epigenetic Modulation of the miR-200 Family Is Associated With Transition to a Breast Cancer Stem Cell-Like State. *J Cell Sci* (2013) 126(Pt 10):2256–66. doi: 10.1242/jcs.122275
204. Shimono Y, Zabala M, Cho RW, Lobo N, Dalerba P, Qian D, et al. Downregulation of miRNA-200c Links Breast Cancer Stem Cells With Normal Stem Cells. *Cell* (2009) 138:592–603. doi: 10.1016/j.cell.2009.07.011
205. Gregory PA, Bert AG, Paterson EL, Barry SC, Tsykin A, Farshid G, et al. The miR-200 Family and miR-205 Regulate Epithelial to Mesenchymal Transition by Targeting ZEB1 and SIP1. *Nat Cell Biol* (2008) 10:593–601. doi: 10.1038/ncb1722
206. Yu F, Yao H, Zhu P, Zhang X, Pan Q, Gong C, et al. Let-7 Regulates Self-Renewal and Tumorigenicity of Breast Cancer Cells. *Cell* (2007) 131:1109–23. doi: 10.1016/j.cell.2007.10.054
207. Sun X, Xu C, Tang S-C, Wang J, Wang H, Wang P, et al. Let-7c Blocks Estrogen-Activated Wnt Signaling in Induction of Self-Renewal of Breast Cancer Stem Cells. *Cancer Gene Ther* (2016) 23:83–9. doi: 10.1038/cgt.2016.3
208. Liu C, Tang DG. MicroRNA Regulation of Cancer Stem Cells. *Cancer Res* (2011) 71:5950–4. doi: 10.1158/0008-5472.CAN-11-1035
209. El Helou R, Pinna G, Cabaud O, Wicinski J, Bhajun R, Guyon L, et al. miR-600 Acts as a Bimodal Switch That Regulates Breast Cancer Stem Cell Fate Through WNT Signaling. *Cell Rep* (2017) 18:2256–68. doi: 10.1016/j.celrep.2017.02.016
210. Park EY, Chang E, Lee EJ, Lee H-W, Kang H-G, Chun K-H, et al. Targeting of Mir34a-NOTCH1 Axis Reduced Breast Cancer Stemness and Chemoresistance. *Cancer Res* (2014) 74:7573–82. doi: 10.1158/0008-5472.CAN-14-1140
211. Yu F, Jiao Y, Zhu Y, Wang Y, Zhu J, Cui X, et al. MicroRNA 34c Gene Down-Regulation via DNA Methylation Promotes Self-Renewal and Epithelial-Mesenchymal Transition in Breast Tumor-Initiating Cells. *J Biol Chem* (2012) 287:465–73. doi: 10.1074/jbc.M111.280768
212. Zuo J, Yu Y, Zhu M, Jing W, Yu M, Chai H, et al. Inhibition of miR-155, a Therapeutic Target for Breast Cancer, Prevented in Cancer Stem Cell Formation. *Cancer Biomark* (2018) 21:383–92. doi: 10.3233/CBM-170642
213. Khan AQ, Ahmed EI, Elareer NR, Junejo K, Steinhoff M, Uddin S. Role of miRNA-Regulated Cancer Stem Cells in the Pathogenesis of Human Malignancies. *Cells* (2019) 8:E840. doi: 10.3390/cells8080840
214. Liu L, Zhou W, Cheng C-T, Ren X, Somlo G, Fong MY, et al. TGFβ Induces “BRCAness” and Sensitivity to PARP Inhibition in Breast Cancer by Regulating DNA-Repair Genes. *Mol Cancer Res* (2014) 12:1597–609. doi: 10.1158/1541-7786.MCR-14-0201
215. Wang Y, Yu Y, Tsuyada A, Ren X, Wu X, Stubblefield K, et al. Transforming Growth Factor-β Regulates the Sphere-Initiating Stem Cell-Like Feature in Breast Cancer Through miRNA-181 and ATM. *Oncogene* (2011) 30:1470–80. doi: 10.1038/onc.2010.531
216. Yan L-X, Huang X-F, Shao Q, Huang M-Y, Deng L, Wu Q-L, et al. MicroRNA miR-21 Overexpression in Human Breast Cancer Is Associated With Advanced Clinical Stage, Lymph Node Metastasis and Patient Poor Prognosis. *RNA* (2008) 14:2348–60. doi: 10.1261/rna.1034808
217. Zhu S, Si M-L, Wu H, Mo Y-Y. MicroRNA-21 Targets the Tumor Suppressor Gene Tropomyosin 1 (TPM1). *J Biol Chem* (2007) 282:14328–36. doi: 10.1074/jbc.M611393200
218. Frankel LB, Christoffersen NR, Jacobsen A, Lindow M, Krogh A, Lund AH. Programmed Cell Death 4 (PDCD4) Is an Important Functional Target of the MicroRNA miR-21 in Breast Cancer Cells. *J Biol Chem* (2008) 283:1026–33. doi: 10.1074/jbc.M707224200
219. Han M, Liu M, Wang Y, Chen X, Xu J, Sun Y, et al. Antagonism of miR-21 Reverses Epithelial-Mesenchymal Transition and Cancer Stem Cell Phenotype Through AKT/ERK1/2 Inactivation by Targeting PTEN. *PLoS One* (2012) 7:e39520. doi: 10.1371/journal.pone.0039520
220. Han M, Liu M, Wang Y, Mo Z, Bi X, Liu Z, et al. Re-Expression of miR-21 Contributes to Migration and Invasion by Inducing Epithelial-Mesenchymal Transition Consistent With Cancer Stem Cell Characteristics in MCF-7 Cells. *Mol Cell Biochem* (2012) 363:427–36. doi: 10.1007/s11010-011-1195-5
221. Song SJ, Poliseno L, Song MS, Ala U, Webster K, Ng C, et al. MicroRNA-Family-Dependent Chromatin Remodeling. *Cell* (2013) 154:311–24. doi: 10.1016/j.cell.2013.06.026

222. Cheng C-W, Yu J-C, Hsieh Y-H, Liao W-L, Shieh J-C, Yao C-C, et al. Increased Cellular Levels of MicroRNA-9 and MicroRNA-221 Correlate With Cancer Stemness and Predict Poor Outcome in Human Breast Cancer. *Cell Physiol Biochem* (2018) 48:2205–18. doi: 10.1159/000492561
223. Wang X, Sun C, Huang X, Li J, Fu Z, Li W, et al. The Advancing Roles of Exosomes in Breast Cancer. *Front Cell Dev Biol* (2021) 9:731062. doi: 10.3389/fcell.2021.731062
224. Raha D, Wilson TR, Peng J, Peterson D, Yue P, Evangelista M, et al. The Cancer Stem Cell Marker Aldehyde Dehydrogenase Is Required to Maintain a Drug-Tolerant Tumor Cell Subpopulation. *Cancer Res* (2014) 74:3579–90. doi: 10.1158/0008-5472.CAN-13-3456
225. Zhang H, Qian DZ, Tan YS, Lee K, Gao P, Ren YR, et al. Digoxin and Other Cardiac Glycosides Inhibit HIF-1 Synthesis and Block Tumor Growth. *Proc Natl Acad Sci* (2008) 105:19579–86. doi: 10.1073/pnas.0809763105
226. Lee K, Zhang H, Qian DZ, Rey S, Liu JO, Semenza GL. Acriflavine Inhibits HIF-1 Dimerization, Tumor Growth, and Vascularization. *Proc Natl Acad Sci* (2009) 106:17910–5. doi: 10.1073/pnas.0909353106
227. Wong CC-L, Zhang H, Gilkes DM, Chen J, Wei H, Chaturvedi P, et al. Inhibitors of Hypoxia-Inducible Factor 1 Block Breast Cancer Metastatic Niche Formation and Lung Metastasis. *J Mol Med* (2012) 90:803–15. doi: 10.1007/s00109-011-0855-y
228. Ikeda H, Kakeya H. Targeting Hypoxia-Inducible Factor 1 (HIF-1) Signaling With Natural Products Toward Cancer Chemotherapy. *J Antibiot* (2021) 74:687–95. doi: 10.1038/s41429-021-00451-0
229. Chun S-Y, Kwon Y-S, Nam K-S, Kim S. Lapatinib Enhances the Cytotoxic Effects of Doxorubicin in MCF-7 Tumorspheres by Inhibiting the Drug Efflux Function of ABC Transporters. *BioMed Pharmacother* (2015) 72:37–43. doi: 10.1016/j.biopha.2015.03.009
230. Nickoloff BJ, Osborne BA, Miele L. Notch Signaling as a Therapeutic Target in Cancer: A New Approach to the Development of Cell Fate Modifying Agents. *Oncogene* (2003) 22:6598–608. doi: 10.1038/sj.onc.1206758
231. Hori K, Sen A, Artavanis-Tsakonas S. Notch Signaling at a Glance. *J Cell Sci* (2013) 126:2135–40. doi: 10.1242/jcs.127308
232. Eyler CE, Rich JN. Survival of the Fittest: Cancer Stem Cells in Therapeutic Resistance and Angiogenesis. *J Clin Oncol* (2008) 26:2839–45. doi: 10.1200/JCO.2007.15.1829
233. Zheng H, Bae Y, Kasimir-Bauer S, Tang R, Ren G, Rymer I, et al. Therapeutic Antibody Targeting Tumor- and Osteoblastic Nichederived Jagged1 Sensitizes Bone Metastasis to Chemotherapy. *Cancer Cell* (2017) 32:731–47. doi: 10.1016/j.ccell.2017.11.002
234. Qiu M, Peng Q, Jiang I, Carroll C, Han G, Rymer I, et al. Specific Inhibition of Notch1 Signaling Enhances the Antitumor Efficacy of Chemotherapy in Triple Negative Breast Cancer Through Reduction of Cancer Stem Cells. *Cancer Lett* (2013) 328:261–70. doi: 10.1016/j.canlet.2012.09.023
235. Kumar S, Nandi A, Singh S, Regulapati R, Li N, Tobias JW, et al. Dll1+ Quiescent Tumor Stem Cells Drive Chemoresistance in Breast Cancer Through NF- κ B Survival Pathway. *Nat Commun* (2021) 12:432. doi: 10.1038/s41467-020-20664-5
236. Kumar S, Srivastav RK, Wilkes DW, Ross T, Kim S, Kowalski J, et al. Estrogen-Dependent DLL1-Mediated Notch Signaling Promotes Luminal Breast Cancer. *Oncogene* (2019) 38:2092–107. doi: 10.1038/s41388-018-0562-z
237. Simões BM, O'Brien CS, Eyre R, Silva A, Yu L, Sarmiento-Castro A, et al. Anti-Estrogen Resistance in Human Breast Tumors Is Driven by JAG1-NOTCH4-Dependent Cancer Stem Cell Activity. *Cell Rep* (2015) 12:1968–77. doi: 10.1016/j.celrep.2015.08.050
238. Cidado J, Park BH. Targeting the PI3K/Akt/mTOR Pathway for Breast Cancer Therapy. *J Mammary Gland Biol Neoplasia* (2012) 17:205–16. doi: 10.1007/s10911-012-9264-2
239. Hu Y, Guo R, Wei J, Zhou Y, Ji W, Liu J, et al. Effects of PI3K Inhibitor NVP-BKM120 on Overcoming Drug Resistance and Eliminating Cancer Stem Cells in Human Breast Cancer Cells. *Cell Death Dis* (2015) 6:e2020–0. doi: 10.1038/cddis.2015.363
240. Gargini R, Cerliani JP, Escoll M, Antón IM, Wandosell F. Cancer Stem Cell-Like Phenotype and Survival Are Coordinately Regulated by A Kt/ F Oxo/ B Im Pathway. *Stem Cells* (2015) 33:646–60. doi: 10.1002/stem.1904
241. Kolev VN, Wright QG, Vidal CM, Ring JE, Shapiro IM, Ricono J, et al. PI3K/mTOR Dual Inhibitor VS-5584 Preferentially Targets Cancer Stem Cells. *Cancer Res* (2015) 75:446–55. doi: 10.1158/0008-5472.CAN-14-1223
242. Solzak JP, Atale RV, Hancock BA, Sinn AL, Pollok KE, Jones DR, et al. Dual PI3K and Wnt Pathway Inhibition is a Synergistic Combination Against Triple Negative Breast Cancer. *NPJ Breast Cancer* (2017) 3:17. doi: 10.1038/s41523-017-0016-8
243. Li H, Prever L, Hirsch E, Gulluni F. Targeting PI3K/AKT/mTOR Signaling Pathway in Breast Cancer. *Cancers* (2021) 13:3517. doi: 10.3390/cancers13143517
244. Zhou H, Yu C, Kong L, Xu X, Yan J, Li Y, et al. B591, a Novel Specific Pan-PI3K Inhibitor, Preferentially Targets Cancer Stem Cells. *Oncogene* (2019) 38:3371–86. doi: 10.1038/s41388-018-0674-5
245. Jang G-B, Kim J-Y, Cho S-D, Park K-S, Jung J-Y, Lee H-Y, et al. Blockade of Wnt/ β -Catenin Signaling Suppresses Breast Cancer Metastasis by Inhibiting CSC-Like Phenotype. *Sci Rep* (2015) 5:12465. doi: 10.1038/srep12465
246. Jang G-B, Hong I-S, Kim R-J, Lee S-Y, Park S-J, Lee E-S, et al. Wnt/ β -Catenin Small-Molecule Inhibitor CWP232228 Preferentially Inhibits the Growth of Breast Cancer Stem-Like Cells. *Cancer Res* (2015) 75:1691–702. doi: 10.1158/0008-5472.CAN-14-2041
247. Yang Y, Hao E, Pan X, Tan D, Du Z, Xie J, et al. Gomis M2 From Baizuan Suppresses Breast Cancer Stem Cell Proliferation in a Zebrafish Xenograft Model. *Aging* (2019) 11:8347–61. doi: 10.18632/aging.102323
248. Braune E-B, Seshire A, Lendahl U. Notch and Wnt Dysregulation and Its Relevance for Breast Cancer and Tumor Initiation. *Biomedicines* (2018) 6:101. doi: 10.3390/biomedicines6040101
249. Chakrabarti R, Celiá-Terrasa T, Kumar S, Hang X, Wei Y, Choudhury A, et al. Notch Ligand Dll1 Mediates Cross-Talk Between Mammary Stem Cells and the Macrophageal Niche. *Science* (2018) 360:eaan4153. doi: 10.1126/science.aan4153
250. Espinosa L, Inglés-Esteve J, Aguilera C, Bigas A. Phosphorylation by Glycogen Synthase Kinase-3 β Down-Regulates Notch Activity, a Link for Notch and Wnt Pathways. *J Biol Chem* (2003) 278:32227–35. doi: 10.1074/jbc.M304001200
251. Hanahan D, Coussens LM. Accessories to the Crime: Functions of Cells Recruited to the Tumor Microenvironment. *Cancer Cell* (2012) 21:309–22. doi: 10.1016/j.ccr.2012.02.022
252. Gascard P, Tlsty TD. Carcinoma-Associated Fibroblasts: Orchestrating the Composition of Malignancy. *Genes Dev* (2016) 30:1002–19. doi: 10.1101/gad.279737.116
253. Su S, Chen J, Yao H, Liu J, Yu S, Lao L, et al. CD10+GPR77+ Cancer-Associated Fibroblasts Promote Cancer Formation and Chemoresistance by Sustaining Cancer Stemness. *Cell* (2018) 172:841–856.e16. doi: 10.1016/j.cell.2018.01.009
254. Costa A, Kieffer Y, Scholer-Dahirel A, Pelon F, Bourachot B, Cardon M, et al. Fibroblast Heterogeneity and Immunosuppressive Environment in Human Breast Cancer. *Cancer Cell* (2018) 33:463–479.e10. doi: 10.1016/j.ccell.2018.01.011
255. Friedman G, Levi-Galibov O, David E, Bornstein C, Giladi A, Dadiani M, et al. Cancer-Associated Fibroblast Compositions Change With Breast Cancer Progression Linking the Ratio of S100A4+ and PDPN+ CAFs to Clinical Outcome. *Nat Cancer* (2020) 1:692–708. doi: 10.1038/s43018-020-0082-y
256. Strell C, Paulsson J, Jin S-B, Tobin NP, Mezheyski A, Roswall P, et al. Impact of Epithelial–Stromal Interactions on Peritumoral Fibroblasts in Ductal Carcinoma *In Situ*. *J Natl Cancer Inst* (2019) 111:983–95. doi: 10.1093/jnci/djy234
257. Valenti G, Quinn HM, Heynen GJJE, Lan L, Holland JD, Vogel R, et al. Cancer Stem Cells Regulate Cancer-Associated Fibroblasts via Activation of Hedgehog Signaling in Mammary Gland Tumors. *Cancer Res* (2017) 77:2134–47. doi: 10.1158/0008-5472.CAN-15-3490
258. Hui M, Cazet A, Jessica Y, Cooper C, McFarland A, Nair R, et al. Targeting the Hedgehog Signalling Pathway in Triple Negative Breast Cancer. *Ann Oncol* (2015) 26:iii31. doi: 10.1093/annonc/mdv121.02
259. Zhu R, Gires O, Zhu L, Liu J, Li J, Yang H, et al. TSPAN8 Promotes Cancer Cell Stemness via Activation of Sonic Hedgehog Signaling. *Nat Commun* (2019) 10:2863. doi: 10.1038/s41467-019-10739-3
260. He M, Fu Y, Yan Y, Xiao Q, Wu H, Yao W, et al. The Hedgehog Signalling Pathway Mediates Drug Response of MCF-7 Mammosphere Cells in Breast Cancer Patients. *Clin Sci (Lond)* (2015) 129:809–22. doi: 10.1042/CS20140592

261. Diehn M, Cho RW, Lobo NA, Kalisky T, Dorie MJ, Kulp AN, et al. Association of Reactive Oxygen Species Levels and Radioresistance in Cancer Stem Cells. *Nature* (2009) 458:780–3. doi: 10.1038/nature07733
262. Zhong G, Qin S, Townsend D, Schulte BA, Tew KD, Wang GY. Oxidative Stress Induces Senescence in Breast Cancer Stem Cells. *Biochem Biophys Res Commun* (2019) 514:1204–9. doi: 10.1016/j.bbrc.2019.05.098
263. Vlashi E, Lagadec C, Vergnes L, Reue K, Frohnen P, Chan M, et al. Metabolic Differences in Breast Cancer Stem Cells and Differentiated Progeny. *Breast Cancer Res Treat* (2014) 146:525–34. doi: 10.1007/s10549-014-3051-2
264. El-Sahli S, Wang L. Cancer Stem Cell-Associated Pathways in the Metabolic Reprogramming of Breast Cancer. *Int J Mol Sci* (2020) 21:E9125. doi: 10.3390/ijms21239125
265. Sun X, Wang M, Wang M, Yu X, Guo J, Sun T, et al. Metabolic Reprogramming in Triple-Negative Breast Cancer. *Front Oncol* (2020) 10:428. doi: 10.3389/fonc.2020.00428
266. Lucantoni F, Düssemann H, Llorente-Folch I, Pehn JHM. BCL2 and BCL(X) L Selective Inhibitors Decrease Mitochondrial ATP Production in Breast Cancer Cells and Are Synthetically Lethal When Combined With 2-Deoxy-D-Glucose. *Oncotarget* (2018) 9:26046–63. doi: 10.18632/oncotarget.25433
267. Ashton TM, McKenna WG, Kunz-Schughart LA, Higgins GS. Oxidative Phosphorylation as an Emerging Target in Cancer Therapy. *Clin Cancer Res* (2018) 24:2482–90. doi: 10.1158/1078-0432.CCR-17-3070
268. Reyes-Castellanos G, Masoud R, Carrier A. Mitochondrial Metabolism in PDAC: From Better Knowledge to New Targeting Strategies. *Biomedicine* (2020) 8:E270. doi: 10.3390/biomedicine8080270
269. Luo M, Shang L, Brooks MD, Jagge E, Zhu Y, Buschhaus JM, et al. Targeting Breast Cancer Stem Cell State Equilibrium Through Modulation of Redox Signaling. *Cell Metab* (2018) 28:69–86.e6. doi: 10.1016/j.cmet.2018.06.006
270. Pindiprolu SKSS, Krishnamurthy PT, Chintamaneni PK, Karri VVSR. Nanocarrier Based Approaches for Targeting Breast Cancer Stem Cells. *Artif Cells Nanomed Biotechnol* (2018) 46:885–98. doi: 10.1080/21691401.2017.1366337
271. Mitchell MJ, Billingsley MM, Haley RM, Wechsler ME, Peppas NA, Langer R. Engineering Precision Nanoparticles for Drug Delivery. *Nat Rev Drug Discov* (2021) 20:101–24. doi: 10.1038/s41573-020-0090-8
272. El-Sahli S, Hua K, Sulaiman A, Chambers J, Li L, Farah E, et al. A Triple-Drug Nanotherapy to Target Breast Cancer Cells, Cancer Stem Cells, and Tumor Vasculature. *Cell Death Dis* (2021) 12:8. doi: 10.1038/s41419-020-03308-w
273. Gao Y, Tang M, Leung E, Svirskis D, Shelling A, Wu Z. Dual or Multiple Drug Loaded Nanoparticles to Target Breast Cancer Stem Cells. *RSC Adv* (2020) 10:19089–105. doi: 10.1039/D0RA02801K
274. Wang D, Huang J, Wang X, Yu Y, Zhang H, Chen Y, et al. The Eradication of Breast Cancer Cells and Stem Cells by 8-Hydroxyquinoline-Loaded Hyaluronan Modified Mesoporous Silica Nanoparticle-Supported Lipid Bilayers Containing Docetaxel. *Biomaterials* (2013) 34:7662–73. doi: 10.1016/j.biomaterials.2013.06.042
275. Rao W, Wang H, Han J, Zhao S, Dumbleton J, Agarwal P, et al. Chitosan-Decorated Doxorubicin-Encapsulated Nanoparticle Targets and Eliminates Tumor Reinitiating Cancer Stem-Like Cells. *ACS Nano* (2015) 9:5725–40. doi: 10.1021/nn506928p
276. Sun R, Shen S, Zhang Y-J, Xu C-F, Cao Z-T, Wen L-P, et al. Nanoparticle-Facilitated Autophagy Inhibition Promotes the Efficacy of Chemotherapeutics Against Breast Cancer Stem Cells. *Biomaterials* (2016) 103:44–55. doi: 10.1016/j.biomaterials.2016.06.038
277. Kanapathipillai M, Mammoto A, Mammoto T, Kang JH, Jiang E, Ghosh K, et al. Inhibition of Mammary Tumor Growth Using Lysyl Oxidase-Targeting Nanoparticles to Modify Extracellular Matrix. *Nano Lett* (2012) 12:3213–7. doi: 10.1021/nl301206p
278. Goodarzi N, Amini M, Ghahremani MH, Atyabi F, Ostad SN, Dinarvand R. Hyaluronic Acid-Drug Conjugate of Docetaxel and Metformin to Target Cancer Cells and Cancer Stem Cells: Synthesis and Characterization. *J Control Release* (2013) 172:e59. doi: 10.1016/j.jconrel.2013.08.122
279. Elster JD, Krishnadas DK, Lucas KG. Dendritic Cell Vaccines: A Review of Recent Developments and Their Potential Pediatric Application. *Hum Vaccin Immunother* (2016) 12:2232–9. doi: 10.1080/21645515.2016.1179844
280. Gabrilovich DI, Corak J, Ciernik IF, Kavanaugh D, Carbone DP. Decreased Antigen Presentation by Dendritic Cells in Patients With Breast Cancer. *Clin Cancer Res* (1997) 3:483–90.
281. Gervais A, Levêque J, Bouet-Toussaint F, Burtin F, Lesimple T, Sulpice L, et al. Dendritic Cells are Defective in Breast Cancer Patients: A Potential Role for Polyamine in This Immunodeficiency. *Breast Cancer Res* (2005) 7:R326. doi: 10.1186/bcr1001
282. Brossart P, Wirths S, Stuhler G, Reichardt VL, Kanz L, Brugger W. Induction of Cytotoxic T-Lymphocyte Responses *In Vivo* After Vaccinations With Peptide-Pulsed Dendritic Cells. *Blood* (2000) 96:3102–8. doi: 10.1182/blood.V96.9.3102.h8003102_3102_3108
283. Avigan D, Vasir B, Gong J, Borges V, Wu Z, Uhl L, et al. Fusion Cell Vaccination of Patients With Metastatic Breast and Renal Cancer Induces Immunological and Clinical Responses. *Clin Cancer Res* (2004) 10:4699–708. doi: 10.1158/1078-0432.CCR-04-0347
284. Qi C-J, Ning Y-L, Han Y-S, Min H-Y, Ye H, Zhu Y-L, et al. Autologous Dendritic Cell Vaccine for Estrogen Receptor (ER)/progesterone Receptor (PR) Double-Negative Breast Cancer. *Cancer Immunol Immunother* (2012) 61:1415–24. doi: 10.1007/s00262-011-1192-2
285. Fuentes-Antràs J, Guevara-Hoyer K, Baliu-Piqué M, García-Sáenz JA, Pérez-Segura P, Pandiella A, et al. Adoptive Cell Therapy in Breast Cancer: A Current Perspective of Next-Generation Medicine. *Front Oncol* (2020) 10:605633. doi: 10.3389/fonc.2020.605633
286. Alhabbab RY. Targeting Cancer Stem Cells by Genetically Engineered Chimeric Antigen Receptor T Cells. *Front Genet* (2020) 11:312. doi: 10.3389/fgene.2020.00312
287. Liu Y, Zhou Y, Huang K-H, Li Y, Fang X, An L, et al. EGFR-Specific CAR-T Cells Trigger Cell Lysis in EGFR-Positive TNBC. *Aging (Albany NY)* (2019) 11:11054–72. doi: 10.18632/aging.102510
288. Priceman SJ, Tilakawardane D, Jeang B, Aguilar B, Murad JP, Park AK, et al. Regional Delivery of Chimeric Antigen Receptor-Engineered T Cells Effectively Targets HER2+ Breast Cancer Metastasis to the Brain. *Clin Cancer Res* (2018) 24:95–105. doi: 10.1158/1078-0432.CCR-17-2041
289. Masoumi J, Jafarzadeh A, Abdolalizadeh J, Khan H, Philippe J, Mirzaei H, et al. Cancer Stem Cell-Targeted Chimeric Antigen Receptor (CAR)-T Cell Therapy: Challenges and Prospects. *Acta Pharm Sin B* (2021) 11:1721–39. doi: 10.1016/j.apsb.2020.12.015
290. Yang L, Tang H, Kong Y, Xie X, Chen J, Song C, et al. LGR5 Promotes Breast Cancer Progression and Maintains Stem-Like Cells Through Activation of Wnt/ β -Catenin Signaling: LGR5 Activation in Breast Cancer Stem Cells. *Stem Cells* (2015) 33:2913–24. doi: 10.1002/stem.2083
291. Li J, Li W, Huang K, Zhang Y, Kupfer G, Zhao Q. Chimeric Antigen Receptor T Cell (CAR-T) Immunotherapy for Solid Tumors: Lessons Learned and Strategies for Moving Forward. *J Hematol Oncol* (2018) 11:22. doi: 10.1186/s13045-018-0568-6
292. Salmon H, Franciszkiewicz K, Damotte D, Dieu-Nosjean M-C, Validire P, Trautmann A, et al. Matrix Architecture Defines the Preferential Localization and Migration of T Cells Into the Stroma of Human Lung Tumors. *J Clin Invest* (2012) 122:899–910. doi: 10.1172/JCI45817
293. Martini V, D'Avanzo F, Maggiora PM, Varughese FM, Sica A, Gennari A. Oncolytic Virotherapy: New Weapon for Breast Cancer Treatment. *Eccancermediscience* (2020) 14:1149. doi: 10.3332/ecancer.2020.1149
294. Zhang B, Wang X, Cheng P. Remodeling of Tumor Immune Microenvironment by Oncolytic Viruses. *Front Oncol* (2021) 10:561372. doi: 10.3389/fonc.2020.561372
295. Liu Y-T, Sun Z-J. Turning Cold Tumors Into Hot Tumors by Improving T-Cell Infiltration. *Theranostics* (2021) 11:5365–86. doi: 10.7150/thno.58390
296. Terawaki S, Chikuma S, Shibayama S, Hayashi T, Yoshida T, Okazaki T, et al. IFN- α Directly Promotes Programmed Cell Death-1 Transcription and Limits the Duration of T Cell-Mediated Immunity. *J Immunol* (2011) 186:2772–9. doi: 10.4049/jimmunol.1003208
297. Li J, Zeng W, Huang Y, Zhang Q, Hu P, Rabkin SD, et al. Treatment of Breast Cancer Stem Cells With Oncolytic Herpes Simplex Virus. *Cancer Gene Ther* (2012) 19:707–14. doi: 10.1038/cgt.2012.49
298. Bernstein V, Ellard SL, Dent SF, Tu D, Mates M, Dhesy-Thind SK, et al. A Randomized Phase II Study of Weekly Paclitaxel With or Without Pelareorep in Patients With Metastatic Breast Cancer: Final Analysis of Canadian Cancer Trials Group IND.213. *Breast Cancer Res Treat* (2018) 167:485–93. doi: 10.1007/s10549-017-4538-4

299. Chaurasiya S, Fong Y. Viroimmunotherapy for Breast Cancer: Promises, Problems and Future Directions. *Cancer Gene Ther* (2021) 28:757–68. doi: 10.1038/s41417-020-00265-6
300. Jiang X, Wang J, Deng X, Xiong F, Ge J, Xiang B, et al. Role of the Tumor Microenvironment in PD-L1/PD-1-Mediated Tumor Immune Escape. *Mol Cancer* (2019) 18:10. doi: 10.1186/s12943-018-0928-4
301. Schmid P, Adams S, Rugo HS, Schneeweiss A, Barrios CH, Iwata H, et al. Atezolizumab and Nab-Paclitaxel in Advanced Triple-Negative Breast Cancer. *N Engl J Med* (2018) 379:2108–21. doi: 10.1056/NEJMoa1809615
302. Nanda R, Chow LQM, Dees EC, Berger R, Gupta S, Geva R, et al. Pembrolizumab in Patients With Advanced Triple-Negative Breast Cancer: Phase Ib KEYNOTE-012 Study. *J Clin Oncol* (2016) 34:2460–7. doi: 10.1200/JCO.2015.64.8931
303. Gou Q, Dong C, Xu H, Khan B, Jin J, Liu Q, et al. PD-L1 Degradation Pathway and Immunotherapy for Cancer. *Cell Death Dis* (2020) 11:955. doi: 10.1038/s41419-020-03140-2
304. Sgouros G, Bodei L, McDevitt MR, Nedrow JR. Radiopharmaceutical Therapy in Cancer: Clinical Advances and Challenges. *Nat Rev Drug Discov* (2020) 19:589–608. doi: 10.1038/s41573-020-0073-9
305. Meredith R, Torgue J, Shen S, Fisher DR, Banaga E, Bunch P, et al. Dose Escalation and Dosimetry of First-in-Human α Radioimmunotherapy With ^{212}Pb -TCMC-Trastuzumab. *J Nucl Med* (2014) 55:1636–42. doi: 10.2967/jnumed.114.143842
306. Meredith RF, Torgue J, Azure MT, Shen S, Saddekni S, Banaga E, et al. Pharmacokinetics and Imaging of ^{212}Pb -TCMC-Trastuzumab After Intraperitoneal Administration in Ovarian Cancer Patients. *Cancer Biother Radiopharm* (2014) 29:12–7. doi: 10.1089/cbr.2013.1531
307. Costantini DL, Bateman K, McLarty K, Vallis KA, Reilly RM. Trastuzumab-Resistant Breast Cancer Cells Remain Sensitive to the Auger Electron-Emitting Radiotherapeutic Agent ^{111}In -NLS-Trastuzumab and Are Radiosensitized by Methotrexate. *J Nucl Med* (2008) 49:1498–505. doi: 10.2967/jnumed.108.051771
308. Leung CN, Canter BS, Rajon D, Bäck TA, Fritton JC, Azzam EI, et al. Dose-Dependent Growth Delay of Breast Cancer Xenografts in the Bone Marrow of Mice Treated With ^{223}Ra : The Role of Bystander Effects and Their Potential for Therapy. *J Nucl Med* (2020) 61:89–95. doi: 10.2967/jnumed.119.227835
309. D'Huyvetter M, Vos JD, Caveliers V, Vaneycken I, Heemskerk J, Duhoux FP, et al. Phase I Trial of ^{131}I -GMIB-Anti-HER2-VHH1, a New Promising Candidate for HER2-Targeted Radionuclide Therapy in Breast Cancer Patients. *J Nucl Med* (2021) 62:1097–105. doi: 10.2967/jnumed.120.255679
310. Saravanan M, Barabadi H, Ramachandran B, Venkatraman G, Ponmurugan K. Emerging Plant-Based Anti-Cancer Green Nanomaterials in Present Scenario. In: *Comprehensive Analytical Chemistry*. Netherlands: Elsevier (2019) 87:291–318. doi: 10.1016/bs.coac.2019.09.001
311. Virmani I, Sasi C, Priyadarshini E, Kumar R, Sharma SK, Singh GP, et al. Comparative Anticancer Potential of Biologically and Chemically Synthesized Gold Nanoparticles. *J Clust Sci* (2020) 31:867–76. doi: 10.1007/s10876-019-01695-5
312. Vahidi H, Barabadi H, Saravanan M. Emerging Selenium Nanoparticles to Combat Cancer: A Systematic Review. *J Clust Sci* (2020) 31:301–9. doi: 10.1007/s10876-019-01671-z
313. Barabadi H, Mahjoub MA, Tajani B, Ahmadi A, Junejo Y, Saravanan M. Emerging Theranostic Biogenic Silver Nanomaterials for Breast Cancer: A Systematic Review. *J Clust Sci* (2019) 30:259–79. doi: 10.1007/s10876-018-01491-7
314. Saravanan M, Vahidi H, Medina Cruz D, Vernet-Crua A, Mostafavi E, Stelmach R, et al. Emerging Antineoplastic Biogenic Gold Nanomaterials for Breast Cancer Therapeutics: A Systematic Review. *Int J Nanomedicine* (2020) 15:3577–95. doi: 10.2147/IJN.S240293

Conflict of Interest: The authors declare that the research was conducted in the absence of any commercial or financial relationships that could be construed as a potential conflict of interest.

Publisher's Note: All claims expressed in this article are solely those of the authors and do not necessarily represent those of their affiliated organizations, or those of the publisher, the editors and the reviewers. Any product that may be evaluated in this article, or claim that may be made by its manufacturer, is not guaranteed or endorsed by the publisher.

Copyright © 2022 Saha and Lukong. This is an open-access article distributed under the terms of the Creative Commons Attribution License (CC BY). The use, distribution or reproduction in other forums is permitted, provided the original author(s) and the copyright owner(s) are credited and that the original publication in this journal is cited, in accordance with accepted academic practice. No use, distribution or reproduction is permitted which does not comply with these terms.



Pyrotinib-Containing Neoadjuvant Therapy in Patients With HER2-Positive Breast Cancer: A Multicenter Retrospective Analysis

Xiaoyun Mao¹, Pengwei Lv², Yiping Gong³, Xiujuan Wu⁴, Peng Tang⁴, Shushu Wang⁴, Dianlong Zhang⁵, Wei You⁶, Ouchen Wang⁷, Jun Zhou⁸, Jingruo Li^{9*} and Feng Jin^{1*}

OPEN ACCESS

Edited by:

Maria Rosaria De Miglio,
University of Sassari, Italy

Reviewed by:

Angel Luis Guerrero-Zotano,
Instituto Valenciano de

Oncología, Spain

Jacek Jassem,

Medical University of Gdansk, Poland

*Correspondence:

Feng Jin
jin.feng@cmu.edu.cn
Jingruo Li
jingruoli@163.com

Specialty section:

This article was submitted to
Breast Cancer,
a section of the journal
Frontiers in Oncology

Received: 15 January 2022

Accepted: 11 March 2022

Published: 07 April 2022

Citation:

Mao X, Lv P, Gong Y, Wu X,
Tang P, Wang S, Zhang D, You W,
Wang O, Zhou J, Li J and Jin F (2022)
Pyrotinib-Containing Neoadjuvant
Therapy in Patients With
HER2-Positive Breast Cancer: A
Multicenter Retrospective Analysis.
Front. Oncol. 12:855512.
doi: 10.3389/fonc.2022.855512

¹ Department of Breast Surgery, The First Affiliated Hospital of China Medical University, Shenyang, China, ² Department of Breast Surgery, The First Affiliated Hospital of Zhengzhou University, Zhengzhou, China, ³ Department of Breast, Renmin Hospital of Wuhan University, Hubei General Hospital, Wuhan, China, ⁴ Department of Breast and Thyroid Surgery, The Southwest Hospital of Army Medical University, Chongqing, China, ⁵ Department of Breast Surgery, Dalian Municipal Central Hospital, Dalian, China, ⁶ First Department of Breast Surgery, Henan Provincial People's Hospital, Zhengzhou, China, ⁷ Department of Breast Surgery, The First Affiliated Hospital of Wenzhou Medical University, Wenzhou, China, ⁸ Department of Thyroid and Breast Surgery, The First People's Hospital of Lianyungang, Lianyungang, China, ⁹ Second Department of Breast Surgery, The First Affiliated Hospital of Zhengzhou University, Zhengzhou, China

Background: Pyrotinib, a small-molecule tyrosine kinase inhibitor, has been investigated as a component of neoadjuvant therapy in phase 2 trials of human epidermal growth factor receptor 2 (HER2)-positive breast cancer. This study aimed to evaluate the effectiveness and safety of pyrotinib-containing neoadjuvant therapy for patients with HER2-positive early or locally advanced breast cancer in the real-world setting.

Methods: Data of 97 patients with HER2-positive breast cancer from 21 centers across China treated with pyrotinib-containing neoadjuvant therapy were reviewed. Neoadjuvant therapy consisted of taxane/carboplatin/trastuzumab plus pyrotinib (TCbH+Py, 30 [30.9%]), anthracycline/cyclophosphamide followed by taxane/trastuzumab plus pyrotinib (AC-TH+Py) or taxane followed by anthracycline/cyclophosphamide/trastuzumab plus pyrotinib (T-ACH+Py, 29 [29.9%]), taxane/trastuzumab plus pyrotinib (TH+Py, 23 [23.7%]), and other pyrotinib-containing neoadjuvant treatment (15 [15.5%]). The primary outcome was breast pathological complete response (bpCR, ypT0/is) rate. Secondary outcomes included total pathological complete response (tpCR, ypT0/is ypN0) rate, objective response rate (ORR), and the incidence of preoperative adverse events.

Results: The ORR of pyrotinib-containing neoadjuvant therapy was 87.6% (85/97). The bpCR and tpCR rates were 54.6% (95% confidence interval [CI], 44.2%-64.7%) and 48.5% [95% CI, 38.2%-58.8%], respectively. The most common grade 3 or 4 treatment-related adverse events included diarrhea (15 [15.5%]), decreased hemoglobin (nine [9.3%]), and decreased neutrophil count (eight [8.2%]). No treatment-related deaths occurred.

Conclusion: Pyrotinib-containing neoadjuvant therapy for patients with HER2-positive early or locally advanced breast cancer shows favorable effectiveness with manageable toxicity in the real-world setting. Trastuzumab plus pyrotinib may be a novel option of dual HER2-targeted blockade.

Keywords: human epidermal growth factor receptor 2, breast cancer, pyrotinib, neoadjuvant, real-world

INTRODUCTION

Breast cancer is the most common malignant tumor in women. Approximately 10%-13% of women will develop breast cancer during their lifetime (1). Human epidermal growth factor receptor 2 (HER2)-positive breast cancer accounts for 15%-20% of all breast cancers (2). HER2-targeted therapy dramatically improved outcomes in HER2-positive breast cancer. Chemotherapy combined with dual HER2-targeted blockade has become a standard neoadjuvant regimen (3–8). Actually, more than half of patients can achieve pathological complete response (pCR) with neoadjuvant chemotherapy plus dual HER2-targeted monoclonal antibodies (trastuzumab and pertuzumab) (9–11). A randomized, open-label phase 3 KRISTINE trial showed a pCR rate of 44.4% (99 of 223) with trastuzumab emtansine plus pertuzumab and 55.7% (123 of 221) with docetaxel, carboplatin, and trastuzumab plus pertuzumab (absolute difference, -11.3%; 95% confidence interval [CI], -20.5% to -2.0%; $P=0.016$) (9). Chemotherapy combined with trastuzumab and a small-molecule tyrosine kinase inhibitor (TKI, such as lapatinib and neratinib) could also result in favorable breast pCR (bpCR) rate (51.3%-62.0%) (12–16) with acceptable safety profile. A meta-analysis demonstrated that pCR was associated with substantially longer event-free survival and overall survival in HER2-positive breast cancer (17). Thus, the dual HER2-targeted blockade with a macromolecular monoclonal antibody and a small-molecule TKI as components of neoadjuvant therapy deserves further investigation.

Pyrotinib is a small-molecule, irreversible TKI, targeting HER1, HER2, and HER4 (18). The phase 3 PHOEBE study confirmed the superiority of pyrotinib over lapatinib when combined with capecitabine in the treatment of HER2-positive relapsed or metastatic breast cancer, with significantly better objective response rate (ORR, 67.2% vs. 51.5%) and progression-free survival (12.5 months vs. 6.8 months) (19). Pyrotinib as a component of HER2-targeted neoadjuvant therapy has been investigated in small phase 2 clinical trials (20–22). We did a multicenter retrospective analysis to assess effectiveness and safety of pyrotinib-containing regimens as neoadjuvant therapy for patients with HER2-positive breast cancer in the real-world setting.

METHODS

Study Design and Participants

This was a retrospective, observational real-world study of female adult patients with HER2-positive breast cancer who received

pyrotinib-containing neoadjuvant therapy and surgery at 21 centers (**Supplementary Table S1**) across China between November 2018 and January 2021. All eligible patients should have histopathologically confirmed stage II-III HER2-positive (immunohistochemistry score of 3+, or 2+ with gene amplification by fluorescence *in-situ* hybridization) invasive breast cancer, with at least one measurable lesion according to the Response Evaluation Criteria In Solid Tumors (RECIST) version 1.1. Pyrotinib must be used for at least one neoadjuvant cycle. Patients who received other neoadjuvant HER2-TKIs were excluded. This study was approved by the ethics committee of the First Hospital of China Medical University (No. [2021]308). Informed consent was waived due to the retrospective nature of the study.

Treatment

The standard dose of pyrotinib was 400 mg once a day. The combination regimen of neoadjuvant therapy and the initial dose of pyrotinib were at the discretion of local investigator. Dose reduction, interruption, and discontinuation of pyrotinib were allowed according to the adverse events (AEs).

Data Collection

Demography, baseline disease characteristics, information of neoadjuvant therapy and surgery, imaging and pathological results, and safety data were all extracted from the medical records. Radiographic images were assessed by the local investigator according to RECIST 1.1. Pathological reports were completed by the local pathologist.

Outcomes

The primary outcome was bpCR rate, defined as the proportion of patients with no histological evidence of residual invasive tumor cells in the breast (ypT0/is). Secondary outcomes included total pCR (tpCR) rate, ORR, and the incidence of AEs before surgery. The tpCR rate was defined as the proportion of patients with no residual invasive tumor cells in breast and axillary lymph nodes (ypT0/is ypN0). ORR was defined as the proportion of patients with best response of complete or partial response before surgery as per RECIST 1.1. The AEs were graded according to the National Cancer Institute Common Terminology Criteria for Adverse Events version 5.0.

Statistical Analysis

Statistical analysis was performed using SPSS 15.0 (SPSS Inc., Chicago, IL, USA). Continuous variables were expressed as median (range), and categorical variables were expressed as frequency (percentage). The 95% CIs of bpCR and tpCR were

calculated using the Clopper-Pearson method. The bpCR and tpCR rates were also described in subgroups by hormone receptor (HR) status and different neoadjuvant regimens. HR-positive was defined as positive estrogen receptor (ER) and/or progesterone receptor (PR), and HR-negative was defined as negative ER and PR. Comparisons of bpCR and tpCR rates between subgroups by ER, PR, or HR status were performed using chi-square test or Fisher exact test, where appropriate. $P < 0.05$ was considered statistically significant.

RESULTS

Patient Characteristics

A total of 119 patients were assessed for eligibility. Twenty-two patients did not meet inclusion criteria or met the exclusion criteria, leaving 97 patients included in the analysis (**Figure 1**). The median age was 51 years (range, 24–68). More than half of patients had T2 (59.8%) and N1 (54.6%) disease. Fourteen (14.4%) of 97 patients switched from other anti-HER2 neoadjuvant regimen to pyrotinib-containing regimen (**Table 1**).

Treatment Exposure

Among the 97 patients, 30 (30.9%) received taxane/carboplatin/trastuzumab plus pyrotinib (TCbH+Py), 29 (29.9%) received anthracycline/cyclophosphamide followed by taxane/trastuzumab plus pyrotinib (AC-TH+Py) or taxane followed by anthracycline/cyclophosphamide/trastuzumab plus pyrotinib (T-ACH+Py), 23 (23.7%) received taxane/trastuzumab plus pyrotinib (TH+Py), and 15 (15.5%) received other neoadjuvant regimens (**Table 2**). Twenty-one (70.0%) of 30 patients with TCbH+Py received standard 6-cycle treatment. Twenty-seven (97.2%) of 29 patients with AC-TH+Py or T-ACH+Py received

standard 8-cycle treatment. Of 23 patients with TH+Py, 4 (17.4%) received standard 4-cycle treatment, and 17 (73.9%) received treatment for more than 4 cycles (one for 5 cycles and 16 for 6 cycles). Eighty-one (83.5%) of 97 patients had available data of initial dose for pyrotinib. Among them, 66 (81.5%) patients received pyrotinib at an initial dose of 400 mg, and 15 (18.5%) at 320 mg. Fifty-seven (70.4%) patients received 400 mg pyrotinib without dose reductions throughout the neoadjuvant therapy period.

Pyrotinib-Containing Neoadjuvant Therapy Outcomes

After pyrotinib-containing neoadjuvant therapy, 22 (22.7%) of 97 patients had a complete response, and 63 (64.9%) had a partial response, with an ORR of 87.6% according to RECIST 1.1. Five patients had stable disease, and seven patients were not evaluable due to no imaging assessment after baseline.

After pyrotinib-containing neoadjuvant therapy and surgery, 53 (54.6% [95% CI, 44.2%–64.7%]) patients had pCR in breast, and 47 (48.5% [95% CI, 38.2%–58.8%]) had pCR in both breast and lymph nodes (**Figure 2A**). Among 45 patients with HR-positive disease, the bpCR and tpCR rates were 42.2% (95% CI, 28.0%–57.8%) and 31.1% (95% CI, 18.6%–46.8%), respectively. The bpCR and tpCR rates were 65.4% (95% CI, 50.8%–77.7%) and 63.5% [95% CI, 48.9%–76.0%] in 52 patients with HR-negative disease, respectively (**Figure 2A**). ER, PR, or HR status correlated with tpCR ($P < 0.05$), HR status correlated with bpCR ($P = 0.022$; **Table 3**). Of 13 patients with ER-positive/PR-negative disease, 61.5% (8/13) had bpCR and 53.8% (7/13) had tpCR. For four patients with ER-negative/PR-positive disease, three (75.0%) had bpCR and tpCR.

For subgroups by different neoadjuvant regimens, the bpCR rate was 76.7% (95% CI, 57.3%–89.4%) in 30 patients with TCbH+Py,

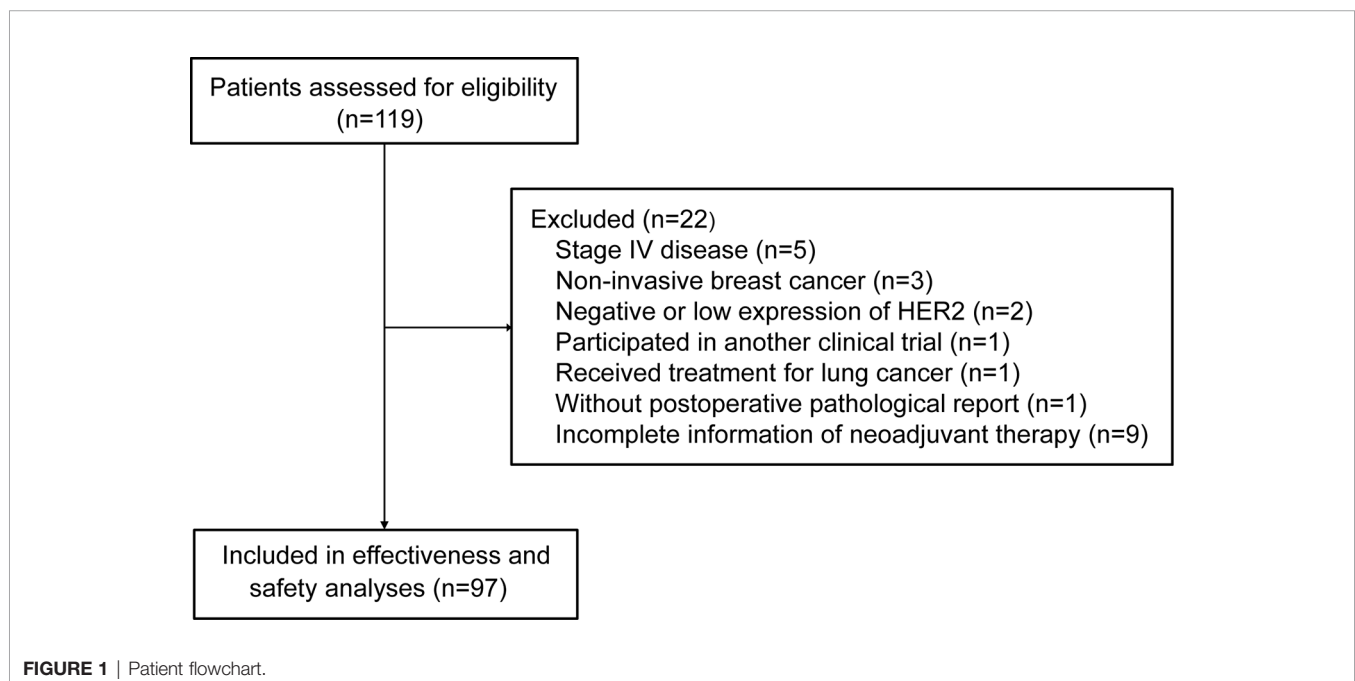


TABLE 1 | Baseline characteristics.

Characteristics	Patients (N = 97)
Median age (range), years ^a	51 (24-68)
T stage, n (%)	
T1	8 (8.2)
T2	58 (59.8)
T3	20 (20.6)
T4	10 (10.3)
Tx	1 (1.0)
N stage, n (%)	
N0	14 (14.4)
N1	53 (54.6)
N2	13 (13.4)
N3	17 (17.5)
Clinical stage, n (%)	
II	52 (53.6)
III	45 (46.4)
ECOG performance status, n (%)	
0	82 (84.5)
1	15 (15.5)
Hormone receptor status, n (%)	
ER and/or PR positive	45 (46.4)
ER and PR negative	52 (53.6)
Ki-67 level, n (%)	
<30%	19 (19.6)
≥30%	78 (80.4)
Menstrual status, n (%)	
Premenopausal	51 (52.6)
Menopausal	39 (40.2)
Unknown	7 (7.2)
Pathological grading, n (%)	
I	2 (2.1)
II-III	54 (55.7)
Unknown	41 (42.3)
Switching from other anti-HER2 neoadjuvant regimens, n (%)	14 (14.4)
Due to intolerable toxicity	3 (3.1)
Due to poor response	11 (11.3)

ECOG, Eastern Cooperative Oncology Group; ER, estrogen receptor; PR, progesterone receptor; HER2, human epidermal growth factor receptor 2.

^aThree patients had missing age.

60.9% (95% CI, 38.8%-79.5%) in 23 patients with TH+Py, and 51.7% (95% CI, 32.9%-70.1%) in 29 patients with AC-TH+Py or T-ACH+Py. The tpCR rate was 73.3% (95% CI, 53.8%-87.0%) in 30 patients with TCbH+Py, 44.8% (95% CI, 27.0%-64.0%) in 29 patients with AC-TH+Py or T-ACH+Py, and 43.5% (95% CI, 23.9%-65.1%) in 23 patients with TH+Py (**Figure 2B**).

Safety

Treatment-related AEs (TRAEs) before surgery occurred in 92.8% (90/97) of patients. Grade ≥3 TRAEs were observed in 35.1% (34/97) of patients. Serious TRAEs were observed in 5.2% (5/97) of patients. The most common TRAEs were diarrhea (62 [63.9%]), decreased hemoglobin (57 [58.8%]), increased alanine transaminase (36 [37.1%]), nausea (34 [35.1%]), decreased neutrophil count (31 [32.0%]), and decreased white blood cell count (30 [30.9%]). The most frequent grade 3 or 4 TRAEs included diarrhea (15 [15.5%]), decreased hemoglobin (nine [9.3%]), and decreased neutrophil count (eight [8.2%]; **Table 4**). There were eight (8.2%) patients having pyrotinib dose reductions due to TRAEs: the dose was reduced to 320 mg

for six patients, 240 mg for one patient, and 160 mg for one patient. No treatment-related deaths occurred.

DISCUSSION

To identify the effectiveness and safety of pyrotinib-containing regimens as neoadjuvant therapy for patients with HER2-positive early or locally advanced breast cancer in the real-world setting, we here made a multicenter retrospective analysis. Lapatinib, neratinib, and pyrotinib are three TKIs investigated in the neoadjuvant setting for patients with HER2-positive breast cancer. Lapatinib is a reversible TKI blocking HER1 and HER2, while pyrotinib is an irreversible pan-ErbB receptor TKI targeting HER2, HER1 and HER4, with similar molecular structure to neratinib (23). In a phase 1 clinical trial, pyrotinib plus capecitabine was well-tolerated and demonstrates promising antitumor activity in patients with HER2-positive metastatic breast cancer (24). Pyrotinib in combination with capecitabine had a significantly higher ORR (78.5% vs. 57.1%, $P=0.01$) and longer progression-free survival (18.1 months vs. 7.0 months, $P<0.001$) compared with lapatinib plus capecitabine in a phase 2 study (25). Results from the phase 3 PHOEBE study confirmed that pyrotinib plus capecitabine could lead to progression-free survival benefit compared with lapatinib plus capecitabine (12.5 months [95% CI, 9.7-not reached] vs. 6.8 months [95% CI, 5.4-8.1]; hazard ratio, 0.39 [95% CI, 0.27-0.56]; $P<0.0001$) in HER2-positive metastatic breast cancer who had previously received anthracycline or taxane chemotherapy (19). Pyrotinib has the advantages of stability, safety, and good tolerance, with encouraging antitumor effects observed in patients with HER2-positive metastatic breast cancer. However, data on its activity in the neoadjuvant setting are still lacking. We supplemented real-world evidence on the basis of previous phase 2 neoadjuvant trials (20–22). The bpCR rate in 97 patients was 54.6% (95% CI, 44.2%-64.7%), and the tpCR rate was 48.5% (95% CI, 38.2%-58.8%). Grade 3 and 4 TRAEs were observed in 35.1% of patients, with the most common events of diarrhea (15.5%), decreased hemoglobin (9.3%), and decreased neutrophil count (8.2%). The safety profile was acceptable.

Taxane/carboplatin/trastuzumab/pertuzumab (TCbHP) and taxane/trastuzumab/pertuzumab (THP) are two class I recommendations in the 2021 version of Chinese Society of Clinical Oncology breast cancer guideline, while other regimens based on anti-HER2 monoclonal antibody and taxane (such as anthracycline/cyclophosphamide followed by taxane/trastuzumab/pertuzumab [AC-THP]) are class II recommendations (3, 4). The National Comprehensive Cancer Network guideline recommended TCbHP as preferred dual anti-HER2 regimens, and recommended the use of AC-THP and taxane followed by anthracycline/cyclophosphamide/trastuzumab/pertuzumab (T-ACHP) in certain circumstances (6). In our study, 84.5% of patients received the common combinations with chemotherapy plus dual HER2-targeted blockade, including 30 patients with TCbH+Py, 29 with AC-

TABLE 2 | Neoadjuvant therapy regimens (N = 97).

Regimens	Number of patients (%)	Median treatment cycles (range)
Dual-target		
TCbH+Py	30 (30.9)	6 (1-6)
AC-TH+Py or T-ACH+Py	29 (29.9)	8 (6-8)
TH+Py	23 (23.7)	6 (1-6)
ACH+Py	2 (2.1)	4 (4-4)
AI+H+Py	1 (1.0)	6
ATH+Py	1 (1.0)	1
N+Pb+H+Py	1 (1.0)	2
OFS+AI+H+Py	1 (1.0)	2
TCH+Py	1 (1.0)	4
AC+Py, then switched to TCbHP ^a	1 (1.0)	8
TCbH+Py, then switched to THP ^b	1 (1.0)	5
Single-target or triple-target		
OFS+EC+Py-T+Py	1 (1.0)	8
Py+X	1 (1.0)	6
T+Py+X	1 (1.0)	6
TC+Py	1 (1.0)	6
TCb+Py	1 (1.0)	6
TCbHP+Py	1 (1.0)	4

T, taxane (docetaxel, albumin-bound paclitaxel, or paclitaxel); Cb, carboplatin; H, trastuzumab; Py, pyrotinib; A, anthracycline (epirubicin, pirarubicin, or doxorubicin); C, cyclophosphamide; AI, aromatase inhibitor (anastrozole or exemestane); N, vinorelbine; Pb, cisplatin; OFS, ovarian function suppression (goserelin); X, capecitabine; P, pertuzumab.

^aThis patient received 2 cycles of AC+Py regimen, then switched to 6 cycles of TCbHP regimen for unknown reason.

^bThis patient received 2 cycles of TCbH+Py regimen, then switched to 3 cycles of THP regimen because of intolerance to Py.

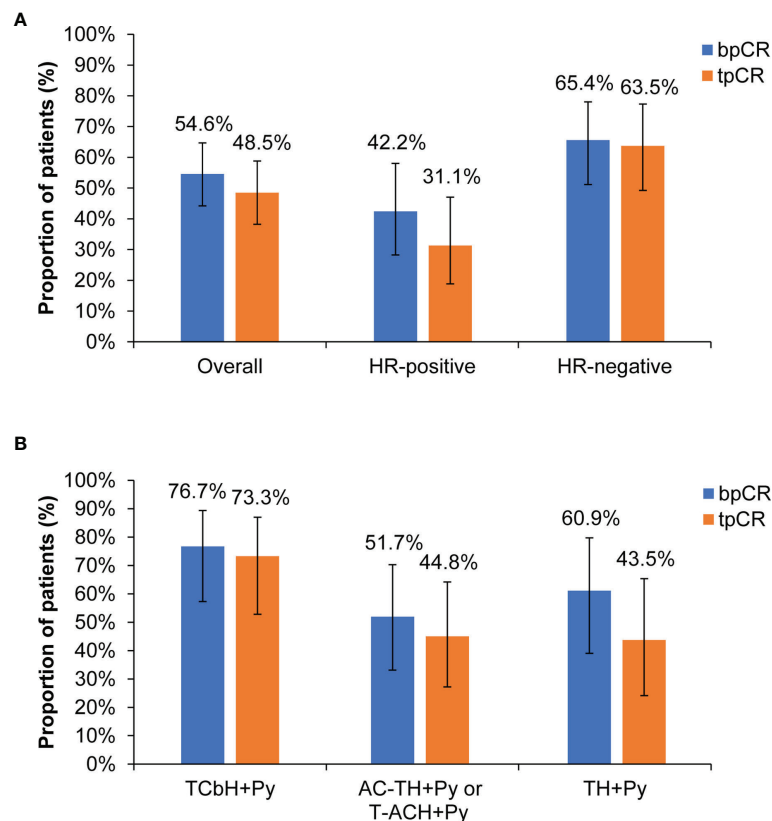


FIGURE 2 | Pathological response. **(A)** Overall population and subgroups by HR status. **(B)** Subgroups by different neoadjuvant regimens. bpCR, breast pathological complete response; tpCR, total pathological complete response; HR, hormone receptor; T, taxane (docetaxel, nanoparticle albumin-bound paclitaxel, or paclitaxel); Cb, carboplatin; H, trastuzumab; Py, pyrotinib; A, anthracycline (epirubicin, pirarubicin, or doxorubicin); C, cyclophosphamide.

TABLE 3 | Comparisons of bpCR and tpCR rates between subgroups by ER, PR, or HR status.

Characteristics	bpCR, n (%)	Non-bpCR, n (%)	P	tpCR, n (%)	Non-tpCR, n (%)	P
ER status			0.069			0.030
Positive (n = 41)	18 (43.9)	23 (56.1)		13 (31.7)	28 (68.3)	
Negative (n = 56)	35 (62.5)	21 (37.5)		34 (60.7)	22 (39.3)	
PR status			0.052			0.005
Positive (n = 32)	13 (40.6)	19 (59.4)		9 (28.1)	23 (71.9)	
Negative (n = 65)	40 (61.5)	25 (38.5)		38 (58.5)	27 (41.5)	
HR status			0.022			0.002
ER and/or PR positive (n = 45)	19 (42.2)	26 (57.8)		14 (31.1)	31 (68.9)	
ER and PR negative (n = 52)	34 (65.4)	18 (34.6)		33 (63.5)	19 (36.5)	

bpCR, breast pathological complete response; tpCR, total pathological complete response; ER, estrogen receptor; PR, progesterone receptor; HR, hormone receptor.

TH+Py or T-ACH+Py, and 23 with TH+Py. The selection of neoadjuvant therapy regimens was in accordance with the guidelines (3, 4, 6). Sixty-nine (84.1%) of 82 patients with these common regimens completed the full course of neoadjuvant therapy, including 17 (73.9%) of 23 patients with TH+Py receiving more than standard 4 cycles. The appropriate selection of neoadjuvant therapy regimens and good compliance might contribute to the high pCR rate. This also reflects a standardized clinical practice environment in China.

In the present study, the tpCR rate in patients with TCbH+Py was 73.3%, higher than docetaxel/carboplatin/trastuzumab/pertuzumab (55.7%) in the KRISTINE study (9) and docetaxel/carboplatin/trastuzumab/lapatinib (51.7%) in the TRIO-US B07 study (15). Patients who received TH+Py had a consistent tpCR rate with paclitaxel/trastuzumab/lapatinib in the NeoALTTO study (43.5% vs. 46.8%) (12). The tpCR rate in patients with AC-TH+Py or T-ACH+Py was 44.8%, similar with paclitaxel/trastuzumab/neratinib followed by doxorubicin/cyclophosphamide (50.0%) in the NSABP FB-7 study (16), and paclitaxel followed by fluorouracil/epirubicin/cyclophosphamide/trastuzumab/lapatinib (46.7%) in the CHER-LOB study (26). A previous phase 2 neoadjuvant trial of

pyrotinib also showed a high tpCR rate with epirubicin/cyclophosphamide/pyrotinib followed by docetaxel/trastuzumab/pyrotinib (73.7%) (20), but the efficacy might be exaggerated due to the limited sample size (n=19; Table 5). Although the cross-study comparisons need to be interpreted in cautions, and the number of patients with different neoadjuvant regimens was small, these results indirectly suggest that trastuzumab plus pyrotinib as dual HER2-targeted blockade is feasible when combined with chemotherapy as neoadjuvant therapy in the real-world setting.

Patients with HR-negative disease accounted for 53.6% of the total population. The bpCR and tpCR rates were 65.4% and 63.5%, respectively, numerically higher than those of patients with HR-positive disease (42.2% and 31.1%). This trend was consistent with previous studies (12–16). Actually, we found that ER status just correlated with tPCR, not bPCR. PR status correlated with both bPCR and tPCR. Compared with PR-positive subgroup, PR-negative patients showed higher bpCR (61.5% vs. 40.6%) and tpCR (58.5% vs. 28.1%) rates with pyrotinib-containing neoadjuvant therapy. PR synthesis requires estrogen and ER, and PR expression is upregulated by ER; thus, ER-positive/PR-positive breast cancer is common (29). PR is also a biomarker used routinely at diagnosis to

TABLE 4 | Treatment-related adverse events before surgery.

Events, n (%)	Patients (N = 97)		
	Any grade	Grade 3	Grade 4
Diarrhea	62 (63.9)	15 (15.5)	0
Hemoglobin decreased	57 (58.8)	9 (9.3)	0
ALT increased	36 (37.1)	2 (2.1)	0
Nausea	34 (35.1)	4 (4.1)	0
Neutrophil count decreased	31 (32.0)	7 (7.2)	1 (1.0)
White blood cell count decreased	30 (30.9)	4 (4.1)	0
Vomiting	28 (28.9)	4 (4.1)	0
AST increased	28 (28.9)	0	0
Hypokalemia	23 (23.7)	2 (2.1)	2 (2.1)
Fatigue	23 (23.7)	2 (2.1)	0
Platelet count decreased	22 (22.7)	0	2 (2.1)
Creatinine increased	13 (13.4)	0	0
Hand-foot syndrome	7 (7.2)	0	0
Hypomagnesemia	7 (7.2)	0	0
Hyponatremia	4 (4.1)	0	0
Rash	2 (2.1)	0	0
Febrile neutropenia	1 (1.0)	0	1 (1.0)
Upper respiratory infection	1 (1.0)	1 (1.0)	0
Weight loss	1 (1.0)	0	0

ALT, alanine transaminase; AST, aspartate transaminase.

TABLE 5 | Pathological response results from current published neoadjuvant trials of tyrosine kinase inhibitor in HER2-positive breast cancer.

Study	Treatment	tpCR rate, n/N (%)			bpCR rate, n/N (%)		
		HR-positive	HR-negative	Total	HR-positive	HR-negative	Total
NSABP FB-7 (16)	TH+Ne-AC	7/23 (30.4)	14/19 (73.7)	21/42 (50.0)	NA	NA	22/42 (52.4)
NeoALTTO (12)	TH+L	NA	NA	68/145 (46.8)	32/77 (41.6)	46/75 (61.3)	78/152 (51.3)
CALGB 40601 (13)	TH+L	28/69 (40.6)	32/47 (68.1)	60/116 (51.7)	28/69 (40.6)	37/47 (78.7)	65/116 (56.0)
NSABP B-41 (14)	AC-TH+L	59/108 (54.6)	44/63 (69.8)	103/171 (60.2)	60/108 (55.6)	46/63 (73.0)	106/171 (62.0)
CHER-LOB (27)	Td-FuECH+L	10/28 (35.7)	10/17 (58.8)	21/45 (46.7)	NA	NA	NA
TRIO-US B07 (15)	TdCbH+L	14/34 (41.2)	16/24 (66.7)	30/58 (51.7)	NA	NA	NA
GBG-70 (28)	H+Af-TH+Af-ECH	20/46 (43.5)	12/19 (63.2)	32/65 (49.2)	NA	NA	36/65 (55.4)
Xuhong et al. (20)	EC+Py-TdH+Py	7/11 (63.6)	7/8 (87.5)	14/19 (73.7)	NA	NA	NA
Zhong et al. (21)	AbTH+Py	3/8 (37.5)	9/13 (69.2)	12/21 (57.1)	NA	NA	NA
Panphila (22)	TdCbH+Py	19/47 (40.4)	19/22 (86.4)	38/69 (55.1)	NA	NA	40/69 (58.0)

HR-positive was defined as positive estrogen receptor and/or progesterone receptor, and HR negative was defined as negative estrogen receptor and progesterone receptor. HER2, human epidermal growth factor receptor 2; T, paclitaxel; H, trastuzumab; Ne, neratinib; A, doxorubicin; C, cyclophosphamide; L, lapatinib; Td, docetaxel; Fu, fluorouracil; E, epirubicin; Cb, carboplatin; Af, afatinib; NA, not available; Py, pyrotinib; AbT, albumin-bound paclitaxel.

characterize breast cancer. It participates in molecular subtyping and plays a determining factor in treatment decisions. The absence of PR reflects a nonfunctional ER pathway, which is less responsive to selective ER modulators (30). Our findings suggest that both ER and PR status are potential prognostic factors for tpCR in HER2-positive breast cancer with pyrotinib-containing neoadjuvant therapy. Further investigation is needed.

The incidence of TRAEs in our study was 92.8%, and the most common TRAEs were diarrhea (63.9%), decreased hemoglobin (58.8%), increased alanine transaminase (37.1%), nausea (35.1%), decreased neutrophil count (32.0%), and decreased white blood cell count (30.9%). The AE profile was consistent with previous neoadjuvant trials of pyrotinib (20–22) and the phase 3 results of pyrotinib in advanced breast cancer (19, 31). The incidence of hand-foot syndrome was 7.2%, and only grade 1 events occurred. Capecitabine is a partner of pyrotinib when used in advanced breast cancer, and one of its frequently reported AEs is hand-foot syndrome. However, capecitabine is not a common component of standard neoadjuvant regimens, with only two (2.1%) patients receiving capecitabine in our study. This might explain the low incidence and severity of hand-foot syndrome. In addition, only 35.1% of patients had grade ≥ 3 TRAEs, mainly grade 3 diarrhea (15.5%). The incidence of serious TRAEs was 5.2%. The overall safety of pyrotinib-containing neoadjuvant therapy was manageable, without new safety signals. Of patients with available data of initial dose for pyrotinib, 70.4% received 400 mg pyrotinib without dose reductions throughout the neoadjuvant therapy period, indicating a good tolerability.

There are some limitations in this multicenter real-world study. First, bias is inevitable due to the retrospective nature. Second, the judgement of AEs needs incorporation of medical records, laboratory test reports, and medical advice. There could be recall bias and missing reports in the real-world setting. Thus, the AE data might be underestimated. Third, some patients could not complete the full course of neoadjuvant therapy due to the impact of coronavirus disease 2019 (COVID-19), leading to reduced effectiveness. Fourth, this study only reported pathological response. The long-term outcomes in patients with HER2-positive breast cancer who received pyrotinib-containing neoadjuvant regimens needs further investigation. Finally, although all patients were treated with

pyrotinib, the effectiveness and safety might be attributed to other components as many combination regimens were included.

CONCLUSIONS

Small-molecule TKI pyrotinib as a component of neoadjuvant therapy for patients with HER2-positive early or locally advanced breast cancer shows effectiveness with manageable toxicity in the real-world setting. Trastuzumab plus pyrotinib may be a novel option of dual HER2-targeted blockade when combined with chemotherapy as neoadjuvant therapy. Our study suggests a trend PR-negative was a significant prognostic factor for tPCR or bPCR in HER2+ breast cancer with pyrotinib-containing neoadjuvant therapy.

DATA AVAILABILITY STATEMENT

The raw data supporting the conclusions of this article will be made available by the authors, without undue reservation.

ETHICS STATEMENT

The studies involving human participants were reviewed and approved by The ethics committee of the First Hospital of China Medical University (No. [2021]308). The patients/participants provided their written informed consent to participate in this study.

AUTHOR CONTRIBUTIONS

FJ and JL contributed to the study conception and design. FJ, JL, XM, PL, YG, XW, PT, SW, DZ, WY, OW, and JZ contributed to the acquisition of data. XM analyzed and interpreted the data. XM drafted the manuscript. FJ and JL contributed to the critical review and revision of the manuscript. All authors contributed to the article and approved the submitted version.

FUNDING

This work was supported by the National Natural Science Foundation of China (No. 81972791). The funders had no role in study design, data collection and analysis, decision to publish, or preparation of the manuscript.

ACKNOWLEDGMENTS

We thank Zheng Pang (medical director, Medical Affairs Department at Jiangsu Hengrui Pharmaceuticals Co., Ltd.) and Bin Liu (senior medical manager, Medical Affairs Department at

Hengrui) for their input in study design, Yufen Xiang (medical manager, Medical Affairs Department at Hengrui) and Ying Li (medical science liaison, Medical Affairs Department at Hengrui) for their input in data interpretation, and Fangzhou Xia (medical writer, Medical Affairs Department at Hengrui) for medical writing assistance according to Good Publication Practice Guidelines.

SUPPLEMENTARY MATERIAL

The Supplementary Material for this article can be found online at: <https://www.frontiersin.org/articles/10.3389/fonc.2022.855512/full#supplementary-material>

REFERENCES

- Harbeck N, Gnant M. Breast Cancer. *Lancet* (2017) 389(10074):1134–50. doi: 10.1016/S0140-6736(16)31891-8
- Loibl S, Gianni L. HER2-Positive Breast Cancer. *Lancet* (2017) 389(10087):2415–29. doi: 10.1016/S0140-6736(16)32417-5
- Hurvitz SA, Martin M, Symmans WF, Jung KH, Huang CS, Thompson AM, et al. Neoadjuvant Trastuzumab, Pertuzumab, and Chemotherapy Versus Trastuzumab Emtansine Plus Pertuzumab in Patients With HER2-Positive Breast Cancer (KRISTINE): A Randomised, Open-Label, Multicentre, Phase 3 Trial. *Lancet Oncol* (2018) 19(1):115–26. doi: 10.1016/S1470-2045(17)30716-7
- Li J, Jiang Z. Chinese Society of Clinical Oncology Breast Cancer Guideline Version 2021: Updates and Interpretations. *Zhonghua Yi Xue Za Zhi* (2021) 101(24):1835–8. doi: 10.3760/cma.j.cn112137-20210421-00954
- Park YH, Senkus-Konefka E, Im SA, Pentheroudakis G, Saji S, Gupta S, et al. Pan-Asian Adapted ESMO Clinical Practice Guidelines for the Management of Patients With Early Breast Cancer: A KSMO-ESMO Initiative Endorsed by CSCO, ISMPO, JSMO, MOS, SSO and TOS. *Ann Oncol* (2020) 31(4):451–69. doi: 10.1016/jannonc.2020.01.008
- National Comprehensive Cancer Network. (NCCN) *Clinical Practice Guidelines in Oncology. Breast Cancer, Version 8* (2021). Available at: https://www.nccn.org/professionals/physician_gls/default.aspx (Accessed 13 Sep 2021).
- Ditsch N, Kolberg-Liedtke C, Friedrich M, Jackisch C, Albert U-S, Banyas-Paluchowski M, et al. AGO Recommendations for the Diagnosis and Treatment of Patients With Early Breast Cancer: Update 2021. *Breast Care (Basel)* (2021) 16(3):214–27. doi: 10.1159/000516419
- Korde LA, Somerfield MR, Carey LA, Crews JR, Denduluri N, Hwang ES, et al. Neoadjuvant Chemotherapy, Endocrine Therapy, and Targeted Therapy for Breast Cancer: ASCO Guideline. *J Clin Oncol* (2021) 39(13):1485–505. doi: 10.1200/JCO.20.03399
- Hurvitz SA, Martin M, Symmans WF, Jung KH, Huang C-S, Thompson AM, et al. Neoadjuvant Trastuzumab, Pertuzumab, and Chemotherapy Versus Trastuzumab Emtansine Plus Pertuzumab in Patients With HER2-Positive Breast Cancer (KRISTINE): A Randomised, Open-Label, Multicentre, Phase 3 Trial. *Lancet Oncol* (2018) 19(1):115–26. doi: 10.1016/S1470-2045(17)30716-7
- van Ramshorst MS, van der Voort A, van Werkhoven ED, Mandjes IA, Kemper I, Dezentjé VO, et al. Neoadjuvant Chemotherapy With or Without Anthracyclines in the Presence of Dual HER2 Blockade for HER2-Positive Breast Cancer (TRAIN-2): A Multicentre, Open-Label, Randomised, Phase 3 Trial. *Lancet Oncol* (2018) 19(12):1630–40. doi: 10.1016/S1470-2045(18)30570-9
- Shao Z, Pang D, Yang H, Li W, Wang S, Cui S, et al. Efficacy, Safety, and Tolerability of Pertuzumab, Trastuzumab, and Docetaxel for Patients With Early or Locally Advanced ERBB2-Positive Breast Cancer in Asia: The PEONY Phase 3 Randomized Clinical Trial. *JAMA Oncol* (2020) 6(3):e193692. doi: 10.1001/jamaoncol.2019.3692
- Baselga J, Bradbury I, Eidtmann H, Di Cosimo S, de Azambuja E, Aura C, et al. Lapatinib With Trastuzumab for HER2-Positive Early Breast Cancer (NeoALTTO): A Randomised, Open-Label, Multicentre, Phase 3 Trial. *Lancet* (2012) 379(9816):633–40. doi: 10.1016/S0140-6736(11)61847-3
- Carey LA, Berry DA, Cirincione CT, Barry WT, Pitcher BN, Harris LN, et al. Molecular Heterogeneity and Response to Neoadjuvant Human Epidermal Growth Factor Receptor 2 Targeting in CALGB 40601, a Randomized Phase III Trial of Paclitaxel Plus Trastuzumab With or Without Lapatinib. *J Clin Oncol* (2016) 34(6):542–9. doi: 10.1200/JCO.2015.62.1268
- Robidoux A, Tang G, Rastogi P, Geyer CE Jr., Azar CA, Atkins JN, et al. Lapatinib as a Component of Neoadjuvant Therapy for HER2-Positive Operable Breast Cancer (NSABP Protocol B-41): An Open-Label, Randomised Phase 3 Trial. *Lancet Oncol* (2013) 14(12):1183–92. doi: 10.1016/S1470-2045(13)70411-X
- Hurvitz SA, Caswell-Jin JL, McNamara KL, Zoeller JJ, Bean GR, Dichmann R, et al. Pathologic and Molecular Responses to Neoadjuvant Trastuzumab and/or Lapatinib From a Phase II Randomized Trial in HER2-Positive Breast Cancer (TRIO-US B07). *Nat Commun* (2020) 11(1):5824. doi: 10.1038/s41467-020-19494-2
- Jacobs SA, Robidoux A, Abraham J, Perez-Garcia JM, La Verde N, Orcutt JM, et al. NSABP FB-7: A Phase II Randomized Neoadjuvant Trial With Paclitaxel + Trastuzumab and/or Neratinib Followed by Chemotherapy and Postoperative Trastuzumab in HER2(+) Breast Cancer. *Breast Cancer Res: BCR* (2019) 21(1):133. doi: 10.1186/s13058-019-1196-y
- Broglio KR, Quintana M, Foster M, Olinger M, McGlothlin A, Berry SM, et al. Association of Pathologic Complete Response to Neoadjuvant Therapy in HER2-Positive Breast Cancer With Long-Term Outcomes: A Meta-Analysis. *JAMA Oncol* (2016) 2(6):751–60. doi: 10.1001/jamaoncol.2015.6113
- Ma F, Li Q, Chen S, Zhu W, Fan Y, Wang J, et al. Phase I Study and Biomarker Analysis of Pyrotinib, a Novel Irreversible Pan-ErbB Receptor Tyrosine Kinase Inhibitor, in Patients With Human Epidermal Growth Factor Receptor 2-Positive Metastatic Breast Cancer. *J Clin Oncol* (2017) 35(27):3105–12. doi: 10.1200/JCO.2016.69.6179
- Xu B, Yan M, Ma F, Hu X, Feng J, Ouyang Q, et al. Pyrotinib Plus Capecitabine Versus Lapatinib Plus Capecitabine for the Treatment of HER2-Positive Metastatic Breast Cancer (PHOEBE): A Multicentre, Open-Label, Randomised, Controlled, Phase 3 Trial. *Lancet Oncol* (2021) 22(3):351–60. doi: 10.1016/S1470-2045(20)30702-6
- Xuhong J, Qi X, Tang P, Fan L, Chen L, Zhang F, et al. Neoadjuvant Pyrotinib Plus Trastuzumab and Chemotherapy for Stage I-III HER2-Positive Breast Cancer: A Phase II Clinical Trial. *Oncologist* (2020) 25(12):e1909–e20. doi: 10.1002/onco.13546
- Zhong X, He P, Chen J, Yan X, Wei B, Zhang Z, et al. Neoadjuvant Pyrotinib Plus Trastuzumab and Nab-Paclitaxel for HER2-Positive Early or Locally Advanced Breast Cancer: An Exploratory Phase II Trial. *Gland Surg* (2022) 11(1):216–25. doi: 10.21037/gs-21-911
- Liu Z, Wang C, Chen X, Zhu J, Sun X, Xia Q, et al. Pathological Response and Predictive Role of Tumour-Infiltrating Lymphocytes in HER2-Positive Early Breast Cancer Treated With Neoadjuvant Pyrotinib Plus Trastuzumab and Chemotherapy (Panphila): A Multicentre Phase 2 Trial. *Eur J Cancer* (2022) 165:157–68. doi: 10.1016/j.ejca.2022.01.022

23. Saura C, Oliveira M, Feng YH, Dai MS, Chen SW, Hurvitz SA, et al. Neratinib Plus Capecitabine Versus Lapatinib Plus Capecitabine in HER2-Positive Metastatic Breast Cancer Previously Treated With ≥ 2 HER2-Directed Regimens: Phase III NALA Trial. *J Clin Oncol* (2020) 38(27):3138–49. doi: 10.1200/JCO.20.00147
24. Li Q, Guan X, Chen S, Yi Z, Lan B, Xing P, et al. Safety, Efficacy, and Biomarker Analysis of Pyrotinib in Combination With Capecitabine in HER2-Positive Metastatic Breast Cancer Patients: A Phase I Clinical Trial. *Clin Cancer Res* (2019) 25(17):5212–20. doi: 10.1158/1078-0432.CCR-18-4173
25. Ma F, Ouyang Q, Li W, Jiang Z, Tong Z, Liu Y, et al. Pyrotinib or Lapatinib Combined With Capecitabine in HER2-Positive Metastatic Breast Cancer With Prior Taxanes, Anthracyclines, and/or Trastuzumab: A Randomized, Phase II Study. *J Clin Oncol* (2019) 37(29):2610–9. doi: 10.1200/JCO.19.00108
26. Guarneri V, Frassoldati A, Bottini A, Cagossi K, Bisagni G, Sarti S, et al. Preoperative Chemotherapy Plus Trastuzumab, Lapatinib, or Both in Human Epidermal Growth Factor Receptor 2-Positive Operable Breast Cancer: Results of the Randomized Phase II CHER-LOB Study. *J Clin Oncol* (2012) 30(16):1989–95. doi: 10.1200/JCO.2011.39.0823
27. Guarneri V, Dieci MV, Frassoldati A, Maiorana A, Ficarra G, Bettelli S, et al. Prospective Biomarker Analysis of the Randomized CHER-LOB Study Evaluating the Dual Anti-HER2 Treatment With Trastuzumab and Lapatinib Plus Chemotherapy as Neoadjuvant Therapy for HER2-Positive Breast Cancer. *Oncologist* (2015) 20(9):1001–10. doi: 10.1634/theoncologist.2015-0138
28. Hanusch C, Schneeweiss A, Loibl S, Untch M, Paepke S, Kümmel S, et al. Dual Blockade With Afatinib and Trastuzumab as Neoadjuvant Treatment for Patients With Locally Advanced or Operable Breast Cancer Receiving Taxane-Anthracycline Containing Chemotherapy-DAFNE (GBG-70). *Clin Cancer Res* (2015) 21(13):2924–31. doi: 10.1158/1078-0432.CCR-14-2774
29. Mohammed H, Russell IA, Stark R, Rueda OM, Hickey TE, Tarulli GA, et al. Progesterone Receptor Modulates $Er\alpha$ Action in Breast Cancer. *Nature* (2015) 523(7560):313–7. doi: 10.1038/nature14583
30. Cui X, Schiff R, Arpino G, Osborne CK, Lee AV. Biology of Progesterone Receptor Loss in Breast Cancer and its Implications for Endocrine Therapy. *J Clin Oncol* (2005) 23(30):7721–35. doi: 10.1200/JCO.2005.09.004
31. Yan M, Bian L, Hu X, Zhang Q, Ouyang Q, Feng J, et al. Pyrotinib Plus Capecitabine for Human Epidermal Factor Receptor 2-Positive Metastatic Breast Cancer After Trastuzumab and Taxanes (PHENIX): A Randomized, Double-Blind, Placebo-Controlled Phase 3 Study. *Trans Breast Cancer Res* (2020) 1:13. doi: 10.21037/tbcr-20-25

Conflict of Interest: The authors declare that the research was conducted in the absence of any commercial or financial relationships that could be construed as a potential conflict of interest.

Publisher's Note: All claims expressed in this article are solely those of the authors and do not necessarily represent those of their affiliated organizations, or those of the publisher, the editors and the reviewers. Any product that may be evaluated in this article, or claim that may be made by its manufacturer, is not guaranteed or endorsed by the publisher.

Copyright © 2022 Mao, Lv, Gong, Wu, Tang, Wang, Zhang, You, Wang, Zhou, Li and Jin. This is an open-access article distributed under the terms of the Creative Commons Attribution License (CC BY). The use, distribution or reproduction in other forums is permitted, provided the original author(s) and the copyright owner(s) are credited and that the original publication in this journal is cited, in accordance with accepted academic practice. No use, distribution or reproduction is permitted which does not comply with these terms.



Augmentation of Extracellular ATP Synergizes With Chemotherapy in Triple Negative Breast Cancer

Jasmine M. Manouchehri, Jharna Datta, Natalie Willingham, Robert Wesolowski, Daniel Stover, Ramesh K. Ganju, William E. Carson, Bhuvaneswari Ramaswamy and Mathew A. Cherian*

Comprehensive Cancer Center, The Ohio State University, Columbus, OH, United States

OPEN ACCESS

Edited by:

Maria Rosaria De Miglio,
University of Sassari, Italy

Reviewed by:

Jane E Cavanaugh,
Duquesne University, United States
Lauren Gollahon,
Texas Tech University, United States

*Correspondence:

Mathew A. Cherian
mathew.cherian@osumc.edu

Specialty section:

This article was submitted to
Breast Cancer,
a section of the journal
Frontiers in Oncology

Received: 14 January 2022

Accepted: 07 March 2022

Published: 20 April 2022

Citation:

Manouchehri JM, Datta J, Willingham N, Wesolowski R, Stover D, Ganju RK, Carson WE, Ramaswamy B and Cherian MA (2022) Augmentation of Extracellular ATP Synergizes With Chemotherapy in Triple Negative Breast Cancer. *Front. Oncol.* 12:855032. doi: 10.3389/fonc.2022.855032

Introduction: Breast cancer affects two million patients worldwide every year and is the most common cause of cancer-related death among women. The triple-negative breast cancer (TNBC) sub-type is associated with an especially poor prognosis because currently available therapies fail to induce long-lasting responses. Therefore, there is an urgent need to develop novel therapies that result in durable responses. One universal characteristic of the tumor microenvironment is a markedly elevated concentration of extracellular adenosine triphosphate (eATP). Chemotherapy exposure results in further increases in eATP through its release into the extracellular space of cancer cells via P2RX channels. eATP is degraded by eATPases. Given that eATP is toxic to cancer cells, we hypothesized that augmenting the release of eATP through P2RX channels and inhibiting extracellular ATPases would sensitize TNBC cells to chemotherapy.

Methods: TNBC cell lines MDA-MB 231, Hs 578t and MDA-MB 468 and non-tumorigenic immortal mammary epithelial MCF-10A cells were treated with increasing concentrations the chemotherapeutic agent paclitaxel in the presence of eATPases or specific antagonists of P2RXs with cell viability and eATP content being measured. Additionally, the mRNA, protein and cell surface expressions of the purinergic receptors P2RX4 and P2RX7 were evaluated in all examined cell lines via qRT-PCR, western blot, and flow cytometry analyses, respectively.

Results: In the present study, we observed dose-dependent declines of cell viability and increases in eATP of paclitaxel-treated TNBC cell lines in the presence of inhibitors of eATPases, but not of the MCF-10A cell line. These effects were reversed by specific antagonists of P2RXs. Similar results, as those observed with eATPase inhibitors, were seen with P2RX activators. All examined cell lines expressed both P2RX4 and P2RX7 at the mRNA, protein and cell surface levels.

Conclusion: These results reveal that eATP modulates the chemotherapeutic response in TNBC cell lines, which could be exploited to enhance the efficacy of chemotherapy regimens for TNBC.

Keywords: ATP, breast cancer, paclitaxel, P2RX4, P2RX7

INTRODUCTION

Breast cancer affects millions of women every year. At 47.8 new cases and 13.6 deaths per 100,000 per year, it has the highest global incidence rate and is the most common cause of cancer-related mortality among women in 2020 (1). Patients with triple-negative breast cancer (TNBC) have a markedly worse outcome in comparison to other breast cancer subtypes due to the aggressive and rapidly progressive nature of the disease and lack of specific targeted therapies (2–4). Hence, there is a critical need for more effective therapeutic strategies.

One universal characteristic of cancer is a marked elevation in extracellular adenosine triphosphate (eATP) (5–7). Under physiological conditions, the concentration of eATP is extremely low, in the 0–10 nanomolar (nM) range as compared to intracellular levels of 3 to 10 millimolar (mM), a difference of more than 10^6 -fold (8). However, eATP concentrations are markedly elevated in neoplastic and inflamed tissues, into the range of 100s of micromoles/liter (8).

Purinergic P2 receptors (P2Rs), integral plasma membrane receptors activated by ATP, are divided into the ionotropic P2 (P2RX) and metabotropic P2 (P2RY) sub-types (9). P2RXs, of which there are seven sub-types, are ATP-gated ion channels that are inducibly permeable to cations. With prolonged activation, P2RX7 channels become non-selectively permeable, resulting in the diffusion of high molecular weight molecules such as ATP; IL-1 β and IL-18 release; large molecular weight dye uptake; K⁺ efflux; Na⁺ and Ca²⁺ influx; membrane phosphatidylserine-flip; membrane blebbing and cell death (10–14). Most P2RXs are activated by ATP concentrations in the nanomolar to low micromolar range, but P2RX7 activation requires millimolar concentrations of eATP (15–17). However, because P2RXs can homo and heterotrimerize to form functional channels with intermediate properties, ATP-dependent interactions between P2RX4 and the C-terminus of P2RX7 can potentiate P2RX7-dependent cell death (18).

Extracellular ATP release occurs through a variety of mechanisms, including tumor necrosis and apoptosis, vesicular exocytosis, active efflux *via* ATP-binding cassette subfamily C member 6 (ABCC6) and the ankylosis gene product ANK and diffusion *via* P2RX7 and Pannexin1 channels (10, 11, 19–24). Multiple pathways for eATP disposal have been described. These pathways hydrolyze nucleotides and limit their availability to activate nucleotide-specific P2Rs while increasing the concentration of extracellular nucleosides such as adenosine (25). There are four major classes of ecto-nucleotidases, including ecto-nucleoside triphosphate diphosphohydrolases (E-NTPDase), 5' nucleotidases, ecto-nucleotide pyrophosphatases/phosphodiesterases (E-NPPase), and tissue non-specific alkaline phosphatases (TNAP) (25). E-NTPDases, which are nucleotide specific, are believed to be the major degradative enzymes for eATP. Extracellular 5' nucleotidase, which is classified as CD73 as per the cluster of differentiation system, catalyzes the conversion of AMP to adenosine and inorganic phosphate. Thus, eATP levels result from a balance between numerous synthetic and secretory pathways and degradative and endocytic pathways.

When cancer cells are exposed to cytotoxic chemotherapy, there is a release of ATP and K⁺ ions through P2RXs such as

P2RX7 and P2RX4 into the extracellular space along with an influx of Ca²⁺ ions (17, 26–28). Exposure of various epithelial cancer cell lines to elevated eATP in culture and xenografts results in growth arrest or cell death (29–31). Notably, P2RX7 activation is a prerequisite for inflammasome activation, IL-1 and IL-18 secretion, and a highly inflammatory form of programmed cell death known as pyroptosis, which can lead to bystander cell death and immune activation (18). In addition, ATP has been administered to patients with advanced cancers with minimal side effects, and ATP administered in mice was associated with inhibitory effects on cancer cells (30, 32, 33).

Overall, these data suggest that the extracellular purinergic signaling pathway may be a promising target for cancer therapeutics. We hypothesized that increased eATP would increase the response to chemotherapy in TNBCs through the activation of P2RX channels, leading to increases in non-selective membrane permeability, the release of eATP and increased cancer cell death.

MATERIALS AND METHODS

Cell Culture and Drugs and Chemicals

Breast cancer cell lines MDA-MB 231 (ATCC HTB-26, RRID : CVCL_0062), MDA-MB 468 (ATCC HTB-132, RRID : CVCL_0419), Hs 578t (ATCC HTB-126, RRID : CVCL_0332), and HEK-293T ATCC Cat# CRL-3216, RRID : CVCL_0063) were maintained in DMEM (Corning) and supplemented with 10% FBS (Cytiva), 1% MEM non-essential amino acids (Gibco), 1 mM sodium pyruvate (Gibco), 4 mM L-glutamine (Gibco) and antimicrobial agents (100 units/ml Penicillin, 100 μ g/ml streptomycin, and 0.25 μ g/ml amphotericin B) (Gibco). Non-tumorigenic immortal mammary epithelial MCF-10A cells (ATCC Cat# CRL-10317, RRID : CVCL_0598) were maintained in DMEM/F12 (Gibco) supplemented with 5% horse serum (Gibco), hydrocortisone (Sigma), epidermal growth factor (Sigma), cholera toxin (Sigma), insulin (Sigma) and antimicrobial agents. All cell lines were authenticated and were maintained in a humidified incubator at 37°C and 5% CO₂.

The following drugs and chemicals were used: dimethyl sulfoxide/DMSO (Sigma), ATP (Sigma), UTP (Sigma), paclitaxel (Calbiochem), sodium polyoxotungstate or POM-1 (Tocris), PSB 069 (Tocris), levamisole hydrochloride (Abcam), A438079 (Tocris), 5-BDBD (Tocris), ENPP1 inhibitor C (Cayman Chemical, Ann Arbor, MI), SBI-425 (MedChemExpress), etidronate disodium and ivermectin (Sigma). ATP and POM-1 were dissolved in nuclease-free water (Invitrogen); paclitaxel, A438079, Iso-PPADS, 5-BDBD, SBI-425, ENPP1 inhibitor C, levamisole hydrochloride, etidronate disodium (Sigma), and ivermectin were dissolved in DMSO. **Table 1** shows drugs' concentrations and functions; we optimized the drug concentrations that were applied for the different assays by using previously described drugs' concentrations as starting points (34–43). Drugs were added to media at designated concentrations and applied to cells in an *in vitro* system.

Cell Viability and eATP Assays

TNBC cell lines, MDA-MB 231, Hs 578t, MDA-MB 468 cells and non-tumorigenic immortal mammary epithelial MCF-10A cells were plated on 96 well plates (Costar) at a high density of 25,000

TABLE 1 | Drug concentrations and functions. The table shows the drugs administered, their concentrations applied and their functions.

Drug	Concentration(s)	Function
Paclitaxel	12.5, 25, 50, 100 $\mu\text{mol/L}$	Chemotherapeutic agent
Iso-PPADs	20 $\mu\text{mol/L}$	P2RX inhibitor
A437809	20 $\mu\text{mol/L}$	P2RX7 inhibitor
5-BDBD	20 $\mu\text{mol/L}$	P2RX4 inhibitor
POM-1	10 $\mu\text{mol/L}$	ecto-nucleoside triphosphate diphosphohydrolases (ENTPDase) inhibitor
PSB 069	10 $\mu\text{mol/L}$	ENTPDase inhibitor
ENNP1 C inhibitor	10 $\mu\text{mol/L}$	ecto-nucleoside pyrophosphatases/ phosphodiesterase 1 (ENPP1) inhibitor
SBI-425	10 $\mu\text{mol/L}$	tissue-nonspecific alkaline phosphatase (TNAP) inhibitor
Levamisole hydrochloride	10 $\mu\text{mol/L}$	TNAP inhibitor
Etidronate disodium	10 $\mu\text{mol/L}$	protein tyrosine phosphatase inhibitor
Ivermectin	20 $\mu\text{mol/L}$	P2RX4 and P2RX7 activator

cells/well and after 24 hours treated with paclitaxel, inhibitors, or ATP for 6 or 48 hours. PrestoBlue™ HS cell viability reagent (Invitrogen) was added to each well according to the manufacturer's instructions. Fluorescence readings (excitation and emission ranges: 540–570 nm and 580–610 nm) were obtained using a Biotech Synergy HT plate reader. ATP was measured in supernatants according to the protocol described by the ATPlite 1 step Luminescence Assay System (PerkinElmer). Luminescence readings were measured on a Biotech Synergy HT plate reader. The student's t-test was applied to the applicable assays (Figures 1, 4, 5) to ascertain significance. * represents $p < 0.05$ and ** represents $p < 0.01$; for Figure 1 comparing ATP to UTP, for Figure 4 comparing PSB alone to PSB 069 and A438079 or to

PSB 069 and 5-BDBD, for Figure 5 comparing vehicle addition (paclitaxel alone) and ivermectin. For Figures 2, 3, one way ANOVA with Tukey's HSD (Honestly Significant Difference) was applied to ascertain significance. For Figure 2 * represents $p < 0.05$ and ** represents $p < 0.01$ when comparing vehicle addition to Iso-PPADS, A438079 or 5-BDBD. For Figure 3 * represents $p < 0.05$ and ** represents $p < 0.01$ when comparing vehicle addition to PSB 069. We highlighted just the significance in the presence of PSB 069 because the cell viability results were consistently significant.

RNA Analysis of P2RX4 and P2RX7

MDA-MB 231, Hs 578t, MDA-MB 468, cell lines and MCF-10A cells were maintained under standard conditions in subconfluent

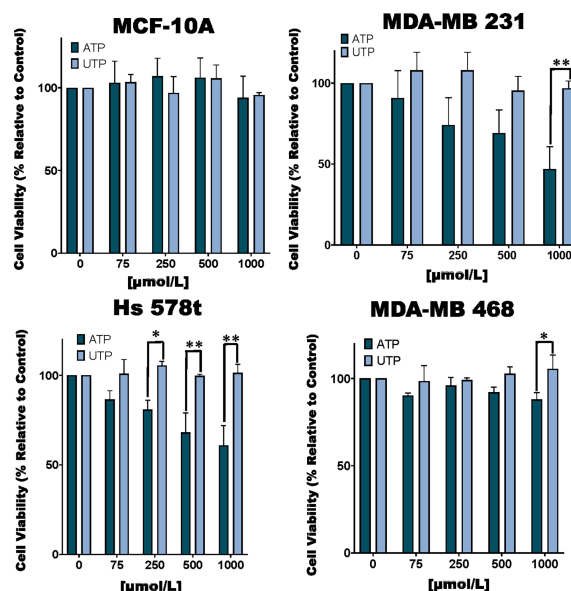


FIGURE 1 | Cell viability of ATP and UTP-treated cells. TNBC MDA-MB 231, Hs 578t and MDA-MB 468 cell lines and non-tumorigenic immortal mammary epithelial MCF-10A cells were treated for 48 hours with increasing concentrations of ATP or UTP, and cell viability was measured with the PrestoBlue HS assay. Error bars represent standard deviations calculated from three independent experiments performed in triplicate. The student's t-test was applied to the to ascertain significance. * represents $p < 0.05$ and ** represents $p < 0.01$ when comparing ATP to UTP.

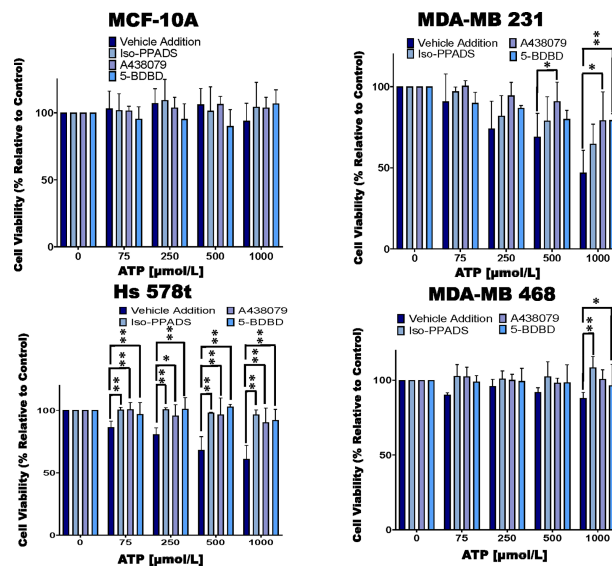


FIGURE 2 | Cell viability of ATP-treated cells in the presence of P2RX inhibitors. TNBC cell lines and MCF-10A cells were treated for 48 hours with increasing concentrations of ATP in the presence of the P2RX inhibitor Iso-PPADS (20 $\mu\text{mol/L}$), the P2RX7 inhibitor A438079 (20 $\mu\text{mol/L}$) or the P2RX4 inhibitor 5-BDBD (20 $\mu\text{mol/L}$) or vehicle addition, and cell viability was measured using the PrestoBlue HS assay. Error bars represent standard deviations calculated from three independent experiments performed in triplicate. One way ANOVA with Tukey's HSD was applied to ascertain significance. * represents $p < 0.05$ and ** represents $p < 0.01$ when comparing vehicle addition to Iso-PPADS, A438079 or 5-BDBD.

cultures. RNA was extracted *via* the TRIzol method (Invitrogen), and qRT-PCR was performed on a Bio-Rad T100 thermal cycler using the following exon-exon junction-spanning primers: for P2RX4, the forward primer TGGCGGATTATGTGATACCAGC and the reverse primer GTCGCATCTGGAATCTCGGG; for P2RX7, the forward primer GTGTCCCGAGTATCCACC and the reverse primer GGCAGTGTCAAGAGAGCAG; and for GAPDH forward primer GTCGTATTGGGCGCCTGGTC and the reverse primer TTTGGAGGGATCTCGTCTCT. The student's t-test was applied to the applicable assays to ascertain significance. * represents $p < 0.05$ and ** represents $p < 0.01$ relative to MCF-10A; + represents $p < 0.05$ and ++ represents $p < 0.01$ relative to HEK293-empty vector transfected.

Western Blot Analysis of P2RX4 and P2RX7

Total cell lysates were prepared in lysis buffer (50 mM Tris HCl at pH 8.0, 1.0 mM EDTA, 1% SDS, and 1% Igepal CA630) with a protease inhibitor cocktail (Thermo Scientific). The lysates were sonicated, placed on ice for 30 minutes, and spun at 10,000 rpm for 10 minutes at 4°C to collect the cleared supernatants for analysis. Protein quantification was performed using the Pierce BCA Protein Assay (Thermo Scientific) and absorbance readings taken at 595 nm. Protein samples (P2RX4: 100 μg , positive control-293T/empty vector 99.5 μg + 293T/O/E P2RX4 0.5 μg and P2RX7: 200 μg , positive control-293T/empty vector 199, 197.5, or 195 μg + 293T/O/E P2RX7 1, 2.5 or 5 μg , respectively, as shown in **Figure 6**) were denatured with 4X Laemmli sample buffer (250 mM Tris-HCl, 8% SDS, 40% glycerol, 8% BME, and 0.06% Bromophenol Blue) at 98°C for 5 minutes and separated

on 12% sodium dodecyl sulfate (SDS)-polyacrylamide gels (Invitrogen). Proteins were transferred to nitrocellulose membranes (Millipore) employing the wet transfer method (Bio-Rad, Hercules, CA). The membranes were blocked with TBS-T (0.15 M NaCl, 0.02 M Tris-HCl, pH 7.4 and 0.1% Tween-20) containing non-fat milk at room temperature for an hour and incubated overnight at 4°C with a primary antibody: P2RX4 (1:500 dilution; Cell Signaling Technology, Cat# 70659, RRID : AB_2799789) and anti-P2RX7 (1:200 dilution; Cell Signaling Technology, Cat# 13809, RRID : AB_2798319), diluted in 5% BSA (GoldBio) or 5% non-fat milk. The membranes were washed in TBS-T (0.15 M NaCl, 0.02 M Tris HCl, pH 7.4), incubated with horseradish peroxidase (HRP)-conjugated secondary anti-rabbit/mouse antibodies diluted in 5% non-fat milk (1:5000) for one hour and washed in TBS-T. The blots were analyzed using enhanced chemiluminescence Immobilon Western Chemiluminescent HRP Substrate (Millipore). The membranes were then stripped and re-probed for GAPDH (Cell Signaling Technology) as the internal loading control. Densitometry was performed on Image Studio (Licor). The student's t-test was applied to the applicable assays to ascertain significance. * represents $p < 0.05$ and ** represents $p < 0.01$ relative to MCF-10A; + represents $p < 0.05$ and ++ represents $p < 0.01$ relative to HEK293-empty vector transfected.

Flow Cytometry Analysis of P2RX4 and P2RX7

MDA-MB 231, MDA-MB 468, Hs 578t, MCF-10A cells, and HEK 293T cells were maintained as previously described. HEK 293T cells were transfected with either P2RX4 or P2RX7 expression plasmids

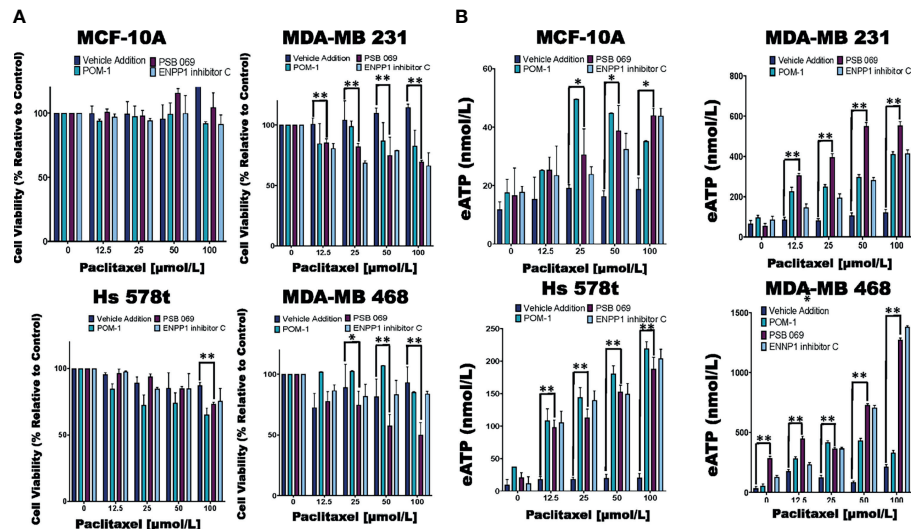


FIGURE 3 | Comparing eATP release from paclitaxel-treated cells in the presence of inhibitors or vehicle addition. **(A)** TNBC and MCF-10A cells were treated with increasing concentrations of paclitaxel and the nucleoside phosphohydrolase inhibitors POM-1 (E-NTPDase inhibitor, 10 $\mu\text{mol/L}$), PSB 069 (E-NTPDase inhibitor, 10 $\mu\text{mol/L}$), ENPP1 inhibitor C (ENPP1 inhibitor, 10 $\mu\text{mol/L}$) or vehicle addition for six hours, and cell viability was measured using the PrestoBlue HS assay. Standard deviation was calculated from three independent experiments performed in triplicate. **(B)** eATP concentrations were measured in the supernatants of TNBC and MCF-10A cells after six hours of treatment with increasing concentrations of paclitaxel and nucleoside phosphohydrolase inhibitors or vehicle addition. Standard deviation was calculated from three independent experiments performed in triplicate. One way ANOVA with Tukey's HSD was applied to ascertain significance. * represents $p < 0.05$ and ** represents $p < 0.01$ when comparing vehicle addition to PSB 069. We highlighted just the significance in the presence of PSB 069 because the cell viability results were consistently significant.

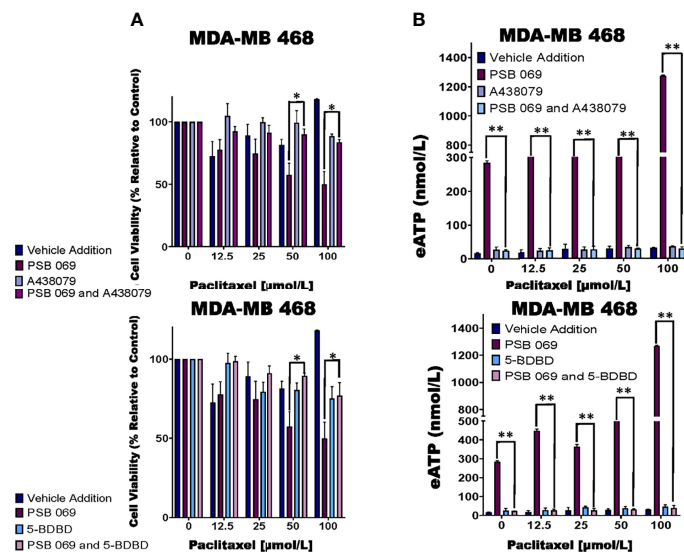


FIGURE 4 | Examining the influence of P2RX inhibitors in combination with E-NTPDase inhibitor on cell viability and eATP release in paclitaxel-treated cells. **(A)** Paclitaxel-treated breast cancer MDA-MB 468 cell lines were treated for six hours with P2RX7 inhibitor A438079 (20 $\mu\text{mol/L}$) or P2RX4 inhibitor 5-BDBD (20 $\mu\text{mol/L}$) in the presence or absence of PSB 069 (10 $\mu\text{mol/L}$), and cell viability was measured by applying PrestoBlue HS assay. Standard deviation was calculated from three independent experiments performed in triplicate. We used the same values for both graphs for vehicle addition and PSB 069. **(B)** eATP concentrations were measured in the supernatants of paclitaxel-treated MDA-MB 468 cells after six hours of treatment. Standard deviation was calculated from three independent experiments performed in triplicate. We used the to the same values for both graphs for vehicle addition and PSB 069. The student's t-test was applied to the applicable assays to ascertain significance. * represents $p < 0.05$ and ** represents $p < 0.01$ for A438079 and PSB 069 or 5-BDBD and PSB 069 when compared to PSB 069 alone.

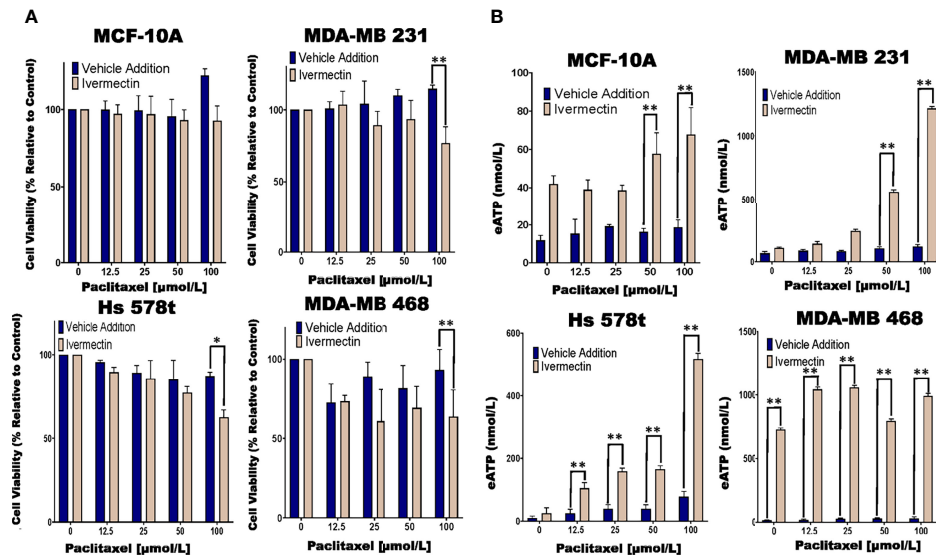


FIGURE 5 | Determining relative eATP content and cell viability in paclitaxel-treated cells in the presence of ivermectin or vehicle addition. **(A)** The graphs represent cell viability as measured using the Presto Blue HS assay +/- standard deviation from three independent experiments performed in triplicate in TNBC and MCF-10A cells after six hours of treatment with increasing concentrations of paclitaxel and the P2RX4 and P2RX7 activator ivermectin (10 $\mu\text{mol/L}$) or vehicle addition. **(B)** eATP content was measured in the supernatants of paclitaxel-treated TNBC and MCF-10A cell lines in the presence of the P2RX4 and P2RX7 activator ivermectin (10 $\mu\text{mol/L}$) or vehicle addition. The student's t-test was applied to the applicable assays to ascertain significance. * represents $p < 0.05$ and ** represents $p < 0.01$ when comparing ivermectin to vehicle addition.

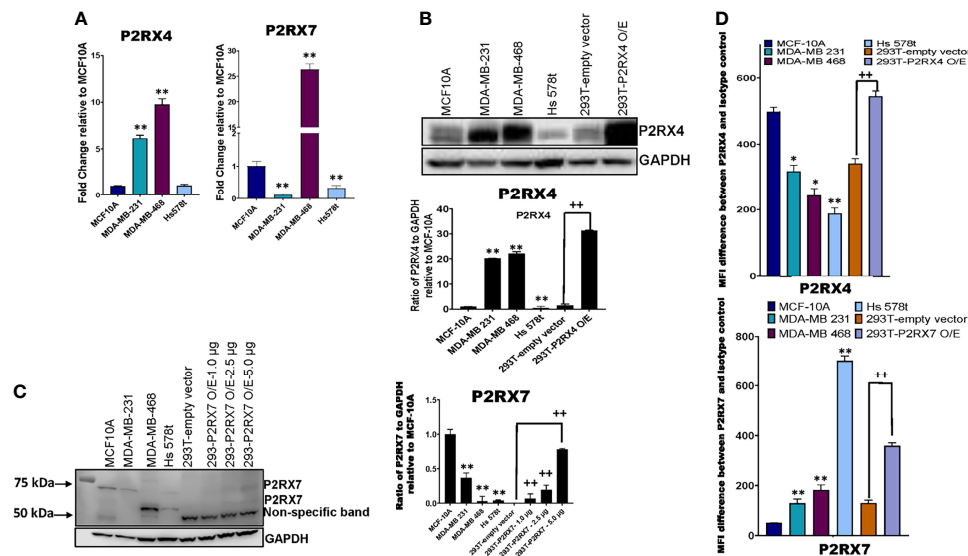


FIGURE 6 | mRNA and protein expression analysis of P2RX4 and P2RX7 for all cell lines. **(A)** qRT-PCR was performed on mRNA of TNBC cell lines and MCF-10A cells using specific primers for P2RX4 and P2RX7. * represents $p < 0.05$ and ** represents $p < 0.01$. TNBC cell lines, MCF-10A cells, and HEK 293T cells transfected with P2RX4 or P2RX7 as positive controls were probed for **(B)** P2RX4 and **(C)** P2RX7, and GAPDH was used as a loading control for western blot analysis repeated twice. HEK 293T cells transfected with P2RX7 were loaded at increasing protein concentrations of 1.0 μg , 2.5 μg , and 5.0 μg combined with lysates of control vector-transfected cells to keep the total loaded protein the same in each lane. Densitometry analysis was performed using Image Studio on the 75 kDa P2RX7 band. The student's t-test was applied to the applicable assays to ascertain significance. * represents $p < 0.05$ and ** represents $p < 0.01$ relative to MCF-10A; + represents $p < 0.05$ and ++ represents $p < 0.01$ relative to HEK293-empty vector transfected. **(D)** The calculated difference in mean fluorescence intensity (MFI) values between TNBC cell lines, MCF-10A cells, and HEK 293T cells transfected with P2RX4 or P2RX7 as positive controls stained with P2RX4 or P2RX7 specific antibody and the isotype control for the different cell lines examined. * represents $p < 0.05$ and ** represents $p < 0.01$ relative to MFI difference in MCF-10A cells; + represents $p < 0.05$ and ++ represents $p < 0.01$ relative to MFI difference in HEK293-empty vector transfected. O/E represents overexpressed.

derived from pcDNA3.1 (RRID: Addgene_79663) using Lipofectamine 3000 (Thermo Fisher Scientific). Cells were detached with accutase (Thermo Fisher Scientific). One million cells were washed in PBS with 0.05% BSA, stained with P2RX7 – FITC (Sigma Aldrich, # P8997, RRID : AB_477416) antibodies or stained with rabbit IgG Isotype Control-FITC (Invitrogen, Cat# PA5-23092, RRID : AB_2540619), or with anti-P2RX4 (Cell Signaling Technology) plus goat anti-rabbit IgG (H+L) secondary antibody-FITC (Novus Biologicals, # NB 7168, RRID : AB_524413) or IgG isotype control plus secondary antibody-FITC in Flow Cytometry Staining Buffer (2% FBS, 0.02% sodium azide and PBS). Analysis was performed on BD FACS Fortessa using the FITC channel (530/30 nm) and Flowjo software (RRID: SCR_008520). The student's t-test was applied to the applicable assays to ascertain significance. * represents $p < 0.05$ and ** represents $p < 0.01$ relative to MFI difference in MCF-10A cells; + represents $p < 0.05$ and ++ represents $p < 0.01$ relative to MFI difference in HEK293-empty vector transfected. O/E represents overexpressed.

RESULTS

Cell Viability of ATP and UTP-Treated Cells and the Impact of P2RX Inhibitors on Cell Viability of ATP-Treated Cells

We examined the toxic effects of ATP using UTP as a control. We observed a dose-dependent loss of viability in TNBC MDA-MB 231, MDA-MB 468 and Hs 578t cell lines upon exposure to ATP but not UTP and not in non-tumorigenic immortal mammary epithelial MCF-10A cells (**Figure 1**). For example, in MDA-MB 231 cells treated with increasing concentrations of ATP, there was a mean loss of viability between 10 and 50%. Similar effects were observed in ATP-treated Hs 578t cells with a mean loss in viability between 15 and 40%. For ATP-treated MDA-MB 468 cells, there was a mean loss of viability between 10 and 13%. We did not see any significant change in cell viability in ATP-treated MCF-10A cells. There were no significant changes in viability in UTP-treated cells.

We next treated the cells with various purinergic receptor antagonists to determine whether P2RX receptors mediate the effects of eATP on cell viability (**Figure 2**). As with **Figure 1**, we did not see any change in cell viability in ATP-treated MCF-10A cells and therefore, did not see any additional changes with exposure to P2RX antagonists. However, for ATP-treated TNBC cells, in the absence of inhibitors we saw decreases in viability that were attenuated by P2RX inhibitors, which decreased their sensitivity to inhibition by ATP. For example, in MDA-MB 231 cells treated with increasing concentrations of ATP, when compared to vehicle addition, there was an improvement in cell viability between 7 and 15% when exposed to the non-specific P2RX inhibitor Iso-PPADS (20 $\mu\text{mol/L}$), an improvement in cell viability between 10 and 30% when exposed to the P2RX7 inhibitor A438079 (20 $\mu\text{mol/L}$), and an improvement in cell viability between 0 and 30% when exposed to the P2RX4 inhibitor 5-BDBD (20 $\mu\text{mol/L}$). Similar effects were seen in ATP-treated Hs 578t cells when compared to vehicle

addition, there was an improvement in cell viability between 14 and 33% when exposed to Iso-PPADS, an improvement in cell viability between 14 and 30% when exposed to A438079, and an improvement in cell viability between 10 and 32% when exposed to 5-BDBD. For ATP-treated MDA-MB 468 cells as compared to vehicle-addition, there was an improvement in cell viability between 12 and 23% when exposed to Iso-PPADS, an improvement in cell viability between 10 and 12% when exposed to A438079, but no significant improvement in cell viability when exposed to 5-BDBD.

Examining the Effects of eATPase Inhibitors on Cell Viability and eATP Release

We next studied the effects of combinations of eATPase inhibitors with chemotherapy (paclitaxel) to determine their effects on the efficacy of chemotherapy. For these experiments, all the cell lines were treated for six hours to simulate the duration of systemic exposure in patients (**Figure 3**). For this reason, we did not see changes in the viability of cells treated with paclitaxel alone. Additionally, there were decreases in cell viability in the paclitaxel-treated TNBC cell lines in the presence of POM-1 and the ENPPase inhibitor ENPP1 inhibitor C, but these results were not consistently significant. For MDA-MB 231 cells treated with increasing concentrations of paclitaxel, there was a mean decrease in cell viability between 15 to 30% in the presence of the E-NTPDase inhibitor PSB 069 when compared to vehicle addition. Similarly for paclitaxel-treated Hs 578t cells in the presence of PSB 069, there was a loss of viability between 0 to 14%. For paclitaxel-treated MDA-MB 468 cells there was a decrease in cell viability between 0 to 50% in the presence of PSB 069 as compared to vehicle addition. However, there was no significant change in the viability of paclitaxel-treated MCF-10A cells in the presence of the three inhibitors (**Figure 3A**). We also confirmed that under these experimental conditions, treatment with the eATPase inhibitors alone did not significantly change cell viability in any of the cell lines (**Supplementary Figure 1**). Therefore, PSB 069 most potently and consistently decreased the viability of TNBC cell lines when combined with paclitaxel.

In the same experiments, we measured the amount of eATP in the supernatants of chemotherapy-treated cells (**Figure 3B**). Treating cells with paclitaxel alone produced quite modest increases in eATP that were generally not statistically significant when compared to vehicle control: for MDA-MB 231 cells treated with increasing concentrations of paclitaxel, eATP increments ranged from 66 to 120 nmol/L, for Hs 578t, from 9 to 20 nmol/L, for MDA-MB 468, eATP increased from 34 to 213 nmol/L, and for MCF-10A, to 12 to 18 nmol/L. However, in the presence of inhibitors, we saw significant increases in eATP levels. For instance, in MDA-MB 231 cells treated with increasing concentrations of paclitaxel, the increments in eATP concentration upon treatment with POM-1 ranged from 130 to 450 nmol/L, with PSB 069 54 to 550 nmol/L and with ENPP1 inhibitor C 86 to 410 nmol/L. Similarly, for Hs 578t cells treated with increasing concentrations of paclitaxel, with POM-1 the increase in eATP ranged from 34 to 219 nmol/L, with PSB 069 21

to 188 nmol/L and with ENPP1 inhibitor C from 12 to 204 nmol/L. For MDA-MB 231 cells treated with increasing concentrations of paclitaxel, the increments in eATP concentration with POM-1 ranged from 84 to 450 nmol/L, with PSB 069 between 284 nmol/L to 1.3 μ mol/L and with ENPP1 inhibitor C 129 nmol/L to 1.4 μ mol/L. For MCF-10A cells treated with increasing concentrations of paclitaxel, the increments in eATP concentration increased with POM-1 ranged from 18 to 40 nmol/L, with PSB 069 16 to 41 nmol/L and with ENPP1 inhibitor C 18 to 39 nmol/L. Thus, ENTPDase and NPPase inhibitors significantly increased eATP release upon chemotherapy treatment although the magnitude of this increase was much higher in TNBC cell lines than in immortal mammary epithelial cells.

Examining the Effects of P2RX Inhibitors on the E-NTPDase Inhibitor-Induced Exaggerated Loss of Cell Viability and eATP Release

Of the eATPase inhibitors tested, we consistently saw an exaggerated loss of cell viability with the E-NTPDase inhibitor PSB 069. Therefore, we sought to determine if the increased loss of cell viability in the presence of PSB 069 is dependent on eATP induced activation of P2RX4 or P2RX7 (**Figure 2**). We chose the MDA-MB 468 cell line because the baseline effects of PSB 069 were maximal and therefore, the reversal of these effects would be most meaningful.

We did see reversal of the effects of PSB 069 on cell viability and eATP release upon concurrent treatment with both the P2RX7 inhibitor A438079 and the P2RX4 inhibitor 5-BDBD (**Figure 4A**). In paclitaxel - treated MDA-MB 468 cells, there was an improvement in viability that ranged from 8 to 34% for the combination of A438079 with PSB 069 when compared to vehicle addition with PSB 069 and an improvement in cell viability ranging from 24 to 27% in the presence of 5-BDBD and PSB 069 when compared to vehicle addition with PSB 069. These results show that the increased loss of cell viability observed when PSB 069 is combined with paclitaxel is dependent on the activation of P2RX4 and P2RX7 by eATP.

In the same experiments, we determined the effects of A438079 and 5-BDBD on eATP release in MDA-MB 468 cells treated with 10 μ mol/L PSB 069 and increasing concentrations of paclitaxel (**Figure 4B**). There was a decrease in eATP from a range of between 284 nmol/L and 1.3 μ mol/L to a range of between 40 and 70 nmol/L when A438079 was combined with PSB 069. There was a decrease in eATP from a range of between 284 nmol/L and 1.3 μ mol/L to a range between 30 to 80 nmol/L when 5-BDBD was combined with PSB 069. These results show that the increased eATP release observed when PSB 069 is combined with paclitaxel is dependent on the activation of P2RX4 and P2RX7 by eATP.

Previous reports indicate that tissue non-specific alkaline phosphatase also metabolizes eATP. We sought to ascertain if two tissue non-specific alkaline phosphatase inhibitors (SBI 425 and levamisole hydrochloride) could augment the effects on cell viability and eATP release in paclitaxel-treated cells while using a protein tyrosine phosphatase inhibitor, etidronate disodium, as a control. Although we observed substantial changes in eATP upon

treatment of the TNBC cell lines, there was no significant change in cell viability (**Supplementary Figure 2**).

Evaluating the Impact of a P2RX Activator on Cell Viability and ATP Release in Chemotherapy-Treated Cells

Previous research had shown that ivermectin is a P2RX4 and P2RX7 activator (44, 45). Hence, we examined the effects of ivermectin on eATP and cell viability in chemotherapy-treated MCF10A cells and TNBC cell lines. We observed significant decreases in cell viability in paclitaxel and ivermectin-treated TNBC cell lines but not in MCF-10A cells (**Figure 5A**). As an example, for ivermectin addition (20 μ mol/L) compared with vehicle addition to cells treated with increasing concentrations of paclitaxel, MDA-MB 231, Hs 578t and MDA-MB 468 cells showed between 3 to 35%, 7 to 38% and 6 to 50% mean decreases in cell viability, respectively.

In the same experiments, we also looked at eATP release upon exposure to the combined treatment of ivermectin and paclitaxel. For paclitaxel-treated cells, there were increases in eATP release in the presence of ivermectin when compared to the vehicle addition. These increases were much more dramatic in the TNBC cell lines than immortal mammary epithelial cells (**Figure 5B**). As an example, for MDA-MB 231 cells in the presence of ivermectin, eATP increased from a range of between 66 and 120 nmol/L (vehicle addition) to a range of between 108 nmol/L and 1.2 μ mol/L, for Hs 578t cells eATP increased from a range of between 9 and 20 nmol/L (vehicle addition) to a range of between 25 and 517 nmol/L and for MDA-MB 468 cells eATP increased from a range of between 34 and 213 nmol/L (vehicle addition) to a range of between 730 nmol/L and 1 μ mol/L. For MCF-10A cells in the presence of ivermectin, eATP increased from a range of between 12 and 18 nmol/L (vehicle addition) to a range of between 42 and 68 nmol/L. Therefore, ivermectin potentiated the effects of paclitaxel on TNBC cell lines.

Expression of P2RX4 and P2RX7 in TNBC Cell Lines

We next sought to assess the expression of P2RX4 and P2RX7 mRNA and protein. qRT-PCR was performed on TNBC and MCF-10A cells with specific exon-exon junction-spanning primers for *P2RX4*, *P2RX7* and *GAPDH*, and fold change was calculated relative to the expression of the receptors in MCF-10A cells (**Figure 6A**). Some TNBC cell lines expressed more *P2RX4* mRNA in comparison to MCF-10A cells: MDA-MB 231 (5-fold; $p=0.0012$ and MDA-MB 468 (10-fold; $p=0.0001$); whereas Hs 578t cells expressed levels that were not significantly different ($p>0.05$). MDA-MB 231 and Hs 578t cells expressed significantly less *P2RX7* mRNA when compared to MCF-10A cells ($p=0.0001$ for both); whereas, MDA-MB 468 cells expressed 25-fold more *P2RX7* mRNA when compared to MCF-10A cells ($p=0.0006$).

Western blot analysis was performed on TNBC cell lines, MCF-10A cells and HEK 293T cells transfected with either a P2RX4 or P2RX7 expression plasmid as positive controls, probing for P2RX4 and P2RX7 with GAPDH as the internal loading control (**Figure 6B**). Two of three TNBC cell lines

expressed more P2RX4 protein when compared to MCF-10A cells when assessed by semi-quantitative densitometry: MDA-MB 231 (20-fold; $p=0.001$), MDA-MB 468 (22-fold; $p=0.001$) while Hs 578t cells expressed significantly less P2RX4 protein ($p=0.01$). We separately probed for P2RX7 protein in the same cell lines. We did detect specific bands corresponding to the full-length glycosylated P2RX7A isoform (75kDa) in the MCF-10A cells but significantly less protein was detected in MDA-MB 231 and Hs 578t cells while a specific 69 kDa band was detected in MDA-MB 468 and Hs 578t cells; we did detect specific bands at 69 and 75 kDa in transfected 293T cells that increased in intensity with increasing loaded mass of lysate from P2RX7-transfected 293T cells. The P2RX7 expression plasmid incorporates the cDNA for the full-length P2RX7A isoform. The P2RX7 protein includes 5 N-linked glycosylation sites. Thus, the 69 kDa band corresponds to the unglycosylated form of the protein and the 75 kDa band likely represents the fully glycosylated form of the protein.

Given that unglycosylated form may not represent the plasma membrane-localized fraction of a protein, we used flow cytometry to quantitate the expression of P2RX7 and P2RX4 at the cell surface. Flow cytometry analysis was performed on TNBC, MCF-10A, and HEK 293T cells transfected with either vector control or P2RX4 expression plasmid as a positive control, probing for cell surface expression P2RX4 (**Figure 6D**) using a primary antibody that targets the extracellular domains of P2RX4. MDA-MB 231, Hs 578t and MDA-MB 468 expressed significantly less cell surface P2RX4 in comparison to MCF-10A cells. The calculated mean fluorescence intensity (MFI) difference between the P2RX4 specific and isotype control antibody for MCF-10A cells was 498, for MDA-MB 231 cells 316 ($p=0.05$ when compared to MFI difference for MCF-10A), for MDA-MB 468 cells 246 ($p=0.02$), and Hs 578t cells 189 ($p=0.01$).

We performed flow cytometry analysis on TNBC, MCF-10A, and HEK 293T cells transfected with either empty vector or P2RX7 expression plasmid as a positive control, probing for cell surface expression P2RX7 (**Figure 6D**) using a primary antibody that targets the extracellular domains of P2RX7. MDA-MB 231, Hs 578t and MDA-MB 468 expressed significantly more cell surface P2RX7 in comparison to MCF-10A cells. The calculated mean fluorescence intensity (MFI) difference between P2RX7 and the isotype control for MCF-10A cells was 51, for MDA-MB 231 cells 129 ($p=0.003$ when compared to MFI difference to MCF-10A), for MDA-MB 468 cells 182 ($p=0.002$), and for Hs 578t cells 703 ($p=0.0001$). Thus, all cell lines expressed both receptors at the cell surface when measured by flow cytometry, and all the TNBC cell lines expressed significantly more P2RX7 protein at the cell surface than immortal mammary epithelial cells.

Additionally, all cell lines were treated with 100 $\mu\text{mol/L}$ paclitaxel and the cell surface expressions of P2RX4 and P2RX7 were examined with the calculated difference in MFI values between cells stained with P2RX4 or P2RX7 specific antibodies to cells stained with the corresponding isotype control (**Supplementary Figure 4**). Upon treatment, cell

surface expression of P2RX7 increased significantly in some TNBC cell lines but this was not a consistent effect.

DISCUSSION

Chemotherapy by itself fails to ablate metastatic TNBC. Extracellular ATP, in the high micromolar to millimolar range, induces cytotoxicity in cancer cell lines. Chemotherapy is known to induce increases in eATP. We hypothesized that interventions that augment chemotherapy-induced increases in eATP would increase cancer cell death.

Our results show that inhibitors of E-NTPDases, ENPPases and TNAP all significantly increased the release of eATP with chemotherapy exposure. However, only the E-NTPDase inhibitor PSB 069, a sulfonated tetracyclic compound, but not POM-1, another E-NTPDase inhibitor, consistently and significantly increased chemotherapy-induced cell death. Both are inhibitors of multiple E-NTPDase isoforms. Some reports suggest that POM-1 also blocks several P2XRs. This may interfere with cell death and may explain their differing effects on chemotherapy-induced cell death. ENPPase and TNAP substrates are not limited to ATP and can affect other nucleotides and cyclic nucleotides, and therefore, inhibition of these enzymes may have ATP non-specific effects (46–48). Each metabolite may have different effects on cell viability, either positive or negative, and this could explain why ENPPase and TNAP increase eATP levels but do not impact cell viability.

We also showed that the addition of exogenous eATP in the absence of chemotherapy significantly reduced TNBC cell viability. Specific inhibitors of P2RX4 and P2RX7, but not a non-specific P2RX inhibitor, attenuated the effects of ATP on cell viability and the effects of E-NTPDase inhibitors on eATP levels and their positive effects on chemotherapy-induced cell death. These data show that ATP-induced cell death and E-NTPDase-inhibitor induced augmentation of chemotherapy-induced cell death are mediated through P2RX4 and P2RX7 channels. However, two observations suggest that P2RX4 and P2RX7 activation alone may not be sufficient for the loss of cell viability observed. Firstly, the addition of eATP to cells was toxic to MDA-MB 231 and Hs 578t cells but minimally affected MDA-MB 468 cells. However, upon chemotherapy treatment, an E-NTPDase inhibitor significantly increased eATP levels and augmented chemotherapy-induced cell death in all the TNBC cell lines. Secondly, the addition of eATP induced loss of TNBC cell viability at concentrations that were higher than those that were observed upon chemotherapy treatment in the presence of eATPase inhibitors. Thus, although P2RX4 and P2RX7 activation are necessary for the augmentation of chemotherapy-induced cell death by eATP, other factors may be required in parallel. For example, the NLRP3 inflammasome is one such death pathway whose activation is dependent on eATP but must also be primed by other factors such as NF- κ B activation. Also, it is important to consider previous research which suggests that eATP concentrations in the immediate pericellular region may far exceed those in the bulk interstitial fluid (21). Thus, our

measurements of eATP in the bulk supernatants may have underestimated pericellular eATP concentrations. In addition, ATP-induced signaling may occur in membrane demarcated intracellular organelles such as lysosomes, where ATP concentrations are independent of eATP concentrations (49).

The effects of eATP on cell viability and the effects of extracellular ATPase inhibitors on eATP levels were reversed by specific P2RX4 and P2RX7 inhibitors suggesting that these receptors are not only necessary for the accentuated cell death downstream of increased eATP but also necessary for increased eATP release. The fact that P2RX4 and P2RX7 antagonists significantly attenuated eATP release even at concentrations of paclitaxel at which cytotoxicity was similar between the treatment groups, suggests that their attenuation of eATP was not due to attenuation of cell death. Given that the P2RX4 and P2RX7 antagonists but not a non-specific P2RX blocker reversed these effects, they are likely specific to these two receptor types.

We aimed to identify clinically approved compounds that modulate eATP levels. The antiparasitic drug ivermectin is an activator of P2RX4 and P2RX7 (44, 45). We showed that consistent with this activity, ivermectin sensitized TNBC cell lines to chemotherapy. Interestingly, we also observed increased eATP release in chemotherapy-treated cells in the presence of ivermectin. This finding is consistent with our data indicating that P2RX4 and P2RX7 channels are not only necessary for ATP-induced loss of viability but also for eATP release.

Concerning expression levels, our western blot data show that P2RX4 is highly expressed in some TNBC cell lines as compared to immortal mammary epithelial cells. However, our flow cytometry data revealed significantly decreased cell surface expression of P2RX4 in the TNBC cell lines as compared to between MCF-10A cells. Previous publications suggest that the

majority of P2RX4 is expressed on lysosomal membranes and that cell surface expression can be increased by stimuli that induce lysosomal exocytosis such as calcium ions (49). This may explain the different expression patterns detected by western blot and flow cytometry.

On western blot analysis of mammary cells, we detected a specific band corresponding to the full-length glycosylated form of P2RX7 in the MDA-MB 231 and MCF-10A cells and lower molecular weight bands that may represent unglycosylated forms of P2RX7 in the MDA-MB 468 and Hs 578t cells. Although expression levels may be low, given that a specific inhibitor of P2RX7 markedly attenuated the cytotoxic effects of eATP and attenuated the positive effects of E-NTPDase inhibitors on eATP levels and loss of cell viability upon chemotherapy exposure, it is possible that even low levels of expression P2RX7 may have functional consequences due to the formation of non-selective macropores in the cell membrane.

On the other hand, our flow cytometry data shows that P2RX7 is expressed at the cell surface of all the TNBC cell lines at higher levels than MCF-10A cells and in the presence of paclitaxel some TNBC cell lines expressed more P2RX7. This suggests there may be selection pressure for higher expression of P2RX7 in TNBC cell lines. Several published data support the facilitator role played by extracellular adenosine, derived from the metabolism of eATP, for the survival of cancer cells by inducing cell-autonomous effects on proliferation and cancer stem cell-like properties as well as paracrine effects on angiogenesis and immunoevasion (50–53). Additionally, this expression analysis was applied to check if expression levels of P2RX4 and P2RX7 could explain the difference in the observed effects between the MDA-MB 468 and other TNBC cell lines; the expression analysis did reveal significant differences in

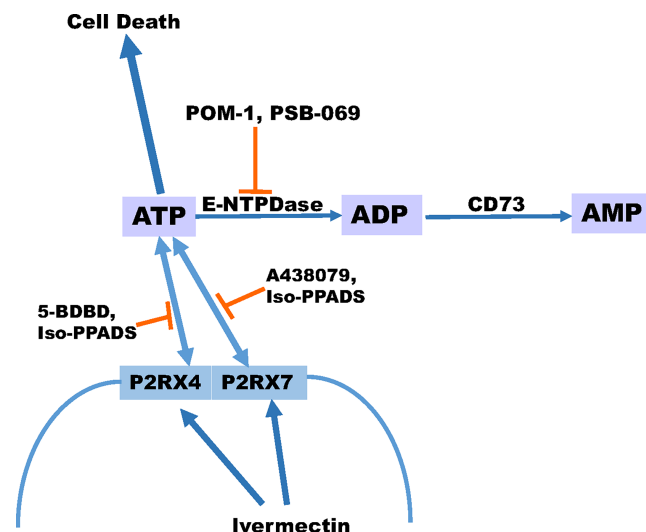


FIGURE 7 | Schematic displaying our proposed model for ATP release. Our proposed model suggests that ivermectin activates P2RX4 and P2RX7 leading to the release of ATP and the more ATP that accumulates extracellular can promote cell death especially in the presence of paclitaxel. In addition, the breakdown of ATP can be prevented in the presence of E-NTPDase inhibitors POM-1 or PSB 069. However, the release of ATP can be prevented in the presence of P2RX4 inhibitors 5-BDBD or Iso-PPADS or P2RX7 inhibitors A438079 or Iso-PPADS.

expression levels. This could explain differences in sensitivity of the cell lines to the eATPase inhibitors and to ivermectin.

In summary, our data indicate that eATP is toxic to several TNBC cell lines and P2RX4 and P2RX7 purinergic channels are necessary for this effect. Chemotherapy exposure induces the release of ATP from TNBC cell lines and inhibitors of eATP metabolism augment chemotherapy-induced loss of TNBC cell viability, and these effects are reversed by specific inhibitors of P2RX4 and P2RX7, suggesting that both eATP release and eATP induced loss of cell viability are mediated by these channels. A heterocyclic-sulphonate inhibitor of multiple E-NTPDases, PSB 069, was most effective at accentuating chemotherapy-induced cell death. A P2RX4 and P2RX7 activator, ivermectin, also accentuated chemotherapy-induced increases in eATP and loss of TNBC cell viability (Figure 7). Although only E-NTPDase inhibitors consistently increased chemotherapy-induced loss of cell viability, all the different classes of extracellular ATPase inhibitors increased eATP levels in the setting of chemotherapy exposure. Thus, to maximally augment eATP levels and reduce adenosine in the tumor microenvironment, inhibitors that have broad inhibitory effects on multiple classes of extracellular ATPases may be necessary. This is in contrast to current monoclonal antibody-based strategies that narrowly focus on E-NTPDase1/CD39 (54). Our future goals are to examine the effects of eATPase inhibition and P2RX4 and P2RX7 activation on TNBC models *in vivo* in the context of an intact tumor microenvironment and functional immune system. These preclinical experiments may lead to therapeutic strategies for TNBC that modulate purinergic signaling in the tumor microenvironment.

DATA AVAILABILITY STATEMENT

The raw data supporting the conclusions of this article will be made available by the authors, without undue reservation.

REFERENCES

1. WHO *Breast Cancer* (2020). Available at: <https://www.who.int/cancer/prevention/diagnosis-screening/breast-cancer/en/>.
2. Dent R, Hanna WM, Trudeau M, Rawlinson E, Sun P, Narod SA. Pattern of Metastatic Spread in Triple-Negative Breast Cancer. *Breast Cancer Res Treat* (2009) 115(2):423–8. doi: 10.1007/s10549-008-0086-2
3. Fisher CS, Ma CX, Gillanders WE, Aft RL, Eberlein TJ, Gao F, et al. Neoadjuvant Chemotherapy is Associated With Improved Survival Compared With Adjuvant Chemotherapy in Patients With Triple-Negative Breast Cancer Only After Complete Pathologic Response. *Ann Surg Oncol* (2012) 19(1):253–8. doi: 10.1245/s10434-011-1877-y
4. Ovaricek T, Frkovic SG, Matos E, Mozina B, Borstnar S. Triple Negative Breast Cancer - Prognostic Factors and Survival. *Radiol Oncol* (2011) 45(1):46–52. doi: 10.2478/v10019-010-0054-4
5. Pellegatti P, Raffaghelli L, Bianchi G, Piccardi F, Pistoia V, Di Virgilio F. Increased Level of Extracellular ATP at Tumor Sites: *In Vivo* Imaging With Plasma Membrane Luciferase. *PLoS One* (2008) 3(7):e2599. doi: 10.1371/journal.pone.0002599
6. Yegutkin GG. Nucleotide- and Nucleoside-Converting Ectoenzymes: Important Modulators of Purinergic Signalling Cascade. *Biochim Biophys Acta* (2008) 1783(5):673–94. doi: 10.1016/j.bbamcr.2008.01.024
7. Fan M, Yan PS, Hartman-Frey C, Chen L, Paik H, Oyer SL, et al. Diverse Gene Expression and DNA Methylation Profiles Correlate With Differential Adaptation

AUTHOR CONTRIBUTIONS

All authors contributed to review and analysis. JMM performed a majority of the assays with NW executing the RNA analysis and JD carrying out the Western blot analysis. JM and MAC conceived of and designed the experiments, reviewed the data, authored and edited the manuscript. All authors contributed to the article and approved the submitted version.

FUNDING

Research reported in this publication was supported by The Ohio State University Comprehensive Cancer Center. Institutions that provided funding support had no role in the design or conduct of this study or the preparation of the manuscript. This publication was also supported, in part, by the National Center for Advancing Translational Sciences of the National Institutes of Health under Grant Numbers KL2TR002734. The content is solely the responsibility of the authors and does not necessarily represent the official views of the National Institutes of Health.

ACKNOWLEDGMENTS

This manuscript is available for preprint: doi: <https://doi.org/10.1101/2022.01.11.475873>.

SUPPLEMENTARY MATERIAL

The Supplementary Material for this article can be found online at: <https://www.frontiersin.org/articles/10.3389/fonc.2022.855032/full#supplementary-material>

- of Breast Cancer Cells to the Antiestrogens Tamoxifen and Fulvestrant. *Cancer Res* (2006) 66(24):11954–66. doi: 10.1158/0008-5472.CAN-06-1666
8. Bakker WW, Donker RB, Timmer A, van Pampus MG, van Son WJ, Aarnoudse JG, et al. Plasma Hemopexin Activity in Pregnancy and Preeclampsia. *Hypertens Pregnancy* (2007) 26(2):227–39. doi: 10.1080/10641950701274896
9. Antonioli L, Pacher P, Vizi ES, Hasko G. CD39 and CD73 in Immunity and Inflammation. *Trends Mol Med* (2013) 19(6):355–67. doi: 10.1016/j.molmed.2013.03.005
10. Chekeni FB, Elliott MR, Sandilos JK, Walk SF, Kinchen JM, Lazarowski ER, et al. Pannexin 1 Channels Mediate 'Find-Me' Signal Release and Membrane Permeability During Apoptosis. *Nature* (2010) 467(7317):863–7. doi: 10.1038/nature09413
11. Brandao-Burch A, Key ML, Patel JJ, Arnett TR, Orriss IR. The P2X7 Receptor is an Important Regulator of Extracellular ATP Levels. *Front Endocrinol (Lausanne)* (2012) 3:41. doi: 10.3389/fendo.2012.00041
12. Ferrari D, Pizzirani C, Adinolfi E, Lemoli RM, Curti A, Idzko M, et al. The P2X7 Receptor: A Key Player in IL-1 Processing and Release. *Jof Immuno* (2006) 176(7):3877–83. doi: 10.4049/jimmunol.176.7.3877
13. Yaron JR, Gangaraju S, Rao MY, Kong X, Zhang L, Su F, et al. K(+) Regulates Ca(2+) to Drive Inflammasome Signaling: Dynamic Visualization of Ion Flux in Live Cells. *Cell Death Dis* (2015) 6(10):e1954. doi: 10.1038/cddis.2015.277
14. Mackenzie AB, Young MT, Adinolfi E, Surprenant A. Pseudopapoptosis Induced by Brief Activation of ATP-Gated P2X7 Receptors. *J Biol Chem* (2005) 280(40):33968–76. doi: 10.1074/jbc.M502705200

15. Gilbert SM, Oliphant CJ, Hassan S, Peille AL, Bronsert P, Falzoni S, et al. ATP in the Tumour Microenvironment Drives Expression of Nfp2x7, a Key Mediator of Cancer Cell Survival. *Oncogene* (2019) 38(2):194–208. doi: 10.1038/s41388-018-0426-6
16. Adinolfi E, Raffaghello L, Giuliani AL, Cavazzini L, Capece M, Chiozzi P, et al. Expression of P2X7 Receptor Increases *In Vivo* Tumor Growth. *Cancer Res* (2012) 72(12):2957–69. doi: 10.1158/0008-5472.CAN-11-1947
17. Haag F, Adriouch S, Brass A, Jung C, Moller S, Scheuplein F, et al. Extracellular NAD and ATP: Partners in Immune Cell Modulation. *Purinergic Signal* (2007) 3(1-2):71–81. doi: 10.1007/s11302-006-9038-7
18. Perez-Flores G, Levesque SA, Pacheco J, Vaca L, Lacroix S, Perez-Cornejo P, et al. The P2X7/P2X4 Interaction Shapes the Purinergic Response in Murine Macrophages. *Biochem Biophys Res Commun* (2015) 467(3):484–90. doi: 10.1016/j.bbrc.2015.10.025
19. Gobeil S, Boucher CC, Nadeau D, Poirier GG. Characterization of the Necrotic Cleavage of Poly(ADP-Ribose) Polymerase (PARP-1): Implication of Lysosomal Proteases. *Cell Death Differ* (2001) 8(6):588–94. doi: 10.1038/sj.cdd.4400851
20. Elliott MR, Cheken FB, Trampont PC, Lazarowski ER, Kadl A, Walk SF, et al. Nucleotides Released by Apoptotic Cells Act as a Find-Me Signal to Promote Phagocytic Clearance. *Nature* (2009) 461:282–6. doi: 10.1038/nature08296
21. Pellegatti P, Falzoni S, Pinton P, Rizzuto R, Di Virgilio F. A Novel Recombinant Plasma Membrane-Targeted Luciferase Reveals a New Pathway for ATP Secretion. *Mol Biol Cell* (2005) 16(8):3659–65. doi: 10.1091/mbc.e05-03-0222
22. Akopova I, Tatur S, Grygorczyk M, Luchowski R, Gryczynski I, Gryczynski Z, et al. Imaging Exocytosis of ATP-Containing Vesicles With TIRF Microscopy in Lung Epithelial A549 Cells. *Purinergic Signal* (2012) 8(1):59–70. doi: 10.1007/s11302-011-9259-2
23. Fader CM, Aguilera MO, Colombo MI. ATP is Released From Autophagic Vesicles to the Extracellular Space in a VAMP7-Dependent Manner. *Autophagy* (2012) 8(12):1741–56. doi: 10.4161/auto.21858
24. Jansen RS, Duijst S, Mahakena S, Sommer D, Szeri F, Varadi A, et al. ABCC6-Mediated ATP Secretion by the Liver is the Main Source of the Mineralization Inhibitor Inorganic Pyrophosphate in the Systemic Circulation-Brief Report. *Arterioscler Thromb Vasc Biol* (2014) 34(9):1985–9. doi: 10.1161/ATVBAHA.114.304017
25. Zimmermann H, Zebisch M, Strater N. Cellular Function and Molecular Structure of Ecto-Nucleotidases. *Purinergic Signal* (2012) 8(3):437–502. doi: 10.1007/s11302-012-9309-4
26. Martins I, Tesniere A, Kepp O, Michaud M, Schlemmer F, Senovilla L, et al. Chemotherapy Induces ATP Release From Tumor Cells. *Cell Cycle* (2009) 8(22):3723–8. doi: 10.4161/cc.8.22.10026
27. Di Virgilio F, Adinolfi E. Extracellular Purines, Purinergic Receptors and Tumor Growth. *Oncogene* (2017) 36(3):293–303. doi: 10.1038/ncr.2016.206
28. Xia J, Yu X, Tang L, Li G, He T. P2X7 Receptor Stimulates Breast Cancer Cell Invasion and Migration via the AKT Pathway. *Oncol Rep* (2015) 34(1):103–10. doi: 10.3892/or.2015.3979
29. Yoshihara K, Shahmoradgoli M, Martinez E, Vegesna R, Kim H, Torres-Garcia W, et al. Inferring Tumour Purity and Stromal and Immune Cell Admixture From Expression Data. *Nat Commun* (2013) 4:2612. doi: 10.1038/ncomms3612
30. Lertsuwan K, Peters W, Johnson L, Lertsuwan J, Marwa I, Sikes RA. Purinergic Receptor Expression and Cellular Responses to Purinergic Agonists in Human Prostate Cancer Cells. *Anticancer Res* (2017) 37(2):529–37. doi: 10.21873/anticancer.11345
31. Rapaport E. Experimental Cancer Therapy in Mice by Adenine Nucleotides. *Eur Jof Cancer Clin Oncol* (1988) 24(9):1491–7. doi: 10.1016/0277-5379(88)90340-9
32. Fontaine E. Anticancer Activities of Adenine Nucleotides in Mice are Mediated Through Expansion of Erythrocyte ATP Pool. *Proc Nati Acad Sci* (1996) 86:1662–6. doi: 10.1073/pnas.86.5.1662
33. Haskell EA. Phase I Trial of Extracellular Adenosine 5'-Triphosphate in Patients With Advanced Cancer. *Med Pediatr Oncol* (1996) 27:165–73. doi: 10.1002/(SICI)1096-911X(199609)27:3<165::AID-MPO6>3.0.CO;2-C
34. du Bois A, Luck HJ, Meier W, Adams HP, Mobus V, Costa S, et al. A Randomized Clinical Trial of Cisplatin/Paclitaxel Versus Carboplatin/Paclitaxel as First-Line Treatment of Ovarian Cancer. *J Natl Cancer Inst* (2003) 95(17):1320–9. doi: 10.1093/jnci/djg036
35. Jacques-Silva MC, Correa-Medina M, Cabrera O, Rodriguez-Diaz R, Makeeva N, Fachado A, et al. ATP-Gated P2X3 Receptors Constitute a Positive Autocrine Signal for Insulin Release in the Human Pancreatic Beta Cell. *Proc Natl Acad Sci USA* (2010) 107(14):6465–70. doi: 10.1073/pnas.0908935107
36. Fleck D, Mundt N, Bruentgens F, Geilenkirchen P, Machado PA, Veitinger T, et al. Distinct Purinergic Signaling Pathways in Prepubescent Mouse Spermatogonia. *J Gen Physiol* (2016) 148(3):253–71. doi: 10.1085/jgp.201611636
37. Balazs B, Danko T, Kovacs G, Koles L, Hediger MA, Zsembery A. Investigation of the Inhibitory Effects of the Benzodiazepine Derivative, 5-BDBD on P2X4 Purinergic Receptors by Two Complementary Methods. *Cell Physiol Biochem* (2013) 32(1):11–24. doi: 10.1159/000350119
38. Pimenta-Dos-Reis G, Torres EJJ, Quintana PG, Vidal LO, Dos Santos BAF, Lin CS, et al. POM-1 Inhibits P2 Receptors and Exhibits Anti-Inflammatory Effects in Macrophages. *Purinergic Signal* (2017) 13(4):611–27. doi: 10.1007/s11302-017-9588-x
39. Draganov D, Gopalakrishna-Pillai S, Chen YR, Zuckerman N, Moeller S, Wang C, et al. Modulation of P2X4/P2X7/Pannexin-1 Sensitivity to Extracellular ATP via Ivermectin Induces a Non-Apoptotic and Inflammatory Form of Cancer Cell Death. *Sci Rep* (2015) 5:16222. doi: 10.1038/srep16222
40. Carozza JA, Brown JA, Bohnert V, Fernandez D, AlSaif Y, Mardjuki RE, et al. Structure-Aided Development of Small-Molecule Inhibitors of ENPP1, the Extracellular Phosphodiesterase of the Immunotransmitter Cgamp. *Cell Chem Biol* (2020) 27(11):1347–58.e5. doi: 10.1016/j.chembiol.2020.07.007
41. Li Q, Huang J, Pinkerton AB, Millan JL, van Zelst BD, Levine MA, et al. Inhibition of Tissue-Nonspecific Alkaline Phosphatase Attenuates Ectopic Mineralization in the Abcc6(-/-) Mouse Model of PXE But Not in the Enpp1 Mutant Mmouse Models of GACI. *J Invest Dermatol* (2019) 139(2):360–8. doi: 10.1016/j.jid.2018.07.030
42. Ramanadham N, Nageshwari B. Anti-Proliferative Effect of Levamisole on Human Myeloma Cell Lines. *Vitro J Immunotoxicol* (2010) 7(4):327–32. doi: 10.3109/1547691X.2010.514871
43. Davidson TG. Conventional Treatment of Hypercalcemia of Malignancy. *Am J Health Syst Pharm* (2001) 58:S8–S15. doi: 10.1093/ajhp/58.suppl_3.S8
44. Khakh BS, Proctor WR, Dunwiddie TV, Labarca C, Lester HA. Allosteric Control of Gating and Kinetics at P2X(4) Receptor Channels. *Jof Neuroscience: Off J Soc Neurosci* (1999) 19(17):7289–99. doi: 10.1523/JNEUROSCI.19-17-07289.1999
45. Nörenberg W, Sobottka H, Hempel C, Plötz T, Fischer W, Schmalzing G, et al. Positive Allosteric Modulation by Ivermectin of Human But Not Murine P2X7 Receptors. *BritishJournal Pharmacol* (2012) 167(1):48–66. doi: 10.1111/j.1476-5381.2012.01987.x
46. Millan JL. Alkaline Phosphatases: Structure, Substrate Specificity and Functional Relatedness to Other Members of a Large Superfamily of Enzymes. *Purinergic Signal* (2006) 2(2):335–41. doi: 10.1007/s11302-005-5435-6
47. Onyedibe KI, Wang M, Sintim HO. ENPP1, an Old Enzyme With New Functions, and Small Molecule Inhibitors-a STING in the Tale of ENPP1. *Molecules* (2019) 24(22):1–18. doi: 10.3390/molecules24224192
48. Sebastian-Serrano A, de Diego-Garcia L, Martinez-Frailes C, Avila J, Zimmermann H, Millan JL, et al. Tissue-Nonspecific Alkaline Phosphatase Regulates Purinergic Transmission in the Central Nervous System During Development and Disease. *Comput Struct Biotechnol J* (2015) 13:95–100. doi: 10.1016/j.csbj.2014.12.004
49. Qureshi OS, Paramasivam A, Yu JC, Murrell-Lagnado RD. Regulation of P2X4 Receptors by Lysosomal Targeting, Glycan Protection and Exocytosis. *J Cell Sci* (2007) 120(Pt 21):3838–49. doi: 10.1242/jcs.010348
50. Lan J, Lu H, Samanta D, Salman S, Lu Y, Semenza GL. Hypoxia-Inducible Factor 1-Dependent Expression of Adenosine Receptor 2B Promotes Breast

- Cancer Stem Cell Enrichment. *Proc Natl Acad Sci* (2018) 115(41):E9640–E8. doi: 10.1073/pnas.1809695115
51. Fernandez-Gallardo M, González-Ramírez R, Sandoval A, Felix R, Monjaraz E. Adenosine Stimulate Proliferation and Migration in Triple Negative Breast Cancer Cells. *PLoS One* (2016) 11(12):e0167445. doi: 10.1371/journal.pone.0167445
 52. Blay J, White TD, Hoskin DW. The Extracellular Fluid of Solid Carcinomas Contains Immunosuppressive Concentrations of Adenosine. *Cancer Res* (1997) 57(13):2602–5.
 53. Du X, Ou X, Song T, Zhang W, Cong F, Zhang S, et al. Adenosine A2B Receptor Stimulates Angiogenesis by Inducing VEGF and Enos in Human Microvascular Endothelial Cells. *Exp Biol Med* (2015) 240(11):1472–9. doi: 10.1177/1535370215584939
 54. Spatola BN, Lerner AG, Wong C, Dela Cruz T, Welch M, Fung W, et al. Fully Human Anti-CD39 Antibody Potently Inhibits Atpase Activity in Cancer Cells via Uncompetitive Allosteric Mechanism. *mAbs* (2020) 12(1):1838036. doi: 10.1080/19420862.2020.1838036

Conflict of Interest: The authors declare that the research was conducted in the absence of any commercial or financial relationships that could be construed as a potential conflict of interest.

Publisher's Note: All claims expressed in this article are solely those of the authors and do not necessarily represent those of their affiliated organizations, or those of the publisher, the editors and the reviewers. Any product that may be evaluated in this article, or claim that may be made by its manufacturer, is not guaranteed or endorsed by the publisher.

Copyright © 2022 Manouchehri, Datta, Willingham, Wesolowski, Stover, Ganju, Carson, Ramaswamy and Cherian. This is an open-access article distributed under the terms of the Creative Commons Attribution License (CC BY). The use, distribution or reproduction in other forums is permitted, provided the original author(s) and the copyright owner(s) are credited and that the original publication in this journal is cited, in accordance with accepted academic practice. No use, distribution or reproduction is permitted which does not comply with these terms.

Frontiers in Oncology

Advances knowledge of carcinogenesis and tumor progression for better treatment and management

The third most-cited oncology journal, which highlights research in carcinogenesis and tumor progression, bridging the gap between basic research and applications to improve diagnosis, therapeutics and management strategies.

Discover the latest Research Topics

[See more →](#)

Frontiers

Avenue du Tribunal-Fédéral 34
1005 Lausanne, Switzerland
frontiersin.org

Contact us

+41 (0)21 510 17 00
frontiersin.org/about/contact

